

Functional renormalization group approach to quantum Heisenberg paramagnets

Dissertation
zur Erlangung des Doktorgrades
der Naturwissenschaften

vorgelegt beim Fachbereich Physik
der Johann Wolfgang Goethe-Universität
in Frankfurt am Main

von
Dmytro Tarasevych
aus
Shitomir, Ukraine

Frankfurt 2023
(D30)

vom Fachbereich Physik der
Johann Wolfgang Goethe-Universität
als Dissertation angenommen.

Dekan: Prof. Dr. Roger Erb

Gutachter: Prof. Dr. Peter Kopietz
Priv. Doz. Dr. Oleksandr Tsyplyatyev
Prof. Dr. Johannes Reuther

Datum der Disputation: 24.06.2024

Abstract

This thesis is concerned with the investigation of static and dynamic properties of quantum Heisenberg paramagnets in the absence of a magnetic field and therefore for vanishing magnetization. For this purpose a new formulation of the spin functional renormalization group (SFRG) is employed. The first manifestations of the SFRG were developed by Krieg and Kopietz [1, 2], motivated by the FRG approach to ordinary field theories [3, 4] and the older works of Vaks, Larkin and Pikin on diagrammatic methods for spin operators [5, 6]. The main idea is to study quantum spin systems by considering the evolution of correlation functions under a continuous deformation of the interaction between magnetic moments, starting from a solvable limit. This leads to nonperturbative results for quantities like the spin-spin correlation function. After a basic introduction to the phenomena and concomitant problems discussed in this thesis, a detailed description of the SFRG method in its initial formulation is given in the second chapter. We start with the generating functional of connected imaginary-time spin-correlation functions $\mathcal{G}_\Lambda[\mathbf{h}]$, for which an exact flow equation is derived. A particular issue, already pointed out by Krieg and Kopietz, arises here, namely the singular non-interacting limit of its subtracted Legendre transform $\Gamma_\Lambda[\mathbf{m}]$. As a consequence the initial condition of that functional does not have a proper series expansion in powers of \mathbf{m} . This prevents us from working directly within a pure one-particle irreducible (1-PI) parametrization of the correlation functions, as is often done in the context of field theories [3, 4]. Thus motivated, we develop a workaround explicitly tailored to paramagnets, which provides us with a functional that has a well-behaved Legendre transform. The new approach is based on a different treatment of fluctuations at zero and finite frequencies, analogous to a previous hybrid formulation for the symmetry-broken phase [7, 8, 9]. Certain properties, considered to be highly relevant for isotropic paramagnets, as well as previous observations, already made in the study of simpler spin systems like the Ising model [1, 2], serve as additional justifications for choosing this construction [10].

In the third chapter our new method is assessed by calculating the dynamic susceptibility $G(\mathbf{k}, i\omega)$ and thus the dynamic structure factor $S(\mathbf{k}, \omega)$ in the symmetric phase. For this purpose an approximate integral equation for the dynamic polarization function $\tilde{\Pi}(\mathbf{k}, i\omega)$ was derived [10]. This equation results from a truncation of the hierarchy of flow equations and contains static quantities, that are assumed to be known from another source. Our first application is the high-temperature limit $T \rightarrow \infty$ in $d \leq 3$ dimensions. Salient features, believed to be part of the spin dynamics in isotropic Heisenberg magnets are also exhibited by our solution, like (anomalous) diffusion in a suitable hydrodynamic limit. Moreover we obtain the same order of magnitude for the diffusion coefficient \mathcal{D} as in experiments and other theoretical calculations. Other aspects do not entirely agree with previous approaches. Afterwards we continue by investigating systems close to the critical point T_c [11]. Dynamic scaling forms for $\tilde{\Pi}(\mathbf{k}, i\omega)$ and $S(\mathbf{k}, \omega)$, which, like spin diffusion, are postulated on the basis of quite general physical arguments, are reproduced. Agreement of the line-shapes

with neutron scattering experiments at $T = T_c$ is found to be satisfying, with deviations for $\omega \rightarrow 0$, that may be attributed to the simplicity of the approximation, like at infinite temperature.

Finally, we focus our attention on the thermodynamic properties of isotropic Heisenberg paramagnets by calculating the static susceptibility $G(\mathbf{k})$. For this purpose we employ simple truncation schemes of the flow equations for the static self-energy $\Sigma_\Lambda(\mathbf{k})$ and four-spin vertex $\Gamma_\Lambda^{(4)}$, together with a basic ansatz for the dynamic polarization $\tilde{\Pi}(\mathbf{k}, i\omega)$ in quantum systems [12]. As a result we obtain transition temperatures T_c of three-dimensional non-frustrated magnets within an accuracy of 5 percent compared to established benchmark values from Quantum Monte Carlo and high temperature expansion series. We conclude this chapter by giving an outlook on the application of our method to frustrated systems, which may require a combined non-trivial calculation of static and dynamic properties.

Publications

This thesis is partially based on the work contained in the following three publications (titles reprinted with permission © [2021-2023] American Physical Society):

Dmytro Tarasevych and Peter Kopietz
Dissipative spin dynamics in hot quantum paramagnets,
Phys. Rev. B **104**, 024423 (2021) [10]

Dmytro Tarasevych and Peter Kopietz
Critical spin dynamics of Heisenberg ferromagnets revisited,
Phys. Rev. B **105**, 024403 (2022) [11]

D. Tarasevych, A. Rückriegel, S. Keupert, V. Mitsiioannou, and P. Kopietz,
Spin-functional renormalization group for the $J_1J_2J_3$ quantum Heisenberg model,
Phys. Rev. B **106**, 174412 (2022);
Erratum: Spin-functional renormalization group for the $J_1J_2J_3$ quantum Heisenberg model,
ibid, **107**, 019904(E) (2023). [12]

Moreover I was one of the authors of the following publications (titles reprinted with permission © [2018-2019] American Physical Society):

D. Tarasevych, J. Krieg, and P. Kopietz,
A rich man's derivation of scaling laws for the Kondo model,
Phys. Rev. B **98**, 235133 (2018)

R. Goll, D. Tarasevych, J. Krieg, and P. Kopietz,
Spin functional renormalization group for quantum Heisenberg ferromagnets: Magnetization and magnon damping in two dimensions,
Phys. Rev. B **100**, 174424 (2019) [7]

The first one resulted from my Bachelor project and the second one included results from my Master project.

Table of Contents

Abstract	2
Publications	3
1 Introduction	8
1.1 The Heisenberg model	8
1.2 Thermodynamics	12
1.2.1 Critical region	15
1.3 Linear response and dynamic correlation functions	18
1.3.1 Linear response	19
1.3.2 Magnetic scattering and dynamic structure factor	20
1.3.3 Matsubara (imaginary-time) formalism	23
1.4 Hydrodynamics and dynamic scaling	25
1.4.1 Hydrodynamics	25
1.4.2 Van Hove Theory of critical scattering and mode-coupling approach	28
1.4.3 Dynamic scaling	30
2 Spin functional renormalization group	34
2.1 Motivation	34
2.2 Initial formulations	35
2.2.1 1-PI formalism	35
2.2.2 1-JI (VLP) formalism	40
2.3 Static-dynamic hybrid functional	43
2.3.1 Amputation with respect to bare coupling	43
2.3.2 Amputation with respect to the inverse propagator	47
3 Dynamic structure factor of a Heisenberg paramagnet	56
3.1 Derivation of an approximation to calculate $\tilde{\Pi}_\Lambda$	56
3.1.1 Flow equations in the high-temperature limit	57
3.1.2 Integral equation	61
3.2 High-temperature limit	69
3.2.1 Spin diffusion above two dimensions	71
3.2.2 Non-analytic corrections to spin diffusion	78
3.2.3 Anomalous diffusion in reduced dimensions	81
3.2.4 General frequency and momentum dependence and correlations in real space	88
3.3 Three-dimensional ferromagnet close to the phase transition	92
3.3.1 Spin diffusion in the vicinity of $T = T_c$	98

3.3.2	Scaling function at the critical point	100
3.3.3	Comparison of the critical scattering with theory	105
3.3.4	Comparison of the critical scattering with experiments	108
3.4	Discussion of the antiferromagnet in $d = 3$ close to T_c	115
3.5	Ferromagnets in reduced dimensions at low temperatures	119
3.5.1	One dimension	119
3.5.2	Two dimensions	124
4	Zero-field thermodynamics of isotropic Heisenberg magnets above $T = T_c$	127
4.1	Static approximation	127
4.1.1	Flow equations	127
4.1.2	Deformation schemes	128
4.1.3	Level 1 truncation	131
4.1.4	Level 2 truncation	135
4.2	Inclusion of dynamic fluctuations	140
5	Conclusion	147
5.1	Summary	147
5.2	Outlook on applying our approach to frustrated systems	149
A	Derivation of initial conditions and relations between vertices	153
A.1	Equations of Motion	153
A.2	Initial condition	155
A.3	Relations arising from symmetries	159
A.4	Hierarchy for interaction-irreducible vertices	161
B	Additional calculations regarding spin dynamics	164
B.1	High temperature spin dynamics on lattices with cubic symmetry	164
B.1.1	$J_1 - J_2$ model on a hypercubic lattice	164
B.1.2	$J_1 - J_2$ model on a body-centered cubic lattice	172
B.2	Time-dependent correlations	175
B.2.1	Non-analytic corrections in $d = 3$	175
B.2.2	Superdiffusion in $d = 1$	177
B.3	Spin dynamics at intermediate temperature in $d = 3$	179
B.4	Spin dynamics in the critical region	181
B.4.1	Dynamic scaling in low-dimensional antiferromagnets	181
B.4.2	Zero-temperature solution for low-dimensional Heisenberg magnets	183
C	Additional calculations concerning thermodynamics	186
C.1	Fixed point in $d \geq 3$	186
C.2	Flow equation of static four-point vertex at finite S	188
C.3	Integration of flow using self-consistent high-temperature spin dynamics	188
C.4	T_c on other cubic lattices	189
C.4.1	Magnets with nearest-neighbor interaction on a bcc lattice	189
C.4.2	Ferromagnet with next-neighbor interaction on a fcc lattice	190

D Deutsche Zusammenfassung	192
D.1 Funktionale Spin-Renormierungsgruppe	192
D.2 Spin-Dynamik im Heisenberg-Paramagneten	194
D.3 Thermodynamik oberhalb der kritischen Temperatur	196
Bibliography	199

Chapter 1

Introduction

1.1 The Heisenberg model

In the following section a short introduction to the isotropic quantum Heisenberg model is given, which is the central topic of this thesis. This model is known to explain the magnetic properties for a plethora of materials. In particular this is the case for insulators, where the interacting magnetic constituents can be assumed as localized. It is a quantum-mechanical model, as it can be only motivated by invoking concepts, that are inherent to a non-classical description, like the Pauli exclusion principle [13, 14]. This should be contrasted with classically motivated dipole-dipole interactions. The typical energies of dipolar contributions are found to be way too small, to account for the observed magnetic energy scales, e.g transition temperatures in ferromagnets [14].

The origin of the Heisenberg or exchange interaction can be, for instance, found in the Coulomb interaction between electrons, which are indistinguishable fermions and carry a spin $S = 1/2$, combined with the aforementioned Pauli principle [13, 14], that prohibits two fermions from assuming a state with the same quantum numbers. Consider the stationary Schrödinger equation for the wavefunction of two interacting electrons bound to two different nuclei I and II with spin projections σ_1 and σ_2 [14, 15, 16]

$$\left(-\frac{\Delta_1 + \Delta_2}{2m} + U(\mathbf{r}_1, \mathbf{r}_2) + \sum_{i=1,2} (V_I(\mathbf{r}_i) + V_{II}(\mathbf{r}_i)) \right) \Psi(\mathbf{r}_1, \mathbf{r}_2, \sigma_1, \sigma_2) = E \Psi(\mathbf{r}_1, \mathbf{r}_2, \sigma_1, \sigma_2). \quad (1.1)$$

Here $U(\mathbf{r}_1, \mathbf{r}_2) = \frac{e^2}{|\mathbf{r}_1 - \mathbf{r}_2|}$ is the Coulomb interaction between the electrons and $V_I(\mathbf{r}_1) = -\frac{e^2}{|\mathbf{r}_1 - \mathbf{r}_I|}$ is a single-electron potential, e.g. the binding energy between the nucleus I and the first electron. The solution is then given by the product of an orbital and spin part [14, 16]

$$\Psi(\mathbf{r}_1, \mathbf{r}_2, \sigma_1, \sigma_2) = \Psi_E(\mathbf{r}_1, \mathbf{r}_2) \chi(\sigma_1, \sigma_2). \quad (1.2)$$

The spin does not appear explicitly in the Hamilton operator $\mathcal{H}(\mathbf{r}_1, \mathbf{r}_2)$. Therefore one can chose $\chi(\sigma_1, \sigma_2)$ as eigenfunctions of the square of the total spin operator $\mathbf{S}^2 = (\mathbf{S}_1 + \mathbf{S}_2)^2$ and its projections along the z -axis $S^z = S_1^z + S_2^z$, which possess the eigenvalues $S(S+1)$ and S^z . The rules for the addition of angular momenta imply in total four states. They are divided among a $S = 0$ and $S = 1$ -subspace for the total spin, where the latter contains three states. The eigenstate with vanishing spin is the antisymmetric singlet

$$\chi_{S=0}(\sigma_1, \sigma_2) = \frac{1}{\sqrt{2}} (\delta_{\sigma_1, \uparrow} \delta_{\sigma_2, \downarrow} - \delta_{\sigma_1, \downarrow} \delta_{\sigma_2, \uparrow}), \quad (1.3)$$

with $\chi_{S=0}(\sigma_1, \sigma_2) = -\chi_{S=0}(\sigma_2, \sigma_1)$. States with $S = 1$ form a triplet and are symmetric under permutations $\sigma_1 \leftrightarrow \sigma_2$

$$\chi_{S=1, m=0}(\sigma_1, \sigma_2) = \frac{1}{\sqrt{2}}(\delta_{\sigma_1, \uparrow} \delta_{\sigma_2, \downarrow} + \delta_{\sigma_1, \downarrow} \delta_{\sigma_2, \uparrow}), \quad (1.4)$$

$$\chi_{S=1, m=\pm 1}(\sigma_1, \sigma_2) = \delta_{\sigma_1, \uparrow/\downarrow} \delta_{\sigma_2, \uparrow/\downarrow}. \quad (1.5)$$

The Pauli principle dictates now, that the total wavefunction has to be antisymmetric under a permutation of the electrons $1 \leftrightarrow 2$. The orbital part of the wavefunction with a singlet is therefore symmetric $\Psi_E = \Psi_{E, \pm}$, while a triplet configuration implies an antisymmetric wavefunction. To account for this property in a simple manner the orbital parts with a distinct symmetry \pm are written as a non-interacting two-body wavefunction [14]

$$\Psi_{E, \pm}(\mathbf{r}_1, \mathbf{r}_2) = \frac{1}{\sqrt{2}}(\psi_A(\mathbf{r}_1)\psi_B(\mathbf{r}_2) \pm \psi_B(\mathbf{r}_1)\psi_A(\mathbf{r}_2)), \quad (1.6)$$

where A, B are single-particle states. One can evaluate then the expectation values of the energy in these states $\langle \mathcal{H} \rangle_{\pm} = \langle \Psi_{\pm} | \mathcal{H} | \Psi_{\pm} \rangle \times \langle \Psi_{\pm} | \Psi_{\pm} \rangle^{-1}$, and finds that they are approximately separated by a difference [14, 17]

$$\langle \mathcal{H} \rangle_{-} - \langle \mathcal{H} \rangle_{+} \approx \int d^3 \mathbf{r}_1 \int d^3 \mathbf{r}_2 [U(\mathbf{r}_1, \mathbf{r}_2) + V_{II}(\mathbf{r}_1) + V_I(\mathbf{r}_2)] \psi_A^*(\mathbf{r}_1) \psi_A(\mathbf{r}_2) \psi_B(\mathbf{r}_1) \psi_B^*(\mathbf{r}_2). \quad (1.7)$$

This expression is known as the exchange integral or Fock-term, abbreviated as J and a consequence of the required antisymmetrization of Ψ [14]. Note that for the above expression we have assumed the overlap between states in $\langle \Psi_{\pm} | \Psi_{\pm} \rangle^{-1}$ to be $\ll 1$. This also allowed us to drop the contribution from the direct Coloumb integral, known as the Hartree term [14], which is just the expectation value of \mathcal{H} in the simple product states, i.e. with the densities of the single-particle states $|\psi_i(x)|^2$. Otherwise one should retain the overlap and Hartree term, which leads to a modified expression for the energy difference. Depending on the sign of J either the singlet with vanishing total spin or the triplet states are energetically favored [16, 17]. Note that this allows for a description by means of an effective model solely for the spin degrees of freedom, namely the Heisenberg Model for two $S = 1/2$ -moments

$$\mathcal{H}_{\text{eff}} = J \mathbf{S}_1 \cdot \mathbf{S}_2. \quad (1.8)$$

The vector operators $\mathbf{S} = (S^x, S^y, S^z)$ satisfy the angular momentum algebra, given by the commutator relations

$$[S^{\alpha}, S^{\gamma}] = i \epsilon_{\alpha\gamma\sigma} S^{\sigma}. \quad (1.9)$$

Here $\epsilon_{\alpha\gamma\sigma}$ is the totally antisymmetric ϵ -tensor, with the properties $\epsilon_{xyz} = 1$, $\epsilon_{\alpha\sigma\gamma} = -\epsilon_{\alpha\gamma\sigma}$. Using the identity $2\mathbf{S}_1 \cdot \mathbf{S}_2 = (\mathbf{S}_1 + \mathbf{S}_2)^2 - \mathbf{S}_1^2 - \mathbf{S}_2^2$, we see that \mathcal{H}_{eff} has the same eigenstates as the operators $S_1^z + S_2^z$ and $(\mathbf{S}_1 + \mathbf{S}_2)^2$, namely the triplet and singlet. For a positive exchange interaction $J > 0$ the singlet $|S = 0, m = 0\rangle$ is the ground state, with the excitation energy exactly given by J . The singlet implies an antiparallel alignment of both spins, and thus the model for positive J is called *antiferromagnetic*. Conversely, for $J < 0$, we have a threefold degenerate ground state, formed by the triplet $|S = 1, m = \pm 1, 0\rangle$. As these configurations include states with parallel alignment, one also calls this type of coupling *ferromagnetic* [17].

Besides referring to the atomistic considerations made above, one can also derive an effective spin model by considering a specific limit in the electronic Hubbard model [15, 16, 18], namely

$$\mathcal{H}_{\text{Hubbard}} = -t \sum_{\sigma} \sum_{\langle i,j \rangle} \left(c_{i\sigma}^{\dagger} c_{j\sigma} + c_{j\sigma}^{\dagger} c_{i\sigma} \right) + U \sum_j c_{j\uparrow}^{\dagger} c_{j\uparrow} c_{j\downarrow}^{\dagger} c_{j\downarrow}. \quad (1.10)$$

$c_{i\sigma}^{\dagger}$ and $c_{i\sigma}$ are fermionic annihilation/creation operators, that represent electrons with two spin projections \uparrow, \downarrow on the N sites, labeled i , of a Bravais lattice. They fulfill the anticommutation relations $\{c_{\alpha}^{\dagger}, c_{\gamma}\} = \delta_{\alpha\gamma}$, $\{c_{\alpha}, c_{\gamma}\} = 0$. The energy t in Eq. (1.10) is a nearest neighbor-hopping energy, that describes the free motion, i.e. delocalization, of the electrons, due to a hybridization of the ion's orbitals. Furthermore the energy $U > 0$ in (1.10) represents the repulsive Coloumb interaction. It yields a contribution, if two electrons occupy the same site. Assuming half-filling, where the number of sites N coincides with the number of electrons, one can show, that in the limit $t/U \ll 1$, the energetically low-lying eigenstates do not include vacant or double-occupied sites, since these are punished by a large contribution $\sim U$. The energy of low-lying eigenstates is then entirely controlled by the relative alignment of the electronic spin projections at single-occupied sites. Thus at low energies one can map the Hamiltonian in (1.10) onto an isotropic $S = 1/2$ -Heisenberg model for the spin degrees of freedom,

$$\mathcal{H}_{\text{Heisenberg}} = J \sum_{\langle i,j \rangle} \mathbf{S}_i \cdot \mathbf{S}_j, \quad (1.11)$$

where $[S_i^{\alpha}, S_j^{\gamma}] = \delta_{ij} [S_i^{\alpha}, S_i^{\gamma}]$ and the nearest neighbor exchange-interaction is $J = 4t^2/U > 0$. The spin operators are expressed in terms of a bilinear form involving the Pauli matrices σ_i , i.e. [15, 18]

$$S^{\alpha} = (c_{\uparrow}^{\dagger}, c_{\downarrow}^{\dagger}) \sigma_{\alpha} (c_{\uparrow}, c_{\downarrow})^T. \quad (1.12)$$

Note that the effective theory for the magnetic degrees of freedom derived from Eq. (1.10) is always an antiferromagnet. This accounts partially for their more frequent occurrence compared to ferromagnets. However, the sketched mechanisms do not always suffice to explain the magnetic properties of realistic materials. One can find examples in systems, where the magnetic moments are separated from each other by non-magnetic ions. This leads to the concept of superexchange mechanisms [19]. Here the magnetic interactions are mediated via the non-magnetic ions, involving hopping between the orbitals of non-magnetic and magnetic constituents. Different signs of the exchange interactions could be explained and predicted based on symmetry properties and electronic configurations [20].

The spectrum of eigenstates for an arbitrary spin- S Heisenberg model

$$\mathcal{H} = \frac{1}{2} \sum_{i,j} J_{ij} \mathbf{S}_i \cdot \mathbf{S}_j, \quad (1.13)$$

depends on the type of exchange coupling J_{ij} . It is usually assumed to be a function of the relative distance $J_{ij} = J_{0j}$, in compliance with homogeneity of the system. Focusing on nearest-neighbor only interactions, we can, as already discussed for the two-site limit, distinguish between the ferro- and antiferromagnet. For the ferromagnet, $J < 0$, the ground state $|0\rangle$ is $(2NS + 1)$ -fold degenerate, including all states that belong to the manifold with

maximum spin $2NS + 1$. A selection of any of these states, is then achieved by switching on an external magnetic field. This amounts to adding the Zeeman term

$$\mathcal{H}_{\text{Zeeman}} = - \sum_i H_i S_i^z, \quad (1.14)$$

to Eq. (1.13). Its eigenstates are product states $|\sigma_1, \dots, \sigma_N\rangle$ with eigenenergy $\sum_i H_i \sigma_i$. Choosing a small uniform field H one therefore selects $|S, \dots, S\rangle$ as the ground state for the Heisenberg ferromagnet. The energy of this state is then given by

$$E_0 = N \left(\frac{cJS^2}{2} - HS \right) \approx \frac{NcJS^2}{2}, \quad (1.15)$$

where c is the number of nearest neighbors. The first excited eigenstates are also exactly known and can be interpreted in terms of a single spin wave or magnon, i.e. a spin flip that propagates like a plane wave in the material [15, 16, 18],

$$|\mathbf{k}\rangle = \sum_j e^{i\mathbf{k}\cdot\mathbf{r}_j} |j\rangle. \quad (1.16)$$

Here $|j\rangle$ is a product state, with spin projections $\sigma_j = S - 1$, $\sigma_i = S$, $i \neq j$, i.e. a total spin that is reduced by one. Its momentum \mathbf{k} assumes values in the first Brillouin Zone of the Bravais lattice. The energy $E(\mathbf{k})$ of a single magnon is then given by [15, 16, 18, 21]

$$E(\mathbf{k}) = H + S(J(\mathbf{k}) - J(\mathbf{0})). \quad (1.17)$$

For a nearest-neighbor ferromagnet on a d -dimensional hypercubic lattice with lattice spacing a the Fourier-transformed exchange coupling is given by

$$J(\mathbf{k}) = \sum_j J_{0j} e^{i\mathbf{k}\cdot\mathbf{r}_j} = 2J \sum_{i=1}^d \cos(k_i a). \quad (1.18)$$

The dispersion $E(\mathbf{k})$ vanishes as k^2 for $k \rightarrow 0$, if $H = 0$. This is readily explained by the transverse magnon being a Goldstone mode, which is a gapless excitation that emerges, due to a spontaneously broken continuous symmetry, in this case, the spin-rotational invariance [14, 16, 22]. The antiferromagnet is more intricate, and its exact ground state is actually unknown. Only in the classical limit $S \gg 1$, $JS^2 = \text{const.}$, where the spin operators are replaced by unit vectors \mathbf{n}_i with a continuous orientation along a spherical surface one can determine the exact configuration. One finds then by minimization of the total energy $\mathcal{H}[\{\mathbf{n}\}]$ on a bipartite lattice, that spins on adjacent sites point in opposite directions, a pattern known as Neel order [15, 16]. This is in complete analogy to the two-site model (dimer) with a singlet ground state. The order parameter is then given by the staggered magnetization, associated with the operator

$$\mathbf{S}(\mathbf{Q}) = \sum_j e^{i\mathbf{Q}\cdot\mathbf{r}_j} \mathbf{S}_j, \quad e^{i\mathbf{Q}\cdot\mathbf{r}} = (-1)^{P(j)} \quad (1.19)$$

where \mathbf{Q} is the Neel ordering vector, i.e. $\mathbf{Q}_N = \frac{\pi}{a}(1, 1, 1)$ for the simple cubic lattice, and $P(j)$ yields either an even or odd number, depending on which sublattice the site j is located. Unfortunately, a product state, constructed from the above prescription, is not an exact eigenstate of the quantum model. The reason for this is the presence of

$$S_i^x S_j^x + S_i^y S_j^y = S_i^+ S_j^- + S_i^- S_j^+, \quad (1.20)$$

in the Hamiltonian (1.13), where we introduced the spherical ladder operators

$$S^\pm = \frac{S^x \pm iS^y}{\sqrt{2}}. \quad (1.21)$$

The transverse terms in (1.20) then do not commute with $\mathbf{S}(\mathbf{Q})$. Nevertheless, many calculations in $d \geq 2$ dimensions still suggest that the expectation value of $\mathbf{S}(\mathbf{Q})$ is non-zero in the corresponding true ground state, albeit smaller than the classical saturation value [16, 23]. Magnon excitations to that vacuum also exist, although they do not belong to exact excited eigenstates. Their dispersion $E(\mathbf{k})$ differs from the ferromagnet, since it is linear for small k [16, 23].

1.2 Thermodynamics

The thermal properties of the Heisenberg model in equilibrium are usually studied within the canonical ensemble, where one keeps the temperature T and the external field H constant as external parameters. The appropriate thermodynamic potential for this ensemble is the free energy $F(T, H)$. One starts with the partition function

$$Z(T, H) = \text{Tr}(e^{-\beta\mathcal{H}}), \quad (1.22)$$

where $\beta = 1/T$ ($k_B = 1$) is the inverse temperature and $\text{Tr}(\dots)$ denotes the trace over the respective Hilbert space. Note that in the classical limit $S \rightarrow \infty$, the trace has to be replaced by continuous integrals over the surfaces of unit spheres on each site, parametrized by angles $\{\theta_i, \phi_i\}$. The thermal probability distribution for the system at a given temperature is then determined by the normalized density operator

$$\rho = \frac{e^{-\beta\mathcal{H}}}{Z}, \quad (1.23)$$

satisfying $\text{Tr}(\rho) = 1$. Using the eigenbasis $\{|n\rangle\}$ of \mathcal{H} to evaluate traces, a thermal expectation value of an operator A is therefore given by

$$\langle A \rangle = \text{Tr}(\rho A) = \sum_n p_n \langle n | A | n \rangle, \quad (1.24)$$

where

$$p_n = \frac{e^{-\beta E_n}}{Z} = \frac{e^{-\beta E_n}}{\sum_m e^{-\beta E_m}}, \quad (1.25)$$

yield the individual probabilities for finding the system in the eigenstate $|n\rangle$ at given temperature T . Note that $p_n = \delta_{0,n}$ for $T = 0$, provided that the ground state $|0\rangle$ is non-degenerate. For example the total energy U of the system is simply the expectation value of the Hamiltonian

$$U(T, H) = \langle \mathcal{H} \rangle = \sum_n p_n E_n. \quad (1.26)$$

The free energy can be obtained by taking the logarithm of Z , namely

$$F(T, H) = -T \ln(Z). \quad (1.27)$$

and is related to the internal energy U via the Legendre transform

$$F = U - TS, \quad (1.28)$$

where S is the entropy and the former natural variable for U , which is initially a function of S and H . In that context $T = T(S, H) = \frac{\partial U}{\partial S}$, which by means of the Legendre transform becomes the new independent variable in F . Note that the free energy depends entirely on intensive variables, i.e. those that do not scale linearly with the system size N . The first partial derivatives of F with respect to T and H are the entropy

$$S(T, H) = -\left(\frac{\partial F}{\partial T}\right)_H, \quad (1.29)$$

and the magnetization per site

$$M(T, H) = \langle S_i^z \rangle = -\frac{1}{N} \left(\frac{\partial F}{\partial H}\right)_T, \quad (1.30)$$

where in the latter case, we already used the homogeneity of the system, meaning that $\langle S_i^z \rangle = \frac{1}{N} \sum_j \langle S_j^z \rangle$. The second order derivatives can be related to the heat capacity at constant magnetic field c_H and the isothermal magnetic susceptibility χ , i.e.

$$c_H(T, H) = T \left(\frac{\partial S}{\partial T}\right)_H = -T \left(\frac{\partial^2 F}{\partial T^2}\right)_H, \quad (1.31)$$

$$\chi(T, H) = \left(\frac{\partial M}{\partial H}\right)_T = -\frac{1}{N} \left(\frac{\partial^2 F}{\partial H^2}\right)_T. \quad (1.32)$$

One can write these quantities in terms of expectation values as mean quadratic deviations from $\langle \mathcal{H} \rangle$ and $\langle S_i^z \rangle$

$$T^2 c_H = \langle (\mathcal{H} - \langle \mathcal{H} \rangle)^2 \rangle = \langle \mathcal{H}^2 \rangle - \langle \mathcal{H} \rangle^2, \quad (1.33)$$

$$T\chi = \frac{1}{N} \sum_{i,j} \langle S_i^z S_j^z \rangle - \langle S_i^z \rangle^2. \quad (1.34)$$

The magnetization behaves for small magnetic fields as

$$M(T, H) = M(T, 0) + \chi(T, 0)H + \mathcal{O}(H^2). \quad (1.35)$$

For temperatures much larger than the magnitude of typical interaction energies, e.g. the exchange coupling J , there is no spontaneous symmetry breaking, so that $M(T, 0) = 0$, implying a direct proportionality between the external field and the magnetization, $M = \chi H$. In this high temperature regime one can systematically evaluate the thermal traces, by expanding $e^{-\beta \mathcal{H}}$ in powers of J/T . During this procedure one has to relate the coefficients at a given order to expectation values of non-interacting spin operators at the same site in an external field. These quantities can be computed exactly by means of a generalized Wick-Theorem [5, 7]. The free energy for an isolated magnetic moment with spin S , is given by [1, 15, 16]

$$F(T, H) = -TB(y = \beta H) = -T \ln \left(\frac{\sinh[(S + 1/2)y]}{\sinh(y/2)} \right), \quad (1.36)$$

which yields the Brillouin function as an expression for the magnetization

$$M(\beta H) = b(y) = B'(y) = \left(S + \frac{1}{2}\right) \coth \left[\left(S + \frac{1}{2}\right)y \right] - \frac{1}{2} \coth \left(\frac{y}{2}\right), \quad (1.37)$$

The zero-field susceptibility can then be determined by expanding the Brillouin function to linear order in y . One obtains

$$\chi(T, 0) = \frac{S(S + 1)}{3T} = \frac{b'_0}{T}, \quad (1.38)$$

where b'_0 is the first derivative of the Brillouin function at vanishing argument. This equation is also known as the Curie-law for a paramagnet [16]. For sufficiently large T , the presence of a finite J implies a first order correction. The susceptibility is then modified as [2, 5]

$$\chi(T, 0) \approx \frac{b'_0}{T} \left[1 - \frac{b'_0 J(\mathbf{0})}{T} \right], \quad (1.39)$$

where for a next-neighbor coupling $J(\mathbf{0}) = cJ$, with c being the number of nearest neighbors. A simple resummation for extrapolating it to lower temperatures is given by

$$\chi(T, 0) = \frac{b'_0}{T + b'_0 J(\mathbf{0})}, \quad (1.40)$$

which is the Curie-Weiss law $\chi(T, 0) \sim \frac{C}{T - T_{CW}}$, with $T_{CW} = -b'_0 J(\mathbf{0})$ [15]. For a ferromagnet, where $J(\mathbf{0}) < 0$, this law implies a singularity of $\chi(T, 0)$ at $T = T_{CW}$. This means that an arbitrarily small magnetic field, will already induce a finite, spontaneous magnetization $M(T, 0)$. To give some more weight to these thoughts, we motivate an approximation, where this is indeed the outcome for $\chi(T, 0)$. This approach is known as mean-field theory and is the simplest way to obtain a non-perturbative description of the model, beyond the high temperature range. Firstly one writes

$$\mathbf{S}_i = \langle \mathbf{S}_i \rangle + \delta \mathbf{S}_i, \quad \delta \mathbf{S}_i = \mathbf{S}_i - \langle \mathbf{S}_i \rangle. \quad (1.41)$$

After insertion into the interacting term of \mathcal{H} in Eq. (1.13), one discards contributions that are quadratic in the fluctuation operators $\delta \mathbf{S}_i$. One obtains then a Zeeman Hamiltonian with an effective, exchange field that is given by [3, 15]

$$\tilde{H}_i = H - \sum_j J_{ij} \langle S_j^z \rangle = H - J(\mathbf{0}) M(T, H) \equiv \tilde{H}. \quad (1.42)$$

It contains the expectation value of the magnetization, which is calculated self-consistently by considering its 'free' expression with the renormalized magnetic field \tilde{H} on the right-hand-side

$$M(T, H) = b(\beta \tilde{H}). \quad (1.43)$$

For $T < b'_0 |J(\mathbf{0})| = T_{CW}$ its solution in the limit $H \rightarrow 0^+$ allows for a finite spontaneous magnetization $M(T, 0) \neq 0$, which vanishes for $T \rightarrow T_{CW}^-$ and is saturated, $M(T, 0) \approx S$, at low temperatures $T \ll |J|$. Differentiating the self-consistency equation (1.43) with respect to H and setting $H = 0$, $T > T_c$, we obtain the approximate formula (1.40) for χ of a paramagnet. Thus T_{CW} turns out to be the critical temperature T_c for a second order phase transition. Such a transition is characterized by a continuous order parameter, here M , at the phase boundary $T = T_c$ and jumps or divergencies in the corresponding susceptibility χ . A second order transition in the thermodynamic limit $N \rightarrow \infty$ is indeed featured by the Heisenberg model in $d = 3$ dimensions [14, 15]. However, the mean-field approximation underestimates thermal fluctuations, as could be inferred from the employed arguments, so that $T_c < T_{CW} = T_c^{\text{MF}}$. Furthermore, the low-temperature asymptotics of, e.g. the magnetization, that are predicted by mean-field theory are at odds with the outcome of spin-wave theory. The reason is the presence of a gap, which actually should vanish as implied by $E(\mathbf{0}) = 0$ in (1.17), leading to an exponentially small correction for $T \ll |J|$ instead of a power law [14, 16, 21]. In reduced dimensions $d \leq 2$, one finds even that thermal fluctuations lead for $H \rightarrow 0$ to divergent corrections to mean-field theory at

any finite temperature, so that $T_c = 0$. The latter statement is known as the *Mermin-Wagner theorem* [15, 16, 24]. In general mean-field theory becomes more accurate with larger interaction ranges or effective coordination numbers, e.g. in high dimensions $d \gg 1$ [1]. Note that for the antiferromagnet $J(\mathbf{0}) > 0$, the mean-field approach has to be adjusted by introducing antiparallel magnetizations on two disjunct sublattices [15]. The magnitude of these fields, the staggered magnetization, also satisfies Eq. (1.43). As a consequence one obtains $T_c = b'_0 |J(\mathbf{Q}_N)|$ with the same temperature dependence of the order parameter and the corresponding susceptibility.

1.2.1 Critical region

The critical region, which is roughly defined by the condition $|T - T_c|/T_c \ll 1$, is dominated by strongly growing correlations between all degrees of freedom in the system, e.g. the magnetic moments sitting on lattice sites in a localized spin model. These correlations extend to a range that is known as the correlation length ξ , which in this regime is much larger than typical microscopic distances like the lattice spacing a . The growth of ξ for $T \rightarrow T_c$ is intimately linked to increasingly singular fluctuations around the ordering vector \mathbf{Q} in momentum space, thus confining the regime of relevant fluctuations to small momenta $|\mathbf{k} - \mathbf{Q}| \ll a^{-1}$. Magnetic moments separated by distances $|\mathbf{r}|$ much larger than ξ are almost uncorrelated, i.e. $|\langle S_{\mathbf{r}} S_{\mathbf{0}} \rangle| \ll b'_0$, like for temperatures far away from the phase transition, where $\xi \lesssim \mathcal{O}(a)$. On the other hand, inside regions of size $\sim \xi^d$ one can treat the system as one entity, due to the strong correlations, i.e. overlap between different constituents. Consequently at the critical temperature $T = T_c$, the system is scale invariant. The leading singular behavior of thermodynamic quantities, like the free energy $F(T, H)$ and its derivatives, is then determined by symmetries that are inherent to a whole universality class of models. Microscopic details, e.g. properties of the interaction at short ranges, cease to play any role in this context [3]. In particular, the large extent of correlations implies that these thermodynamic quantities have to be homogeneous functions of $|T - T_c|/T_c$ and H [3]. This means that multiplication of $|T - T_c|$ and H in the argument by powers of a scaling factors u , should just produce an external factor, that is again a power of u . The homogeneity relation for the singular part of the free energy $f = F/N$ per site, that is assumed by scaling theory, reads explicitly [3, 25]

$$f(u^{n_t} (|T - T_c|/T_c), u^{n_h} H) = u^d f(|T - T_c|/T_c, H). \quad (1.44)$$

Such properties are only realized by power laws in the variables $|T - T_c|/T_c$ and H , with critical exponents, that are characteristic of the universality class, and are related to n_t, n_h in the homogeneity relation [3, 25]. From the aforementioned behavior, one can also infer, that ultimately, the t, h -dependence of $f(T, H)$, can be combined into a single scaling variable [3]

$$f(t, H) = (|T - T_c|/T_c)^{d/n_t} \Phi_{\pm} \left(\frac{H}{(|T - T_c|/T_c)^{n_h/n_t}} \right), \quad (1.45)$$

where $\text{sgn}(t) = \pm$ denotes the side from which one approaches T_c . A similar hypothesis was formulated for quantities, which involve a spatial dependence, i.e. correlations between spin operators on different lattice sites, like the two-point function [3, 27]

$$G^{zz}(\mathbf{r}_i) = \langle S_i^z S_0^z \rangle - \langle S_0^z \rangle^2 \sim (|T - T_c|/T_c)^{2(d-n_h)/n_t} \Psi_{\pm} \left(\frac{|\mathbf{r}_i|}{(|T - T_c|/T_c)^{-1/n_t}} \right). \quad (1.46)$$

From these postulates one can derive algebraic relations between critical exponents [3]. Assuming their validity, these relations allow one to obtain exponents without explicitly calculating the whole set.

A first attempt to calculate critical exponents can be already made in the previously introduced mean-field approximation. For the spontaneous magnetization one can define the critical exponent β , associated with its vanishing close to T_c , via [3, 14]

$$M(T, 0) \sim |T - T_c|^\beta, \quad T < T_c, \quad (1.47)$$

In mean-field theory one obtains $\beta = 1/2$ by expanding the right-hand side of the self-consistency equation (1.43) up to cubic order in M . Conversely, above T_c one can study the divergence of the magnetic susceptibility for $T \rightarrow T_c$ with an exponent γ , e.g. [3, 14]

$$\chi^{-1} \sim |T - T_c|^\gamma, \quad T > T_c. \quad (1.48)$$

Here one reads off from the Curie-Weiss law (1.40) that $\gamma = 1$. Right at $T = T_c$ the magnetization behaves for small fields as $M(T, H) \sim H^{1/\delta}$, and one thus obtains $\delta = 3$ in mean-field [3]. Finally, the exponent of the heat capacity at vanishing magnetic field is introduced as $c_H \sim |T - T_c|^{-\alpha}$. Considering the second T -derivative of the free energy in mean-field theory one obtains a finite jump, implying $\alpha = 0$ [3]. From the conjectured scaling form of the free energy, one can derive via differentiation, the following relations between the critical exponents [3]

$$2 - \alpha = 2\beta + \gamma = \beta(\delta + 1), \quad (1.49)$$

which are both satisfied by the mean-field exponents. However, these exponents still deviate significantly from the actual results for the Heisenberg universality class, with the most accurate results available from Monte Carlo simulations [26].

For an analysis of space-resolved correlations the mean-field approximation alone is insufficient, since the expressions for the spin correlation functions are still purely local. Near the critical point one expects that long wavelength fluctuations, connected to singularities in the susceptibility near the ordering vector \mathbf{Q} , dominate, so that fluctuations with $|\mathbf{k} - \mathbf{Q}|$ larger than a cutoff $k_0 \ll a^{-1}$ can be discarded. Furthermore, only static degrees of freedom will be relevant for the universal properties in this regime, even if there are non-trivial dynamics induced by a finite S . The reason for this lies in *critical slowing down*, which is the effective freezing of any time dependence, i.e. decay, of fluctuations around the ordering vector, allowing us to retain only the static components of the spin degrees of freedom [3]. This already yields a classical theory of a long wavelength field ϕ , so that the partition function Z can be written as a path integral $\int \mathcal{D}[\phi] e^{-S_{k_0}[\{\phi\}]}$ with an effective action $S_{k_0}[\{\phi\}]$ [3]. However, $S_{k_0}[\{\phi\}]$ still features infinitely many powers of the field. Close to T_c the field is expected to fluctuate around a small or vanishing thermal mean $\langle \phi \rangle$. As a consequence one usually truncates the action $S_{k_0}[\{\phi\}]$ to the fourth order in ϕ [3]. That yields the simplest possible interacting field theory, the ϕ^4 -theory of a three-component field. It is expected to produce accurate results for the critical properties of the $\mathcal{O}(3)$ -universality class, which includes the Heisenberg Model. The corresponding action is referred to as the Ginzburg-Landau-Wilson functional and reads [3]

$$S_{k_0}[\{\phi\}] = \int d^d r \left[f_0 + \frac{r_0}{2} \phi(\mathbf{r}) \cdot \phi(\mathbf{r}) + \frac{w_0}{2} \sum_{i=1}^d \partial_i \phi(\mathbf{r}) \cdot \partial_i \phi(\mathbf{r}) + \frac{u_0}{24} (\phi(\mathbf{r}) \cdot \phi(\mathbf{r}))^2 - h_0 \cdot \phi(\mathbf{r}) \right], \quad (1.50)$$

where in real space all fluctuations on length scales smaller than k_0^{-1} are neglected, so that the field $\phi(\mathbf{r})$ represents actually a magnetization averaged over a cell of size k_0^{-d} . The parameters f_0, r_0, w_0, u_0 can be related to the small momentum-limit of the exchange constant and the temperature, e.g. [3]

$$w_0 \sim 1/c \sim 1/(2d), \quad r_0 \sim T - T_c, \quad u_0 \sim \beta J(\mathbf{0}), \quad (1.51)$$

while h_0 is proportional to the external magnetic field. The neglect of terms $\mathcal{O}(\phi^6)$ is typically justified by arguing that these contributions can be dropped in the relevant regions of the path integral, i.e. that the decay, caused by $e^{-S[\phi]}$ is sufficiently strong for large amplitudes of the field. Here the renormalization group approach provides a better explanation in terms of the relevance of the interaction vertices in $S_{k_0}[\phi]$ [3]. The effect of all irrelevant terms beyond a given order is then just a numeric renormalization of the relevant couplings w_0, r_0, u_0, \dots , i.e. modified critical temperatures or stiffness constants. Note that one recovers the free energy from the mean-field approximation by neglecting the spatial variation of the order parameter field and assuming that the path integral is dominated by spatially uniform configurations [3]. Going beyond plain mean-field theory one can obtain analytic expressions for the partition function and arbitrary correlations by means of a Gaussian approximation to the action $S_{k_0}[\phi]$, which requires that all terms of $\mathcal{O}(\delta\phi^3)$ in a fluctuation field $\delta\phi = \phi(\mathbf{r}) - M_0$, where M_0 is the uniform order parameter, are dropped [3]. This is a consequence of the resulting integrand being $\sim \exp(-\frac{1}{2}(\phi, A, \phi))$. Above T_c , where $M_0 = 0$, the quartic term does not contribute at all to the new action. The two-point function, which measures the correlation between the fields, for instance at a given momentum \mathbf{k} , can then be directly read off from the matrix in the approximate non-interacting action, namely [3]

$$\langle S^z(\mathbf{k})S^z(-\mathbf{k}) \rangle \approx \langle \phi(\mathbf{k})\phi(-\mathbf{k}) \rangle = \frac{1}{r_0 + w_0|\mathbf{k} - \mathbf{Q}|^2} = \frac{1}{w_0(|\mathbf{k} - \mathbf{Q}|^2 + \xi^{-2})}, \quad (1.52)$$

which is also known as the Ornstein-Zernike form. It can be written in terms of the scaling law

$$\langle S^z(\mathbf{k})S^z(-\mathbf{k}) \rangle \sim \chi g(|\mathbf{k} - \mathbf{Q}|\xi), \quad (1.53)$$

where $\chi \sim \xi^2$ is the magnetic susceptibility and $g(x) = [1 + x^2]^{-1}$. For $T = T_c$, where $r_0 = 0$ or $\xi^{-1} = 0$ one obtains

$$\langle S^z(\mathbf{k})S^z(-\mathbf{k}) \rangle = \frac{1}{c_0|\mathbf{k} - \mathbf{Q}|^2}, \quad (1.54)$$

which can be compared with the general assumption for the critical correlation function

$$\langle S^z(\mathbf{k})S^z(-\mathbf{k}) \rangle \sim |\mathbf{k} - \mathbf{Q}|^{\eta-2}, \quad (1.55)$$

thus yielding $\eta = 0$ for the anomalous dimension. A finite $\eta > 0$ indicates the breakdown of an analytic \mathbf{k} -dependence in the inverse correlation function, i.e. the Ornstein-Zernike ansatz. Note that for classical systems the two-point function is equivalent to $TG(\mathbf{k})$, where $G(\mathbf{k})$ is the momentum-resolved static susceptibility, defined via

$$\langle S^z(\mathbf{k}) \rangle = G(\mathbf{k})H(\mathbf{k}) + \mathcal{O}(H^2) \rightarrow G(\mathbf{k}) = \partial_{H(\mathbf{k})}\langle S^z(\mathbf{k}) \rangle|_{H(\mathbf{k})=0}, \quad (1.56)$$

where $H(\mathbf{k})$ is a small, inhomogeneous magnetic field that couples linearly to $S^z(\mathbf{k})$, i.e. via $\sum_{\mathbf{k}} H(\mathbf{k})S^z(\mathbf{k})$. For quantum systems with an intrinsic time dependence, this holds only for

vanishing momentum, $\langle S^z(\mathbf{0})S^z(\mathbf{0}) \rangle = T\chi$, or infinite temperatures. However, as expected from critical slowing down, dynamic corrections that arise from this, do not qualitatively alter the analytic structure, i.e. the leading singularity of $G(\mathbf{k})$, and amount at most to $\mathcal{O}(1)$ renormalizations of numeric constants. From Eq. (1.52) one reads off

$$\xi \sim \sqrt{r_0^{-1}} \sim |T - T_c|^{-1/2}, \quad (1.57)$$

and the corresponding critical exponent, defined via $\xi \sim |T - T_c|^{-\nu}$, is therefore $\nu = 1/2$. It also implies $\gamma = 1$ for the susceptibility, like in mean-field theory. That one can identify ξ with the correlation length, i.e. the range which separates correlated from uncorrelated regions, can be seen by calculating the correlation function in real space. For separations much larger than ξ one arrives at an exponential decay [3]

$$\langle S^z(\mathbf{r})S^z(0) \rangle \sim \cos(\mathbf{Q} \cdot \mathbf{r})|\mathbf{r}|^{-1} \exp(-|\mathbf{r}|/\xi) \ll 1, \quad (1.58)$$

indicating only a weak overlap between spins separated by this distance. In the opposite limit $|\mathbf{r}| \ll \xi$ it falls off as a much slower algebraic power-law [3]

$$\langle S^z(\mathbf{r})S^z(0) \rangle \sim \cos(\mathbf{Q} \cdot \mathbf{r})|\mathbf{r}|^{-1}, \quad (1.59)$$

which for $T = T_c$ is valid for arbitrary \mathbf{r} , a consequence of the vanishing gap $\sim \xi^{-2} \rightarrow 0$ in the two-point function. In general the scaling law satisfied by the correlation function is

$$\langle S_r^z S_0^z \rangle \sim \cos(\mathbf{Q} \cdot \mathbf{r})|\mathbf{r}|^{-1} \tilde{g}(|\mathbf{r}|/\xi). \quad (1.60)$$

Hence calling ξ a correlation range is justified with the observed properties. In $d = 3$ dimensions it is consistent with hyperscaling relations, that result from combining both scaling hypotheses, e.g. $\gamma = (2 - \eta)\nu$ [3]. However, the values of ν , η are, like the thermodynamic exponents, wrong in $d = 3$ [26], since it is smaller than the upper critical dimension $d_c = 4$. A simple explanation attributes this failure to the divergence of an effective dimensionless four-point interaction \tilde{u}_0 [3]. It is obtained after rescaling fields and momenta with properly chosen powers ξ , i.e. such that the new coefficient of the k^2 -term \tilde{w}_0 and the momentum-independent part \tilde{r}_0 in the quadratic contribution to the action are both of the order unity. Comparing \tilde{u}_0 directly to the free, Gaussian, contribution, one sees that it diverges as ξ^{4-d} . This indicates its relevance in a renormalization group sense [3]. In fact the true critical properties in $d < 4$ are determined by the eigenvalues of the linearized RG flow of relevant couplings with respect to a non-Gaussian fixed point, the Wilson-Fisher fixed point [3]. Simple approximation schemes to the flow, i.e. truncations to finite loop order, suffice for a controlled calculation of the critical properties for $\epsilon = 4 - d \ll 1$ [3].

1.3 Linear response and dynamic correlation functions

In our discussion of the thermodynamics and critical properties of the systems we have already introduced the magnetic susceptibility χ and more general the momentum-resolved static susceptibility $G(\mathbf{k})$, see Eq. (1.56). Such quantities yield information about the response of the system to first order in a static perturbation \mathbf{H} , as embodied for instance by the Zeeman-term (1.14). From their behavior one can draw conclusions regarding the presence of phase transitions, but dynamic properties of the system remain inaccessible. As a consequence an extension of the linear response framework to time-dependent phenomena is required, which is described below. One can then link the introduced generalized dynamic susceptibilities to experimentally measurable quantities like the scattering cross section of magnetic samples, and therefore correlations between spin operators at different times.

1.3.1 Linear response

Consider a Hamiltonian, which is now perturbed by a weak, time-dependent and spatially inhomogeneous external field $\mathbf{H}_j(t)$, e.g. [16, 18, 28]

$$\mathcal{H}(t) = \mathcal{H}_0 + \mathcal{V}(t), \quad (1.61)$$

where \mathcal{H}_0 is the initial, static Hamiltonian of the system and $\mathcal{V}(t) = -\sum_j \mathbf{S}_j \cdot \mathbf{H}_j(t)$ is the perturbation. As already discussed, the expectation value of any operator is given by calculating $\text{Tr}(\rho(t)A)$, but now the density matrix $\rho(t)$ is time-dependent due to the finite perturbation. The time evolution of $\rho(t)$ is governed by the von Neumann equation

$$i\partial_t \rho(t) = [\mathcal{H}(t), \rho(t)], \quad (1.62)$$

with the boundary condition, that initially our $\rho(t)$ is given by the thermal probability operator in the canonical ensemble

$$\rho(t \rightarrow -\infty) = \frac{e^{-\beta \mathcal{H}_0}}{Z} = \rho_0. \quad (1.63)$$

Note that this is usually combined with an adiabatic, i.e. slow, increase of the magnetic field, implying that $\mathbf{H}(t)$ is multiplied with $e^{\delta t}$, $\delta = 0^+$, thus also ensuring $H(t \rightarrow -\infty) = 0$. Switching to the interaction picture, where the time-evolution of any operator is given by

$$A^I(t) = e^{i\mathcal{H}_0 t} A(t) e^{-i\mathcal{H}_0 t}, \quad (1.64)$$

the differential equation obeyed by the perturbed density matrix becomes

$$i\partial_t \rho^I(t) = [\mathcal{V}^I(t), \rho^I(t)], \quad (1.65)$$

which can be integrated to

$$\rho^I(t) = \rho_0 - i \int_{-\infty}^t dt' [\mathcal{V}^I(t'), \rho^I(t')]. \quad (1.66)$$

Expanding $\rho(t)$ in powers of H as

$$\rho^I(t) = \rho_0 + \rho_1^I(t) + \mathcal{O}(H^2), \quad (1.67)$$

which amounts to iterating the right-hand side of Eq. (1.65) in powers of \mathcal{V} , one obtains for the first order correction

$$\rho_1^I(t) = -i \int_{-\infty}^t dt' [\mathcal{V}^I(t'), \rho_0] = i \sum_j \int_{-\infty}^t dt' \sum_{\gamma} [S_j^{\gamma}(t'), \rho_0] H_j^{\gamma}(t'). \quad (1.68)$$

The expectation value of S_i^{α} in the presence of the perturbation \mathcal{V} reads then [28]

$$\langle S_i^{\alpha} \rangle(t) \approx \text{Tr}(\rho_0 S_i^{\alpha}) + \text{Tr}(\rho_1^I(t) S_i^{\alpha, I}(t)) = \langle S_i^{\alpha} \rangle_0 + \sum_j \int_{-\infty}^{\infty} dt' G_{ret, ij}^{\alpha\gamma}(t-t') H_j^{\gamma}(t'). \quad (1.69)$$

Here we introduced the retarded magnetic susceptibility

$$G_{ret, ij}^{\alpha\gamma}(t) = i\Theta(t) \text{Tr}(\rho_0 [S_i^{\alpha}(t), S_j^{\gamma}(0)]) = i\Theta(t) \langle [S_i^{\alpha}(t), S_j^{\gamma}(0)] \rangle_0, \quad (1.70)$$

where the cyclic property of the trace was used, in order to transfer the density matrix ρ_0 outside the commutator. Note that $\langle \dots \rangle_0$ denotes the equilibrium expectation value and we have dropped the superscript I for operators that have no explicit time-dependence, like S^α . The tensor $G_{ret,ij}^{\alpha\gamma}(t)$, first appearing in Eq. (1.69), thus relates the induced change in their expectation values to a small perturbing external field $\mathbf{H}(t)$, that couples linearly to the spin operators. The relation (1.69) is also known as the Kubo formula [28]. More insights can be extracted from the Fourier transform of the retarded susceptibility to frequency and momentum space

$$G_{ret}^{\alpha\gamma}(\mathbf{k}, \omega) = \sum_j e^{i\mathbf{k}\cdot\mathbf{r}_j} \int_{-\infty}^{\infty} dt e^{i(\omega+i\delta)t} G_{ret,0j}^{\alpha\gamma}(t), \quad (1.71)$$

which couples then to the corresponding components of the external field $H^\gamma(\mathbf{k}, \omega)$. Here we have already set $\hbar = 1$, which will be maintained throughout this thesis. Moreover we have transferred the infinitesimal δ from the adiabatic increase of H , which is necessary for ensuring convergence of the integral in the time domain and the avoidance of singularities directly on the real frequency axis. The susceptibility in Fourier space is of particular interest, as it contains crucial information about the system described by \mathcal{H}_0 . For instance, poles in the transverse part defined by $[G_{ret}^{+-}(\mathbf{k}, \omega = E(\mathbf{k}))]^{-1} = 0$ may indicate the existence of excitations given by propagating quasiparticles with dispersion $E(\mathbf{k})$, e.g. magnons, with small but finite deviations of the inverse from 0, i.e. shifts of the pole along the imaginary axis, being related to their inverse lifetime [18, 29]. Conversely, large imaginary parts of the roots imply a strong damping and therefore dissipative behavior, which is anticipated deep in the disordered phase where longitudinal ($\parallel \mathbf{e}_z$) and transverse fluctuations are indistinguishable [31, 32].

1.3.2 Magnetic scattering and dynamic structure factor

The most common way of probing magnetic systems is inelastic neutron scattering, because these particles, while having no electric charge, carry a magnetic moment, thus interacting with the moments in the target, i.e. the localized spins. Employing the Born approximation one can show that the differential cross section satisfies [31, 32, 33]

$$\frac{d^2\sigma}{d\Omega d\omega} \propto \frac{k_1}{k_0} \sum_{\alpha,\gamma} \left(\delta_{\alpha\gamma} - \frac{k^\alpha k^\gamma}{k^2} \right) S^{\alpha\gamma}(\mathbf{k}, \omega). \quad (1.72)$$

Here k_1, k_0 are the initial/final momentum of the neutrons, $\mathbf{k} = \mathbf{k}_1 - \mathbf{k}_0$ is the momentum and $\omega = \frac{k_1^2 - k_0^2}{2m_n}$ the frequency (energy) transfer of the scattered neutrons. Note that the neutrons couple only to fluctuations in the direction perpendicular to the momentum transfer \mathbf{k} , as implied by $\left(\delta_{\alpha\gamma} - \frac{k^\alpha k^\gamma}{k^2} \right)$. $S^{\alpha\gamma}(\mathbf{k}, \omega)$ is known as the dynamic structure factor, which is the Fourier transform of a time-dependent spin-spin correlation function

$$S^{\alpha\gamma}(\mathbf{k}, \omega) = \frac{1}{2\pi} \sum_i \int_{-\infty}^{\infty} dt e^{i\omega t + i\mathbf{k}\cdot\mathbf{r}_i} \langle S_i^\alpha(t) S_0^\gamma(0) \rangle. \quad (1.73)$$

The dynamic structure factor is related to the retarded spin susceptibility by means of the fluctuation-dissipation theorem [16, 34, 35]

$$S^{\alpha\gamma}(\mathbf{k}, \omega) = \frac{1}{\pi} \frac{1}{1 - e^{-\beta\omega}} \text{Im} G_{ret}^{\alpha\gamma}(\mathbf{k}, \omega). \quad (1.74)$$

The above equation establishes a connection between thermal fluctuations of the spins in the unperturbed system in equilibrium, represented by the dynamic structure factor, and dissipation, implied by the retarded susceptibility. The relation between $S(\mathbf{k}, \omega)$ and $G_{\text{ret}}(\mathbf{k}, \omega)$ can be derived from the spectral representation of these quantities, which is obtained by inserting an identity $\mathbf{1} = \sum_n |n\rangle\langle n|$ between the operators in the expectation values. In the time-domain they are given by

$$G_{\text{ret},ij}^{\alpha\gamma}(t) = iZ^{-1}\Theta(t) \sum_{n,m} (e^{-\beta E_n} - e^{-\beta E_m}) \langle n|S_i^\alpha|m\rangle \langle m|S_j^\gamma|n\rangle e^{i(E_n - E_m)t}, \quad (1.75)$$

$$S_{\text{ret},ij}^{\alpha\gamma}(t) = (2\pi Z)^{-1} \sum_{n,m} e^{-\beta E_n} \langle n|S_i^\alpha|m\rangle \langle m|S_j^\gamma|n\rangle e^{i(E_n - E_m)t}. \quad (1.76)$$

Taking the Fourier transform to momenta and real frequencies, they read with $\frac{1}{2\pi} \int_{-\infty}^{\infty} e^{ixy} dy = \delta(x)$

$$\begin{aligned} G_{\text{ret}}^{\alpha\gamma}(\mathbf{k}, \omega) &= \sum_i \int_0^\infty dt G_{\text{ret},ij}^{\alpha\gamma}(t) e^{i\omega t + i\mathbf{k}\cdot(\mathbf{r}_i - \mathbf{r}_j) - \delta t} \\ &= -\frac{1}{Z} \sum_{n,m} \frac{\langle n|S^\alpha(\mathbf{k})|m\rangle \langle m|S^\gamma(-\mathbf{k})|n\rangle (e^{-\beta E_n} - e^{-\beta E_m})}{E_n - E_m + \omega + i\delta}, \end{aligned} \quad (1.77)$$

$$\begin{aligned} S^{\alpha\gamma}(\mathbf{k}, \omega) &= \sum_i \int_0^\infty dt S_{ij}^{\alpha\gamma}(t) e^{i\omega t + i\mathbf{k}\cdot(\mathbf{r}_i - \mathbf{r}_j)} \\ &= \frac{1}{Z} \sum_{n,m} \langle n|S^\alpha(\mathbf{k})|m\rangle \langle m|S^\gamma(-\mathbf{k})|n\rangle e^{-\beta E_n} \delta(E_n - E_m + \omega), \end{aligned} \quad (1.78)$$

where we introduced $S^\alpha(\mathbf{k}) = \sum_i e^{i\mathbf{k}\cdot\mathbf{r}_i} S_i^\alpha$. Inserting the Sokhotski-Plemelj formula $[x + i\delta]^{-1} = \mathcal{P}(1/x) - i\pi\delta(x)$ [29], when taking the imaginary part of G_{ret} , one sees that with the constraint $E_m = E_n + \omega$ from the δ -function one arrives at $\text{Im}G_{\text{ret}}(\mathbf{k}, \omega) = \pi(1 - e^{-\beta\omega})S(\mathbf{k}, \omega)$. In an isotropic paramagnet with vanishing external field, the two-point functions are all proportional to unity with respect to the Cartesian components. Hence for $\alpha = \gamma$ one can use that the spin operators satisfy $S(\mathbf{k}) = S^\dagger(-\mathbf{k})$, which implies that $S(\mathbf{k}, \omega)$ is real and ≥ 0 . In this context one also often introduces the spectral density [16, 29]

$$\rho(\mathbf{k}, \omega) = 2\text{Im}G_{\text{ret}}(\mathbf{k}, \omega) = \frac{2\pi(1 - e^{-\beta\omega})}{Z} \sum_{n,m} |\langle n|S^\alpha(\mathbf{k})|m\rangle|^2 e^{-\beta E_n} \delta(E_n - E_m + \omega), \quad (1.79)$$

which for $\omega > 0$ yields the frequency dependence of the scattering intensity at $T = 0$. Furthermore it provides information about excitations from the ground state, i.e. the low-energy sector of the spectrum, as can be inferred from the transition matrix elements $\langle n|S^\alpha(\mathbf{k})|m\rangle$ in front of the δ -distribution. Note that the spectral density is, at least for non-conserved operators, an odd function of ω , i.e. $\rho(\mathbf{k}, \omega) = -\rho(\mathbf{k}, -\omega)$, as can be seen by using $\delta(x) = \delta(-x)$ and $|\langle n|S^\alpha(\mathbf{k})|m\rangle| = |\langle m|S^\alpha(\mathbf{k})|n\rangle|$, with the latter requiring inversion symmetry on the lattice [36]. Under the latter conditions one can also infer that $\text{Re}G_{\text{ret}}$ is an even function of ω . Moreover $\rho(\mathbf{k}, \omega)$ is positive for $\omega > 0$ and negative for $\omega < 0$, as can be read off from the factor $1 - \exp(-\beta\omega)$. For constant operators like the total spin

$\mathbf{S}(\mathbf{k} = \mathbf{0}) = \frac{1}{N} \sum_i \mathbf{S}_i$, which are diagonal in the eigenbasis $\{|n\rangle\}$, it contains a Dirac-peak at vanishing frequency [36].

Another type of correlation function, which was often studied in the literature, is the so-called Kubo relaxation function [28, 33]

$$\mathcal{R}_{ij}^{\alpha\gamma}(t) = \int_0^\beta ds \langle S_j^\gamma(0) e^{-s\mathcal{H}} S_i^\alpha(t) e^{s\mathcal{H}} \rangle. \quad (1.80)$$

A simple interpretation for this quantity can be given if one considers a constant external perturbation H in $t \in (-\infty, 0)$ that is abruptly switched off at $t = 0$. The time-dependence of $\mathcal{R}_{ij}^{\alpha\gamma}(t)$ describes then the change of $\langle S_i^\alpha(t) \rangle$ as it relaxes to the equilibrium state [28, 33], which will be shown below. Consistent with that statement its value at $t = 0$ in \mathbf{k} -space is given by the zero-field static susceptibility $G^{\alpha\gamma}(\mathbf{k})$, defined in Eq. (1.56). Assuming for simplicity no symmetry breaking, so that $\mathcal{R}^{\alpha\gamma}(\mathbf{k}, \omega) = \delta_{\alpha\gamma} \mathcal{R}(\mathbf{k}, \omega)$, one can see this by using the derivative rule [28, 37]

$$\partial_{H(\mathbf{k})} e^{-\beta[\mathcal{H}-H(\mathbf{k})S^z(\mathbf{k})]} = e^{-\beta[\mathcal{H}-H(\mathbf{k})S^z(\mathbf{k})]} \int_0^\beta ds e^{s[\mathcal{H}-H(\mathbf{k})S(\mathbf{k})]} S^z(\mathbf{k}) e^{-s[\mathcal{H}-H(\mathbf{k})S^t(\mathbf{k})]}, \quad (1.81)$$

whose non-trivial shape is a consequence of $[S^z(\mathbf{k}), \mathcal{H}] \neq 0$. With the cyclic property of the trace the expectation value reads

$$\langle S^z(\mathbf{k}) \rangle = Z^{-1} \text{Tr}(e^{-\beta\mathcal{H}} S^z(\mathbf{k})), \quad (1.82)$$

whereas the following expression is obtained for its derivative [37]

$$\partial_{H(-\mathbf{k})} \langle S^z(\mathbf{k}) \rangle_{H=0} = Z^{-1} \int_0^\beta ds \text{Tr}(e^{-\beta\mathcal{H}} S^z(-\mathbf{k}) e^{-s\mathcal{H}} S^z(\mathbf{k}) e^{s\mathcal{H}}), \quad (1.83)$$

which is simply $\mathcal{R}(\mathbf{k}, t = 0)$. Turning to the spectral representation of the relaxation function one obtains

$$\mathcal{R}_{ij}^{\alpha\gamma}(t) = \frac{1}{Z} \sum_{n,m} (e^{-\beta E_n} - e^{-\beta E_m}) \langle n | S_i^\alpha | m \rangle \langle m | S_j^\gamma | n \rangle \frac{e^{i(E_n - E_m)t}}{E_m - E_n}. \quad (1.84)$$

from which one reads off for $t > 0$

$$\frac{d}{dt} \mathcal{R}_{ij}^{\alpha\gamma}(t) = -G_{\text{ret},ij}^{\alpha\gamma}(t). \quad (1.85)$$

Note that with $\mathbf{H}_j(t) = \mathbf{H}_j \Theta(-t)$, the assumption $\mathcal{R}_{ij}^{\alpha\gamma}(t \rightarrow \infty) = 0$ and the linear-response relation (1.69) it implies the aforementioned relaxation of $\langle S_i^\alpha(t) \rangle$, i.e.

$$\langle S_i^\alpha(t) \rangle - \langle S_i^\alpha \rangle_0 = \sum_j \mathcal{R}_{ij}^{\alpha\gamma}(t) H_j^\gamma. \quad (1.86)$$

Continuing with the Fourier-transform of the relaxation-function given by

$$\mathcal{R}^{\alpha\gamma}(\mathbf{k}, \omega) = \frac{2\pi}{Z} \sum_{n,m} (e^{-\beta E_n} - e^{-\beta E_m}) \langle n | S^\alpha(\mathbf{k}) | m \rangle \langle m | S^\gamma(-\mathbf{k}) | n \rangle \frac{\delta(\omega - E_n + E_m)}{E_m - E_n}. \quad (1.87)$$

one can relate it to the retarded spin susceptibility via

$$\omega \mathcal{R}^{\alpha\gamma}(\mathbf{k}, \omega) = 2\text{Im} G_{\text{ret}}^{\alpha\gamma}(\mathbf{k}, \omega), \quad (1.88)$$

so that we can write

$$S^{\alpha\gamma}(\mathbf{k}, \omega) = \frac{1}{2\pi} \frac{\omega}{1 - e^{-\beta\omega}} \mathcal{R}^{\alpha\gamma}(\mathbf{k}, \omega). \quad (1.89)$$

Note that for $\beta\omega \ll 1$ the relaxation function yields directly the frequency dependence of the scattering cross section and therefore for arbitrary ω at infinite temperature. In those limit structure factor $S^{\alpha\gamma}$ and relaxation function $\mathcal{R}^{\alpha\gamma}$ are the same up to a factor of $T/2\pi$. Note also that in general

$$\langle S^\alpha(\mathbf{k}, t) S^\gamma(-\mathbf{k}, 0) \rangle = 2\pi S^{\alpha\gamma}(\mathbf{k}, t) = \int_{-\infty}^{\infty} \frac{d\omega}{2\pi} \frac{\omega e^{-i\omega t}}{1 - e^{-\beta\omega}} \mathcal{R}^{\alpha\gamma}(\mathbf{k}, \omega), \quad (1.90)$$

confirming that only at $T = \infty$ the classical relation $T\mathcal{R}(\mathbf{k}, t) = \langle S(\mathbf{k}, t) S(-\mathbf{k}, 0) \rangle$, in particular between equal-time correlation function and static susceptibility $G(\mathbf{k})$, is valid. In the opposite limit $T = 0$ one finds $S(\mathbf{k}, t) \sim \int_0^\infty d\omega \omega \mathcal{R}(\mathbf{k}, \omega) e^{i\omega t}$. In the symmetric phase $\mathcal{R}(\mathbf{k}, \omega) = \rho(\mathbf{k}, \omega)/\omega$ is a real-valued, positive definite, and even function of frequency, in accordance with the properties of the spectral density. The Kubo relaxation function was frequently employed in non-perturbative calculations of the spin dynamics in the symmetric phase, especially at $T = \infty$, in the framework of the so-called memory function formalism [38, 39]. One solves then an integro-differential equation of Langevin type for $\mathcal{R}(\mathbf{k}, t)$, that describes mainly dissipative processes. Such processes are believed to govern the long-time ($t \gg \mathcal{O}(|J|^{-1})$) dynamics of isotropic paramagnets [33, 39], in contrast to the oscillatory behavior in the ordered phase, implied by long-lived, propagating quasiparticles.

1.3.3 Matsubara (imaginary-time) formalism

In the context of fermionic or bosonic many-body systems it was found that diagrammatic expansions of retarded susceptibilities around a free limit cannot be formulated for $T \neq 0$ in a straightforward way. This can be explained by the fact that $\exp(-\beta\mathcal{H})$ appears in a non-trivial fashion, so that calculations of these quantities turn out to be rather cumbersome [18, 29]. Note that this has also bearings on quantum spin systems like the Heisenberg model, even though there are no kinetic, i.e. free, terms in \mathcal{H} , meaning that there is no small parameter at low temperatures to expand in. By invoking the spin wave picture, which is believed to be correct for $T \ll |J|$, one can introduce however an effective bosonic model for magnon excitations from the ground state and expand in powers of $1/S$ [16, 30]. Hence one faces similar technical problems at finite temperatures as for true fermions/bosons, if one is interested in corrections to the non-interacting limit.

Fortunately, there exists a remedy, first developed by Matsubara [40]. It is based on an analytic continuation of the time evolution operator $\mathcal{U}(t, 0) = e^{i\mathcal{H}t}$, by substituting the real-valued time variable via [18, 29, 40]

$$t \rightarrow -i\tau, \quad (1.91)$$

so that one is entirely located on the imaginary axis. The evolution in imaginary time is therefore

$$A(t) \rightarrow A(t = -i\tau) = e^{\tau\mathcal{H}} A e^{-\tau\mathcal{H}}, \quad (1.92)$$

meaning that the new time-evolution operator is non-unitary, i.e. $\mathcal{U}^{-1}(\tau, 0) = \mathcal{U}(0, \tau) \neq \mathcal{U}^\dagger(\tau, 0)$. Obviously, it has a functional form that is similar to the Boltzmann operator $e^{-\beta\mathcal{H}}$

in the equilibrium density matrix ρ_0 , in contrast to the 'oscillatory' real-time evolution operator. In order to obtain proper correlation functions in imaginary time, we first introduce time-ordering, via the action of an operator \mathcal{T} , e.g. [1, 2]

$$\mathcal{T}(S_i^\alpha(\tau)S_j^\gamma(0)) = \Theta(\tau)S_i^\alpha(\tau)S_j^\gamma(0) + \Theta(-\tau)S_j^\gamma(0)S_i^\alpha(\tau), \quad (1.93)$$

which is easily generalized to an arbitrary number of operators, with arguments τ_1, \dots, τ_n under the time-ordering symbol \mathcal{T} . Note that equal-time expressions of non-commuting spin operators, e.g. S_i^x, S_i^y , are obtained by setting their relative time difference to $\delta = 0^{+/-}$. An imaginary-time two-spin correlation function is then defined as [2]

$$G_{ij}^{\alpha\gamma}(\tau) = \langle \mathcal{T}(S_i^\alpha(\tau)S_j^\gamma(0)) \rangle = \text{Tr}(\rho_0 \mathcal{T}(S_i^\alpha(\tau)S_j^\gamma(0))). \quad (1.94)$$

From the cyclic property of the trace, one can show then that it satisfies Kubo-Martin-Schwinger boundary conditions

$$G_{ij}^{\alpha\gamma}(\tau) = G_{ij}^{\alpha\gamma}(\tau + \beta), \quad (1.95)$$

i.e. that is periodic, and therefore has to be only calculated explicitly in $[0, \beta]$. This periodicity extends to each time argument of higher order-correlation functions. As a consequence one can introduce a discrete Fourier transform

$$G_{ij}^{\alpha\gamma}(i\omega) = \int_0^\beta d\tau G_{ij}^{\alpha\gamma}(\tau) e^{i\omega\tau}, \quad (1.96)$$

where the discretized Matsubara frequencies are given by $\omega = 2\pi nT$, $n \in \mathbf{Z}$, like for bosons. Only for $T \rightarrow 0$ ($\beta \rightarrow \infty$) the set of thermal frequencies becomes continuous again. Conversely we have

$$G_{ij}^{\alpha\gamma}(\tau) = T \sum_\omega G_{ij}^{\alpha\gamma}(i\omega) e^{-i\omega\tau}. \quad (1.97)$$

The spectral representation of the two-spin Matsubara function in an isotropic paramagnet, where $G^{\alpha\gamma}(\mathbf{k}, i\omega) = \delta_{\alpha\gamma} G(\mathbf{k}, i\omega)$, is given by

$$G(\mathbf{k}, i\omega) = -\frac{1}{Z} \sum_{n,m} |\langle n | S^\alpha(\mathbf{k}) | m \rangle|^2 \frac{(e^{-\beta E_n} - e^{-\beta E_m})}{E_n - E_m + i\omega}. \quad (1.98)$$

From this expression one reads off that the retarded susceptibility is the analytical continuation of the Matsubara function slightly above the real axis

$$G_{\text{ret}}(\mathbf{k}, \omega) = G(\mathbf{k}, i\omega \rightarrow \omega + i0^+), \quad (1.99)$$

and

$$G(\mathbf{k}, i\omega = 0) = \mathcal{R}(\mathbf{k}, t = 0), \quad (1.100)$$

which thus implies that the zero-frequency value of $G(\mathbf{k}, i\omega)$ is the static susceptibility from Eq. (1.56)

$$G(\mathbf{k}, i\omega = 0) = G(\mathbf{k}). \quad (1.101)$$

Hence one can extract the same physical information from the Matsubara correlation function. The analytic structure of the imaginary-time functions is, compared to G_{ret} , relatively

benign, as it does very seldom involve poles in the immediate vicinity of the real ω -axis. Defining a so-called dynamic susceptibility in the complex frequency plane [18, 29]

$$\tilde{G}(\mathbf{k}, s) = \int_{-\infty}^{\infty} \frac{d\nu}{2\pi} \frac{\rho(\mathbf{k}, \nu)}{\nu - s} = \int_{-\infty}^{\infty} \frac{d\nu}{\pi} \frac{1}{\nu - s} \text{Im}G_{\text{ret}}(\mathbf{k}, \nu), \quad (1.102)$$

one sees by inserting the spectral representation of the spectral density, Eq. (1.79), that the inverse relation between the Matsubara function and the retarded susceptibility is given by setting $s = i\omega$. This expression features a branch cut for $\text{Im}(s) = 0$, meaning that approaching the real axis from above and below $s = \omega \pm i0^+$ produces a discontinuity, with the difference given by $i\rho(\mathbf{k}, \omega)$. Note that depending on the sign of $\text{Im}(s)$ the susceptibility $\tilde{G}(\mathbf{k}, s)$ can be expressed via a one-sided Fourier (or Laplace) transform of the time-dependent spectral density $\rho(\mathbf{k}, t)$ for either $t > 0$ or < 0 , e.g. $G_L(\mathbf{k}, s) = i \int_0^{\infty} dt e^{ist} \rho(\mathbf{k}, t) = i\rho_L(\mathbf{k}, s)$, $\text{Im}(s) > 0$, and hence [35]

$$\rho(\mathbf{k}, \omega) = \rho_L(\mathbf{k}, \omega + i0^+) - \rho_L(\mathbf{k}, \omega - i0^+) = 2\text{Re}(\rho_L(\mathbf{k}, \omega + i0^+)). \quad (1.103)$$

In terms of the relaxation function the Matsubara function reads

$$G(\mathbf{k}, i\omega) = \int_{-\infty}^{\infty} \frac{d\nu}{2\pi} \frac{\nu}{\nu - i\omega} \mathcal{R}(\mathbf{k}, \nu). \quad (1.104)$$

Note that from this relation and the properties of $\mathcal{R}(\mathbf{k}, \nu)$ one can infer that in the disordered phase $\text{Im}G(\mathbf{k}, i\omega) = 0$, $\text{Re}G(\mathbf{k}, i\omega) > 0$ and $G(\mathbf{k}, i\omega) = G(\mathbf{k}, -i\omega)$. Furthermore the above relation implies that $G(\mathbf{k}, i\omega)$ is a monotonously decreasing function of frequency, since

$$\text{Re}G(\mathbf{k}, i\omega) = \int_{-\infty}^{\infty} \frac{d\nu}{2\pi} \frac{\nu^2}{\nu^2 + \omega^2} \mathcal{R}(\mathbf{k}, \nu). \quad (1.105)$$

Note that it depends solely on ω^2 which in turn leads to an explicit dependence on $|\omega|$ for small frequencies. For large frequencies $G(\mathbf{k}, i\omega)$ falls off as $1/\omega^2$. A perturbation theory for the Matsubara function can be formally setup by switching to an interaction picture, where the operators evolve with a non-interacting \mathcal{H}_0 , and one expands a suitable time-ordered exponential, which contains the separated, interacting part \mathcal{J} [1, 2]. For fermions and bosons this provides us with finite-temperature diagrammatic expansions, that are similar to the ones at $T = 0$ [18, 29]. For the Heisenberg Model or other purely localized spin models such an expansion can only be reasonably used for high temperatures, where $\beta|J| \ll 1$, since free terms are absent in \mathcal{H} . Due to the already presented advantages in its analytic structure compared to the real-time approach, the Matsubara framework facilitates formulating and applying non-perturbative methods. Hence we will use it in our further investigations.

1.4 Hydrodynamics and dynamic scaling

1.4.1 Hydrodynamics

The phenomenological concept of hydrodynamics in the context of correlation functions of many-body systems was first introduced by Kadanoff and Martin [41] to describe the properties of many-body systems in non-equilibrium. The main assumption is that the variation of relevant quantities, i.e. those that are conserved in a suitable long wavelength-limit, is very slow in time and space for inhomogeneous perturbations from equilibrium

[35, 41]. As a consequence the system can be regarded as being everywhere in a local quasiequilibrium. This description requires sufficiently large times t (\leftrightarrow small frequencies ω) and distances $|\mathbf{r}|$ (\leftrightarrow large wavelengths $\lambda \sim k^{-1}$) in order to be valid, i.e. those that are much bigger than all other relevant scales in the problem. The corresponding crossover scales can be for instance purely microscopic and therefore can be read off from parameters in the Hamiltonian, e.g. the typical magnitude of the interaction $|U|$ and its effective range. For $T = \infty$ a hydrodynamic description should therefore be applicable for macroscopically small momenta and frequencies if the interaction is short-ranged. At lower temperatures additional scales emerge dynamically, like the aforementioned correlation length ξ and a corresponding relaxation time for the decay of fluctuations $\tau(\xi)$. Both become macroscopically large in the critical region, $\xi \gg a$, $\tau(\xi) \gg \mathcal{O}(|U|^{-1})$, leading to a continuous shrinking of the hydrodynamic regime for $T \rightarrow T_c$. In the context of a fluid, the relevant crossover scales can be understood as a mean free path, i.e. interatomic distance λ_f and flight time τ_f between collisions of particles. The hydrodynamic regime is thus often referred to as collision-dominated regime, since such events occur frequently on macroscopic space-time scales $\gg \lambda_f$, τ_f and ensure the aforementioned local equilibrium. If these conditions are met, one can reduce the problem in the hydrodynamic regime to the solution of a finite set of partial differential equations. First we have conservation laws, that are written in terms of a continuity equation [35]

$$\partial_t n(\mathbf{r}, t) + \nabla \cdot \mathbf{j}(\mathbf{r}, t) = 0, \quad (1.106)$$

where $n(\mathbf{r}, t)$ is a density and $\mathbf{j}(\mathbf{r}, t)$ is the corresponding current. For a normal fluid consisting of particles with mass m , we have densities of their number $\rho(\mathbf{r}, t)$, momentum $\mathbf{g}(\mathbf{r}, t)$ and energy $\epsilon(\mathbf{r}, t)$ which lead to the following equations [41]

$$\partial_t n(\mathbf{r}, t) + \nabla \cdot \mathbf{g}(\mathbf{r}, t)/m = 0, \quad (1.107)$$

$$\partial_t g_j(\mathbf{r}, t) + \partial_i T_{ij}(\mathbf{r}, t) = 0, \quad (1.108)$$

$$\partial_t \epsilon(\mathbf{r}, t) + \nabla \cdot \mathbf{j}_\epsilon(\mathbf{r}, t) = 0, \quad (1.109)$$

where $T_{ij}(\mathbf{r}, t)$ is the stress tensor and $\mathbf{j}_\epsilon(\mathbf{r}, t)$ the energy current. These equations are supplemented by expressions for T_{ij} and \mathbf{j}_ϵ on top of additional conditions for the gradients of the inhomogeneous temperature and pressure $T(\mathbf{r}, t)$, $P(\mathbf{r}, t)$ [41].

Spin Diffusion and other types of magnetic transport

In the context of the isotropic Heisenberg Model it suffices to restrict our discussion of hydrodynamics to one particular equation, describing the dynamics of the magnetization at elevated temperatures and asymptotically large space-time variables (\mathbf{r}, t) , i.e. $|\mathbf{r}| \gg \max\{\xi, a\}$, $t \gg \max\{\tau, \text{const} \times |J|^{-1}\}$. Note that spins separated by these distances are therefore weakly correlated, $|\langle S_{\mathbf{r}}(t) S_{\mathbf{0}} \rangle| \ll b'_0$. The corresponding equation for the variation of the inhomogeneous magnetization $M(\mathbf{r}, t) = \langle S_{\mathbf{r}}^z(t) \rangle$ in the symmetric phase reads then [41]

$$\partial_t M(\mathbf{r}, t) = -\mathcal{D}(i\nabla)^2 M(\mathbf{r}, t), \quad (1.110)$$

which follows from the corresponding continuity equation, if one assumes $\mathbf{j}_M = \mathcal{D}\nabla M$ [35, 41] for the magnetization current. Here $\mathcal{D} > 0$ is the spin diffusion coefficient, since one can readily discern that this partial differential equation has the same shape as the

diffusion equation, known from the theory of Brownian motion [35]. Note that \mathcal{D} has to be calculated by some other means, with its explicit numeric value depending on microscopic details [41]. For $T \rightarrow \infty$ one expects $\mathcal{D} \propto |J|$ [42]. Transforming to momentum space, where $(i\nabla)^2 \rightarrow k^2$ one obtains for its solution

$$M(\mathbf{k}, t) = M(\mathbf{k}, 0) \exp(-\mathcal{D}k^2 t). \quad (1.111)$$

Such an exponential decay is an irreversible and, for the assumed hydrodynamic times and momenta, slow process, describing the dissipation of an inhomogeneous initial configuration $M(\mathbf{k}, 0)$, caused by disturbing equilibrium. Note that transforming the expression for $M(\mathbf{k}, t)$ to real space yields a normalized Gaussian $\propto \exp(-\frac{r^2}{2(\Delta r)^2})$ with squared mean displacement $(\Delta r)^2 = \mathcal{D}t$, which describes the time-dependent spreading of a sharply localized initial magnetization $M(\mathbf{r}, 0) \propto \delta(r)$ [35]. Taking a one-sided Fourier or Laplace-transform of the above solution to the complex upper plane $M_L(\mathbf{k}, s) = \int_0^\infty dt e^{ist} M(\mathbf{k}, t)$ one finds [35, 41]

$$M_L(\mathbf{k}, s) = \frac{M(\mathbf{k}, 0)}{\mathcal{D}k^2 - is}, \quad (1.112)$$

implying an imaginary pole at $s = -i\mathcal{D}k^2$. One can also calculate the two-spin correlation function and therefore scattering intensity $S(\mathbf{k}, \omega)$, by essentially assuming that the diffusion equation (1.110) holds on the level of operator or fields too, without taking the non-equilibrium expectation value with respect to a perturbed density matrix $\neq \rho_0$ [35]. From that one immediately concludes, by taking the equilibrium average, that the two-spin correlation function $S(\mathbf{k}, t) \sim \langle S^\alpha(\mathbf{k}, t) S^\alpha(-\mathbf{k}, 0) \rangle$ satisfies the diffusion equation

$$\partial_t S(\mathbf{k}, t) = -\mathcal{D}k^2 S(\mathbf{k}, t), \quad (1.113)$$

which yields the previous exponential decay. Note that for $\mathbf{k} = \mathbf{0}$ it does not decay, since the total spin is conserved as implied by the continuity equation. One obtains a similar expression for its Laplace-transform

$$S_L(\mathbf{k}, s) \propto [\mathcal{D}k^2 - is]^{-1}, \quad (1.114)$$

featuring again the imaginary diffusion pole. The dynamic structure factor $S(\mathbf{k}, \omega) = 2\text{Re}(S_L(\mathbf{k}, s \rightarrow \omega + i0^+))$ is then proportional to a Lorentzian, centered at $\omega = 0$ [35, 41]

$$S(\mathbf{k}, \omega) \propto \frac{\mathcal{D}k^2}{(\mathcal{D}k^2)^2 + \omega^2}, \quad (1.115)$$

which also implies [35]

$$\mathcal{D} \sim \lim_{\omega \rightarrow 0} \lim_{k \rightarrow 0} \frac{\omega^2}{k^2} S(\mathbf{k}, \omega). \quad (1.116)$$

Furthermore we want to note that alternatively the diffusion coefficient \mathcal{D} can be written in terms of a static ($\omega = 0$) and homogeneous ($k \rightarrow 0$) limit for the current-current correlation function, i.e. its spatial and temporal average [28, 35, 42, 43].

There are no rigorous proofs on the existence of spin diffusion in the isotropic Heisenberg Model. Whether hydrodynamics in the laid out version is indeed a valid description of the long-time and wavelength asymptotics, may depend also on additional properties of the system, like its dimensionality [44, 45, 46] and further conservation laws, that arise for instance from integrability in some particular one-dimensional systems [47, 48, 49, 50].

Furthermore the aforementioned asymptotic behavior may be restricted to specific scaling limits, requiring as an example some fixed relation between t and k [44], with the asymptotic long-time behavior being more intricate. Besides ordinary diffusion described above, one also encounters anomalous diffusion, which amounts to a time-dependent diffusion coefficient $\mathcal{D}(t)$, that does not converge to a finite long-time value $\mathcal{D}(t = \infty) = \mathcal{D} \neq 0$. Depending on whether it diverges for $t \rightarrow \infty$ or approaches zero one can distinguish between super- and subdiffusion [47, 48, 51]. Conversely, $\mathcal{D}(\omega)$ approaches zero for $\omega \rightarrow 0$ in the case of subdiffusion and diverges in the low-frequency limit for superdiffusion [44, 47, 51, 53], often as a power-law. Note that the low- ω asymptotics of $\mathcal{D}(\omega)$, implied by anomalous diffusion, are covered by Eq. (1.116) as well, relating \mathcal{D} to a specific zero-momentum/frequency limit of the scattering intensity $S(\mathbf{k}, \omega)$ [42]. In real space such a behavior of the diffusion coefficient would manifest itself via a modified law for the time-dependent spread or variance

$$\Delta r^2 \sim t^{2m}, \quad (1.117)$$

of magnetization profiles, with $m > 1/2$ for super- and $m < 1/2$ for subdiffusion [48]. m is directly related to the divergence or vanishing of $\mathcal{D}(t)$, $\mathcal{D}(\omega)$, whose asymptotics also determine a dynamic index $z = 1/m$ such that one obtains $\omega \sim k^z$ as a characteristic energy at small k and ω [51]. For instance, the diffusion form (1.115) for $S(\mathbf{k}, \omega)$ implies $z = 2$. Note that m is bounded from above by 1, with that limit describing ballistic transport, i.e. $\sqrt{\Delta r^2} \sim vt$. Ballistic behavior in magnets at high temperatures is explicitly found in the spin-1/2 XXZ-chain with weak or vanishing Ising-anisotropy [47, 48, 51, 52, 53], but is also argued to occur frequently in classical integrable systems [47, 48]. Moreover one can associate ballistic transport, as is the case for electrons, with a perfect conductor, i.e. ideal transport unhampered by a finite scattering rate τ_s^{-1} [42, 52, 53]. The form for the corresponding dynamic conductivity

$$\sigma(\omega) = D_R \delta(\omega) + \sigma_{\text{reg}}(\omega) \quad (1.118)$$

is shown to host a Dirac-peak with a finite Drude weight $D_R > 0$, that is given by the long-time limit of the aforementioned current-current autocorrelation [42, 51], besides a regular, dissipative contribution $\sigma_{\text{reg}}(\omega)$ that can be related to $\mathcal{D}(\omega)$ [42, 43, 51]. Conversely ordinary diffusion is characterized by a non-zero τ_s^{-1} and the removal of the Drude peak, $D_R = 0$ [42, 52], with $\sigma_{\text{reg}}(0) \neq 0$, analogous to a realistic conductor [42]. A vanishing diffusion coefficient or static conductivity, as is the case for subdiffusion, implies transport like in an insulator, e.g. a disordered electronic system with a high concentration of impurities and the fully localized limit given by $\Delta x^2 \sim t^0$ [42, 43, 51]. Finally, for superdiffusion the Drude weight remains zero as for diffusion [53], thus still being dissipative, although with faster growth of Δx^2 due to $\lim_{\omega \rightarrow 0} \sigma_{\text{reg}}(\omega) = \infty$ [51].

1.4.2 Van Hove Theory of critical scattering and mode-coupling approach

The van Hove theory was a first attempt to give a phenomenological description of the scattering at magnetic materials [32]. In particular it provided predictions for the critical T -dependence of decay rates for quantities like the magnetization in a ferromagnet. Van Hoves starting point concerning the magnetic scattering in the vicinity of the critical point, is again a phenomenological equation for the variation of the magnetization $\mathbf{M}(\mathbf{r}, t)$ of a paramagnet at macroscopically large distances and times, which in momentum space reads

$$\partial_t \mathbf{M}(\mathbf{k}, t) = -G^{-1}(\mathbf{k}) L(\mathbf{k}) \mathbf{M}(\mathbf{k}, t). \quad (1.119)$$

Here, the dimensionless quantity $L(\mathbf{k}) > 0$ is a so-called Onsager-coefficient and $G(\mathbf{k})$ the momentum-resolved static susceptibility defined in Eq. (1.69). In the vicinity of $k = 0$, i.e. long wavelengths, this coefficient satisfies

$$L(\mathbf{k}) = Lk^2, \quad (1.120)$$

so that this equation describes, as already discussed, spin diffusion, with a diffusion constant given by

$$\mathcal{D} = G^{-1}(\mathbf{0})L. \quad (1.121)$$

For a ferromagnet $G^{-1}(\mathbf{0})$ is the inverse of the order parameter susceptibility χ and goes to zero as ξ^{-2} for $T \rightarrow T_c$. van Hove argued now that $L(\mathbf{k})$ remains finite for $T = T_c$ [32, 54], as it should be determined by fluctuations on all length scales, including microscopic ones, regardless of the strong correlations, associated with a singular static susceptibility. He explicitly related L to the change of entropy δS in the irreversible process of dissipating a spatially inhomogenous magnetization, e.g. [32]

$$\delta S \sim \frac{L}{T\chi^2} \left(\sum_{\alpha,\gamma} \frac{\partial M_\alpha}{\partial x_\gamma} \right)^2. \quad (1.122)$$

It was then imposed that after insertion of $M_\alpha = \chi H_\alpha$, the change δS should not depend on the susceptibility χ , meaning that δS is non-singular, if L is also taken as a finite constant. The consequence of all this is that \mathcal{D} vanishes as χ^{-1} [32], i.e. the decay rate of fluctuations around the ordering vector goes to 0, which is a manifestation of the aforementioned critical slowing down, see section 1.2.1, that allows us to ignore the effect of dynamics on universal properties of static quantities near a critical point. In an antiferromagnet this also applies to the decay rate of the staggered magnetization, which is non-conserved and at large temperatures a fast mode due to $L(\mathbf{Q}) \neq 0$, but becomes as a consequence of $G^{-1}(\mathbf{Q}) \rightarrow 0$ also slowly varying in the vicinity of T_c . Note also that fluctuations near the origin do not exhibit critical slowing down in an antiferromagnet, since $G^{-1}(\mathbf{0}) = \mathcal{O}(J) \neq 0$ at T_c , implying $\mathcal{D} \neq 0$.

Mode-coupling approach to critical dynamics

It turns out that, while critical slowing down is observed in experiments and also found in other calculations [55, 56], a non-singular Onsager-coefficient L is not always guaranteed for $T \rightarrow T_c$. If one allows for a divergent L , the vanishing of \mathcal{D} or other decay rates of interest, occurs with a smaller exponent, and this was indeed measured in experiments [54, 55, 56]. The reason for this failure may be traced back to the neglect of certain terms in the dynamics of the magnetization as described by Eq. (1.119), which will induce singular anomalies in the T -dependence of L . These contributions correspond to reversible and nondissipative processes, in contrast to the irreversible, dissipative diffusion term, as introduced in hydrodynamics. They are rooted in interactions between proper *slow* modes M_i , namely the order parameter and other quantities, whose decay rates approach zero for $k \rightarrow 0$ or $\mathbf{k} \rightarrow \mathbf{Q}$ and $T \rightarrow T_c$. Hence even without being conserved the order parameter is of relevance, due to $G^{-1}(\mathbf{Q}) \rightarrow 0$ for $T \rightarrow T_c$, so that its relaxation rate vanishes eventually too. Note that all other *fast* variables, which do not satisfy these conditions, are projected out via a suitable procedure, as first introduced in the Mori-Zwanzig formalism [33, 38, 39, 55]. The scalar product between modes (M_i^*, M_j) is then defined in terms of a relaxation function of these two quantities (operators) and the projection separates degrees of freedom which

are orthogonal to the relevant modes in the sense of this scalar product [39, 55]. Note that the aforementioned interactions between relevant modes are nonlinear and persist at macroscopic distances k^{-1} of the same order as the correlation length $\xi \gg a$, with the reversible terms known as *mode-coupling* contributions [54, 55, 56, 57]. The shape of these terms is determined by generalized Poisson brackets $\{M_i, M_j\}$ between slow variables. In the case of magnetic moments, one can obtain those via the correspondence principle by using the commutator relations (1.9) for spin operators [56]. The structure of the reversible coupled-mode terms, is thus the same, as in the equation of motion for the quantum-mechanical operators. For the Heisenberg Model this amounts to the Larmor precession of a single spin in an effective exchange field, that is determined by all other spins, which couple to it via the interaction J_{ij} [56]. The dissipative term, which is also a consequence of interactions between slow modes, acts then as a damping of this precession. It is proportional to the variation of the free energy functional $F[\{\mathbf{M}\}]$ with respect to \mathbf{M} . In the case of a Heisenberg magnet the functional is simply given by the one for a three-component M^4 -theory, a static Ginzburg-Landau-Wilson functional (1.50). The extracted dynamic equation for the slowly varying magnetization in an isotropic ferromagnet reads for instance [55, 56, 57]

$$\frac{\partial}{\partial t} \mathbf{M}(\mathbf{r}, t) = C \mathbf{M} \times \frac{\delta F[\{\mathbf{M}\}]}{\delta \mathbf{M}(\mathbf{r}, t)} - L(i\nabla)^2 \frac{\delta F[\{\mathbf{M}\}]}{\delta \mathbf{M}(\mathbf{r}, t)} + \zeta(\mathbf{r}, t). \quad (1.123)$$

The first two terms on the right-hand side were already identified as the spin precession and its damping. The third one is a stochastic noise term [56], representing random forces, which is a consequence of integrating out all fast modes, that are orthogonal to the slow subspace. It is usually taken as White Noise, i.e. a Gaussian distribution for these random forces with variance L [55, 57]. Eq. (1.123) can then be treated for instance by means of the renormalization group to extract its scaling properties near the upper critical dimension, which for a ferromagnet is $d_c = 6$ [56, 57]. Usually one neglects, at least for the ferromagnet, terms of the order $(\mathbf{M}^2)^2$ in $F[\{\mathbf{M}\}]$, which are irrelevant above $d = 4$. The dissipative term is then purely linear. Conversely the coupled-mode term is quadratic like in the equations of motion for the spin operators. Moreover it is $\propto \nabla^2$, due to $\mathbf{M} \times \mathbf{M} = 0$, which is consistent with spin conservation [57]. Note that Eq. (1.123) includes additional approximations, like neglecting memory effects, via a retarded kernel in the dissipative part, and a possible dependence of L on \mathbf{M} [55, 56, 57].

1.4.3 Dynamic scaling

The *dynamic scaling hypothesis* (DSH), as formulated by Halperin and Hohenberg [54, 58], postulates that in the vicinity of a second order finite-temperature phase transition dynamic correlation functions at macroscopically large length- and timescales, have to be, analogous to static correlations, continuous along boundaries between asymptotic regions in a (\mathbf{k}, ξ^{-1}) -parameter space. Such an assumption for the dynamics at long wavelengths and low frequencies leads to results, which differ significantly from van Hoves predictions in Sec. 1.4.2. Its tremendous effect may be readily explained by explicitly taking the singular behavior of static order parameter correlations into account. In fact one of the central outcomes of dynamic scaling is that below a critical dimension d_c , which is inherent to a dynamic universality class of models, the leading temperature dependence of relevant decay rates, like the spin diffusion constant \mathcal{D} in a magnet, is strongly modified due to singularities in the corresponding Onsager coefficients [54, 58]. Such singularities were ruled out a priori in van Hoves description [32]. As time eventually showed dynamic scaling proved to be a

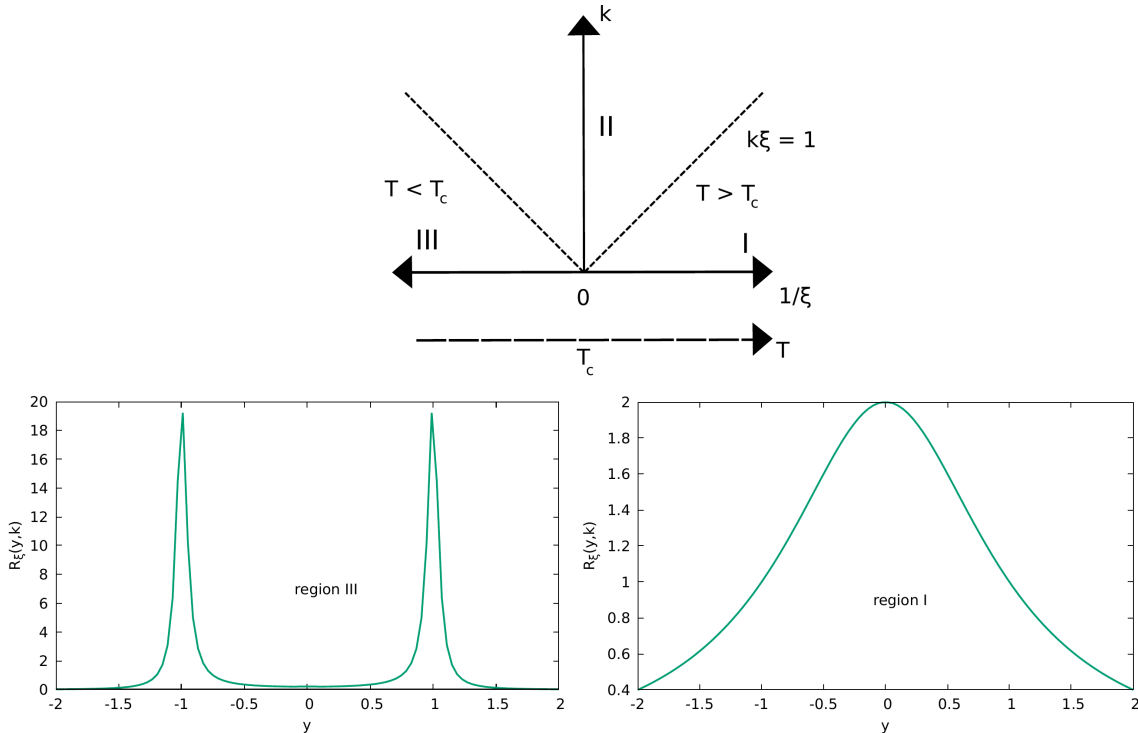


Figure 1.1: Upper plot: The three relevant asymptotics regions in the (k, ξ^{-1}) -plane as described in the main text. I and III are hydrodynamic regions above and below T_c whereas II is the critical region. Below: Typical line-shapes $\mathcal{R}_\xi(y = \omega/\omega_\xi(\mathbf{k}), k)$ for the frequency dependence of the dynamic structure factor $S(\mathbf{k}, \omega)$ in the regions III (left) and I (right).

powerful concept in describing the properties of models near their critical point. Its validity was repeatedly confirmed in other theoretical investigations, e.g. within the previously described effective field dynamics [55, 56, 57, 60], and, more important, experimental studies of magnetic systems [61, 62].

One starts by defining the regions of interests in a plane, spanned by a k and ξ^{-1} -axis, with the conditions that both $ka \ll 1$ and $\xi/a \gg 1$, i.e. the wavelengths of fluctuations and correlation length are much larger than all microscopic scales. Note that ξ^{-1} measures also the distance to the phase transition, since $|T - T_c| \sim \xi^{-1/\nu}$. Coming from above T_c and assuming $k\xi \ll 1$ one is located in the hydrodynamic regime of the symmetric phase, region I, where on length scales $\lambda \sim k^{-1} \gg \xi$ the system appears largely disordered, i.e. fluctuations are mostly uncorrelated. It can then be still appropriately described by the aforementioned phenomenological picture, as is the case at elevated temperatures, where ξ is small and the relevant constraint for hydrodynamics is relaxed to $ka \ll 1$. Taking as an example magnetic systems, spin dynamics in this region are, as previously discussed, dominated by processes like diffusion of the magnetic moment, implying dissipative, non-propagating, modes as purely imaginary poles in the dynamic two-spin correlation function at low frequencies [33, 35, 41]. Increasing $k\xi$ to values exceeding unity, one arrives in the so-called critical regime $k\xi \gg 1$, region II. Here the assumptions of a hydrodynamic theory cease to be valid, as degrees of freedom on the sufficiently short length scale $k^{-1} \ll \xi$ are now highly correlated. At the critical point where $\xi^{-1} = 0$ this is the sole available regime.

The boundary between both the regions I and II is roughly given by the line $k = \xi^{-1}$ and is alleged to lie in a smooth crossover between them (see below). In contrast to region I not even qualitative statements can be made on the dynamics exhibited in II, due to the lack of a simple phenomenological picture [58]. Finally one can also move into the symmetry-broken phase, below T_c . Leaving the critical region, by trespassing the left line $k\xi = 1$ one is again in a regime, that is suited for a hydrodynamic description, region III. However, in contrast to I, it is dominated by well-defined, propagating modes, where the real part of their dispersion $E(\mathbf{k})$ is much larger than the imaginary part, i.e. the damping $\Gamma(\mathbf{k})$ for small momenta $k \ll \xi^{-1}$ [6, 58, 59]. In magnets these modes can then be identified with spin waves. For a better overview we have sketched the different regions in the centre of Fig. 1.1.

The aforementioned continuity relations, which are also known as the *weak* formulation of this hypothesis, can be written as conditions enforced on correlations at the boundaries between the critical and hydrodynamic regions. Before formulating them explicitly, let us first write the dynamic structure factor as follows for small momentum and frequency [58]

$$S_\xi(\mathbf{k}, \omega) = TG_\xi(\mathbf{k})[2\pi\omega_\xi(\mathbf{k})]^{-1}\mathcal{R}_\xi(\omega/\omega_\xi(\mathbf{k}), k). \quad (1.124)$$

Here the subscript ξ indicates again the correlation length and thus the temperature at which one evaluates these quantities. $\mathcal{R}_\xi(y, k)$ is a normalized shape-function of the frequency-dependence, while $\omega_\xi(\mathbf{k})$ is a characteristic frequency, which can for instance be determined via a half-area constraint

$$\int_{-1}^1 \frac{dy}{2\pi} \mathcal{R}_\xi(y, k) = \frac{1}{2}. \quad (1.125)$$

In region I this frequency can be identified with the width $\Gamma(\mathbf{k})$ of a broad Lorentzian for the relaxation function \mathcal{R} . On the other hand for region III it is, in the limit $k \rightarrow 0$, where the damping is negligible, given by a single-magnon energy, e.g. $E(\mathbf{k}) \sim \rho_s k^2$ for the ferromagnet. The corresponding line-shape \mathcal{R} is dominated by the transverse part, which is quite close to sharp δ -peaks at $\omega = \pm E(\mathbf{k})$. The line-shapes in the hydrodynamic regions I and III are shown on the left and right of Fig. 1.1. Assuming sufficiently small frequencies in addition to the constraints already formulated for k , ξ^{-1} , we introduce asymptotic expressions of the momentum-dependent functions $\omega_\xi(\mathbf{k})$, $\mathcal{R}_\xi(y, k)$ and $G_\xi(\mathbf{k})$ in each of the regions I ($k\xi \rightarrow 0$, $T > T_c$), II ($k\xi \rightarrow \infty$) and III ($k\xi \rightarrow 0$, $T < T_c$). We demand that they coincide up to $\mathcal{O}(1)$ -factors W , W' at the lines given by $|k\xi| = 1$, e.g. for the characteristic frequency [54, 58]

$$\omega^{II}(\mathbf{k}) = W\omega_{\xi=k^{-1}}^I(\mathbf{k}), \quad (1.126)$$

$$\omega^{III}(\mathbf{k}) = W'\omega_{\xi=k^{-1}}^{III}(\mathbf{k}). \quad (1.127)$$

Note that one can recover static scaling relations from section 1.2.1, if one considers the respective conditions for the static susceptibility $G_\xi(\mathbf{k})$ [58]. While the weak formulation is sufficient to derive well-known results, there exists a more famous version of the DSH, which is fully compatible with the above continuity conditions. The *strong* formulation is given by postulating that the characteristic frequency and shape function obey the scaling laws [54, 58]

$$\omega_\xi(\mathbf{k}) = k^z \Omega(k\xi), \quad (1.128)$$

$$\mathcal{R}_\xi(y, k) = \mathcal{R}(y, k\xi), \quad (1.129)$$

where $z > 0$ is the dynamic exponent belonging to the respective dynamic universality class. Note that the limit $\Omega(\infty)$ is finite, thus implying that the line-shape at T_c can be written solely as a function of $\omega/\omega_\infty(\mathbf{k}) \sim \omega/k^z$ [58].

Taking a look at the correlations of an order parameter, whose decay rate in the hydrodynamic regime scales as $\tau^{-1}(k) \sim \Gamma(\xi)k^n$, one can read off from the matching condition above T_c

$$\Gamma(\xi) \sim \xi^{n-z}, \quad \Omega(k\xi \ll 1) \sim (k\xi)^{n-z}. \quad (1.130)$$

Normally $z > n$ [56, 58], so that $\Gamma(\xi)$ vanishes and is therefore compatible with the critical slowing down of order parameter fluctuations, although z will be smaller than the van Hove value, reflecting the aforementioned divergence of Onsager-coefficients for $T \rightarrow T_c$ [58]. The dynamic index z can be explicitly extracted by considering the behavior in the ordered phase, i.e. the hydrodynamic expressions for the spin wave dispersion [5, 6, 59] and using the postulated continuity relations. One can therefore predict from the knowledge of dynamic properties on one side of the phase transition some scaling properties for the approach from the other side. Note that measuring ω in terms $\omega_\xi(\mathbf{k})$ is not a unique choice to write down a scaling law. Other scaling variables for the frequency may be introduced as well, which leads to different scaling functions \mathcal{R}' that can be related to each other by means of simple rescalings of the argument and a possible prefactor. For instance one can measure the frequency in units of the $k\xi \ll 1$ (region I/III) or $k\xi \gg 1$ (region II)-limits of the characteristic frequency. This allows one to interpret plots of the scaling functions \mathcal{R}' directly in terms of dependences on a variable at fixed momentum k , frequency ω or temperature T .

We want to close on the note that one can distinguish between a *restricted* and *extended* scaling hypothesis [58]. The former is exclusively concerned with fluctuations of the order parameter, for instance the magnetization in a ferromagnet. In that case, the above considerations appear to be most justified, given that its own static correlations are singular. Extended scaling formulates similar statements for other operators of interest. Those are also part of the aforementioned slow variables, i.e. constants of motion like the total energy. A system where this is of relevance is the Heisenberg antiferromagnet, whose order parameter is not the total spin but the non-conserved staggered magnetization with ordering vector \mathbf{Q}_N . In that case extended scaling makes statements about the dynamics of the uniform magnetization. Independent calculations indeed predicted scaling forms for the dynamics of fluctuations around $\mathbf{0}$ and \mathbf{Q}_N that share a common characteristic frequency [56, 60], in agreement with extended dynamic scaling.

Chapter 2

Spin functional renormalization group

2.1 Motivation

The main goal of the spin functional renormalization group (SFRG) lies in establishing a non-perturbative method to determine thermodynamic and dynamic properties of quantum magnets, that works directly with the physical spin operators \mathbf{S} and their correlation functions. A major obstacle in transferring common methods for fermions or bosons to spin operators are their commutator relations, i.e. the $SU(2)$ algebra (1.9), since instead of a complex number like for the (anti-)commutators of canonical annihilation and creation operators, the commutator is again a spin operator. Thus the corresponding Wick theorem has a more complicated form [5, 7]. For the same reason one also cannot write the partition function Z like for fermions or bosons as a path integral over the spin degrees of freedom, i.e. in terms of Grassmann-valued or complex fields. Nevertheless Vaks, Larkin and Pikin (VLP) developed and used a diagrammatic expansion of spin correlation functions in terms of loop integrations, which is controlled by an associated small parameter like the inverse range of interactions [5, 6]. It went beyond high temperature expansion series, since it amounts already at zeroth order to an infinite resummation in J . This method was successfully employed to confirm findings of other approaches. One example is the occurrence of spin waves at low temperatures and their persistence in a hydrodynamic regime of sufficiently long wavelengths up to $T = T_c$ [6, 59].

However, the technique of VLP did not find widespread use, probably due to its unusual and therefore unwieldy diagrammatics. Other approximate approaches involve the solution of non-linear integro-differential equations for time-dependent correlations, which are derived in a memory-function formalism by means of separating properly chosen slow and fast degrees of freedom [38, 39, 60]. They are especially successful in describing relaxational dynamics in the disordered phase, but need an input for the thermodynamics and are also somewhat restricted in the way of conducting analytic investigations. Conversely, static properties are often approximately calculated by means of Green's function methods. These approaches use some simple decoupling scheme for the equations of motion, requiring only the calculation of a handful parameters, i.e. correlation functions up to a finite upper limit for the spatial separation between spins in these correlations [63, 64, 65, 66]. However, they give only a qualitative description of the critical behavior, i.e. wrong critical exponents, and do not perform better than mean-field theory in this regard. Furthermore on

their own, i.e. without the notion of memory effects, they are inconvenient for the description of dissipative phenomena in paramagnets like diffusion. A method which is capable of treating both sectors, static and dynamic, is therefore highly desired.

A different direction of approximate methods, that achieved some success, is based on expressing the spin operators via auxiliary degrees of freedom, i.e. canonical fermions c^\dagger , c or bosons b^\dagger , b with additional constraints. The most famous example is spin-wave theory for ordered magnets at low temperatures. In that case the magnon excitations can be described in terms of bosonic operators [16, 18, 30], whose number is limited by kinematic interactions at sufficiently large temperatures in order to account for the finite spin length on the otherwise unrestrained bosonic Fock space. Other ways to represent the spin operators, that are more tailored to the disordered phase, like Schwinger bosons [67] or Abrikosov pseudofermions [68] suffer from the same artificial increase of the Hilbert space, leading as an example to states with a vanishing S that are not part of the initial model [69]. Furthermore, the calculation of correlations between spin operators requires in general the knowledge of higher order correlation functions for these auxiliary operators, which introduces an additional complication.

Working directly with physical spin operators in the correct Hilbert space remains therefore quite tempting. In fact, some common mathematical objects like a path integral are not necessary for setting up a non-perturbative FRG. This was used by Krieg and Kopietz to formulate first an approach using the spin operators in their correct Hilbert space. In that context the whole non-trivial spin algebra (1.9) is then accounted for via the initial condition of the FRG flow, with its diagrammatic structure dictated by the FRG for bosonic systems [1, 2]. In the following we will start with the SFRG in its first formulation. Afterwards we construct, on that foundation, an approach which is especially suited for the paramagnetic phase and was introduced in our first publication, Ref. [10].

2.2 Initial formulations

2.2.1 1-PI formalism

We start by introducing a deformation into the isotropic Heisenberg Hamiltonian $\mathcal{H} \rightarrow \mathcal{H}_\Lambda$ which is decomposed as

$$\mathcal{H}_\Lambda = \mathcal{H}_0 + \mathcal{J}_\Lambda, \quad (2.1)$$

where the role of the non-interacting part is played by the Zeeman term coupling to a finite, spatially homogeneous external field H in the z-direction

$$\mathcal{H}_0 = -H \sum_i S_i^z, \quad (2.2)$$

and the contribution of the exchange interaction on a d -dimensional Bravais lattice with $N = \prod_{i=1}^d N_i$ sites and basis $\{\mathbf{a}_i\}$

$$\mathcal{J}_\Lambda = \frac{1}{2} \sum_{i,j} J_{ij}^\Lambda \mathbf{S}_i \cdot \mathbf{S}_j, \quad (2.3)$$

now depends on the flow parameter Λ by substituting $J_{ij} \rightarrow J_{ij}^\Lambda$. The latter is accomplished by introducing a regulator function R^Λ , which is added to the bare coupling J , i.e.

$$J_{ij}^\Lambda = J_{ij} + R_{ij}^\Lambda. \quad (2.4)$$

The coupling at the initial scale $\Lambda = \Lambda_0$ should be chosen such that the model in the corresponding limit is exactly solvable or can be treated in an approximate but controlled way. The simplest example is the non-interacting limit of isolated spins, $J_{ij}^{\Lambda_0} = 0$, for which one can calculate the eigenspectrum and thus thermodynamic observables and correlation functions exactly. In the following we will assume that $J_{ij}^{\Lambda} = J_{\Lambda}(\mathbf{r}_i - \mathbf{r}_j)$ depends only on the relative separation of lattice sites, implying discrete translational invariance on the Bravais Lattice. For convenience we impose periodic boundary conditions, e.g. $f(\mathbf{r} + N_i \mathbf{a}_i) = f(\mathbf{r})$, which however play no role in the thermodynamic limit $N \rightarrow \infty$. The Fourier transform of the spin operators and the exchange coupling is given by

$$\mathbf{S}(\mathbf{k}) = \sum_i e^{i\mathbf{k}\cdot\mathbf{r}_i} \mathbf{S}_i, \quad (2.5)$$

$$J_{\Lambda}(\mathbf{k}) = \sum_i e^{i\mathbf{k}\cdot\mathbf{r}_i} J_{\Lambda}(\mathbf{r}_i), \quad (2.6)$$

whereas the inverse Fourier transformation to a quantity f_i on the Bravais lattice reads

$$f_i = \int_{\mathbf{k}} f(\mathbf{k}) e^{-i\mathbf{k}\cdot\mathbf{r}_i}. \quad (2.7)$$

Here $\int_{\mathbf{k}} \equiv \frac{1}{N} \sum_{\mathbf{k}}$ is a shorthand-notation and the momenta can be for instance discretized as $k_i = \frac{\pi n_i}{N_i}$, $i = 1 \dots d$, $n_i = -N_i/2 + 1 \dots N_i/2$, which in the limit $N_i \rightarrow \infty$ implies that $\frac{1}{N} \sum_{\mathbf{k}}$ are replaced by integral averages over the first Brillouin Zone, $\frac{1}{V_{BZ}} \int d^d k$. The Hamiltonian can then be written as

$$\mathcal{J}_{\Lambda} = \frac{1}{2} \sum_{\mathbf{k}} J_{\Lambda}(\mathbf{k}) \mathbf{S}(\mathbf{k}) \cdot \mathbf{S}(-\mathbf{k}). \quad (2.8)$$

Note that orthogonality relations for the lattice transforms came in handy here, namely $\sum_{\mathbf{k}} e^{i\mathbf{k}\cdot(\mathbf{r}_i - \mathbf{r}_j)} = N \delta_{i,j}$ and $\sum_i e^{i(\mathbf{k} + \mathbf{k}')\cdot\mathbf{r}_i} = N \delta_{\mathbf{k} + \mathbf{k}', 0}$. In our further studies we will consider solely the zero-field limit $H = 0$, so that $\mathcal{H}_0 = 0$, and assume that we are in the symmetric phase, thus excluding a priori a finite vacuum expectation value, i.e. $\langle S_i^z \rangle = 0$.

The flowing generating functional of connected time-ordered spin correlation functions is given by [1]

$$\mathcal{G}_{\Lambda}[\mathbf{h}] = \ln \text{Tr} \left(\mathcal{T} \left(e^{(h,S) - \int_0^{\beta} d\tau \mathcal{J}_{\Lambda}(\tau)} \right) \right), \quad (2.9)$$

where (h, S) is a short-hand notation for

$$(h, S) = \int_0^{\beta} d\tau \sum_i \mathbf{h}_i(\tau) \cdot \mathbf{S}_i(\tau) = \int_0^{\beta} d\tau \sum_{i,\alpha} h_i^{\alpha}(\tau) S_i^{\alpha}(\tau), \quad (2.10)$$

with space-time dependent magnetic sources $\mathbf{h}_i(\tau)$ and the interaction part

$$\mathcal{J}_{\Lambda}(\tau) = \frac{1}{2} \sum_{i,j} J_{ij}^{\Lambda} \sum_{\alpha} S_i^{\alpha}(\tau) S_j^{\alpha}(\tau). \quad (2.11)$$

The imaginary time-evolution of the spin operators is given by the interaction picture

$$S_i^{\alpha}(\tau) = e^{\mathcal{H}_0 \tau} S_i^{\alpha} e^{-\mathcal{H}_0 \tau}. \quad (2.12)$$

Note that for $\mathcal{H}_0 = 0$, as considered by us, the exponentials $e^{\pm\mathcal{H}_0\tau}$ can be only set to zero, after the time-ordering is explicitly evaluated, meaning that one has to retain them under the \mathcal{T} -symbol. The time-ordered exponential has to be understood as

$$\mathcal{T}(e^{\int_0^\beta d\tau A(\tau)}) = 1 + \sum_{n=1}^{\infty} \frac{1}{n!} \int_0^\beta d\tau_1 \dots \int_0^\beta d\tau_n \mathcal{T}(A(\tau_1) \dots A(\tau_n)). \quad (2.13)$$

The physical limit of the model is recovered by setting $\mathbf{h} = \mathbf{0}$, where

$$\mathcal{G}_\Lambda[\mathbf{0}] = \ln Z_\Lambda = -\beta F_\Lambda. \quad (2.14)$$

By repeated functional differentiation of $G_\Lambda[\mathbf{h}]$ with respect to the magnetic sources and setting afterwards $\mathbf{h} = \mathbf{0}$, one can generate physical connected correlation functions to arbitrary order, namely

$$G_{\Lambda, X_1, \dots, X_n}^{\alpha_1, \dots, \alpha_n} = \langle \mathcal{T}(S_{X_1}^{\alpha_1} \dots S_{X_n}^{\alpha_n}) \rangle_{\Lambda, conn} = \left(\frac{\delta^n \mathcal{G}_\Lambda}{\delta h_{X_1}^{\alpha_1} \dots \delta h_{X_n}^{\alpha_n}} \right)_{\mathbf{h}=\mathbf{0}}, \quad (2.15)$$

where we introduced space-time labels $X_i = (\mathbf{r}_i, \tau_i)$. In accordance with the homogeneity of the system for vanishing sources, one can reduce them to functions of $n - 1$ space-time arguments, with the n -th argument set to a reference point $X = 0$

$$G_{\Lambda, X_1, \dots, X_n}^{\alpha_1, \dots, \alpha_n} = G_{\Lambda, X_1 - X_n, \dots, 0}^{\alpha_1, \dots, \alpha_n}. \quad (2.16)$$

The Fourier transform to the $K = (\mathbf{k}, i\omega)$ -representation acquires therefore an energy-momentum-conserving factor, e.g.

$$G_{\Lambda, K_1, \dots, K_n}^{\alpha_1, \dots, \alpha_n} = \delta_{\sum_{i=1}^n K_i, 0} \int_{X_1} (\dots) \int_{X_{n-1}} \prod_{j=1}^{n-1} e^{i\mathbf{k}_j \cdot \mathbf{r}_j + i\omega_j \tau_j} G_{\Lambda, X_1, \dots, 0}^{\alpha_1, \dots, \alpha_n}. \quad (2.17)$$

where the short-hand notation $\int_X = \sum_i \int_0^\beta d\tau$ was introduced. In particular the two-point function is diagonal $\sim \delta_{K, -K}$ in K -space. Note that these quantities can then be also written as functional derivatives with respect to properly defined sources h_K in the Fourier domain. The inverse relation is

$$G_{\Lambda, X_1, \dots, 0}^{\alpha_1, \dots, \alpha_n} = \int_{K_1} (\dots) \int_{K_{n-1}} \prod_{j=1}^{n-1} e^{-i\mathbf{k}_j \cdot \mathbf{r}_j - i\omega_j \tau_j} G_{\Lambda, K_1, \dots, K_{n-1}, -\sum_{i=1}^{n-1} K_i}^{\alpha_1, \dots, \alpha_n}, \quad (2.18)$$

where we introduced $\int_K = \frac{1}{\beta N} \sum_k \sum_\omega$. The connected expressions $\langle \dots \rangle_{conn}$ are cumulants and therefore include products of lower order expectation values, which is a result of taking the derivative of the logarithm and not Z_Λ itself. For uncorrelated degrees of freedom the multi-spin expectation values factorize, e.g. $\langle \mathcal{T}(S^\alpha S^\beta) \rangle \approx \langle \mathcal{T}(S^\alpha) \rangle \langle \mathcal{T}(S^\beta) \rangle$ such that the corresponding connected correlations will be zero. In fact one can cast the latter in the form $\langle \mathcal{T} \prod_i (S_i - \langle \mathcal{T} S_i \rangle) \rangle$, being therefore thermal averages of products of deviations from the one-point expectation value. As an example the two-point function is given by the following 'variance'

$$\begin{aligned} G_{\Lambda, X_1, X_2}^{\alpha_1, \alpha_2} &= \langle \mathcal{T}(S_{\mathbf{r}_1}^{\alpha_1}(\tau_1) S_{\mathbf{r}_2}^{\alpha_2}(\tau_2)) \rangle - \langle \mathcal{T} S_{\mathbf{r}_1}^{\alpha_1}(\tau_1) \rangle \langle \mathcal{T} S_{\mathbf{r}_2}^{\alpha_2}(\tau_2) \rangle \\ &= \langle \mathcal{T}(S_{\mathbf{r}_1}^{\alpha_1}(\tau_1) - \langle \mathcal{T} S_{\mathbf{r}_1}^{\alpha_1}(\tau_1) \rangle) (S_{\mathbf{r}_2}^{\alpha_2}(\tau_2) - \langle \mathcal{T} S_{\mathbf{r}_2}^{\alpha_2}(\tau_2) \rangle) \rangle, \end{aligned} \quad (2.19)$$

where time-ordered expectation values in the interaction picture are calculated with the help of

$$\begin{aligned} \mathcal{T}(B_1(\tau'_1)\dots B_m(\tau'_m)e^{\int_0^\beta d\tau A(\tau)}) &= \mathcal{T}(B_1(\tau'_1)\dots B_m(\tau'_m)) \\ &+ \sum_{n=1}^{\infty} \frac{1}{n!} \int_0^\beta d\tau_1 \dots \int_0^\beta d\tau_n \mathcal{T}(B_1(\tau'_1)\dots B_m(\tau'_m)A(\tau_1)\dots A(\tau_n)). \end{aligned} \quad (2.20)$$

The notion of a functional derivative is thus also justified, because all operators commute under the time-ordering symbol \mathcal{T} . Note that above T_c the physical one-point functions are zero, so that the two-point function is just the two-spin expectation value. This also means that the two-point function is equivalent to the Matsubara function $G_{\Lambda,ij}(\tau)$ introduced in section 1.3.3. Assuming an analytic-in- \mathbf{h} shape of $\mathcal{G}_\Lambda[\mathbf{h}]$, in particular around $\mathbf{h} = \mathbf{0}$, the physical connected correlation functions are also the Taylor coefficients in a functional series expansion of $\mathcal{G}_\Lambda[\mathbf{h}]$ in powers of h , which up to quadratic order reads

$$\mathcal{G}_\Lambda[\mathbf{h}] = -\beta F_\Lambda + \frac{1}{2} \int_X \int_{X'} G_{\Lambda, X-X', 0} \mathbf{h}_X \cdot \mathbf{h}_{X'} + \mathcal{O}(h^3). \quad (2.21)$$

Here we used that $G_{\Lambda, X-X', 0}^{\alpha_1, \alpha_2} = \delta_{\alpha_1, \alpha_2} G_{\Lambda, X-X', 0}$ for an intact symmetry with respect to rotations around an arbitrarily chosen axis.

Differentiating $e^{\mathcal{G}_\Lambda[\mathbf{h}]}$ with respect to Λ yields an exact flow equation for $\mathcal{G}_\Lambda[\mathbf{h}]$

$$\partial_\Lambda \mathcal{G}_\Lambda[\mathbf{h}] = -\frac{1}{2} \int_0^\beta d\tau \sum_{i,j} \partial_\Lambda R_{ij}^\Lambda \sum_\alpha \left[\frac{\delta^2 \mathcal{G}_\Lambda[\mathbf{h}]}{\delta h_i^\alpha(\tau) \delta h_j^\alpha(\tau)} + \frac{\delta \mathcal{G}_\Lambda[\mathbf{h}]}{\delta h_i^\alpha(\tau)} \frac{\delta \mathcal{G}_\Lambda[\mathbf{h}]}{\delta h_j^\alpha(\tau)} \right]. \quad (2.22)$$

This equation can be cast into a more compact form, using a supermatrix notation. Defining

$$\mathbf{G}_\Lambda^{(2)}[\mathbf{h}] = \left[\frac{\delta}{\delta \mathbf{h}} \otimes \frac{\delta}{\delta \mathbf{h}} \right] \mathcal{G}_\Lambda[\mathbf{h}], \quad (2.23)$$

and

$$[\mathbf{R}_\Lambda]_{X, X'}^{\alpha, \alpha'} = \delta_{\alpha, \alpha'} \delta(\tau - \tau') R_{ij}^\Lambda, \quad (2.24)$$

we can then write

$$\partial_\Lambda \mathcal{G}_\Lambda[\mathbf{h}] = -\frac{1}{2} \text{Tr} \left(\partial_\Lambda \mathbf{R}_\Lambda \mathbf{G}_\Lambda^{(2)}[\mathbf{h}] \right) - \frac{1}{2} \left(\frac{\delta \mathcal{G}_\Lambda}{\delta \mathbf{h}}, \partial_\Lambda \mathbf{R}_\Lambda \frac{\delta \mathcal{G}_\Lambda}{\delta \mathbf{h}} \right), \quad (2.25)$$

where now $\text{Tr}(\dots) = \sum_\alpha \int_X (\dots)$ denotes the sum over all field indices and (A, B) is a scalar product as in the magnetic source-term (2.10). Inserting for instance the functional Taylor expression of $\mathcal{G}_\Lambda[\mathbf{h}]$ on both sides of (2.25) and comparing properly symmetrized coefficients of monomials in \mathbf{h} one arrives at an infinite hierarchy of coupled integro-differential equations for the connected spin correlation functions $G_\Lambda^{(n)}$. Choosing the K -representation for the trace and scalar products the term $\sim \mathbf{G}_\Lambda^{(2)}$ in Eq. (2.25) contains only one sum $\int_K(\dots)$, while the bilinear contribution is purely local in momenta and frequencies. Note that in a field-theoretical language $\mathbf{G}_\Lambda^{(2)}$ is often known as the propagator [3].

A conceptually simple application of the flow hierarchy is to iterate it in power of βJ_Λ , thus reproducing the exact high-temperature expansion of any imaginary-time correlation function. In practice, the calculation of higher order terms becomes quite cumbersome,

due to a strong growth of the number of contributing diagrams and, being an asymptotic series in βJ_Λ , it is even then of little use beyond the limit $|\beta J_\Lambda| \ll 1$, without some prudent extrapolation scheme. Hence we have to find a way of resumming infinite orders in J in order to obtain nonperturbative results. While one can achieve this by truncating the hierarchy of flow equations, it is not really recommended, especially due to the tree-level contributions implied by the scalar product in (2.25). In fact the presence of the latter leads us to consider the Legendre transform of $\mathcal{G}_\Lambda[\mathbf{h}]$, which is given by [2, 3]

$$\mathcal{L}_\Lambda[\mathbf{m}] = (\mathbf{m}, \mathbf{h}) - \mathcal{G}_\Lambda[\mathbf{h}], \quad (2.26)$$

where we introduced the magnetization field, a one-point expectation value in the presence of magnetic sources

$$\mathbf{m} = \frac{\delta \mathcal{G}_\Lambda[\mathbf{h}]}{\delta \mathbf{h}} = \langle \mathcal{T}(\mathbf{S}) \rangle. \quad (2.27)$$

Conversely, the magnetic sources are the first functional derivatives of the Legendre transform

$$\mathbf{h} = \frac{\delta \mathcal{L}_\Lambda[\mathbf{m}]}{\delta \mathbf{m}}. \quad (2.28)$$

Furthermore one can infer from writing by means of the chain rule $\frac{\delta \mathbf{h}}{\delta \mathbf{h}} = \left(\frac{\delta \mathbf{h}}{\delta \mathbf{m}}, \frac{\delta \mathbf{m}}{\delta \mathbf{h}} \right) = \mathbf{1}$ that the second derivatives are related to each other via [3]

$$\mathbf{L}_\Lambda^{(2)}[\mathbf{m}] = [\mathbf{G}_\Lambda^{(2)}[\mathbf{h}]]^{-1}, \quad (2.29)$$

where

$$\mathbf{L}_\Lambda^{(2)}[\mathbf{m}] = \left[\frac{\delta}{\delta \mathbf{m}} \otimes \frac{\delta}{\delta \mathbf{m}} \right] \mathcal{L}_\Lambda[\mathbf{m}]. \quad (2.30)$$

Relation (2.29) already hints at a major issue, which will be later elucidated on. Note that $\mathcal{L}_\Lambda[\mathbf{m}]$ corresponds to the Gibbs' free energy $G(T, M)$ in thermodynamics, where one transforms from H to M [3]. Differentiating \mathcal{L}_Λ with respect to the flow parameter at constant \mathbf{m} we obtain

$$\partial_\Lambda \mathcal{L}_\Lambda[\mathbf{m}] = \frac{1}{2} \text{Tr} \left(\partial_\Lambda \mathbf{R}_\Lambda [\mathbf{L}_\Lambda^{(2)}[\mathbf{m}]]^{-1} \right) + \frac{1}{2} (\mathbf{m}, \partial_\Lambda \mathbf{R}_\Lambda \mathbf{m}), \quad (2.31)$$

where a chain rule $\partial_\Lambda \mathcal{G}_\Lambda[\mathbf{h}] = \partial_\Lambda \mathcal{G}_\Lambda[\mathbf{h}]_{\mathbf{h}=\mathbf{h}_\Lambda} + (\delta \mathbf{h} \mathcal{G}_\Lambda, \partial_\Lambda \mathbf{h}_\Lambda)$ was used, since the source field is now Λ -dependent, leading to the cancellation of terms $\sim (\mathbf{m}, \partial_\Lambda \mathbf{h})$. Introducing the subtracted Legendre transform

$$\Gamma_\Lambda[\mathbf{m}] = \mathcal{L}_\Lambda[\mathbf{m}] - \frac{1}{2} (\mathbf{m}, \mathbf{J}_\Lambda \mathbf{m}), \quad (2.32)$$

so that $\Gamma_\Lambda^{(2)}[\mathbf{m}] + \mathbf{R}_\Lambda = [\mathbf{G}_\Lambda^{(2)}[\mathbf{h}]]^{-1}$ we can also eliminate the, now admittedly trivial, tree-contribution to the flow equation, leading to

$$\partial_\Lambda \Gamma_\Lambda[\mathbf{m}] = \frac{1}{2} \text{Tr} \left(\partial_\Lambda \mathbf{R}_\Lambda [\Gamma_\Lambda^{(2)}[\mathbf{m}] + \mathbf{R}_\Lambda]^{-1} \right), \quad (2.33)$$

which is the Wetterich equation for $\Gamma_\Lambda[\mathbf{m}]$ [1, 2, 3, 4]. The functional, defined in Eq. (2.32), is also known as the 1-particle irreducible (1-PI) effective average action, because its functional derivatives at the physical configuration in a paramagnet, $\mathbf{m} = 0$, are the 1-PI vertex functions $\Gamma_\Lambda^{(n)}$. These are comprised of all diagrams which cannot be split into a product

of lower order diagrams by cutting a single $\mathbf{G}_\Lambda^{(2)}$ -line [2, 3]. Hence the flow equation (2.33) features only terms with at least one loop integration, as indicated by the trace, whereas purely local tree contributions like in the flow of the correlation functions $G_\Lambda^{(n)}$ are now absent. Analogous to \mathcal{G}_Λ an infinite hierarchy of equations for the 1-PI vertices $\Gamma_\Lambda^{(n)}$ can be derived from the Wetterich equation by either comparing properly symmetrized coefficients of monomials in \mathbf{m} or successively differentiating the flow equation (2.33) with respect to \mathbf{m} and evaluating these derivatives at $\mathbf{m} = \mathbf{0}$ [1, 3, 4]. The relation between $\Gamma_\Lambda^{(n)}$ and $G_\Lambda^{(n)}$, also known as tree expansion, is obtained by differentiating Eq. (2.29), which also allows one to determine the initial condition of the vertices. Note that we have chosen \mathbf{J}_Λ instead of $\mathbf{R}_\Lambda = \mathbf{J}_\Lambda - \mathbf{J}$ in order to avoid a finite magnetization at the initial scale which is implied by the minimization condition for the flowing effective average action [2]

$$\left(\frac{\delta\Gamma_\Lambda}{\delta\mathbf{m}}\right)_{\mathbf{m}=\mathbf{M}_\Lambda} = \mathbf{h}_\Lambda - \mathbf{R}_\Lambda\mathbf{M}_\Lambda = 0, \quad (2.34)$$

and is equivalent to demanding that the one-point vertex $\Gamma_\Lambda^{(1)}$ is zero for arbitrary Λ . One sees now that for $\mathbf{R}_{\Lambda_0} = \mathbf{J}$, a finite source field $h_0 = -J(\mathbf{Q})M_Q$ is generated, which corresponds to the mean-field solution for the magnetization and therefore symmetry breaking below T_c^{MF} , thus serving as an additional complication. Choosing \mathbf{J}_Λ one avoids this issue, and can, by assuming $\mathbf{M}_\Lambda = \mathbf{0} \rightarrow \mathbf{h}_\Lambda = \mathbf{0}$, stay in the symmetric phase, as long as there are no singularities in the static susceptibility $G_\Lambda(\mathbf{k})$.

Unfortunately the flow equations for $\Gamma_\Lambda^{(n)}$ cannot be straightforwardly used, at least if one chooses simple initial conditions for the flow. Consider the limit of decoupled spins, $\mathcal{H}_{\Lambda_0} = 0$: Here we obtain for the connected two-point function of one magnetic moment

$$G(\tau - \tau') = \langle \mathcal{T}(S^\alpha(\tau - \tau')S^\alpha(0)) \rangle = \langle S^\alpha S^\alpha \rangle = \frac{\langle (\mathbf{S})^2 \rangle}{3} = \frac{S(S+1)}{3}, \quad (2.35)$$

due to $\partial_\tau \mathbf{S}(\tau) \sim [\mathcal{H}, \mathbf{S}(\tau)] = 0$. Hence the Fourier transform to frequency space is

$$G(\omega) = \int_0^\beta d\tau G(\tau) = \beta \delta_{\omega,0} \frac{S(S+1)}{3}. \quad (2.36)$$

As a consequence, the inverse of $G(\omega)$ which determines the two-point vertex $\Gamma^{(2)}(\omega)$ according to (2.29) is singular for $\omega \neq 0$. From this we conclude that $\Gamma_\Lambda[\mathbf{m}]$ is a non-analytic functional at the initial scale and does not have a proper series expansion around $\mathbf{m} = \mathbf{0}$. The fundamental issue here, leading to a non-invertible propagator, are conservation laws for any operator corresponding to one power of the field, here \mathbf{m} . For instance, even by turning on an external magnetic field, the component of the spin parallel to the field is conserved, so that longitudinal correlations $G^{zz}(\omega)$ still do not acquire a time dependence on the local level [7]. Consequently we have to search for other parametrizations of the connected correlation functions, where the respective vertices are well-defined for initial configurations like the aforementioned isolated spins. In the next section such a workaround is described. Note that this issue does not occur on the static sector. Hence in the absence of any equilibrium dynamics, which is the case for classical spin models with $S \rightarrow \infty$, $JS^2 = \text{const.}$, since $[S^\alpha, S^\gamma]/S^2 \sim S^{-1} \rightarrow 0$, one can reliably stay within the 1-PI framework.

2.2.2 1-JI (VLP) formalism

An alternative to the 1-PI approach is not to start with pure connected correlation function, but their amputated pendants, as first introduced by Krieg and Kopietz. The corresponding

generating functional is defined as follows [1, 2]

$$\mathcal{F}_\Lambda[\mathbf{s}] = \mathcal{G}_\Lambda[-\mathbf{J}_\Lambda \mathbf{s}] - \frac{1}{2}(\mathbf{s}, \mathbf{J}_\Lambda \mathbf{s}). \quad (2.37)$$

The amputation is performed with respect to \mathbf{J}_Λ , whose components are defined by

$$[\mathbf{J}_\Lambda]_{X, X'}^{\alpha, \alpha'} = \delta_{\alpha, \alpha'} \delta(\tau - \tau') J_{ij}^\Lambda. \quad (2.38)$$

Its consequences are relatively easy to tackle: The amputated correlation functions are the functional derivatives with respect to the new source \mathbf{s} , evaluated at $\mathbf{s} = \mathbf{0}$. Hence any $F_\Lambda^{(n)}$, with $n \neq 2$, is simply given by the corresponding $G_\Lambda^{(n)}$ which is multiplied by factors of $-\mathbf{J}_\Lambda$, i.e.

$$F_{\Lambda, X_1, \dots, X_n}^{\alpha_1, \dots, \alpha_n} = \left(\frac{\delta^n \mathcal{F}_\Lambda}{\delta h_{X_1}^{\alpha_1} \dots \delta h_{X_n}^{\alpha_n}} \right)_{\mathbf{s}=\mathbf{0}} = (-1)^n \sum_{j_1, \dots, j_n} (J_{i_1, j_1}^\Lambda \dots J_{i_n, j_n}^\Lambda) \left(\frac{\delta^n \mathcal{G}_\Lambda}{\delta h_{(j_1, \tau_1)}^{\alpha_1} \dots \delta h_{(j_n, \tau_n)}^{\alpha_n}} \right)_{\mathbf{h}=\mathbf{0}}, \quad (2.39)$$

while the two-point function acquires an additional term

$$\mathbf{F}_\Lambda = \mathbf{F}_\Lambda^{(2)}[\mathbf{s} = \mathbf{0}] = -\mathbf{J}_\Lambda + \mathbf{J}_\Lambda \mathbf{G}_\Lambda \mathbf{J}_\Lambda, \quad (2.40)$$

and is commonly referred to as effective interaction [1, 5]. Note that in the past $\mathcal{F}_\Lambda[\mathbf{s}]$ was also represented via a path integral $\int \mathcal{D}[\varphi] e^{-S[\varphi] + \frac{1}{2}(\varphi, \mathbf{J}_\Lambda^{-1} \varphi) + (s, \varphi)}$, running over a bosonic auxiliary field φ , which makes use of the quadratic-in- \mathbf{S} form of \mathcal{H} [1, 2]. It is introduced by means of a Hubbard-Stratonovich transformation i.e. an inverse Gaussian integration

$$\mathcal{T} \exp \left(- \frac{(S + s, \mathbf{A}(S + s))}{2} \right) \sim \int \mathcal{D}[\varphi] \exp \left(- \frac{(\varphi, \mathbf{A}^{-1} \varphi)}{2} + (s, \varphi) \right) \mathcal{T} \left(\exp(S, \varphi) \right), \quad (2.41)$$

of the time ordered exponential $\mathcal{T} e^{(\dots)}$ in the trace over the Hilbert space. Note that $\exp(S, \varphi)$ has to be kept under the trace and time-ordering symbol, since S is operator-valued. As a result one arrives at an interacting action $S[\varphi]$ that is up to a sign given by the generating functional $\mathcal{G}_0[\varphi]$ of connected correlations for an isolated spin [1, 2]. The exchange coupling assumes then the role of the Gaussian propagator for the new field φ , justifying to call the above procedure amputation as in the context of field-theoretical approaches [3]. The amputated correlation functions $F_\Lambda^{(n)}$ can then be identified with connected path-integral averages of products in φ [2]. Turning \mathbf{J}_Λ off via a deformation, amounts then to increasing the flowing mass of the φ -field, i.e. it becoming infinitely heavy for $\Lambda = \Lambda_0$. On the level of the φ -field the deformation of the interaction is thus analogous to the usual FRG procedure for bosons or fermions, where fluctuations are successively frozen out with increasing mass [3].

Taking the Λ -derivative of \mathcal{F}_Λ , we obtain with the help of the relation

$$\frac{\delta \mathcal{F}_\Lambda[\mathbf{s}]}{\delta \mathbf{s}} = -\mathbf{J}_\Lambda \left(\frac{\delta \mathcal{G}_\Lambda[\mathbf{h}]}{\delta \mathbf{h}} + \mathbf{s} \right), \quad (2.42)$$

its exact flow equation,

$$\partial_\Lambda \mathcal{F}_\Lambda[\mathbf{s}] = \frac{1}{2} \text{Tr} \left(\partial_\Lambda \mathbf{J}_\Lambda^{-1} \mathbf{F}_\Lambda^{(2)}[\mathbf{s}] \right) + \frac{1}{2} \left(\frac{\delta \mathcal{F}_\Lambda[\mathbf{s}]}{\delta \mathbf{s}}, \partial_\Lambda \mathbf{J}_\Lambda^{-1} \frac{\delta \mathcal{F}_\Lambda[\mathbf{s}]}{\delta \mathbf{s}} \right) + \frac{1}{2} \text{Tr}(\mathbf{J}_\Lambda \partial_\Lambda \mathbf{J}_\Lambda^{-1}), \quad (2.43)$$

which is also known as the Polchinski equation [3]. Its subtracted Legendre transform is then defined as

$$\Phi_\Lambda[\boldsymbol{\eta}] = (\boldsymbol{\eta}, \mathbf{s}) - \mathcal{F}_\Lambda[\mathbf{s}] + \frac{1}{2}(\boldsymbol{\eta}, \mathbf{J}_\Lambda^{-1}\boldsymbol{\eta}), \quad (2.44)$$

with the magnetic exchange field

$$\boldsymbol{\eta} = \frac{\delta \mathcal{F}_\Lambda[\mathbf{s}]}{\delta \mathbf{s}} = -\mathbf{J}_\Lambda \langle \mathcal{T} \mathcal{S} \rangle - \mathbf{J}_\Lambda \mathbf{s}, \quad (2.45)$$

and conversely

$$\mathbf{s} = \frac{\delta \Phi}{\delta \boldsymbol{\eta}} - \mathbf{J}_\Lambda^{-1} \boldsymbol{\eta}. \quad (2.46)$$

This functional generates, in contrast to $\Gamma_\Lambda[\mathbf{m}_j]$, vertices that are irreducible with respect to cutting a single effective interaction line, $\mathbf{F}_\Lambda^{(2)}$. Its second derivative is, for instance,

$$\Phi_\Lambda^{(2)}[\boldsymbol{\eta}] = \mathbf{J}_\Lambda^{-1} + [\mathbf{F}_\Lambda^{(2)}[\mathbf{s}]]^{-1} = -[\mathbf{J}_\Lambda + [\mathbf{G}_\Lambda^{(2)}[\mathbf{h}]]^{-1}]^{-1}. \quad (2.47)$$

and conversely

$$\mathbf{G}_\Lambda^{(2)}[\mathbf{h}] = -\Phi_\Lambda^{(2)}[\boldsymbol{\eta}][\mathbf{1} - \mathbf{J}_\Lambda \Phi_\Lambda^{(2)}[\boldsymbol{\eta}]]^{-1}. \quad (2.48)$$

which has the structure of a Dyson, i.e. geometric series [18, 29], in $\mathbf{J}_\Lambda \Phi_\Lambda^{(2)}$, featuring infinitely many powers of \mathbf{J}_Λ . Relations between higher order vertices $\Phi_\Lambda^{(n)}$ and the connected correlation functions $G_\Lambda^{(n)}$ can be obtained by taking derivatives of Eq. (2.48) with respect to $\boldsymbol{\eta}$. Note that we have chosen $-\mathbf{J}_\Lambda^{-1}$ as the regulator matrix instead of $\mathbf{R}_\Lambda = \mathbf{J}^{-1} - \mathbf{J}_\Lambda^{-1}$, for the same reason as in the 1-PI average effective action, namely avoiding a finite magnetization at the initial scale, that is generated by the condition $\Phi_\Lambda^{(1)} = 0$. The flow equation of $\Phi_\Lambda[\boldsymbol{\eta}]$ reads [1, 2]

$$\partial_\Lambda \Phi_\Lambda[\boldsymbol{\eta}] = -\frac{1}{2} \text{Tr} \left(\partial_\Lambda \mathbf{J}_\Lambda^{-1} [\Phi_\Lambda^{(2)}[\boldsymbol{\eta}] - \mathbf{J}_\Lambda^{-1}]^{-1} \right) - \frac{1}{2} \text{Tr} (\mathbf{J}_\Lambda \partial_\Lambda \mathbf{J}_\Lambda^{-1}). \quad (2.49)$$

This equation has also the form of the Wetterich equation [2, 4]. The initial condition of the vertices $\Phi_{\Lambda_0}^{(n)}$ in the case of decoupled sites is simply given by the corresponding connected correlation functions $G_{\Lambda_0}^{(n)}$ of a single spin. This is easily seen on the level of the tree expansion because all diagrams that are proportional to two or more correlation functions of lower order vanish as $\mathcal{O}(J_\Lambda)$ for $J_\Lambda \rightarrow 0$, due to at least one power of \mathbf{F}_Λ [2]. Note that this is a consequence of the Legendre-transform $\Phi_\Lambda[\boldsymbol{\eta}]$ reducing to the aforementioned bare Hubbard-Stratonovich action for $\mathbf{J}_\Lambda \rightarrow 0$. Hence this functional is well-behaved even in the non-interacting limit, which was pathological for the 1-PI effective average action. Regarding the usefulness of this new functional we note that $\mathbf{F}_\Lambda = \mathcal{O}(J_\Lambda)$ allows to setup a high temperature expansion more efficiently than using $\mathcal{G}_\Lambda[\mathbf{h}]$. For once, there are no tree-level terms, implying an infinite resummation in J even in the simplest approximation $\Phi_\Lambda^{(n)} \approx \Phi_{\Lambda_0}^{(n)}$. Furthermore less contributions have to be taken into account at a given order, since diagrams containing a number of internal lines $\dot{F}_\Lambda, F_\Lambda$ which is larger than the order in βJ can be neglected. A far more interesting observation is the fact that $\Phi_\Lambda^{(n)} \approx \Phi_{\Lambda_0}^{(n)}$ amounts to a solution of the infinite hierarchy of equations $G_\Lambda^{(n)}$ in the absence of terms containing at least one closed loop integration. Therefore, if integrals over momentum, or sums over frequencies, are associated with a small parameter, the hierarchy of flow

equations can be iterated in \int_K to set up an expansion of $\Phi_\Lambda^{(n)}$ in powers of the parameter [1, 2]. Such a small parameter may be an inverse interaction range, if the exchange coupling is sufficiently long-ranged, or, similarly, an inverse coordination number, for instance on higher-dimensional lattices, $d \gg 1$. This FRG approach is thus equivalent to the spin-diagrammatic method, set up by Vaks *et al.* [5, 6], although less cumbersome, since it uses the relatively straightforward language of the Wetterich equation, instead of relying on their complicated rules.

The above observations make a great case for employing this framework in situations where the presence of a small quantity, associated with loop integrals, enables a controlled expansion in powers of it. On the other hand, if such parameters are absent, one has to rely on less controlled approximations when truncating the hierarchy of flow equations. Experience shows then that it performs rather poorly whenever it can be benchmarked against a 1-PI approach or established methods. For instance, Vaks, Larkin and Pikin [5] found, that their expansion inevitably breaks down in the critical region, as can be expected from the large range of correlations. From this alone one anticipates that simple one-loop equations for, e.g., the static two and four-point vertices are inferior to their 1-PI pendants [2, 3]. Krieg and Kopietz [1, 2] compared explicitly in the case of classical Ising and Heisenberg models the results of inserting a d^{-1} -expansion for $\Phi^{(2)}(\mathbf{k})$ and $\Gamma^{(2)}(\mathbf{k})$ into the static static susceptibility $G(\mathbf{k})$ and found the latter choice to be always superior to the VLP parametrization. It is likely that many problems in the study of static quantities within simple approximation schemes can be traced back to $\Phi_\Lambda^{(2)}$ appearing also in the numerator of $G_\Lambda(\mathbf{k})$, see Eq. (2.48), as opposed to the 1-PI self-energy, which is the negative of its inverse.

2.3 Static-dynamic hybrid functional

The points made in the previous sections suggest that one has to seek for alternatives to the pure interaction-irreducible approach. Fortunately we found that the static sector can and should be treated as 1-PI with no intricacies arising from an ill-defined initial condition. On the other hand, this is not the case for anything involving dynamic fluctuations, whose existence is implied by the non-trivial commutation relations (1.9) between spin operators. Hence a hybrid parametrization, with the quantum sector treated in a similar manner to VLP, as 1-interaction irreducible, is a prudent choice. Note that such an approach will always reduce to the pure 1-PI framework in the classical limit, $S \rightarrow \infty$.

2.3.1 Amputation with respect to bare coupling

We begin with a straightforward hybrid formulation, which runs along similar lines to a previous hybrid approach, albeit constructed in an entirely different context, the symmetry-broken phase [2, 7]. Appropriate to that configuration one distinguishes between transverse and longitudinal spin fluctuations, where the former are treated as 1-PI while the latter are amputated in the same manner as by Krieg and Kopietz, with respect to the flowing coupling \mathbf{J}_Λ [2, 7]. Afterwards we argue that in our case applying the same procedure to the dynamic sector, is not necessarily the most convenient one. Thus adjustments to the 'naive' implementation will be made, leading to a modified approach.

The starting point of the hybrid formalism, is the auxiliary functional, defined as,

$$\mathcal{A}_\Lambda[s] = \mathcal{G}_\Lambda[\mathbf{h}^c, \mathbf{h}^q = -\mathbf{J}_\Lambda \mathbf{s}^q] - \frac{1}{2}(\mathbf{s}^q, \mathbf{J}_\Lambda \mathbf{s}^q). \quad (2.50)$$

Here we introduced the following decomposition of the magnetic sources in terms of static (classical) and dynamic (quantum) components

$$\mathbf{h}_{i,\omega} = \mathbf{h}_i^c \beta \delta_{\omega,0} + \mathbf{h}_{i,\omega}^q (1 - \delta_{\omega,0}) \rightarrow \mathbf{h}_i(\tau) = \mathbf{h}_i^c + T \sum_{\omega \neq 0} e^{i\omega\tau} \mathbf{h}_{i,\omega}^q, \quad (2.51)$$

and expressed \mathbf{h}^q via the magnetization sources \mathbf{s}^q . Its functional derivatives are partially amputated on the quantum sector, i.e. all arguments at $\omega \neq 0$ imply a multiplication with $-\mathbf{J}_\Lambda$. In particular the two-point function at vanishing sources are in momentum-energy representation given by

$$A_\Lambda^{(2)}(\mathbf{k}, 0) = G_\Lambda(\mathbf{k}), \quad (2.52)$$

$$A_\Lambda^{(2)}(\mathbf{k}, i\omega \neq 0) = F_\Lambda(\mathbf{k}, i\omega) = -J_\Lambda(\mathbf{k}) + (J_\Lambda(\mathbf{k}))^2 G_\Lambda(\mathbf{k}, i\omega). \quad (2.53)$$

In general all purely static quantities are just the corresponding connected spin correlation functions. Introducing the regulator as

$$\mathbf{R}_\Lambda = \begin{pmatrix} \mathbf{R}_\Lambda^c & 0 \\ 0 & \mathbf{R}_\Lambda^q \end{pmatrix}, \quad (2.54)$$

$$\mathbf{R}_\Lambda^c = \mathbf{J}_\Lambda \rightarrow [\mathbf{R}_\Lambda^c]^{\alpha\alpha'}(K, K') = \delta_{K+K',0} \delta_{\alpha,\alpha'} J_\Lambda(\mathbf{k}), \quad (2.55)$$

$$\mathbf{R}_\Lambda^q = -\mathbf{J}_\Lambda^{-1} \rightarrow [\mathbf{R}_\Lambda^q]^{\alpha\alpha'}(K, K') = -\delta_{K+K',0} \delta_{\alpha,\alpha'} J_\Lambda^{-1}(\mathbf{k}), \quad (2.56)$$

we can write the flow equation satisfied by \mathcal{A}_Λ as

$$\begin{aligned} \partial_\Lambda \mathcal{A}_\Lambda[\mathbf{h}^c, \mathbf{s}^q] &= -\frac{1}{2} \text{Tr} \left(\partial_\Lambda \mathbf{R}_\Lambda \mathbf{A}_\Lambda^{(2)}[\mathbf{h}^c, \mathbf{s}^q] \right) - \frac{1}{2} \left(\frac{\delta \mathcal{A}_\Lambda}{\delta \mathbf{h}^c}, \partial_\Lambda \mathbf{R}_\Lambda \frac{\delta \mathcal{A}_\Lambda}{\delta \mathbf{h}^c} \right)_{\omega=0} \\ &\quad - \frac{1}{2} \left(\frac{\delta \mathcal{A}_\Lambda}{\delta \mathbf{s}^q}, \partial_\Lambda \mathbf{R}_\Lambda \frac{\delta \mathcal{A}_\Lambda}{\delta \mathbf{s}^q} \right)_{\omega \neq 0} - \frac{1}{2} \text{Tr}_{\omega \neq 0} (\mathbf{J}_\Lambda \partial_\Lambda \mathbf{R}_\Lambda^q), \end{aligned} \quad (2.57)$$

where the subscripts $\omega = 0$, $\omega \neq 0$ indicate that we take only the static or dynamic subspace when calculating the sum over field components. Introducing then the subtracted Legendre transform of \mathcal{A}_Λ , defined as

$$\Gamma_\Lambda[\mathbf{m}^c, \boldsymbol{\eta}^q] = (\mathbf{m}^c, \mathbf{h}^c) + (\boldsymbol{\eta}^q, \mathbf{s}^q) - \mathcal{A}_\Lambda[\mathbf{h}^c, \mathbf{s}^q] - \frac{1}{2} (\mathbf{m}^c, \mathbf{R}_\Lambda^c \mathbf{m}^c) - \frac{1}{2} (\boldsymbol{\eta}^q, \mathbf{R}_\Lambda^q \boldsymbol{\eta}^q), \quad (2.58)$$

with the classical magnetization

$$\mathbf{m}^c = \frac{\delta \mathcal{A}_\Lambda[\mathbf{h}^c, \mathbf{s}^q]}{\delta \mathbf{h}^c}, \quad (2.59)$$

and the quantum exchange field corrections

$$\boldsymbol{\eta}^q = \frac{\delta \mathcal{A}_\Lambda[\mathbf{h}^c, \mathbf{s}^q]}{\delta \mathbf{s}^q}, \quad (2.60)$$

one obtains then its version of the Wetterich equation

$$\partial_\Lambda \Gamma_\Lambda[\mathbf{m}^c, \boldsymbol{\eta}^q] = \frac{1}{2} \text{Tr} \left(\partial_\Lambda \mathbf{R}_\Lambda [\Gamma_\Lambda^{(2)}[\mathbf{m}^c, \boldsymbol{\eta}^q] + \mathbf{R}_\Lambda]^{-1} \right) + \frac{1}{2} \text{Tr}_{\omega \neq 0} (\mathbf{J}_\Lambda \partial_\Lambda \mathbf{R}_\Lambda^q). \quad (2.61)$$

Note that the hybrid functional $\Gamma_\Lambda[\mathbf{m}^c, \boldsymbol{\eta}^q]$ is related to $\Phi_\Lambda[\boldsymbol{\eta}]$ via a Legendre-Transformation from static exchange fields $\boldsymbol{\eta}^c$ to the classical magnetization \mathbf{m}^c . Introducing the static spin self energy as

$$\Sigma_\Lambda(\mathbf{k}) = \Gamma_\Lambda^{(2)}(\mathbf{k}), \quad (2.62)$$

and the dynamic polarization as

$$\Pi_\Lambda(\mathbf{k}, i\omega) = -\Phi_\Lambda^{(2)}(K), \quad (2.63)$$

we can write the corresponding two-point functions in K -space as

$$G_\Lambda(\mathbf{k}) = \frac{1}{\Sigma_\Lambda(\mathbf{k}) + J_\Lambda(\mathbf{k})}, \quad (2.64)$$

$$F_\Lambda(\mathbf{k}, i\omega) = -\frac{J_\Lambda(\mathbf{k})}{1 + \Pi_\Lambda(\mathbf{k}, i\omega)J_\Lambda(\mathbf{k})}. \quad (2.65)$$

The latter parametrization is reminiscent of the Random Phase Approximation, e.g. a screened Coloumb interaction in electronic systems [18, 29], which explains why one often calls $F(\mathbf{k}, i\omega)$ an effective interaction and $\Pi_\Lambda(\mathbf{k}, i\omega)$ a polarization. The Matsubara function can then be written as

$$\begin{aligned} G_\Lambda(\mathbf{k}, i\omega) &= \frac{1}{\Pi_\Lambda^{-1}(\mathbf{k}, i\omega) + J_\Lambda(\mathbf{k})} \\ &= \frac{\Pi_\Lambda(\mathbf{k}, i\omega)}{1 + \Pi_\Lambda(\mathbf{k}, i\omega)J_\Lambda(\mathbf{k})}. \end{aligned} \quad (2.66)$$

Assuming $J_{\Lambda_0} = 0$ the initial conditions are

$$G_{\Lambda_0}(\mathbf{k}, i\omega) = \beta b'_0 \delta_{\omega,0}, \quad (2.67)$$

$$\Sigma_{\Lambda_0}(\mathbf{k}) = (\beta b'_0)^{-1}, \quad (2.68)$$

$$\Pi_{\Lambda_0}(\mathbf{k}, i\omega) = 0. \quad (2.69)$$

For negligible quantum dynamics, one obtains, intuitively, the 1-PI effective average action $\Gamma_\Lambda[\mathbf{m}^c, \boldsymbol{\eta}^q] \approx \Gamma_\Lambda[\mathbf{m}^c, 0]$. On the level of vertices, i.e. the tree expansion, this is easily discerned from the lack of mixing between static and dynamic sector, which is a consequence of translational invariance in time and therefore conservation of frequency. Hence the above construction is warranted. Turning to the dynamic sector we will now explain why the chosen treatment of quantum fluctuations is still inconvenient. One starts by noting that due to the lack of dynamics the associated spectral density is simply a Dirac-delta

$$\text{Im}G_{\Lambda_0}(\mathbf{k}, \omega + i0^+) = b'_0 \delta(\omega). \quad (2.70)$$

This is trivial, given that the spin is conserved for $\mathcal{H} = 0$. Measuring a time-ordered correlation between two spin components at different times produces then always the same result. On the other hand in an interacting many-body system the individual spins acquire a non-trivial time evolution. Hence the correlations between corresponding modes in \mathbf{k} -space will also depend on time, implying a non-trivial frequency dependence of $G(\mathbf{k}, i\omega)$ and $G_{\text{ret}}(\mathbf{k}, \omega)$ for $\omega \neq 0$. The only exception is the $\mathbf{k} = 0$ -mode, i.e. the total spin $\sum_i \mathbf{S}_i$ which satisfies $\partial_t S(\mathbf{0}) \sim [S(\mathbf{0}), \mathcal{H}] = 0$, so that the Matsubara function fulfills

$$G_\Lambda(\mathbf{0}, i\omega \neq 0) = 0. \quad (2.71)$$

Hence, the uniform retarded susceptibility $G_{\text{ret}}(\mathbf{0}, \omega)$ of an interacting system is still a δ -distribution multiplied by the isothermal magnetic susceptibility $\chi = \partial_H M|_{H=0}$ [28]. Indeed one can show that the zero-frequency limit of $G_{\text{ret}}(\mathbf{k}, \omega)$, the isolated Kubo susceptibility,

is always $\leq \partial_H M_{H=0}$ [37] and in fact is even $\leq \chi_S = \partial_H M(H)_{S=\text{const.}} \leq \chi$, where χ_S is the adiabatic magnetic susceptibility [70, 71].

A question that still lingers: Is there a discontinuity, e.g a Dirac-delta, in the static limit $i\omega \rightarrow 0$ of susceptibilities for non-conserved operators, i.e. those at $\mathbf{k} \neq \mathbf{0}$? For instance Kwok *et al.* derived for the prefactor of the zero-frequency Dirac-peak in the difference between $G(\mathbf{k}, i\omega \rightarrow 0) - G(\mathbf{k}, 0)$, i.e. the *anomaly* the following expression [36, 71]

$$A(\mathbf{k}) = \frac{1}{2} \left[\lim_{t \rightarrow \infty} \langle S^z(\mathbf{k}, 0) S^z(-\mathbf{k}, t) \rangle + \lim_{t \rightarrow -\infty} \langle S^z(\mathbf{k}, 0) S^z(-\mathbf{k}, t) \rangle \right]. \quad (2.72)$$

For $\mathbf{k} = \mathbf{0}$ this is obviously non-zero, due to the absent time-dependence. On the other hand, the anomaly $A(\mathbf{k})$ vanishes, if the expectation value in (2.72) approaches zero for $t = \pm\infty$ [36]. The absence of an anomaly is thus consistent with the statement that degrees of freedom which are not constants of motion, should become uncorrelated for asymptotically large times. Considering the presumed dissipative dynamics at elevated temperatures, as laid out by hydrodynamics for a thermodynamic system, $N \rightarrow \infty$, it seems suggestive that at finite momentum $A(\mathbf{k})$ should vanish [35, 41]. An alternative and less handy expression for the anomaly reads [36],

$$A(\mathbf{k}) = \frac{1}{Z} \sum_{m,n} e^{-\beta E_n} |\langle n | S^\alpha(\mathbf{k}) | m \rangle|^2 \delta_{E_n, E_m}, \quad (2.73)$$

where one notes the 'same energy'-constraint $E_n = E_m$.

Moreover one can invoke the concept of *ergodicity* for thermodynamically large systems, $N \rightarrow \infty$ [28, 71]. Roughly speaking, one expects, if it holds, that starting from any initially prepared macrostate with fixed energy or temperature, the system relaxes for long enough times to a steady state, that is determined by the respective statistical ensemble (micro-canonical, canonical) [28]. More precisely, the time-average of an evolving observable S over an interval $[0, T_m]$, approaches in the limit $T_m \rightarrow \infty$ its statistical average $\langle S \rangle$ [28, 71], i.e. on the classical level $\langle S \rangle = \lim_{T_m \rightarrow \infty} \frac{1}{T_m} \int_0^{T_m} dt S(t)$, regardless of the initial value $S(0)$. A similar statement has to apply to two-point correlation functions $S(\mathbf{k}, t)$ or relaxation functions $\mathcal{R}(\mathbf{k}, t)$ (in the quantum case), which are also written in terms of a time-averaged quantity, where the averaging is performed over a second initial time t' contained in both observables [28]. From the fulfillment of ergodicity in the outlined sense one can deduce then that the long-time limit of the autocorrelation functions in Eq. (2.72) should converge to a product of one-point functions and thus go to zero for finite \mathbf{k} [28, 71]. A more recent analysis by Chiba *et al.* [72] suggests, that the different static spin susceptibilities are equal for $\mathbf{k} \neq \mathbf{0}$, if conditions similar to but also weaker than the *eigenstate thermalization hypothesis* (ETH) [73] are satisfied, with the latter being also concerned with ergodicity in the context of quantum systems. The imposed conditions in Ref. [72] require then that for $\mathbf{k} \neq \mathbf{0}$ off-diagonal terms of a narrow slice of states in the spectral representation of the aforementioned anomaly in Eq. (2.73) vanish sufficiently fast in the thermodynamic limit.

While there exists no rigorous proof that the presented conditions hold and the concept of ergodicity applies to the systems in question [28, 71], we assume that they are valid in the discussed sense. Thus the dynamic spin susceptibility at finite momentum $\mathbf{k} \neq \mathbf{0}$ is taken as continuous in the low-frequency limit, i.e.

$$G(\mathbf{k} \neq \mathbf{0}, i\omega \rightarrow 0) = G(\mathbf{k} \neq \mathbf{0}, i\omega = 0) = G(\mathbf{k}). \quad (2.74)$$

For the corresponding 1-line irreducible vertices it reads

$$\Pi(\mathbf{k}, i\omega \rightarrow 0) = \Sigma^{-1}(\mathbf{k}). \quad (2.75)$$

Hence the isolated Kubo susceptibility $G_{\text{ret}}(\mathbf{k}, 0)$ will be equivalent to the isothermal static susceptibility $G(\mathbf{k}, 0)$ [28] as introduced in Eq. (1.56). Note that $\text{Im}G_{\text{ret}}(\mathbf{k}, \omega)$ thus has to vanish for $\omega \rightarrow 0$. The restoration of continuity in $G(\mathbf{k}, i\omega)$ can be connected to a broadening of $\delta_{\omega,0}$ via the introduction of a finite width $\Delta(\mathbf{k})$ for $J \neq 0$ and $\mathbf{k} \neq 0$, i.e. [6, 36]

$$\delta_{\omega,0} \rightarrow \frac{\Delta(\mathbf{k})}{|\omega| + \Delta(\mathbf{k})}, \quad (2.76)$$

which in real frequencies translates to a Lorentzian

$$\delta(\omega) \rightarrow \frac{1}{\pi} \frac{\Delta(\mathbf{k})}{\omega^2 + \Delta(\mathbf{k})^2}. \quad (2.77)$$

Here the width $\Delta(\mathbf{k})$ may be for instance related to typical energy scales, i.e. relaxation rates, of dissipative processes in paramagnets, e.g. $\Delta(\mathbf{k}) \sim \mathcal{D}k^2$ in the case of spin diffusion [6]. Suppose now that we are explicitly interested in the dynamics of the system at arbitrary time scales. The continuity condition for Π_Λ (2.75) requires then meticulous fine-tuning for all $J_\Lambda \neq 0$. It does not work to enforce, via suitable vertex corrections or other auxiliary quantities, that their derivatives coincide

$$\partial_\Lambda \Sigma_\Lambda^{-1}(\mathbf{k}) = \partial_\Lambda \Pi_\Lambda(\mathbf{k}, i\omega \rightarrow 0), \quad (2.78)$$

because the initial conditions are different as a consequence of the discontinuity in an isolated spin. With this relatively straightforward ansatz already disqualified it is hard to discern another simple approximation for ensuring (2.75).

Another aspect, that hints at potential issues and appears at first less obvious, concerns the fact, that $J_\Lambda(\mathbf{k})$ is negative definite in a large region of the Brillouin Zone. For instance, in the case of an antiferromagnet where $J > 0$, the vicinity of the global minimum is also the region where $\Pi_\Lambda(\mathbf{k}, i\omega)$ is not suppressed in $|\mathbf{k} - \mathbf{Q}|$, in contrast to the origin, where it vanishes. Moreover the thermal frequencies $2\pi nT$ become successively smaller with decreasing temperature. Applying then a simple approximation for $\Pi_\Lambda(\mathbf{k}, i\omega)$, e.g. a high-frequency limit $\propto \omega^{-2}$, leads to a breakdown of the flow for sufficiently low temperatures, because $[1 + \Pi_\Lambda(\mathbf{k}, i\omega)J_\Lambda(\mathbf{k})]$ becomes negative, thus implying divergencies in $F_\Lambda(\mathbf{k}, i\omega)$. Hence a stable flow can be only guaranteed if $\Pi_\Lambda(\mathbf{k}, i\omega) < \Sigma_\Lambda^{-1}(\mathbf{k})$, otherwise one may hit singularities at finite frequencies and earlier than the order parameter susceptibility $G_\Lambda(\mathbf{Q})$, which is non-physical. This is consistent with the continuity condition (2.75): The zero-frequency limit also provides an upper bound for $\Pi_\Lambda(\mathbf{k}, i\omega)$, if one assumes $\Pi_\Lambda(\mathbf{k}, i\omega)$ to be a monotonous function of $|\omega|$. More importantly, the above discussion implies that continuity should always be ensured, even if one only wants to calculate thermodynamic properties and is not explicitly interested in dynamics.

2.3.2 Amputation with respect to the inverse propagator

To remedy the aforementioned issues we propose the following substitution: Instead of using J_Λ for the amputation, we take the inverse of the flowing static susceptibility $G_\Lambda(\mathbf{k})$. The new auxiliary functional is

$$\tilde{\mathcal{A}}_\Lambda[s] = \mathcal{G}_\Lambda[\mathbf{h}^c, \mathbf{h}^q = -\tilde{\mathbf{J}}_\Lambda \mathbf{s}^q] - \frac{1}{2}(\mathbf{s}^q, \tilde{\mathbf{J}}_\Lambda \mathbf{s}^q), \quad (2.79)$$

where the components of the subtracted coupling $\tilde{\mathbf{J}}_\Lambda$ on the quantum sector are defined as

$$[\tilde{\mathbf{J}}_\Lambda]_{K,K'}^{\alpha\alpha'} = G_\Lambda^{-1}(\mathbf{k})\delta_{K+K',0}\delta_{\alpha,\alpha'}. \quad (2.80)$$

Note that the dynamic effective interaction is then given by

$$\tilde{F}_\Lambda(\mathbf{k}, i\omega) = -G_\Lambda^{-1}(\mathbf{k}) + (G_\Lambda^{-1}(\mathbf{k}))^2 G_\Lambda(\mathbf{k}, i\omega), \quad (2.81)$$

and n -point correlations with $n \neq 2$ are multiplied by $-G_\Lambda^{-1}$ at finite frequency, while the purely static n -point functions are not affected by this change in the amputation. Since $\partial_\Lambda \tilde{J}_\Lambda(\mathbf{k}) \neq \partial_\Lambda J_\Lambda(\mathbf{k})$, additional terms are generated in the flow of $\tilde{\mathcal{A}}_\Lambda$, containing at finite frequency the derivative of a residue $\partial_\Lambda \Sigma_\Lambda(\mathbf{k})$. We obtain for its flow equation

$$\begin{aligned} \partial_\Lambda \tilde{\mathcal{A}}_\Lambda[\mathbf{h}^c, \mathbf{s}^q] &= -\frac{1}{2} \left(\frac{\delta \tilde{\mathcal{A}}_\Lambda}{\delta \mathbf{h}^c}, \partial_\Lambda \mathbf{J}_\Lambda \frac{\delta \tilde{\mathcal{A}}_\Lambda}{\delta \mathbf{h}^c} \right)_{\omega=0} - \frac{1}{2} \text{Tr}_{\omega=0} (\partial_\Lambda \mathbf{J}_\Lambda \mathbf{A}_\Lambda^{(2)}) - \frac{1}{2} \text{Tr}_{\omega \neq 0} (\tilde{\mathbf{J}}_\Lambda [\partial_\Lambda \mathbf{J}_\Lambda] \tilde{\mathbf{J}}_\Lambda \mathbf{A}_\Lambda^{(2)}) \\ &\quad - \frac{1}{2} \text{Tr}_{\omega \neq 0} (\tilde{\mathbf{J}}_\Lambda \partial_\Lambda \mathbf{J}_\Lambda) - \frac{1}{2} \left(\tilde{\mathbf{J}}_\Lambda \frac{\delta \tilde{\mathcal{A}}_\Lambda}{\delta \mathbf{s}^q}, [\partial_\Lambda \mathbf{J}_\Lambda] \tilde{\mathbf{J}}_\Lambda \frac{\delta \tilde{\mathcal{A}}_\Lambda}{\delta \mathbf{s}^q} \right)_{\omega \neq 0} \\ &\quad + \frac{1}{2} (\mathbf{s}^q, [\partial_\Lambda \Sigma_\Lambda] \mathbf{s}^q)_{\omega \neq 0} + \left(\mathbf{s}^q, [\partial_\Lambda \Sigma_\Lambda] \tilde{\mathbf{J}}_\Lambda \frac{\delta \tilde{\mathcal{A}}_\Lambda}{\delta \mathbf{s}^q} \right)_{\omega \neq 0}. \end{aligned} \quad (2.82)$$

The corresponding subtracted Legendre transform is defined as

$$\tilde{\Gamma}_\Lambda[\mathbf{m}^c, \boldsymbol{\eta}^q] = (\mathbf{m}^c, \mathbf{h}^c) + (\boldsymbol{\eta}^q, \mathbf{s}^q) - \tilde{\mathcal{A}}_\Lambda[\mathbf{h}^c, \mathbf{s}^q] - \frac{1}{2} (\mathbf{m}^c, \mathbf{R}_\Lambda^c \mathbf{m}^c) - \frac{1}{2} (\boldsymbol{\eta}^q, \mathbf{R}_\Lambda^q \boldsymbol{\eta}^q), \quad (2.83)$$

with

$$\mathbf{m}^c = \frac{\delta \tilde{\mathcal{A}}_\Lambda[\mathbf{h}^c, \mathbf{s}^q]}{\delta \mathbf{h}^c}, \quad (2.84)$$

$$\boldsymbol{\eta}^q = \frac{\delta \tilde{\mathcal{A}}_\Lambda[\mathbf{h}^c, \mathbf{s}^q]}{\delta \mathbf{s}^q}, \quad (2.85)$$

and \mathbf{R}_Λ^c chosen as in section 2.3.1, whereas $\mathbf{J}_\Lambda^{-1} \rightarrow \tilde{\mathbf{J}}_\Lambda^{-1}$ in \mathbf{R}_Λ^q . Accordingly, $\tilde{\Gamma}_\Lambda$ generates hybrid vertices which are 1- \tilde{J} -irreducible for dynamic degrees of freedom and 1-propagator-line-irreducible on the static sector. Furthermore $\tilde{\Gamma}_\Lambda[\mathbf{m}^c, \boldsymbol{\eta}^q]$ reduces, as the functional of Sec. 2.3.1, to the classical 1-PI effective action $\Gamma_\Lambda[\mathbf{m}^c]$ in the limit $S \rightarrow \infty$. Using

$$\mathbf{m}^c = \frac{\delta \tilde{\Gamma}_\Lambda[\mathbf{m}^c, \boldsymbol{\eta}^q]}{\delta \mathbf{h}^c} + \mathbf{R}_\Lambda^c \mathbf{h}^c, \quad (2.86)$$

$$\mathbf{s}^q = \frac{\delta \tilde{\Gamma}_\Lambda[\mathbf{m}^c, \boldsymbol{\eta}^q]}{\delta \boldsymbol{\eta}^q} + \mathbf{R}_\Lambda^q \boldsymbol{\eta}^q, \quad (2.87)$$

one arrives at the flow equation satisfied by $\tilde{\Gamma}_\Lambda[\mathbf{m}^c, \boldsymbol{\eta}^q]$

$$\begin{aligned} \partial_\Lambda \tilde{\Gamma}_\Lambda[\mathbf{m}^c, \boldsymbol{\eta}^q] &= \frac{1}{2} \text{Tr} (\dot{\mathbf{R}}_\Lambda [\tilde{\Gamma}_\Lambda^{(2)}[\mathbf{m}^c, \boldsymbol{\eta}^q] + \mathbf{R}_\Lambda]^{-1}) + \frac{1}{2} \text{Tr}_{\omega \neq 0} (\tilde{\mathbf{J}}_\Lambda \partial_\Lambda \mathbf{J}_\Lambda) \\ &\quad - \frac{1}{2} \left(\frac{\delta \tilde{\Gamma}_\Lambda}{\delta \boldsymbol{\eta}^q}, [\partial_\Lambda \Sigma_\Lambda] \frac{\delta \tilde{\Gamma}_\Lambda}{\delta \boldsymbol{\eta}^q} \right)_{\omega \neq 0}, \end{aligned} \quad (2.88)$$

where we have introduced as a generalization of $\partial_\Lambda \mathbf{R}_\Lambda$ the matrix

$$\dot{\mathbf{R}}_\Lambda \equiv \begin{pmatrix} \partial_\Lambda \mathbf{J}_\Lambda & 0 \\ 0 & \tilde{\mathbf{J}}_\Lambda^{-1} [\partial_\Lambda \mathbf{J}_\Lambda] \tilde{\mathbf{J}}_\Lambda^{-1} \end{pmatrix}. \quad (2.89)$$

The generalized Wetterich equation (2.88) still involves a residual term $\propto \partial_\Lambda \Sigma_\Lambda$. Formally, the additional contribution retains a tree-structure, with a product of two vertices that

have the same K -arguments as on the left-hand side, linked by $\partial_\Lambda \Sigma_\Lambda$. Due to conservation of total frequency, implied by translational symmetry in time, this term will not appear in the flow equation of any static vertex, in particular the self-energy Σ_Λ . Therefore, its contribution to the flow of vertices with at least two dynamic legs is at least of first order in loops.

All vertices $\tilde{\Gamma}_\Lambda^{(n)}$ that are generated by $\tilde{\Gamma}_\Lambda[\mathbf{m}^c, \boldsymbol{\eta}^q]$ can be, as already mentioned, related to the connected correlation functions by means of the tree expansion. The subtracted dynamic polarization is again defined as

$$\tilde{\Pi}_\Lambda(\mathbf{k}, i\omega) = -\tilde{\Gamma}_\Lambda^{(2)}(\mathbf{k}, i\omega). \quad (2.90)$$

Thus one can write the dynamic two-point functions as

$$\tilde{F}_\Lambda(\mathbf{k}, i\omega \neq 0) = -\frac{G_\Lambda^{-1}(\mathbf{k})}{1 + G_\Lambda^{-1}(\mathbf{k})\tilde{\Pi}_\Lambda(\mathbf{k}, i\omega)}, \quad (2.91)$$

$$G_\Lambda(\mathbf{k}, i\omega) = \frac{\tilde{\Pi}_\Lambda(\mathbf{k}, i\omega)}{1 + G_\Lambda^{-1}(\mathbf{k})\tilde{\Pi}_\Lambda(\mathbf{k}, i\omega)}, \quad (2.92)$$

or more suggestive

$$G_\Lambda(\mathbf{k}, i\omega) = G_\Lambda(\mathbf{k}) \frac{G_\Lambda^{-1}(\mathbf{k})\tilde{\Pi}_\Lambda(\mathbf{k}, i\omega)}{1 + G_\Lambda^{-1}(\mathbf{k})\tilde{\Pi}_\Lambda(\mathbf{k}, i\omega)}. \quad (2.93)$$

Hence by comparing $\tilde{F}_\Lambda(\mathbf{k}, i\omega \neq 0)$ with $F_\Lambda(\mathbf{k}, i\omega \neq 0)$ in (2.65) we find the new dynamic vertex to be related to $\Pi_\Lambda(\mathbf{k}, i\omega)$ via

$$\tilde{\Pi}_\Lambda^{-1}(\mathbf{k}, i\omega) = \Pi_\Lambda^{-1}(\mathbf{k}, i\omega) - \Sigma_\Lambda(\mathbf{k}, 0). \quad (2.94)$$

Enforcing continuity (2.74) thus implies

$$\tilde{\Pi}_\Lambda^{-1}(\mathbf{k} \neq \mathbf{0}, i\omega \rightarrow 0) = 0, \quad (2.95)$$

meaning that $G_\Lambda^{-1}(\mathbf{k})\tilde{\Pi}_\Lambda(\mathbf{k}, i\omega)$ has to diverge for $\omega \rightarrow 0$, so that the frequency-dependent factor in Eq. (2.93) becomes unity to ensure (2.74). This condition is certainly easier to realize than the one for the bare coupling amputation, where the static and dynamic part in $G_\Lambda(\mathbf{k}, i\omega)$ are harder to separate from each other. Furthermore we note that $[1 + G_\Lambda^{-1}(\mathbf{k})\tilde{\Pi}_\Lambda(\mathbf{k}, i\omega)]^{-1} > 0$ is always ensured if $\tilde{\Pi}_\Lambda(\mathbf{k}, i\omega) > 0$, because $G_\Lambda^{-1}(\mathbf{k}) \geq 0$. We already deduced in Sec. 1.3.3 that $G_\Lambda(\mathbf{k}, i\omega)$ is a real, positive and monotonously decaying function of $|\omega|$, implying that $\tilde{\Pi}_\Lambda(\mathbf{k}, i\omega) = [G_\Lambda^{-1}(\mathbf{k}, i\omega) - G_\Lambda^{-1}(\mathbf{k})]^{-1}$ is also real, > 0 and a monotonous function of $|\omega|$. Positivity is therefore a generic property of $\tilde{\Pi}_\Lambda$ and should be satisfied by the outcome of any sound approximation. These properties also transfer to the unsubtracted polarization $\Pi_\Lambda(\mathbf{k}, i\omega) = \frac{\tilde{\Pi}_\Lambda(\mathbf{k}, i\omega)}{1 + \tilde{\Pi}_\Lambda(\mathbf{k}, i\omega)\Sigma_\Lambda(\mathbf{k})}$, given that $\Sigma_\Lambda(\mathbf{k}) > 0$.

Another aspect which makes the amputation with $G_\Lambda^{-1}(\mathbf{k})$ in place of $J_\Lambda(\mathbf{k})$ more feasible can be seen by considering the limit of large temperatures, $T \gg |J|$. In this limit the static susceptibility $G_\Lambda(\mathbf{k})$ is asymptotically given by the result for an isolated spin and is formally an even function of the exchange interaction J . The same symmetry with respect to $J \leftrightarrow -J$ should be present in $G_\Lambda(\mathbf{k}, i\omega)$. This is intuitive, given that a system with Hamiltonian $-\mathcal{H}$ has the same spectrum of eigenstates, except that their order is inverted. At infinite temperature, where $\exp(-\beta\mathcal{H}) = 1$, the latter does not matter anymore, since all states are equally probable, so that all expectation values are indeed independent

of $\text{sign}(J)$. In the new parametrization this is clearly reflected, as long as $\tilde{\Pi}_\Lambda(\mathbf{k}, i\omega)$ also exhibits this symmetry. In contrast to that the much needed symmetry is not apparent in the previous parametrization, due to the explicit presence of $J_\Lambda(\mathbf{k})$ in $G_\Lambda(\mathbf{k}, i\omega)$, see its parametrization in Eq. (2.66), which is obviously asymmetric, regardless of temperature. From that difference in structure alone one concludes that proper approximations for $\Pi_\Lambda(\mathbf{k}, i\omega)$ are more difficult to construct than for $\tilde{\Pi}_\Lambda(\mathbf{k}, i\omega)$. Note also here that $\tilde{\Pi}_\Lambda(\mathbf{k}, i\omega)$ has to vanish as T^{-1} for $T \gg |J|$ and fixed ω , because the respective expectation values in real-time $\sim T \int d\omega \text{Im}G_{\text{ret}}(\mathbf{k}, \omega)/\omega$ are finite [31]. The ω -dependent function in Eq. (2.93) converges then to a non-zero limit, reflecting the non-trivial dynamics even at $T = \infty$ [33]. An additional, although more specific reason, for using the new amputation, can be given by considering low-dimensional systems for $T \rightarrow 0$, e.g. nearest-neighbor magnets on the square lattice. In that case we know that the most prominent feature in the dynamic structure factor $S(\mathbf{k}, \omega)$ are sharp peaks at the energy of a single magnon $E(\mathbf{k})$. For both signs of J , the dispersion is roughly proportional to $\sqrt{G^{-1}(\mathbf{k})\tilde{\Pi}(\mathbf{k})}$ [21, 23], with $\tilde{\Pi}(\mathbf{k}) \sim k^2$, $ka \ll 1$ and $\tilde{\Pi}(\mathbf{k}) \sim |J|^{-1}$, $ka \sim \mathcal{O}(1)$. Taking the generic high-frequency ansatz $\tilde{\Pi}(\mathbf{k}, i\omega) \sim \tilde{\Pi}(\mathbf{k})J^2/\omega^2$, we are able to reproduce this basic result for $S(\mathbf{k}, \omega)$.

Looking at the higher order vertices we will focus on three- and four-point quantities, since those appear directly in the flow of the two-point vertices, Σ_Λ and $\tilde{\Pi}_\Lambda$. We will use the Cartesian representation, because in the absence of symmetry-breaking it is less redundant than the spherical representation, which in turn is a more convenient choice if spin-rotational invariance is broken. Their initial condition can be obtained from the connected correlation functions of an isolated spin, which are explicitly given in appendix A.2. The functional series expansion of $\tilde{\Gamma}_\Lambda[\mathbf{m}, \boldsymbol{\eta}]$ up to fourth order in the fields $\mathbf{m}, \boldsymbol{\eta}$ is given by

$$\begin{aligned}
 \tilde{\Gamma}_\Lambda[\mathbf{m}, \boldsymbol{\eta}] = & \tilde{\Gamma}_\Lambda[\mathbf{0}, \mathbf{0}] + \frac{\beta}{2} \int_{\mathbf{k}} [J_\Lambda + \Sigma_\Lambda(\mathbf{k})] \mathbf{m}_{\mathbf{k}} \cdot \mathbf{m}_{-\mathbf{k}} - \frac{1}{2} \int_K [G_\Lambda^{-1}(\mathbf{k}) + \tilde{\Pi}_\Lambda(K)] \boldsymbol{\eta}_K \cdot \boldsymbol{\eta}_{-K} \\
 & + [\eta^x \eta^y m^z] + [\eta^x m^y \eta^z] + [m^x \eta^y \eta^z] + [\eta^x \eta^y \eta^z] + \frac{1}{(2!)^2} \left([m^x m^x m^y m^y] \right. \\
 & + [m^x m^x m^z m^z] + [m^y m^y m^z m^z] \left. \right) + \frac{1}{4!} \left([m^x m^x m^x m^x] \right. \\
 & + [m^y m^y m^y m^y] + [m^z m^z m^z m^z] \left. \right) + \frac{1}{(2!)^2} \left([m^x m^x \eta^y \eta^y] \right. \\
 & + [m^x m^x \eta^z \eta^z] + [m^y m^y \eta^z \eta^z] + [m^x m^x \eta^x \eta^x] \\
 & + [m^y m^y \eta^y \eta^y] + [m^z m^z \eta^z \eta^z] \left. \right) + [m^x m^y \eta^x \eta^y] \\
 & + [m^x m^z \eta^x \eta^z] + [m^y m^z \eta^y \eta^z] \\
 & + \frac{1}{(2!)^2} \left([\eta^x \eta^x \eta^y \eta^y] + [\eta^x \eta^x \eta^z \eta^z] + [\eta^y \eta^y \eta^z \eta^z] \right) \\
 & + \frac{1}{4!} \left([\eta^x \eta^x \eta^x \eta^x] + [\eta^y \eta^y \eta^y \eta^y] + [\eta^z \eta^z \eta^z \eta^z] \right) + [\eta \eta \eta \eta] \text{-vertices} + \dots, \quad (2.96)
 \end{aligned}$$

$[\eta \eta \eta \eta]$ are shorthand notations for the integrals over the respective monomials, e.g.

$$[m^x \eta^y \eta^z] = \int_{K_1} \int_{K_2} \int_{K_3} \delta(K_1 + K_2 + K_3) \tilde{\Gamma}_\Lambda^{xyz}(K_1, K_2, K_3) \beta \delta_{\omega_1} m_{\mathbf{k}_1}^x \eta_{K_2}^y \eta_{K_3}^z, \quad (2.97)$$

$$[\eta^x \eta^y \eta^z] = \int_{K_1} \int_{K_2} \int_{K_3} \delta(K_1 + K_2 + K_3) \tilde{\Gamma}_\Lambda^{xyz}(K_1, K_2, K_3) \eta_{K_1} \eta_{K_2} \eta_{K_3}, \quad (2.98)$$

where $\delta(K) = \beta N \delta_{\omega,0} \delta_{\mathbf{k},0} = \delta(\omega) \delta(\mathbf{k})$, $\mathbf{m}_K = \mathbf{m}_k \delta(\omega)$. Here we already used that all zero-frequency correlation functions and therefore vertices with an odd number of legs satisfy

$$\tilde{\Gamma}_{\Lambda}^{(2n+1)}(\mathbf{k}_1, \dots, \mathbf{k}_{2n+1}) = 0, \quad (2.99)$$

due to an intact spin-rotation symmetry. This relation is a special case of the odd vertices' antisymmetry under a simultaneous inversion of sign in all frequencies. Furthermore the terms containing $[m\eta\eta\eta]$ are not considered explicitly, because the associated 4-vertex functions do not contribute directly to the flow of the two-point vertices. The structure of the three-point vertex with respect to the spin components is

$$\tilde{\Gamma}_{\Lambda}^{\alpha\beta\gamma}(K_1, K_2, K_3) = \epsilon_{\alpha\beta\gamma} \tilde{\Gamma}_{\Lambda}^{xyz}(K_1, K_2, K_3), \quad (2.100)$$

implying that the corresponding term in the series expansion can be written as a triple product, e.g $m_1 \cdot (\eta_2 \times \eta_3)$. Its tree expansion reads

$$\tilde{\Gamma}_{\Lambda}^{\alpha\beta\gamma}(K_1, K_2, K_3) = -[\tilde{A}_{\Lambda}^{(2)}(K_1)]^{-2} [\tilde{A}_{\Lambda}^{(2)}(K_2)]^{-1} [\tilde{A}_{\Lambda}^{(2)}(K_3)]^{-1} \tilde{A}_{\Lambda}^{\alpha\beta\gamma}(K_1, K_2, K_3), \quad (2.101)$$

and its initial condition at finite frequencies is therefore

$$\tilde{\Gamma}_{\Lambda_0}^{\alpha\beta\gamma}(\omega, -\omega, 0) = -\frac{\epsilon_{\alpha\beta\gamma}}{\omega}, \quad (2.102)$$

$$\tilde{\Gamma}_{\Lambda_0}^{\alpha\beta\gamma}(\omega, \nu, -\omega - \nu) = 0, \quad \omega, \nu, \omega + \nu \neq 0. \quad (2.103)$$

These expressions are retained in its zero-momentum limit for an interacting system. The mixed 4-legged vertex $\tilde{\Gamma}_{\Lambda}^{\alpha\alpha\gamma\gamma}(K_1, K_2, K_3, K_4)$ does not depend explicitly on α, γ and has the following tree expansion

$$\begin{aligned} \tilde{\Gamma}_{\Lambda}^{\alpha\alpha\gamma\gamma}(K_1, K_2, K_3, K_4) &= -[\tilde{A}_{\Lambda}^{(2)}(K_1)]^{-2} [\tilde{A}_{\Lambda}^{(2)}(K_2)]^{-1} [\tilde{A}_{\Lambda}^{(2)}(K_3)]^{-1} [\tilde{A}_{\Lambda}^{(2)}(K_4)]^{-1} \\ &\quad \times \tilde{A}_{\Lambda}^{\alpha\alpha\gamma\gamma}(K_1, K_2, K_3, K_4) + \sum_{\sigma} \tilde{\Gamma}_{\Lambda}^{\alpha\gamma\sigma}(K_1, K_3, -K_1 - K_3) \\ &\quad \times \tilde{A}_{\Lambda}^{(2)}(K_1 + K_3) \tilde{\Gamma}_{\Lambda}^{\alpha\gamma\sigma}(K_2, K_4, -K_2 - K_4), \end{aligned} \quad (2.104)$$

whereas the longitudinal vertex does not involve lower order tree diagrams, due to $\Gamma_{\Lambda}^{\alpha\alpha\alpha} = 0$. Note that due to an intact spin-rotation invariance it is possible to express the longitudinal vertex solely via the mixed one, namely

$$\tilde{\Gamma}_{\Lambda}^{\alpha\alpha\alpha\alpha}(K_1, K_2, K_3, K_4) = \mathcal{S}_{K_2;K_3,K_4} \tilde{\Gamma}_{\Lambda}^{\alpha\alpha\gamma\gamma}(K_1, K_2, K_3, K_4), \quad (2.105)$$

where the operator $\mathcal{S}_{K_1, \dots; K'_1, \dots}$ symmetrizes the expression with respect to two disjoint tuples $\{K\}$, $\{K'\}$ of arguments. Considering then solely vertices whose combinations of frequencies appear directly in the flow of $\Sigma_{\Lambda}(\mathbf{k})$ and $\tilde{\Pi}_{\Lambda}(K)$ we obtain for their initial conditions

$$\tilde{\Gamma}_{\Lambda_0}^{\alpha\alpha\alpha\alpha}(\omega_1, \omega_2, \omega_3, \omega_4) = -[G_{\Lambda_0}(0)]^{-4} G_{\Lambda_0}^{\alpha\alpha\alpha\alpha}(0, 0, 0, 0) = \delta_{\omega_1,0} \delta_{\omega_2,0} \delta_{\omega_3,0} \frac{|b_0''''|}{\beta(b_0')^4}, \quad (2.106)$$

$$\tilde{\Gamma}_{\Lambda_0}^{\alpha\alpha\gamma\gamma}(0, 0, 0, 0) = -[G_{\Lambda_0}(0)]^{-4} G_{\Lambda_0}^{\alpha\alpha\gamma\gamma}(0, 0, 0, 0) = \frac{|b_0''''|}{3\beta(b_0')^4}, \quad (2.107)$$

$$\begin{aligned}
 \tilde{\Gamma}_{\Lambda_0}^{\alpha\alpha\gamma\gamma}(\omega, -\omega, 0, 0) &= - [G_{\Lambda_0}(0)]^{-2} G_{\Lambda_0}^{\alpha\alpha\gamma\gamma}(\omega, -\omega, 0, 0) \\
 &\quad + 2\tilde{\Gamma}_{\Lambda_0}^{xyz}(\omega, 0, -\omega)\tilde{\Gamma}_{\Lambda_0}^{xyz}(-\omega, 0, \omega)(-G_{\Lambda_0}^{-1}(0)) \\
 &= 0 \\
 &= -2\tilde{\Gamma}_{\Lambda_0}^{\alpha\alpha\gamma\gamma}(\omega, 0, -\omega, 0),
 \end{aligned} \tag{2.108}$$

$$\begin{aligned}
 \tilde{\Gamma}_{\Lambda_0}^{\alpha\alpha\gamma\gamma}(\omega, -\omega, \omega, -\omega) &= -G_{\Lambda_0}^{xyyy}(\omega, -\omega, -\omega, \omega) + \tilde{\Gamma}_{\Lambda_0}^{xyz}(\omega, -\omega, 0)\tilde{\Gamma}_{\Lambda_0}^{xyz}(-\omega, \omega, 0)G_{\Lambda_0}(0) \\
 &= 0 \\
 &= -2\tilde{\Gamma}_{\Lambda_0}^{\alpha\alpha\gamma\gamma}(\omega, \omega, -\omega, -\omega),
 \end{aligned} \tag{2.109}$$

$$\begin{aligned}
 \tilde{\Gamma}_{\Lambda_0}^{\alpha\alpha\gamma\gamma}(\omega, \nu, -\omega, -\nu) &= -G_{\Lambda_0}^{\alpha\alpha\gamma\gamma}(\omega, \nu, -\omega, -\nu) + \tilde{\Gamma}_{\Lambda_0}^{xyz}(\nu, -\nu, 0)\tilde{\Gamma}_{\Lambda_0}^{xyz}(\omega, -\omega, 0)G_{\Lambda_0}^{(2)}(0) \\
 &= 0 \\
 &= -2\tilde{\Gamma}_{\Lambda_0}^{\alpha\alpha\gamma\gamma}(\omega, -\omega, \nu, -\nu).
 \end{aligned} \tag{2.110}$$

From the above initial conditions we conclude that only the mixed 3-vertex and static 4-vertex contribute to leading order in βJ_Λ to the flow equations of the self-energy $\Sigma_\Lambda(\mathbf{k})$ and polarization $\tilde{\Pi}_\Lambda(\mathbf{k}, i\omega)$. The static self-energy $\Sigma_\Lambda(\mathbf{k})$ satisfies in general

$$\begin{aligned}
 \partial_\Lambda \Sigma_\Lambda(\mathbf{k}) &= \frac{T}{2} \int_{\mathbf{q}} \dot{G}_\Lambda(\mathbf{q}) [3\tilde{\Gamma}_\Lambda^{\alpha\alpha\gamma\gamma}(\mathbf{k}, -\mathbf{k}, \mathbf{q}, -\mathbf{q}) + 2\tilde{\Gamma}_\Lambda^{\alpha\alpha\gamma\gamma}(\mathbf{k}, \mathbf{q}, -\mathbf{k}, -\mathbf{q})] \\
 &\quad + \frac{T}{2} \int_{\mathbf{q}} \sum_{\nu \neq 0} \dot{F}_\Lambda(Q) [3\tilde{\Gamma}_\Lambda^{\alpha\alpha\gamma\gamma}(\mathbf{k}, -\mathbf{k}, Q, -Q) + 2\tilde{\Gamma}_\Lambda^{\alpha\alpha\gamma\gamma}(\mathbf{k}, Q, -\mathbf{k}, -Q)] \\
 &\quad + T \int_{\mathbf{q}} \sum_{\nu \neq 0} [\tilde{F}_\Lambda(Q)\tilde{F}_\Lambda(Q+\mathbf{k})] \bullet [\tilde{\Gamma}_\Lambda^{xyz}(\mathbf{k}, Q, -Q-\mathbf{k})]^2,
 \end{aligned} \tag{2.111}$$

whereas the flow of the interaction-irreducible subtracted polarization $\tilde{\Pi}_\Lambda(K)$ reads

$$\begin{aligned}
 \partial_\Lambda \tilde{\Pi}_\Lambda(\mathbf{k}, i\omega) &= -\frac{T}{2} \int_{\mathbf{q}} \sum_{\nu \neq 0} \dot{F}_\Lambda(\mathbf{q}, i\nu) [3\tilde{\Gamma}_\Lambda^{xyyy}(K, -K, Q, -Q) + 2\tilde{\Gamma}_\Lambda^{xyyy}(K, Q, -K, -Q)] \\
 &\quad - \frac{T}{2} \int_{\mathbf{q}} \dot{G}_\Lambda(\mathbf{q}) [3\tilde{\Gamma}_\Lambda^{xyyy}(K, -K, \mathbf{q}, -\mathbf{q}) + 2\tilde{\Gamma}_\Lambda^{xyyy}(K, \mathbf{q}, -K, -\mathbf{q})] \\
 &\quad - T \int_{\mathbf{q}} \sum_{\nu \neq 0, -\omega} [\tilde{F}_\Lambda(\mathbf{q}, i\nu)\tilde{F}_\Lambda(\mathbf{q}+\mathbf{k}, i\nu+i\omega)] \bullet [\tilde{\Gamma}_\Lambda^{xyz}(-Q, Q+K, -K)]^2 \\
 &\quad - T \int_{\mathbf{q}} [\tilde{F}_\Lambda(\mathbf{q}, i\omega)G_\Lambda(\mathbf{q}+\mathbf{k})] \bullet [\tilde{\Gamma}_\Lambda^{xyz}(-\mathbf{q}+i\omega, \mathbf{q}+\mathbf{k}, -\mathbf{k}-i\omega)]^2 \\
 &\quad - T \int_{\mathbf{q}} [G_\Lambda(\mathbf{q})\tilde{F}_\Lambda(\mathbf{q}+\mathbf{k}, i\omega)] \bullet [\tilde{\Gamma}_\Lambda^{xyz}(-\mathbf{q}, \mathbf{q}+\mathbf{k}+i\omega, -\mathbf{k}-i\omega)]^2 \\
 &\quad + \tilde{\Pi}_\Lambda^2(\mathbf{k}, i\omega)\partial_\Lambda \Sigma_\Lambda(\mathbf{k}).
 \end{aligned} \tag{2.112}$$

Here we introduced the static and dynamic single scale propagators

$$\dot{G}_\Lambda(\mathbf{q}) \equiv -\partial_\Lambda J_\Lambda(\mathbf{q})G_\Lambda^2(\mathbf{q}) = -\frac{\partial_\Lambda J_\Lambda(\mathbf{q})}{[\Sigma_\Lambda(\mathbf{q}) + J_\Lambda(\mathbf{q})]^2}, \tag{2.113}$$

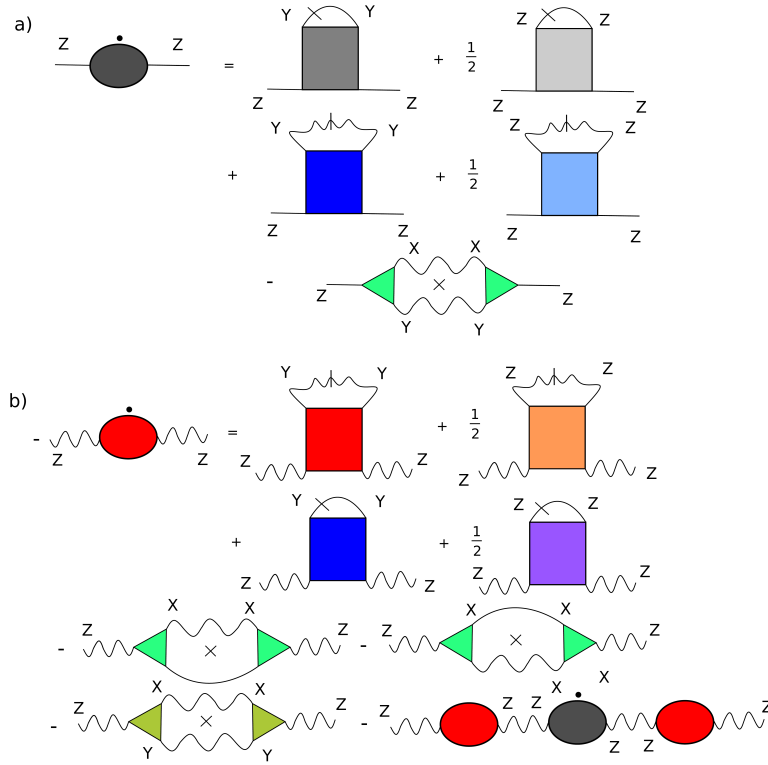


Figure 2.1: Diagrammatic representation of flow equations for a) the static self-energy Σ_Λ (2.111) and b) the dynamic polarization $\tilde{\Pi}_\Lambda$ (2.112). A straight line denotes here a static fluctuation, while wiggly lines represent dynamic components. Internal lines are the corresponding two-point functions in these channels, with the slashed ones being the single-scale propagators. A cross between two internal lines forming a loop indicates the 'product rule', e.g. $[G(\mathbf{q})G(\mathbf{q} + \mathbf{k})]^\bullet$.

$$\dot{\tilde{F}}_\Lambda(\mathbf{q}, i\nu) \equiv -\frac{\partial_\Lambda J_\Lambda(\mathbf{q})}{[1 + G_\Lambda^{-1}(\mathbf{q})\tilde{\Pi}_\Lambda(\mathbf{q}, i\nu)]^2}, \quad (2.114)$$

and the corresponding 'product rule' appearing in the flow equations as

$$[\tilde{F}_\Lambda(Q)\tilde{F}_\Lambda(Q + \mathbf{k})]^\bullet = \dot{\tilde{F}}_\Lambda(Q)\tilde{F}_\Lambda(Q + \mathbf{k}) + \tilde{F}_\Lambda(Q)\dot{\tilde{F}}_\Lambda(Q + \mathbf{k}), \quad (2.115)$$

$$[\tilde{F}_\Lambda(\mathbf{q}, i\omega)G_\Lambda(\mathbf{q} + \mathbf{k})]^\bullet = \dot{\tilde{F}}_\Lambda(\mathbf{q}, i\omega)G_\Lambda(\mathbf{q} + \mathbf{k}) + \tilde{F}_\Lambda(\mathbf{q}, i\omega)\dot{G}_\Lambda(\mathbf{q} + \mathbf{k}), \quad (2.116)$$

$$[G_\Lambda(\mathbf{q})G_\Lambda(\mathbf{q} + \mathbf{k})]^\bullet = \dot{G}_\Lambda(\mathbf{q})G_\Lambda(\mathbf{q} + \mathbf{k}) + G_\Lambda(\mathbf{q})\dot{G}_\Lambda(\mathbf{q} + \mathbf{k}). \quad (2.117)$$

Both flow equations, (2.111) and (2.112) are depicted in a diagrammatic representation in Fig. 2.1. Now one should remember the structure of the non-interacting three and four-legged vertices $\tilde{\Gamma}_0^{(n)}(\{\omega_i\})$, which all diverge for $\omega_i \rightarrow 0$. Together with the flow of $\tilde{\Pi}_\Lambda(\mathbf{k}, i\omega)$ which is 'proportional' to powers of these vertices, it seems that at least with the explicit loop diagrams in (2.112) one can arrive at $\lim_{\omega \rightarrow 0} \tilde{\Pi}_\Lambda(\mathbf{k}, i\omega) = \infty$, as required by the continuity conditions (2.74) and (2.75). Further below, we will see that by ignoring the renormalization of higher order vertex corrections the flow of $\tilde{\Pi}_\Lambda(K)$ does not couple to other frequencies. Hence the loop-terms, which depend then only on the external frequency ω

and diverge for $\omega \rightarrow 0$, are indeed compatible with these conditions. Note that the required $\omega \rightarrow 0$ -singularity is not entirely removed by the self-consistent coupling to $\tilde{\Pi}_\Lambda(K)$, which is contained in $\tilde{F}_\Lambda, \dot{\tilde{F}}$. Instead it only mitigates the divergence caused by the vertices $\Gamma_0^{(n)}(\omega)$, since one expects that for $|J_\Lambda| \gg |\omega|$ its flow equation has roughly the qualitative structure

$$\partial_\Lambda \tilde{\Pi}_\Lambda \propto \Gamma_0^{(n)}(\omega) \tilde{\Pi}_\Lambda^{-l}, \quad l > 0, \quad (2.118)$$

which implies $\tilde{\Pi}_\Lambda \sim (\Gamma_0^{(n)}(\omega))^{-1/(l+1)}$ for $\omega \rightarrow 0$. On the other hand, a term, which still may prevent us from achieving continuity, is the tree-like contribution $\sim \tilde{\Pi}_\Lambda^2(\mathbf{k}, i\omega) \partial_\Lambda \Sigma_\Lambda$. Its presence may simply cause an unstable flow for $|J_\Lambda| \gtrsim |\omega|$, via a premature singularity at finite ω as is anticipated with differential equations of the form $\partial_\Lambda f_\Lambda = A_\Lambda[f_\Lambda] + B_\Lambda[f_\Lambda] f_\Lambda^2$, where A_Λ and B_Λ are > 0 and bounded from above. However, at least in contrast to the pure J_Λ hybrid-formalism, the problematic contribution with respect to continuity is easily identified in the new framework. Hence by, e.g., ignoring the local term $\propto \partial_\Lambda \Sigma_\Lambda$ one already arrives at an approximate flow equation that is compatible with continuity of $G_\Lambda(\mathbf{k}, i\omega)$.

In the following section we will calculate $\tilde{\Pi}_\Lambda(\mathbf{k}, i\omega)$ in the whole range of frequencies. Before we turn to that, let us consider first some simple truncations and see whether they are sound, i.e. consistent with the imposed conditions of spin conservation (2.71) and continuity (2.95). We start by setting $\tilde{\Gamma}_\Lambda^{(3/4)} \approx \tilde{\Gamma}_{\Lambda_0}^{(3/4)}$. The flow equation of $\tilde{\Pi}_\Lambda(\mathbf{k}, i\omega)$ is then given by

$$\partial_\Lambda \tilde{\Pi}_\Lambda(\mathbf{k}, i\omega) = -\frac{2T}{\omega^2} \int_{\mathbf{q}} [\tilde{F}_\Lambda(\mathbf{q}, i\omega) G_\Lambda(\mathbf{q} + \mathbf{k})]^\bullet + \tilde{\Pi}_\Lambda^2(\mathbf{k}, i\omega) \partial_\Lambda \Sigma_\Lambda(\mathbf{k}). \quad (2.119)$$

Besides the already discussed local term, which prevents us from restoring continuity, we also note that in general $\partial_\Lambda \tilde{\Pi}_\Lambda(\mathbf{0}, i\omega) \neq 0$, which is incompatible with conservation of the total spin (2.71). By ignoring the renormalization of the two-legged vertices $\Sigma_\Lambda(\mathbf{k})$ and $\tilde{\Pi}_\Lambda(\mathbf{k})$ on the right-hand side, so that $\dot{\tilde{F}}_\Lambda \approx \partial_\Lambda \tilde{F}_\Lambda, \dot{G}_\Lambda \approx \partial_\Lambda G_\Lambda$, we can perform the Λ -integration exactly to obtain the one-loop result

$$\tilde{\Pi}_\Lambda(\mathbf{k}, i\omega) = \frac{2T}{\omega^2} \int_{\mathbf{q}} [G_\Lambda^{-1}(\mathbf{q} + \mathbf{k}) G_\Lambda(\mathbf{q}) - 1]. \quad (2.120)$$

One sees that it is compatible with continuity, since $\tilde{\Pi}_\Lambda^{-1}(\mathbf{k}, i\omega \rightarrow 0) \sim \omega^2 \rightarrow 0$. Furthermore it now satisfies the exact relation

$$\tilde{\Pi}_\Lambda(\mathbf{0}, i\omega \neq 0) = 0, \quad (2.121)$$

implied by total spin conservation (2.71). Note that this property is still preserved if we allow for a renormalized $\Sigma_\Lambda(\mathbf{k}) \neq T/b'_0$ on the right-hand side of the flow equation, i.e.

$$\begin{aligned} \partial_\Lambda \tilde{\Pi}_\Lambda(\mathbf{k}, i\omega) &= -\frac{2T}{\omega^2} \int_{\mathbf{q}} (G_\Lambda^{-1}(\mathbf{q}) G_\Lambda^2(\mathbf{q} + \mathbf{k}) \partial_\Lambda J_\Lambda(\mathbf{q} + \mathbf{k}) - G_\Lambda(\mathbf{q} + \mathbf{k}) \partial_\Lambda J_\Lambda(\mathbf{q})) \\ &= \frac{2T}{\omega^2} \int_{\mathbf{q}} (G_\Lambda(\mathbf{q} + \mathbf{k}) - G_\Lambda^{-1}(\mathbf{q} + \mathbf{k}) G_\Lambda^2(\mathbf{q})) \partial_\Lambda J_\Lambda(\mathbf{q}). \end{aligned} \quad (2.122)$$

A closer scrutiny reveals that the right-hand side is > 0 , consistent with the positivity of $\tilde{\Pi}_\Lambda$, e.g. for a ferromagnet both the expression in brackets and the derivative of the coupling are negative in the vicinity of $\mathbf{q} = \mathbf{0}$, so that their product is positive. Taking a $1/\omega^2$ -expression for $\tilde{\Pi}(\mathbf{k}, i\omega)$ at arbitrary ω , implies with $\omega^2 \rightarrow -\omega^2$ sharp δ -peaks in

$\text{Im}G_{\text{ret}}(\mathbf{k}, \omega)$ and therefore $S(\mathbf{k}, \omega)$, which is an unsatisfying result for the spin dynamics, in particular at high temperatures. Nevertheless there are instances where such an outcome is encountered. One such case are Green's function methods, that use undamped T -dependent auxiliary dynamics to mimick the effect of quantum fluctuations on static properties [65, 66]. Without any feedback from $\tilde{\Pi}_\Lambda$ the solution of (2.122) is only a good approximation for large frequencies $\omega \gg |J|$, where the leading frequency dependence is indeed $\propto \omega^{-2}$ [31]. In such a limit, one also does not have to bother with the tree-term $\propto \Pi_\Lambda^2(\mathbf{k}, i\omega)$, since it is $\mathcal{O}(\omega^{-4})$ and therefore subleading. To leading order in J_Λ/T the flow equation (2.122) reproduces the one-loop result (2.120) which reads

$$\tilde{\Pi}_\Lambda(\mathbf{k}, i\omega) = \frac{2(b'_0)^2}{T\omega^2} \int_{\mathbf{q}} J_\Lambda(\mathbf{q}) [J_\Lambda(\mathbf{q}) - J_\Lambda(\mathbf{q} + \mathbf{k})], \quad (2.123)$$

and is consistent with $\tilde{\Pi}_\Lambda \sim T^{-1}$. It has a simple \mathbf{k} -dependence for finite-ranged couplings and indeed is exact for $\omega, T \gg |J|$ [31].

To go beyond the high-frequency limit, a self-consistent coupling to $\tilde{\Pi}_\Lambda(K)$ is necessary, thus implying an infinite resummation in ω^{-2} . As already discussed such a coupling will reduce the leading low-frequency singularity in $\tilde{\Pi}_\Lambda(K)$, resulting in dissipative dynamics with a large damping, in contrast to the ω^{-2} -approximation. However, the presence of $\tilde{\Pi}_\Lambda(\mathbf{q}, i\omega)$ in the integral of, e.g. (2.122), leads also to a violation of the constraint (2.121) implied by spin conservation. Note that going to the next-highest order, ω^{-4} , in a high-frequency expansion, requires a lot more effort than the ω^{-2} -expression, namely finite corrections to higher order vertices. All of these terms have to be kept or at least treated such that Eq. (2.121) and other constraints like $\tilde{\Pi}_\Lambda(K) > 0$ are fulfilled. This can be arranged exactly as long as $|J_\Lambda|/T \ll 1$, where the inverse loop frequencies $\nu^{-1} \sim 1/T$, in powers of which one can expand (partially) dynamic vertices, are thermally suppressed. We should also note here, that truncating at $\mathcal{O}(\omega^{-4})$ will, in contrast to the $1/\omega^{-2}$ -limit, cause severe problems in the low-frequency sector. One can explain this with the observation that the accompanying coefficient is negative [31, 74], see Sec. 3.2.1 and Eq. (1.105), thus contradicting the positivity of $\tilde{\Pi}_\Lambda(K)$ for too small ω and inducing an unstable flow. Judicious extrapolations of these truncated high-frequency series are thus necessary to keep $\tilde{\Pi}_\Lambda(K)$ physical for smaller frequencies [33]. Quite generally the necessity of resumming infinitely many powers of J on the vertex level, even in the high-temperature limit, due to $\omega \ll |J|$ being a perturbatively inaccessible region, sets the problem of calculating dynamic properties significantly apart from the computation of thermodynamic quantities.

Chapter 3

Dynamic structure factor of a Heisenberg paramagnet

3.1 Derivation of an approximation to calculate $\tilde{\Pi}_\Lambda$

As observed, a truncation where vertices of third and higher order are kept at their initial values, while the response of $\tilde{\Pi}_\Lambda(K)$ on the right-hand side is fully retained, violates in general two major constraints: The vanishing of $\tilde{\Pi}_\Lambda(\mathbf{k}, i\omega)$ at zero momentum and finite frequency (2.121) and its divergence at finite momentum and vanishing frequency (2.95). To ensure their fulfillment we propose to replace (2.119) by

$$\partial_\Lambda \tilde{\Pi}_\Lambda(\mathbf{k}, i\omega) = -\frac{2T}{\omega^2} \int_{\mathbf{q}} \left([\tilde{F}_\Lambda(\mathbf{q}, i\omega) G_\Lambda(\mathbf{q} + \mathbf{k})]^\bullet - [\tilde{F}_\Lambda(\mathbf{q}, i\omega) G_\Lambda(\mathbf{q})]^\bullet \right). \quad (3.1)$$

As with the approximations in the previous section Eq. (3.1) remains purely local in frequency, since it does not contain any frequency sums, which couple to modes with $\nu \neq \omega$. This also implies that one can directly consider its analytical continuation and solve for $\tilde{\Pi}_\Lambda(\mathbf{k}, \omega + i0^+)$ in real frequencies and thus the retarded spin-spin correlation function $G_{ret,\Lambda}(\mathbf{k}, \omega)$, at least if an expression for the flowing static susceptibility $G_\Lambda(\mathbf{k})$ is available.

About the origins of (3.1): First, we removed, as suggested before, the tree-contribution to ensure continuity (2.75). Second, we subtracted from the loop-diagram in (2.119) its value at vanishing momentum transfer \mathbf{k} , which in general is $\neq 0$ due to $\tilde{\Pi}_\Lambda(\mathbf{q}, i\omega) \neq 0$ in $\tilde{F}_\Lambda(\mathbf{q}, i\omega)$, thus always enforcing (2.121). Formally, the above can be accomplished by setting up an appropriate flowing four-point vertex, that cancels the contribution $\sim \partial_\Lambda \Sigma_\Lambda$ and replaces it with the subtracted $\mathbf{k} = \mathbf{0}$ -loop. Such a form should be at the very least consistent with the initial condition of the vertex in question. The explicit form for the relevant combination of 4-point vertices is then chosen as follows

$$\tilde{\Gamma}_\Lambda^{(4)}(K) \equiv \frac{3\tilde{\Gamma}_\Lambda^{\alpha\alpha\gamma\gamma}(0, 0, -K, K) + 2\tilde{\Gamma}_\Lambda^{\alpha\alpha\gamma\gamma}(0, K, 0, -K)}{2} = \frac{1}{\omega^2} [W_\Lambda(i\omega) + C_\Lambda(\mathbf{k}, i\omega)], \quad (3.2)$$

where the Ward identity (2.121) is enforced by the contribution

$$W_\Lambda(i\omega) \equiv \frac{2 \int_{\mathbf{q}} [\tilde{F}_\Lambda(\mathbf{q}, i\omega) G_\Lambda(\mathbf{q})]^\bullet}{\int_{\mathbf{q}} \dot{G}_\Lambda(\mathbf{q})}, \quad (3.3)$$

while the continuity condition (2.95) is enforced by

$$C_\Lambda(\mathbf{k}, i\omega) \equiv \frac{\omega^2 \tilde{\Pi}_\Lambda^2(\mathbf{k}, i\omega) \partial_\Lambda \Sigma_\Lambda(\mathbf{k})}{T \int_{\mathbf{q}} \dot{G}_\Lambda(\mathbf{q})}. \quad (3.4)$$

Using that $\partial_\Lambda J_\Lambda(\mathbf{q}) \sim J$ one can first check that the denominator behaves in both cases as

$$\int_{\mathbf{q}} \dot{G}_\Lambda(\mathbf{q}) \approx \left(\frac{b'_0}{T}\right)^3 \int_{\mathbf{q}} \partial_\Lambda J_\Lambda^2(\mathbf{q}) \sim \beta^3 J \mathcal{O}(J_\Lambda). \quad (3.5)$$

For the numerators we start with the dynamic susceptibility, which satisfies for $|J_\Lambda| \ll \omega, T$

$$\tilde{\Pi}_\Lambda(\mathbf{k}, i\omega) \sim \frac{\beta J_\Lambda^2}{\omega^2}, \quad (3.6)$$

and therefore its square is $\sim \mathcal{O}(J_\Lambda^4)$. Together with $\partial_\Lambda \Sigma_\Lambda \sim J \mathcal{O}(J_\Lambda)$, we thus find that the momentum-dependent contribution behaves as $C_\Lambda(\mathbf{k}, i\omega) \sim \mathcal{O}(J_\Lambda^4)$ for $J_\Lambda \rightarrow 0$. The second term is less suppressed, but we still obtain

$$\int_{\mathbf{q}} [\tilde{F}_\Lambda(\mathbf{q}, i\omega) G_\Lambda(\mathbf{q})]^\bullet = - \int_{\mathbf{q}} \tilde{\Pi}_\Lambda(\mathbf{q}, i\omega) \dot{F}_\Lambda(\mathbf{q}, i\omega) \approx \int_{\mathbf{q}} \tilde{\Pi}_\Lambda(\mathbf{q}, i\omega) \partial_\Lambda J_\Lambda(\mathbf{q}) = \beta J \mathcal{O}(J_\Lambda^2), \quad (3.7)$$

so that $W_\Lambda(i\omega) \sim J_\Lambda$, implying that

$$\tilde{\Gamma}_\Lambda^{\alpha\alpha\gamma\gamma}(0, 0, -K, K) = \mathcal{O}(J_\Lambda), \quad (3.8)$$

in accordance with its initial condition. Note that we assumed throughout

$$\int_{\mathbf{q}} \partial_\Lambda J_\Lambda(\mathbf{q}) = 0. \quad (3.9)$$

However, this is not mandatory for every conceivable cutoff scheme, for instance the average of the derivative can be non-zero, although an on-site coupling is never generated during the flow. In that case one has to lower the order of each integral and $\tilde{\Pi}_\Lambda$ by one, namely $\tilde{\Pi}_\Lambda(\mathbf{k}, i\omega) \sim J_\Lambda$ and $\int_{\mathbf{q}} \dot{G}_\Lambda(\mathbf{q}) \sim J = \mathcal{O}(\Lambda^0)$. Hence the 4-vertex still vanishes to leading order like $J_\Lambda \rightarrow 0$. In the next section, we will see that further modifications will be necessary to ensure that $\tilde{\Pi}_\Lambda(K)$ complies with all conditions for a physical solution.

3.1.1 Flow equations in the high-temperature limit

Let us take a closer look at the behavior of the right-hand side in (3.1) for large temperatures $T \gg |J_\Lambda|$. As discussed in Sec. 2.3.2, $G_\Lambda^{-1}(\mathbf{k}) \tilde{\Pi}_\Lambda(\mathbf{k}, i\omega)$ has to approach a finite limit for $T \rightarrow \infty$ at any non-zero frequency. Therefore one can write

$$\tilde{\Pi}_\Lambda(\mathbf{k}, i\omega) = \beta b'_0 \pi_\Lambda(\mathbf{k}, i\omega/J), \quad (3.10)$$

where $\pi_\Lambda(\mathbf{k}, i\omega/J)$ is assumed to be finite at $T = \infty$. Furthermore we inferred that it should not depend on $\text{sign}(J)$, is real-valued and positive definite

$$\pi_\Lambda(\mathbf{k}, i\omega/J) = \pi_\Lambda(\mathbf{k}, |\omega/J|) > 0. \quad (3.11)$$

This implies that the right-hand side of $\partial_\Lambda \tilde{\Pi}_\Lambda$ has to be > 0 . Expanding all static quantities to the first non-trivial orders in βJ_Λ in Eq. (3.1), the contribution from the amputated single-scale propagator becomes

$$-T^2 \tilde{F}_\Lambda(\mathbf{q}, i\omega)[G_\Lambda(\mathbf{q} + \mathbf{k}) - G_\Lambda(\mathbf{q})] \sim (b'_0)^2 \partial_\Lambda J_\Lambda(\mathbf{q})[J_\Lambda(\mathbf{q}) - J_\Lambda(\mathbf{q} + \mathbf{k})][1 + \pi_\Lambda(\mathbf{q}, i\omega/J)]^{-2} + \mathcal{O}(J_\Lambda^3), \quad (3.12)$$

which fulfills all of the aforementioned criteria. For a ferromagnetic coupling, $J < 0$, it is straightforward to argue that at arbitrary temperatures this term containing $G_\Lambda(\mathbf{q} + \mathbf{k}) - G_\Lambda(\mathbf{q})$ will remain consistent with the condition $\pi_\Lambda(\mathbf{q}, i\omega) > 0$. The reason for this is that the integrand always has, due to the behavior of $G_\Lambda^{-1}(\mathbf{q})\tilde{\Pi}_\Lambda(\mathbf{q}, i\omega)$, more weight in the region around the origin $\mathbf{q} = \mathbf{0}$, where $G_\Lambda(\mathbf{q} + \mathbf{k}) - G_\Lambda(\mathbf{q})$ and $\partial_\Lambda J_\Lambda(\mathbf{q})$ are both < 0 . Similar considerations for the antiferromagnet, $J > 0$, have also to take singular fluctuations at $\mathbf{q} = \mathbf{Q} \neq \mathbf{0}$ into account. Nevertheless we also find that the integrand is positive in the vicinity of both, e.g. for $\mathbf{q} \approx \mathbf{0}$, $\partial_\Lambda J_\Lambda(\mathbf{q})$ and the difference are positive, while for $\mathbf{q} \approx \mathbf{Q}$ both signs flip simultaneously, which is consistent with the integral remaining > 0 . Performing the same expansion for the term containing \dot{G}_Λ we obtain

$$\begin{aligned} -T^2 \tilde{F}_\Lambda(\mathbf{q}, i\omega)[\dot{G}_\Lambda(\mathbf{q} + \mathbf{k}) - \dot{G}_\Lambda(\mathbf{q})] &\sim b'_0 T \partial_\Lambda [J_\Lambda(\mathbf{q}) - J_\Lambda(\mathbf{q} + \mathbf{k})][1 + \pi_\Lambda(\mathbf{q}, i\omega/J)]^{-1} \\ &\quad + (b'_0)^2 J_\Lambda(\mathbf{q}) \partial_\Lambda [J_\Lambda(\mathbf{q}) - J_\Lambda(\mathbf{q} + \mathbf{k})][1 + \pi_\Lambda(\mathbf{q}, i\omega/J)]^{-1} \\ &\quad - (b'_0)^2 \partial_\Lambda [J_\Lambda^2(\mathbf{q}) - J_\Lambda^2(\mathbf{q} + \mathbf{k})][1 + \pi_\Lambda(\mathbf{q}, i\omega/J)]^{-1}. \end{aligned} \quad (3.13)$$

Except the first line of (3.13), the generated terms are also compatible with the postulated T -dependence and parity in J . A net contribution of the former, which is $\sim T$ and odd in J_Λ , is only produced for finite $\pi_\Lambda(\mathbf{q}, i\omega)$, i.e. to subleading order in J_Λ^2/ω^2 . The contribution $\sim J_\Lambda(\mathbf{q})\partial_\Lambda [J_\Lambda(\mathbf{q}) - J_\Lambda(\mathbf{q} + \mathbf{k})]$ in the second line of (3.13), implied by $J_\Lambda(\mathbf{q})$ in the numerator of $\tilde{F}_\Lambda(\mathbf{q}, i\omega)$, is positive definite. In fact this term is needed to obtain the correct result for $\pi_\Lambda(\mathbf{q}, i\omega)$ at infinite temperature and $\mathcal{O}(\omega^{-2})$, see Eq. (2.123). This will not be the case for the last line $\sim \partial_\Lambda [J_\Lambda^2(\mathbf{q}) - J_\Lambda^2(\mathbf{q} + \mathbf{k})]$, which is created by the temperature dependence of $\dot{G}_\Lambda(\mathbf{q})$ and again starts to contribute at subleading order in $\pi_\Lambda(\mathbf{q}, i\omega)$. For $\omega \rightarrow 0$ and $ka \ll 1$ the magnitude of the last term will be larger than the positive definite contribution in the second line, hence resulting definitely in a negative contribution of (3.13). Considering also the different weighting $[1 + \pi_\Lambda(\mathbf{q}, i\omega)]^{-1}$ in the $\dot{G}(\mathbf{q} + \mathbf{k}) - \dot{G}(\mathbf{q})$ -term, compared to $[1 + \pi_\Lambda(\mathbf{q}, i\omega)]^{-2}$ in (3.12), it may lead in total to a negative right-hand side of Eq. (3.1). This contradicts the conditions that π_Λ is real-valued and > 0 , implying a non-physical solution even without the obviously inadequate term in the first line of (3.13). From this we infer that terms, involving the static single-scale propagator $\dot{G}_\Lambda(\mathbf{q})$, are prone to issues beyond the leading order in $1/\omega^2$. In principle we can take care of these contributions via suitable momentum-dependent counterterms in the condition-fixing mixed 4-vertex $\tilde{\Gamma}_\Lambda^{(4)}(K)$, as was the case for fulfilling spin conservation (2.71) and continuity (2.75).

Let us consider first the case where the contributions implied by the presence of the static single-scale propagator $\dot{G}_\Lambda(\mathbf{q})$ are completely removed. The corresponding four-point vertex reads

$$\tilde{\Gamma}_\Lambda^{(4)}(K) \rightarrow \tilde{\Gamma}_\Lambda^{(4)}(K) + \frac{2 \int_{\mathbf{q}} \tilde{F}_\Lambda(\mathbf{q}, i\omega)[\dot{G}_\Lambda(\mathbf{q} + \mathbf{k}) - \dot{G}_\Lambda(\mathbf{q})]}{\omega^2 \int_{\mathbf{q}} \dot{G}_\Lambda(\mathbf{q})}, \quad (3.14)$$

where the additional contribution on top of (3.2) vanishes for $J_\Lambda \rightarrow 0$ too. Considering now the $T = \infty$ -limit, we arrive at the following flow equation

$$\partial_\Lambda \pi_\Lambda(\mathbf{k}, |\omega/J|) \approx \frac{2b'_0}{\omega^2} \int_{\mathbf{q}} \left(\frac{\partial_\Lambda J_\Lambda(\mathbf{q}) [J_\Lambda(\mathbf{q}) - J_\Lambda(\mathbf{q} + \mathbf{k})]}{[1 + \pi_\Lambda(\mathbf{q}, |\omega/J|)]^2} \right), \quad (3.15)$$

where one sees that $\pi_\Lambda(\mathbf{k}, \omega) \sim k^2$, $ka \rightarrow 0$, as anticipated from (2.121). Now we can make some further statements regarding its actual behavior, i.e. frequency dependence. Assuming for simplicity a linear deformation $J_\Lambda = \Lambda J$ [2] and small frequencies $|\omega| \ll |J_\Lambda|$, for whom $\pi_\Lambda(\mathbf{k}, |\omega/J|)$ will diverge, together with the small momentum expansion

$$\pi_\Lambda(\mathbf{k}, |\omega/J|) = \pi_\Lambda(|\omega/J|)k^2, \quad ka \ll 1, \quad (3.16)$$

we see that for $d < 4$ the integral in (3.15) is dominated by small momenta $q \lesssim \pi_\Lambda^{-1/2}(|\omega/J|)$, so that one obtains

$$\pi_\Lambda(|\omega/J|)^{d/2} \partial_\Lambda \pi_\Lambda(|\omega/J|) \propto \Lambda \left(\frac{J\sqrt{b'_0}}{|\omega|} \right)^2, \quad (3.17)$$

implying

$$\pi_\Lambda(|\omega/J|) \sim \left(\frac{J_\Lambda \sqrt{b'_0}}{|\omega|} \right)^{\frac{4}{d+2}}. \quad (3.18)$$

Conversely above $d = 4$

$$\pi_\Lambda(|\omega/J|) \sim \left(\frac{J_\Lambda \sqrt{b'_0}}{|\omega|} \right)^{\frac{2}{3}}, \quad (3.19)$$

since here one can set the denominator of $\dot{F}_\Lambda(\mathbf{q}, i\omega)$ directly to $\pi_\Lambda^2(\mathbf{q}, |\omega/J|)$ without risking an infrared divergence for $q \rightarrow 0$. Here we have also used that with the linear deformation the \mathbf{k} -dependence of $\pi_\Lambda(\mathbf{k}, |\omega/J|)$ is on the same simple level as for the plain $1/\omega^2$ -limit (2.123), whose result is, up to a factor of two, reproduced for $\omega \rightarrow \infty$, e.g. $\pi_\Lambda(\mathbf{k}, |\omega/J|) \propto [J(\mathbf{0}) - J(\mathbf{k})]$ for a nearest neighbor-coupling J . Moreover a ΛJ -deformation allows one to write (3.15) at $T = \infty$ as a differential equation with respect to a frequency variable $(\tilde{\omega}_\Lambda)^{-2} = (J_\Lambda \sqrt{b'_0}/\omega)^2$, i.e.

$$\partial_{(\tilde{\omega}_\Lambda)^{-2}} \pi_\Lambda(\mathbf{k}, |\omega/J|) = \frac{1}{J^2} \int_{\mathbf{q}} \frac{J(\mathbf{q}) [J(\mathbf{q}) - J(\mathbf{q} + \mathbf{k})]}{[1 + \pi_\Lambda(\mathbf{q}, |\omega/J|)]^2}, \quad (3.20)$$

thus solving for the dynamics during integration of the flow. For $d = 3$, the low-frequency limit of $\pi_\Lambda(|\omega/J|)$ diverges as $|\omega|^{-4/5}$. This is incompatible with spin diffusion, whose existence is not rigorously proven but nevertheless anticipated in three dimensions [41, 42, 74, 77]. In that case one expects $\pi_\Lambda \sim \mathcal{D}_\Lambda |\omega|^{-1}$, given that $G_\Lambda(\mathbf{k}, i\omega)$ assumes then the form

$$G_\Lambda(\mathbf{k}, i\omega) = \frac{b'_0}{T} \frac{|\omega| \pi_\Lambda(|\omega/J|) k^2}{|\omega| \pi_\Lambda(|\omega/J|) k^2 + |\omega|} = \frac{b'_0}{T} \frac{\mathcal{D}_\Lambda k^2}{\mathcal{D}_\Lambda k^2 + |\omega|}, \quad (3.21)$$

which via analytic continuation $|\omega| \rightarrow -i\omega$ leads to a centered Lorentzian for $S(\mathbf{k}, \omega) \sim \text{Im} G_{\text{ret}}(\mathbf{k}, \omega)/\omega$, consistent with the diffusion form in Eq. (1.115) [35, 41]. In place of the above one finds for $d > 2$ subdiffusion, for which the divergence of π_Λ is weaker than $|\omega|^{-1}$, so that the diffusion coefficient $\mathcal{D}_\Lambda(i\omega) \propto |\omega| \pi_\Lambda(|\omega/J|)$ vanishes for $\omega \rightarrow 0$. The corresponding scattering intensity $S(\mathbf{k}, \omega)$ diverges then as $|\omega|^{\frac{2-d}{2+d}}$ for $\omega \rightarrow 0$ [51], a feature which is not observed in experiments. Diffusion is solely present in two dimensions, while for $d = 1$, we obtain $\pi_\Lambda \sim |\omega|^{-4/3}$, which, due to the stronger singularity, is superdiffusive. The results

in $d > 2$ imply for small momenta scaling $k \sim \omega^{1/z}$ with a dynamic exponent $z = \frac{d+2}{2} > 2$, whereas $z = 2$ is required for diffusion, as seen in (3.21) and discussed in Sec. 1.4.1. The outcome of (3.15) is obviously not supported by the phenomenological assumptions of hydrodynamics for isotropic magnets. Based on homogeneity relations for the solution of the mode-coupling equations in the long-time region several publications suggested subdiffusive exponents $z > 2$, but their explicit values $z = \frac{d+4}{2}$ [78, 79, 80] do not agree with the predictions of Eq. (3.15) in $d > 2$. For reduced dimensions the outcomes seem to be more in line with previous calculations. While there is a paucity of results for the long-time dynamics in $d = 2$, there seems to be mounting evidence [48, 49, 50, 51, 81, 82, 83, 84, 85, 86], that at least for the integrable $S = 1/2$ -model with nearest-neighbor interaction, the behavior is superdiffusive too, with the same dynamic index $z = 3/2$.

The results of (3.15) above $d = 2$ are disappointing, as they do not agree with the outlined hydrodynamic picture, on top of lacking corroboration from other methods. The subdiffusive behavior arises from the quadratic denominator of $\tilde{F}_\Lambda(\mathbf{q}, i\omega)$ in Eq. (3.15). Reducing its power, hypothetically, to $[1 + \pi_\Lambda(\mathbf{q}, |\omega/J|)]^{-1}$, the integral becomes IR-singular in the low- ω -limit only for $d \leq 2$, with the result in $d > 2$ always being consistent with diffusion, since setting $F_\Lambda(\mathbf{q}, i\omega) \rightarrow \pi_\Lambda(\mathbf{q}, |\omega/J|)^{-1}$ becomes valid in the latter case. However, it turns out that a modification of the \tilde{F} -term by virtue of this raise is not necessary. Instead we can change the above high-temperature equation (3.15) by simply retaining the sole fully compatible term in the $[\dot{G}_\Lambda(\mathbf{q}) - \dot{G}_\Lambda(\mathbf{q} + \mathbf{k})]$ -contribution, which thus also reproduces the leading behavior for $\omega \rightarrow \infty$, see Eq. (2.123). We obtain

$$\partial_\Lambda \pi_\Lambda(\mathbf{k}, |\omega/J|) \approx \frac{2b'_0}{\omega^2} \int_{\mathbf{q}} \left(\frac{\partial_\Lambda J_\Lambda(\mathbf{q}) [J_\Lambda(\mathbf{q}) - J_\Lambda(\mathbf{q} + \mathbf{k})]}{[1 + \pi_\Lambda(\mathbf{q}, |\omega/J|)]^2} + \frac{J_\Lambda(\mathbf{q}) \partial_\Lambda [J_\Lambda(\mathbf{q}) - J_\Lambda(\mathbf{q} + \mathbf{k})]}{[1 + \pi_\Lambda(\mathbf{q}, |\omega/J|)]} \right), \quad (3.22)$$

which as (3.15) can be recast into a differential equation with respect to J_Λ^2/ω^2 . Note that this fixing amounts to the following substitution in the effective interaction

$$\tilde{F}_\Lambda(\mathbf{q}, i\omega) \rightarrow -J_\Lambda(\mathbf{q}) [1 + G_\Lambda^{-1}(\mathbf{q}) \tilde{\Pi}_\Lambda(\mathbf{q}, i\omega)]^{-1}, \quad (3.23)$$

i.e. ignoring the self-energy initially contained in the numerator of $\tilde{F}_\Lambda(\mathbf{q}, i\omega)$, whose presence leads to contributions with wrong asymptotic properties for $T \rightarrow \infty$ and $\omega \rightarrow 0$. The elimination of the unphysical contributions, can, as already described, be realized via a properly chosen higher order vertex

$$\tilde{\Gamma}_\Lambda^{(4)}(K) \rightarrow \tilde{\Gamma}_\Lambda^{(4)}(K) - \frac{2 \int_{\mathbf{q}} \Sigma_\Lambda(\mathbf{q}) [1 + G_\Lambda^{-1}(\mathbf{q}) \tilde{\Pi}_\Lambda(\mathbf{q}, i\omega)]^{-1} [\dot{G}_\Lambda(\mathbf{q} + \mathbf{k}) - \dot{G}_\Lambda(\mathbf{q})]}{\omega^2 \int_{\mathbf{q}} \dot{G}_\Lambda(\mathbf{q})}. \quad (3.24)$$

For $d > 2$ the right term in (3.22) will dominate and therefore lead to diffusion $\pi_\Lambda \propto |\omega|^{-1}$, while the initial contribution from (3.15) will be suppressed by a relative factor $\sim \pi_\Lambda^{(2-d)/2} \sim |\omega|^{(d-2)/2}$. This also strengthens the previous argument, that keeping terms $\sim \Sigma_\Lambda(\mathbf{q}) [1 + G_\Lambda^{-1}(\mathbf{q}) \tilde{\Pi}_\Lambda(\mathbf{q}, i\omega)]^{-1}$ leads in total to a contradiction, as negative contributions will dominate compared to the \tilde{F}_Λ -term. For a nearest-neighbor coupling on a d -dimensional hypercubic lattice, the \mathbf{k} -dependence is, as for Eq. (3.15), simply given by

$$\pi_\Lambda(\mathbf{k}, i\omega) = \pi_\Lambda(\omega) \left[1 - \frac{1}{d} \sum_{i=1}^d \cos(k_i a) \right], \quad (3.25)$$

and the low-frequency solution for the sole Fourier amplitude is

$$\pi_\Lambda(\omega) = \frac{2\sqrt{2}d\sqrt{b'_0}|J_\Lambda|}{|\omega|} \left(\int_{\mathbf{q}} \frac{\left(\frac{1}{d} \sum_{i=1}^d \cos(q_i a) \right)^2}{\left[1 - \frac{1}{d} \sum_{i=1}^d \cos(q_i a) \right]} \right)^{1/2}. \quad (3.26)$$

The corresponding diffusion coefficient can then be obtained from

$$\mathcal{D}_\Lambda = \lim_{\omega \rightarrow 0} \frac{|\omega| \pi_\Lambda(\omega) a^2}{2d}. \quad (3.27)$$

With the above integral it is in $d = 3$ given by $\mathcal{D}_\Lambda \approx |J_\Lambda| \sqrt{b'_0} a^2$. For both $S = 1/2$ and $S \rightarrow \infty$ this is too large by about 70 percent compared to previous estimates in the literature, but at least it has the same leading dependence on the model parameters J, S [42, 74]. The simple momentum dependence of the solution may be one of the reasons for the large numeric deviation. Note also the absent spin-dependence [42] beyond the scaling with $|J_\Lambda| \sqrt{b'_0}$. In the marginal case of two dimensions, one induces a superdiffusive logarithmic divergence via the new contribution, whereas for $d = 1$ both terms contribute equally, leading to the already discussed $|\omega|^{-1/3}$ -singularity. We have shown numeric results for the frequency dependence of $\pi(\omega)|\omega|$ obtained from the solution of the first equation (3.15) in Fig. 3.1 for $d = 2, 3$ and from the modified flow (3.22) in Fig. 3.2 for $d = 1, 2, 3$. The applicability of (3.22) at lower temperatures, especially in the vicinity of the critical point, is harder to assess, in particular with respect to the scaling behavior, that is expected in this regime on the ground of definite predictions by the dynamic scaling hypothesis [54, 56, 58]. Note that in this region it is impossible to resolve the flow solely with respect to frequency due to the non-perturbative built-up of static correlations with J_Λ , in contrast to $T \gg |J_\Lambda|$. A tentative analysis of the integrand around $\mathbf{q} = \mathbf{Q}, \mathbf{0}$ suggests that the additional \dot{G} -term keeps the same, positive, sign for lower temperatures, i.e. $J_\Lambda(\mathbf{q})$ and the \dot{G} -difference in (3.13) have the same signs as their pendants with switched derivatives in (3.12). Eq. (3.22) should therefore stay physical in this regard. On top of the crude numeric estimate for \mathcal{D} at $T = \infty$, the partial neglect of terms in the numerator of $\tilde{F}_\Lambda(\mathbf{q}, i\omega)$ seems somewhat artificial and one would still like to work with the full expression for the effective interaction. Hence we will continue our search for alternatives to the equations (3.15) and (3.22).

3.1.2 Integral equation

Returning to the idea of 'raising' the power in the denominator of \tilde{F}_Λ , in order to restore diffusion, we will take a look at integrated equations, where \dot{F}_Λ , \dot{G}_Λ and $\partial_\Lambda \tilde{\Pi}_\Lambda$ are replaced by \tilde{F}_Λ , G_Λ and $\tilde{\Pi}_\Lambda$. The simplest way of achieving that is to substitute

$$[\tilde{F}_\Lambda(\mathbf{q}, i\omega) G_\Lambda(\mathbf{q} + \mathbf{k})]^\bullet \rightarrow \partial_\Lambda [\tilde{F}_\Lambda(\mathbf{q}, i\omega) G_\Lambda(\mathbf{q} + \mathbf{k})], \quad (3.28)$$

in Eq. (3.1) at the beginning of section 3.1. The above prescription is also known as the Katanin substitution [7, 75, 76], meaning that the single-scale propagators are replaced by total derivatives with respect to the flow parameter,

$$\dot{\tilde{F}}_\Lambda(Q) \rightarrow \partial_\Lambda \tilde{F}_\Lambda(Q) = \dot{\tilde{F}}_\Lambda(Q) + \tilde{F}_\Lambda^2(Q) \partial_\Lambda \tilde{\Pi}_\Lambda(Q) - \frac{\partial_\Lambda \Sigma_\Lambda(\mathbf{q})}{[1 + \tilde{\Pi}_\Lambda(Q) G_\Lambda^{-1}(\mathbf{q})]^2}, \quad (3.29)$$

$$\dot{G}_\Lambda(\mathbf{q}) \rightarrow \partial_\Lambda G_\Lambda(\mathbf{q}) = \dot{G}_\Lambda(\mathbf{q}) - G_\Lambda^2(\mathbf{q}) \partial_\Lambda \Sigma_\Lambda(\mathbf{q}). \quad (3.30)$$

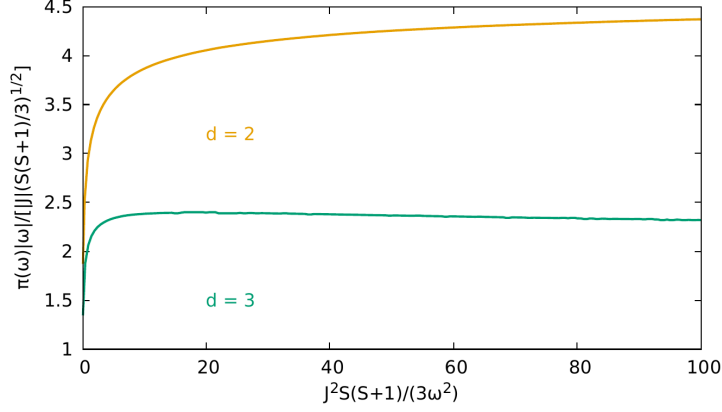


Figure 3.1: $\pi(\omega)|\omega|/(|J|\sqrt{b'_0})$, which for $\omega \rightarrow 0$ corresponds to $\mathcal{D}(i\omega)/(|J|\sqrt{b'_0})$, as a function of the effective flow parameter $J^2 b'_0 / \omega^2$ obtained from the solution of the first flow equation (3.15) for the nearest-neighbor Heisenberg magnet on a hypercubic lattice with $d = 2$ and $d = 3$. In the latter case one sees the subdiffusive trend $\sim |\omega|^{1/5}$, i.e. a continuous decrease for $1/\omega^2 \rightarrow \infty$.

This substitution amounts to effective vertex corrections of finite loop order and can be in principle taken care off via appropriate choice of higher order vertices, like in the previous section. Such a procedure was first motivated in the context of the fermionic FRG. There it was found, that its implementation in the flow of the two-fermion interaction accounted via the derivative of the self-energy for additional loop corrections, whose presence reduced in turn the error in some Ward identities, implied by conservation laws [68, 75, 76]. The self-consistency equation for $\tilde{\Pi}(\mathbf{k}, i\omega)$ reads then

$$\tilde{\Pi}(\mathbf{k}, i\omega) = -\frac{2T}{\omega^2} \int_{\mathbf{q}} \left(G(\mathbf{q} + \mathbf{k}) - G(\mathbf{q}) \right) \tilde{F}(\mathbf{q}, i\omega). \quad (3.31)$$

This is not a differential equation and can be directly evaluated at the final scale, hence not depending on a particular deformation scheme at intermediate scales. The computational burden is then shifted to solving a integral equation, for instance by iterating it until convergence is achieved. To leading order in $1/\omega^2$ it has the same shape as the one-loop expression (2.120), being also compatible with a renormalized $\Sigma_{\Lambda}(\mathbf{k})$. A closer scrutiny reveals that beyond $\mathcal{O}(\omega^{-2})$ problems are reintroduced via this manipulation, of which we already took care of in the previous approximations. Firstly, the kernel is not an even function of J in the high-temperature limit. Secondly that equation also implies a non-physical asymptotic behavior of the dynamic polarization for $T \rightarrow \infty$, i.e. $\tilde{\Pi}(\mathbf{k}, i\omega) \sim \mathcal{O}(1)$, instead of $\mathcal{O}(T^{-1})$. Hence the equation in its current form cannot be used.

A potential remedy is the introduction of an appropriate vertex correction into Eq. (3.31), namely

$$\begin{aligned} \tilde{\Pi}(\mathbf{k}, i\omega) = & -2T \int_{\mathbf{q}} \left(G(\mathbf{q} + \mathbf{k}) (\tilde{\Gamma}^{xyz}(\mathbf{q} + \mathbf{k}, -\mathbf{q} + i\omega, K))^2 \right. \\ & \left. - G(\mathbf{q}) (\tilde{\Gamma}^{xyz}(\mathbf{q}, -\mathbf{q} + i\omega, -i\omega))^2 \right) \tilde{F}(\mathbf{q}, i\omega). \end{aligned} \quad (3.32)$$

Instead of taking a look at the flow equation of the the three-point vertex $\tilde{\Gamma}_{\Lambda}^{(3)}$, we resort

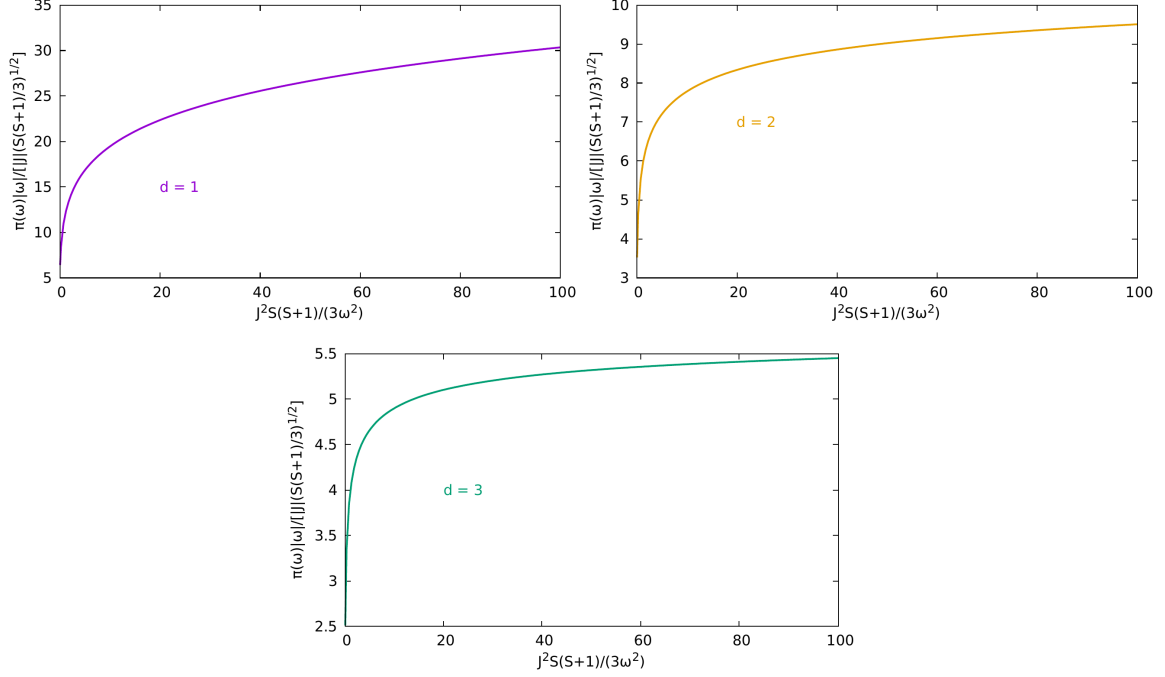


Figure 3.2: $\pi(\omega)|\omega|/(|J|\sqrt{b'_0})$ as a function of $J^2 b'_0/\omega^2$ obtained from the solution of the second flow equation (3.22) for the nearest-neighbor Heisenberg magnet on a hypercubic lattice in $d = 1, 2, 3$ (counterclockwise, starting top left).

to considering one of the equations of motion for the corresponding three-point function, which for general combinations of its arguments is given by

$$\begin{aligned}
 -\omega G^{xyz}(Q+K, -Q, -K) &= G(Q) - G(Q+K) + [J(\mathbf{q}) - J(\mathbf{q}+\mathbf{k})]G(Q)G(Q+K) \\
 &\quad - \int_{Q'} [J(\mathbf{q}') - J(\mathbf{q}'+\mathbf{k})]G^{\alpha\alpha\gamma\gamma}(Q+K, -Q'-K, Q', -Q).
 \end{aligned}
 \tag{3.33}$$

The method for writing down these equations is described in Appendix A.1. We have differentiated here with respect to a designated frequency ω , contained in the argument K , which will be later fixed to the external frequency in the equation for $\tilde{\Pi}_\Lambda(\mathbf{k}, i\omega)$ (3.32). The expression on the right-hand side lacks therefore a symmetry under arbitrary permutations of the vertex' arguments. Symmetry can then be only restored by considering the derivative with respect to the second independent frequency, e.g. ν in the argument Q and matching the right-hand sides, implying additional conditions for the involved quantities. For our purpose it is, however, sufficient to consider only one equation of motion, with the indicated choice of derivative. This particular choice will be justified afterwards. To progress further, we first have to eliminate the coupling to the connected four-point function. For this, we set it, only on the right-hand side of the equation of motion (3.33), to its initial or more general a momentum-independent, and thus local, expression, since then the momentum integrals $\sim \int_{\mathbf{q}} J(\mathbf{q})$ cancel each other. After this, the expression for G^{xyz} simplifies a lot, since it can be solely expressed via the propagator $G(K)$ and therefore the two-point vertices. Note that the neglect of the fourth order correlation function in the equation of motion is mainly

motivated by this simplification, as we ignore the fact that a momentum-independent four-point correlation function is not entirely consistent with the vertices $\tilde{\Gamma}_\Lambda^{(3)}$, $\tilde{\Gamma}_\Lambda^{(4)}$ used in the flow equations, via whom one can also construct this quantity.

Let us now write the approximate expression for the three-point function in a different way

$$\begin{aligned} \omega G^{xyz}(Q+K, -Q, -K) \approx & -G(Q) \left(1 + \frac{[J(\mathbf{q}) - J(\mathbf{q} + \mathbf{k})]G(Q+K)}{2} \right) \\ & + G(Q+K) \left(1 + \frac{[J(\mathbf{q} + \mathbf{k}) - J(\mathbf{q})]G(Q)}{2} \right). \end{aligned} \quad (3.34)$$

To be consistent with the local-in- ω structure of Eq. (3.32), the three-point function and corresponding vertex should be, as its initial condition, only finite if one out of the three frequencies is zero. Since we choose $\omega \neq 0$ as the external frequency of (3.32), that means either $\nu = 0$ or $\nu + \omega = 0$. Thus

$$\begin{aligned} \omega G^{xyz}(Q+K, -Q, -K) \approx & -\delta_{\nu,0} G(\mathbf{q}) \left(1 + \frac{[J(\mathbf{q}) - J(\mathbf{q} + \mathbf{k})]G(\mathbf{q} + K)}{2} \right) \\ & + \delta_{\nu+\omega,0} G(\mathbf{q} + \mathbf{k}) \left(1 + \frac{[J(\mathbf{q} + \mathbf{k}) - J(\mathbf{q})]G(\mathbf{q}, i\omega)}{2} \right), \end{aligned} \quad (3.35)$$

which, as expected, is consistent with its initial value

$$G_0^{xyz}(Q+K, -Q, -K) = -\frac{\beta b'_0 \delta_{\nu,0}}{\omega} + \frac{\beta b'_0 \delta_{\nu,-\omega}}{\omega}. \quad (3.36)$$

One obtains then for the relevant 3-point vertex via the tree expansion (2.101)

$$\begin{aligned} \tilde{\Gamma}^{xyz}(\mathbf{q} + \mathbf{k}, -\mathbf{q} + i\omega, -K) \approx & -\frac{1}{\omega} \left(1 + \frac{[J(\mathbf{q} + \mathbf{k}) - J(\mathbf{q})]G(\mathbf{q}, i\omega)}{2} \right) \\ & \times [1 + \tilde{\Pi}(\mathbf{q}, i\omega)G^{-1}(\mathbf{q})][1 + \tilde{\Pi}(\mathbf{k}, i\omega)G^{-1}(\mathbf{k})]. \end{aligned} \quad (3.37)$$

However, we will also approximate $[1 + \tilde{\Pi}(\mathbf{q}, i\omega)G^{-1}(\mathbf{q})][1 + \tilde{\Pi}(\mathbf{k}, i\omega)G^{-1}(\mathbf{k})]$ by unity, i.e. explicitly neglect $\tilde{\Pi}$ in these factors. Furthermore we set $G(\mathbf{q}, i\omega) \approx G(\mathbf{q})$. Hence

$$\tilde{\Gamma}^{xyz}(\mathbf{q} + \mathbf{k}, -\mathbf{q} + i\omega, -K) \approx -\frac{1}{\omega} \left(1 + \frac{[J(\mathbf{q} + \mathbf{k}) - J(\mathbf{q})]G(\mathbf{q})}{2} \right). \quad (3.38)$$

Note that

$$\tilde{\Gamma}^{xyz}(\mathbf{q}, -\mathbf{q} + i\omega, -i\omega) \approx -\frac{1}{\omega}, \quad (3.39)$$

which for $\mathbf{q} = \mathbf{0}$ is an exact relation, see appendix A.1. In general the three-point vertex (3.38) is simply a product of $\frac{1}{\omega}$ and a factor that is determined by the static susceptibility and exchange interaction. To justify the above simplifications consider

$$\begin{aligned} G(\mathbf{q} + \mathbf{k})(\omega \tilde{\Gamma}(\mathbf{q} + \mathbf{k}, -\mathbf{q} + i\omega, -K))^2 - G(\mathbf{q}) &= G(\mathbf{q} + \mathbf{k}) - G(\mathbf{q}) \\ &+ G(\mathbf{q})G(\mathbf{q} + \mathbf{k})[J(\mathbf{q} + \mathbf{k}) - J(\mathbf{q})] \\ &+ G(\mathbf{q})^2 G(\mathbf{q} + \mathbf{k})[J(\mathbf{q} + \mathbf{k}) - J(\mathbf{q})]^2. \end{aligned} \quad (3.40)$$

Now, using

$$G(\mathbf{q})G(\mathbf{q} + \mathbf{k})[J(\mathbf{q} + \mathbf{k}) - J(\mathbf{q})] = G(\mathbf{q}) - G(\mathbf{q} + \mathbf{k}) + G(\mathbf{q})G(\mathbf{q} + \mathbf{k})[\Sigma(\mathbf{q}) - \Sigma(\mathbf{q} + \mathbf{k})], \quad (3.41)$$

we see that the undesired contribution $G(\mathbf{q}) - G(\mathbf{q} + \mathbf{k})$ encountered in (3.31) is cancelled with the help of the vertex correction (3.38), so that

$$G(\mathbf{q} + \mathbf{k})(\omega\tilde{\Gamma}(\mathbf{q} + \mathbf{k}, -\mathbf{q} + i\omega, -K))^2 - G(\mathbf{q}) = G(\mathbf{q})G(\mathbf{q} + \mathbf{k})[\Sigma(\mathbf{q}) - \Sigma(\mathbf{q} + \mathbf{k})] + G(\mathbf{q})^2G(\mathbf{q} + \mathbf{k})[J(\mathbf{q} + \mathbf{k}) - J(\mathbf{q})]^2. \quad (3.42)$$

The term in the second line is positive and $\sim J^2/T^3$, therefore having the correct properties after insertion into (3.32). The contribution from the self-energy reads to leading order in a high temperature-expansion, see also Sec. 3.2 [1, 2]

$$G(\mathbf{q})G(\mathbf{q} + \mathbf{k})[\Sigma(\mathbf{q}) - \Sigma(\mathbf{q} + \mathbf{k})] \propto \frac{1}{T^3} \int_{\mathbf{q}} [J^2(\mathbf{q}) - J(\mathbf{q})J(\mathbf{q} + \mathbf{k})], \quad (3.43)$$

which is $\sim J^2/T^3$ and positive definite. Hence the kernel exhibits all properties, which are necessary for a physical equation at high temperatures. Taking the derivative with respect to K , see Eq. (3.33), was therefore warranted. Note that by keeping the frequency finite in $G(\mathbf{q}, i\omega)$, which is contained in the first form of the 3-vertex in Eq. (3.37), we acquire a residue besides the above contributions, that is proportional to $\frac{G(\mathbf{q} + \mathbf{k}) - G(\mathbf{q})}{1 + G^{-1}(\mathbf{q})\tilde{\Pi}(\mathbf{q}, i\omega)}$ which for $\omega \neq 0$ is $\propto J/T^2$, and thus non-physical. Similarly the factors $\sim [1 + G^{-1}(\mathbf{k})\tilde{\Pi}(K)]$ featured in Eq. (3.37) will generate beyond $\mathcal{O}(\omega^{-2})$ additional contributions, that are not cancelled out, with a spurious leading dependence on T , for instance $TG(\mathbf{q} + \mathbf{k})[2\tilde{\Pi}(K)G^{-1}(\mathbf{k}) + (\tilde{\Pi}(K)G^{-1}(\mathbf{k}))^2] \sim T^0$, hence contradicting $\tilde{\Pi} \sim T^{-1}$. Note also that a factor $[1 + \tilde{\Pi}(\mathbf{q}, i\omega)G^{-1}(\mathbf{q})]^2$ implied by Eq. (3.37) would fully eliminate the denominator in $F(\mathbf{q}, i\omega)$ and therefore destroy the non-linear structure $\tilde{\Pi} \sim \tilde{\Pi}^{-m}/\omega^2$, $m > 0$ encountered up to this point. A linear structure in its place would then be inconsistent with dissipative dynamics and prone to breakdowns at $\omega \neq 0$. Hence the omission of these ω -dependent factors is also justified. Finally we want to emphasize, that we motivated our approximation for the irreducible 3-point vertex via the equation of motion for the three-point correlation function and not $\tilde{\Gamma}^{(3)}$ itself. The latter equation has on the level of tree-diagrams a simpler shape, featuring no explicit dependence on J and depending on the two-point vertices instead of the propagator. On the other hand it also contains more intricate diagrams with explicit loop integrations, that couple to $\tilde{\Gamma}^{(3)}$ itself and do not vanish in a local approximation to the vertices appearing under these integrals. Even in the absence of the loops the direct dependence on $\tilde{\Pi}(\mathbf{q}, i\omega)$ with its divergent low-frequency limit rather than $G(K)$, would destroy again the benign structure of the integral equation, in a similar vein to the previously neglected $[1 + \tilde{\Pi}(\mathbf{q}, i\omega)G^{-1}(\mathbf{q})]$ -factors from the tree expansion.

Plugging the vertex correction (3.38) into the self-consistency equation for $\tilde{\Pi}(\mathbf{k}, i\omega)$ we finally arrive at

$$\tilde{\Pi}(\mathbf{k}, i\omega) = \frac{1}{2\omega^2} \int_{\mathbf{q}} \frac{G(\mathbf{q} + \mathbf{k})}{1 + G^{-1}(\mathbf{q})\tilde{\Pi}(\mathbf{q}, i\omega)} \left(G(\mathbf{q})[J(\mathbf{q}) - J(\mathbf{q} + \mathbf{k})]^2 + [\Sigma(\mathbf{q}) - \Sigma(\mathbf{q} + \mathbf{k})] \right). \quad (3.44)$$

Note that by introducing the 3-point vertex from Eq. (3.38) as a Λ -dependent quantity in the initial flow equation (3.1) instead of Eq. (3.32), one will not obtain correct high-temperature asymptotics. Firstly one additional power of J/T is generated with the replacement of $\tilde{F}_{\Lambda}(\mathbf{q}, i\omega)$ by the single-scale propagator $\tilde{F}_{\Lambda}(\mathbf{q}, i\omega)$, turning it thus subleading for $T \rightarrow \infty$. Secondly the term $\sim \hat{G}(\mathbf{q} + \mathbf{k}) - \hat{G}(\mathbf{q})$ is not eliminated by the vertex, in contrast to the

difference of propagators, see Eq. (3.41), so that its problems in the $T \rightarrow \infty$ -limit are retained. In principle one can salvage it as in the case of the second approximate flow equation (3.22), by neglecting Σ_Λ in the numerator of $\tilde{F}_\Lambda(\mathbf{q}, i\omega)$, see (3.23). In that case one is left with a flow equation similar to Eq. (3.22) in the $T \rightarrow \infty$ -limit, differing only by the absence of the $\dot{\tilde{F}}_\Lambda$ -term, which in turn formed the core of Eq. (3.15). Note that by introducing the Katanin-substitution (3.28) in the propagators in (3.1) and extending the Λ -derivative to the now present vertex correction (3.38), while dropping the residue from the product rule, containing $\partial_\Lambda(\tilde{\Gamma}_\Lambda^{(3)})^2 \sim \mathcal{O}(J/T)$, we also arrive at the above integral equation (3.44). The neglected residue, whose presence prevents us from trivially integrating with respect to Λ , shares similar issues with the \dot{G} -contribution without vertex correction, discussed in the previous section 3.1.1. As an example it boasts a term $\sim T\partial_\Lambda[J_\Lambda(\mathbf{q}) - J_\Lambda(\mathbf{q} + \mathbf{k})]F_\Lambda(\mathbf{q}, i\omega)G_\Lambda(\mathbf{q})G_\Lambda(\mathbf{q} + \mathbf{k})$ which has spurious high-temperature asymptotics $\sim \mathcal{O}(T^0)$. As seen several times before the most straightforward way to eliminate such issues is by dropping $\Sigma_\Lambda(\mathbf{q})$ in the numerator of $\tilde{F}_\Lambda(\mathbf{q}, i\omega)$. We conclude, that from the presented choices for approximations solely the integral equation (3.44) is capable of keeping the structure of both propagators intact, while having a physical solution.

Let us conclude this discussion by pointing out, that our assessment of the equations discussed up to this point relied mostly upon the limit $T \gg |J_\Lambda|$. The paramagnetic phase extends much beyond this limit, in particular for systems in $d \leq 2$ dimensions, which are disordered at any finite temperature [24]. Fortunately, the $[J(\mathbf{q}) - J(\mathbf{q} + \mathbf{k})]^2$ -term in (3.44) is positive definite, regardless of temperature, and will lead on its own to outcomes that are in full agreement with the predictions of the dynamic scaling hypothesis [55, 58, 60]. On the other hand, taking a closer look at the vicinity of the phase transition, we note that $\Sigma(\mathbf{q}) - \Sigma(\mathbf{q} + \mathbf{k})$ is for small momenta proportional to the negative change of the spin stiffness $-\Sigma'' = -\nabla_{\mathbf{k}}^2 \Sigma(\mathbf{k})_{\mathbf{k}=\mathbf{Q}}$, with the bare stiffness determined by $J''_Q \sim \nabla_{\mathbf{k}}^2 J(\mathbf{k})_{\mathbf{k}=\mathbf{Q}}$. Usually, the renormalized spin stiffness is, due to loop corrections, larger than the bare one, so that Σ'' is positive [3]. Thus the contribution would be, in contrast to the high-temperature limit (3.43), negative definite. In fact this term will dominate in $d \leq 2$ the right-hand-side for $\omega \rightarrow 0$, implying a non-physical result. An issue with similar severity occurs in $d = 3$ too, because there the self energy at $T = T_c$ is known to behave non-analytically as $|\mathbf{k} - \mathbf{Q}|^{2-\eta}$, $\eta > 0$, so that it does not have a proper series expansion around $\mathbf{k} = \mathbf{Q}$. The negative definite term $\Sigma(\mathbf{q}) - \Sigma(\mathbf{q} + \mathbf{k})$ dominates thus again, implying also a breakdown of the approximation. Even with a positive sign, the term would introduce an additional dependence on a non-universal ratio $\sim \Sigma''/J''_Q$ in the critical regime, thus contradicting a dynamic scaling form for $\tilde{\Pi}(\mathbf{k}, i\omega)$. Such issues do not occur for $T \gg |J|$. In this limit the contribution from the self-energy is positive definite. Moreover there are no singular critical fluctuations at $T \rightarrow \infty$ which are for instance necessary for the arguments laid out in the dynamic scaling hypothesis [54, 56, 58]. Furthermore, since we neglect a lot of terms in our derivation of the vertex correction $\tilde{\Gamma}_\Lambda^{(3)}$, that translate to higher order contributions in J_Λ , our approximation cannot be expected to remain controlled for lower temperatures. Thus we will work with (3.44), involving explicitly the $\Sigma(\mathbf{k})$ -term, only in the high- T limit.

Note that Eq. (3.44) still remains applicable to any other temperature, if one neglects the momentum dependence of $\Sigma(\mathbf{k})$, i.e. $\Sigma(\mathbf{k}) \approx \Sigma$, since then one is left with the J^2 -contribution. In fact, since $\eta \ll 1$ in $d = 3$ [26], the effect of neglecting it should be of minor significance for the qualitative behavior of the dynamic structure factor $S(\mathbf{k}, \omega)$. Corrections from the small anomalous dimension can not be reasonably captured by experiments anyways [61]. Moreover one can eliminate the aforementioned issues, generated by a finite

Σ'' , via the following replacement in the renormalized 3-legged vertex (3.38)

$$J(\mathbf{q}) - J(\mathbf{q} + \mathbf{k}) \rightarrow G^{-1}(\mathbf{q}) - G^{-1}(\mathbf{q} + \mathbf{k}), \quad (3.45)$$

with the new self-consistency equation becoming

$$\tilde{\Pi}(\mathbf{k}, i\omega) = \frac{1}{2\omega^2} \int_{\mathbf{q}} \frac{G(\mathbf{q} + \mathbf{k})G(\mathbf{q})}{1 + G^{-1}(\mathbf{q})\tilde{\Pi}(\mathbf{q}, i\omega)} [G^{-1}(\mathbf{q}) - G^{-1}(\mathbf{q} + \mathbf{k})]^2. \quad (3.46)$$

The proposed substitution eliminates the 'culprit' $\propto \Sigma(\mathbf{q}) - \Sigma(\mathbf{q} + \mathbf{k})$ and reduces to (3.44) for $\Sigma(\mathbf{k}) \approx \Sigma$. It will also produce an equation that for arbitrary $\Sigma(\mathbf{k})$ will be consistent with dynamic scaling in the critical regime. Note that a similar substitution was proposed in the context of mode-coupling theory [55, 60], to reproduce correct dynamic exponents of ferromagnets for $\eta \neq 0$. However, in contrast to us, the unmodified equation was still fine by itself, as it did not feature an isolated self-energy term.

We conclude this section by introducing the quantity $\Delta(\mathbf{k}, i\omega)$ via

$$G^{-1}(\mathbf{k})\tilde{\Pi}(\mathbf{k}, i\omega) = \frac{\Delta(\mathbf{k}, i\omega)}{|\omega|}, \quad (3.47)$$

which we will refer to as the *dissipation energy*. As $\tilde{\Pi}(\mathbf{k}, i\omega)$ it is real-valued and > 0 . Roughly speaking it determines characteristic energies (rates) and thus timescales on which the decay of spin fluctuations with momentum \mathbf{k} takes place. The Matsubara function can then be written in terms of $\Delta(\mathbf{k}, i\omega)$ as

$$G(\mathbf{k}, i\omega) = G(\mathbf{k}) \frac{\Delta(\mathbf{k}, i\omega)}{|\omega| + \Delta(\mathbf{k}, i\omega)}. \quad (3.48)$$

The multiplication of $\tilde{\Pi}(\mathbf{k}, i\omega)$ with $G^{-1}(\mathbf{k})$ also implies that $\Delta(\mathbf{k}, i\omega)$ has a finite limit for $T \rightarrow \infty$, which makes it thus the proper quantity to study in this limit, where it is equivalent to $|\omega|\pi_{\Lambda}(\mathbf{k}, |\omega|/J)$ used for the flow equations in Sec. C.3. Note that the product $G(\mathbf{k})\Delta(\mathbf{k}, i\omega) = |\omega|\tilde{\Pi}(\mathbf{k}, i\omega)$ may be understood as a generalized Onsager coefficient [28, 32], see Sec. 1.4.2. Continuity (2.74) of the susceptibility at $\mathbf{k} \neq \mathbf{0}$, is fulfilled if $\Delta(\mathbf{k}, i\omega)/|\omega| \rightarrow \infty$ for $\omega \rightarrow 0$, which is the case for the solution of (3.44), a consequence of its $\tilde{\Pi} \sim \tilde{\Pi}^{-l}/\omega^2$ -structure at low frequencies. Furthermore spin conversation (2.121) implies

$$\Delta(\mathbf{0}, i\omega) = 0. \quad (3.49)$$

$\Delta(\mathbf{k}, i\omega)$ itself satisfies the integral equation

$$\Delta(\mathbf{k}, i\omega) = \int_{\mathbf{q}} \frac{V(\mathbf{k}, \mathbf{q})}{\Delta(\mathbf{q}, i\omega) + |\omega|}, \quad (3.50)$$

where the kernel $V(\mathbf{k}, \mathbf{q})$ has units of energy squared and is defined as

$$V(\mathbf{k}, \mathbf{q}) = \frac{TG^{-1}(\mathbf{k})G(\mathbf{q} + \mathbf{k})}{2} \left(G(\mathbf{q})[J(\mathbf{q}) - J(\mathbf{q} + \mathbf{k})]^2 + [\Sigma(\mathbf{q}) - \Sigma(\mathbf{q} + \mathbf{k})] \right). \quad (3.51)$$

For small, i.e. hydrodynamic, momenta $k \ll \xi^{-1}$ one can deduce from the expansion of the static quantities that, as long as $G^{-1}(\mathbf{0}) \neq 0$, the right-hand side of (3.50) will behave

analytically, in particular as k^2 to leading order, with odd contributions in q and k vanishing under the integral due to inversion symmetry. As an example for $\Sigma(\mathbf{k}) \approx \Sigma$

$$\int_{\mathbf{q}} \frac{V(\mathbf{k}, \mathbf{q})}{\Delta(\mathbf{q}, i\omega) + |\omega|} = \frac{TG^{-1}(\mathbf{0})}{2} \int_{\mathbf{q}} \frac{G(\mathbf{q})^2 [\nabla_{\mathbf{q}} J(\mathbf{q}) \cdot \mathbf{k}]^2}{\Delta(\mathbf{q}, i\omega) + |\omega|} + \mathcal{O}(k^4). \quad (3.52)$$

Therefore the dissipation energy satisfies for $k \rightarrow 0$

$$\Delta(\mathbf{k}, i\omega) = \mathcal{D}(i\omega)k^2 + \mathcal{O}(k^4), \quad (3.53)$$

where we already identified the k^2 -coefficient with a, possibly frequency-dependent, diffusion constant $\mathcal{D}(i\omega)$ by comparing the expressions for the Matsubara function in (3.48) and (3.21). One can then write the diffusion coefficient, in complete analogy to its previously derived relation with $S(\mathbf{k}, \omega)$ given by (1.116), as

$$\mathcal{D} = \mathcal{D}(0) = \lim_{i\omega \rightarrow 0} \lim_{k \rightarrow 0} \frac{\Delta(\mathbf{k}, i\omega)}{k^2}. \quad (3.54)$$

Anomalous sub- or superdiffusion is characterized by a vanishing or infinite right-hand side. Note however that (3.53) actually implies that the occurrence of spin diffusion is in our case equivalent to $\Delta(\mathbf{k}, 0)$ being non-singular and finite. This means that for diffusion, one simply has

$$\mathcal{D} = \lim_{k \rightarrow 0} \frac{\Delta(\mathbf{k}, 0)}{k^2}. \quad (3.55)$$

On the other hand for anomalous diffusion the low-momentum behavior of $\Delta(\mathbf{k}, i\omega)$ as k^2 always requires a suppression or singularity in its leading ω -dependence to obtain scaling with a non-diffusive exponent $z \neq 2$. In that case it is therefore consistent with

$$\mathcal{D}(i\omega) = \lim_{k \rightarrow 0} \frac{\Delta(\mathbf{k}, i\omega)}{k^2} \sim |\omega|^{(z-2)/z}, \quad (3.56)$$

and obviously at odds with $0 < \Delta(\mathbf{k}, 0) < \infty$.

As already mentioned $\Delta(\mathbf{k}, i\omega)$ is a purely real and positive function of $|\omega|$, if the frequency is treated as a continuous parameter, but in contrast to $\tilde{\Pi}(\mathbf{k}, i\omega)$ it may be non-monotonous-in- ω due to the multiplication with $|\omega|$. Its analytic continuation to frequencies slightly above the real axis, is in general a complex quantity

$$\Delta_{\text{ret}}(\mathbf{k}, \omega) = \Delta(\mathbf{k}, i\omega \rightarrow \omega + i0^+) = \Delta_R(\mathbf{k}, \omega) + i\Delta_I(\mathbf{k}, \omega). \quad (3.57)$$

Knowledge of $\Delta_{\text{ret}}(\mathbf{k}, \omega)$ can then be used to determine the retarded spin-response function $G_{\text{ret}}(\mathbf{k}, \omega)$

$$\begin{aligned} G_{\text{ret}}(\mathbf{k}, \omega) &= G(\mathbf{k}, i\omega \rightarrow \omega + i0^+) = G(\mathbf{k}) \frac{\Delta_R(\mathbf{k}, \omega) + i\Delta_I(\mathbf{k}, \omega)}{\Delta_R(\mathbf{k}, \omega) - i(\omega - \Delta_I(\mathbf{k}, \omega))} \\ &= G(\mathbf{k}) \frac{\Delta_R^2(\mathbf{k}, \omega) + \Delta_I^2(\mathbf{k}, \omega) - \omega\Delta_I(\mathbf{k}, \omega) + i\Delta_R(\mathbf{k}, \omega)\omega}{\Delta_R^2(\mathbf{k}, \omega) + (\omega - \Delta_I(\mathbf{k}, \omega))^2}, \end{aligned} \quad (3.58)$$

which as anticipated fulfills $G_{\text{ret}}(\mathbf{k}, 0) = G(\mathbf{k})$. Note that we used $|\omega| = -i(i\omega)\text{sgn}(\omega)$ which is analytically continued to $-i\omega$, i.e. $i\omega \rightarrow \text{sgn}(\omega)\omega$, because the spectral density $2\text{Im}G_{\text{ret}}(\mathbf{k}, \omega)$ has to be an odd function of ω , whereas $\text{Re}G_{\text{ret}}(\mathbf{k}, \omega)$ is symmetric. This also

requires $\Delta_{R/I}(\mathbf{k}, i\omega)$ to be an even/odd function [28], and in general amounts to choosing the 'correct' branch for determining $\Delta_{\text{ret}}(\mathbf{k}, \omega)$ from its Matsubara pendant, since $\Delta(\mathbf{k}, i\omega)$ depends for small frequencies explicitly on $|\omega|$. The dynamic structure factor $S(\mathbf{k}, \omega)$ written in terms of $\Delta_{\text{ret}}(\mathbf{k}, \omega)$ is then given by

$$\begin{aligned} S(\mathbf{k}, \omega) &= \frac{1}{\pi} \frac{G(\mathbf{k})}{1 - e^{-\beta\omega}} \text{Im} G_{\text{ret}}(\mathbf{k}, \omega) \\ &= \frac{1}{\pi} \frac{\omega G(\mathbf{k})}{1 - e^{-\beta\omega}} \frac{\Delta_R(\mathbf{k}, \omega)}{\Delta_R^2(\mathbf{k}, \omega) + (\omega - \Delta_I(\mathbf{k}, \omega))^2}, \end{aligned} \quad (3.59)$$

also implying $\Delta_R(\mathbf{k}, \omega) > 0$, due to $S(\mathbf{k}, \omega) > 0$.

3.2 High-temperature limit

We start our investigations with large temperatures $T \gg |J|$, see also our first publication, Ref. [10]. For that we first have to determine the explicit shape of the kernel $V(\mathbf{k}, \mathbf{q})$, that is generally given by Eq. (3.51). For the static two-point function it is sufficient to set $G(\mathbf{k}) \approx b'_0/T$ in $V(\mathbf{k}, \mathbf{q})$. Furthermore we need the high temperature behavior of the static self energy $\Sigma(\mathbf{k})$ to calculate explicitly the second contribution in $V(\mathbf{k}, \mathbf{q})$. It is given by

$$\Sigma(\mathbf{k}) = \frac{T}{b'_0} + \frac{\Sigma_2(\mathbf{k})}{T} + \mathcal{O}\left(\frac{J^3}{T^2}\right), \quad (3.60)$$

where the $\mathcal{O}(J^2/T)$ -contribution reads [2]

$$\Sigma_2(\mathbf{k}) = \frac{1}{12} \int_{\mathbf{q}} J(\mathbf{q})J(\mathbf{q} + \mathbf{k}) + \left(b'_0 + \frac{1}{6}\right) \int_{\mathbf{q}} J^2(\mathbf{q}), \quad (3.61)$$

which can be obtained by solving iteratively the flow equation of $\Sigma_\Lambda(\mathbf{k})$, (2.111), to order J_Λ^2 , where it suffices to keep the vertices on the right-hand side at their initial values. The kernel $V(\mathbf{k}, \mathbf{q})$ in Eq. (3.51) can thus be written as

$$V(\mathbf{k}, \mathbf{q}) = \frac{b'_0}{2} [J(\mathbf{q}) - J(\mathbf{q} + \mathbf{k})]^2 + 2[\Sigma_2(\mathbf{q}) - \Sigma_2(\mathbf{q} + \mathbf{k})] + \mathcal{O}\left(\frac{J^3}{T}\right). \quad (3.62)$$

For the modified kernel in Eq. (3.46), featuring a difference of $G^{-1}(\mathbf{k})$, only the first term is present, since the self-energy corrections are subleading in J/T relative to $J(\mathbf{q})$ in that difference. Note that for a short-ranged exchange coupling J_{ij} its Fourier transform $J(\mathbf{k})$ is constructed from a finite number of terms. Products of $J(\mathbf{q})$ involve higher order exponentials, but still have a finite range on the respective Bravais lattice. Furthermore, exponentials that are created by $J(\mathbf{q})J(\mathbf{q} + \mathbf{k})$ and $J(\mathbf{q} + \mathbf{k})^2$ can be also written as a product of \mathbf{q} and \mathbf{k} -dependent harmonics. As a consequence the kernel $V(\mathbf{k}, \mathbf{q})$ can be expanded in the following form

$$V(\mathbf{k}, \mathbf{q}) = \sum_{\mu=1}^M e^{i\mathbf{k} \cdot \mathbf{R}_\mu} V_\mu(\mathbf{q}), \quad (3.63)$$

where $\{\mathbf{R}_\mu\}$ is a set of M vectors on the Bravais lattice. Hence one can also write the dissipation energy as a finite Fourier series

$$\Delta(\mathbf{k}, i\omega) = \sum_{\mu=1}^M e^{i\mathbf{k} \cdot \mathbf{R}_\mu} \Delta_\mu(i\omega), \quad (3.64)$$

with the frequency-dependent amplitudes $\tilde{\Delta}_\mu(i\omega)$ given by the solution of

$$\Delta_\mu(i\omega) = \int_{\mathbf{q}} \frac{V_\mu(\mathbf{q})}{\sum_{\mu'=1}^M e^{i\mathbf{k}\cdot\mathbf{R}_{\mu'}} \Delta_{\mu'}(i\omega) + |\omega|}. \quad (3.65)$$

This greatly facilitates the calculation, since now one only has to deal with a relatively small number of coupled self-consistency equations for $\tilde{\Delta}_\mu(i\omega)$. The fact that our solution for $\Delta(\mathbf{k}, i\omega)$ can be expanded in a finite Fourier series means that it is analytic in the whole Brillouin Zone, which in particular is consistent with the small-momentum expansion of $\Delta(\mathbf{k}, i\omega)$ in Eq. (3.53).

To proceed further one has to specify the type of interaction and Bravais lattice. A good starting point is to consider a nearest neighbor interaction J on a d -dimensional hypercubic lattice with spacing a . The exchange coupling is then

$$J(\mathbf{k}) = J \sum_{\delta} e^{i\mathbf{k}\cdot\delta} = 2dJ\gamma(\mathbf{k}), \quad (3.66)$$

where the sum runs over all $2d$ vectors $\delta = \pm a\mathbf{e}_i$, $i = 1, \dots, d$, connecting the arbitrarily chosen origin to its nearest neighbors, and we have introduced the normalized nearest neighbor form factor on a hypercubic lattice

$$\gamma(\mathbf{k}) = \frac{1}{2d} \sum_{\delta} e^{i\mathbf{k}\cdot\delta} = \frac{1}{d} \sum_{\alpha=1}^d \cos(k_\alpha a). \quad (3.67)$$

Using the following factorization

$$\int_{\mathbf{q}} \gamma(\mathbf{q})\gamma(\mathbf{q} + \mathbf{k}) = \int_{\mathbf{q}} \gamma^2(\mathbf{q})\gamma(\mathbf{k}) = \frac{\gamma(\mathbf{k})}{2d}, \quad (3.68)$$

the $\mathcal{O}(J^2/T)$ -term in the self-energy becomes then

$$\Sigma_2(\mathbf{k}) = \frac{dJ^2}{6} [\gamma(\mathbf{k}) + 12b'_0 + 2], \quad (3.69)$$

and thus its contribution to $V(\mathbf{k}, \mathbf{q})$ is proportional to

$$\Sigma_2(\mathbf{q}) - \Sigma_2(\mathbf{q} + \mathbf{k}) = \frac{dJ^2}{6} [\gamma(\mathbf{q}) - \gamma(\mathbf{q} + \mathbf{k})]. \quad (3.70)$$

For our further analysis it is convenient to introduce dimensionless quantities, defined as

$$\tilde{\Delta}(\mathbf{k}, i\omega) \equiv \frac{\Delta(\mathbf{k}, i\omega)}{|J|\sqrt{b'_0}}, \quad \tilde{\omega} \equiv \frac{\omega}{|J|\sqrt{b'_0}}. \quad (3.71)$$

The newly defined dissipation energy is therefore a function of $\tilde{\omega}$. Writing $\tilde{\omega} = \omega\tau$ we already extract the characteristic timescale $\tau = (|J|\sqrt{b'_0})^{-1}$ of the crossover between the short and long-time regime at large temperatures. Hydrodynamic frequencies then satisfy $\tilde{\omega} \ll 1 \leftrightarrow \omega \ll \tau^{-1}$ at $T = \infty$, forming together with $ka \ll 1$ the collision-dominated regime. The form of τ could be anticipated from the shape of \mathcal{H} and the corresponding equations of motion, given that time-derivatives of spin operators generate terms $\propto J \times [S^\alpha, S^\gamma]$, where the commutator is $\propto S$. The corresponding dimensionless kernel $\tilde{V}(\mathbf{k}, \mathbf{q})$ is given by

$$\tilde{V}(\mathbf{k}, \mathbf{q}) = \frac{[\gamma(\mathbf{q}) - \gamma(\mathbf{q} + \mathbf{k})]^2}{2} + \frac{d}{3b'_0} [\gamma(\mathbf{q}) - \gamma(\mathbf{q} + \mathbf{k})]. \quad (3.72)$$

Note that the contribution from $\Sigma_2(\mathbf{k})$ generates an additional dependence on the spin quantum number S , which otherwise is fully absorbed in the rescaled frequency variable $\tilde{\omega}$. Turning to the Fourier expansion of $\tilde{\Delta}(\mathbf{k}, i\tilde{\omega})$ we find that for $d \geq 2$ it can be solely expressed via three independent amplitudes

$$\tilde{\Delta}(\mathbf{k}, i\tilde{\omega}) = (1 - \gamma(\mathbf{k}))\tilde{\Delta}_1(i\tilde{\omega}) + (1 - \gamma(2\mathbf{k}))\tilde{\Delta}_2^{\parallel}(i\tilde{\omega}) + (1 - \gamma^{\perp}(\mathbf{k}))\tilde{\Delta}_2^{\perp}(i\tilde{\omega}). \quad (3.73)$$

Here $\gamma^{\perp}(\mathbf{k})$ is the normalized off-diagonal next-nearest neighbor form factor on a hypercubic lattice in $d \geq 2$

$$\gamma^{\perp}(\mathbf{k}) = \frac{2}{d(d-1)} \sum_{1 \leq \alpha < \alpha' \leq d} \cos(k_{\alpha}a) \cos(k_{\alpha'}a). \quad (3.74)$$

It is generated by terms $\sim J(\mathbf{q} + \mathbf{k})^2$ in the kernel, same as $\gamma(2\mathbf{k})$, where the latter is the form factor of fourth-nearest (next-nearest in $d = 1$, third-nearest in $d = 2$) neighbors on the hypercubic lattice. In one dimension there is no perpendicular direction, so that only two amplitudes have to be calculated

$$\tilde{\Delta}(\mathbf{k}, i\tilde{\omega}) = (1 - \gamma(\mathbf{k}))\tilde{\Delta}_1(i\tilde{\omega}) + (1 - \gamma(2\mathbf{k}))\tilde{\Delta}_2^{\parallel}(i\tilde{\omega}). \quad (3.75)$$

The self-consistency equations for $d \geq 2$ are given by

$$\begin{aligned} \tilde{\Delta}_1(i\omega) = 2d \int_{\mathbf{q}} \frac{1}{|\tilde{\omega}| + \tilde{\Delta}(\mathbf{q}, i\omega)} + \frac{d}{3b'_0} \int_{\mathbf{q}} \frac{\gamma(\mathbf{q})}{|\tilde{\omega}| + \tilde{\Delta}(\mathbf{q}, i\omega)} \\ - 2\tilde{\Delta}_2^{\parallel}(i\omega) - 2\tilde{\Delta}_2^{\perp}(i\omega), \end{aligned} \quad (3.76a)$$

$$\tilde{\Delta}_2^{\parallel}(i\omega) = -d \int_{\mathbf{q}} \frac{\gamma(2\mathbf{q})}{|\tilde{\omega}| + \tilde{\Delta}(\mathbf{q}, i\omega)}, \quad (3.76b)$$

$$\tilde{\Delta}_2^{\perp}(i\omega) = -2d(d-1) \int_{\mathbf{q}} \frac{\gamma^{\perp}(\mathbf{q})}{|\tilde{\omega}| + \tilde{\Delta}(\mathbf{q}, i\omega)}, \quad (3.76c)$$

whereas for $d = 1$, the third equation simply reads $\tilde{\Delta}_2^{\perp}(i\omega) = 0$. The above system of equations can be evaluated numerically with modest effort. In the following sections we will discuss their solution in different dimensions and compare their performance to approaches, previously used in older publications.

3.2.1 Spin diffusion above two dimensions

For $d > 2$ one finds that these equations imply a finite static dissipation energy $\Delta(\mathbf{k}, 0)$, consistent with spin diffusion, because the behavior of the integrands for small $|\mathbf{q}| = q$ is $\sim q^{d-3}$, and therefore non-singular. The corresponding amplitudes are solutions of

$$\begin{aligned} \tilde{\Delta}_1(0) = 2d \int_{\mathbf{q}} \frac{1}{\tilde{\Delta}(\mathbf{q}, 0)} + \frac{d}{3b'_0} \int_{\mathbf{q}} \frac{\gamma(\mathbf{q})}{\tilde{\Delta}(\mathbf{q}, 0)} \\ - 2\tilde{\Delta}_2^{\parallel}(0) - 2\tilde{\Delta}_2^{\perp}(0), \end{aligned} \quad (3.77a)$$

$$\tilde{\Delta}_2^{\parallel}(0) = -d \int_{\mathbf{q}} \frac{\gamma(2\mathbf{q})}{\tilde{\Delta}(\mathbf{q}, 0)}, \quad (3.77b)$$

$$\tilde{\Delta}_2^{\perp}(0) = -2d(d-1) \int_{\mathbf{q}} \frac{\gamma^{\perp}(\mathbf{q})}{\tilde{\Delta}(\mathbf{q}, 0)}, \quad (3.77c)$$

and the finite spin diffusion coefficient can be extracted from $\tilde{\Delta}(\mathbf{k}, 0)$ to $\mathcal{O}(k^2)$ as

$$\mathcal{D} = \frac{|J|\sqrt{b'_0}a^2}{2d} [\tilde{\Delta}_1(0) + 4\tilde{\Delta}_2^{\parallel}(0) + 2\tilde{\Delta}_2^{\perp}(0)], \quad (3.78)$$

where we used $\gamma(\mathbf{k}) \approx 1 - \frac{(ka)^2}{2d}$ and $\gamma^{\perp}(\mathbf{k}) \approx 1 - \frac{(ka)^2}{d}$ for the form factors. The dominant scaling with $\tau^{-1} \sim |J|\sqrt{b'_0}$, which is $\propto JS$ for $S \gg 1$, is the same as in the result (3.26) from the last flow equation (3.22) and consistent with previous estimates provided by older calculations [42, 74]. Setting $\Delta(\mathbf{k}, i\omega) \approx \Delta(\mathbf{k}, 0) = \Delta_R(\mathbf{k}, 0)$, which we also call Lorentzian approximation [55], one obtains for the dynamic structure factor $S(\mathbf{k}, \omega)$

$$S(\mathbf{k}, \omega) = \frac{b'_0}{\pi} \frac{\Delta_R(\mathbf{k}, 0)}{(\Delta_R(\mathbf{k}, 0))^2 + \omega^2}. \quad (3.79)$$

Here we already used that for $T \rightarrow \infty$, the detailed-balance factor from the fluctuation-dissipation theorem is given by the classical expression $[1 - e^{-\beta\omega}]^{-1} \approx (\beta\omega)^{-1}$. For small momenta $ka \ll 1$, $S(\mathbf{k}, \omega)$ is equivalent to the generic diffusion form in Eq. (1.115) [35, 41]

$$S(\mathbf{k}, \omega) = \frac{b'_0}{\pi} \frac{\mathcal{D}k^2}{(\mathcal{D}k^2)^2 + \omega^2}, \quad (3.80)$$

which consists of a single elastic peak at $\omega = 0$ with a half-width $\sim \mathcal{D}k^2$ and a peak height $\propto (\mathcal{D}k^2)^{-1}$. As expected it can be cast into the scaling form $S(\mathbf{k}, \omega) = k^{-2}s(\omega/k^2)$ with dynamic exponent $z = 2$ and is consistent with the outcomes of other theoretical approaches [74], besides being argued for by hydrodynamics as discussed in Sec. 3.2.1 [41]. The Fourier transform to the time-domain of the diffusion form (3.80) yields then the previously discussed exponential decay of the spin-correlation function [35, 41]

$$\langle S^z(\mathbf{k}, t)S^z(-\mathbf{k}, 0) \rangle \sim S(\mathbf{k}, t) \propto \int \frac{d\omega}{2\pi} \frac{e^{i\omega t}\mathcal{D}k^2}{(\mathcal{D}k^2)^2 + \omega^2} \propto e^{-\mathcal{D}k^2 t} = \tilde{s}(k^2 t), \quad (3.81)$$

generated by the imaginary pole at $\omega = -i\mathcal{D}k^2$. The autocorrelation function in d dimensions decays then via an algebraic long-time tail as

$$\langle S_{\mathbf{0}}^z(t)S_{\mathbf{0}}^z(0) \rangle \sim S(\mathbf{r} = \mathbf{0}, t) \propto \int_{\mathbf{q}} S(\mathbf{q}, t) \sim (\mathcal{D}t)^{-d/2}. \quad (3.82)$$

For finite displacements the Fourier transform contains a Gaussian function of $|\mathbf{r}|(\mathcal{D}t)^{-1/2}$, which approaches unity for $t \rightarrow \infty$ [35, 41]. We shall come back to the last two expressions, and see that at asymptotically large times neither Eq. (3.81) nor Eq. (3.82) tell the whole story and that one has to consider the ω -dependence of $\Delta(\mathbf{k}, i\omega)$ beyond its static limit.

As a first quantitative test of the self-consistency equations, we consider the limit of high dimensions $d \gg 1$, where one can solve for the dynamics, without relying on numerics, by using that integrals over powers of normalized form factors are small in this limit [2]

$$\int_{\mathbf{q}} \gamma^{(i)}(\mathbf{q})^n = \mathcal{O}(d^{-1}). \quad (3.83)$$

This property can be explained by the fact that only collinear terms in the integrand do contribute to these sums, while products of orthogonal exponentials vanish. The number of these combinations scales then with a smaller power of d than d^n , leading to the suppression

of these integrals. As a consequence only the integral without form factor in Eq. (3.77) matters to leading order in $1/d$, meaning that the amplitudes are given by

$$\tilde{\Delta}_1(0) = \sqrt{2d}, \quad \tilde{\Delta}_2^{\parallel}(0) = \tilde{\Delta}_2^{\perp}(0) = 0, \quad (3.84)$$

so that

$$\mathcal{D} = |J|a^2 \sqrt{\frac{b'_0}{2d}}. \quad (3.85)$$

Note that $2d$ is just the coordination number c on the hypercubic lattice. We therefore may extend this formula to the case of any lattice with a large c , by just replacing $2d$ with c . The scaling of \mathcal{D} with $c^{-1/2}$ was also found in the literature [42] and in some sense is intuitive, i.e. that the rate of dissipation should decrease with growing dimensionality.

Results in three dimensions and comparison to previous calculations

Theoretical results for the high-temperature diffusion coefficient are mainly available from methods pursuing two different paths: *first principles* and a more *phenomenological* line. The first direction usually involves the solution of an integro-differential equation [74, 87, 88, 89, 90, 91, 92, 93], that results from truncating an infinite hierarchy of coupled equations [74, 87, 89, 91, 93]. The neglect of higher order diagrams is often justified by using the inverse coordination number $1/c$ as a small parameter. The leading approximation has then the shape of a non-linear generalized Langevin equation [33, 39, 74] for the Kubo relaxation-shape function $\tilde{\mathcal{R}}(\mathbf{k}, t) \equiv G^{-1}(\mathbf{k})\mathcal{R}(\mathbf{k}, t)$, namely

$$\partial_t \tilde{\mathcal{R}}(\mathbf{k}, t) = - \int_0^t dt' \mathcal{K}(\mathbf{k}, t-t') \tilde{\mathcal{R}}(\mathbf{k}, t'). \quad (3.86)$$

Here the memory kernel or 'friction function' $\mathcal{K}(\mathbf{k}, t)$ is related to a two-point relaxation-shape function for the time derivatives of the spin operators $\partial_t \mathbf{S}$ [74]. Those are determined by the equations of motion for \mathbf{S} , yielding a four-operator relaxation function in $\mathcal{K}(\mathbf{k}, t)$, that is in the simplest approximation written as a product of two spin-spin relaxation functions [74]. Note also that $\tilde{\mathcal{R}}(\mathbf{k}, t) = S(\mathbf{k}, t)/b'_0$ for $T \gg |J|$, which helps in applying such decoupling procedures. Assuming $\mathcal{K}(\mathbf{k}, t < 0) = 0$, in accordance with the retarded nature of (3.86), and taking the one-sided Fourier or Laplace-Transform of Eq. (3.86) with $\text{Im}(s) > 0$ one obtains [55]

$$\tilde{\mathcal{R}}_L(\mathbf{k}, s) = \frac{1}{\mathcal{K}_L(\mathbf{k}, s) - is}, \quad (3.87)$$

Hence the full Fourier-transform is with $\mathcal{K}_L(\mathbf{k}, \omega + i0^+) = \mathcal{K}(\mathbf{k}, \omega)$ given by [74]

$$\tilde{\mathcal{R}}(\mathbf{k}, \omega) = 2\text{Re}\left(\tilde{\mathcal{R}}_L(\mathbf{k}, s = \omega + i0^+)\right) = \frac{2\mathcal{K}_R(\mathbf{k}, \omega)}{\mathcal{K}_R^2(\mathbf{k}, \omega) + (\omega - \mathcal{K}_I(\mathbf{k}, \omega))^2}, \quad (3.88)$$

from which we read off by comparing with $S(\mathbf{k}, \omega)$ in Eq. (3.59) that $\mathcal{K}(\mathbf{k}, \omega)$ fulfills an analogous role to the retarded dissipation energy $\Delta_{\text{ret}}(\mathbf{k}, \omega)$ in our case, i.e. that equivalent expressions for both quantities lead to the same outcome for $S(\mathbf{k}, \omega)$. In the same sense $\Delta(\mathbf{k}, i\omega)$ assumes a role similar to $\mathcal{K}_L(\mathbf{k}, s = i\omega)$, the Laplace-transformed memory kernel for purely imaginary frequencies, given that $G(\mathbf{k})\text{Re}[\Delta(\mathbf{k}, i\omega \rightarrow \omega + i0^+) - i\omega]^{-1} = \text{Im}G_{\text{ret}}(\mathbf{k}, \omega)/\omega$. In the leading mode-coupling approximation $\mathcal{K}(\mathbf{k}, t)$ is purely local in time, implying a mixing of frequencies in the self-consistency equation for $\mathcal{K}(\mathbf{k}, \omega)$, contrary to

our local-in- ω equation for $\Delta(\mathbf{k}, i\omega)$. The diffusion coefficient can then be, analogous to our method, determined from its static limit [74]

$$\mathcal{D} = \lim_{k \rightarrow 0} \frac{1}{k^2} \int_0^\infty dt \mathcal{K}(\mathbf{k}, t), \quad (3.89)$$

provided that the $k \rightarrow 0$ -limit is finite, which was assumed by most authors solving these equations [74, 88]. It is however controversial, whether the mode-coupling equation indeed hosts spin diffusion at asymptotically large times [80]. Scaling arguments for the spin-correlation function in the $t \rightarrow \infty$, utilizing in part also the mode-coupling equations, predict dynamic exponents larger than $z = 2$, incompatible with diffusion [78, 80]. Provided that the integral in Eq. (3.89) is convergent, one can determine \mathcal{D} numerically from integrating Eq. (3.86) forward in time with the initial condition $\tilde{\mathcal{R}}(\mathbf{k}, 0) = 1$.

Turning to the *phenomenological* methods, one notes that all of them rely on the high-frequency or short-time expansion of $\tilde{\mathcal{R}}$, and assume that the long-time or low-frequency limit is governed by spin diffusion [42, 77, 87, 88, 94, 95, 96, 97, 98]. The relaxation-shape function at arbitrary times is then obtained via a prudent extrapolation of the short-time expression. In our language one often makes an ansatz for $\Delta(\mathbf{k}, i\omega)$ which amounts to a terminated continuous fraction [33, 98, 99, 100], e.g.

$$\Delta(\mathbf{k}, i\omega) = \frac{\delta_1(\mathbf{k})}{|\omega| + \frac{\delta_2(\mathbf{k})}{|\omega| + \dots}} \approx \frac{\delta_1(\mathbf{k})}{|\omega| + \frac{\delta_2(\mathbf{k})}{|\omega| + \tau^{-1}(\mathbf{k})}}. \quad (3.90)$$

In fact there is a formal motivation for this, since an infinite fraction for $\Delta(\mathbf{k}, i\omega)$ is indeed an exact way to write $\tilde{\mathcal{R}}(\mathbf{k}, \omega)$. Such an expansion can be derived via a memory-function formalism [39, 99], based on a projection procedure with suitable Kubo relaxation functions to define overlaps (A_i, A_j) . More accurately, the fraction is built from an infinite number of dynamic self-energies, which are defined via scalar products between time-evolved quantities and their initial value; for $n > 1$ between components, orthogonal to the $(n - 1)$ -th quantity at $t = 0$ [33, 99] and for $n = 1$ by the overlap $(\mathcal{S}(t), \mathcal{S}(0))$. Each of them satisfies then a Langevin equation, with the corresponding friction kernel proportional to the $(n + 1)$ -th self-energy and $\delta_n(\mathbf{k})$. After successive Laplace-transformations one thus arrives at the structure in (3.90). Eq. (3.90) is often referred to as the *three-pole approximation*, because the denominator of $\tilde{\mathcal{R}}(\mathbf{k}, \omega)$ is a third order polynomial in ω^2 , thus implying three complex poles for ω^2 . For $r(\mathbf{k}) \sim \delta_2(\mathbf{k})/\delta_1(\mathbf{k}) \gg 1$ the line-shape consists of a sole central peak, whereas for $r(\mathbf{k}) \ll 1$ it features two symmetric maxima at finite frequencies. Note that $r(\mathbf{k})^{1/2}$ can be interpreted as the ratio of a damping $\sim \delta_2^{1/2}(\mathbf{k})/\delta_1(\mathbf{k})$ to a dispersion $\sim \delta_1^{1/2}(\mathbf{k})$. Such an approach is often used to complement mode-coupling calculations at lower temperatures and/or larger momenta, where the results of these methods tend to deviate more from experiments [98]. The parameters $\delta_1(\mathbf{k}), \delta_2(\mathbf{k})$ are extracted by demanding that the first two terms to order t^2 and t^4 , in the short-time expansion of $\tilde{\mathcal{R}}(\mathbf{k}, t)$ are reproduced. A popular choice for the decay rate and termination constant of the fraction $\tau^{-1}(\mathbf{k})$ is $\sim \sqrt{\delta_2(\mathbf{k})}$ [98]. Hence $\Delta(\mathbf{k}, i\omega) \sim \delta_1(\mathbf{k})/\delta_2(\mathbf{k})^{1/2} f(|\omega|\tau(\mathbf{k}))$, and $\tau(\mathbf{k})$ separates a low and high-frequency region. At $T = \infty$ it is $\sim (|J| \sqrt{b'_0})^{-1}$, similar to our characteristic time scale. The required short-time coefficients of $\tilde{\mathcal{R}}(\mathbf{k}, t)$ are known as its first two moments $\langle \omega^2 \rangle_{\mathbf{k}}, \langle \omega^4 \rangle_{\mathbf{k}}$, i.e. [95, 98]

$$\langle \omega^{2n} \rangle_{\mathbf{k}} = \int_{-\infty}^{\infty} \frac{d\omega}{2\pi} \omega^{2n} \tilde{\mathcal{R}}(\mathbf{k}, \omega) = (-1)^n \frac{d^{2n}}{dt^{2n}} \tilde{\mathcal{R}}(\mathbf{k}, t) |_{t=0}, \quad (3.91)$$

and can be calculated exactly for $T \gg |J|$ [31, 97, 101]. One can express them via the coefficients $\Delta^{(n)}(\mathbf{k})$ in a high-frequency expansion of $\Delta(\mathbf{k}, i\omega)$ [95],

$$\Delta(\mathbf{k}, i\omega) = \Delta^{(1)}(\mathbf{k})/|\omega| + \Delta^{(2)}(\mathbf{k})/|\omega|^3 + \mathcal{O}(|\omega|^{-5}), \quad (3.92)$$

as

$$\langle \omega^2 \rangle_{\mathbf{k}} = \Delta^{(1)}(\mathbf{k}), \quad (3.93)$$

$$\langle \omega^4 \rangle_{\mathbf{k}} = (\Delta^{(1)}(\mathbf{k}))^2 - \Delta^{(2)}(\mathbf{k}), \quad (3.94)$$

which can for instance be deduced from the relation (1.105) between $G(\mathbf{k}, i\omega)$ and $\mathcal{R}(\mathbf{k}, \omega)$. This also implies $\delta_1(\mathbf{k}) = \Delta^{(1)}(\mathbf{k})$, $\delta_2(\mathbf{k}) = -\Delta^{(2)}(\mathbf{k})/\Delta^{(1)}(\mathbf{k})$ for the parameters in the three-pole ansatz (3.90). Note that the ω^{-6} -decay of $\mathcal{R}(\mathbf{k}, \omega)$ implied by (3.90) leads to all moments beyond $\langle \omega^4 \rangle_{\mathbf{k}}$ being ∞ in this approximation. Common to all extrapolation schemes one finds expressions of the type [77, 87, 88, 95, 98]

$$\mathcal{D} \propto \lim_{k \rightarrow 0} k^{-2} \frac{\langle \omega^2 \rangle_{\mathbf{k}}^{3/2}}{\langle \omega^4 \rangle_{\mathbf{k}}^{1/2}}. \quad (3.95)$$

In contrast to first principles calculations the expression (3.95) is analytically known due to knowledge of the high-temperature moments, which are linear combinations of lattice harmonics [101]. Extensions, which took the conservation of the sixth order moment into account were also discussed, and found only a modest effect on the value of \mathcal{D} [102]. Note that an extrapolation scheme yielding equivalent results for \mathcal{D} is given by assuming a two-parameter Gaussian for $\Delta_R(\mathbf{k}, \omega) \propto \mathcal{N}_{\mathbf{q}} \exp(-(\omega/(2\omega_{\mathbf{q}}^*))^2)$ with $\Delta_I(\mathbf{k}, \omega)$ determined from $\Delta_R(\mathbf{k}, \omega)$ via a Kramers-Kronig relation [88, 94, 95].

For the physical case of $d = 3$, where $c = 6$ is relatively small, our asymptotic $d \rightarrow \infty$ -expression (3.85) is too rough to serve as a reliable estimate. Hence we have to solve numerically for the zero-frequency amplitudes to obtain \mathcal{D} . For this procedure the result for large dimensions (3.85), evaluated at $d = 3$, is still used as an initial guess. The primary amplitude $\Delta_1(0)$, also present in the second approximate flow equation (3.22), turns out to be positive. On the other hand the additional quantities $\Delta_2^{\perp}(0)$ and $\Delta_2^{\parallel}(0)$ are negative, thus reducing \mathcal{D} compared to the simpler form for $\Delta(\mathbf{k}, 0)$ in (3.22), which contains only $\Delta_1(0)$. Our results for the dimensionless quantity $\frac{\mathcal{D}}{|J|a^2\sqrt{4b'_0}}$ as a function of S on the simple cubic lattice are given in Table 3.1. Comparing the outcome $\mathcal{D} = 0.217|J|a^2$ for $S = 1/2$ to previous results, which are listed in Table 3.2, we find it to be about 30 percent smaller than the estimates of mode-coupling theory and extrapolation schemes, using exact moments. It therefore does not surprise us, that it is closer to estimates, which operate either with approximate expressions for the moments $\langle \omega^{2n} \rangle_{\mathbf{k}}$ [88, 90, 91], e.g the leading $1/c$ -expression, or use an entirely different ansatz to relate high and low-frequency regions in the spectral density, e.g. via a truncated Lorentzian for $\mathcal{R}(\mathbf{k}, \omega)$ as done by de Gennes [77]. For $S \rightarrow \infty$ the deviation of our result $\mathcal{D} = 0.193S|J|a^2$ to established values is about 40 percent. Our tendency to underestimate \mathcal{D} could be anticipated from the fact that the leading expression for $\Delta(\mathbf{k}, i\omega)$ at large frequencies, which is $\langle \omega^2 \rangle_{\mathbf{k}}/|\omega|$, is too small by a factor of 2, i.e.

$$\begin{aligned} \Delta(\mathbf{k}, i\omega) &\approx \frac{1}{|\omega|} \int_{\mathbf{q}} V(\mathbf{k}, \mathbf{q}) \approx \frac{b'_0}{|\omega|} \int_{\mathbf{q}} [J(\mathbf{q})^2 - J(\mathbf{q})J(\mathbf{q} + \mathbf{k})] \\ &\rightarrow \langle \omega^2 \rangle_{\mathbf{k}} = c|J|^2 b'_0 (1 - \gamma(\mathbf{k})). \end{aligned} \quad (3.96)$$

One may consider this as a payoff of converting the flow entirely into an integral equation, by neglecting some residual terms, see Sec. 3.1.2. Multiplication of $V(\mathbf{k}, \mathbf{q})$ with two would then increase \mathcal{D} by a factor of $\sqrt{2}$, for instance $\mathcal{D} = 0.307|J|a^2$ for $S = 1/2$ and $\mathcal{D} = 0.273|J|Sa^2$ for $S \gg 1$. This still leaves us with a residual deviation of about 20 percent for $S = \infty$. The fact that these rescaled values are still smaller than the estimate from the flow equation (3.22), which yields the correct second moment, aligns with the observation that a more intricate momentum dependence of $\Delta(\mathbf{k})$ decreases the magnitude of \mathcal{D} . Note that not all of the older estimates involve an explicit dependence on S , beyond the dominant scaling with $|J|\sqrt{b'_0}$. An example is the outcome (3.89) from a numeric integration of the mode-coupling equation (3.86), which reads $\mathcal{D} = 0.57|J|\sqrt{b'_0}a^2$ for the simple cubic lattice [74]. In the context of extrapolation schemes a spin dependence is introduced via a term $\sim 1/b'_0$ in the fourth moment $\langle \omega^4 \rangle_{\mathbf{k}}$ [95]. According to (3.94) it can be written in terms of $\Delta^{(2)}(\mathbf{k})$ and $\Delta^{(1)}(\mathbf{k})$, where the former is in our case given by

$$\Delta^{(2)}(\mathbf{k}) = -\left(c^2 - \frac{c}{6b'_0}\right)|J|^4(b'_0)^2(1 - \gamma(\mathbf{k})). \quad (3.97)$$

As in the exact result [42, 95] we have an additional term $\sim 1/(b'_0) \times (1 - \gamma(\mathbf{k}))$ with the correct sign, which depends explicitly on S . Furthermore this expression has up to prefactors the same \mathbf{k} -dependence as the mode-coupling result for $\Delta^{(2)}(\mathbf{k})$ [74]. The S -dependence $\propto (1 - A/b'_0)^{1/2}$ of $\mathcal{D}/(|J|\sqrt{b'_0})$ from the extrapolation formula (3.95), is much less pronounced than for us though [42, 95]. The larger effect of the Σ -term may be partly explained by the q^0 -weighting at small loop momentum relative to the J^2 -contribution to \mathcal{D} , which scales as $(\mathbf{q} \cdot \mathbf{k})^2$ for $qa \ll 1$, since $[J(\mathbf{q}) - J(\mathbf{q} + \mathbf{k})] \propto 2(\mathbf{q} \cdot \mathbf{k}) + k^2$. We have compared the explicit spin dependence of the diffusion coefficient with the result of extrapolation schemes in Tab. 3.3 to illustrate this difference. Accordingly, estimating \mathcal{D} with our moments from a ratio $\tilde{\Delta}^{(1)}(\mathbf{k})^{3/2}(-\tilde{\Delta}^{(2)}(\mathbf{k}))^{-1/2}$ as in Eq. (3.95), yields also a much weaker magnitude for the S -dependence than the direct solution of our self-consistency equation. This serves as a first demonstration that for us the low and high-frequency sector are not as easily related to each other, as is the case for extrapolation schemes. One may argue on these grounds that one should not divert too much attention to outcomes in the high- ω sector, if one is focused on low-frequency properties, that cannot be reliably estimated from the high-frequency behavior. Note that the strong effect of the contribution $\sim \Sigma(\mathbf{q}) - \Sigma(\mathbf{q} + \mathbf{k})$ in $V(\mathbf{k}, \mathbf{q})$ will become even more apparent in low dimensions $d \leq 2$, where it changes the qualitative behavior in the limit $\omega \rightarrow 0$.

Another way to gain insights are spin dynamics simulations [103, 104], i.e. by solving a classical equation of motion for an ensemble of interacting unit vectors, which represent the spins, using a sufficiently large number of initial randomly generated configurations. However, results at asymptotically long times are mostly inaccessible, in particular in three dimensions, where the computational cost increases rapidly for sufficiently large lattice sizes. Thus one is mostly unable to conclusively determine even the type of the long-time behavior, which is usually read off from the decay of autocorrelations in the time-domain [104, 105, 106], with the diffusive case given by Eq. (3.82). As an example the exponents γ in the long-time tail of $S(\mathbf{r} = \mathbf{0}, t) \sim t^{-\gamma}$ still evolved with t in the largest available time windows [104, 105, 106]. Only in recent years significant progress was made for numerical simulations of one-dimensional systems [85]. We have also repeated the calculation of \mathcal{D} for another three-dimensional isotropic lattice, namely the body-centered cubic (bcc) lattice, including also for both lattices a next-nearest neighbor coupling. The corresponding results can be found in Appendix B.1.

S	$\frac{1}{2}$	1	$\frac{3}{2}$	2	$\frac{5}{2}$	3	$\frac{7}{2}$	∞
$\frac{\mathcal{D}}{ J a^2\sqrt{4b'_0}}$	0.217	0.189	0.179	0.175	0.172	0.171	0.170	0.167

Table 3.1: Our results for the diffusion coefficient \mathcal{D} of the nearest-neighbor spin- S Heisenberg model on a simple cubic lattice with spacing a at $T = \infty$, obtained from the numerical solution of (3.77). Note that we have chosen the normalization factor $\sqrt{4b'_0} = \sqrt{4S(S+1)/3}$ such that it is unity for $S = 1/2$. For the modified kernel in (3.46), this ratio does not depend on S and is equal to the value at $S = \infty$.

Method	$\frac{\mathcal{D}}{ J a^2\sqrt{4b'_0}}$
de Gennes [77]	0.199
Mori <i>et al.</i> [87]	0.295
Bennett <i>et al.</i> [88]	0.225
Redfield <i>et al.</i> [94]	0.296
Resibois <i>et al.</i> [90]	0.255
Blume <i>et al.</i> [74]	0.286
Reiter [92]	0.205
Tucker [102]	0.297
Myles <i>et al.</i> [93]	0.326
Morita [97]	0.317
our method	0.217

Table 3.2: Comparison of our outcome with other theoretical $T = \infty$ -estimates for \mathcal{D} of the nearest-neighbor $S = 1/2$ Heisenberg model on the simple cubic lattice.

S	$\frac{1}{2}$	1	$\frac{3}{2}$	2	$\frac{5}{2}$	∞
$\frac{\mathcal{D}(S)}{\mathcal{D}(S=1/2)\sqrt{4b'_0}}$	1.0	0.871	0.825	0.806	0.793	0.770
Extrapolation scheme	1.0	0.967	0.958	0.955	0.953	0.949

Table 3.3: Comparison of the dependence on S between our results for \mathcal{D} in Table 3.1 and extrapolation schemes, that use the exact second and fourth moment in their expression [42, 87, 95], see (3.95). In our case the contribution $\propto 1/b'_0$ has a much larger effect compared to moment-based approaches.

3.2.2 Non-analytic corrections to spin diffusion

Since we are not limited to $\omega \neq 0$ we continue on taking a closer look at $\Delta(\mathbf{k}, i\omega)$ for finite frequencies, which reveals additional features of interest, in particular concerning the long-time dynamics. Looking at our equations (3.76) for the amplitudes we can first rewrite

$$\frac{1}{|\tilde{\omega}| + \tilde{\Delta}(\mathbf{q}, i\omega)} = \left[1 - \frac{|\tilde{\omega}|}{|\tilde{\omega}| + \tilde{\Delta}(\mathbf{q}, i\omega)} \right] \frac{1}{\tilde{\Delta}(\mathbf{q}, i\omega)}. \quad (3.98)$$

From the presence of the second term we infer, that the leading correction for $\omega \neq 0$ is non-analytic in $d \leq 4$. The reason for this lies in an additional power of $\tilde{\Delta}(\mathbf{q}, i\omega)$, implying an infrared divergence at small momenta $\int dq q^{d-5} \sim 1/q_{\text{low}}^{4-d}$, so that for instance in $d = 3$ the relevant contribution to the integral is cut above $k_{\omega}^* a \sim (|\tilde{\omega}|/\tilde{\mathcal{D}})^{1/2}$. We therefore obtain in three dimensions a correction which is $\sim |\tilde{\omega}|^{1/2}$, i.e.

$$\tilde{\Delta}(\mathbf{k}, i\omega) = \tilde{\Delta}(\mathbf{k}, 0) + \tilde{\Delta}'(\mathbf{k})|\omega|^{1/2} + \mathcal{O}(|\tilde{\omega}|), \quad (3.99)$$

or for the corresponding ω -dependent diffusion coefficient

$$\mathcal{D}(i\omega) \approx \mathcal{D} + \mathcal{D}'|\tilde{\omega}|^{1/2}, \quad (3.100)$$

while in $d = 4$ the correction is logarithmic $\sim \tilde{\omega} \ln(\tilde{\omega})$. $\Delta'(\mathbf{k})$ still has to be determined self-consistently, via linear equations for its amplitudes, which are easily solved, after $\Delta(\mathbf{k}, 0)$ is calculated. For the simple cubic lattice the corrections satisfy

$$\begin{aligned} \tilde{\Delta}'_1 &= -6 \int_{\mathbf{q}} \frac{\tilde{\Delta}'(\mathbf{q})}{\tilde{\Delta}^2(\mathbf{q}, 0)} - \frac{1}{b'_0} \int_{\mathbf{q}} \frac{\gamma(\mathbf{q})\tilde{\Delta}'(\mathbf{q})}{\tilde{\Delta}^2(\mathbf{q}, 0)} \\ &\quad - \frac{6 + 1/b'_0}{4\pi\tilde{\mathcal{D}}^{3/2}} - 2\tilde{\Delta}'_{2,\parallel} - 2\tilde{\Delta}'_{2,\perp}, \end{aligned} \quad (3.101a)$$

$$\tilde{\Delta}'_{2,\parallel} = 3 \int_{\mathbf{q}} \frac{\gamma(2\mathbf{q})\tilde{\Delta}'(\mathbf{q})}{\tilde{\Delta}^2(\mathbf{q}, 0)} + \frac{3}{4\pi\tilde{\mathcal{D}}^{3/2}}, \quad (3.101b)$$

$$\tilde{\Delta}'_{2,\perp} = 12 \int_{\mathbf{q}} \frac{\gamma^\perp(\mathbf{q})\tilde{\Delta}'(\mathbf{q})}{\tilde{\Delta}^2(\mathbf{q}, 0)} + \frac{3}{\pi\tilde{\mathcal{D}}^{3/2}}, \quad (3.101c)$$

where we used $\int_0^\infty \frac{dx}{1+x^2} = \frac{\pi}{2}$ for the terms $\sim \tilde{\mathcal{D}}^{-3/2}$, created by the aforementioned singularity. Explicitly solving those equations, we find that $\Delta'(\mathbf{k})$ is positive for small momenta $ka \ll 1$ and becomes negative for $ka \sim 1$. The solution along one path in the Brillouin Zone is shown in Fig. 3.3. Inserting the result involving a finite $\Delta'(\mathbf{k})$ into $S(\mathbf{k}, \omega)$ we obtain

$$S(\mathbf{k}, \omega) = \frac{b'_0}{\pi} \frac{\Delta(\mathbf{k}, 0) + \Delta'(\mathbf{k})\sqrt{|\tilde{\omega}|/2}}{(\Delta(\mathbf{k}, 0) + \Delta'(\mathbf{k})\sqrt{|\tilde{\omega}|/2})^2 + (\text{sgn}(\omega)\Delta'(\mathbf{k})\sqrt{|\tilde{\omega}|/2} + \omega)^2}, \quad (3.102)$$

where we used for the analytic continuation that $(\tilde{\omega})^{1/2} \rightarrow (1 - i\text{sgn}(\omega))(|\tilde{\omega}|/2)^{1/2}$ to ensure that $\text{Im}G_{\text{ret}}(\mathbf{k}, \omega)$ is an odd function of ω . Obviously, the square-root distorts the previous Lorentzian, implying a non-analytic narrowing for $\omega \rightarrow 0$, instead of a smooth maximum. Indeed, we saw that $\mathcal{D}' > 0$, so that $S(\mathbf{k}, \omega)$ is for small momenta still peaked at $\omega = 0$, whereas for $ka = \mathcal{O}(1)$, the correction is negative, implying a downward slope. At small momentum one still finds a regime of frequencies, where this non-analytic term is negligible. This is the case for the so-called *strict hydrodynamic* limit, given by the prescription $k \rightarrow$

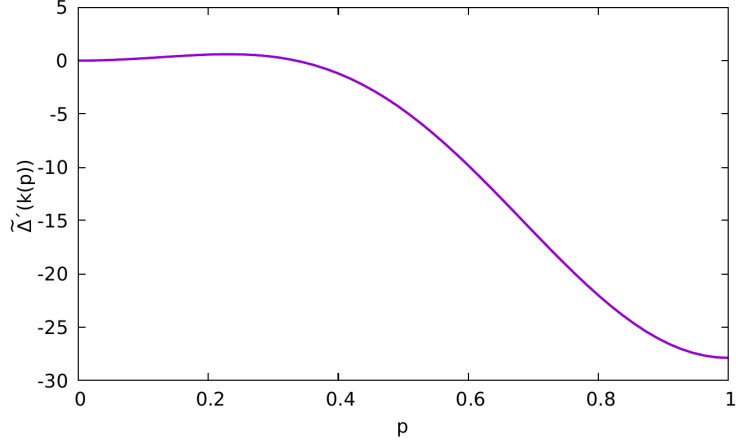


Figure 3.3: $\tilde{\Delta}'(\mathbf{k})$ for a $S = 1/2$ -Heisenberg Model with nearest neighbor-coupling J on a simple cubic lattice, from the solution of (3.101), plotted along the path $\mathbf{k}(p) = \frac{p\pi}{a}(1, 1, 1)$. We obtain $\mathcal{D}' = 0.393|J|a^2$ for the k^2 -coefficient in the low momentum expansion.

0 and $\omega \propto k^2 \rightarrow 0$, so that the leading correction to $\mathcal{D}(i\omega \propto k^2)$ scales as k and can thus be dropped [44, 107]. Going to the time-domain this limiting procedure amounts to asymptotically small k and long times restricted by $\mathcal{D}k^2t = \text{const}$. In that case one still finds that the diffusion pole dominates $S(\mathbf{k}, t) \sim \exp(-\mathcal{D}k^2t)$, while corrections to it can be dropped due to their scaling as $\mathcal{O}(k)$. This is also the limit, which is often implicitly assumed in theoretical discussions concerning diffusion [44, 74, 90, 107]. In the opposite case, at fixed momentum \mathbf{k} and for small ω or long times free of any constraints the asymptotics are driven by the contribution $\sim |\tilde{\omega}|^{1/2}$ in $\Delta(\mathbf{k}, i\omega)$, since it generates a branch point at $\omega = 0$ [44, 107]. As a consequence a term $\sim \mathcal{D}'k(\mathcal{D}k^2t)^{-3/2}$ is created in $S(\mathbf{k}, t)$ [44], which as a power-law exhibits a much weaker decrease than the contribution from the diffusion pole for $t \rightarrow \infty$. Note that the non-analytic square-root correction occurs in our case for any momentum \mathbf{k} , so that $S(\mathbf{k}, t)$ is in general $\propto \Delta'(\mathbf{k})(\Delta(\mathbf{k}, 0)t)^{-3/2}$ for $t \rightarrow \infty$. Since there is no exponential suppression, all momenta in the first Brillouin Zone have a similar non-negligible weight in a \mathbf{k} -integral over this branch cut correction, which makes it thus a non-hydrodynamic contribution. Moreover a potential $1/k^2$ -singularity for $k \ll \mathcal{O}(t^{-1/2})$ in the non-hydrodynamic term is regularized by the integration over \mathbf{k} in $d > 2$. In particular this implies that the long-time tail of the autocorrelation function $S(\mathbf{r} = \mathbf{0}, t)$ in $d = 3$ still falls off as $t^{-3/2}$, but is accompanied by a modified coefficient $\neq \mathcal{D}^{-3/2}$, which is renormalized via the leading non-analytic term in $\Delta(\mathbf{k}, i\omega)$ in the aforementioned manner. Conversely long-time tails of pair-correlation functions $S(\mathbf{r} \neq \mathbf{0}, t)$ would therefore decay with different coefficients, determined by the real space transform of the branch cut correction to $S(\mathbf{k}, t)$.

We want to emphasize that terms with such effects, will be also generated by our equation in higher dimensions, even though above $d = 4$ the first correction to $\Delta(\mathbf{k}, i\omega)$ is always $\propto \tilde{\omega}$, so that $S(\mathbf{k}, \omega)$ retains a Lorentzian shape for small frequencies. This is simply due to the creation of zero-frequency branch points, by multi-valued roots or logarithms, no matter how strong their suppression is in the strict hydrodynamic limit [108], which will lack any exponential decay for $t \rightarrow \infty$. For an odd dimension $d = 2l + 1$ the first non-analytic term is of the form

$$\mathcal{D}(i\omega) - \mathcal{D} \sim (\tilde{\omega})^{l-1/2} \sim (\tilde{\omega})^{(d-2)/2}, \quad (3.103)$$

and in even dimensions $d = 2l$ the correction contains a logarithm

$$\mathcal{D}(i\omega) - \mathcal{D} \sim (\tilde{\omega})^l \ln(\tilde{\omega}) \sim (\tilde{\omega})^{d/2} \ln(\tilde{\omega}), \quad (3.104)$$

Both types lead to an additional contribution $\sim t^{-d/2}$ in $S(\mathbf{k}, t)$ [108] and therefore $S(\mathbf{r}, t)$. These terms appear also as subleading corrections in lower dimensions. However, the change implied by them in $S(\mathbf{r}, t)$ is negligible for $t \rightarrow \infty$ compared to the diffusion pole and leading branch-cut term, since the respective exponents in their algebraic tails are larger. A singular k^{-2} -behavior is then regularized by a \mathbf{k} -integration in $d > 2$, so that their contribution to $S(\mathbf{r}, t)$ retains the exponent from the tail in $S(\mathbf{k}, t)$. The involvement of all length scales in the branch-point contribution to $S(\mathbf{r}, t)$ contradicts the assumption of hydrodynamics [35, 41], namely that the long-time behavior should be governed solely by fluctuations at long wavelengths. Hence one cannot exclude the possibility of even negative autocorrelations in the long-time limit, thus implying at least one damped oscillation. Such a behavior was previously observed in the solution of an approximate kinetic equation, derived by Résibois and De Leener (RDL) [89, 90]. However, their result for $S(\mathbf{0}, t)$ approaches zero via exponentially damped oscillations, not an algebraic long-time tail [90]. Blume and Hubbard (BH) [74] showed later that the RDL equation is only applicable for times $t \lesssim (|J|\sqrt{b'_0})^{-1}$, with their numerical result for $S(\mathbf{0}, t)$ staying positive for all times [74].

Note that similar corrections to $\Delta(\mathbf{k}, i\omega)$ were also found and discussed in the context of mode-coupling theory [109, 110]. At vanishing momentum the leading correction to $\mathcal{D}(i\omega)$ is found to be $\sim |\omega|^{3/2}$ for the Heisenberg model in $d = 3$ [109, 110], smaller than our $|\omega|^{1/2}$, which in turn is a common prediction of mode-coupling theory for fluids [44, 108]. Another difference is the behavior at finite momentum. In that case these non-analyticities occur as functions of $\bar{\mathcal{D}}k^2 - i\omega$, e.g. in $d = 3$ [109, 110, 111]

$$\mathcal{D}(i\omega) - \mathcal{D} \sim \mathcal{D}k^2 \left(\bar{\mathcal{D}}k^2 - i\omega \right)^{3/2}. \quad (3.105)$$

As a consequence the branch points are now located at finite frequencies for $\mathbf{k} \neq \mathbf{0}$, so that in the time-domain an exponential modulation is introduced on top of the algebraic tails [44], for example a term $\sim t^{-5/2} \exp(-\bar{\mathcal{D}}k^2 t)$ [109, 110, 111]. One finds $\bar{\mathcal{D}} < \mathcal{D}$, implying that these corrections still exhibit a slower decay than the diffusive contribution to $S(\mathbf{k}, t)$. In fact the exponential damping becomes weaker with increasing order [107, 110], so that each term is eventually becoming more dominant than its predecessors, even if the algebraic tails fall off more rapidly. This is a highly non-uniform series, so that the exact long-time behavior of $S(\mathbf{k}, t)$ cannot be determined via a truncation at finite order [107, 110]. Nevertheless, that intricacy does not matter for $S(\mathbf{r}, t)$, because the damping with $\bar{\mathcal{D}}k^2 \neq 0$ cuts off the momentum integrals over the branch point corrections for sufficiently large timescales and, as already sketched, divergent pre-factors $\sim 1/k^2$ are regularized by the \mathbf{k} -integration in $d > 2$. Considering that these corrections are already accompanied by the aforementioned decaying long-time tails, these terms are therefore suppressed in $S(\mathbf{r}, t)$. Hence the long-time limit of space-resolved correlations is governed by the purely diffusive expression [44], as postulated by hydrodynamics. In our case the momentum dependence of $\Delta(\mathbf{k}, i\omega)$ is, as a finite superposition of lattice harmonics, incompatible with masked corrections at $k \neq 0$, thus leading to an absent damping in the time-domain. Despite this shortcoming our result still serves as an illustration on how behavior at asymptotically long times or low frequencies is not solely driven by hydrodynamics in a naive sense, which are formally only valid in the aforementioned scaling regime. We have added a more detailed discussion of the long-time asymptotics, which arise from the non-analytic contributions to $\Delta(\mathbf{k}, i\omega)$, in appendix B.2.1.

Note that in contrast to our approach, extrapolation schemes, e.g. (3.90), which assume a definite low-frequency limit, based on high-frequency properties, also exclude the possibility of non-analytic corrections to $\Delta(\mathbf{k}, i\omega)/k^2$. The first correction to \mathcal{D} is then usually of the order $|\omega|$. Such contributions amount then to simple renormalizations of the diffusion pole $\mathcal{D}k^2$, i.e. small relative corrections $\sim \mathcal{O}(k^2)$ in the exponential decay of $S(\mathbf{k}, t)$ [109]. The behavior of the strict hydrodynamic limit can therefore be extended without problems to asymptotically large times [98].

3.2.3 Anomalous diffusion in reduced dimensions

In low dimensions $d \leq 2$ we find that $\Delta(\mathbf{k}, i\omega)$ cannot have a finite static limit, therefore ruling out spin diffusion. As a consequence one has to consider the leading frequency dependence of the dissipation energy, which turns out to diverge for $\omega \rightarrow 0$. The reason for this lies in the infra-red behavior of the integrals, which prevents us from directly setting $\omega = 0$ in $[\Delta(\mathbf{k}, i\omega) + |\omega|]$. Instead, the singular behavior of $\int \frac{dq q^{d-1}}{|\tilde{\omega}| + \tilde{\Delta}(\mathbf{q}, i\omega)}$ for $\omega \rightarrow 0$ implies that the integrations are cut above

$$k_\omega^* a = (\omega/\mathcal{D}(i\omega))^{1/2}. \quad (3.106)$$

In this region one can accordingly truncate the expansion of the dissipation energy after quadratic order

$$\tilde{\Delta}(\mathbf{k}, i\omega) \approx \tilde{\mathcal{D}}(i\omega)k^2 + \mathcal{O}(k^4). \quad (3.107)$$

Furthermore we note that one can also approximate in all integrals

$$\int_{\mathbf{q}} \frac{f(\mathbf{q})}{|\tilde{\omega}| + \tilde{\mathcal{D}}(i\omega)q^2} \approx f(\mathbf{0}) \int_{\mathbf{q}} \frac{1}{|\tilde{\omega}| + \tilde{\mathcal{D}}(i\omega)q^2}, \quad (3.108)$$

where $f(\mathbf{q})$ is assumed to be a slowly varying function for momenta $k \ll k_\omega^*$, for instance a form factor. Finite- q corrections to $f(\mathbf{q})$ as well as $\mathcal{O}(q^4)$ -terms in $\tilde{\Delta}(\mathbf{q}, i\omega)$ are then suppressed as some power of $k_\omega^* a \ll 1$. Note that the integral runs over the whole \mathbf{q} -space in this limit, since it is ultraviolet convergent due to the confinement for small q . The dissipation energy satisfies therefore in the low-frequency limit

$$\tilde{\Delta}(\mathbf{k}, i\omega) = \int_{\mathbf{q}} \frac{\tilde{V}(\mathbf{k}, \mathbf{0})}{|\tilde{\omega}| + \tilde{\mathcal{D}}(i\omega)q^2}, \quad (3.109)$$

with its momentum dependence for $\tilde{\omega} \ll 1$ entirely generated by

$$\tilde{V}(\mathbf{k}, \mathbf{0}) = \frac{[\gamma(\mathbf{0}) - \gamma(\mathbf{k})]^2}{2} + \frac{d}{3b'_0}[\gamma(\mathbf{0}) - \gamma(\mathbf{k})]. \quad (3.110)$$

Note that the first term is $\mathcal{O}(k^4)$, because the contribution at $\mathcal{O}(k^2)$ behaves as $(\mathbf{k} \cdot \mathbf{q})^2$ thus removing the IR-singularity on that level and featuring an additional suppressed power of $k_*(\omega)a \ll 1$ relative to the leading term. Hence the singular contribution to $\mathcal{D}(i\omega)$ is solely determined by the static self-energy correction $\sim (b'_0)^{-1}$. This also means that in the absence of the latter the approximation (3.107) is inapplicable, and therefore has to be tweaked. Continuing now with a finite $(b'_0)^{-1}$ -term, we are left with determining $\mathcal{D}(i\omega)$. Using the small- k expansion of the form factor $\gamma(\mathbf{k})$, we obtain the self-consistent relation

$$\tilde{\mathcal{D}}(i\omega) = \frac{a^2}{6b'_0} \int_{\mathbf{q}} \frac{1}{|\tilde{\omega}| + \tilde{\mathcal{D}}(i\omega)q^2}. \quad (3.111)$$

One dimension

Evaluating the right-hand side of (3.111) in $d = 1$ yields

$$\mathcal{D}(i\omega) = \left(\frac{|J|}{144|\omega|} \right)^{1/3} |J|a^2, \quad (3.112)$$

and its analytic continuation is therefore

$$\mathcal{D}(i\omega \rightarrow \omega + i0^+) = \left(\frac{|J|}{144|\omega|} \right)^{1/3} \left(\frac{\sqrt{3}}{2} + i \frac{\text{sgn}(\omega)}{2} \right) |J|a^2 = \mathcal{D}_1 \left(\sqrt{3} + i \text{sgn}(\omega) \right) \left(\frac{|J|}{\omega} \right)^{1/3}, \quad (3.113)$$

implying $k_\omega^* \sim \omega^{2/3}$ for the cutoff or characteristic momentum. Note that $\mathcal{D}(i\omega)$ just scales as $|J|$ instead of $|J|\sqrt{b_0}$, since the dominant small- ω contribution to $\mathcal{D}(i\omega)$ is $\propto (b_0')^{-1}$. The divergence of the frequency-dependent diffusion coefficient with $|\tilde{\omega}|^{-1/3}$ is equivalent to anomalous superdiffusion. Since the exponent in the singularity is < 1 , both imaginary and real part are of the same order, in accordance with dissipative dynamics. The corresponding dynamic structure factor reads

$$S(\mathbf{k}, \omega) = \frac{\sqrt{3}\mathcal{D}_1 k^2 |\omega/|J||^{1/3}}{(\sqrt{3}\mathcal{D}_1 k^2)^2 + (\omega|\omega/J|^{1/3} - \text{sgn}(\omega)\mathcal{D}_1 k^2)^2}, \quad (3.114)$$

which yields $\lim_{k \rightarrow 0} \omega^2/k^2 S(\mathbf{k}, \omega) \sim |\omega|^{-1/3} \sim \mathcal{D}(\omega)$, consistent with Eq. (1.116). $S(\mathbf{k}, \omega)$ vanishes non-analytically as $|\tilde{\omega}|^{1/3}$ for $\omega \rightarrow 0$ and exhibits as a function of ω a broad maximum at a finite characteristic frequency $\omega_*(k) \sim k^z$, with a dynamic index $z = 3/2$ in contrast to $z = 2$ for diffusion. This can be seen by casting Eq. (3.114) into the form

$$S(\mathbf{k}, \omega) \sim k^{-3/2} \tilde{s}_1^{k,\omega} (\omega(\mathcal{D}_1)^{-3/4} k^{-3/2}). \quad (3.115)$$

The dependence on the scaling variable $\omega k^{-3/2}$ for small momenta and frequencies implies accordingly that in the time-domain the scaling form is

$$S(\mathbf{k}, t) \sim \tilde{s}_1^{k,t} ((\mathcal{D}_1)^{3/4} k^{3/2} t), \quad (3.116)$$

with the corresponding scaling function

$$\tilde{s}_1^{k,t}(y) = \int_0^\infty \frac{du \sqrt{3} u^{1/3} \cos(uy)}{\pi (3 + (u^{4/3} - 1)^2)}, \quad (3.117)$$

where $u = \mathcal{D}_1 k^2 / (\omega(\omega/J)^{1/3})$. This will not result in a simple exponential (3.81) at asymptotically large times like for ordinary diffusion. In fact one should note here the simultaneous presence of branching points at $u = 0$ and complex poles in the denominator, due to the non-analytic u -dependence. One can contrast that with the diffusion form for $S(\mathbf{k}, \omega)$ in Eq. (3.80) which implies purely imaginary poles without any branch points. Transforming to real space one sees that $S(\mathbf{r}, t)$ decays as $t^{-2/3}$ for long times, i.e.

$$S(\mathbf{r}, t) \sim t^{-2/3} \tilde{s}_1^{r,t} (r \mathcal{D}_1^{-1} t^{-2/3}), \quad (3.118)$$

implying also $\int dr S(\mathbf{r}, t) r^2 / \int dr S(\mathbf{r}, t) \sim (\Delta r)^2 \sim t^{2/3}$ for the spread in real space. Note that $\tilde{s}_1^{r,t}(rt^{-2/3})$ is not a Gaussian, opposed to initial findings in numerical calculations, which simply suggested a diffusion law in non-linear time $\sim t^{4/3}$ [48].

A scaling with exponent $z = 3/2$ is characteristic of the Kardar-Parisi-Zhang (KPZ) universality class [81, 86]. For instance the solution of the eponymous non-linear stochastic partial differential equation in $(1 + 1)$ dimensions [112, 113] belongs to this class. Besides having the same dynamic exponent it is also believed that the spin-correlation function for integrable isotropic linear magnets at asymptotically large times is given by the KPZ scaling function [81, 86]. A scaling form for $S(\mathbf{k}, \omega)$ like in Eq. (3.115) with a vanishing scattering intensity for $\omega \rightarrow 0$, was also found by Sanchez *et al.* [51, 84] in a semiphenomenological treatment of the frequency-dependent spin conductivity $\sigma(\omega)$, which can be identified with our $\mathcal{D}(i\omega)$ [51]. However, other authors arrive at the result that the $\omega^{-1/3}$ -divergence of $\Delta(\mathbf{k}, i\omega)$ is regularized at $k \neq 0$ [49, 113]. In particular this is the case for the exact KPZ scaling function [113], whose (\mathbf{k}, t) -representation is well described by an exponential decay with a superimposed oscillation [113]. A simple way to account for this is to replace $\omega^{-1/3} \rightarrow (Ck^{3/2} + \omega)^{-1/3}$, so that $\mathcal{D}(i\omega) \rightarrow \mathcal{D}(Ck^{3/2} + \omega)$ [45, 46]. Our result would thus be equivalent to the limit $Ck^{3/2} \ll \omega$, which is also the relevant one to determine the type of dissipative mechanism as in (1.116) or (3.54). Conversely for $\omega \ll Ck^{3/2}$ the dissipation energy scales in the presence of screening as $k^{3/2}$ instead of k^2 [45, 46, 49]. This cannot happen in our case, because the \mathbf{k} -dependence of our solution is determined by a finite-ranged Fourier expansion. In some sense this is analogous to the situation in $d > 2$, where such modifications at non-zero momentum \mathbf{k} appear in the corrections to the static limit $\Delta(\mathbf{k}, 0)$ and shift the branch points to finite values, see Eq. (3.105). In our case without screening the branch cut contribution to $S(\mathbf{k}, t)$, is a power-law for $k^2 t \rightarrow \infty$, i.e. $(kt^{1/z})^{-2}$. It will always either dominate or be of the same order, compared to terms generated by poles, i.e. roots of the denominator of $\tilde{s}_1^{k, \omega}$, which imply exponentially damped oscillations. This is due to the fact that in contrast to $d > 2$, where the cuts are not part of the hydrodynamic scaling form for $S(\mathbf{k}, \omega)$ at small k and ω , one cannot neglect them here for any value of the scaling variable $k^z t$. Correlations $S(\mathbf{r}, t)$ in real space and long times are determined by both, pole and branch cut, as in higher dimensions. However, there is a salient difference, namely that the contribution from the branch cut to $S(\mathbf{r}, t)$ will be also dominated by small momenta $k \lesssim \mathcal{O}(t^{-z})$ in the \mathbf{k} -integral analogous to the (super-)diffusion pole. One can infer this from the $1/k^2$ -behavior of the branch-cut term for $t \rightarrow \infty$, which implies an infrared singularity $\sim 1/k$ and thus the confinement to small k . We have laid out in appendix B.2.2 the effect of branch-cut contributions in $S(\mathbf{k}, \omega)$ on the time-resolved dynamics in $d = 1$. Note that a vanishing elastic scattering $S(\mathbf{k}, 0)$, implies, according to the spectral representation of $S(\mathbf{k}, \omega)$ (1.78) that the contribution of terms with vanishing energy difference, in particular transitions between degenerate states, remains negligible in the thermodynamic limit, in contrast to normal diffusion, where $S(\mathbf{k}, 0) \neq 0$.

In Fig. 3.4 we display the frequency dependence at a small momentum, including also a correction $\sim \omega^{1/3}$ to $\Delta(\mathbf{k}, i\omega)$, beyond the aforementioned scaling limit, defined by $\omega \sim k^z$, $k \rightarrow 0$, where it is negligible. It has no effect on the superdiffusive form (3.114) for $\omega \rightarrow 0$, i.e. its vanishing, but changes the curve for frequencies $\omega \gtrsim \omega_{\text{Peak}}$. Furthermore this term does not, in contrast to $d > 2$, contribute to leading order in $t^{-1/z}$ to $S(\mathbf{r}, t)$. As already mentioned anomalous superdiffusion, characterized by the long-time scaling with dynamic exponent $z = 3/2$, is at least in agreement with calculations for the isotropic Heisenberg spin-1/2 chain with nearest neighbor-coupling [47, 48, 49, 50, 51, 81, 82, 84, 85, 86]. Note that this model is integrable, i.e. exactly solvable by means of the Bethe-ansatz [114]. Integrability is associated with additional symmetries and in fact with a macroscopic number of conservation laws. Generalizations of hydrodynamic descriptions, developed specifically for integrable systems, established arguments for the occurrence of superdiffusion in the

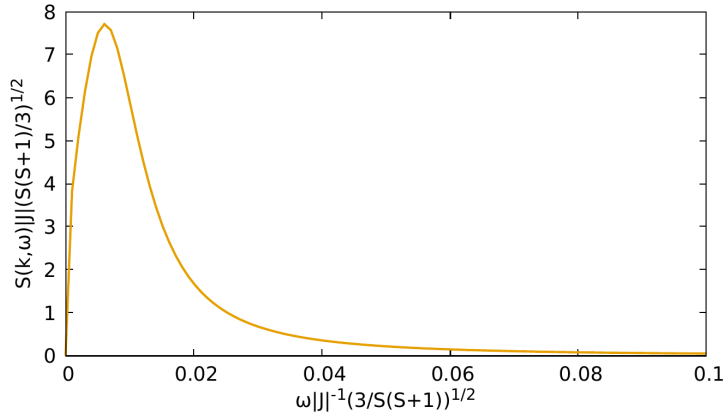


Figure 3.4: Frequency dependence of the dynamic structure factor, built from the first two low-frequency terms in $\Delta(\mathbf{k}, i\omega) = \Delta'(\mathbf{k})|\omega|^{-1/3} + \Delta''(\mathbf{k})|\omega|^{1/3} + \dots$, at $T = \infty$ of the $S = 1/2$ -Heisenberg Model nearest-neighbor-chain for a fixed momentum $ka = 0.1$. One clearly sees the suppression of $S(\mathbf{k}, \omega)$ for $\omega \rightarrow 0$.

isotropic limit of the Heisenberg Model [49, 50]. On the other hand chains with a finite next-nearest neighbor coupling or $S > 1/2$ are non-integrable and therefore do not possess the above symmetries. For these models the situation regarding the long-time dynamics is more controversial. In fact some methods predicted superdiffusion for arbitrary spin chains [82]. Ultimately the overall evidence favors in this case diffusive dynamics $z = 2$ for sufficiently large times, so that $S(\mathbf{0}, t) \sim t^{-1/2}$, see also Eq. (3.82), crossing over from the superdiffusive $z = 3/2$ at intermediate timescales. This was convincingly demonstrated in numerical calculations of the autocorrelation function by Dupont and Moore [85] based on tensor networks methods. On phenomenological assumptions Nardis *et al.* argued [83], that while there is a crossover from $z = 3/2$ to some weaker decay in $S(\mathbf{0}, t)$, the diffusion constant still diverges logarithmically for $t \rightarrow \infty$, which is, however, numerically hard to resolve for the accessible time windows. Note that in our case, integrability does not play any role at all, and the behavior of the system is entirely tied to its dimensionality, similar to normal fluids in mode-coupling theory [44, 45, 46]. One reason for the deviations in the non-integrable cases, may be the local-in- ω shape of our equation (3.50), accounting only for elastic processes, which may be an insufficient approximation for too low frequencies. Older calculations within a modified mode-coupling approximation [79] obtained $S(\mathbf{0}, t) \sim t^{-2/3}$ in an intermediate time-window, similar to the aforementioned numerical simulations [85] of non-integrable systems. However, a scaling analysis of the mode-coupling equations suggests an exponent $z = 5/2$ instead of $z = 2$ for asymptotically large times, thus indicative of a subdiffusive long-time tail in $S(\mathbf{0}, t)$ [79, 80].

Two dimensions

In two dimensions the leading singularity is logarithmic, and Eq. (3.111) implies therefore

$$\mathcal{D}(i\omega) = \sqrt{\ln\left(\frac{\mathcal{D}(i\omega)}{a^2|\omega|}\right)} \frac{|J|a^2}{\sqrt{24\pi}}. \quad (3.119)$$

In the limit $\omega \rightarrow 0$ we can solve this equation by iterating the logarithm, i.e. replacing $\mathcal{D}(i\omega)$ on the right-hand side by the prefactor, hereby neglecting nested terms $\ln \ln(|J|/\omega)$ at subleading order. We thus obtain for the anomalous diffusion coefficient in real frequencies

$$\mathcal{D}(\omega) = \frac{|J|a^2}{\sqrt{24\pi}} \sqrt{\ln\left(\frac{|J|}{\sqrt{24\pi}|\omega|}\right) + i\frac{\pi}{2}\text{sgn}(\omega)} \approx \mathcal{D}_2 \ln^{1/2}\left(\frac{|J|}{\sqrt{24\pi}|\omega|}\right), \quad (3.120)$$

where we used that the imaginary part under the square-root is logarithmically suppressed compared to the real part. Keeping it to leading order in $\ln^{-1}(|J|/\omega)$, we simply obtain

$$\mathcal{D}(\omega) \approx \mathcal{D}_2 \left(\sqrt{\ln\left(\frac{|J|}{\sqrt{24\pi}|\omega|}\right) + i\frac{\pi}{4}\text{sgn}(\omega)} \right). \quad (3.121)$$

The scattering intensity is thus given by

$$S(\mathbf{k}, \omega) = \frac{\mathcal{D}_2 k^2 \ln\left(\frac{|J|}{\sqrt{24\pi}|\omega|}\right)^{-1/2}}{(\mathcal{D}_2 k^2)^2 + \omega^2 \ln^{-1}\left(\frac{|J|}{\sqrt{24\pi}|\omega|}\right)}, \quad (3.122)$$

with spectral weight suppressed like $\ln^{-1/2}(|J|/\omega)$ in the low-frequency limit. The logarithmic correction arises from $d = 2$ being the marginal dimension in Eq. (3.77). The scaling of the characteristic frequency for $ka \rightarrow 0$ is thus approximatively given by $\omega_*(k) \sim k^2 \ln^{1/2}(1/(ka))$ for $k \rightarrow 0$, yielding also the position of the broad peak in $S(\mathbf{k}, \omega)$, or conversely $k \sim \omega^{1/2} \ln^{-1/4}(1/\tilde{\omega}) \sim k_\omega^* \sim (\omega/\mathcal{D}(i\omega))^{1/2}$, i.e.

$$S(\mathbf{k}, \omega) \sim k^{-2} \ln^{-1/2}(1/(ka)) \tilde{s}_2^{k,\omega}(\omega/\omega_*(k)). \quad (3.123)$$

This implies in turn

$$S(\mathbf{k}, t) \sim \tilde{s}_2^{k,t}(k^2 \ln^{1/2}(1/(ka))t), \quad (3.124)$$

which yields a characteristic time scale via $k \sim t^{-1/2} \ln(t/|J|)^{-1/4}$, i.e. $t_*(k) \sim \omega_*(k)^{-1}$, leading in the end to

$$S(\mathbf{r}, t) \sim \ln(t)^{-1/2} t^{-1} \tilde{s}_2^{r,t}(r \ln(t/|J|)^{-1/4} t^{-1/2}). \quad (3.125)$$

Hence the autocorrelation function vanishes as $t^{-1} \ln^{-1/2}(t)$ [115] in contrast to the result for normal diffusion, which is $S(\mathbf{0}, t) \sim t^{-1}$, see Eq. (3.82). For $\tilde{s}_2^{r,t}$ we expect, as for the linear chain, contributions from the branch cut at zero frequency and superdiffusion poles in $\tilde{s}_2^{k,\omega}$, with the relevant region in the \mathbf{k} -integration again being confined to small arguments of the scaling function $\tilde{s}_2^{k,t}$, i.e. $k \lesssim t^{-1/2} \ln^{-1/4}(t)$. Note that our outcomes for the divergence of $\mathcal{D}(i\omega)$ in $d = 1$ and 2 , were also found in the context of mode-coupling theory applied to fluids [44, 115]. In that context one neglected screening at finite momentum too, thus implying the same divergence for $\omega \rightarrow 0$ and arbitrary k . As in $d = 1$, it is not a bold proposition to regularize this singularity by means of $\ln^{1/2}((\tilde{\omega})^{-1}) \rightarrow \ln^{1/2}(1/(ka)^2 + \tilde{\omega}^{-1})$, implying a non-analytic correction $\sim \ln^{1/2}(ka)$ to the dispersion. This was later taken care of in a dynamic renormalization group analysis by Forster *et al.* using $\epsilon = 2 - d$ as a small parameter for normal fluids [45, 46], where asymptotics expressions of $\Delta(\mathbf{k}, i\omega)/k^2$ were given for $\omega \rightarrow 0$ or $k \rightarrow 0$ in reduced dimensions. We emphasize again that the onset of superdiffusion in reduced dimensions is solely a consequence of the q^0 -behavior

of $\Sigma(\mathbf{q}) - \Sigma(\mathbf{q} + \mathbf{k})$ for $q \rightarrow 0$. This shows how, on a moment-based level seemingly inconspicuous, terms like the $(b'_0)^{-1}$ -contribution [42, 95], which is also not accounted for in mode-coupling theory for magnets [74], may alter the whole structure of the solution.

Unfortunately, converged results regarding the long-time or low-frequency behavior of the dissipation energy and therefore spin-correlation functions are not available up to this point in two dimensions, in contrast to $d = 1$. Extrapolation schemes are based on the assumption of diffusive long-time asymptotics [95, 97, 116]. Numerical solutions of the mode-coupling equations, as first performed by Blume and Hubbard [74], are consistent with normal diffusion in low dimensions [117], while a more recent scaling analysis by Lovesey and Balcar [80] rules out ordinary diffusion, although with a subdiffusive exponent $z > 2$. An explicit numerical evaluation of the mode-coupling equations, again by Lovesey [80], predicts in an intermediate time-window a dynamic exponent z that is slightly below 2, thus indicative of superdiffusion. For $t \rightarrow \infty$ it is then expected to change over to the subdiffusive value from the scaling argument. Superdiffusive intermediate behavior was also found in an experiment by Hild *et al.* performed on ultracold atoms, where the setup is reasonably described by an isotropic Heisenberg ferromagnet [118]. There are no available numerical simulations of the spin dynamics, that can give conclusive results on the $t \rightarrow \infty$ -asymptotics, with the more recent ones still being unable to leave intermediate times [106], i.e. achieve convergence. In any case a numeric corroboration of a logarithmic divergence in the time-domain, as found here, is a challenging endeavour.

Alternative equation

Let us also briefly discuss the changes to our solutions in reduced dimensions if one removes the contribution generated by the momentum dependence of $\Sigma(\mathbf{k})$, which amounts to solving (3.46). Since this term is $\propto (b'_0)^{-1}$, the results here can be formally considered as an intermediate frequency dependence in the initial equation (3.50) as long as $S \gg 1$, so that the self-energy term is suppressed. For $\omega \rightarrow 0$ one would still arrive at the previously discussed behavior. As mentioned, the k^2 -term in $\Delta(\mathbf{k}, 0)$ is suppressed compared to all terms of higher order in k , due to the accompanying q^2 -factor. Hence a truncation, retaining only $\mathcal{D}(i\omega)k^2$ in its expansion does not work out. It turns out that, at least in $d = 1$, it is sufficient to include the k^4 -term. Thus we approximate

$$\Delta(\mathbf{k}, i\omega) \approx \mathcal{D}(i\omega)k^2 + \mathcal{D}''(i\omega)k^4, \quad (3.126)$$

$$\mathcal{D}(i\omega) = \frac{2b'_0(J'')^2 a^2}{\pi} \int_0^{\pi/a} \frac{dq q^2}{|\omega| + \mathcal{D}(i\omega)q^2 + \mathcal{D}''(i\omega)q^4}, \quad (3.127)$$

$$\mathcal{D}''(i\omega) = \frac{b'_0(J'')^2 a^4}{2\pi} \int_0^{\pi/a} \frac{dq}{|\omega| + \mathcal{D}(i\omega)q^2 + \mathcal{D}''(i\omega)q^4}. \quad (3.128)$$

These two equations can be solved by the following ansatz

$$\mathcal{D}(i\omega) = \mathcal{D}^{(1)} |\omega/J''|^{1/5} |J''| a^2, \quad (3.129)$$

$$\mathcal{D}''(i\omega) = \mathcal{D}^{(2)} |\omega/J''|^{-3/5} |J''| a^4. \quad (3.130)$$

with the numeric coefficients satisfying $\mathcal{D}^{(1/2)}$ satisfying

$$(\mathcal{D}^{(1)})^{\frac{5}{2}} = \frac{2b'_0}{\pi} \int_0^\infty \frac{du u^2}{1 + u^2 + \left(\frac{\mathcal{D}^{(1)}}{\sqrt{\mathcal{D}^{(2)}}}\right)^4 u^4}, \quad (3.131)$$

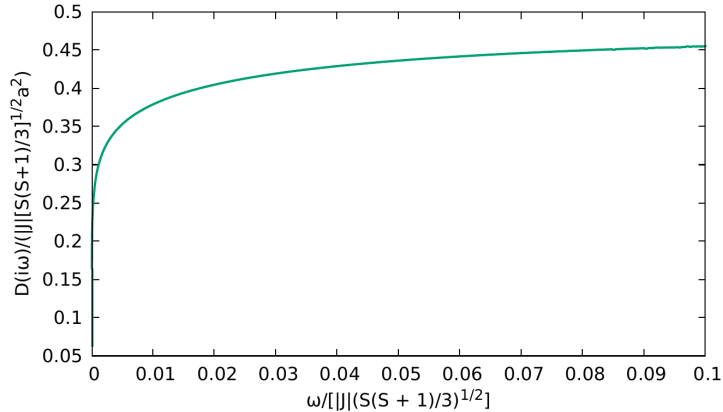


Figure 3.5: Frequency dependence of the k^2 -coefficient $\mathcal{D}(i\omega)$ at $T = \infty$ of the Heisenberg Model on a square lattice with nearest neighbor interaction J , obtained by solving the modified integral equation (3.46) without $(b'_0)^{-1}$ -contribution.

$$\mathcal{D}^{(2)} = \frac{b'_0}{2\pi\sqrt{\mathcal{D}^{(2)}}} \int_0^\infty \frac{du}{1 + u^2 + \left(\frac{\mathcal{D}^{(1)}}{\sqrt{\mathcal{D}^{(2)}}}\right)^4 u^4}, \quad (3.132)$$

where we performed the substitution $u = q(\mathcal{D}(i\omega)/\omega)^{1/2}$ and used that the resulting integrals are UV-convergent, allowing us to extend their boundaries to infinity. The regime of validity for 'nearly' classical systems with $S \gg 1$ is therefore $\mathcal{O}(S^{-2}) \ll |\omega/J|^{4/5} \ll 1$, before one would again encounter a singular increase of $\mathcal{D}(i\omega)$ together with a crossover of $\Delta(\mathbf{k}, i\omega)$ from $\omega^{-3/5}$ to a weaker $\omega^{-1/3}$ -divergence. This is somewhat peculiar, as a decrease in the zero-frequency singularity of $\Delta(\mathbf{k}, i\omega)$ leads to a crossover from subdiffusive to superdiffusive behavior, instead of the other way round, as observed in the decay of the autocorrelation function $S(\mathbf{0}, t)$ in computer simulations [85, 104]. We therefore obtain in $d = 1$ a scaling of the characteristic energy $\omega_*(k) \sim k^{5/2}$, i.e. the subdiffusive exponent $z = 5/2$. Note that $S(\mathbf{k}, \omega)$ vanishes like $|\omega|^{3/5}$ for $\omega \rightarrow 0$, even though $\mathcal{D}(i\omega)$ has an entirely different behavior compared to the previous superdiffusive solution. This can be contrasted with the subdiffusive solutions of the flow eq. (3.15), where $S(\mathbf{k}, \omega)$ diverges for $\omega \rightarrow 0$. The respective scaling function $s_1^{k,\omega}$ involves two terms in contrast to the previous superdiffusion form (3.115). In the end this amounts to a $t^{-2/5}$ -tail in the time-resolved autocorrelation function, with a modulation that depends on $rt^{-2/5}$ for finite r . Such an exponent in the long-time asymptotics was also found in the context of the aforementioned scaling analysis of the mode-coupling equations by Lovesey *et al.* [79, 80].

The situation in $d = 2$ is more complex, being the marginal case. On a qualitative level we expect results analogous to $d = 1$, namely that $\mathcal{D}(i\omega) \rightarrow 0$ and $\mathcal{D}''(i\omega) \rightarrow \infty$ for $\omega \rightarrow 0$, with $S(\mathbf{0}, t)$ exhibiting a weaker decay than t^{-1} . We have confirmed numerically, that $\Delta(\mathbf{k}, i\omega)$ diverges in the zero-frequency limit, while in $\mathcal{D}(i\omega)$ the singularities of the amplitudes cancel each other, leading to its vanishing and therefore subdiffusion. The behavior of $\mathcal{D}(i\omega)$ is demonstrated in Fig. 3.5. The singularities of $\Delta(\mathbf{k}, i\omega)$ beyond $\mathcal{O}(k^2)$ imply again that $S(\mathbf{k}, \omega)$ vanishes for $\omega \rightarrow 0$. Note that the exponent in two dimensions, proposed by Lovesey's analysis in mode-coupling theory $z = 3$ [80] is, in contrast to $d = 1$, inconsistent with our new equation. Same goes for $d > 2$, where the modified equation still

predicts diffusion, also at odds with the mode-coupling analysis of Ref. [80]. One would obtain $z = \frac{d+4}{2}$ for the exponents by applying the same approximation (3.126) as in $d = 1$, but due to the previously stated reasons, it is invalid.

3.2.4 General frequency and momentum dependence and correlations in real space

We will conclude our discussion of the dynamics at $T = \infty$ by taking a look at the frequency and momentum dependence of $S(\mathbf{k}, \omega)$ for arbitrary \mathbf{k} and ω , i.e. going beyond the hydrodynamic regime. For this purpose one solves directly the analytically continued self-consistency equations for the Fourier amplitudes of the dissipation energy. The continuation can be easily performed, because ω is simply an external parameter in each equation. This procedure doubles the number of quantities, because now $\Delta(\mathbf{k}, \omega)$ also has a finite imaginary part. On a hypercubic lattice the set of equations is given by

$$\begin{aligned} \tilde{\Delta}_1(\omega) = 2d \int_{\mathbf{q}} \frac{\tilde{\Delta}_R(\mathbf{q}, \omega) - i\tilde{\Delta}_I(\mathbf{q}, \omega) + i\tilde{\omega}}{(\tilde{\omega} - \tilde{\Delta}_I(\mathbf{q}, \omega))^2 + \tilde{\Delta}_R(\mathbf{q}, \omega)^2} + \frac{d}{3b'_0} \int_{\mathbf{q}} \frac{\gamma(\mathbf{q})[\tilde{\Delta}_R(\mathbf{q}, \omega) - i\tilde{\Delta}_I(\mathbf{q}, \omega) + i\tilde{\omega}]}{(\tilde{\omega} - \tilde{\Delta}_I(\mathbf{q}, \omega))^2 + \tilde{\Delta}_R(\mathbf{q}, \omega)^2} \\ - 2\tilde{\Delta}_2^{\parallel}(\omega) - 2\tilde{\Delta}_2^{\perp}(\omega), \end{aligned} \quad (3.133a)$$

$$\tilde{\Delta}_2^{\parallel}(\omega) = -d \int_{\mathbf{q}} \frac{\gamma(2\mathbf{q})[\tilde{\Delta}_R(\mathbf{q}, \omega) - i\tilde{\Delta}_I(\mathbf{q}, \omega) + i\tilde{\omega}]}{(\tilde{\omega} - \tilde{\Delta}_I(\mathbf{q}, \omega))^2 + \tilde{\Delta}_R(\mathbf{q}, \omega)^2}, \quad (3.133b)$$

$$\tilde{\Delta}_2^{\perp}(\omega) = -2d(d-1) \int_{\mathbf{q}} \frac{\gamma^{\perp}(\mathbf{q})[\tilde{\Delta}_R(\mathbf{q}, \omega) - i\tilde{\Delta}_I(\mathbf{q}, \omega) + i\tilde{\omega}]}{(\tilde{\omega} - \tilde{\Delta}_I(\mathbf{q}, \omega))^2 + \tilde{\Delta}_R(\mathbf{q}, \omega)^2}. \quad (3.133c)$$

In experiments one often measures the intensity of inelastic neutron scattering on a magnetic sample [31, 33]. As given by Eq. (1.72) in Sec. 1.3.2, the scattering cross sections are proportional to the dynamic structure factor $S(\mathbf{k}, \omega)$. Scans are performed at a fixed energy (frequency) or momentum transfer. We can also take a look at such line-shapes, by plotting $S(\mathbf{k}, \omega)$ at fixed \mathbf{k} or ω as a function of ω or \mathbf{k} . However, we will refrain here from an explicit comparison to experimentally determined inelastic neutron scattering. Firstly, there is a scarcity of such measurements in an effective high temperature regime, with T being at most three to four times larger than the critical temperature T_c [119, 120, 121], thus requiring that corrections at finite temperature are taken into account. Secondly, salient features of the theoretical curves, like the non-analytic cusp around $\omega = 0$, can be obscured by a, necessarily, finite experimental resolution δ_{ω} [92, 119]. Note that satisfying agreement was found between the outcomes of mode-coupling theory [74] and related approaches [92] for $S(\mathbf{k}, \omega)$, which predict a Lorentzian for small k , ω , and fixed momentum scans recorded for the simple cubic antiferromagnet RbMnF_3 at $T = 3.5T_c$ [92, 119]. Instead we focus on the comparison of our results for the spin diffusion coefficient with the extracted values from experiments on isotropic magnets at large temperatures [120, 122, 123]. These results are presented in the corresponding appendix B.1 concerned with different cubic lattices. In Sec. 3.3.4 we will actually compare experimentally measured line-shapes in the critical region with our results.

Frequency dependence - $k = \text{const.}$

As already discussed, $S(\mathbf{k}, \omega)$ has in three or more dimensions, as a function of ω , a single maximum at $\omega = 0$ with height $\sim [\mathcal{D}k^2]^{-1}$ for small momentum $ka \ll 1$. In $d = 3$ it is approached via a non-analytic square-root cusp with a (half-)width that is $\sim \mathcal{D}k^2$.

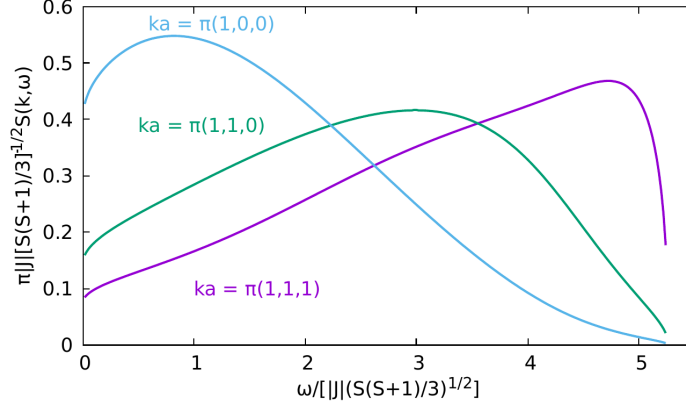


Figure 3.6: Frequency dependence of the dynamic structure factor at $T = \infty$ of the $S = 1/2$ -Heisenberg Model with nearest-neighbor interaction J on the simple cubic lattice for fixed momenta $\mathbf{k}a = \pi(1, 0, 0)$, $\pi(1, 1, 0)$, $\pi(1, 1, 1)$ from the numerical solution of (3.133). Especially for the largest momentum we observe a sharp flank, somewhat reminiscent of Blumes mode-coupling solution [74] and a simpler analytic approximation by Reiter [92], with the latter also sharing the abrupt vanishing above a finite frequency.

Conversely, for momenta far away from the origin, i.e. sufficiently short wavelengths, we observe a minimum at $\omega = 0$, with a similar non-analytic narrowing and two broad humps located at finite frequencies $\pm \omega_{\text{peak}} \sim \mathcal{O}(|J|\sqrt{b'_0})$. The latter peaks cannot be ascribed to propagating excitations, since their width is of the same magnitude as the peak position, indicating overdamped modes. In lower dimensions $S(\mathbf{k}, \omega)$ exhibits, regardless of the value of k , two peaks at finite frequencies $\pm \omega_{\text{Peak}}$ and a vanishing elastic scattering $S(\mathbf{k}, 0) = 0$. For hydrodynamic momenta the peak position ω_{Peak} scales as k^z with a height $\sim k^{-z}$ and a width $\sim \omega_{\text{Peak}}$. Results for the ω -dependence of $S(\mathbf{k}, \omega)$ at a few select momenta $ka \sim \mathcal{O}(1)$ are shown in Fig. 3.6, 3.7 and 3.8 for nearest-neighbor Heisenberg models on hypercubic lattices in $d = 1, 2, 3$. In contrast to the low-frequency behavior, where the solutions in reduced dimensions imply a vanishing $S(\mathbf{k}, 0)$, the qualitative behavior is qualitatively similar at larger frequencies $\omega \sim \mathcal{O}(J)$. In all cases one observes broad peaks. For momenta at the corner of the Brillouin zone, the maxima exhibit a pronounced asymmetry with a strong decrease for $\omega > \omega_{\text{Peak}}$, meaning that most of the spectral weight is concentrated in $|\omega| < \omega_{\text{Peak}}$. Such a flank at short wavelengths in $S(\mathbf{k}, \omega)$ should be reflected in the time-domain by oscillations of $S(\mathbf{k}, t)$ [74]. Note also that a rapid decay of $S(\mathbf{k}, \omega)$ is consistent with all high-frequency moments being finite, in contrast to the three-pole approximation (3.90). In fact above a cutoff frequency ω_c we obtain $\Delta_R(\mathbf{k}, \omega > \omega_c) = 0$, so that

$$S(\mathbf{k}, \omega) \propto \delta(\omega - \Delta_I(\mathbf{k}, \omega)) = 0, \quad (3.134)$$

since $\omega > \Delta_I(\mathbf{k}, i\omega)$. Such a sharp cutoff is reminiscent of de Gennes' ansatz for the relaxation-shape function [77]. This could have been expected from the form of the high-frequency expansion for $\Delta(\mathbf{k}, i\omega)$ which contains only odd powers of $|\omega|^{-1}$. After analytic continuation the asymptotic large- ω expression is therefore a purely imaginary quantity, so that a finite real part can be only realized via a kink at an intermediate frequency ω_c . We obtained $\omega_c \times (|J|\sqrt{b'_0})^{-1} \approx 3.1, 4.4, 5.3$ for the hypercubic lattice in $d = 1, 2, 3$. This

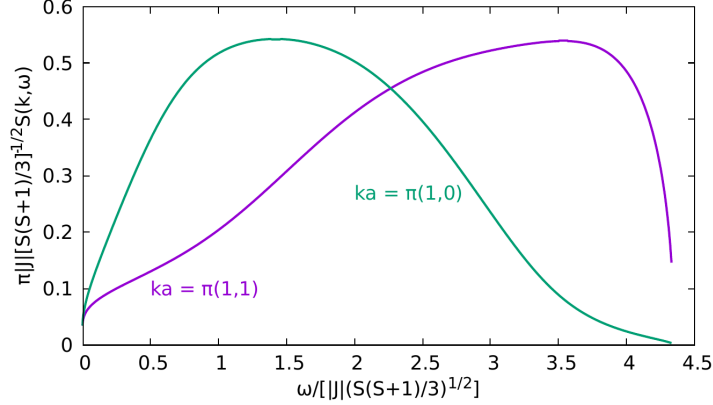


Figure 3.7: Frequency dependence of the dynamic structure factor at $T = \infty$ of the $S = 1/2$ -Heisenberg Model with nearest-neighbor interaction J on the square lattice for fixed momenta $\mathbf{k} = \frac{\pi}{a}(1, 0)$, $\frac{\pi}{a}(1, 1)$ from the numerical solution of (3.133). Note that in contrast to $d = 3$ the scattering intensity goes to zero for $\omega \rightarrow 0$.

should be contrasted with extrapolation formulas, like (3.90), where $S(\mathbf{k}, \omega) > 0$ for any $|\omega| < \infty$. Note that this feature of our solution is another sign of how low and high- ω sectors do not connect to each other by means of a simple interpolation.

Momentum dependence - $\omega = \text{const.}$

For the \mathbf{k} -dependence at constant ω , one first notes that, due to total spin conservation (2.71), $S(\mathbf{k}, \omega)$ will always vanish for $k \rightarrow 0$, namely as k^2 like $\Delta(\mathbf{k}, i\omega)$. For hydrodynamic frequencies single peaks occur at long wavelengths with their location scaling as $k_* \sim (\tilde{\omega})^{1/z}$, a width of the same order and a height $\sim \omega^{-1}$. Note that non-analytic corrections to $\Delta(\mathbf{k}, i\omega)$, e.g. the $|\omega|^{1/2}$ -term in $d = 3$, are only small corrections in the regime of small $ka \lesssim (\tilde{\omega})^{1/z}$. At larger $\tilde{\omega} \sim \mathcal{O}(1)$ a broad single peak is located at a momentum $ka \sim 1$. For brevity we show in this section only the momentum dependence on a linear nearest-neighbor chain in Fig. 3.9, because it suffices for illustrating the main aspects and there is only one \mathbf{k} -direction in this case. In appendix B.1 we also show results for the momentum dependence of the dissipation energy and its inverse in the (quasi-)static limit $\omega \ll |J|$ for select paths in the first Brillouin Zone, with $\Delta^{-1}(\mathbf{k}, \omega)$ being proportional to $S(\mathbf{k}, \omega)$, i.e.

$$\tilde{S}(\mathbf{k}, \omega) \approx \frac{b'_0}{\pi} \frac{\tilde{\Delta}_R(\mathbf{k}, \omega)}{|\tilde{\Delta}(\mathbf{k}, \omega)|^2}, \quad (3.135)$$

for Heisenberg models with couplings J_1 and J_2 between nearest and next-nearest neighbors on hypercubic lattices. Note that constant frequency scans can help with identifying different line shapes, since ω_{peak} is $\neq 0$ for arbitrary \mathbf{k} and therefore depends on the corresponding profile for $S(\mathbf{k}, \omega)$. We will make use of this property when discussing neutron scattering in the critical region, see Sec. 3.3.4.

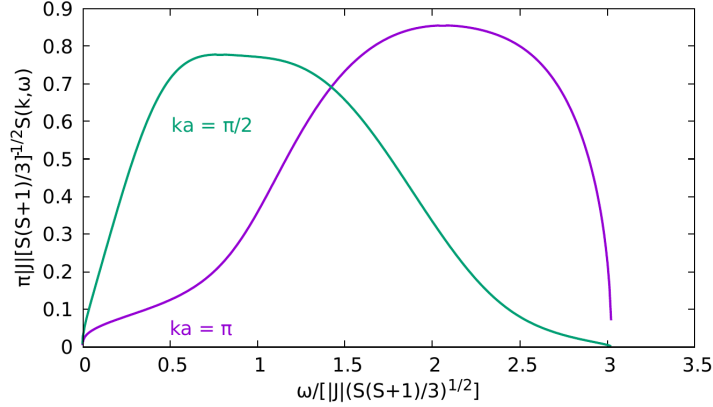


Figure 3.8: Frequency dependence of the dynamic structure factor at $T = \infty$ of the $S = 1/2$ -Heisenberg Model with nearest-neighbor interaction J on the linear chain for constant momenta $\mathbf{k} = \frac{\pi}{2a}, \frac{\pi}{a}$ from the numerical solution of (3.133).

Frequency-dependent correlation functions in real space

Besides $S(\mathbf{k}, \omega)$, let us shortly discuss ω -dependent correlations in real space. One example is the autocorrelation function

$$S(\mathbf{r} = \mathbf{0}, \omega) = \int_{\mathbf{k}} S(\mathbf{k}, \omega) \geq 0. \quad (3.136)$$

In the case of normal diffusion this quantity has a finite static limit. Its value at $\omega = 0$ is then proportional to the Brillouin zone average of $\Delta(\mathbf{k}, 0)^{-1}$. In lower dimensions, we find that due to IR-singular behavior of the integrand $\sim k^{d-2}$ the above quantity diverges for $\omega \rightarrow 0$. We obtain $\omega^{-1/3}$ for its leading singularity in $d = 1$ and $\ln(|J|/\omega)$ in two dimensions. The coefficient of that singularity is thus solely determined by the numeric constant in the divergent $\mathcal{D}(i\omega)$, as the integrals are confined to $k \lesssim k_{\omega}^* \sim (\omega/\mathcal{D}(i\omega))^{1/2}$. Note that in reduced dimensions low-frequency singularities also occur for normal diffusion, due to the same low-momentum asymptotics $\Delta(\mathbf{k}, i\omega) \sim k^2$, implying $\omega^{-1/2}$ in $d = 1$ and again $\ln(|J|/\omega)$ in $d = 2$ [124, 125]. The same leading dependences in the low-frequency limit $\omega \ll |J|$ can be found for pair-correlation functions with $\mathbf{r} \neq \mathbf{0}$,

$$S(\mathbf{r}, \omega) = \int_{\mathbf{k}} e^{i\mathbf{k}\cdot\mathbf{r}} S(\mathbf{k}, \omega), \quad (3.137)$$

e.g. between nearest neighbors on a cubic lattice, where $e^{i\mathbf{k}\cdot\mathbf{r}} \rightarrow \gamma(\mathbf{k})$. In $d > 2$ these quantities are finite at zero frequency as the autocorrelation function, whereas in reduced dimensions their divergence does not depend on \mathbf{r} , due to the $k \rightarrow 0$ singularity, so that $e^{i\mathbf{k}\cdot\mathbf{r}} \approx 1$. For larger frequencies $\tilde{\omega} \gtrsim 1$, correlations between spins at different sites feature damped oscillations. Note that as for $S(\mathbf{k}, \omega)$ these correlations vanish above $\omega > \omega_c$ in our approximation. Results for the frequency dependence of $S(\mathbf{r}, \omega)$ on distances $|\mathbf{r}| \sim \mathcal{O}(a)$ are shown in Fig. 3.10 and 3.11 for a nearest-neighbor magnet on the simple cubic lattice and linear chain. We want to point out that one can write our solution, see (3.77), for the zero-frequency amplitudes $\tilde{\Delta}(0)$ in $d > 2$ as a linear combination of short-ranged $S(\mathbf{r}, 0)$, since $S(\mathbf{k}, 0) \sim \frac{1}{\Delta(\mathbf{k}, 0)}$. Hence the diffusion coefficient \mathcal{D} is also a finite sum of auto- and

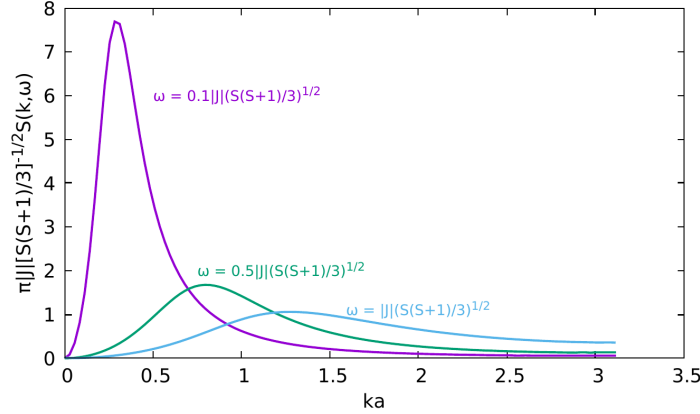


Figure 3.9: \mathbf{k} -dependence of the dynamic structure factor at $T = \infty$ of the $S = 1/2$ -Heisenberg Model with nearest-neighbor interaction J on the linear chain for fixed frequencies $\tilde{\omega} = 0.1, 0.5, 1.0$.

pair-correlations at vanishing frequency. For $\omega \neq 0$ one can interpret the terms on the right-hand-sides of (3.76) as Laplace-transforms of the relaxation-shape function in real space, i.e. $\tilde{\mathcal{R}}_L(\mathbf{r}, \omega) = \int_{\mathbf{k}} e^{i\mathbf{k}\cdot\mathbf{r}} [\Delta(\mathbf{k}, i\omega) + \omega]^{-1}$ [124, 125].

As an alternative route for measuring spin dynamics, one can extract the discussed real-space correlation functions via nuclear magnetic resonance (NMR) experiments, which determine the spin relaxation rates τ_N^{-1} of the nuclei that form the magnetic compound. The linewidths τ_N^{-1} can then be written as a linear combination of zero-frequency correlations at short distances, analogous to $\Delta(\mathbf{k}, 0)$ in our case [122, 123]. Note that the ω -dependence of $S(\mathbf{r}, \omega)$ in a paramagnet, at least for $T \gg |J|$, can be accessed via the dependence of τ_N^{-1} on sufficiently weak external fields $|H| \ll T$ [123].

3.3 Three-dimensional ferromagnet close to the phase transition

We will consider now the critical region above the transition, where $(T - T_c)/T_c \ll 1$, including the critical point itself, $T = T_c$, describing hereby calculations contained in our second publication Ref. [11]. In this regime the static susceptibility $G(\mathbf{k}) = [\Sigma(\mathbf{k}) + J(\mathbf{k})]^{-1}$ is strongly peaked around the ordering vector \mathbf{Q} , which is equal to $\mathbf{0}$ for the ferromagnet. Its singular behavior allows, at least in the physical case $d = 3$, the application of additional approximations during the study of the integral equation (3.50) at small frequencies $\omega \ll |J|$ and momenta $ka \ll 1$, as will be demonstrated below. Neglecting the momentum dependence of $\Sigma(\mathbf{k})$ and expanding the exchange interaction on a lattice with cubic symmetry to leading order around $\mathbf{k} = \mathbf{0}$

$$J(\mathbf{k}) \approx J(\mathbf{0}) + J''(ka)^2 + \mathcal{O}(k^4), \quad (3.138)$$

one can write $G(\mathbf{k})$ for small momenta $ka \ll 1$ as

$$G(\mathbf{k}) \approx \frac{\chi}{1 + (k\xi)^2} = \chi g(k\xi). \quad (3.139)$$

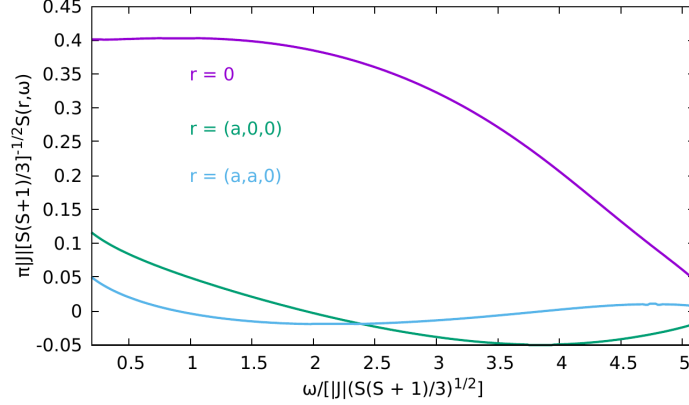


Figure 3.10: Frequency-dependent two-spin correlations $S(\mathbf{r}, \omega)$ on the same site (purple) or between nearest (green) and next-nearest neighbors (blue) at $T = \infty$ from the numerical solution of (3.133) for a $S = 1/2$ Heisenberg model with a nearest-neighbor interaction J on a simple cubic lattice. The ω -dependences below ω_c , in particular for $\mathbf{r} \neq \mathbf{0}$, are in qualitative agreement with results of mode-coupling theory [74] and extrapolation schemes [95]. Note however that we obtain a plateau with a slight increase in $S(\mathbf{0}, \omega)$, followed by a region with negative curvature. Such features are absent in outcomes of the aforementioned theoretical approaches in $d = 3$ [74, 95].

Here $\chi = G(\mathbf{0})$ is the magnetic susceptibility and $\xi \gg a$ is the correlation length, defined as

$$\xi = \sqrt{\rho_0 \chi}, \quad (3.140)$$

with the spin stiffness given by the bare expression

$$\rho_0 = J'' a^2, \quad (3.141)$$

since $\Sigma'' = 0$. At the critical point, where $\chi^{-1} = 0$, the correlation length ξ is infinitely large so that $G(\mathbf{k}) = [\rho_0 k^2]^{-1}$. The above shape of $G(\mathbf{k})$ is the Ornstein-Zernicke form (1.52) with static scaling function $g(x) = [1 + x^2]^{-1}$. This form is automatically implied by $\Sigma(\mathbf{k}) \approx \Sigma$ so that the anomalous dimension η is assumed to be zero. As already discussed, neglecting η is justified in $d = 3$, since the actual numeric value ≈ 0.03 [26] is quite small and therefore of almost no relevance in experiments. In the same vein one can expand the difference in the kernel $V(\mathbf{k}, \mathbf{q})$ from Eq. (3.51) as

$$[J(\mathbf{q}) - J(\mathbf{q} + \mathbf{k})]^2 \approx (\rho_0)^2 [k^2 + 2\mathbf{k} \cdot \mathbf{q}]^2, \quad (3.142)$$

leading therefore to

$$V(\mathbf{k}, \mathbf{q}) = \frac{T\rho_0}{2} \frac{[1 + (k\xi)^2][k^2 + 2\mathbf{k} \cdot \mathbf{q}]^2 \xi^2}{[1 + (q\xi)^2][1 + (\mathbf{k} + \mathbf{q})^2 \xi^2]}, \quad (3.143)$$

and the following self-consistency equation for the dissipation energy $\Delta(\mathbf{k}, i\omega)$ in d dimensions

$$\Delta(\mathbf{k}, i\omega) = \frac{T\rho_0 v a^d}{2} \int \frac{d^d q}{(2\pi)^d} \frac{[1 + (k\xi)^2][k^2 + 2\mathbf{k} \cdot \mathbf{q}]^2 \xi^2}{[1 + (q\xi)^2][1 + (\mathbf{k} + \mathbf{q})^2 \xi^2]} \frac{1}{|\omega| + \Delta(\mathbf{q}, i\omega)}. \quad (3.144)$$

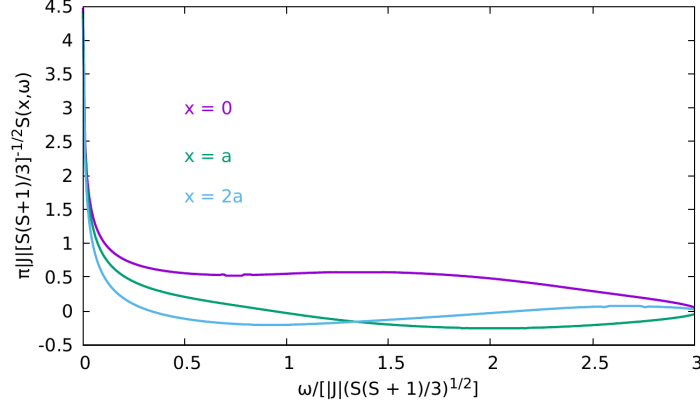


Figure 3.11: Frequency dependence of $S(\mathbf{r} = x, \omega)$ for a linear $S = 1/2$ -chain at $T = \infty$, with $x = 0, a, 2a$ and $\omega \lesssim \omega_c$. One clearly discerns the low-frequency divergence, which is the same for all x . The qualitative agreement in $d = 1$ with other methods is better than in $d = 3$, even if extrapolation schemes [95], for instance, assume a diffusion form, leading to a different exponent in the $\omega \rightarrow 0$ singularity. The only feature not shared by, e.g. Ref. [95] is a weak growth in $S(\mathbf{r}, \omega)$ at intermediate ω .

Here we have introduced the ratio v of the volume of the primitive unit cell of the isotropic Bravais lattice to the volume of the conventional unit cell, given by a^d , since it is a cube that may contain more than one atom.

Confining ourselves to a small momentum expansion of $G^{-1}(\mathbf{q})$ and $V(\mathbf{k}, \mathbf{q})$ is a justified approximation below a critical dimension $d = d_c$, which in the case of a ferromagnet is $d_c = 6$ [57], larger than the upper critical dimension for static properties $d = 4$ [3]. This can be deduced from the fact that in the small frequency-region $\Delta(\mathbf{k}, i\omega)$ behaves for $k \gg \xi^{-1}$ as k^4 , since the integrand in Eq. (3.144) becomes $\propto k^4 G^{-1}(\mathbf{k}) G(\mathbf{q} + \mathbf{k})$. Then the ultraviolet behavior, $qa \gg 1$, is in d dimensions $\int d^d q q^2 / q^8 \sim q_c^{d-6}$, so that the integrand shows a stronger decay than q^{-1} for $d < d_c = 6$. Thus the integrals are UV-convergent, allowing us to extend their boundaries to ∞ . Contributions to higher order in q , contained in $G^{-1}(\mathbf{q})$ and $J(\mathbf{q})$, are negligible near T_c , because they are suppressed in ξ^{-1} or another, e.g. ω -dependent, cutoff momentum $\ll 1$, depending on which is larger. On the other hand for $d > d_c$ one has to take the full momentum dependence of $G(\mathbf{k})$ and $J(\mathbf{k})$ into account, as the integrals are not restricted to small momenta $ka \ll 1$ anymore.

Substituting $r = q\xi$ in the integral Eq. (3.144) and introducing a characteristic timescale

$$\tau = \sqrt{\frac{2}{TvJ''}} (\xi/a)^z, \quad (3.145)$$

where the dynamic exponent reads

$$z = \frac{d+2}{2}, \quad (3.146)$$

one sees that the dissipation energy satisfies

$$\Delta(\mathbf{k}, i\omega) = \tau^{-1} A(x = k\xi, iy = i\omega\tau), \quad (3.147)$$

with the dimensionless scaling function $A(x, iy)$ being the solution of

$$A(x, iy) = [1 + x^2] \int \frac{d^d r}{(2\pi)^d} \frac{(x^2 + 2\mathbf{x} \cdot \mathbf{r})^2}{(1 + r^2)[1 + (\mathbf{x} + \mathbf{r})^2]} \frac{1}{A(r, iy) + |y|}. \quad (3.148)$$

The Matsubara function is then given by the scaling form

$$G(\mathbf{k}, i\omega) = \chi g(k\xi) \frac{A(k\xi, i\omega\tau)}{A(k\xi, i\omega\tau) + |\omega|\tau}. \quad (3.149)$$

The energy scale τ^{-1} marks the crossover between a hydrodynamic $\omega\tau \ll 1$ and collisionless regime $\omega\tau \gg 1$. It assumes therefore the same role as at high temperatures, with the difference that now τ^{-1} is $\ll |J|$, thus leaving room for another low-frequency regime in $\tau^{-1} \ll \omega \ll |J|$. For $T \rightarrow T_c$, the hydrodynamic region shrinks steadily, due to $\tau \sim \xi^z \rightarrow \infty$ until one is left, at $T = T_c$, with the collisionless regime in the whole low-frequency sector. Taking the analytic continuation of $G(\mathbf{k}, i\omega)$ and using the fluctuation-dissipation theorem (3.59), where for small frequencies $\omega \ll |J| \lesssim T_c \approx T$ the detailed-balance factor is equal to the classical expression

$$(1 - e^{-\omega/T})^{-1} \approx T/\omega, \quad (3.150)$$

we obtain for the dynamic structure factor

$$S(\mathbf{k}, \omega) = \frac{T\chi g(k\xi)}{\pi\omega} \text{Im} \left[\frac{A(k\xi, \omega\tau + i0)}{A(k\xi, \omega\tau + i0) - i\omega\tau} \right]. \quad (3.151)$$

It can also be written in terms of a scaling function $\Phi(x, y)$ for its frequency dependence

$$\Phi(x, y) = \frac{1}{y} \text{Im} \left[\frac{A(x, y + i0)}{A(x, y + i0) - iy} \right]. \quad (3.152)$$

as

$$S(\mathbf{k}, \omega) = \frac{T\tau\chi g(x)}{\pi} \Phi(x, y). \quad (3.153)$$

Note that $\Phi(x, y)$ is, up to a factor of two, the scaling form for the corresponding Kubo relaxation-shape function $\tilde{\mathcal{R}}(\mathbf{k}, \omega)$, and $S(\mathbf{k}, \omega)$ is thus an even function of ω in the low-frequency region $\omega \ll T$. The dominance of fluctuations on macroscopic length and time scales below the critical dimension d_c , leading to the above scaling forms, was also found in the coupled-mode approach to critical dynamics, see Sec. 1.4.2. Furthermore it is central to the dynamic scaling hypothesis. The dynamic exponent $z = (d + 2)/2$ fully agrees with its predictions for the dynamic universality class of Heisenberg ferromagnets [54, 58]. Note also that the decay rate $\tau^{-1} \sim \xi^{-z}$ in the above scaling forms corresponds to the characteristic frequency in the hydrodynamic limit as proposed by the DSH [58], see Sec. 1.4.3. Incorporating $\eta \neq 0$, which requires in our case the aforementioned modified equation (3.46), we obtain $z = (d + 2 - \eta)/2$, thus agreeing with dynamic scaling too [55, 58, 60]. Note that above $d = d_c$ there is no singular coupling to long wavelength fluctuations and therefore the dynamic exponent is $z = 4$ as predicted by the older and simpler van Hove theory, which rests on the assumption that Onsager coefficients are determined by fluctuations on all length scales, similar to the behavior far away from T_c [32, 56]. On top of that above d_c the scaling function for $S(\mathbf{k}, \omega)$ at asymptotically small k, ω has a simple form like for $T \gg T_c$, featuring only the leading term $\Delta_{\text{ret}}(\mathbf{k}, \omega) \propto G^{-1}(\mathbf{k})k^2$. Conversely for $d < d_c$ the scaling functions $A(x, iy)$, $\Phi(x, y)$ in the critical region have a non-trivial shape, which will be determined by us.

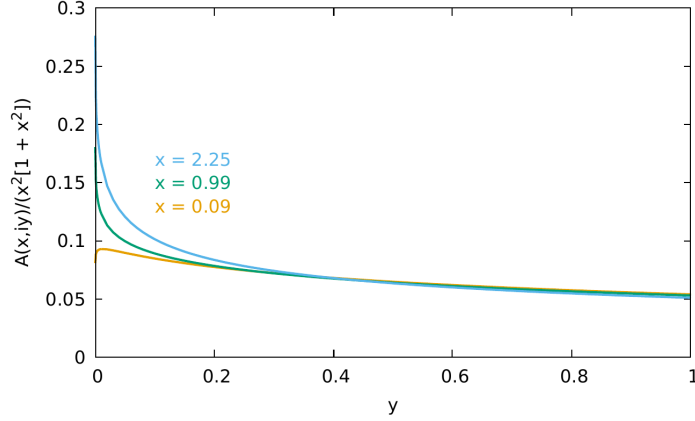


Figure 3.12: The numerical solution of Eq. (3.154) for the scaling function $A(x, iy)$ of the dissipation energy $\Delta(\mathbf{k}, i\omega)$, defined via (3.147), in $d = 3$ as a function of dimensionless frequency $y = \omega\tau$ for different values of the momentum variable $x = k\xi$. Note that we divided $A(x, iy)$ by $x^2[1 + x]$, since this factor contains most of the dependence on x . Reprinted with permission from Ref. [10] © [2021] American Physical Society.

To calculate the scaling function $\Phi(x, y)$ we have to solve the self-consistency equation for $A(x, iy)$. In the physically relevant case of $d = 3$ the angular integrations over ϕ , θ can be performed exactly, leaving us with the integral equation

$$A(x, iy) = \frac{1 + x^2}{2\pi^2} \int_0^\infty \frac{dr r^2}{A(r, iy) + |y|} \left[\frac{x^2}{1 + r^2} + \frac{1 + r^2}{4xr} \ln \left(\frac{1 + |r + x|^2}{1 + |r - x|^2} \right) - 1 \right]. \quad (3.154)$$

This is a simplification compared to the mode-coupling equations [55, 60], where the integration over the angle θ between \mathbf{x} and \mathbf{r} has to be performed numerically too. Eq. (3.154) was solved by simply iterating it, starting from $y = 0$. For the initial estimate of $A(x, 0)$ we have ignored anything beyond x^2 in the integral on the right-hand-side, thus allowing us to obtain an analytic expression for the starting point. In Fig. 3.12 numerical results for the y -dependence of $A(x, iy)$ at chosen values for x are displayed, where we have scaled out the dominant momentum dependence $\sim x^2[1 + x^2]$. The resulting scaling function $\Phi(x, y)$ is plotted as a function of y at different x in Fig. 3.13. Note that the latter plots are directly proportional to the frequency dependence on constant momentum scans of the scattering intensity at a fixed correlation length and thus temperature. Conversely, the x -dependence for different values y may be interpreted as the k -dependence in constant energy scans at the same T . For sufficiently large $x \gtrsim \mathcal{O}(1)$ the scaling function $\Phi(x, y)$ exhibits peaks, whose position y_* and halfwidth Δy_* increase rapidly as a function of x . In fact, one finds that y_* , $\Delta y_* \sim x^{5/2}$ for $x \gg 1$, which translates into a dispersion $\omega_k \propto k^{5/2}$ for $k \gg \xi^{-1}$ with damping of the same order of magnitude. To demonstrate this explicitly, one should use another scaling variable ν for the frequency, so that the aforementioned features occur at values $|\nu| \lesssim \mathcal{O}(1)$, with accompanying new scaling functions in place of $A(x, iy)$ and $\Phi(x, y)$. A prudent choice for the new variable is

$$\nu = \frac{y}{x^z} = \frac{\omega\tau}{(k\xi)^z} = \frac{\omega}{\omega_k}, \quad (3.155)$$

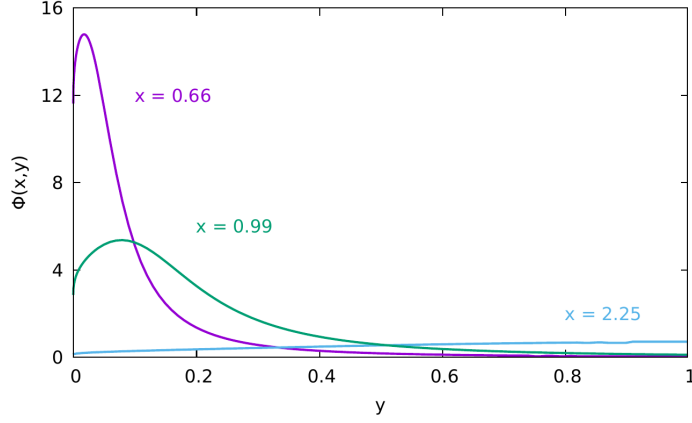


Figure 3.13: Plot of the scaling function $\Phi(x, y)$ of $S(\mathbf{k}, \omega)$ in $d = 3$, obtained from $A(x, y + i0^+)$, see also Eq. (3.153), as a function of y for different values of x . As discussed in the main text, it describes the frequency dependence of the dynamic structure factor at fixed T . Reprinted with permission from Ref. [10] © [2021] American Physical Society.

where we introduced the characteristic frequency, see also Sec. 1.4.3,

$$\omega_k = (k\xi)^z \tau^{-1} = \omega_*(ka)^z, \quad (3.156)$$

which contains a non-universal energy scale ω_* , already encountered in the definition of τ

$$\omega_* = \sqrt{\frac{T\nu J''}{2}} \approx \sqrt{\frac{T_c \nu J''}{2}}. \quad (3.157)$$

The dissipation energy and dynamic structure factor can then be written in terms of new scaling functions as

$$\Delta(\mathbf{k}, i\omega) = \omega_k B(k\xi, i\omega/\omega_k), \quad (3.158a)$$

$$S(\mathbf{k}, \omega) = \frac{T\chi g(k\xi)}{\pi\omega_k} \Psi(k\xi, \omega/\omega_k). \quad (3.158b)$$

From a comparison of the expressions for $\Delta(\mathbf{k}, i\omega)$ and $S(\mathbf{k}, \omega)$ in (3.147) and (3.153) with (3.158) we obtain the following relations

$$B(x, i\nu) = x^{-z} A(x, i\nu x^z), \quad (3.159a)$$

$$\Psi(x, \nu) = x^z \Phi(x, \nu x^z), \quad (3.159b)$$

with the scaling form for the frequency dependence of $S(\mathbf{k}, \omega)$ now given by

$$\Psi(x, \nu) = \frac{1}{\nu} \text{Im} \left[\frac{B(x, \nu + i0)}{B(x, \nu + i0) - i\nu} \right]. \quad (3.160)$$

After the substitution $r = x\rho$ in Eq. (3.154) we arrive at the following self-consistency equation for the new scaling function $B(x, i\nu)$ in $d = 3$

$$B(x, i\nu) = \frac{1+x^2}{2\pi^2 x^2} \int_0^\infty \frac{d\rho\rho^2}{\rho^{5/2} B(x\rho, i\nu/\rho^{5/2}) + |\nu|} \left[\frac{x^2}{1+x^2\rho^2} + \frac{1+x^2\rho^2}{4x^2\rho} \ln \left(\frac{1+x^2|\rho+1|^2}{1+x^2|\rho-1|^2} \right) - 1 \right]. \quad (3.161)$$

As for $A(x, iy)$ we solve this equation by taking as an initial estimate $B(x, 0) \sim x^{2-z}[1+x^2]$, which amounts to $\Delta(\mathbf{k}, 0) \sim k^2 G^{-1}(\mathbf{k})$. Results for the ν -dependence $B(x, i\nu)$ and $\Psi(x, \nu)$ at different values of x from the numerical solution of (3.161) are shown in the Figures 3.14 and 3.15. Conversely to $\Phi(x, y)$, the ν -dependence of $\Psi(x, \nu)$ at different $x = \text{const.}$ can be directly interpreted as the frequency dependence of $S(\mathbf{k}, \omega)$ at different temperatures and the same momentum. We see then in Fig. 3.15 that the position of the peaks ν_* , together with their width $\Delta\nu_*$, indeed have a finite limit for $T \rightarrow T_c$, so that one can interpret $\omega_k \sim k^{5/2}$ as the dispersion of an overdamped, i.e. dissipative mode. Note that the elastic scattering reduces with increasing x and therefore diminishing distance to T_c , approaching the behavior of the solution at the critical point, which will be explicitly discussed.

3.3.1 Spin diffusion in the vicinity of $T = T_c$

In the limit of hydrodynamic frequencies $|y| \ll 1$ one can, analogous to $T = \infty$, set $A(x, iy) \approx A(x, 0)$, yielding the following equation for the static dissipation energy

$$A(x, 0) = \frac{1+x^2}{2\pi^2} \int_0^\infty \frac{dr r^2}{A(r, 0)} \left[\frac{x^2}{1+r^2} + \frac{1+r^2}{4xr} \ln \left(\frac{1+|r+x|^2}{1+|r-x|^2} \right) - 1 \right]. \quad (3.162)$$

According to (3.53) we can expand $A(x, 0)$ for hydrodynamic momenta $x \ll 1$ as

$$A(x, 0) = A_2 x^2 + \mathcal{O}(x^4), \quad (3.163)$$

where the numerical solution of Eq. (3.162) yields $A_2 \approx 0.078$ in $d = 3$. For general $d < d_c$ this numeric constant is given by

$$A_2 = \frac{[1+x^2]}{d} \int \frac{d^d r}{(2\pi)^d} \frac{r^2}{[1+r^2]^2} \frac{1}{A(r, 0)}, \quad (3.164)$$

where we used $(\mathbf{x} \cdot \mathbf{r}) \rightarrow x^2 r^2 / d$ due to isotropy. Hence we find that to leading order in $x \ll 1$ and $y \ll 1$ the dissipation energy is given by the diffusive result

$$\Delta(\mathbf{k}, 0) \approx A_2 (k\xi)^2 \tau^{-1} = \mathcal{D} k^2, \quad (3.165)$$

from which we read off the spin diffusion coefficient as

$$\mathcal{D} = A_2 \xi^2 \tau^{-1} = \frac{A_2 \omega_* a^2}{(\xi/a)^{(d-2)/2}}. \quad (3.166)$$

We thus see that the diffusion coefficient vanishes for $T \rightarrow T_c$ as $\xi^{-1/2} \propto \chi^{-1/4}$ in three dimensions, or $\mathcal{D} \sim \xi^{2-z} \sim \xi^{(2-d)/2}$ for arbitrary d , i.e. $\mathcal{D} \sim (T - T_c)^{(d-2)\nu/2}$, with $\xi \sim (T - T_c)^{-\nu}$. One therefore obtains a divergence $\sim \xi^{3/2}$ for the corresponding Onsager-coefficient $L \sim \lim_{k \rightarrow 0} k^{-2} |\omega| \tilde{\Pi}(\mathbf{k}, i\omega)$ in $d = 3$, a consequence of coupling to singular order parameter fluctuations. As expected this dependence on $T - T_c$ agrees fully with the predictions made by dynamic scaling in the hydrodynamic regime [58]. With $\nu \approx 0.7$ it is in $d = 3$ explicitly given by $\mathcal{D} \sim (T - T_c)^{0.35}$, in reasonable agreement with experiments [121]. This has to be contrasted with the stronger decay $\mathcal{D} \sim \chi^{-1} \sim \xi^{-2}$ postulated by van Hove, which assumed a finite Onsager coefficient, yielding $\mathcal{D} \sim (T - T_c)^{2\nu}$. The van Hove expression can already be ruled out visually in measurements, since it implies a vanishing slope for $T \rightarrow T_c$ due to $\nu > 1/2$. Our result for \mathcal{D} in Eq. (3.166) is also an outcome of more sophisticated mode-coupling calculations [88, 126, 127, 128], with a similar dependence on

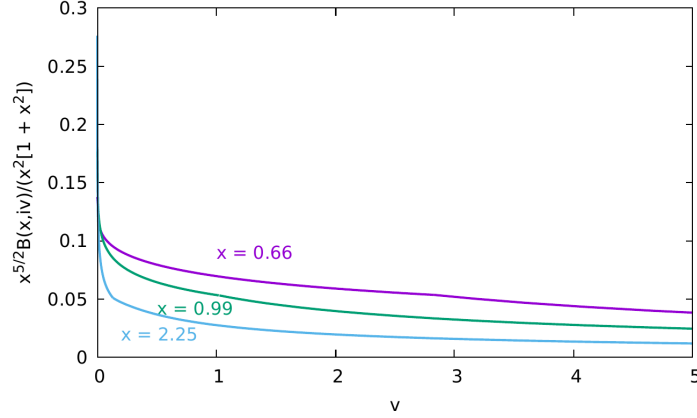


Figure 3.14: Numerical solution of Eq. (3.161) for the alternative scaling function $B(x, i\nu)$ of the dissipation energy in $d = 3$, defined in Eq. (3.159a), plotted as a function of the new frequency variable $\nu = \omega/\omega_k$ for different x . We show $B(x, i\nu)/(x^{2-z}[1 + x^2])$, equivalent to $A(x, i\nu x^z)/(x^2[1 + x^2])$, because this eliminates again the dominant dependence on x . Reprinted with permission from Ref. [11] © [2022] American Physical Society.

microscopic parameters in ω_* . The generic fact of \mathcal{D} vanishing at T_c is a manifestation of critical slowing down, as the decay rate of fluctuations in the vicinity of the ordering vector tends to zero for $T \rightarrow T_c$. From the autocorrelation function at vanishing frequency, a Brillouin zone average of the elastic scattering $S(\mathbf{k}, 0)$, one obtains one of the contributions to the NMR linewidth [58]. In $d < d_c$ dimensions it diverges near T_c as

$$S(\mathbf{r} = \mathbf{0}, \omega = 0) \propto \tau \int \frac{dk k^{d-1}}{A(k\xi, 0)} \frac{\chi}{[1 + (k\xi)^2]} \propto \xi^{z-d+2} \sim \xi^{(6-d)/2}. \quad (3.167)$$

Here we used that the integral is cut above $k\xi \sim 1$, due to $A(x, 0) \propto x^4$ for large momentum. In three dimensions the asymptotic behavior is $\sim \xi^{3/2} \approx |T - T_c|^{-1}$, in agreement with [58]. For $d > 6$, where van Hove theory is valid, it is finite.

Employing the same reasoning as for $T \gg |J|$, non-analytic corrections to $A(x, 0)$ occur at finite y , which are $\sim |y|^{1/2}$ in $d = 3$, i.e.

$$A(x, iy) = A(x, 0) + A_1(x)|y|^{1/2} + \mathcal{O}(y). \quad (3.168)$$

Again they can be dropped in the strict hydrodynamic limit $k\xi \rightarrow 0$, $\omega\tau \sim (k\xi)^2$ or equivalently $\tau \ll t \lesssim \mathcal{O}((Dk^2)^{-1})$, i.e. $(\xi/a)^z \ll \omega_* t \lesssim k^{-2}\xi^{z-2}$, yielding thus the exponential $\exp(-Dk^2 t)$ for $S(\mathbf{k}, t)$, generated by the diffusion pole. Conversely one expects for larger times again a $t^{-3/2}$ -decay due to the zero-frequency branch point implied by the square-root. The distortion of the Lorentzian in the frequency domain via a non-analytic cusp at small frequencies is clearly seen in plots of the scaling functions $\Phi(x, y)$ and $\Psi(x, \nu)$ in Fig. 3.13 and 3.15. Like at $T = \infty$ there is a crossover at finite k between a positive sign of $A_1(x)$ for $x \ll 1$ and a negative one for $x \gg 1$. The different low-frequency behavior of $A(x)$ for small and large x can be discerned in Fig. 3.12.

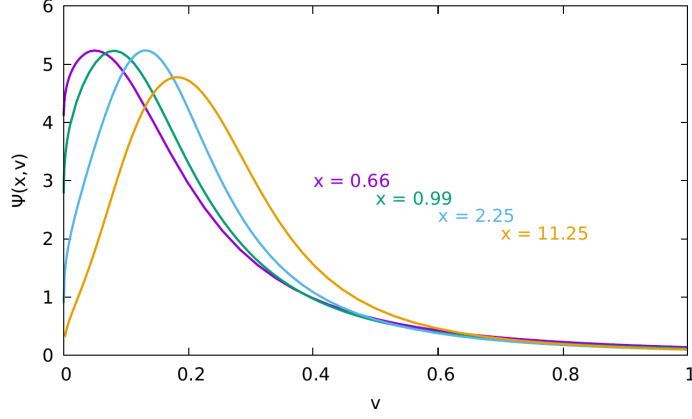


Figure 3.15: Alternative scaling function $\Psi(x, \nu)$, defined in Eq. (3.160), of $S(\mathbf{k}, \omega)$ as a function ν , shown for different values of x . Reprinted with permission from Ref. [11] © [2022] American Physical Society.

3.3.2 Scaling function at the critical point

At the critical point $T = T_c$, where $k\xi = \infty$, the scaling functions depend only on one residual variable, i.e.

$$B_c(i\nu) = B(\infty, i\nu), \quad (3.169)$$

$$\Psi_c(\nu) = \Psi(\infty, \nu), \quad (3.170)$$

with the critical line-shape given by

$$\Psi_c(\nu) = \frac{1}{\nu} \text{Im} \left[\frac{B_c(\nu + i0)}{B_c(\nu + i0) - i\nu} \right]. \quad (3.171)$$

The dissipation energy and dynamic structure factor for $T = T_c$ are therefore

$$\Delta(\mathbf{k}, i\omega) = \omega_k B_c(i\omega/\omega_k), \quad (3.172)$$

$$S(\mathbf{k}, \omega) = \frac{T_c G(\mathbf{k})}{\pi \omega_k} \Psi_c(\omega/\omega_k). \quad (3.173)$$

Setting $x = \infty$ in the integral equation (3.161) for $B(x, i\nu)$ we obtain the following self-consistency equation for the scaling function of the critical dissipation energy in $d = 3$

$$B_c(i\nu) = \frac{1}{2\pi^2} \int_0^\infty \frac{d\rho}{\rho^{5/2} B_c(i\nu/\rho^{5/2}) + |\nu|} \left[1 + \frac{\rho^3}{2} \ln \left| \frac{\rho + 1}{\rho - 1} \right| - \rho^2 \right]. \quad (3.174)$$

Before turning to the explicit numerical solution of (3.174), one can already infer the behavior the dissipation energy for small and large ν . For $|\nu| \ll 1$ we can use that the integral is cut above $\rho \sim \mathcal{O}(|\nu|^{2/5})$. This means that we can set the slowly varying expressions in the brackets of (3.174) approximately to their value at $\rho = 0$, which is equal to unity.

Substituting $s = |\nu|/\rho^{5/2}$ in Eq. (3.174) we thus extract for $|\nu| \rightarrow 0$

$$\begin{aligned} B_c(i\nu) &= \frac{1}{2\pi^2} \int_0^\infty \frac{d\rho}{\rho^{5/2} B_c(i\nu/\rho^{5/2}) + |\nu|} \\ &= \frac{|\nu|^{(2/5)-1}}{5\pi^2} \int_0^\infty \frac{ds s^{-2/5}}{B_c(is \operatorname{sgn}\nu) + |s|} \\ &= \frac{B_0}{|\nu|^{3/5}}, \end{aligned} \quad (3.175)$$

where the numeric prefactor B_0 is determined self-consistently by the full solution,

$$B_0 = \frac{1}{5\pi^2} \int_0^\infty \frac{ds s^{-2/5}}{B_c(is \operatorname{sgn}\nu) + |s|}. \quad (3.176)$$

For the high-frequency asymptotics $|\nu| \gg 1$, one can expand the term in the brackets in (3.174) to leading order in $1/\rho$,

$$1 + \frac{\rho^3}{2} \ln \left| \frac{\rho+1}{\rho-1} \right| - \rho^2 = \frac{4}{3} + \mathcal{O}(1/\rho^2), \quad (3.177)$$

because the integral is now dominated by $\rho \gtrsim |\nu|^{2/5} \gg 1$. Hence $B_c(i\nu)$ has in this limit up to a modified numeric constant the same shape as for $|\nu| \rightarrow 0$, i.e.

$$B_c(i\nu) \sim \frac{4}{3} \frac{B_0}{|\nu|^{3/5}}. \quad (3.178)$$

Note that above T_c one obtains the same behavior of $B(x, i\nu)$ for $|\nu| \gg 1$, if $(\omega/\omega_*)^{1/z} \gg \max\{(\xi/a)^{-1}, ka\}$ or equivalently $|\nu|^{1/z} \gg \max\{x^{-1}, 1\}$, i.e. when a frequency-dependent characteristic momentum, see further below, is the largest scale. We conclude from the high- ν asymptotics of $B_c(i\nu)$ in Eq. (3.178) that the dynamic structure factor decays for $|\omega| \gg \omega_k$ as

$$S(\mathbf{k}, \omega) \propto |\omega|^{-13/5}, \quad (3.179)$$

consistent with older calculations [127, 132] and in contrast to a Lorentzian, like in the diffusion form (1.115), whose large-frequency tail is $\propto \omega^{-2}$. Conversely the low-frequency behavior of $B_c(i\nu)$ yields for the scattering intensity in the limit $|\omega| \rightarrow 0$

$$S(\mathbf{k}, \omega) \propto |\omega|^{3/5}, \quad (3.180)$$

i.e. a non-analytic vanishing of $S(\mathbf{k}, \omega)$, analogous to the line-shapes found by us in $d \leq 2$ at elevated temperatures. This differs from the outcome of mode-coupling theory [127, 128] and extrapolated perturbative renormalization group expansions [131, 132]. Instead one arrives in those cases at $0 < \lim_{\nu \rightarrow 0} B_c(i\nu) < \infty$, such that the elastic scattering is non-zero $S(\mathbf{k}, 0) \neq 0$. Hence contrary to a singular frequency dependence, one obtains a modified \mathbf{k} -dependence for $k > k_\omega$, i.e. $\Delta(\mathbf{k}, i\omega) \sim \omega_k \sim k^{5/2}$, implying $\tilde{\Pi}(\mathbf{k}, i\omega) \sim k^{1/2}/|\omega|$. The dynamic structure factor around $\omega = 0$, i.e. for $\omega \lesssim \omega_k$ is then approximately given by a centered Lorentzian [133] with a half-width $\propto k^{5/2}$, instead of $\mathcal{D}k^2 \sim k^2 \xi^{-1/2}$ as in the hydrodynamic regime. In our case this is prevented by the low-frequency divergence in $B_c(i\nu)$, leading to $\Delta(\mathbf{k}, i\omega) \propto k^4$.

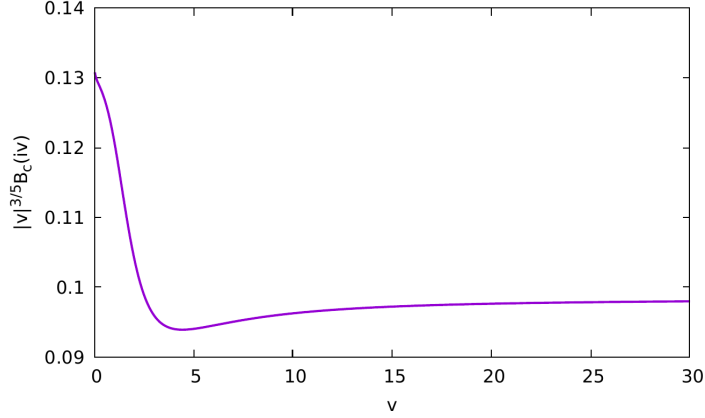


Figure 3.16: Numerical solution of (3.174) for the critical scaling function $B_c(i\nu) = B(\infty, i\nu)$ of the dissipation energy in $d = 3$. We display the quantity $|\nu|^{3/5} B_c(i\nu)$, as it approaches finite values for $\nu = 0$ and $\nu \rightarrow \infty$ due to the derived behavior of $B_c(i\nu)$ in Eq. (3.175) and Eq. (3.178). Reprinted with permission from Ref. [11] © [2022] American Physical Society.

For the sake of completeness, let us state the general asymptotics for $d < d_c$ in both cases of small and large frequencies

$$B_c(i\nu) \sim |\nu|^{1-4/z} \sim |\nu|^{(d-6)/(d+2)}, \quad \nu \rightarrow 0, \quad (3.181)$$

$$B_c(i\nu) \sim |\nu|^{(d-6)/(d+2)}, \quad \nu \rightarrow \infty, \quad (3.182)$$

implying

$$S(\mathbf{k}, \omega) \propto |\omega|^{(6-d)/(d+2)}, \quad \omega \ll \omega_k, \quad (3.183)$$

$$S(\mathbf{k}, \omega) \propto |\omega|^{(10+d)/(d+2)}, \quad \omega \gg \omega_k. \quad (3.184)$$

Results for the ν -dependence of $B_c(i\nu)$ and $\Psi_c(\nu)$ in $d = 3$ are shown in the figures 3.16 and 3.17. We observe the previously described behavior at small and large frequencies with a broad maximum at $\nu \approx 0.2$, which is a consequence of the asymptotics exhibited by $B_c(i\nu)$. Similar to the solutions for $A(x, iy)$ and $B(x, i\nu)$, we have first inserted an estimate from a truncation, where only the k^4 -term in $\Delta(\mathbf{k}, i\omega)$ is retained, serving as a starting point for iterations, which converge rapidly to the full solution of (3.174).

Turning explicitly to the momentum dependence of the critical scattering intensity at fixed frequency, we first introduce a corresponding momentum variable p via

$$\nu = \frac{\omega}{\omega_k} = \left(\frac{k_\omega}{k} \right)^z = p^{-z}, \quad (3.185)$$

yielding $k_\omega a = (\omega/\omega_*)^{1/z}$ for the characteristic momentum and therefore

$$p = k/k_\omega = \nu^{-1/z}. \quad (3.186)$$

We find then that the k -dependence is proportional to a function, defined by

$$\tilde{\Psi}_c(p) = p^{-9/2} \Psi_c(p^{-5/2}), \quad (3.187)$$

which is shown in Fig. 3.18. For $k \rightarrow 0$ the dynamic structure factor vanishes as

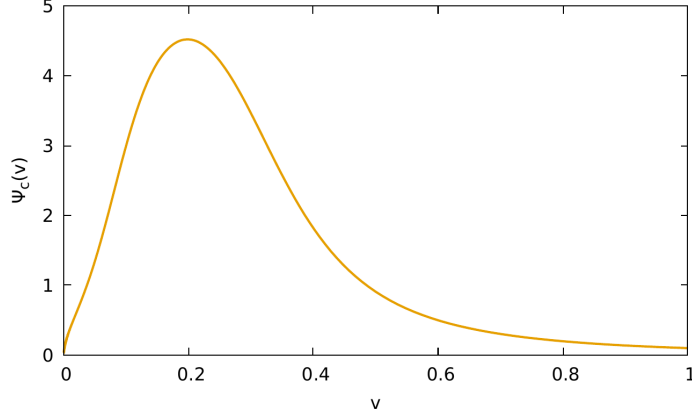


Figure 3.17: Scaling function $\Psi_c(\nu)$, defined in Eq. (3.171), of the dynamic structure factor in three dimensions, yielding the frequency dependence of $S(\mathbf{k}, \omega)$ at $T = T_c$. Reprinted with permission from Ref. [11] © [2022] American Physical Society.

$$S(\mathbf{k}, \omega \neq 0) \propto k^2, \quad (3.188)$$

due to total spin conservation (2.71). A Lorentzian shape leads to a non-analyticity $S(\mathbf{k}, \omega) \sim k^{1/2}$, i.e. $k^{z-2} = k^{\frac{d-2}{2}}$ for arbitrary d , in accordance with dynamic scaling. In the opposite limit $k \gg k_\omega$ the function $S(\mathbf{k}, \omega)$ decays in any dimension as k^{-6} , stronger than for a Lorentzian, which in turn vanishes in $d = 3$ as $k^{-9/2}$ for large momenta, or more general $k^{-2-z} = k^{-(d+6)/2}$. Between both limits one encounters a single broad peak. Since $\omega \ll \omega_k \leftrightarrow k \gg k_\omega$ the Lorentzian behavior for large momenta is also exhibited by the line-shapes of the leading mode-coupling approximations [127, 128, 129] and extrapolated RG expansions [131, 132, 134, 135], in disagreement with our outcome. Conversely the vanishing as k^2 for $k \ll k_\omega$ is, as the high-frequency behavior, consistent with the aforementioned line-shapes [127, 134]. Note that the one-peak structure in $\omega = \text{const.}$ scans is fairly generic. On the other hand, the fact that the maximum is located at a finite $k = k_*(\omega)$, means that not only its width $\Delta k(\omega)$ but also its position are sensitive to the precise line-shape. Thus one can better distinguish between different results for the scaling function. This becomes particularly useful for comparisons to experimental data, where low-frequency features may be concealed in the measured scattering intensity due to a finite resolution. We will discuss this in more detail in section 3.3.4, which is explicitly concerned with measurements of the scattering intensity at constant k and ω .

The scaling function $\tilde{\Psi}_c(p)$, defined via Eq. (3.187), is also a convenient starting point for calculating the Fourier transform of $S(\mathbf{k}, \omega)$ to real space, thus yielding scaling forms for ω -dependent correlation functions at large distances $|\mathbf{r}| \gg a$. One obtains then

$$S(\mathbf{r}, \omega) \sim \int_{\mathbf{k}} k_\omega^{-9/2} \tilde{\Psi}_c(k/k_\omega) e^{i\mathbf{k}\cdot\mathbf{r}} \sim k_\omega^{-3/2} \int_{\mathbf{u}} u^{-9/2} \tilde{\Psi}_c(u^{-5/2}) e^{ik_\omega \mathbf{u}\cdot\mathbf{r}} = k_\omega^{-3/2} \tilde{s}^{k,\omega}(k_\omega |\mathbf{r}|), \quad (3.189)$$

where the convergence of the integral is ensured by strong oscillations of the exponential for $|\mathbf{r}| \gg k_\omega^{-1} \rightarrow \infty$, as $S(\mathbf{k}, \omega)$ decays like k^{-6} , confining it in $d < d_c$ to $|\mathbf{k}| \lesssim k_c(r) \ll k_\omega$, or for $|\mathbf{r}|^{-1} \gg k_\omega \rightarrow 0$ by the k^4 -behavior of the dissipation energy, meaning that the integral is cut above $k \sim k_\omega$. In both cases it is therefore sufficient to retain only the

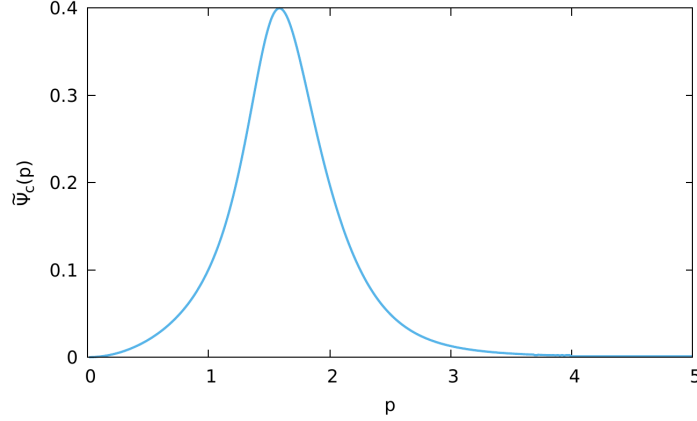


Figure 3.18: Scaling function for the momentum dependence of $S(\mathbf{k}, \omega)$ at $T = T_c$, defined in Eq. (3.187). Reprinted with permission from Ref. [11] © [2022] American Physical Society.

low momentum limit $p \ll 1$ of our scaling function. Conversely we can evaluate it at short distances, i.e. the auto- or pair correlation function between adjacent sites, where we can use again that for small frequencies the integral is restricted to $k \lesssim k_\omega$. We find then that short-distance correlations diverge as $k_\omega^{-3/2} \sim \omega^{-3/5}$ for $\omega \rightarrow 0$ or $\omega^{(d-6)/(d+2)}$ in arbitrary dimensions, which is consistent with the behavior of the zero-frequency limit $\sim \xi^{(6-d)/2}$ above T_c for a ferromagnet [58]. This could be anticipated since the behavior of our solution is corroborated by other methods for $k \lesssim k_\omega$. Note that the solution at large $|\mathbf{r}|$, i.e. the scaling regime, has the same low-frequency asymptotics, if $k_\omega |\mathbf{r}| \ll 1$.

For an investigation of k -dependent correlations in the time-domain $\Psi_c(\nu)$ itself is the appropriate starting point. Assuming $t \gg |JS|^{-1}$ one finds then for the time-dependent correlation function

$$S(\mathbf{k}, t) \sim \int_{-\infty}^{\infty} \frac{d\omega}{2\pi} S(\mathbf{k}, \omega) e^{i\omega t} \sim G(\mathbf{k}) \int_{-\infty}^{\infty} \frac{d\nu}{2\pi} e^{i\omega_k \nu t} \Psi_c(\nu) \sim k^{-2} \tilde{s}^{k,t}(\omega_k t) \quad (3.190)$$

The actual behavior of the critical scaling function $\tilde{s}^{k,t}(\omega_k t)$ is controversial, besides the fact that it is not a simple exponential [33]. Here the main question is whether it exhibits damped oscillations or approaches zero monotonously, with more recent numeric integrations of the mode-coupling equations predicting the former for $k\xi \rightarrow \infty$ [55, 129, 130]. In our case, $\tilde{s}^{k,t}(\omega_k t)$, should due to the branch point of $\Psi_c(\nu)$ at $\nu = 0$, caused by the non-analytic ν -dependence, fall off as a power-law for $t \rightarrow \infty$, namely $(kt^{1/z})^{-4}$. Note that the frequency dependence of $B_c(i\nu)$, shown in Fig. 3.16, does not allow for an analytic calculation of $S(\mathbf{k}, t)$, in contrast to the high- T results for the scaling forms in reduced dimensions. Doing otherwise, i.e. by neglecting the full dependence of $B_c(i\nu)$ and following the calculation in appendix B.2.2 one produces an error $\sim \mathcal{O}(1)$. We found that such a crude approximation results in an exponentially damped oscillation in the time-domain, similar to Ref. [129]. For the transform to real space we have to take the factor $1/k^2$ from $G(\mathbf{k})$ into account. $S(\mathbf{r}, t)$ is in $d < d_c$ then given by $t^{-(d-2)/z} \tilde{s}^{r,t}(rt^{-1/z})$. The spatial scaling function $\tilde{s}^{r,t}$ should then be determined by contributions with $k \lesssim t^{-1/z}$ in the k -integral over $\tilde{s}^{k,t}(\omega_k t)$, similar to the behavior in $d \leq 2$ for $T = \infty$.

3.3.3 Comparison of the critical scattering with theory

Returning to the frequency dependence of the dynamic structure factor, we found that $\lim_{\omega \rightarrow 0} S(\mathbf{k} \neq \mathbf{0}, \omega) = 0$ is at odds with previous calculations. All these methods predict a single maximum at $\nu = 0$ in the scaling function $\Psi_c(\nu)$, albeit of a broader shape and a steeper decay for $\omega \gtrsim \omega_k$, compared to a Lorentzian [55, 128]. The bell or Gaussian-like shape of $S(\mathbf{k}, \omega)$ can be interpreted in terms of a strong overlap between a dissipative component at $\omega = 0$ and overdamped 'spin waves' with hidden peaks at $\omega \neq 0$ [121].

Mode-coupling approaches boil down to the solution of an integro-differential equation for the relaxation-shape function $\tilde{\mathcal{R}}(\mathbf{k}, t)$ [60, 127, 128, 129, 130]. Here one uses an analogous decoupling of higher order spin relaxation functions as for $T \rightarrow \infty$, so that one arrives at the same high- T equation (3.86) as solved by Blume and Hubbard [74]. This approximation, together with using a classical fluctuation-dissipation theorem, i.e. its low-frequency limit (3.150), for the relation between $S(\mathbf{k}, \omega)$ and $\tilde{\mathcal{R}}(\mathbf{k}, \omega)$ was argued to produce only a small error for $T \gtrsim T_c$ in $d = 3$ [128], invoking in this process the limit of a sufficiently large coordination number c and therefore large $T_c \propto c|J|$. The Fourier-transform of the memory kernel, which, as discussed in Sec. 3.2.1, plays the same role as the analytically continued dissipation energy $\Delta_{\text{ret}}(\mathbf{k}, \omega)$, assumes then the form [127, 128]

$$\mathcal{K}(\mathbf{k}, \omega) \propto G^{-1}(\mathbf{k}) \int_{-\infty}^{\infty} \frac{d\nu}{2\pi} \int_{\mathbf{q}} [J(\mathbf{q}) - J(\mathbf{q} + \mathbf{k})]^2 G(\mathbf{q}) G(\mathbf{q} + \mathbf{k}) \tilde{\mathcal{R}}(\mathbf{q}, \nu) \tilde{\mathcal{R}}(\mathbf{q} + \mathbf{k}, \nu + \omega), \quad (3.191)$$

which exhibits the same dependence on static quantities as our equation. For $ka \ll 1$ and $\omega \ll |J|S$ one can show that $\mathcal{K}(\mathbf{k}, \omega)$ satisfies dynamic scaling with the predicted dynamic exponent for this universality class [127, 128]. Eq. (3.191) is a convolution in frequency space and follows from the purely local-in- t form of $\mathcal{K}(\mathbf{k}, t)$, whereas $\Delta_{\text{ret}}(\mathbf{k}, t)$ in our approximation would satisfy a non-local equation. One can also study the short-wavelength region with (3.191), although mode-coupling-theory is known to compete worse in this regard compared to extrapolation schemes [55], like the three-pole approximation (3.90) [98, 136]. These schemes also made use of similar approximations to obtain closed expressions for the moments $\langle \omega^2 \rangle_{\mathbf{k}}$, $\langle \omega^4 \rangle_{\mathbf{k}}$ and therefore $\Delta(\mathbf{k}, i\omega)$ at arbitrary temperatures. However, an analysis based on high-frequency properties is unsuitable for providing reliable results in the scaling regime. In particular they do not reproduce the correct dynamic exponent z below d_c due to an absence of singularities in the moments used for the low-frequency extrapolation [87, 88], leading therefore to Van Hove-behavior.

The other path for calculating $S(\mathbf{k}, \omega)$ close to T_c is based on an extrapolation of the expansion for the dissipation energy in powers of $\epsilon = 6 - d$. It was explicitly calculated within a perturbative renormalization group treatment of an effective equation of motion (1.123) for the spin degrees of freedom \mathbf{S} at long wavelengths [57, 131, 132], under the assumption of a Ginzburg-Landau theory (1.50) of its static properties. The structure of this equation and basic aspects of its derivation were sketched in section 1.4.2 about the coupled-mode approach to critical dynamics. Note that these effective field dynamics and mode-coupling theory, as described in the paragraph above, can be derived along similar lines, based on the memory-function framework by means of projections to separate 'slow' and 'fast' variables [55, 56], as mentioned in Section 1.4.2. In fact the outcomes for the two-spin correlation function in the scaling region turn out to be quite similar, which may be attributed to the common origin of these methods [55, 129].

Besides finding to $\mathcal{O}(\epsilon)$ the predicted value for the dynamic exponent $z = (8 - \epsilon)/2 = (d + 2)/2$ [57], it was shown in this context that the scaling function is finite and analytic for

$\omega \rightarrow 0$ [57, 131, 132] in contrast to our findings, which acquire a non-analytic suppression for any $\epsilon > 0$. This can be already seen as a strong argument against our low-frequency results in $d < d_c$. Note also that except for one calculation [137], where the authors presumably made a computational error and predicted a two-peak structure, it is recognized that to linear order in ϵ the scaling function has, down to $\epsilon = 3$, a sole maximum at $\omega = 0$ [132], in agreement with mode-coupling theory [127, 128]. The $\mathcal{O}(\epsilon)$ -result is properly extrapolated by enforcing that the correct behavior for $\nu \rightarrow \infty$ is reproduced [132, 135]. Technically this requires knowledge of infinitely many higher orders in ϵ to obtain the exact numeric value $2 + \epsilon/(8 - \epsilon)$ for the exponent in the high-frequency tail [131, 132]. For instance this can be realized by exponentiating the result for the dissipation energy to first order in frequency with $\epsilon/(\epsilon - 8)$, where the free parameters of this ansatz are fixed by the conditions that the zero-frequency amplitude and linear-in- ω term are exactly reproduced [132, 135]. Using our language one obtains [132, 134]

$$\Psi_c(\nu) \sim \text{Re}\left(\frac{1}{\Delta(\nu) - i\nu}\right), \quad (3.192)$$

$$\Delta(\nu) = \Delta(0)[1 + b\epsilon i\nu + \mathcal{O}(\nu^2)] \rightarrow \Delta(0)(1 + b(8 - \epsilon)i\nu)^{-\epsilon/(8-\epsilon)}, \quad (3.193)$$

where the arrow in the second line denotes the extrapolation. b is a numeric constant which follows from the expansion of the integrals in the effective equations of motion to $\mathcal{O}(\epsilon)$ [132]. As in our case the characteristic frequency behaves like $\omega_k = \omega_* k^z$ with a non-universal energy scale ω_* . The above form for the dissipation energy is analogous to the one discussed in Sec. 3.2.3 for reduced dimensions [45, 46]. In general one may consider extrapolating to $\epsilon = 3$ as an audacious move, because besides ϵ being large, one trespasses $d = 4$, the static critical dimension. Then the quartic coupling u in ϕ^4 -theory becomes relevant, implying a non-Gaussian fixed point, contrary to $d > 4$ where u was ignored due to its irrelevance [131, 135]. In spite of these subtleties the scaling form implied by Eq. (3.193) is in good agreement with mode-coupling theory and gives a satisfactory description of the measured critical scattering [55]. We will refer to (3.193) also as the interpolation formula of asymptotic RG, since this expression is a simple way to connect both limits $\nu \ll 1$ and $\nu \gg 1$. Note that its usage is restricted to the scaling region, i.e. one cannot study properties at large momenta and frequencies. Let us emphasize again that the dynamic scaling hypothesis itself does not make any definite statements about the line-shape $\Psi_c(\nu)$ at $T = T_c$, contrary to the hydrodynamic region, where a diffusion form is anticipated. However, it usually assumes that the elastic scattering is finite [58, 131], which lacks a rigorous argument in its favour, although it is corroborated by the ϵ -expansion and mode-coupling theory.

Numerical simulations of the spin dynamics, by integrating the equations of motion for an ensemble of classical spins, can, in principle, provide clarification of this issue. However up to now, no definite results could be extracted for the line-shape at $T = T_c$ in the scaling regime of very small momenta [138], given that large lattice sizes are necessary to obtain a good resolution, implying large computational costs in $d = 3$. Instead those calculations were mainly focused on confirming the fulfillment of dynamic scaling laws by analyzing the dependence on the finite system size [138, 139], or the behavior at short wavelengths, i.e. the non-universal region [140]. Investigations concerned with the latter found for instance evidence for the existence of propagating spin waves at short wavelengths $\lambda \lesssim \mathcal{O}(a)$ and large energies $\omega \sim |J|$ above T_c in a Heisenberg ferromagnet [140], agreeing with older neutron scattering data on iron [141]. A one-peak structure of $S(\mathbf{k}, \omega)$ for small momenta

was mentioned by the authors of Ref. [140], but never explicitly shown and a scrutiny of the corresponding PhD Thesis [142] did not reveal anything further concerning this aspect. A later review by Folk and Moser about critical dynamics in the scaling regime [56] did not reference this simulation, perhaps due to the focus of [140] on non-universal properties. The issue regarding the explicit form of the critical scaling function was therefore still seen as unresolved, but no further attempts were made thereafter to calculate $\Psi_c(\nu)$. Considering also the satisfying agreement of the mode-coupling and RG results with energy/momentum-resolved neutron scattering data, see the following Sec. 3.3.4, the available evidence is suggestive of our results being incorrect for $\omega \ll \omega_k$, although a residual ambiguity persists.

Proposals for refinement

Focusing for a moment on the mode-coupling results, the modified k -dependence of $\Delta(\mathbf{k}, i\omega)$ at $T = T_c$ for $\omega \ll \omega_k$, i.e. large k , arises there because the q -integral in the corresponding equation for $\Psi_c(\nu)$ [127, 128] was cut above momenta $q \sim k$, as evidenced by an ultra-violet behavior $\sim \int \frac{d^3q}{q^{9/2}} \sim q_c^{-3/2}$ [127], or $q_c^{(d-6)/2}$ for $d < 6$. In the opposite high-frequency limit $\omega \gg \omega_k$ the q -integral is cut by the frequency, i.e for $q \sim k_\omega \sim (\omega/\omega_*)^{1/z}$. While the latter is also realized in our context, the former situation cannot occur for our equation, due to an insufficient damping of the integrand in the infra-red limit $q \rightarrow 0$. Inserting $\Delta(\mathbf{q}, i\omega) \sim q^{5/2}$ would then produce an IR-singularity $\int \frac{d^3q}{q^{9/2}} \sim q_{\text{low}}^{-3/2}$. Hence, the integrals are cut above $k \sim k_\omega$ too, even if the largest scale is given by the external momentum, leading to the $k^4/\omega^{8/5}$ -behavior of the dissipation energy in both limits. For $T > T_c$ one also has to take $\xi^{-1} \neq 0$ as a potential cutoff into account. The hydrodynamic region would then be given by $\xi^{-1} \gg \max\{k, k_\omega\}$, the critical region by $k \gg \max\{\xi^{-1}, k_\omega\}$ and the high-frequency regime is $k_\omega \gg \max\{\xi^{-1}, k\}$, as previously mentioned. Our equation reproduces then two out of the three possible cases correctly.

One should note that one contribution to $V(\mathbf{k}, \mathbf{q})$ is compatible with a finite $\Delta(\mathbf{k}, 0)$, namely the term $\sim (\mathbf{k} \cdot \mathbf{q})^2$, since $\int \frac{d^3q}{q^{5/2}} \sim q^{1/2}$ is non-singular. Hence by replacing

$$[k^2 + 2\mathbf{k} \cdot \mathbf{q}]^2 \rightarrow 4[\mathbf{k} \cdot \mathbf{q}]^2, \quad (3.194)$$

one induces a sufficient suppression, to allow for setting $[\omega + \Delta(\mathbf{k}, i\omega)] \rightarrow \Delta(\mathbf{k}, 0)$ with $\Delta(\mathbf{k}, 0) \propto k^z$. We have checked on its effect and found that, although now $S(\mathbf{k}, 0) \neq 0$, the modified scaling form does not feature an elastic peak. In its place we obtained a minimum with a non-analytic narrowing caused by corrections at finite frequency. Obviously the proposed raise in the leading power of loop momentum for $q \rightarrow 0$ does not introduce a masking of deviations from analytic behavior in $|\omega|$. Furthermore the above change moves our equation further away from our own three-point vertex (3.38) and the mode-coupling approximation, which contained the same static part $\sim [J(\mathbf{q}) - J(\mathbf{q} + \mathbf{k})]^2 G(\mathbf{q})G(\mathbf{q} + \mathbf{k})$ on the right-hand side.

While the non-local coupling between different frequencies in the mode-coupling kernel (3.191) is the most conspicuous difference between our equations, the origin of the screening at finite momentum is, more likely, found in additional momentum transfers, that appear directly in the dissipation energy. A modification of (3.50) may look like this

$$\Delta(\mathbf{q}, i\omega) \rightarrow \frac{1}{2} \left(\Delta(\mathbf{q}, i\omega) + \Delta(\mathbf{q} + \mathbf{k}, i\omega) \right). \quad (3.195)$$

For $\mathbf{k} \neq \mathbf{0}$ all previously encountered $q \rightarrow 0$ -singularities are regularized, so that $\Delta(\mathbf{k}, 0)$ always has a finite limit. The modification (3.195) also introduces for $\mathbf{k} \neq \mathbf{0}$ a screening of

non-analytic corrections to diffusion above two dimensions [44, 109], which were discussed in 3.2.2. Note that one cannot perform in $d = 3$ the integration over the angle between \mathbf{k} and \mathbf{q} analytically like in the previous case. At elevated temperatures the above substitution will prevent us from writing $\Delta(\mathbf{k}, i\omega)$ as a finite-ranged Fourier series like in Eq. (3.64). The dissipation energy will not have a form as simple as in the RG interpolation formula (3.193) from Ref. [134]. Furthermore it is a priori unclear, whether the solution for $\Delta(\mathbf{k}, i\omega)$ from an accordingly modified equation indeed leads to a elastic peak or a central dip in $S(\mathbf{k}, \omega)$ at T_c . Note that a similar type of equation was also proposed for lowest-order coupled-mode contributions to the dissipation energy at long wavelengths [44, 109]. In that context the equations were formulated using the hydrodynamic dispersion $\lambda(\mathbf{q})$ under the integral, which is defined by the solution of the self-consistency equation $\lambda(\mathbf{q}) = \Delta(\mathbf{q}, -i\lambda(\mathbf{q}))$ [44], i.e. the poles of the relaxation function.

3.3.4 Comparison of the critical scattering with experiments

We have established, that our line-shape does not agree for small frequencies $\omega \ll \omega_k$ with the result from mode-coupling theory and asymptotic RG. For experiments the feature of a non-analytic suppression of spectral weight at small frequencies is likely obscured by a finite energy resolution [61, 144], which turns out to be of the same order as the characteristic frequency ω_k . As a consequence of that smoothing spectral weight is transferred to $\omega = 0$, so that the measured scattering exhibits either a two-peak structure with a finite, analytic minimum or blends both maxima into a single peak at $\omega = 0$. Hence qualitative differences of the theoretical line-shapes cannot be reasonably discerned in the convoluted cross section at low frequencies. The same reasoning applies to the non-analytic distortion of spin diffusion above T_c , which by this means also becomes practically invisible. Hence one is not able to rule out salient low-frequency features as found in our scaling functions by purely visual cues in the experimental data. Nevertheless one can assess the applicability of our result for the critical line-shape by fitting it to available data from inelastic neutron scattering experiments at $T = T_c$.

Experimental data of neutron scattering intensities can be for instance found in Ref. [61, 144] for the magnetic insulator EuO at $T_c = 69.25$ K. This material is aptly described by an isotropic Heisenberg Model on a face-centered cubic lattice with nearest and next-nearest neighbor interactions, $J_1 = 1.21$ K and $J_2 = 0.24$ K and a lattice spacing $a = 5.12$ Å. Here the spacing a refers to the conventional unit cell, which is four times larger than the primitive cell, implying $v = 1/4$ [143]. To explicitly enable a comparison, we have to perform the aforementioned smoothing of our theoretical result for $S(\mathbf{k}, \omega)$. For that purpose one convolutes $S(\mathbf{k}, \omega)$ with the experimental resolution function $E(\omega)$ [61], so that the measured intensity due to magnetic scattering is up to a conversion factor given by

$$S_{\text{con}}(\mathbf{k}, \omega) = \int_{-\infty}^{\infty} d\omega' E(\omega - \omega') S(\mathbf{k}, \omega'). \quad (3.196)$$

A common choice for $E(\omega)$ is a normalized Gaussian [139]

$$E(\omega) = \frac{1}{\sqrt{2\pi\delta_\omega^2}} \exp\left[-\frac{\omega^2}{2\delta_\omega^2}\right], \quad (3.197)$$

with its width δ_ω being the aforementioned energy resolution. In the second experiment by Böni *et al.* on EuO in Ref. [144] it is given by $\delta_\omega = 0.05$ meV. For the measured neutron

scattering intensity at fixed momentum $\mathbf{k} = \text{const.}$ the following ansatz is made, analogous to the procedure used in Ref. [144],

$$\mathcal{I}_k(\omega) = CS_{\text{con}}(\mathbf{k}, \omega) + B. \quad (3.198)$$

This quantity has units of counts per time interval, see the following figures. For the unconvoluted $S(\mathbf{k}, \omega)$ we take corrections up to quadratic order in ω/T to the classical detailed-balance factor (3.150) into account. The $(\omega/T)^2$ -contribution is then already found to be very small, i.e negligible. Note that non-magnetic scattering at $\omega = 0$ was subtracted from the data given in Ref. [144]. This leaves us with the background scattering B as the sole source of contributions not covered by the Heisenberg description. It is then, together with the normalization constant C , a parameter of a χ^2 -fit, using Eq. (3.198). Furthermore the characteristic frequency ω_k and thus the non-universal energy scale $\omega_* = \omega_k(ka)^{-5/2}$ is also determined from the fit, like for the RG formula [134, 144]. Adjusting ω_k can be interpreted as allowing for corrections to the bare spin stiffness ρ_0 from a non-trivial but still analytic momentum dependence of the static self-energy $\Sigma(\mathbf{k})$, i.e. $0 < \Sigma'' < \infty$. In our context the latter can be considered a consequence of taking the solution of the equation with modified G^{-1} -kernel (3.46). Afterwards one proceeds to the data recorded at $\omega = \text{const.}$, by fitting it to [144]

$$\mathcal{I}_\omega(k) = CS_{\text{con}}(\mathbf{k}, \omega) + B', \quad (3.199)$$

with the background B' being the sole free parameter of the fixed- ω fit, whereas C , ω_k are determined via the previous scan at constant momentum. One anticipates that our result for the line-shape can be only applied for sufficiently large ω , so that data at too low frequencies should be excluded from our fit. The explicit prescription is given by removing all data points fulfilling the condition $|\omega| \lesssim \Gamma_k$, where $\Gamma_k = \Gamma'(ka)^{5/2}$ is the measured linewidth for a Lorentzian curve, i.e. [61, 133, 144]

$$S(\mathbf{k}, \omega) \propto \frac{\Gamma_k}{(\Gamma_k)^2 + \omega^2}. \quad (3.200)$$

For the material EuO the non-universal constant is given by $\Gamma' = 0.139$ MeV [61]. Note that before one employed more theoretically grounded line-shapes, like Eq. (3.193), for the analysis of experimental data the Lorentzian was empirically modified as [61, 146]

$$S(\mathbf{k}, \omega) \propto \left(\frac{\Gamma_k}{(\Gamma_k)^2 + \omega^2} \right)^{\epsilon(\omega)}. \quad (3.201)$$

The exponent $\epsilon(\omega)$ is given by [61, 146]

$$\epsilon(\omega) = 1 + \frac{\alpha(|\omega| - \Gamma_k)}{\Gamma_k} \Theta(|\omega| - \Gamma_k), \quad \alpha > 0, \quad (3.202)$$

where α is a non-universal fit parameter, that depends on the studied material [61, 146] and therefore cannot be properly connected to a dynamic scaling ansatz [134]. This form decays much faster than the simple Lorentzian for $|\omega| > \Gamma_k$. The motivation for Eq. (3.201) was to provide a better description of the data at large frequencies, since the Lorentzian has a too large tail for $|\omega| \gg \Gamma_k$ [61] and is therefore only a reasonable approximation in the vicinity of $\omega = 0$. This also explains, why we use the same condition for separating low and high-frequency data, since our prediction for the line-shape is presumably valid in the latter Non-Lorentzian region. The heuristic ansatz (3.201) was shown to yield quite similar

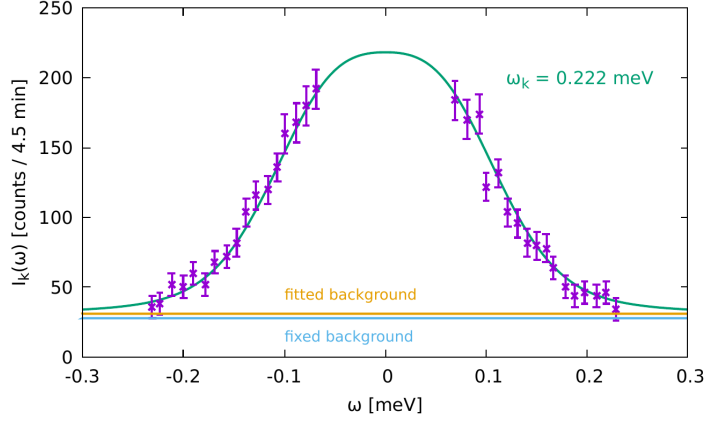


Figure 3.19: Fit to experimental neutron scattering data at $T = T_c$ and a fixed momentum $k = 0.15 \text{ \AA}^{-1}$, shown in Fig. 2 of Ref. [144], using our theoretical prediction for the convoluted neutron scattering intensity in Eq. (3.198). Data with small frequencies $|\omega| \lesssim \Gamma_k = 0.072 \text{ meV}$ was dropped, as described in the text. Note that Ref. [144] provided the error bars only for select data points. We therefore assigned the same error bars to adjacent points as an estimate of the remaining ones. Reprinted with permission from Ref. [11] © [2022] American Physical Society.

results to the interpolation formula from asymptotic RG (3.193), which superseded it in subsequent analyses of the data [134].

Returning to our result for the convoluted scattering cross section, we show in Fig. 3.19 a fit to measured data, displayed in Fig. 2 of Ref. [144], at fixed momentum $k = 0.15 \text{ \AA}^{-1}$ with a determined Lorentzian half-width $\Gamma_k \approx 0.072 \text{ MeV}$. We obtain $\omega_k = 0.222 \text{ MeV}$ for the characteristic frequency and therefore $\omega_* = 0.429 \text{ MeV}$. This is larger than the estimates $\omega_k = 0.158 \text{ MeV}$, $\omega_* = 0.306 \text{ MeV}$ from the solution of the integral equation, if one takes only the contribution from $J'' = J_1 + J_2 = 1.45 \text{ K}$ to the stiffness into account. The position of the broad peak in the theoretical curve with fitted ω_k would thus lie at $\omega_*(k) = 0.2 \times \omega_k \approx 0.045 \text{ MeV} \approx 0.62\Gamma_k$, which is even smaller than δ_ω . This explains why the convoluted line-shape exhibits only a single elastic peak. Hence a non-analytic low-frequency suppression of $S(\mathbf{k}, \omega)$ is, together with a two-peak structure, entirely hidden. Our result for the background $B = 31$ counts is relatively close to the fixed value $B \approx 28$ counts. The latter was extracted from the measured scattering at low temperatures, since this baseline can be accurately determined due to almost all spectral weight being concentrated in sharp spin-wave peaks [144]. Fitting the data to the interpolation formula (3.193) yields directly $B = 28$ counts, suggesting that it performs a bit better in the considered region [144]. However, if we use the low-temperature background for our fit the remaining parameters C and ω_k change only modestly. A Lorentzian fit, also shown in Fig. 2 of Ref. [144] yields $B \approx 0$ counts, which is obviously way too low and caused by the too slow decrease for $|\omega| \gg \Gamma_k$. Altogether the fit in Fig. 3.19 indicates that beyond $\omega \sim \Gamma_k$ the experimental scattering intensity can be, as anticipated, adequately described by our line-shape. To check that our ansatz becomes less applicable for small frequencies we fit it to the whole set of data, which is shown in Fig. 3.20. The relevant fit parameters are now given by $\omega_k = 0.177 \text{ MeV} \rightarrow \omega_* = 0.342 \text{ MeV}$, which is much closer to the theoretical

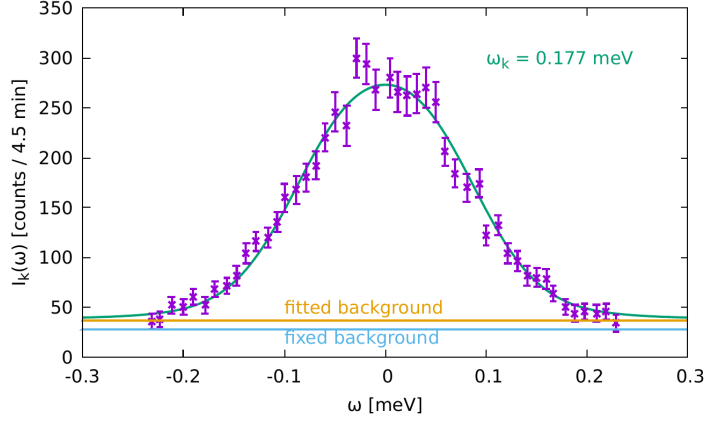


Figure 3.20: Fit to the **full** data at $k = 0.15 \text{ \AA}^{-1}$ shown in Fig. 2 of Ref. [144] using our prediction for the convoluted scattering intensity. Reprinted with permission from Ref. [11] © [2022] American Physical Society.

estimate, and $B = 37$ counts. The significant enlargement of the fitted background hints at the fact, that our line-shape lacks spectral weight for $\omega \rightarrow 0$, and thus indicates that it may not properly describe the low-frequency behavior.

An alternative method of assessing our result for $S(\mathbf{k}, \omega)$, is given by a fit of the convoluted line-shape to scattering data at fixed frequency transfer by means of Eq. (3.199). As already mentioned, these scans are much more shape-specific due to the location of the peak at finite momentum $k_*(\omega)$. The theoretical results for the peak position and width are for our solution given by

$$k_*(\omega)a = [3.25\omega/\omega_*]^{2/5} > k_\omega a, \quad \Delta k(\omega) = 0.5k_*(\omega), \quad (3.203)$$

as can be inferred from $\tilde{\Psi}_c(p)$ depicted in Fig. 3.18. Conversely for the Lorentzian one finds $k_*(\omega)a = [\omega/(3\Gamma')]^{2/5}$ and $\Delta k(\omega) = 1.57k_*(\omega)$, while the peak parameters from the line-shape in the RG interpolation formula (3.193) are given by $k_*(\omega)a = [\omega/(1.3\Gamma')]^{2/5}$ and $\Delta k(\omega) = 0.75k_*(\omega)$ [134, 135]. The latter is close to the experimentally determined $k_*(\omega)a = [\omega/(1.27\Gamma')]^{2/5}$ [144]. The values of the RG formula and the Lorentzian can be compared directly for arbitrary values of Γ' , due to Γ' being approximately the same for both types of line-shapes [144]. One finds then that $k_*(\omega)a$ for the Lorentzian is too small by 30 percent and the width is larger by 50 percent, another indication that a Lorentzian is inferior to the RG result (3.193). For a comparison to our line-shape, one explicitly needs the ratio ω_*/Γ' , which depends on the material. From the fit to data at fixed k , we obtain $\omega_*/\Gamma' \approx 3$. Our peak position is thus 15 percent larger than the RG result, with a width that is too slim by about 30 percent. As before, we exclude data from the $\omega = \text{const.}$ -fit, for which our ansatz presumably does not work. Consistent with the scans at constant momentum we only keep data points with momenta satisfying $ka \lesssim (\omega/\Gamma')^{2/5} \approx 1.36$, which is equivalent to ignoring frequencies below $\Gamma'(ka)^{5/2}$ in scans at constant momentum. In Fig. 3.21 a fit to a scan at fixed $\omega = 0.3$ meV, see Fig. 3 of Ref. [144], is shown. Note that the boundary momentum lies almost at the position of the maximum of our line-shape, $k_*(\omega)a \approx 1.4$, which remains practically unaltered after convolution with the resolution function. We obtain $B' = 92$ counts for the background, fairly close to $B' = 83$ counts given in Ref. [144],

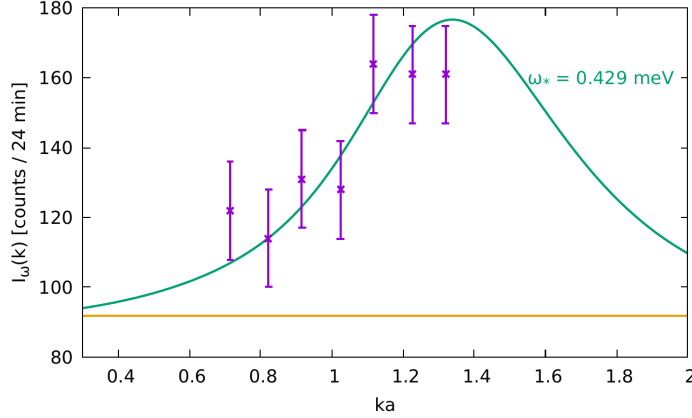


Figure 3.21: Fit to experimental scattering data at $T = T_c$ and fixed frequency $\omega = 0.3$ meV shown in Fig. 3 of Ref. [144] using our theoretical prediction for the convoluted scattering intensity given in Eq. (3.199). Only data fulfilling $ka < (\omega/\Gamma')^{2/5} \approx 1.36$ was taken into account, since for $k \gtrsim k_\omega$ we expect that our ansatz fails. Note that the data displayed here is collected during a larger time-interval than in Fig. 3.19, hence the larger values. Reprinted with permission from Ref. [11] © [2022] American Physical Society.

extracted by using the RG interpolation formula (3.193) for the fit. Overall, the data does not appear to contradict our prediction for the line-shape. The number of available points is quite small though. In conjunction with the large statistical errors, it is therefore hard to assess the compatibility of our result with the measured data of Ref. [144]. Fitting our ansatz to an intensity recorded at the smaller frequency $\omega = 0.2$ MeV, see also Fig. 3 of Ref. [144], the agreement with the data is significantly reduced. However, in that case the number of data points, satisfying $ka < (\omega/\Gamma')^{2/5}$, is even smaller. Hence the available data for EuO does not suffice to make definite statements regarding the applicability of our approximation in the low-momentum region $k \lesssim k_\omega$. For the sake of completeness we have also fitted our ansatz to the full data at fixed $\omega = 0.3$ MeV, which is shown in Fig. 3.22, using ω_* from the fixed k -fit in Fig. 3.20. In contrast to the full-data scan at constant momentum it decisively confirms that our result is inappropriate for too large momenta or too small frequencies, due to the strong dislocation of the peak.

Fortunately, EuO is not the only magnetic material, for which experimental data is available in the critical region. The spin dynamics near T_c of the related compound EuS were also investigated via inelastic neutron scattering [145]. Like EuO it is a Heisenberg ferromagnet on a fcc lattice with spacing $a = 5.95$ Å, nearest / next-nearest neighbor interactions $J_1 = 0.47$ K, $J_2 = -0.24$ K and a transition temperature $T_c = 16.5$ K [143]. Analogous to the analysis concerning EuO only data at sufficiently large frequencies or small momenta is kept, with the same criteria $|\omega| \gtrsim \Gamma_k = \Gamma'(ka)^{5/2}$ and $ka \lesssim (\omega/\Gamma')^{2/5}$, where $\Gamma' = 0.026$ MeV for EuS. The experimental resolution of Ref. [145] is $\delta_\omega = 0.035$ MeV. In Fig. 3.23 a fit, using (3.198), to a scan at fixed $k = 0.22$ Å⁻¹ is shown, see Fig. 2 of Ref. [145], where frequencies $|\omega| \lesssim 0.051$ MeV are omitted. We obtain $\omega_* = 0.079$ MeV $\rightarrow \omega_k = 0.154$ MeV, which is again larger than the estimates $\omega_* = 0.058$ MeV, $\omega_k = 0.113$ MeV. Our fit shows a similar agreement to the data as for EuO. The obtained background almost coincides with $B \approx 15$ counts for EuS, where the latter is extracted from the measured low-

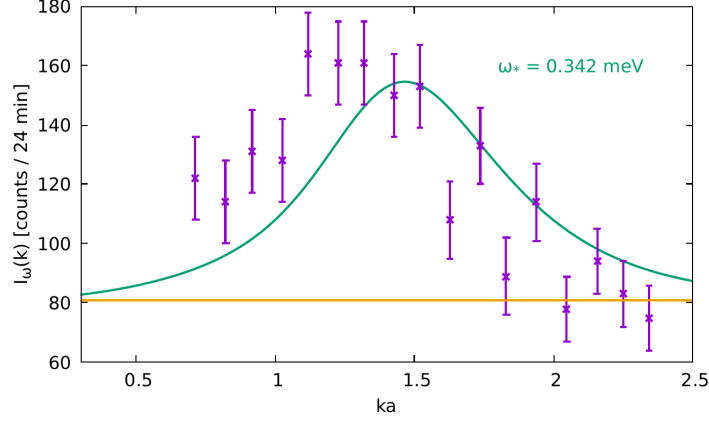


Figure 3.22: Fit to a scan at fixed $\omega = 0.3$ meV, where the **whole** data of Fig. 3 in Ref [144] is retained. One can discern that our ansatz is inadequate for this purpose, as indicated by the too large peak position, resulting in a systematic deviation of the fitting curve from the data.

temperature scattering. Like in the case of EuO the putative peaks featured by our $\Psi_c(\nu)$ lie at about 60 percent of the Lorentzian width $\Gamma_k = 0.051$ MeV. This is smaller than the energy resolution δ_ω , so that again we observe a broad single peak at $\omega = 0$ in the convoluted line-shape. In fact, $\delta_\omega/\omega_k \approx 0.22$ is practically the same for EuO and EuS. Furthermore the ratio $\omega_*(\text{EuO})/\omega_*(\text{EuS}) \approx 5.4$ of non-universal constants in both materials is nearly identical with $\Gamma'(\text{EuO})/\Gamma'(\text{EuS})$, which supports the conclusion that our result is suited for describing the high-frequency behavior. Turning to the data collected at constant frequency $\omega = 0.15$ MeV, which is shown in Fig. 3 of Ref. [145], we find that even after excluding large momenta $ka > (\omega/\Gamma')^{2/5} = 2.0$, a significantly larger number of points can be used for the fit in the presumed low-momentum region. In Fig. 3.24 a fit to the reduced data, using (3.199), is shown. Our prediction shows satisfying agreement with the scattering data, in particular for the lowest-lying momenta. Only close to the peak discernible deviations set in, given that our prediction $k_*(\omega)a \approx 2.1$ for the location of the maximum is, like for EuO, 15 percent larger than the experimental / RG value and lies again in the vicinity of the crossover between low and high-momentum regime.

The main takeaway of our analysis is, that the interpolation formula from the asymptotic RG approach, Eq. (3.193), which was previously used for analyzing the experimental data performs better at explaining measured scattering intensities. This is especially the case for scans at constant frequency transfer. The non-analytic suppression of spectral weight in $S(\mathbf{k}, \omega \rightarrow 0)$ is therefore in all likeliness an artifact of our approximation. Still, for large frequencies or small momenta our line-shapes are consistent with the experimental scattering data and clearly superior to a Lorentzian in these regions. As noticed in previous investigations, and also found by us, the region where the experimental scattering satisfies dynamic scaling laws is quite extended [144, 145]. For instance the fixed k -scans analyzed here were taken at $ka = 0.768$ for EuO and $ka = 1.309$ for EuS. This is somewhat unexpected, since these values are close to or larger than the boundaries set by theoretical approaches, which demand that $ka \ll 1$ has to hold for the scaling region [55].

Note that we have focused on data for only two materials, since it sufficed for checking on the validity of our line-shape. We explicitly chose these two compounds, because they

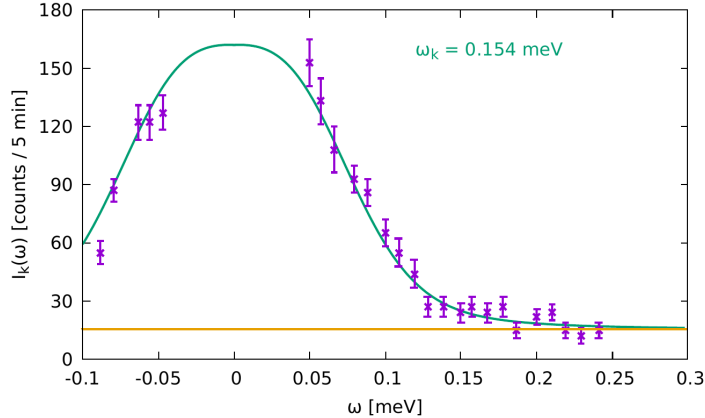


Figure 3.23: Fit to a scan of the experimentally measured scattering of EuS at $T = T_c$ and $k = 0.22 \text{ \AA}^{-1}$, shown in Fig. 2 of Ref. [145], using our prediction for the convoluted scattering intensity in Eq. (3.198). Small frequencies $|\omega| \lesssim \Gamma_k = 0.051 \text{ meV}$ were for the sake of consistency already removed from the data. As in the case of EuO, error bars were assigned to groups of adjacent points, since only a few were indicated in Ref. [145]. Reprinted with permission from Ref. [11] © [2022] American Physical Society.

are not conductors [121, 143], so that the major cause of their magnetism is likely the interaction between localized moments, as represented by the Heisenberg model. On the other hand a substantial amount of neutron scattering experiments were performed on metals like Iron (Fe) and Nickel (Ni) [146, 147, 148]. For these systems one would expect that their magnetism may be partially attributed to itinerant conduction electrons [14, 18]. Nevertheless data in the critical region revealed, that the scattering is consistent with dynamic scaling for the universality class of isotropic ferromagnets with $z = 5/2$ [146, 147, 148]. In fact, energetic considerations suggest that the magnetic properties of Fe and Ni can be explained by exchange between localized moments [150, 151]. Data from Ni for $T \geq T_c$ was also found to be satisfactorily described by a modified RG interpolation formula for $S(\mathbf{k}, \omega)$ with multiple adjustable parameters [148, 153]. Furthermore the exponent in the high-frequency decay of the dynamic structure factor was explicitly measured for Ni. It was found to be ≈ 2.3 , which corroborates again that the line-shape is non-Lorentzian, although with a weaker tail compared to the theoretical prediction $S(\mathbf{k}, \omega) \sim |\omega|^{-2.6}$ [148].

Finally we like to point out a caveat in the analysis of experimental data for ferromagnets. Long-ranged dipolar interactions, present in realistic materials, that have a much smaller magnitude than the exchange coupling J [14], still induce a crossover to different critical behavior at very long wavelengths [55, 149]. This is accompanied by a change in the dynamic universality class, as now the order parameter is not conserved. The Heisenberg results thus become inappropriate for momenta below a cutoff wave vector k_D , that is determined by the dipolar interaction strength [55, 149]. Such deviations from the theoretical results for exchange-based magnets were indeed measured for EuO at T_c [152], where the line-shape for $k \rightarrow 0$ resembled again a Lorentzian and not the critical scaling function of the Heisenberg ferromagnet. Hence a description that takes solely short-ranged exchange into account retains its validity only for $k > k_D$, which fortunately holds true for the data analyzed by us. At temperatures slightly above T_c , the effect of dipolar forces on the scat-

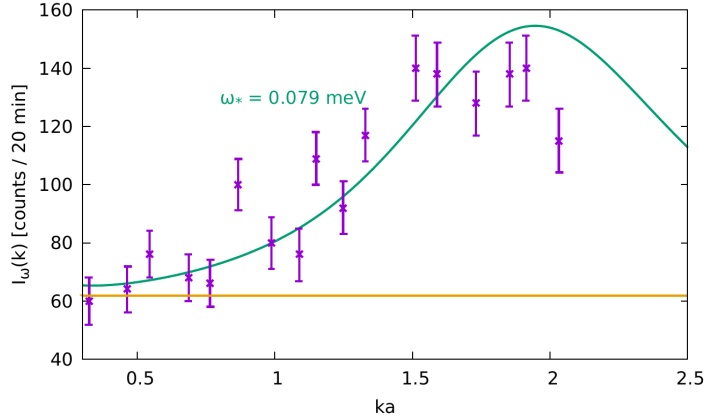


Figure 3.24: Fit to a scan at $T = T_c$ and fixed frequency $\omega = 0.15$ meV of the experimentally determined scattering of EuS, shown in Fig. 3 of Ref. [145], using our own theoretical prediction given by (3.199). Large momenta $ka \gtrsim (\omega/\Gamma')^{2/5} \approx 2.0$ were omitted for this fit. Reprinted with permission from Ref. [11] © [2022] American Physical Society.

tering becomes even more pronounced. For instance the temperature dependence of the peak positions and width in scans at $\omega = \text{const.}$ for EuS [145] could not be explained by the prediction of asymptotic RG for exchange-based magnets [154]. Mode-coupling calculations taking dipole-dipole interactions into account confirmed that the presence of dipolar terms causes these changes [149].

3.4 Discussion of the antiferromagnet in $d = 3$ close to T_c

In section 3.3 we investigated the critical dynamics of a ferromagnet, where the magnetization is also the order parameter, leading to only one relevant slow mode. The antiferromagnet, on the other hand, has a non-conserved order parameter at finite momentum $\mathbf{Q} = \mathbf{Q}_N$ and the conserved magnetization at $\mathbf{q} = 0$, implying therefore two types of slow fluctuations coupling to each other. Hence close to the critical temperature T_c , one has to compute two different scaling functions [56, 58, 60]. A compelling reason to study the antiferromagnet is that numeric benchmark calculations [155], including the regime of arbitrarily small momenta, are readily available, thus giving conclusive evidence regarding the line-shape, in contrast to the ferromagnet. Furthermore the presence of dipolar forces in real antiferromagnets does not alter the critical properties and therefore the dynamic universality class. Employing a Heisenberg description therefore suffices for studying the scaling regime and explain the corresponding experiments on real materials. Note that this section is mainly concerned with the scaling behavior and does not contain explicit results for the shape function. In appendix B.3 we have given results for the T -dependence of key quantities, like \mathcal{D} , in the whole paramagnetic phase for a Heisenberg magnet with nearest-neighbor coupling $J > 0$.

For the explicit treatment of an antiferromagnet one first needs to introduce the relevant static susceptibilities. We assume a non-frustrated antiferromagnet with nearest-neighbor interaction $J > 0$ on a bipartite lattice, thus enabling a Néel-ordered ground state with $\mathbf{Q} = \mathbf{Q}_N$, i.e. a finite staggered magnetization. Valid isotropic lattices are therefore simple

cubic (sc) or body-centered cubic (bcc), but not the face-centered cubic (fcc) lattice [156]. For such systems the exchange interaction satisfies

$$J(\mathbf{q} + \mathbf{Q}) = -J(\mathbf{q}), \quad (3.204)$$

and in particular $J(\mathbf{0}) = |J(\mathbf{Q})|$. For the non-singular (uniform) region around $q = 0$, we simply have

$$G(\mathbf{q}) \approx \chi, \quad qa \ll 1, \quad (3.205)$$

where $\chi \sim J^{-1}$ is the magnetic susceptibility. For $\Sigma(\mathbf{k}) \approx \Sigma$ it is $\chi \approx 1/(2|J(\mathbf{Q})|)$. Conversely, in the vicinity of the ordering vector \mathbf{Q} we assume again an Ornstein-Zernicke form

$$G(\mathbf{q} + \mathbf{Q}) \approx \frac{\chi_N}{1 + (q\xi)^2}, \quad qa \ll 1, \quad (3.206)$$

with the staggered susceptibility $\chi_N = \xi^2/\rho_0$, where ξ and ρ_0 are the correlation length and bare spin stiffness with $\rho_0 = J_Q'' a^2 = |J|a^2$. The coupling to the uniform region arises from the momentum transfer $\sim \mathbf{Q}$ in the equation for the dissipation energy $\Delta(\mathbf{Q}, i\omega)$ at the Néel ordering vector. Hence one susceptibility in the product $G(\mathbf{q})G(\mathbf{q} + \mathbf{Q})$ is singular, namely $G(\mathbf{q} + \mathbf{Q})$, which is the same divergence $1/q^2$ as in the contribution around \mathbf{Q} where $G(\mathbf{q})$ is singular. In the equation for the diffusive component in $\Delta(\mathbf{k} \rightarrow 0, i\omega) \propto k^2$ only terms in the vicinity of \mathbf{Q} have relevant weight, with $G(\mathbf{q})G(\mathbf{q} + \mathbf{k})$ yielding a singularity $\sim 1/q^4$. Finally one needs that for $k\xi \gg 1$, $ka \ll 1$, where k is either the distance to $\mathbf{0}$ or \mathbf{Q} , both $\Delta(\mathbf{k}, i\omega)$ and $\Delta(\mathbf{Q} + \mathbf{k}, i\omega)$ behave as k^2 . From this information one can infer that the upper critical dimension, where the integrals are solely determined by small momenta around the singularities of $G(\mathbf{q})$, $G(\mathbf{q} + \mathbf{k})$ is now given by $d_c = 4$, because the integrals are only UV-convergent as $\int d^d q/q^4 \sim 1/q_c^{4-d}$. Then one can set $q_c \rightarrow \infty$ in the integrations and use $J(\mathbf{q} + \mathbf{Q}) \approx J_Q''(qa)^2$. Note that in contrast to a ferromagnet the critical dimensions for statics and dynamics do coincide. This implies that a renormalization group analysis of the equations of motion to first in order $\epsilon = 4 - d$, already has to take into account that the static critical properties are described by the non-Gaussian Wilson-Fisher fixed point.

With the above results one can now explicitly show that both types of dissipation energies satisfy dynamic scaling relations, at least if one neglects the momentum dependence of the static self-energy. For the hydrodynamic region $k, \omega \rightarrow 0$ it is then convenient to write them in terms of the following scaling functions

$$\Delta(\mathbf{k}, i\omega) = \tau^{-1} A_0(x = k\xi, iy = i\omega\tau), \quad (3.207)$$

$$\Delta(\mathbf{Q} + \mathbf{k}, i\omega) = \tau^{-1} A_N(x, iy). \quad (3.208)$$

Here the characteristic timescale is given by

$$\tau = \sqrt{\frac{1}{|J(\mathbf{Q})|vT}} (\xi/a)^{d/2} = \frac{(\xi/a)^{d/2}}{\omega_*}, \quad (3.209)$$

implying the dynamic exponent $z = 3/2$ in $d = 3$, in contrast to van Hove theory where $z = 2$ and in agreement with the predictions of the dynamic scaling hypothesis [54, 58]. Furthermore the qualitative form of the non-universal constant ω_* agrees with mode-coupling theory [60, 157]. In this context one also notes that, in contrast to the ferromagnet, the dynamic exponent z remains the same if the anomalous dimension η is finite [58, 60]. Note that for a momentum-dependent self-energy one has to fulfill the constraint $4\chi|J(\mathbf{Q})|^2 = \chi^{-1}$,

in order to get rid of non-universal parameter ratios, which implies $\chi = (2|J(\mathbf{Q})|)^{-1}$ and is thus equivalent to the intuitive condition $\Sigma(\mathbf{0}) = \Sigma(\mathbf{Q}) \approx |J(\mathbf{Q})|$. The self-consistency equations for the dissipation energies are then given by

$$A_0(x, iy) = \int \frac{d^d r}{(2\pi)^d} \frac{(x^2 + 2\mathbf{x} \cdot \mathbf{r})^2}{(1+r^2)(1+(\mathbf{x}+\mathbf{r})^2)} \frac{1}{A_N(r, iy) + |y|}, \quad (3.210)$$

$$A_N(x, iy) = [1 + x^2] \int \frac{d^d r}{(2\pi)^d} \left(\frac{1}{(1+(\mathbf{x}+\mathbf{r})^2)} \frac{1}{A_0(r, iy) + |y|} + \frac{1}{(1+r^2)} \frac{1}{A_N(r, iy) + |y|} \right), \quad (3.211)$$

where we approximated for the second equation $J(\mathbf{q})^2 \approx J(\mathbf{0})^2 = J(\mathbf{Q})^2$. Note that the contribution from the Néel region onto itself has a trivial momentum dependence $\propto [1+x^2]$. The scaling functions of the frequency dependence of the dynamic structure factor around $\mathbf{k} = \mathbf{0}$ and $\mathbf{k} = \mathbf{Q}_N$ are

$$\Phi_0(x, y) = \frac{1}{y} \text{Im} \left(\frac{A_0(x, y + i0)}{A_0(x, y + i0) - iy} \right), \quad (3.212)$$

$$\Phi_N(x, y) = \frac{1}{y} \text{Im} \left(\frac{A_N(x, y + i0)}{A_N(x, y + i0) - iy} \right), \quad (3.213)$$

so that the corresponding scattering intensities can be written as

$$S_0(\mathbf{k}, \omega) = \frac{T\tau\chi}{\pi} \Phi_0(x, y), \quad (3.214)$$

$$S_N(\mathbf{k}, \omega) = \frac{T\tau\chi_N}{\pi[1+x^2]} \Phi_N(x, y). \quad (3.215)$$

Diffusion coefficient and order parameter relaxation for $T \rightarrow T_c$

For the zero-frequency limit $y \rightarrow 0$, we obtain finite solutions $A_0(x, 0)$ and $A_N(x, 0)$. From the expansion of $A_0(x, 0)$ to $\mathcal{O}(x^2)$ we extract the spin diffusion coefficient

$$\mathcal{D} = A_{0,2} \xi^2 \tau^{-1} = A_{0,2} \omega_* a^2 \xi^{(4-d)/2}, \quad (3.216)$$

with a numeric constant $A_{0,2}$ that is determined from the numerical solution of the integral equations. We see that \mathcal{D} diverges for $T \rightarrow T_c$ in three dimensions as $\xi^{1/2} \sim (T - T_c)^{-\nu/2}$, which can be interpreted as a form of *critical speeding up*. This agrees with the extended dynamic scaling hypothesis [58], mode-coupling theory [158] and was also confirmed by neutron scattering experiments [120]. The conventional van Hove theory predicts a finite diffusion coefficient for $T \rightarrow T_c$, i.e. a change by $\mathcal{O}(1)$ from the $T = \infty$ -value [32]. The relaxation rate of the staggered magnetization behaves as

$$\Gamma_N = \tau^{-1} A_N(0, 0) \propto \xi^{-d/2}. \quad (3.217)$$

Its vanishing is, like for \mathcal{D} in the ferromagnet, a manifestation of critical slowing down [58, 158]. Note that in the conventional theory $\Gamma_N \propto \xi^{-2}$, a generic result for the transport coefficient associated with the order parameter. The autocorrelation function at $\omega = 0$ can then be estimated as

$$S(\mathbf{r} = \mathbf{0}, 0) \propto \int dk k^{d-1} \frac{\chi_N \tau}{A_N(x)[1+(k\xi)^2]} \propto \xi^{z+2-d} \sim \xi^{(4-d)/2}, \quad (3.218)$$

where we used that $A_N \propto x^2$ at large $x = k\xi$, acting thus as a UV-cutoff to the integral. Note that the contribution from the uniform region is negligible as it lacks a divergence in the susceptibility. In $d = 3$ the linewidth diverges as $\xi^{1/2} \sim |T - T_c|^{-1/3}$, again in agreement with [58]. Above $d = 4$ the integral remains non-singular for $T \rightarrow T_c$.

Scaling behavior at $T = T_c$

The scaling functions at the critical point, where $\xi = \infty \rightarrow \tau = \infty$, depend on a sole variable $\nu = \omega/\omega_k$, in complete analogy to the ferromagnet. The characteristic frequency is in this context given by

$$\omega_k = \omega_*(ka)^z, \quad z = d/2. \quad (3.219)$$

As before one can also introduce a corresponding momentum variable $p = k/k_\omega$ with the characteristic wave-vector given by

$$k_\omega = (\omega/\omega_*)^{1/z}. \quad (3.220)$$

The dissipation energies can thus be written in terms of critical scaling functions as

$$\Delta(\mathbf{k}, i\omega) = \omega_k B_{0,c}(i\omega/\omega_k), \quad (3.221)$$

$$\Delta(\mathbf{k} + \mathbf{Q}, i\omega) = \omega_k B_{N,c}(i\omega/\omega_k), \quad (3.222)$$

with the corresponding self-consistency equations

$$B_{0,c}(i\nu) = \int \frac{d^d u}{(2\pi)^d} \frac{(p^2 + 2\mathbf{u} \cdot \mathbf{p})^2}{u^2 (\mathbf{u} + \mathbf{p})^2 [u^z B_{N,c}(i|\nu|u^{-z}) + |\nu|]}, \quad (3.223)$$

$$B_{N,c}(i\nu) = p^2 \int \frac{d^d u}{(2\pi)^d} \left(\frac{1}{(\mathbf{u} + \mathbf{p})^2 [u^z B_{0,c}(i|\nu|u^{-z}) + |\nu|]} + \frac{1}{u^2 [u^z B_{N,c}(i|\nu|u^{-z}) + |\nu|]} \right), \quad (3.224)$$

where $\mathbf{p} = |\nu|^{-1/z} \hat{\mathbf{p}}$. Again one can infer the asymptotic behavior of the scaling functions for $\nu \gg 1$ ($p \ll 1$) and $\nu \ll 1$ ($p \gg 1$) from these equations. In the high-frequency limit one obtains for both scaling functions $B_{0,c} \sim |\nu|^{1/z-1}$ and $B_{N,c} \sim |\nu|^{1/z-1}$. In three dimensions this implies a Non-Lorentzian decay $\propto |\nu|^{-4/3}$ for both scaling functions in full agreement with previous calculations [157], leading to a structure factor decaying as $\omega^{-7/3}$. Accordingly this translates into a $k_\omega^{-1/2} \sim \omega^{-1/3}$ -divergence in the critical auto- and pair-correlation functions in real space, consistent with the divergence at $\omega = 0$ as $\xi^{1/2}$ for $T \rightarrow T_c$. In the low-frequency sector $\nu \ll 1$ we encounter the same problem as for the ferromagnet, namely that the contributions from the order parameter region are insufficiently damped for $\mathbf{q} \rightarrow \mathbf{Q}$, thus implying that one cannot set $\nu \rightarrow 0$ on the right-hand side. The contribution from the uniform region to $B_{N,c}$ allows for this though and is therefore suppressed in this regime. We therefore obtain divergent dissipation energies $B_{0/N,c} \sim |\nu|^{1/z-1}$, implying that $S(\mathbf{k}, \omega)$ vanishes in the whole Brillouin zone as $|\omega|^{1/3}$ for $\omega \rightarrow 0$. The branch point at $\nu = 0$ should then produce in the time-domain a $1/(kt^{1/z})^2$ long-time decay for both types of fluctuations. In real space one has $S(\mathbf{r}, t) \sim t^{-(d-2)/z}$, due to the dominant staggered fluctuations.

A non-analytic suppression in the zero-frequency limit is, like for the ferromagnet, at odds with predictions by mode-coupling theory [157, 158], RG calculations [159, 160] to first order in $\epsilon = 4 - d$ and in particular spin dynamics simulations [155], which were

able to access, in contrast to ferromagnets, the line-shape in the scaling region. From this we conclude that these ubiquitous low-frequency divergences are an artifact of our approximation. Interestingly an RG analysis of the $O(n)$ -model at arbitrary n [160] obtained to $\mathcal{O}(\epsilon)$ that the zero-frequency spectral weight at the Néel point is continuously reduced with increasing n . This does not apply to scattering in the vicinity of $\mathbf{q} = \mathbf{0}$, which will always exhibit an elastic peak [56, 159]. Note that in contrast to the ferromagnet, mode-coupling theory and RG calculations did not yield a critical line-shape, which is fully consistent with experiments [62]. Their outcome is a two-peak structure for $S(\mathbf{k}, \omega)$ close to \mathbf{Q}_N , analogous to high-temperature scattering at the zone boundary. On the other hand, numerical simulations and experiments clearly showed a three-peak structure around the Néel vector [62, 155], i.e. an additional maximum at zero frequency. In the context of the renormalization group it was noted that two-loop calculations alter significantly the position of the dynamic fixed point [56]. The result is then approximately the same as for the $O(2)$ -model at $\mathcal{O}(\epsilon)$ which exhibits only a central peak. Up to this point no successful reconciliation between numeric simulations/experiments and simpler theoretical approximations was achieved.

3.5 Ferromagnets in reduced dimensions at low temperatures

We conclude our studies of the spin dynamics by taking a look at isotropic ferromagnets below three dimensions in the low-temperature regime $T \ll |J|$. In contrast to systems in $d > 2$ there is no phase transition at a finite temperature, as a consequence of the Mermin-Wagner theorem [24], so that $T_c = 0$. Thus one is always located in the symmetric phase for $T > 0$, with a singular magnetic susceptibility and correlation length for $T \rightarrow 0$. Note that we will use directly the alternative integral equation (3.46) with the $G^{-1}(\mathbf{q}) - G^{-1}(\mathbf{q} + \mathbf{k})$ -kernel. As pointed out earlier, Eq. (3.44), which contains the contribution $\Sigma(\mathbf{q}) - \Sigma(\mathbf{q} + \mathbf{k})$, guarantees physical results only in the high-temperature limit $T \gg |J|$. Also remember that the solution of the alternative equation (3.46) exhibits different dynamics for hydrodynamic frequencies, compared to the initial equation (3.44), as discussed for $T = \infty$.

3.5.1 One dimension

The static susceptibility $G(\mathbf{k})$ for small momenta $ka \ll 1$ is in $d = 1$ given by a Ornstein-Zernicke form ($\eta = 0$) [161, 162]. The correlation length diverges for $T \rightarrow 0$ as

$$\xi \sim 1/T, \tag{3.225}$$

and the magnetic susceptibility behaves thus as

$$\chi = \rho^{-1} \xi^2 \sim 1/T^2, \tag{3.226}$$

where $\rho = J'' + \Sigma''$ is the full, i.e. renormalized, spin stiffness. The numeric constants in the quantities χ and ξ have been calculated by means of several methods. A quite straightforward one is the modified spin-wave theory by Takahashi [161, 162]. It differs from orthodox spin-wave theory by the introduction of a self-consistent non-zero chemical potential in the magnon dispersion, thus regularizing the ubiquitous infra-red divergences

implied by the naive method in $d \leq 2$ [16, 161, 162]. His results for a ferromagnetic chain with nearest-neighbor coupling J are given by

$$\chi = \frac{2|J|S^4}{3T^2}, \quad (3.227)$$

$$\frac{\xi}{a} = \frac{|J|S}{T}, \quad (3.228)$$

which agrees with χ obtained from a numeric evaluation of the thermodynamic Bethe-ansatz equations for the $S = 1/2$ -chain [163]. Note that Arovas and Auerbach found on the basis of a Schwinger-Boson mean-field theory that χ is larger by a factor of $3/2$, while obtaining the same expression for ξ [164]. A combination of a one-loop renormalization group calculation together with a Quantum Monte Carlo simulation of the ferromagnetic $S = 1/2$ -chain obtained that the result for ξ lies almost within the error bars, while the pre-factor for χ is found to be smaller than Takahashi's result [165]. The question of the exact numeric pre-factor is, however, not pertinent to the present analysis, given that all these approaches arrive at the same asymptotic T -dependence.

Repeating the steps from the previous sections we first introduce the scaling function of the dissipation energy

$$\Delta(\mathbf{k}, i\omega) = \tau^{-1} A(k\xi, i\omega\tau), \quad (3.229)$$

where we assumed again small frequencies and momenta, leading therefore to a singular coupling to critical fluctuations in the integral equation and the onset of dynamic scaling, as implied by (3.229). The characteristic timescale τ of the hydrodynamic regime is here given by

$$\tau = \sqrt{\frac{2\chi\xi}{aT}} \propto \xi^2, \quad (3.230)$$

since $\xi \sim T^{-1}$. The dynamic exponent is therefore $z = 2$, and not $z = (d + 2)/2 = 3/2$ as suggested by dimensional analysis of the integral above two dimensions. This is a consequence of $T_c = 0$, implying that the factor of T in front of the integral contributes to the low-temperature asymptotics as well. Such an exponent is the most straightforward result, if the solution features spin waves with a k^2 -dispersion in the ground state [21], and a scaling form continuously connecting to the zero-temperature limit is also satisfied. Note in this context that the dynamic scaling hypothesis as formulated by Halperin and Hohenberg [54, 58] does not consider transitions at zero temperature, but only at elevated temperatures, i.e. with a classical critical point, as for Heisenberg magnets in $d > 2$. The self-consistency equation satisfied by the scaling function is in $d = 1$ given by

$$A(x, iy) = [1 + x^2] \int_{-\infty}^{\infty} \frac{dr}{2\pi} \frac{(x^2 + 2xr)^2}{(1 + r^2)[1 + (x + r)^2]} \frac{1}{A(r, iy) + |y|}. \quad (3.231)$$

Furthermore we consider again the scaling function of the line-shape $\Phi(x, y)$, i.e.

$$\Phi(x, y) = \frac{1}{y} \text{Im} \left(\frac{A(x, y + i0^+)}{A(x, y + i0^+) - iy} \right), \quad (3.232)$$

from which one can directly read off the frequency dependence of the dynamic structure factor $S(\mathbf{k}, \omega)$ in the classical limit $\omega \ll T \sim \xi^{-1}$. Note that the classical regime includes the whole range of hydrodynamic frequencies $\omega \ll \tau^{-1} \sim T^2$. In addition to the hydrodynamic region, the classical regime shrinks also as one approaches $T \rightarrow 0$, so that for $\omega \gtrsim T$

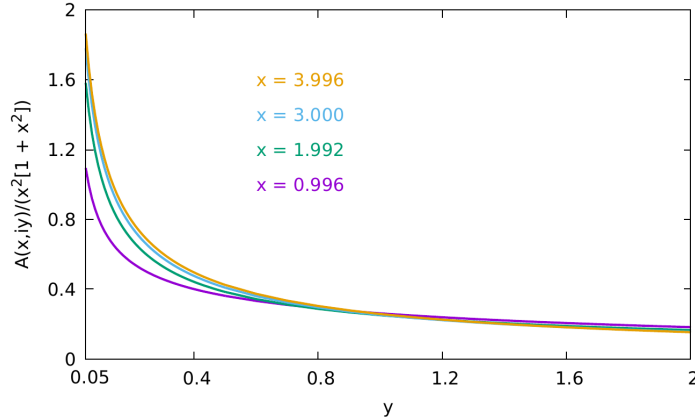


Figure 3.25: Numerical solution of (3.231) for the scaling function $A(x, iy)$, defined in Eq. (3.229), of the dissipation energy in $d = 1$. Like in Fig. 3.12 we plot $A(x, iy)/(x^2[1+x^2])$ because this quantity exhibits only a modest x -dependence. Reprinted with permission from Ref. [11] © [2022] American Physical Society.

one has to take the full detailed-balance factor $[1 - e^{-\beta\omega}]^{-1}$ into account. $\Phi(x, y)$ can also be used directly for the ω -dependence in the collisionless region $k\xi$, $\omega\tau \gg 1$, as long as $T^2/|J| \ll \omega \ll T$. Anticipating a 'dispersion' $\omega\tau \sim (k\xi)^2$ this implies the condition $(\xi/a)^{-1} \ll ka \ll (T/|J|)^{1/2}$ for the associated momenta.

In Fig. 3.25 and 3.26 we display results for $A(x, iy)$ and $\Phi(x, y)$. One can compare the latter for instance with modified spin-wave theory [166], which also predicts line-shapes that are consistent with dynamic scaling with the same index z . In fact modified spin-wave theory provides an analytic expression for $\Phi(x, y)$, with a similar structure for the relaxation time τ^{-1} as in our case, i.e. its dependence on microscopic parameters. The most salient difference to our result is the low-frequency behavior of $\Phi(x, y)$. For $x, y \ll 1$, i.e. the hydrodynamic region, our solution behaves as

$$A(x, iy) \sim A_1 x^2 |y|^{1/5} + A_2 \frac{x^4}{|y|^{3/5}}. \quad (3.233)$$

This result is analogous to the prediction of (3.46) for small k, ω and elevated temperatures discussed in Sec. 3.2.3, that can be considered as subdiffusive due to the vanishing of the x^2 -coefficient for $y \rightarrow 0$. The leading divergence for $y \rightarrow 0$ persists at arbitrary x , e.g. for large momenta $x \gg 1$ the dissipation energy is $\propto x^4 |y|^{-3/5}$. Hence $S(\mathbf{k}, \omega)$ always goes to zero as $|\omega|^{3/5}$ for $\omega \rightarrow 0$ and finite \mathbf{k} . Contrary to our result Takahashi's solution for $\Phi(x, y)$ consists of a single elastic peak for $x \lesssim 1$ [166]. Conversely at larger momenta $x \gtrsim 1$ the elastic scattering is still finite, being now an analytic local minimum of $S(\mathbf{k}, \omega)$. Note however that Takahashi's scaling function $\Phi(x, y)$ does not reduce to a simple Lorentzian in the hydrodynamic regime $x, y \ll 1$. Moreover it has dissipative poles at $y \sim \pm ix$, so that the relevant decay rate is $x/\tau \sim k/\xi$ instead of $x^2/\tau \sim \mathcal{D}k^2$ [166]. A mode-coupling analysis found spin diffusion in the hydrodynamic region [167]. In that context one obtains a finite $T = 0$ -limit of \mathcal{D} , consistent with $z = 2$, which is not surprising given the structure of the mode-coupling kernel [167]. This is incompatible with critical slowing down of spin fluctuations, as exhibited above $d = 2$ near $T_c \neq 0$ [3, 58]. Given that our solution does

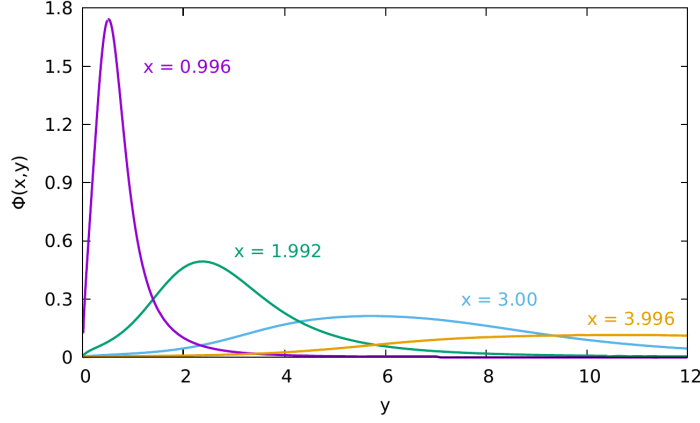


Figure 3.26: Dependence on $y = \omega\tau$ of the scaling function $\Phi(x, y)$, defined in Eq. (3.232), of $S(\mathbf{k}, \omega)$ for linear Heisenberg ferromagnets, evaluated at different values of $x = k\xi$. As discussed such a plot yields for $\omega \ll T$ directly the frequency dependence of $S(\mathbf{k}, \omega)$ for different momenta k . Reprinted with permission from Ref. [11] © [2022] American Physical Society.

not feature spin diffusion, a direct comparison is impossible. The k^2 and k^4 -coefficient of $\Delta(\mathbf{k}, i\omega)$ diverge in our case for $T \rightarrow 0$ as $T^{-2/5}$ and $T^{-4/5}$, again a consequence of scaling, but now even as a critical speeding up. Note that there is no consensus on the predicted T -dependence of \mathcal{D} or even the type of long-time/low-energy behavior. For the former, a violation of dynamic scaling, leads automatically to a different outcome, as found for instance by the three-pole approximation (3.90), using classical moments, where $\mathcal{D} \propto T$ for $T \rightarrow 0$ [168]. However, being based on an extrapolation of a short-time expansion, it is prone to errors in the critical region. As already discussed, recent calculations suggest at high temperatures anomalous diffusion with a divergent diffusion coefficient $\mathcal{D}(i\omega) \sim |\omega|^{-1/3}$ at least for integrable spin chains [85]. Extensions to low temperatures for the antiferromagnet show that this mechanism is still present in the asymptotic long-time limit [82, 169], with the time-scale at which it occurs becoming increasingly larger, due to the narrowing of the hydrodynamic region for $T \rightarrow 0$. Note that the question on whether $S(\mathbf{k}, \omega)$ is finite or vanishes for $\omega \rightarrow 0$ in the absence of normal diffusion cannot be definitely answered at this point, although the former is more likely [113]. At least for critical three-dimensional systems we have conclusive evidence to the contrary. A modification of our equation to avoid the non-analytic vanishing of $S(\mathbf{k}, \omega \rightarrow 0)$ was described in Eq. (3.195).

Returning to our comparison with Takahashi's line-shapes, we find for $k\xi \gg 1$, that our result exhibits, as his solution for $\Phi(x, y)$ [166], peaks with a position scaling as $y \sim x^2$, i.e. $\omega_*(k) \sim k^2$, reminiscent of a magnon dispersion. As discussed for $d = 3$, this can be seen more clearly if one introduces a different scaling form

$$\Psi(x, \nu) = x^2 \Phi(x, \nu x^2), \quad (3.234)$$

with the new variable

$$\nu = \omega/\omega_k, \quad \omega_k = (k\xi)^2/\tau = \omega_* k^2. \quad (3.235)$$

In Fig. 3.27 we show a plot of the ν -dependence of $\Psi(x, \nu)$ for different x . These curves collapse for $x \gg 1$, thus confirming our assumption for the 'spin-wave' dispersion. However,

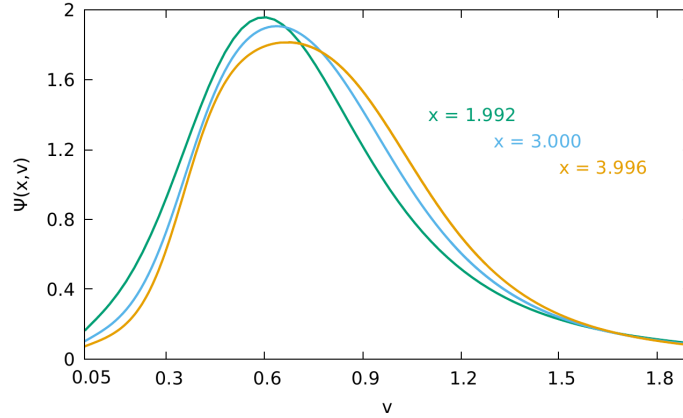


Figure 3.27: Dependence on $\nu = \omega/\omega_k$ of the alternative scaling function $\Psi(x, \nu)$ of $S(\mathbf{k}, \omega)$, see Eq. (3.234), for a linear ferromagnet, evaluated at different values of x . Such plots are equivalent to the ω -dependence of $S(\mathbf{k}, \omega)$ for different temperatures and $\omega/T \ll 1$. Reprinted with permission from Ref. [11] © [2022] American Physical Society.

one sees that their maxima are broad, i.e. the width $\Delta\omega(k)$ is of same order as the associated energy. Such an outcome is heavily at odds with Takahashi's results. In his approximation the ratio $\Delta\omega(k)/\omega_*(k)$ vanishes for $x \rightarrow \infty$ as $x\tau^{-1} \sim 1/x$. The line-shape at $T = 0$ is then simply given by a δ -peak at the classical one-magnon energy $E(\mathbf{k})$ (1.17) for arbitrary momenta in the Brillouin zone [166]. Note that in the language of the high- ω expansion for $\Delta(\mathbf{k}, i\omega)$, such a solution implies that all coefficients of higher order in its expansion should vanish for $T \rightarrow 0$, i.e. $\Delta(\mathbf{k}, i\omega) \sim |\omega|^{-1}$. Other approximate calculations also predict that the width of the associated peaks in $S(\mathbf{k}, \omega)$ and therefore the quasiparticle damping Γ_k are zero at $T = 0$ [168, 170, 171]. Since for generic ferromagnets [21] the zero-magnon vacuum is indeed the ground state, and states containing one spin wave excitation anywhere in the first Brillouin zone are exact eigenstates, the absence of a damping seems quite reasonable. Note that otherwise transition matrix elements between the vacuum state and some high energy multimagnon states have to be finite as can be inferred from the spectral representation of $S(\mathbf{k}, \omega)$ (1.78). In the appendix B.4.2 a short description of our zero-temperature solution in reduced dimensions is given, which turns out to be a sharply cut, broad continuum, around the spin-wave energies.

The $T = 0$ -failure is fully shared by the solution of the conventional mode-coupling integro-differential equation [167]. That is not unexpected, given the similar dependence on static quantities in both cases, so that for instance higher order terms in a large- ω expansion of $\Delta(\mathbf{k}, i\omega)$ do not vanish for $T \rightarrow 0$. Ad hoc changes to the mode-coupling equations had to be implemented as a remedy. One approach by McLean and Blume introduced magnetic short-range order for the spin-wave region $k\xi \gtrsim 1$ [167], thus explicitly distinguishing between transverse and longitudinal fluctuations. Another approximation by Lovesey and Megann was based on appropriate rescalings of the time-variable and the prefactor $G^{-1}(\mathbf{k})$, enforcing that the first two moments, at least in the classical limit $S \rightarrow \infty$, are exactly reproduced [170]. However, these procedures, in particular the second one, lead to solutions that are inconsistent with dynamic scaling. For instance $\mathcal{D} \sim T^{-1/4}$ is predicted by the latter refinement of the mode-coupling equations [170]. In fact, the

question whether dynamic scaling relations are obeyed in low-dimensional systems remains unsettled [171, 172, 173]. Unfortunately there are no calculations of the dynamic structure factor available for integrable linear ferromagnets, which utilize the exact Bethe-ansatz solution and are therefore capable of clarifying the above issues.

3.5.2 Two dimensions

Although the main features of the low-temperature dynamics were outlined in the previous section about $d = 1$, let us also take a look at the marginal case of two-dimensional ferromagnets. These systems are of some interest, because the static susceptibility $G(\mathbf{k})$ is not given by an Ornstein-Zernicke form. As an example, modified spin-wave theory predicts the following scaling function for $G(\mathbf{k}) = \chi g(k\xi)$ in the vicinity of $\mathbf{k} = \mathbf{0}$ [161, 162]

$$g(x) = \frac{\ln(x + \sqrt{x^2 + 1})}{x\sqrt{x^2 + 1}}. \quad (3.236)$$

The magnetic susceptibility and correlation length are known to diverge exponentially for $T \rightarrow 0$, i.e.

$$\chi \sim C_\chi e^{2\alpha/T}, \quad (3.237)$$

$$\xi/a \sim C_\xi e^{\alpha/T}. \quad (3.238)$$

Assuming a nearest neighbor-coupling $J < 0$ on a square lattice the constant α in the exponent is given by $2\pi|J|S^2$. The pre-factors C_χ and C_ξ are in modified spin-wave theory given by $C_\chi = 1/(12\pi|J|S)$ and $C_\xi = \sqrt{|J|S/T}$ [161, 162], implying the following relation for $T \ll |J|$

$$\frac{\chi}{T(\xi/a)^2} = \text{const.} \quad (3.239)$$

Note that C_χ , C_ξ coincide with the predictions of a one-loop RG calculation [174] and the Schwinger boson-mean field theory [164], with the one-loop momentum shell RG shown to be actually equivalent to modified spin-wave theory and the Schwinger boson approach [165]. A two-loop RG calculation predicts modified T -dependences, i.e. $C_\chi \sim T^2$ and $C_\xi \sim T^{1/2}$ [174], but the relation (3.239) between χ and ξ is preserved. This relation is also the reason, for why the Ornstein-Zernicke ansatz $g(x) = [1 + x^2]^{-1}$ cannot be used, as it would imply that $G(\mathbf{k}) \sim (T/J^2)/(ka)^2$ for $k\xi \rightarrow \infty$. On the other hand the modified form for $g(x)$ ensures that $G(\mathbf{k}) \propto 1/(ka)^2$ is finite for $T = 0$. Using the modified $g(x)$ yields the following integral equation for the scaling function of $\Delta(\mathbf{k}, i\omega)$

$$A(x, iy) = g^{-1}(x) \int \frac{d^2r}{(2\pi)^2} g(r) g(|\mathbf{x} + \mathbf{r}|) \frac{[g^{-1}(r) - g^{-1}(|\mathbf{x} + \mathbf{r}|)]^2}{A(r, iy) + |y|}, \quad (3.240)$$

where the hydrodynamic crossover scale is now

$$\tau = \sqrt{\frac{2\chi}{T}} \left(\frac{\xi}{a}\right) = \sqrt{\frac{2\chi a^2}{T\xi^2}} \left(\frac{\xi}{a}\right)^2. \quad (3.241)$$

As a consequence of (3.239) one obtains $\tau = \omega_*^{-1}\xi^2$, i.e. scaling with a dynamic index $z = 2$ as in one dimension. This agrees with the result from dimensional analysis $z = (d+2)/2$ and modified spin-wave theory [166], exhibiting a similar dependence on microscopic parameters in ω_* as Ref. [166]. Note that for an Ornstein-Zernicke form of the static susceptibility,

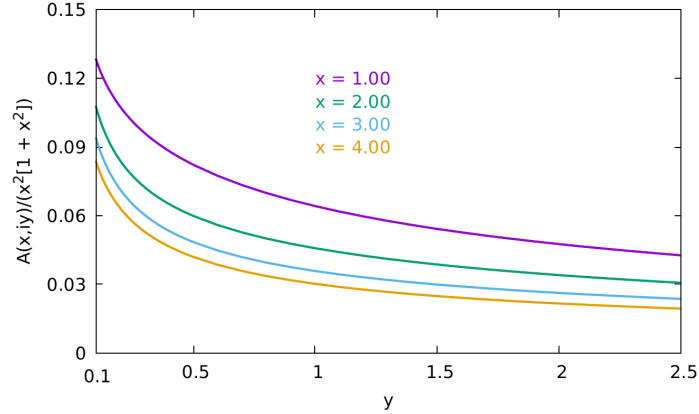


Figure 3.28: Numerical solution of Eq. (3.240) for the scaling function $A(x, iy)$ of the dissipation energy in $d = 2$, defined as in Eq. (3.229). Like in Fig. 3.25 we show $A(x, iy)/(x^2[1+x^2])$, which has a much weaker x -dependence than $A(x, iy)$. Reprinted with permission from Ref. [11] © [2022] American Physical Society.

where $\chi/\xi^2 = \text{const.}$ the factor $T \sim \ln^{-1}(\xi/a)$ would generate an additional logarithmic dependence on ξ in the relaxation time $\tau \sim \xi^2 \ln^{1/2}(\xi/a)$. Compared to the equations in $d = 1$ and 3 the modified scaling function in two dimensions, does not allow for an analytic evaluation of the angular integration, which was therefore performed numerically.

In Fig. 3.28 and 3.29 results for the frequency dependence of the scaling functions $A(x, iy)$ and $\Phi(x, y)$, defined as in one dimension, are shown for different values of x . Like in $d = 1$ and at larger temperatures the low-frequency behavior is characterized by a vanishing $\Phi(x, 0)$, i.e. a divergent dissipation energy for $y \rightarrow 0$, always leading to maxima at $\omega \neq 0$, which is at odds with normal diffusion. Again this differs from Takahashi's analytic result [166], where $S(\mathbf{k}, 0) \neq 0$. Note that like in $d = 1$ his analytic solution for $\Phi(x, y)$ does not yield a simple Lorentzian for $x, y \rightarrow 0$, featuring the same hydrodynamic decay rate $\sim x/\tau$ instead of $\mathcal{D}k^2 \sim x^2/\tau$. A Schwinger-Boson approach by Chubukov lead to diffusion in the hydrodynamic regime, but with a singular logarithmic-in- ξ dependence of \mathcal{D} , i.e. additional corrections to scaling with plain $z = 2$ [175].

For large x , the positions of the peaks $\omega_*(k)$ is $\propto x^2 \sim k^2$, similar to $d = 1$, which we demonstrate explicitly by plotting again the alternative scaling function $\Psi(x, \nu)$ from Eq. (3.234) with $\nu = y/x^2 = \omega/(\omega_*k^2)$ in Fig. 3.30. Similar to one dimension, our solution suffers from a width $\Delta\omega(k)$, which has the same order of magnitude as $\omega_*(k)$ for $x \rightarrow \infty$. Again this is at odds with the predictions of modified spin-wave theory [166] or other approaches, also working within a spin-wave picture [171]. In those cases the zero-temperature result for $S(\mathbf{k}, \omega)$ is again given by a sharp δ -peak corresponding to well-defined magnon excitations [166]. As already argued for one dimension, this seems reasonable, given the structure of the eigenspectrum [21]. We conclude that our equation shares some problems with the conventional mode-coupling theory in low dimensions [117, 167, 171], that can be attributed to the similar structure regarding the feedback of static quantities onto the spin dynamics. The fulfillment of scaling relations is in accordance with modified spin-wave theory [166], although like in $d = 1$, the question on whether they really hold is not definitely answered [171, 172, 173, 175].

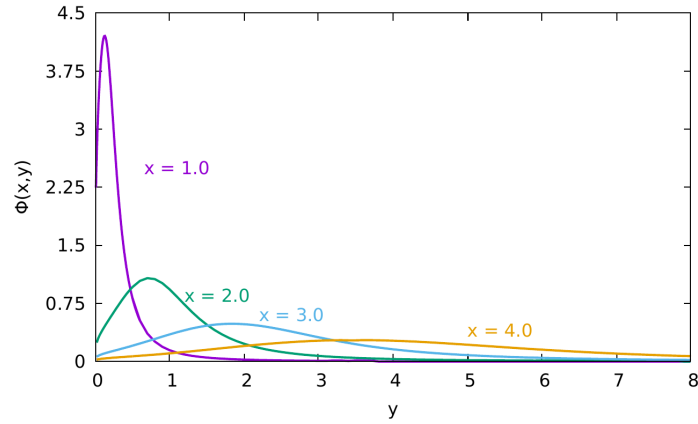


Figure 3.29: Dependence on the frequency variable y of the scaling function $\Phi(x, y)$ of $S(\mathbf{k}, \omega)$ in $d = 2$, defined as in Eq. (3.232), evaluated at different x . Reprinted with permission from Ref. [11] © [2022] American Physical Society.

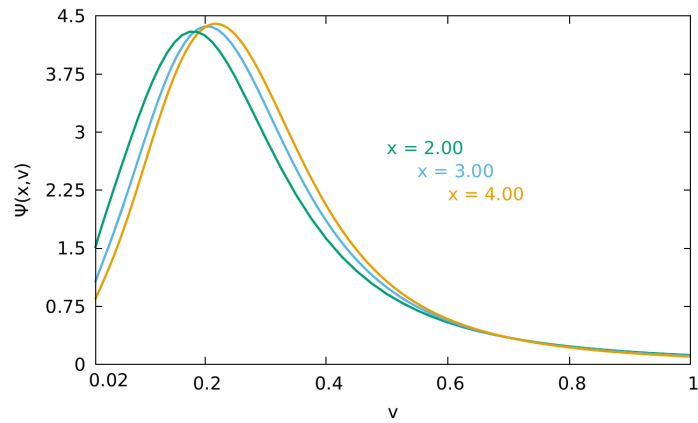


Figure 3.30: Dependence on the frequency variable ν of the alternative scaling function $\Psi(x, \nu)$ of $S(\mathbf{k}, \omega)$, introduced in Eq. (3.234), in $d = 2$ evaluated at different x . Reprinted with permission from Ref. [11] © [2022] American Physical Society.

Chapter 4

Zero-field thermodynamics of isotropic Heisenberg magnets above $T = T_c$

In Chapter 3 we have calculated the spin dynamics of isotropic Heisenberg models in the symmetric phase under some basic assumptions about the static behavior of the system, i.e. the shape of the static susceptibility $G(\mathbf{k})$. Conversely we can calculate thermodynamic properties above T_c in a vanishing external field $H = 0$. This entails solving the flow equation of the static self-energy $\Sigma_\Lambda(\mathbf{k})$, which in turn determines the static susceptibility $G_\Lambda(\mathbf{k}) = [\Sigma_\Lambda(\mathbf{k}) + J_\Lambda(\mathbf{k})]^{-1}$. We will discuss several approximations to the flow equations of $\Sigma_\Lambda(\mathbf{k})$, starting from a purely classical approach, which completely ignores dynamic fluctuations that arise from the non-trivial spin algebra (1.9). Most of these calculations are based on the work described in Ref. [12].

4.1 Static approximation

Considering only static fluctuations one can work entirely within a 1-PI parametrization, i.e. with the vertices generated by the classical effective average action $\Gamma_\Lambda[\mathbf{m}^c] = \tilde{\Gamma}_\Lambda[\mathbf{m}^c, \boldsymbol{\eta}^q = \mathbf{0}]$. This becomes exact in limit $S \rightarrow \infty$, while for finite S the neglect of quantum contributions amounts to an approximation. As such it cannot reproduce some additional dependencies on S , with these corrections potentially having a large effect in the quantum limit $S = 1/2$. For a description of universal critical properties of classical phase transitions at finite temperature, such a description is sufficient though, a consequence of critical slowing down [3]. For instance one thus should be able to obtain the renormalization group fixed point associated with the transition in the Heisenberg universality class [3]. Quantum diagrams, representing the effect of spin dynamics, affect then only non-universal parameters, like the explicit value of the critical temperature T_c or the spin stiffness ρ .

4.1.1 Flow equations

In the static approximation $\Sigma_\Lambda(\mathbf{k})$ satisfies the flow equation

$$\partial_\Lambda \Sigma_\Lambda(\mathbf{k}) = \frac{T}{2} \int_{\mathbf{q}} \dot{G}_\Lambda(\mathbf{q}) [3\tilde{\Gamma}_\Lambda^{\alpha\alpha\gamma\gamma}(\mathbf{k}, -\mathbf{k}, \mathbf{q}, -\mathbf{q}) + 2\tilde{\Gamma}_\Lambda^{\alpha\alpha\gamma\gamma}(\mathbf{k}, \mathbf{q}, -\mathbf{k}, -\mathbf{q})], \quad (4.1)$$

while the mixed static 4-legged vertex obeys

$$\begin{aligned}
 \partial_\Lambda \tilde{\Gamma}_\Lambda^{\alpha\alpha\gamma\gamma}(\mathbf{k}_1, \mathbf{k}_2, \mathbf{k}_3, \mathbf{k}_4) &= \frac{T}{2} \int_{\mathbf{q}} \dot{G}_\Lambda(\mathbf{q}) [\tilde{\Gamma}_\Lambda^{\alpha\alpha\gamma\gamma\gamma\gamma}(\mathbf{k}_1, \mathbf{k}_2, \mathbf{k}_3, \mathbf{k}_4, \mathbf{q}, -\mathbf{q}) \\
 &+ \tilde{\Gamma}_\Lambda^{\alpha\alpha\alpha\alpha\gamma\gamma}(\mathbf{k}_1, \mathbf{k}_2, \mathbf{q}, -\mathbf{q}, \mathbf{k}_3, \mathbf{k}_4) + \tilde{\Gamma}_\Lambda^{xyyyzz}(\mathbf{k}_1, \mathbf{k}_2, \mathbf{q}, -\mathbf{q}, \mathbf{k}_3, \mathbf{k}_4)] \\
 &- \frac{T}{2} \int_{\mathbf{q}} [\dot{G}_\Lambda(\mathbf{q}) G_\Lambda(\mathbf{q} + \mathbf{k}_1 + \mathbf{k}_2)] \bullet \tilde{\Gamma}_\Lambda^{\alpha\alpha\gamma\gamma}(\mathbf{k}_1, \mathbf{k}_2, \mathbf{q}, -\mathbf{q} - \mathbf{k}_1 - \mathbf{k}_2) \\
 &\times \tilde{\Gamma}_\Lambda^{\alpha\alpha\gamma\gamma}(-\mathbf{q}, \mathbf{q} + \mathbf{k}_1 + \mathbf{k}_2, \mathbf{k}_3, \mathbf{k}_4) - \frac{T}{2} \int_{\mathbf{q}} \mathcal{S}_{\mathbf{k}_1; \mathbf{k}_2} \mathcal{S}_{\mathbf{k}_3; \mathbf{k}_4} [\dot{G}_\Lambda(\mathbf{q}) G_\Lambda(\mathbf{q} - \mathbf{k}_1 - \mathbf{k}_3)] \bullet \\
 &\times \tilde{\Gamma}_\Lambda^{\alpha\alpha\gamma\gamma}(\mathbf{k}_1, \mathbf{q} - \mathbf{k}_1 - \mathbf{k}_3, \mathbf{k}_3, -\mathbf{q}) \tilde{\Gamma}_\Lambda^{\alpha\alpha\gamma\gamma}(\mathbf{k}_2, \mathbf{q}, -\mathbf{q} + \mathbf{k}_1 + \mathbf{k}_3, \mathbf{k}_4) \\
 &- \frac{T}{2} \int_{\mathbf{q}} [\dot{G}_\Lambda(\mathbf{q}) G_\Lambda(\mathbf{q} - \mathbf{k}_1 - \mathbf{k}_2)] \bullet \tilde{\Gamma}_\Lambda^{\alpha\alpha\gamma\gamma}(\mathbf{k}_1, \mathbf{k}_2, \mathbf{q} - \mathbf{k}_1 - \mathbf{k}_2, -\mathbf{q}) \\
 &\times [\tilde{\Gamma}_\Lambda^{\alpha\alpha\gamma\gamma}(-\mathbf{q} + \mathbf{k}_1 + \mathbf{k}_2, \mathbf{q}, \mathbf{k}_3, \mathbf{k}_4) + \tilde{\Gamma}_\Lambda^{\alpha\alpha\gamma\gamma}(-\mathbf{q} + \mathbf{k}_1 + \mathbf{k}_2, \mathbf{k}_4, \mathbf{k}_3, \mathbf{q}) \\
 &+ \tilde{\Gamma}_\Lambda^{\alpha\alpha\gamma\gamma}(-\mathbf{q} + \mathbf{k}_1 + \mathbf{k}_2, \mathbf{k}_3, \mathbf{q}, \mathbf{k}_4)] + (\mathbf{k}_1, \mathbf{k}_2 \leftrightarrow \mathbf{k}_3, \mathbf{k}_4). \tag{4.2}
 \end{aligned}$$

Here we have also expressed the longitudinal 4-vertex $\tilde{\Gamma}_\Lambda^{\alpha\alpha\gamma\gamma}$ via its mixed pendant, see Eq. (2.105). A graphical representation of Eq. (4.2) is shown in Fig. 4.1. A popular strategy to truncate the hierarchy of flow equations, amounts to neglecting the renormalization of the six-point vertices, i.e. replacing them by their initial values $\tilde{\Gamma}_{\Lambda_0}^{(6)}$ [1, 2, 3]. However, we will start our investigation, by truncating on an even lower level, namely by setting the 4-point vertex to its initial value $\tilde{\Gamma}_{\Lambda_0}^{(4)}$. It turns out that such a primitive approximation is already able to provide valuable insight. Note that for $S \rightarrow \infty$ the dependence on S has to be eliminated, by defining appropriate energy scales, which remain finite in this limit, i.e. one should keep $J_\Lambda S^2 = \text{const}$, $\Sigma_\Lambda S^2 = \text{const}$, $\tilde{\Gamma}_\Lambda^{(4)} S^4 = \text{const}$ and so on.

For the sake of completeness let us briefly state what happens under full neglect of the flow equations, which amounts to setting $\Sigma_\Lambda \approx \Sigma_{\Lambda_0}$. The expression for the static susceptibility reads thus

$$G_\Lambda(\mathbf{k}) = \frac{1}{T/b'_0 + J_\Lambda(\mathbf{k})} = \frac{b'_0/T}{1 + b'_0 J_\Lambda(\mathbf{k})/T}, \tag{4.3}$$

which is equivalent to the tree-approximation [2, 5, 6, 7]. It yields a phase transition at the mean-field critical temperature $T_c^{\text{MF}} = b'_0 |J(\mathbf{Q})|$ with the corresponding values for the critical indices $\gamma = 2\nu = 1$. It is more reliable for large dimensions, if not too close to T_c [1, 2, 5], while being very rough in physical dimensions $d \leq 3$. This is particularly true for $d \leq 2$, where finite-temperature order is a priori excluded [24].

4.1.2 Deformation schemes

Before solving explicitly the flow of Σ_Λ and $\tilde{\Gamma}_\Lambda^{(4)}$ one has to specify the deformation scheme for the flowing exchange coupling $J_\Lambda(\mathbf{k})$. We have considered two different schemes, which satisfy the conditions $J_{\Lambda=0}(\mathbf{k}) = 0$ and $J_{\Lambda=1}(\mathbf{k}) = J(\mathbf{k})$. The first is the so-called *interaction-switch* cutoff scheme

$$J_\Lambda(\mathbf{k}) = \Lambda J(\mathbf{k}), \tag{4.4}$$

so that $\partial_\Lambda J_\Lambda(\mathbf{k}) = J(\mathbf{k})$, which was already used in the study of dynamics in Sec. 3.1.1. A linear deformation may be directly interpreted in terms of an infinite resummation of

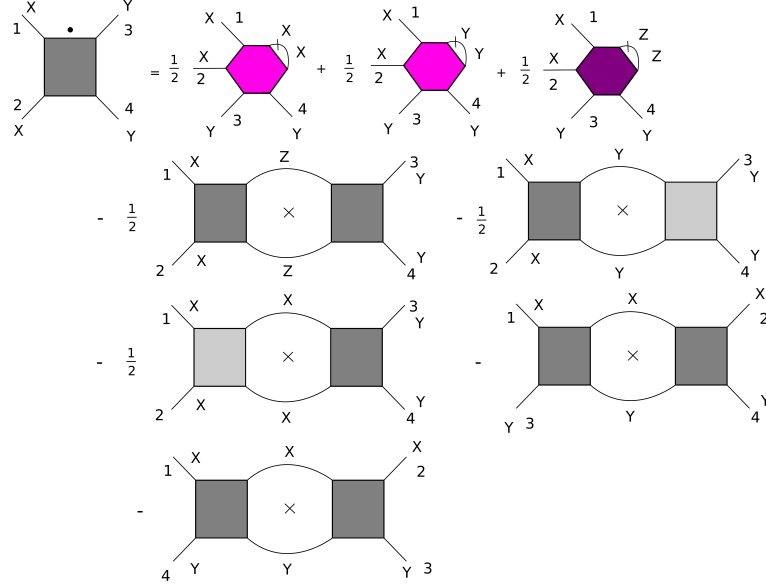


Figure 4.1: Flow equation of the mixed static 4-legged vertex $\Gamma_{\Lambda}^{xyyy}(\mathbf{k}_1, \mathbf{k}_2, \mathbf{k}_3, \mathbf{k}_4)$, see also Eq. (4.2), within a purely static approximation, where all diagrams involving fluctuations at finite frequencies are neglected.

diagrams in a high-temperature expansion. This can be seen by means of rescaling all quantities with powers of T^{-1} , in order to make them dimensionless, i.e.

$$\Sigma_{g_{\Lambda}}(\mathbf{k}) = (b'_0/T)\Sigma_{\Lambda}(\mathbf{k}), \quad (4.5)$$

$$\tilde{\Gamma}_{g_{\Lambda}}^{\alpha\alpha\gamma\gamma}(\mathbf{k}_1, \mathbf{k}_2, \mathbf{k}_3, \mathbf{k}_4) = (b'_0/T)\tilde{\Gamma}_{\Lambda}^{\alpha\alpha\gamma\gamma}(\mathbf{k}_1, \mathbf{k}_2, \mathbf{k}_3, \mathbf{k}_4), \quad (4.6)$$

$$\tilde{J}_{\Lambda}(\mathbf{k}) = (b'_0/T)J_{\Lambda}(\mathbf{k}) = g_{\Lambda}\gamma_{NN}(\mathbf{k}), \quad (4.7)$$

where

$$g_{\Lambda} = c\Lambda Jb'_0/T, \quad \partial_{\Lambda}g_{\Lambda} = cJb'_0/T. \quad (4.8)$$

Here we assumed for simplicity that $J(\mathbf{k}) = c\gamma_{NN}(\mathbf{k})$, i.e. a nearest-neighbor interaction on a lattice with coordination number c . From the shape of g_{Λ} we infer that it assumes the role of an inverse flowing temperature, which is initially zero and is increased to some finite value during the flow, i.e. $|g_{\Lambda}| = T_c^{\text{MF}}/T$. Dividing the flow equations of the rescaled quantities by $\partial_{\Lambda}g_{\Lambda}$, they can then be cast into the form $\partial_{g_{\Lambda}}\Sigma_{g_{\Lambda}} = \dots$, $\partial_{g_{\Lambda}}\tilde{\Gamma}_{g_{\Lambda}}^{(4)} = \dots$ and so on. Hence one can directly solve for the temperature dependence of any quantity in a set window $[0, |g_{\Lambda=1}|]$. This is a significant advantage compared to other deformation schemes. However, one should not ignore drawbacks of this somewhat primitive procedure. The most conspicuous one is that one cannot interpret it in terms of a mode elimination process, which is the foundation of the conventional momentum-shell RG or its FRG pendants [3]. Hence it cannot be employed to search directly for renormalization group fixed points with their corresponding eigenvalues, i.e. by studying properly rescaled flow equations in a logarithmic RG time l . This may be seen as an encumbrance in the investigation of critical properties, which is strongly facilitated if one can relate the FRG flow to ordinary RG equations. A

scheme which remedies this issue, is given by [176]

$$J_\Lambda(\mathbf{k}) = J_{\mathbf{k}} - \Theta(J(\mathbf{k})) (J(\mathbf{k}) - J_{\max}\Lambda) \Theta(J(\mathbf{k}) - J_{\max}\Lambda) \\ + \Theta(-J(\mathbf{k})) (-J(\mathbf{k}) + J_{\min}\Lambda) \Theta(-J(\mathbf{k}) + J_{\min}\Lambda). \quad (4.9)$$

Such a deformation with *Litim*-type regulator [3, 177] turns on gradually the bandwidth of the coupling $\Delta J_\Lambda = \Lambda(J_{\max} - J_{\min})$. The exchange interaction is then given by the non-deformed result $J(\mathbf{k})$ in the window $J(\mathbf{k}) \in [\Lambda J_{\min}, \Lambda J_{\max}]$, whereas beyond these boundaries it is replaced by a flat value $J_{\max}\Lambda$, $J_{\min}\Lambda$. Hence the interaction vanishes for $\Lambda \rightarrow 0$, in accordance with the enforced initial condition. The scale derivative of the deformed coupling is

$$\partial_\Lambda J_\Lambda(\mathbf{k}) = J_{\max} \Theta(J(\mathbf{k})) \Theta(J(\mathbf{k}) - J_{\max}\Lambda) + J_{\min} \Theta(-J(\mathbf{k})) \Theta(-J(\mathbf{k}) + J_{\min}\Lambda). \quad (4.10)$$

It is only non-zero outside the flowing edges of the band. Note that the single-scale propagator can be written as

$$\dot{G}_\Lambda(\mathbf{k}) = -\frac{J_{\max} \Theta(J(\mathbf{k})) \Theta(J_{\mathbf{k}} - J_{\max}\Lambda)}{[\Sigma_\Lambda(\mathbf{k}) + J_{\max}\Lambda]^2} - \frac{J_{\min} \Theta(-J(\mathbf{k})) \Theta(J_{\min}\Lambda - J(\mathbf{k}))}{[\Sigma_\Lambda(\mathbf{k}) + J_{\min}\Lambda]^2}. \quad (4.11)$$

For the case of $\Sigma_\Lambda(\mathbf{k}) \approx \Sigma_\Lambda$ only the numerator is momentum-dependent, meaning that everything else can be moved in front of integrals in the classical flow equations. Multiplying the above expressions with additional powers of $G_\Lambda(\mathbf{k})$ will just create additional factors $[\Sigma_\Lambda + J_{\max/\min}\Lambda]^{-1}$. Such diagrams occur in approximations where all vertices do not carry a momentum dependence, i.e. where the external momentum transfer of the loops is always zero, which will be discussed in more detail in the next sections. In these situations one only has to deal with integrals of the type

$$I_\Lambda^> = \int_{\mathbf{k}} \Theta(J(\mathbf{k})) \Theta(J(\mathbf{k}) - J_{\max}\Lambda), \quad I_\Lambda^< = \int_{\mathbf{k}} \Theta(-J(\mathbf{k})) \Theta(J_{\min}\Lambda - J(\mathbf{k})), \quad (4.12)$$

i.e. the corresponding diagrams are simply

$$\int_{\mathbf{q}} \dot{G}_\Lambda(\mathbf{q}) [G_\Lambda(\mathbf{q})]^n = -\frac{J_{\max}}{[\Sigma_\Lambda + J_{\max}\Lambda]^{n+2}} I_\Lambda^> - \frac{J_{\min}}{[\Sigma_\Lambda + J_{\min}\Lambda]^{n+2}} I_\Lambda^<. \quad (4.13)$$

The meaning of these integrals can be understood in terms of the number of states in the first Brillouin zone, with energies $J_{\max} > J(\mathbf{k}) > J_{\max}\Lambda$ and $J_{\min} < J(\mathbf{k}) < J_{\min}\Lambda$. Introducing explicitly the density of states for the exchange interaction

$$\rho(\epsilon) = \int_{\mathbf{k}} \delta(\epsilon - J(\mathbf{k})), \quad (4.14)$$

which yields the number of states at a fixed energy ϵ , we can instead write $I_\Lambda^{>,<}$ in terms of integrals over energy

$$I_\Lambda^> = \int_{J_{\max}\Lambda}^{J_{\max}} d\epsilon \rho(\epsilon), \quad I_\Lambda^< = \int_{J_{\min}}^{J_{\min}\Lambda} d\epsilon \rho(\epsilon). \quad (4.15)$$

This clearly confirms the identification in terms of a total number in the given intervals. Note that for systems with interactions on bipartite lattices, i.e. those that fulfill $J(\mathbf{q} + \mathbf{Q}_N) = -J(\mathbf{q})$, both integrals are equivalent $I_\Lambda^> = I_\Lambda^<$ since the density of states is symmetric,

$\rho(-\epsilon) = \rho(\epsilon)$. Assuming $J(\mathbf{k}) - J_{\min} \propto k^2$ the behavior of $\rho(\epsilon)$ in the vicinity of the global minimum, is in d dimensions given by

$$\rho(\epsilon) \sim (\epsilon + J_{\min})^{(d-2)/2}, \quad |\epsilon + J_{\min}|/|J_{\min}| \ll 1, \quad (4.16)$$

and the total number of states in the vicinity of the band edge scales therefore as $(\Delta\epsilon)^{d/2}$. Note that the mathematical expressions for $\rho(\epsilon)$ are equivalent to the density of states for free fermions with a tight-binding dispersion [15]. Writing the diagrams in terms of an energy integration, which contains $\rho(\epsilon)$, is also possible for the ΛJ -cutoff (4.4) with the same assumptions for the momentum dependence of the vertices. The resulting integrals do not have a simple interpretation in terms of a number of states though, since they involve powers of $[\epsilon + \Sigma]^{-1}$ in the integrand. In contrast to a linear deformation, the bandwidth-scheme clearly distinguishes between two types of fluctuations, i.e. those that lie within and beyond these Λ -dependent boundaries, that define manifolds in momentum space. Indeed we can take a look at the dependence of the vertices on $1 - \Lambda = e^{-2l}$ and rescale Σ_Λ , $\Gamma_\Lambda^{(4)}$, ... with powers of Λ according to their respective canonical dimension [3]. For $e^{-2l} \ll 1$ one can then recover equations which are equivalent to the ordinary (one-loop) RG flow equations for the Heisenberg universality class, yielding the same fixed points and eigenvalues, as will be shown in Appendix C.1. In contrast to the linear cutoff, this procedure suffers, however, from a more intricate intermediate \mathbf{k} -dependence of the deformed interaction. In particular this means that one cannot solve as a function of T^{-1} during the flow and has to integrate the differential equations individually for each temperature.

4.1.3 Level 1 truncation

We start by considering the so-called level-one truncation, a term coined by Metzner *et al.* in the study of the FRG flow for fermionic systems [178]. Here 'level- n ' refers to the number of pairs of external legs, beyond which one discards the renormalization of the corresponding vertices. Thus a level-one truncation amounts to neglecting the flow of the four-point vertex, which is then approximated by its initial value

$$\tilde{\Gamma}_\Lambda^{\alpha\alpha\gamma\gamma}(\mathbf{k}_1, \mathbf{k}_2, \mathbf{k}_3, \mathbf{k}_4) \approx \tilde{\Gamma}_0^{\alpha\alpha\gamma\gamma}(\mathbf{k}_1, \mathbf{k}_2, \mathbf{k}_3, \mathbf{k}_4) = -\frac{Tb_0'''}{3(b_0')^4} \equiv \frac{U_0}{3}, \quad (4.17)$$

where the third derivative of the Brillouin function $b(y)$ at vanishing argument is given by

$$b_0''' = -\frac{(2S+1)^4 - 1}{120} = -\frac{6}{5}b_0' \left(b_0' + \frac{1}{6} \right) < 0. \quad (4.18)$$

As a consequence the static self-energy does not acquire a momentum dependence in this approximation. Its flow equation reads

$$\partial_\Lambda \Sigma_\Lambda = -\frac{5TU_0}{6} \int_{\mathbf{q}} \frac{\partial_\Lambda J_\Lambda(\mathbf{q})}{[J_\Lambda(\mathbf{q}) + \Sigma_\Lambda]^2}. \quad (4.19)$$

The right-hand side is positive definite, since the integrand is peaked at $\mathbf{q} = \mathbf{Q}$, where $\partial_\Lambda J_\Lambda(\mathbf{q}) < 0$. Thus we observe an enhancement of the self-energy due to thermal fluctuations, i.e. a decrease of the transition scales compared to the mean-field result, as expected. In fact Eq. (4.19) does not predict a finite T_c below four dimensions. In its place the inverse of the order parameter susceptibility $G_\Lambda^{-1}(\mathbf{Q})$ vanishes only for $T \rightarrow 0$, so that $T_c = 0$.

Using for instance the ΛJ -scheme one can determine the leading temperature dependence for $T \ll |J|$. For this we consider the flow of

$$\partial_\Lambda G_\Lambda^{-1}(\mathbf{Q}) = \partial_\Lambda(\Sigma_\Lambda + J_\Lambda(\mathbf{Q})) = \partial_\Lambda J_\Lambda(\mathbf{Q}) + \frac{5TU_0}{6} \int_{\mathbf{q}} \dot{G}_\Lambda(\mathbf{q}), \quad (4.20)$$

and write

$$G_\Lambda(\mathbf{q}) = [G_\Lambda^{-1}(\mathbf{Q}) + J_\Lambda(\mathbf{q}) - J_\Lambda(\mathbf{Q})]^{-1}, \quad (4.21)$$

with the low momentum expansion

$$J_\Lambda(\mathbf{q}) - J_\Lambda(\mathbf{Q}) = \Lambda J_Q'' |\mathbf{q} - \mathbf{Q}|^2. \quad (4.22)$$

Assuming $G_\Lambda^{-1}(\mathbf{Q})|J|^{-1} \ll 1$ one can approximate the loop in $d \leq 4$ as

$$\int_{\mathbf{q}} \dot{G}_\Lambda(\mathbf{q}) \approx K_d |J(\mathbf{Q})| \int_0^\infty \frac{dq q^{d-1}}{[G_\Lambda^{-1}(\mathbf{Q}) + \Lambda J_Q'' q^2]^2} = \frac{K_d |J(\mathbf{Q})| (G_\Lambda^{-1}(\mathbf{Q}))^{(d-4)/2}}{(\Lambda J_Q'')^{d/2}} \int_0^\infty \frac{dq q^{d-1}}{[1 + q^2]^2}, \quad (4.23)$$

where $K_d = \Omega_d / (2\pi)^d$. Setting $G_\Lambda^{-1}(\mathbf{Q}) = 0$ does not work below $d = 4$, because one runs into an infra-red singularity in the integral for $|\mathbf{q} - \mathbf{Q}| \rightarrow 0$. Since the above term, which diverges as $G_\Lambda(\mathbf{Q})^{(4-d)/2}$, is positive definite a transition for a $T_c \neq 0$ cannot occur. Only in the low-temperature limit the factor $TU_0 \sim T^2$ in front of the integral is able to suppress this divergence. Enforcing now for $|\Lambda J/T| \rightarrow \infty$ the stationary condition

$$\partial_\Lambda G_\Lambda^{-1}(\mathbf{Q}) = 0, \quad (4.24)$$

which in turn implies

$$|J(\mathbf{Q})| = \frac{5TU_0}{6} \int_{\mathbf{q}} \dot{G}_\Lambda(\mathbf{q}), \quad (4.25)$$

and using the previous expression for the low- T limit of that integral, we obtain

$$G_\Lambda^{-1}(\mathbf{Q}) \sim (T/(\Lambda J_Q''))^{4/(4-d)}. \quad (4.26)$$

From the above expression one reads off $\xi \sim T^{-2/(4-d)}$ for the corresponding correlation length. In low dimensions this implies $\xi \sim T^{-2/3}$ ($d = 1$) and $\xi \sim T^{-1}$ ($d = 2$) which in both cases is a too weak divergence, compared to the true behavior as T^{-1} and $\exp(\alpha/T)$ in one and two dimensions [165, 174]. This could be anticipated given the strong enhancement of thermal fluctuations, thus destroying long-range order at $T \neq 0$ in three dimensions too. In fact by solving these equations in both schemes numerically we corroborated the derived low-temperature behavior, which is also exhibited by the Litim-solution, showing that this feature is intrinsic to the truncation. Note that by considering the corresponding RG flow of the rescaled interaction $u_l \sim e^{(4-d)l} \tilde{\Gamma}_\Lambda^{(4)}$ at large $2l = -\ln(1 - \Lambda)$ one can also see that the Level-1 truncation is incompatible with $T_c \neq 0$, because below $d = 4$ the fixed point is repulsive, i.e. $\partial_l u_l \sim (4 - d)u_l > 0$, implying a runaway flow.

Nevertheless the numerical solution of the flow equation (4.19) is still able to give valuable information, even about the ordering scales T_c . We have solved it explicitly for a non-frustrated $J_1 - J_3$ Heisenberg Model on a simple cubic lattice, where $J_{1/3} > 0$. The exchange interaction is given by

$$J(\mathbf{k}) = 6J_1\gamma^{(1)}(\mathbf{k}) + 8J_3\gamma^{(3)}(\mathbf{k}), \quad (4.27)$$

where

$$\gamma^{(1)}(\mathbf{k}) = \frac{(\cos(k_x a) + \cos(k_y) + \cos(k_z a))}{3}, \quad (4.28)$$

$$\gamma^{(3)}(\mathbf{k}) = \cos(k_x a) \cos(k_y a) \cos(k_z a). \quad (4.29)$$

We observe that the resulting curves for $G^{-1}(\mathbf{Q})$ exhibit a turn or kink at a temperature of the order $T \sim c|J|b'_0$, thus preventing the susceptibility from becoming 0, in line with the above arguments. The position of this kink is thus 'the crossover scale' between the high-temperature behavior of $G^{-1}(\mathbf{Q})$ and its vanishing $\sim T^{4/(4-d)}$ for $T \ll |J''_{\mathbf{Q}}|$. As a kink, i.e. a point where the curvature has its extremal value, it is given by the maximum of $\frac{d^2 G^{-1}(\mathbf{Q})}{dT^2} = \frac{d^2 \Sigma}{dT^2}$ or a turning point in the first derivative $\frac{d\Sigma}{dT}$. Given that in three dimensions the solution behaves as T^4 for $T \rightarrow 0$, implying that the curvature vanishes as T^2 and one starts with $G^{-1}(\mathbf{Q}) \propto T$, i.e. zero curvature, there is indeed an intermediate maximum in the second derivative. Using a RG picture one can also say that the influence of the 'true' critical fixed point is already felt at this temperature, before one is ultimately repelled from it. Hence we use this scale in $d = 3$ to estimate transition temperatures of the system.

In Fig. 4.2 plots of the inverse susceptibility and its second T -derivative are shown for the nearest neighbor Heisenberg model with $S = 1/2, \infty$, utilizing the bandwidth cutoff (4.9). Crossover scales obtained via the prescription above are listed in Table 4.1 for both types of cutoffs. In the case of the bandwidth deformation scheme one obtains reasonable agreement with benchmark results for T_c , extracted from Quantum Monte Carlo simulations [179, 180, 181] or high temperature expansion series [182]. Especially for larger spin values the agreement is very good. Note the absent dependence of T_c on $\text{sgn}(J)$. This follows from the $J(\mathbf{q}) = -J(\mathbf{q} + \mathbf{Q})$ - property of couplings on bipartite lattices, meaning that one integrates in Eq. (4.19) over the same contributions but in reversed locations of the Brillouin zone. For the interaction-switch scheme the deviations from the benchmark values are more spread out. This is not very surprising, because the RG interpretation in terms of 'feeling' the vicinity of the fixed point, appears less justified within this scheme.

In lower dimensions, $d \leq 2$, one may be also inclined to interpret kinks of the $G^{-1}(\mathbf{Q})$ -curve at $T \neq 0$ in terms of a transition at the respective temperature. However one can still infer in these cases that the true critical temperature is zero, in agreement with the Mermin-Wagner theorem. To justify that, one takes a look at the low-temperature behavior of $G^{-1}(\mathbf{Q})$. In two dimensions the inverse susceptibility behaves as $\sim T^2$ for $T \rightarrow 0$. This means that $d^2 \Sigma/dT^2$ has a finite value at $T = 0$, instead of approaching zero like in $d > 2$. For one dimension one observes a divergence for $T \rightarrow 0$, since $d^2 \Sigma/dT^2 \sim T^{-2/3} \rightarrow \infty$. Hence the different $T \rightarrow 0$ -behavior compared to $d > 2$ may be used to argue for the absence of long-range order at finite T_c . Note that the Level 1-approximation may be also applied, without further adjustments, to systems with finite frustrating couplings J_i to neighbors of higher order, that introduce a competition between different states \mathbf{Q}_j . However, it does not offer any new insights, compared to a discussion of the extremal field configurations for the classical total energy. As long as $J''_{\mathbf{Q}} \neq 0$ we find the same qualitative behavior for $G^{-1}(\mathbf{Q})$ and thus its T -derivatives. Only in the case of degenerate ground states, one may encounter distinct behavior, due to $J''_{\mathbf{Q}} = 0$, meaning that $J(\mathbf{q}) - J(\mathbf{Q})$ vanishes with a larger power in $|\mathbf{q} - \mathbf{Q}|$. In turn this leads to a reduction of the effective dimensionality in the integral $\int_{\mathbf{q}} \hat{G}_{\Lambda}(\mathbf{q})$, so that in three dimensions one also extracts $T_c = 0$ at the classical phase boundaries in the plane of couplings.

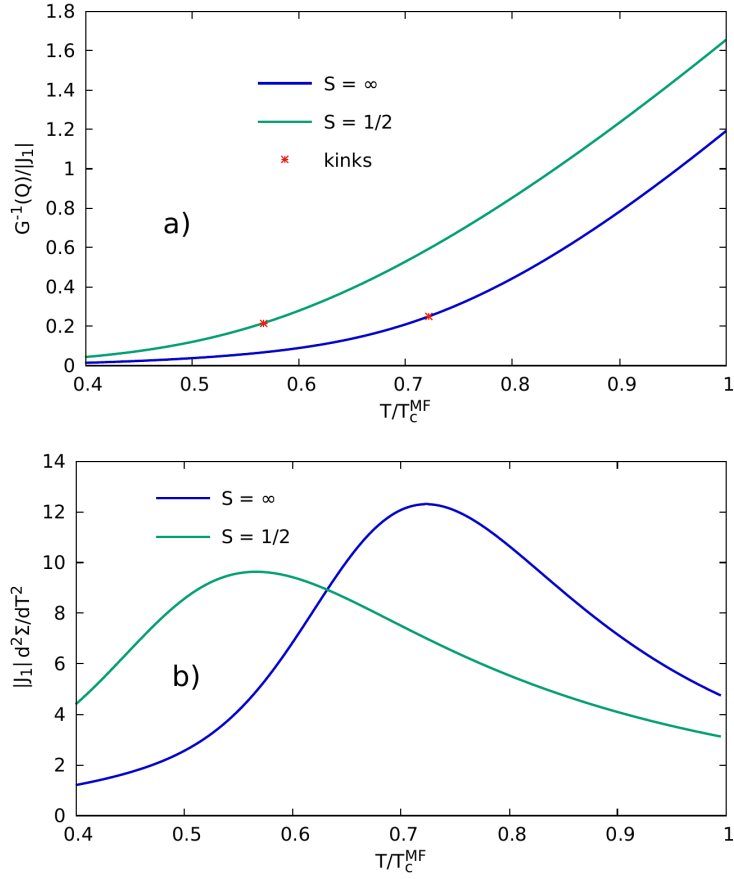


Figure 4.2: T -dependence of a) the inverse order parameter susceptibility $G^{-1}(\mathbf{Q})$ and b) $d^2\Sigma/dT^2$ of the $S = 1/2$ and classical ($S = \infty$) nearest neighbor Heisenberg magnet on a simple cubic lattice in a Level 1-truncation (4.19), using the Litim-cutoff scheme (4.9) for the deformed coupling. The red crosses in the upper plot mark the kinks and correspond to the maxima in the lower figure.

S	J_1	J_3/J_1	T_c/T_c^{MF}			rel. error / %	
			switch	Litim	benchmark	switch	Litim
1/2	< 0	0	0.651	0.568	0.559	16.5	1.6
1/2	> 0	0	0.651	0.568	0.629	3.5	9.7
1	< 0	0	0.726	0.668	0.650	11.7	2.8
1	> 0	0	0.726	0.668	0.684	6.1	2.3
3/2	< 0	0	0.745	0.695	0.685	8.8	1.5
3/2	> 0	0	0.745	0.695	0.702	6.1	1.0
1/2	> 0	0.2	0.746	0.701	0.722	3.3	2.9
1/2	> 0	0.4	0.782	0.753	0.768	1.8	2.0
1/2	> 0	0.6	0.800	0.776	0.794	0.8	2.3
1/2	> 0	0.8	0.807	0.787	0.808	0.1	2.6
∞	$\neq 0$	0	0.766	0.725	0.722	6.1	0.4

Table 4.1: Critical temperatures obtained for the $J_1 - J_3$ model on a simple cubic lattice within a Level 1-truncation (4.19), which are given by turning points / peak positions of $d\Sigma/dT$, $d^2\Sigma/dT^2$. For the cases with $S = 1/2$ the benchmark values are Quantum Monte Carlo results [179, 180, 181], while for larger spins the values are taken from an Padé-approximated high temperature series [182].

4.1.4 Level 2 truncation

In the previous section it was demonstrated that without a flowing four-point vertex one does not obtain a phase transition at finite temperature below $d = 4$. Hence one should proceed one level further in the hierarchy and retain the flow equation of $\Gamma_\Lambda^{\alpha\alpha\gamma\gamma}$. In the classical approximation the hierarchy is closed by neglecting the flow of the six-point vertices, whose local initial values are given by

$$\tilde{\Gamma}_0^{\alpha\alpha\gamma\gamma\gamma\gamma} = 3\tilde{\Gamma}_0^{xyyz} = \frac{T}{5(b'_0)^6} \left(\frac{10(b''_0)^2}{b'_0} - b^{(5)} \right) = \frac{V_0}{5}, \quad (4.30)$$

where the fifth derivative of the spin- S Brillouin function at vanishing argument reads

$$b^{(5)} = \frac{(2S+1)^6 - 1}{252}. \quad (4.31)$$

One still has to deal with the momentum dependence of the four-point vertex. Fortunately, running along similar lines, as one-loop approximations to conventional momentum shell RG calculations [2, 3] it is sufficient for our purposes to approximate

$$\tilde{\Gamma}_\Lambda^{\alpha\alpha\gamma\gamma}(\mathbf{k}_1, \mathbf{k}_2, \mathbf{k}_3, \mathbf{k}_4) \approx \tilde{\Gamma}_\Lambda^{\alpha\alpha\gamma\gamma}(\mathbf{Q}, -\mathbf{Q}, \mathbf{Q}, -\mathbf{Q}) = \frac{U_\Lambda}{3}. \quad (4.32)$$

Here \mathbf{Q} is the classical ordering vector, i.e. for either the ferromagnetic $\mathbf{Q} = \mathbf{0}$ or Néel ground state $\mathbf{Q} = \mathbf{R} = \frac{\pi}{a}(1, 1, 1)$. This is certainly justified in the absence of frustrating interactions, i.e. non-competing classical ground states. As a consequence, $\Sigma_\Lambda(\mathbf{k})$ loses again its momentum dependence, i.e

$$\Sigma_\Lambda(\mathbf{k}) \approx \Sigma_\Lambda(\mathbf{Q}) = \Sigma_\Lambda. \quad (4.33)$$

Hence one arrives at the following two differential equations

$$\partial_\Lambda \Sigma_\Lambda = -\frac{5TU_\Lambda}{6} \int_{\mathbf{q}} \frac{\partial_\Lambda J_\Lambda(\mathbf{q})}{[J_\Lambda(\mathbf{q}) + \Sigma_\Lambda]^2}, \quad (4.34)$$

$$\partial_\Lambda U_\Lambda = T \int_{\mathbf{q}} \dot{G}_\Lambda(\mathbf{q}) \left[\frac{7}{10} V_0 - \frac{11}{3} U_\Lambda^2 G_\Lambda(\mathbf{q}) \right]. \quad (4.35)$$

The term $\propto \int_{\mathbf{q}} \dot{G}_\Lambda(\mathbf{q})$ in (4.35) is due to $V_0 > 0$ positive definite as in the flow of Σ_Λ , countering the decrease of U_Λ , which is driven by the quadratic term $\propto \int_{\mathbf{q}} \dot{G}_\Lambda(\mathbf{q}) G_\Lambda(\mathbf{q})$. The latter decrease of U_Λ is responsible for restoring magnetic order below $d = 4$, i.e. the reduction of the sole diagram in $\partial_\Lambda \Sigma_\Lambda$, which previously prevented a transition at $T_c \neq 0$. Note that we used for (4.35) that $\mathbf{Q} \pm \mathbf{Q}$, which appears as a momentum transfer in the quadratic diagrams, is always a reciprocal lattice vector \mathbf{G} . Given that all vertices in \mathbf{k} -space have the periodicity of the reciprocal lattice, one concludes that the effective momentum transfer is always zero. Thus one obtains the same flow equations for the ferro- and antiferromagnet. In fact, for systems where the exchange coupling fulfills $J(\mathbf{q} + \mathbf{Q}) = -J(\mathbf{q})$, i.e. next-neighbor models on bipartite cubic lattices, one arrives at the same temperature dependence of the order parameter susceptibility, regardless of the global sign of $J(\mathbf{k})$. This is an exact property for classical models, satisfying the aforementioned conditions. In the static approximation it is also retained for finite S . One already observed this in the Level-1 truncation. Such behavior for $S < \infty$ is not correct anymore, given that the symmetry with respect to $J \leftrightarrow -J$ is destroyed by quantum fluctuations. The latter can be inferred for instance from the fact that staggered degrees of freedom are time-dependent in contrast to the conserved total spin.

The Level-2 flow equations (4.34) and (4.35) are analogous to the ones derived by Krieg [2] in the context of the spin- S Ising model. They only differ by the prefactors in front of each loop integration, since we have $n = 3$ instead of only one direction. In fact these factors are consistent with the coefficients in the one-loop momentum shell RG equations for the n -component ϕ^4 -model [3]. These RG equations host the non-Gaussian Wilson-Fisher (WF) fixed point ($u_* \neq 0$) in $d < 4$, that describes the critical properties of models in the $\mathcal{O}(n)$ -universality class. Note, however, the additional presence of the six-point vertex in our case, which, in a RG sense, turns out to be marginal in $d = 3$ and irrelevant for $d > 3$, consistent with its canonical dimension $6 - 2d$ [3]. In principle this can lead to additional fixed points in $d = 3$ besides the Wilson-Fisher fixed point [183]. In appendix C.1 we show by employing the Litim-cutoff that one indeed recovers equations equivalent to the one-loop RG equations for the $\mathcal{O}(3)$ -model which feature the WF fixed point.

Solving the flow equations numerically in both cutoff schemes for the $J_1 - J_3$ model on the simple cubic lattice we obtain, as anticipated, a true phase transition, indicated by $G^{-1}(\mathbf{Q}) = 0$ at a temperature $T = T_c$. Results for $G^{-1}(\mathbf{Q})$ and the effective four-spin interaction U calculated within the interaction-switch scheme (4.4) are shown in Fig. 4.3. The four-vertex vanishes 'square-root'-like, i.e. with an exponent smaller than unity, for $T \rightarrow T_c$, which is expected, given that it has to regularize the divergence of $\int_{\mathbf{q}} \dot{G}_\Lambda(\mathbf{Q}) \propto G_\Lambda(\mathbf{Q})^{(4-d)/2}$ in $\partial_\Lambda \Sigma_\Lambda$. In fact, assuming

$$G_\Lambda^{-1}(\mathbf{Q}) \sim (1 - \Lambda)^\gamma, \quad (4.36)$$

and

$$U_\Lambda \sim (1 - \Lambda)^\alpha, \quad (4.37)$$

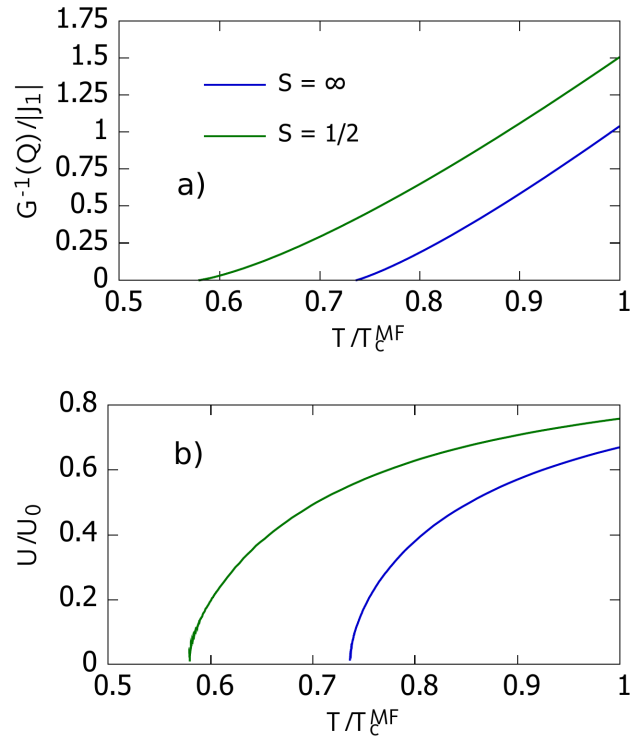


Figure 4.3: T -dependence of the a) inverse order parameter susceptibility $G^{-1}(\mathbf{Q})$ and b) dimensionless effective four-spin interaction U/U_0 of the $S = 1/2$ and classical nearest neighbor Heisenberg magnet on a simple cubic lattice in a Level 2-truncation, using the interaction deformation scheme (4.4) for the numeric integration of the respective flow equations, (4.34) and (4.35).

at $T = T_c$ we obtain by enforcing $\partial_\Lambda G_\Lambda^{-1}(\mathbf{Q}) = 0$ ($\gamma > 1$) or $\partial_\Lambda G_\Lambda^{-1}(\mathbf{Q}) = \text{const.}$ ($\gamma = 1$) the following relation

$$\alpha = \left(\frac{4-d}{2}\right)\gamma, \quad (4.38)$$

i.e. $\alpha = \gamma/2$ for $d = 3$. An analysis of the corresponding one-loop RG flow, which as sketched in appendix C.1, can be recovered within the bandwidth scheme, yields in $d = 3 + \epsilon'$ dimensions $\gamma \approx 1.12$, which is too small [26], given that the one-loop approximation is only accurate in the vicinity of $d = 4$ [3]. Inserting the Λ -dependence of $G_\Lambda^{-1}(\mathbf{Q})$ and U_Λ into the flow equation of U_Λ (4.35) we find that for $d \geq 3$ they are fully consistent with $\partial_\Lambda U_\Lambda \propto (1 - \Lambda)^{\alpha-1}$ with α given by Eq. (4.38), where we made use of

$$\int_{\mathbf{q}} \dot{G}_\Lambda(\mathbf{q}) G_\Lambda(\mathbf{q}) \propto G_\Lambda^{-1}(\mathbf{Q})^{(d-6)/2}. \quad (4.39)$$

Note that above three dimensions and in the vicinity of T_c the contribution from the six-point vertex becomes negligible compared to the term $\propto U_\Lambda^2$, in accordance with its irrelevance, while in $d = 3$ it is marginal and thus contributes equally to $\partial_\Lambda U_\Lambda$. Above $d = 4$ the integral in $\partial_\Lambda \Sigma_\Lambda$ is non-singular. Furthermore U_Λ approaches a finite value for T_c , given that its Λ -derivative is not sufficiently singular due to the exponent in the quadratic term fulfilling $(d-6)/2 > -1$. This is consistent with the irrelevance of the four-vertex with respect to the Gaussian fixed point. Thus one obtains $\partial_\Lambda G_\Lambda^{-1}(\mathbf{Q}) = \text{const.}$, i.e. the mean-field exponent $\gamma = 1$, as expected above the critical dimension.

The extracted critical temperatures for the $J_1 - J_3$ model on a simple cubic lattice are given in Table 4.2 and are in relatively good agreement with the benchmark values, in particular for the interaction-switch cutoff at larger spin values. Larger deviations for $S = 1/2$ are not surprising, given that the purely classical approach completely ignores the feedback of quantum dynamics. The accuracy of a classical approximation is thus inferior to an application to the Ising model [2]. The Ising Hamiltonian does not contain non-commuting operators so that taking only static fluctuations into account does not amount to an additional approximation. Even for $S = \infty$ the deviation is still larger [2], but this also does not surprise us, since the stronger effect of fluctuations due to a larger n may be underestimated in the same type of truncation. Integrating the Level-2 flow with the Litim-cutoff yields lower T_c in all listed cases, performing worse than the interaction-switch deformation.

Let us briefly discuss reduced dimensions, in which the effect of the six-spin vertex is more pronounced than in $d = 3$. In fact its inclusion leads to a vanishing T_c , i.e. the fulfillment of the Mermin-Wagner-Theorem [24]. This is a consequence of $\int_{\mathbf{q}} \dot{G}_\Lambda(\mathbf{q})$ being too singular, which prevents U_Λ and thus $G_\Lambda^{-1}(\mathbf{Q})$ from flowing to zero at any finite temperature. One can estimate the leading T -dependence of Σ_Λ like in the Level-1 truncation by enforcing a vanishing flow of $G_\Lambda^{-1}(\mathbf{Q})$ and U_Λ for $\Lambda \rightarrow \infty$, i.e. the $T = 0$ -limit in the linear deformation scheme (4.4). First we find

$$G_\Lambda^{-1}(\mathbf{Q}) \propto (TU_\Lambda)^{2/(4-d)}. \quad (4.40)$$

From $\partial_\Lambda U_\Lambda = 0$ we read off

$$TU_\Lambda^2 G_\Lambda^{-1}(\mathbf{Q})^{(d-6)/2} \sim T^2 G_\Lambda^{-1}(\mathbf{Q})^{(d-4)/2} \rightarrow U_\Lambda \sim (TG_\Lambda^{-1}(\mathbf{Q}))^{1/2}, \quad (4.41)$$

which is solved by

$$G_\Lambda^{-1}(\mathbf{Q}) \propto T^{3/(3-d)} \sim T^{2\nu}, \quad (4.42)$$

S	J_1	J_3/J_1	T_c/T_c^{MF}			rel. error / %	
			switch	Litim	benchmark	switch	Litim
1/2	< 0	0	0.578	0.525	0.559	3.4	6.1
1/2	> 0	0	0.578	0.525	0.629	8.1	16.5
1	< 0	0	0.672	0.625	0.650	3.4	3.8
1	> 0	0	0.672	0.625	0.684	1.8	8.6
3/2	< 0	0	0.701	0.658	0.685	2.3	3.9
3/2	> 0	0	0.701	0.658	0.702	0.1	6.3
1/2	> 0	0.2	0.712	0.676	0.722	1.4	6.4
1/2	> 0	0.4	0.768	0.740	0.768	0.0	3.7
1/2	> 0	0.6	0.795	0.771	0.794	0.1	2.9
1/2	> 0	0.8	0.808	0.787	0.808	0.0	2.6
∞	$\neq 0$	0	0.736	0.700	0.722	1.9	3.0

Table 4.2: Critical temperatures of the same Heisenberg models, as in Table 4.1, obtained within a Level 2-Truncation, given by the flow equations (4.34) and (4.35).

$$U_\Lambda \propto T^{\frac{(6-d)}{2(3-d)}}. \quad (4.43)$$

This yields $\nu = \frac{3}{2(3-d)}$ for the correlation length exponent, i.e. $\xi \sim T^{-3/4}$ and $\xi \sim T^{-3/2}$ in $d = 1$ and $d = 2$. That is still a too weak singularity for $T \rightarrow 0$, compared to the correct behavior in ferromagnets [165, 174]. Note that the latter can already be estimated from the spin length constraint $\langle S_i^\alpha S_i^\alpha \rangle = S(S+1)/3$ in the symmetric phase

$$b'_0 = T \int_{\mathbf{q}} \sum_{\nu} G(Q) \approx T \int_{\mathbf{q}} G(\mathbf{q}), \quad (4.44)$$

where the latter \approx holds exactly in the classical $S \rightarrow \infty$ limit. One sees than that it is violated by our low-temperature expressions, leading to a vanishing right-hand side for $T \rightarrow 0$. The effective interaction U_Λ approaches zero in our case as $T^{5/4}$ in one dimension and T^2 in two dimensions. We have corroborated this limiting behavior by a numerical integration of the flow. As for the Level-1 truncation the same asymptotics are predicted when a bandwidth cutoff is used. Results for the temperature dependence of $G^{-1}(\mathbf{Q})$ and the four-point vertex, using the Litim-deformation scheme (4.9), are shown in Fig. 4.4 for Heisenberg models on the linear chain and the square lattice with nearest neighbor coupling (1.18).

Note that the fulfillment of the sum rule (4.44), can, in principle, be realized by the introduction of a suitable counterterm C_Λ or higher order vertex correction. One can add for instance an on-site coupling $C_\Lambda = J_{ii}^\Lambda$, that is generated during the flow, in order to enforce $\partial_\Lambda \int_K G_\Lambda(K) = 0$. The absence of long-range order for $T > 0$ is in some sense a 'lucky' coincidence in the Heisenberg case. For the Ising model, where the flow equations have the same structure, it does not hold, i.e $T_c \neq 0$, since there is no continuous rotational symmetry to be broken, whereas the Level-2 truncation still predicts $T_c = 0$ [2]. The general inadequacy of this truncation in low dimensions, can be readily explained by the fact, that arguments regarding the relevance of vertices, that are justified in $d > 2$, where $T_c \neq 0$, cannot be applied here, e.g. arbitrary n -point vertices turn out to be all relevant in $d \leq 2$ according to the simple classification scheme [3]. Note that with reasonable expressions for the \mathbf{k} -dependence of $\Sigma_\Lambda(\mathbf{k})$ the sum rule (4.44) should always ensure the

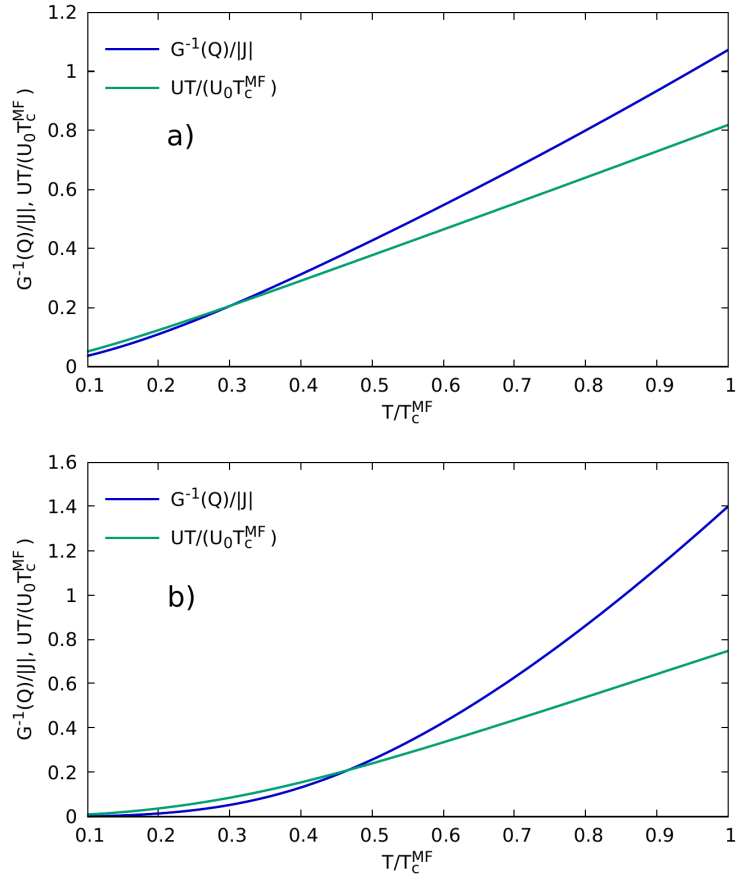


Figure 4.4: T -dependence of the inverse order parameter susceptibility $G^{-1}(\mathbf{Q})$ (blue) and the four-point vertex U (green) of the $S = 1/2$ and $S = \infty$ nearest neighbor Heisenberg magnet on a) a linear chain and b) a square lattice, using the Level 2-truncation, (4.34) and (4.35), for the flow equations and a bandwidth cutoff (4.9). Note that U vanishes with a larger-than-linear power in $T - T_c$, in contrast to $d > 2$.

Mermin-Wagner-Theorem for the Heisenberg model in $d \leq 2$. Otherwise the integral over the static component in the frequency sum will simply diverge, leading to a violation of (4.44). Its implementation should be therefore crucial in reduced dimensions.

4.2 Inclusion of dynamic fluctuations

Up to now the feedback of fluctuations at finite frequency onto the flow of Σ_Λ , $\tilde{\Gamma}_\Lambda^{(4)}$ was utterly neglected. As a consequence some features are not captured, like the different critical temperatures for quantum ferro- and antiferromagnets. Taking dynamic terms into account introduces frequency sums in the flow of purely static quantities, which contain higher order vertices, including odd ones, with legs at finite frequency. It turns out that for our purpose these partially dynamic vertices may be safely approximated by their initial values. Using the same simplifications for the momentum dependence of the four-vertex, Eq. (4.32), and

self-energy, Eq. (4.33), one arrives at the flow equations

$$\partial_\Lambda \Sigma_\Lambda = \frac{5T}{6} U_\Lambda \int_{\mathbf{q}} \dot{G}_\Lambda(\mathbf{q}) + T \sum_{\omega \neq 0} \int_{\mathbf{q}} \frac{2}{\omega^2} \dot{F}_\Lambda(\mathbf{q}, i\omega) \tilde{F}_\Lambda(\mathbf{q} + \mathbf{Q}, i\omega), \quad (4.45)$$

and

$$\begin{aligned} \partial_\Lambda U_\Lambda &= T \int_{\mathbf{q}} \dot{G}_\Lambda(\mathbf{q}) \left[\frac{7}{10} V_0 - \frac{11}{3} U_\Lambda^2 G_\Lambda(\mathbf{q}) \right] \\ &+ \frac{3T}{2} \sum_{\omega \neq 0} \int_{\mathbf{q}} \dot{F}_\Lambda(\mathbf{q}, i\omega) [2\tilde{\Gamma}_0^{xxxxzz}(\omega, -\omega, 0, 0, 0, 0) + \tilde{\Gamma}_0^{xyyyzz}(\omega, -\omega, 0, 0, 0, 0)] \\ &- 24T \sum_{\omega \neq 0} \int_{\mathbf{q}} \dot{F}_\Lambda(\mathbf{q}, i\omega) \tilde{F}_\Lambda(\mathbf{q}, i\omega) \tilde{F}_\Lambda^2(\mathbf{q} + \mathbf{Q}, i\omega) \left[\tilde{\Gamma}_0^{xyz}(-\omega, \omega, 0) \right]^4. \end{aligned} \quad (4.46)$$

Here we have already inserted the expression for the mixed three-point vertex $\propto \omega^{-1}$ and also used that the four-point vertex with two dynamic legs vanishes at the initial scale as seen in Sec. 2.3.2. Furthermore diagrams with the mixed five-point vertices featuring two quantum legs are also absent in (4.46) due to

$$\tilde{\Gamma}_0^{xyzzz}(\omega, 0, -\omega, 0, 0, 0) = 0. \quad (4.47)$$

On the other hand the mixed six-point vertices needed for Eq. (4.46) are finite

$$\tilde{\Gamma}_0^{xxxxzz}(\omega, -\omega, 0, 0, 0, 0) = \frac{2b_0'''}{3(\beta b_0')^4 \omega^2}, \quad \tilde{\Gamma}_{\Lambda_0}^{xyyyzz}(\nu, -\nu, 0, 0, 0, 0) = \frac{4b_0'''}{3\beta(\beta b_0')^4 \omega^2}, \quad (4.48)$$

so that their diagrams still contribute at this level of approximation. The full flow equation for the static 4-point vertex is given in appendix C.2.

One still has to deal with finding an appropriate treatment for the dynamic polarization $\tilde{\Pi}_\Lambda(\mathbf{k}, i\omega)$, which is contained in the effective interaction $\tilde{F}_\Lambda(\mathbf{k}, i\omega)$. Setting it to ≈ 0 works only for very large temperatures $|J_\Lambda| \ll T$, whereas for $|J_\Lambda| \sim \mathcal{O}(T)$, i.e. the region where one anticipates a phase transition, one runs into problems. These issues are caused by an insufficient inhibition of the associated diagrams. At least for an antiferromagnet, one can show that the contribution in $\partial_\Lambda \Sigma_\Lambda(\mathbf{k})$ will grow exponentially for low temperatures without being mitigated by a finite $\tilde{\Pi}_\Lambda(\mathbf{k}, i\omega)$. As an example the quantum contribution to the flow of $\Sigma_\Lambda(\mathbf{k})$ becomes

$$\begin{aligned} T \sum_{\omega \neq 0} \int_{\mathbf{q}} \frac{2}{\omega^2} \dot{F}_\Lambda(\mathbf{q}, i\omega) F_\Lambda(\mathbf{q} + \mathbf{k}, i\omega) &= \frac{1}{6T} \int_{\mathbf{q}} (\partial_\Lambda J_\Lambda(\mathbf{q})) G_\Lambda^{-1}(\mathbf{q} + \mathbf{k}) \\ &= \frac{1}{12T} \partial_\Lambda \int_{\mathbf{q}} J_\Lambda(\mathbf{q}) J_\Lambda(\mathbf{q} + \mathbf{k}) + \frac{1}{6T} \int_{\mathbf{q}} \Sigma_\Lambda(\mathbf{q}) \partial_\Lambda J_\Lambda(\mathbf{q} + \mathbf{k}). \end{aligned} \quad (4.49)$$

Assuming a linear deformation (4.4) one can separate the momentum-dependent contribution to $\Sigma_\Lambda(\mathbf{k})$, i.e. for a nearest neighbor interaction $J(\mathbf{k}) = cJ\gamma(\mathbf{k})$

$$(b_0'/T) \Sigma_\Lambda(\mathbf{k}) = \Sigma_g(\mathbf{k}) = \Sigma_g + \Sigma_g^{(1)} \gamma(\mathbf{k}), \quad (4.50)$$

with $\Sigma_g^{(1)}$ satisfying

$$\partial_g \Sigma_g^{(1)} = \frac{1}{6b_0'} \int_{\mathbf{q}} \gamma(\mathbf{q})^2 [g + \Sigma_g^{(1)}], \quad \Sigma_0^{(1)} = 0, \quad (4.51)$$

where we introduced the new variable $g = (c\Lambda J b'_0)/T$. The solution is then given by

$$\Sigma_g^{(1)} = [C]^{-1} \left(1 - (1 + Cg) \exp(-Cg) \right) \exp(Cg), \quad (4.52)$$

where

$$C = \frac{1}{6b'_0} \int_{\mathbf{q}} \gamma(\mathbf{q})^2 > 0. \quad (4.53)$$

For $|g| \ll 1$ it reduces to the leading high-temperature expression, obtained by dropping the momentum dependence of $\Sigma_{\Lambda}(\mathbf{k})$ in the integral, i.e. $\Sigma_g^{(1)} \approx \frac{Cg^2}{2}$. In the limit $|g| \gg 1$ its asymptotics depend on the sign of J . For a ferromagnet, $g < 0$, it is $\propto |g|$, which is not too problematic. On the other hand for antiferromagnets with $g > 0$, the aforementioned exponential explosion occurs, so that the flow will break down. Note that in the approximation $\Sigma_{\Lambda}(\mathbf{k}) \approx \Sigma_{\Lambda}(\mathbf{Q})$ one would simply obtain the high-T limit of this diagram, which grows as J_{Λ}^2/T , is negative for $\mathbf{Q} = \mathbf{Q}_N$ and therefore still causes similar issues for the antiferromagnet.

Fortunately, in the case of systems which have a finite $T_c = \mathcal{O}(c|J|b'_0)$, one is able to obtain reasonable results with a fairly simple ansatz for the dynamics. It is explicitly given by the leading order for $\tilde{\Pi}_{\Lambda}(\mathbf{k}, i\omega)$ in a high-frequency and high-temperature expansion, see Eq. (2.123), i.e. $\tilde{\Pi}_{\Lambda}(\mathbf{k}, i\omega) \propto J_{\Lambda}^2/(\omega^2 T)$. Note that at large temperatures, its contribution to $\partial_{\Lambda} \Sigma_{\Lambda}$, Eq. (4.45) is of the order J^4/T^3 , due to the Matsubara frequencies behaving as $\omega_n = 2\pi nT$ in (4.45). This approximation still loses its validity for $T \lesssim |J_{\Lambda}|$, as $\tilde{\Pi}_{\Lambda}$ grows with increasing $|J_{\Lambda}|/T$, but in contrast to $\tilde{\Pi}_{\Lambda} = 0$, it does not cause any severe issues, since its mitigating effect on that diagram is actually enhanced with decreasing T . A generalization of Eq. (2.123) for arbitrary temperatures, keeping only the leading $1/\omega^2$ -dependence in the high-frequency limit, is given by replacing the \mathbf{k} -dependent coefficient with an exact expression for the second moment [98, 100], i.e.

$$\tilde{\Pi}_{\Lambda}(\mathbf{k}, i\omega) = \frac{2}{\omega^2} \int_{\mathbf{q}} [J_{\Lambda}(\mathbf{q} + \mathbf{k}) - J_{\Lambda}(\mathbf{q})] \langle S^z(\mathbf{q}) S^z(-\mathbf{q}) \rangle_{\Lambda}. \quad (4.54)$$

This would also introduce a self-consistent coupling to $\tilde{\Pi}_{\Lambda}(\mathbf{q}, i\nu)$ via the static structure factor

$$\langle S^z(\mathbf{q}) S^z(-\mathbf{q}) \rangle_{\Lambda} = T \sum_{\nu} G_{\Lambda}(\mathbf{q}, i\nu), \quad (4.55)$$

on the right-hand side, while still exhibiting the same simple momentum dependence for finite-ranged exchange couplings. Note that negligence of finite frequencies in Eq. (4.55) is incompatible with a non-singular susceptibility. $\tilde{\Pi}_{\Lambda}(\mathbf{k}, i\omega)$ would then vanish for $T \rightarrow 0$, potentially causing an explosion of the quantum diagrams in (4.45) and (4.46), as discussed above. Even if $\tilde{\Pi}_{\Lambda}(\mathbf{k}, i\omega)$ has a finite limit for $T \rightarrow 0$, a $1/\omega^2$ -ansatz appears to be inadequate for mimicking the influence of quantum fluctuations at low temperatures. The reason for this is that a successively growing number of Matsubara frequencies $\sim 2\pi T$ contained in frequency sums becomes for $T \ll |J|$ much smaller than $|J|$, so that one crosses into the low-frequency sector for the dynamics. Interestingly, in the context of a second order Green's function theory, the damping of spin waves, or any kind of relaxational processes, are entirely ignored. However, this did not prevent the authors of Ref. [66] from finding disordered phases in the spin-1/2 J_1 - J_2 model on the square lattice, in fact considerably overestimating the extent of the disordered phase [66]. We have corroborated this tendency by solving for a \mathbf{k} -independent Σ_{Λ} fixed via the sum rule (4.44) and the above choice (4.54) for the dynamics of the same model.

As an alternative to the self-consistent second moment (4.54), one could solve a flow equation, e.g. Eq. (2.122), whose right-hand side is $\propto 1/\omega^2$ too, but does not contain any frequency sums, while still being free of outright non-physical properties down to $T = 0$. One may also try to improve upon the $1/\omega^2$ -ansatz, by retaining the ω^{-4} -term in $\tilde{\Pi}_\Lambda(\mathbf{k}, i\omega)$, i.e. the fourth moment $\langle \omega^4 \rangle_{\mathbf{k}}$, which is a three-loop expression involving four-spin correlations [31, 98]. The additional term can then be used for an extrapolation to a diffusive $|\omega|^{-1}$ -low frequency shape, e.g. in the sense of the previously discussed three-pole approximation (3.90) [98, 100]. The last and most sophisticated path one can pursue is to work with an a priori unknown frequency dependence for $\Pi(\mathbf{k}, i\omega)$. Note that this requires a finite cutoff ω_{\max} for the number of frequencies used in numeric calculations. For too low temperatures $T \lesssim \mathcal{O}(J)$ this will not suffice, because the largest frequency becomes of the same order as J , with ω_{\max}/J_Λ eventually scaling to 0, if the frequency cutoff remains fixed. Note that we have provided results for such a case, using the self-consistency equation (3.44) for $\tilde{\Pi}_\Lambda(K)$, which exhibits a non-trivial ω -dependence, in appendix C.3.

However, as already stated, for our purpose of investigating non-frustrated magnets in $d \geq 3$ the high- T/ω -limit (2.123) is a sufficient approximation, with the proposed refinements presumably having only a modest impact. In fact, the more sophisticated ansatz based on (3.44) and discussed in appendix C.3 does not perform better than (2.123). Having a fixed, analytic dependence on $1/\omega^2$ allows us to evaluate the Matsubara sums in the flow equations analytically by using the theorem of residues [18, 29]. Writing

$$G_\Lambda^{-1}(\mathbf{k})\tilde{\Pi}_\Lambda(\mathbf{k}, i\omega) = \frac{\tilde{\Omega}_\Lambda(\mathbf{k})}{(\beta\omega)^2}, \quad (4.56)$$

one arrives at the following set of equations

$$\partial_\Lambda \Sigma_\Lambda = \frac{5T}{6} U_\Lambda \int_{\mathbf{q}} \dot{G}_\Lambda(\mathbf{q}) + \frac{2}{T} \int_{\mathbf{q}} \frac{\partial_\Lambda J_\Lambda(\mathbf{q})}{G_\Lambda(\mathbf{q} + \mathbf{Q})} S_1 \left(\tilde{\Omega}_\Lambda(\mathbf{q}), \tilde{\Omega}_\Lambda(\mathbf{q} + \mathbf{Q}) \right), \quad (4.57a)$$

$$\begin{aligned} \partial_\Lambda U_\Lambda = T \int_{\mathbf{q}} \dot{G}_\Lambda(\mathbf{q}) \left[\frac{7}{10} V_0 - \frac{11}{3} U_\Lambda^2 G_\Lambda(\mathbf{q}) \right] - 4 \int_{\mathbf{q}} [\partial_\Lambda J_\Lambda(\mathbf{q})] \left[\frac{b_0'''}{(b_0')^4} S_2 \left(\tilde{\Omega}_\Lambda(\mathbf{q}) \right) \right] \\ - \frac{24}{T^3 (b_0')^4} \int_{\mathbf{q}} \frac{\partial_\Lambda J_\Lambda(\mathbf{q})}{G_\Lambda(\mathbf{q}) G_\Lambda^2(\mathbf{q} + \mathbf{Q})} S_4 \left(\tilde{\Omega}_\Lambda(\mathbf{q}), \tilde{\Omega}_\Lambda(\mathbf{q} + \mathbf{Q}) \right). \end{aligned} \quad (4.57b)$$

Three distinct Matsubara sums appear in the above equations. Together with the auxiliary

quantity $S_3(x, y)$ used for calculating $S_4(x, y)$ these sums are for $x, y \geq 0$ given by

$$\begin{aligned} S_1(x, y) &= \sum_{\omega \neq 0} \frac{(\beta\omega)^4}{[(\beta\omega)^2 + x]^2 [(\beta\omega)^2 + y]} \\ &= \frac{1}{8(x-y)^2} \left[2\sqrt{x}(x-3y) \coth(\sqrt{x}/2) \right. \\ &\quad \left. - x(x-y) \operatorname{csch}^2(\sqrt{x}/2) + 4y^{3/2} \coth(\sqrt{y}/2) \right], \end{aligned} \quad (4.58a)$$

$$S_2(x) = \sum_{\omega \neq 0} \frac{(\beta\omega)^2}{[(\beta\omega)^2 + x]^2} = \frac{\sqrt{x} - \sinh(\sqrt{x})}{4\sqrt{x}[1 - \cosh(\sqrt{x})]}, \quad (4.58b)$$

$$\begin{aligned} S_3(x, y) &= \sum_{\omega \neq 0} \frac{(\beta\omega)^2}{[(\beta\omega)^2 + x]^2 [(\beta\omega)^2 + y]} \\ &= \frac{1}{8\sqrt{x}(x-y)^2} \left[2(x+y) \coth(\sqrt{x}/2) + \sqrt{x}(x-y) \operatorname{csch}^2(\sqrt{x}/2) \right. \\ &\quad \left. - 4\sqrt{xy} \coth(\sqrt{y}/2) \right], \end{aligned} \quad (4.58c)$$

$$\begin{aligned} S_4(x, y) &= \sum_{\omega \neq 0} \frac{(\beta\omega)^6}{[(\beta\omega)^2 + x]^3 [(\beta\omega)^2 + y]^2} \\ &= S_3(x, y) + \frac{x}{2} \partial_x S_3(x, y) + y \partial_y S_3(x, y) + \frac{xy}{2} \partial_x \partial_y S_3(x, y). \end{aligned} \quad (4.58d)$$

In the following we will solely consider the interaction-switch cutoff (4.4) for the integration of the flow equations (4.57). As in the purely static case one can then map the flow onto an integration with respect to inverse temperature, i.e. $g = \pm T_c^{\text{MF}}/T$. For that one simply works with the dimensionless quantities $\tilde{\Omega}_\Lambda(\mathbf{k})$ and $\beta\omega = 2\pi n$. The reason for restricting ourselves to a linear deformation is that $\tilde{\Pi}_\Lambda(\mathbf{k}, i\omega)$, given by (2.123), can be straightforwardly evaluated with $J_\Lambda = \Lambda J$. For the aforementioned $J_1 - J_3$ -model one obtains

$$\tilde{\Omega}_\Lambda(\mathbf{k}) = \frac{G_\Lambda^{-1}(\mathbf{k})(6\Lambda b'_0 J_1)^2}{3T^3} \left(1 - \gamma^{(1)}(\mathbf{k}) + \frac{4}{3} \left(\frac{J_3}{J_1} \right)^2 (1 - \gamma^{(3)}(\mathbf{k})) \right), \quad (4.59)$$

which is consistent with its initial condition $\tilde{\Omega}_{\Lambda_0}(\mathbf{k}) = 0$. On the other hand for the Litim-cutoff (4.9) the deformed coupling $J_\Lambda(\mathbf{k})$ exhibits a complicated \mathbf{k} -dependence at intermediate values of Λ . Hence a factorization of exponentials which works for an intact momentum dependence of $J_\Lambda(\mathbf{k})$ does not occur, so that one cannot decompose $\tilde{\Omega}_\Lambda(\mathbf{k})$ into a finite Fourier series. As a consequence one can calculate the momentum and cutoff dependence of $\tilde{\Omega}_\Lambda(\mathbf{k})$ only numerically. An alternative would be to consider $\tilde{\Pi}(\mathbf{k}, i\omega)$ at the final scale, where $J_\Lambda(\mathbf{k}) = J(\mathbf{k})$. However, this artificial procedure is inconsistent with the initial condition $\tilde{\Pi}_{\Lambda_0}(\mathbf{k}, i\omega) = 0$. Note, that in general one cannot write the quantum diagrams in terms of an energy integration, involving the density of states, due to both the momentum dependence of $\tilde{\Pi}_\Lambda(\mathbf{k}, i\omega)$ and the finite momentum transfer for antiferromagnets. Only in the case of a nearest-neighbor coupling on a bipartite lattice, it is possible to write the high-temperature approximation for $\tilde{\Pi}_\Lambda(\mathbf{k}, i\omega)$ and $J(\mathbf{k} + \mathbf{Q})$ in terms of $J(\mathbf{k})$.

Numerical results for $G^{-1}(\mathbf{Q})$ as a function of T/T_c^{MF} for nearest-neighbor Heisenberg models on a simple cubic lattice with $S = 1/2$, 1 and different signs of the exchange interaction are shown in Fig. 4.5. As anticipated the degeneracy of the curves for opposing

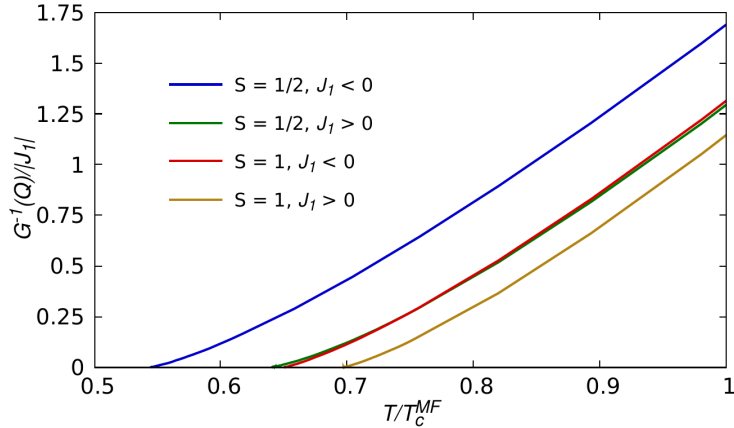


Figure 4.5: T -dependence of the inverse order parameter susceptibility $G^{-1}(\mathbf{Q})$ including dynamic spin fluctuations from the numerical solution of (4.57) using the interaction-switch deformation scheme (4.4) for quantum Heisenberg Models with nearest neighbor interaction J_1 and $S = 1/2, 1$.

signs of J_1 is lifted by the presence of finite-frequency diagrams, with different momentum transfers $\mathbf{k} = \mathbf{Q}$. For the ferromagnet ($J_1 < 0$) with $\mathbf{Q} = \mathbf{0}$ quantum fluctuations enhance the static self-energy and therefore T_c is decreased, compared to the purely static approximation. The opposite effect occurs for the antiferromagnet, $J_1 > 0$, with $\mathbf{Q} = \mathbf{Q}_N$, where the spin self energy is reduced by these terms, leading in turn to an increase of T_c relative to the classical truncation. Note that this effect is primarily driven by the diagram in the flow of Σ_Λ (4.57a), containing the square of the mixed three-point vertex $\tilde{\Gamma}_\Lambda^{(3)}(\nu, -\nu, 0)$, whose sign can already be read off from its high temperature limit. The frequency sums in the flow equation of U_Λ (4.57b) have, compared to that, only a minor impact on Σ_Λ .

Results for the transition temperatures in the J_1 - J_3 model are given in Table 4.3. The agreement with the benchmark values is quite satisfactory as our results deviate by five percent at most. Our accuracy is thus similar or even better than in typical truncations of the pseudofermion FRG (PF-FRG), where usually the deviation from benchmark values lies above that threshold [181, 184, 185, 186, 188, 190]. Furthermore our approximation has the advantage of being numerically much less expensive, requiring only the solution of two differential equations, opposed to computing complicated functions of one momentum and three frequency variables [68, 181]. Residual differences may be traced back to neglecting the momentum dependence of the self-energy and four-point vertex, together with dropping higher order diagrams. Results for the critical temperatures of magnets on other cubic lattices, are given in appendix C.4.

Note that in the first implementations of the PF-FRG by Reuther *et al.*, which extracted the T -dependence directly from the dependence on an ultraviolet frequency cutoff in a flow at zero temperature [181], the four-spin interaction, an eight-point pseudofermion vertex in their formalism, was not generated. The Katanin substitution [75], which is a relatively successful weak coupling approximation for fermionic systems applied by them to the flow of the four-fermion vertex, accounted only for corrections generated by three-spin correlations. These corrections were found to be crucial in order to obtain disorder at $T = 0$ though [68]. Hence a (non-Gaussian) critical fixed point was, technically speaking, inaccessible in their approximation. Note that this PF-FRG truncation reduces in the classical

S	J_1	J_3/J_1	T_c/T_c^{MF}		rel. error / %
			switch	benchmark	switch
1/2	< 0	0	0.545	0.559	2.5
1/2	> 0	0	0.640	0.629	1.7
1	< 0	0	0.651	0.650	0.2
1	> 0	0	0.697	0.684	1.9
3/2	< 0	0	0.688	0.685	0.4
3/2	> 0	0	0.715	0.702	1.9
1/2	> 0	0.2	0.752	0.722	4.2
1/2	> 0	0.4	0.799	0.768	4.0
1/2	> 0	0.6	0.823	0.794	3.7
1/2	> 0	0.8	0.834	0.808	3.2

Table 4.3: Same as Tables 4.1 and 4.2, but now including the feedback of quantum dynamics onto static properties via a high-temperature ansatz (2.123) for $\tilde{\Pi}_\Lambda(\mathbf{k}, i\omega)$, i.e. the solution of (4.57). Note that the limit $S \rightarrow \infty$ is not shown here, because the corresponding flow reduces to the static Level-2 truncation. Furthermore we only used the interaction-switch cutoff (4.4) as discussed in the main text.

limit $S \rightarrow \infty$ [187] to the tree approximation for the static spin susceptibility (4.3), which is clearly inferior to our Level-2 truncation, which is relatively insensitive to the value of S . Indeed, the different Hilbert space sizes, determined by S , are fully accounted for via our initial condition, whereas the PF-FRG requires a less trivial construction to deal with this [187]. Furthermore, the Mermin-Wagner theorem is violated in low dimensions within these PF-FRG truncations [68, 184], again in contrast to our, admittedly coincidental, fulfillment. Additional loop corrections then only alleviate the issue by lowering the breakdown scales but do not eliminate it entirely [184]. In a more recent FRG formalism, based on a Majorana fermion representation of $S = 1/2$ operators, one was able to account for the four-point vertex, by making use of exact operator identities. One therefore obtained a real, non-Gaussian, fixed point with the correct critical exponents in $d = 3$ [188, 189, 190]. Note also that this new implementation does not, in contrast to the initial pseudofermion method, introduce non-physical states and is therefore more suitable for calculations at finite temperature. However, it trades this deficiency for a redundancy which is of high relevance for low temperatures. As a consequence typical truncations of the Majorana fermion flow cannot reach down all the way to $T = 0$ [188, 189, 190].

Chapter 5

Conclusion

5.1 Summary

In this thesis we have investigated the thermodynamic properties and the spin dynamics of quantum Heisenberg paramagnets in a vanishing magnetic field by means of a new iteration of the non-perturbative SFRG. In contrast to the first formulations of the SFRG as laid out in Ref. [1], we managed to treat dynamic and static degrees of freedom, using the same framework without resorting to perturbative expansions in some small parameter. The major results will be recapitulated in the following paragraphs.

The original version of the SFRG, a pure one-particle irreducible approach, suffered from a major flaw, which prevented its application to quantum systems. We presented and discussed the pure 'VLP'-FRG, which was developed by Krieg and Kopietz to eliminate that issue and relied on an amputation of correlation functions with respect to the flowing coupling \mathbf{J}_Λ [1, 2]. Here we explained, based on previous observations, why working with the corresponding irreducible vertices $\Phi_\Lambda^{(n)}$ is not recommended for calculations, which are non-perturbative with respect to loop integrations or J/T . Hence we introduced in Chapter 2 a hybrid 1-PI / amputated formalism, where static ($\omega = 0$) and dynamic ($\omega \neq 0$) fluctuations are treated differently, which is the only natural division in the symmetric phase. A first naive formulation, using \mathbf{J}_Λ for the amputation at $\omega \neq 0$, was shown to be inconvenient for implementing crucial properties of the solution, in particular concerning the dynamic susceptibility $G(\mathbf{k}, i\omega \neq 0)$. Some of these properties are

- continuity at vanishing frequency $G(\mathbf{k}, i\omega \rightarrow 0) = G(\mathbf{k})$, often connected to assuming ergodicity [28, 72],
- a sensible high-temperature limit of $G(\mathbf{k}, i\omega)$ for arbitrary ω , e.g. that it is
 - symmetric under $J \rightarrow -J$,
 - and $\propto 1/T$ for $T \gg |J|$,
- and the positivity of denominators in the dynamic two-point function $F(K)$ in order to avoid non-physical singularities in the flow.

From this we inferred that a reasonable modification is given by replacing $J_\Lambda(\mathbf{k}) \rightarrow G_\Lambda^{-1}(\mathbf{k})$ in the amputation on the dynamic sector [10]. The Legendre-transform of the new hybrid functional $\tilde{\Gamma}_\Lambda[\mathbf{m}^c, \boldsymbol{\eta}^q]$ was shown to satisfy a modified Wetterich equation (2.88).

Subsequently, in Chapter 3, we truncated the infinite hierarchy of flow equations for the 1-line irreducible vertex functions to obtain several closed flow equations, given in Eq. (3.15) and Eq. (3.22), as well as an integral equation (3.44) for the dynamic two-point vertex $\tilde{\Pi}_\Lambda(\mathbf{k}, i\omega)$. All these equations were local-in- ω , thus also allowing for a direct solution in the real frequency-domain. Properly chosen higher order vertex corrections ensured that these approximations are compatible with the properties listed above, as well as additional ones like total spin conservation, see Eq. (2.71). For convenience we introduced in Eq. (3.47) the so-called dissipation energy $\Delta(\mathbf{k}, i\omega)$, which was shown to fulfill the same role as the memory kernel in mode-coupling theory, a non-perturbative method for calculating spin dynamics [33, 74]. In the following we focused on the integral equation (3.44) and solved it in different regimes, under basic assumptions for static quantities, namely the static susceptibility $G(\mathbf{k})$.

We began with the high-temperature limit $T \gg |J|$ where we obtained

- spin diffusion in $d > 2$, i.e. $\Delta(\mathbf{k}, 0) \sim k^2$ for $ka \ll 1$, implying a finite diffusion coefficient $\mathcal{D} \propto |J| \sqrt{b_0}$,
- non-analytic corrections to spin diffusion, which can be only dropped in specific scaling limits and otherwise alter the asymptotic long-time dynamics,
- anomalous diffusion in $d \leq 2$, so that $\mathcal{D} = \mathcal{D}(\omega)$ either diverges or goes to zero for $\omega \rightarrow 0$, depending on the version of our integral equation.

Most of these features were also found in one form or the other in previous theoretical calculations [74, 80, 85, 95, 109], with diffusion being argued for on the grounds of a hydrodynamic picture [35, 41, 77]. The order of magnitude of our estimates for quantities like D also agreed with the literature and experiments [74, 95, 123]. Some deviations still occurred, like non-analytic terms for small but finite ω which were insufficiently screened for $\mathbf{k} \neq 0$. These downsides were attributed to the simple shape of our approximate self-consistency equation (3.44).

Afterwards we proceeded to the critical region of ferro- and antiferromagnets. Here we obtained in all physical dimensions results that are consistent with the dynamic scaling hypothesis, especially above $d = 2$ [54, 58]. These include

- scaling forms for $\Delta(\mathbf{k}, i\omega)$ and thus the dynamic structure factor $S(\mathbf{k}, \omega)$ at small k and ω ,
- with the same predicted dynamic index z , connected to the scaling of a critical characteristic frequency $\omega_k \sim k^z$ and a diverging hydrodynamic relaxation time $\tau \sim \xi^z$,
- and anomalous temperature-dependences of decay rates near T_c , implied by z deviating from the predictions of van Hove theory [32], for instance $\mathcal{D} \sim \xi^{-1/2}$ in the 3D ferromagnet.

The actual line-shapes for $S(\mathbf{k}, \omega)$, which we have computed for ferromagnets, showed in $d = 3$ at $T = T_c$ good agreement with neutron scattering experiments [144, 145] and other theoretical calculations for $\omega \gtrsim \omega_k$ [127, 134]. In the opposite low-frequency limit, we obtained a suppression of spectral weight, such that $S(\mathbf{k}, 0) = 0$, which is not exhibited by other theoretical predictions. A comparison with experimental data [144] suggested that this is likely an artifact of our approximation, which probably shares its origin with the deviations found for $T = \infty$. An analysis for the antiferromagnet, where high-precision spin

dynamics simulations are available [155], corroborated such a conclusion. In reduced dimensions, where $T_c = 0$, our results fulfilled, like in the modified spin-wave theory developed by Takahashi [166], dynamic scaling relations. The low-frequency behavior of $S(\mathbf{k}, \omega)$ still differed, although for $d \leq 2$ there is no consensus on the actual low-temperature results in the hydrodynamic regime. A more conspicuous deviation was the absence of sharp excitation peaks in the $T = 0$ -limit of $S(\mathbf{k}, \omega)$, similar to the solution of the standard mode-coupling equations [167].

All in all our approach produced results for the spin dynamics, especially in $d = 3$, which included many salient aspects, that were predicted by a plethora of other methods and were also found in experiments. Note that the pseudofermion method, which is the other recent FRG approach to quantum spin systems, did not attempt an explicit calculation of spin dynamics in thermodynamic systems and up to this point limited itself to static quantities [68, 181, 188].

Finally, in Chapter 4 we took a look at thermodynamic properties, using the same hybrid formalism. We calculated the static susceptibility $G(\mathbf{k})$ for non-frustrated Heisenberg models, by means of several non-perturbative truncations of the flow equations. Running along similar lines to the work by Krieg and Kopietz [1] we first considered a purely static 1-PI approach, which is formally exact in the limit $S \rightarrow \infty$. We then employed two truncations of the classical flow equations:

- A level-one truncation, where only the static self-energy $\Sigma_\Lambda(\mathbf{k}) \approx \Sigma_\Lambda$ is renormalized,
- and a level-two truncation, where the flow of the static 4-vertex $\Gamma_\Lambda^{(4)}(\mathbf{k}_1, \mathbf{k}_2, \mathbf{k}_3, \mathbf{k}_4) \approx \Gamma_\Lambda^{(4)}(\mathbf{0}, \mathbf{0}, \mathbf{0}, \mathbf{0}) = U_\Lambda$ is also taken into account.

The first approximation did not produce a phase transition in $d \leq 4$, but we were still able to obtain estimates for critical temperatures by determining the location of kinks in the T -dependence of $G^{-1}(\mathbf{Q})$. The accuracy of our estimates was found to be quite good, in particular for sufficiently large S and for a bandwidth-cutoff for the deformed coupling (4.9). A true critical point, characterized by $G^{-1}(\mathbf{Q}) = 0$ at $T = T_c$, emerged in the next-level approximation for $d > 2$. In this context a ΛJ -cutoff for integrating the flow equations produced T_c , that were closest to established benchmark values [179, 182]. However, these classical truncations neglected any quantum effects like different T_c for ferro- and antiferromagnets. Thus we took the spin dynamics via the leading high-temperature and frequency approximation for $\tilde{\Pi}_\Lambda(\mathbf{k}, i\omega)$ into account, see Eq. (2.123). The effect of the quantum diagrams in the flow equations of $\Sigma_\Lambda(\mathbf{Q})$ and U_Λ turned out to be as expected. Our results for T_c showed a similar, or even superior accuracy compared to the auxiliary fermion FRG, with the latter method having significantly higher numerical costs [181, 190].

Altogether we have demonstrated in this work that our new SFRG approach is capable of yielding meaningful results for the static and dynamic properties of quantum spin systems in the absence of symmetry breaking. Hence we gained confidence in extending our method to more complicated models, beyond the thoroughly studied cases discussed in this thesis.

5.2 Outlook on applying our approach to frustrated systems

For more complex systems, i.e. those featuring frustrating interactions, the employed approximations in Chapter 3 and Chapter 4, both for the static and dynamic sector, are probably insufficient to give sensible results. As already mentioned, results from a second

order Green's function theory [66] and our own investigation, with a similar approximation based on Eq. (4.44) and (4.54) both suggest that a $1/\omega^2$ -ansatz may overestimate the effect of finite frequency terms, leading to a much larger disordered phase in the phase space of couplings J_i . One can probably trace back these failures to the emerging low frequency sector $2\pi nT \ll |J|$ on the Matsubara axis. It is unclear whether generic approximations like an extrapolated high-frequency series are able to accurately represent the effect of quantum fluctuations on the phase diagram. Moreover it is quite doubtful that they produce satisfying results for the dynamic structure factor $S(\mathbf{k}, \omega)$ at low temperatures. As an example, even for a non-frustrated square-lattice antiferromagnet, the system is believed to host high-frequency continua above sharp single magnon peaks in its scattering spectrum [191, 192]. Such structures can not be generated by the more sophisticated three-pole ansatz (3.90), which interpolates between a purely relaxational, diffusive regime, as found in paramagnets at high temperatures and weakly interacting quasiparticles at low temperatures [99, 98]. Note that the self-consistency equation (3.44) derived by us for $\tilde{\Pi}_\Lambda(\mathbf{k}, i\omega)$, and solved with known thermodynamics, is, besides overestimating the damping in ordered, low-dimensional systems [117, 167, 170], inconsistent with a non-singular $G(\mathbf{k})$ for $T \rightarrow 0$ due to the absence of frequency sums. This is also an issue within the usual mode-coupling equations that make use of the classical fluctuation-dissipation theorem (3.150) [128]. In our framework this amounts to neglecting dynamic contributions in the relation between the Matsubara function $G(\mathbf{q}, i\nu)$ and the static structure factor $\langle S(\mathbf{q})S(-\mathbf{q}) \rangle$ in Eq. (4.55).

For the static quantities, i.e. the spin self-energy $\Sigma_\Lambda(\mathbf{k})$ and the effective interaction $\tilde{\Gamma}_\Lambda^{(4)}$, the neglect of a momentum dependence is certainly a rough approximation, that is hard to justify in the presence of a strong competition between different near-degenerate ordering instabilities $\mathbf{Q}_1, \mathbf{Q}_2, \dots$ in the Brillouin zone. Thus one should take at least the momentum dependence of the frequency sums in the flow equation (2.111) of $\Sigma_\Lambda(\mathbf{k})$ into account. Note that the diagram $\sim (\tilde{\Gamma}_\Lambda^{(3)})^2$ in (2.111) has to change its sign at low temperatures, if one assumes it to be responsible for the destruction of magnetic order via a finite gap $\sim \mathcal{O}(|J|)$. As observed in Sec. 4.2 for sufficiently high temperatures this diagram generates a negative contribution to the flow of $\Sigma_\Lambda(\mathbf{Q})$, i.e. at typical antiferromagnetic ordering vectors.

Turning to the four-spin vertex, a dependence on momentum may already be necessary on the classical level, albeit it should not contain more than one independent momentum, as otherwise computational costs increase rapidly. That may be achieved by neglecting the mixing of three different channels, i.e. the dependence of the quadratic diagrams $\sim (\Gamma_\Lambda^{(4)})^2$ on the transfer momenta $\mathbf{q}_i + \mathbf{q}_j$. However it is difficult to assess the reliability of such an approximation. Note that the total neglect of any but one channel, in contrast to the symmetry-broken phase [8], cannot be justified, i.e. all these contributions have to be treated on an equal footing. Furthermore, some properties in the classical limit $S \rightarrow \infty$ may be harder to conserve with an explicit \mathbf{k} -dependence. These are for instance equal thermodynamics on bipartite lattices for different signs of J and the topology of the phase diagram for frustrated systems, which may be altered, and thus contradict the result of minimizing the total energy. The fulfillment of sum rules, like in Eq. (4.44), is also highly relevant for systems which do not order at finite temperature. This was already discussed in the purely classical case, and may probably help in preserving some of the known features in the $S \rightarrow \infty$ -limit. The presence of quantum diagrams in the flow of $\tilde{\Gamma}_\Lambda^{(4)}$ is an additional complication, since the loop integrations acquire themselves more intricate dependences on transfer momentum. One example is the diagram with four powers of the effective interaction F_Λ , which is a function of two single and one combined momentum. In

such a situation it may be prudent to ignore these terms even for finite S .

Note that studying the four-point vertex and thus the corresponding four-spin correlation functions would be helpful in identifying weak order, that is for instance induced by a pattern of dimerized spins, which is encoded in an enhanced response function of the respective, composite operators [68]. Otherwise one can only extract information about the two-spin correlation function, because the four-point vertex will not have a meaningful limit for $T \rightarrow 0$. This also includes (partially) dynamic three and four-point vertices, which were left at their initial values in Chapter 4 and are all required for computation of four-point correlation functions. In this context one should also note that one cannot conclusively determine, even in the case of a singular order parameter susceptibility $G(\mathbf{Q})$, whether the system exhibits true long range order at $T = 0$. In fact a spin liquid state can still be gapless [193, 194, 195], implying an infinite correlation length $\xi = \infty$. As a consequence spatial spin-spin correlations $\langle S_r S_0 \rangle$ decay as a power-law and one expects that $G(\mathbf{k})$ diverges somewhere in the Brillouin zone, i.e. at one or several of the ordering vectors \mathbf{Q}_i [194, 195]. A more thoroughly studied example of such systems are half-integer antiferromagnetic chains, which are also gapless, but do not exhibit true long-range order, leading to the same behavior of $G(\mathbf{k})$ and $\langle S_r S_0 \rangle$ [164, 196, 197]. A method relying solely on the behavior of the susceptibility in the paramagnetic phase is thus insufficient. At that level one can only make definite statements about the absence of order for a truly gapped system with a finite zero-temperature correlation range and static susceptibility $G(\mathbf{k})$, as is the case for the aforementioned dimerized order [193, 194, 195].

All in all, it would certainly be a great accomplishment if one were able to predict the ground states of frustrated spin models with relatively modest computational efforts, compared to e.g. the PF-FRG method [68] or its more recent Majorana implementation [190]. In general our SFRG approach seems to be physically more transparent, since it works directly with the physical spin operators. It therefore avoids unphysical, i.e. spinless (pseudofermion), or redundant (Majorana) sectors in the Hilbert space. The latter redundancy was for instance shown to lead to complications in flows at too low temperatures [188, 189], complementary to the thermal problems in the original PF-FRG [69]. Higher order vertices and the corresponding correlations, necessary for identifying different disordered ground states, are also more accessible in our approach. Furthermore different S are easily incorporated via the initial values for the vertices, whereas methods working with auxiliary operators require more effort for implementing $S > 1/2$. However, our initial condition is also more complex than for these methods, because the hybrid functional for an isolated spin $\tilde{\Gamma}_{\Lambda_0}[\mathbf{m}^c, \boldsymbol{\eta}^q]$ contains infinitely many terms in its series expansion. One can contrast this with the bare auxiliary fermion actions, which do not go beyond fourth order in the fermion field [68, 189]. Furthermore, we employ an interaction cutoff, where in particular the ΛJ -scheme does not have an interpretation as an UV cutoff for coarse-grained degrees of freedom in the RG sense. On the other hand, the auxiliary fermion methods work with a frequency cutoff in the Gaussian propagator of the fermion field [68, 189]. Finding a suitable approximation for lower temperatures and/or frustrated systems may thus prove to be more challenging in our context. In the pseudofermion or Majorana framework one applies for instance fairly generic truncation schemes for fermionic systems with a two-body interaction, regardless of the actual configuration of exchange interactions [68, 75, 76].

Note that there is conflicting evidence on the question, whether the results from PF-FRG for thermodynamics, obtained within a Katanin truncation, are always converged. For the $J_1 - J_2$ model on a square lattice this seems to be the case [68, 184], in agreement with other methods [193, 194]. On the other hand, for the $J_1 - J_2 - J_3$ model in $d = 3$

multi-loop corrections reduce significantly the extent of an intermediate paramagnetic phase in parameter space [185, 188] predicted within the standard truncation in Ref. [181]. The multi-loop result shows then better agreement with an independent high temperature series analysis [198]. It remains to be seen, whether our method leads to outcomes that are sufficiently robust with respect to higher order corrections, whatever the latter may entail.

Appendix A

Derivation of initial conditions and relations between vertices

The following appendix is mostly concerned with the formally exact hierarchy of equations of motion for correlation functions and vertices, that is employed for various purposes in this thesis. For instance we can use it to determine the initial condition of the correlation functions $G^{(n)}$ and corresponding irreducible vertices $\tilde{\Gamma}^{(n)}$, which is needed before solving explicitly the flow equations. As already stated, at the beginning of our flow, the model is given by a set of N decoupled, localized spins, with an optional external field, coupling to them via a Zeeman term (1.14). Given that our investigations are primarily concerned with paramagnets we will focus on the zero-field limit $H = 0$, in order to exclude any explicit symmetry breaking in advance. For the case of $H \neq 0$ we have already calculated the non-interacting correlation functions $G_{\Lambda_0}^{(n)}$ [7], also known as *generalized blocks* [2, 5]. The quantities for $H = 0$ may thus be obtained by taking the appropriate zero-field limits. While this is a legitimate procedure, we will not take this path. Firstly, the finite field correlations, are most conveniently formulated in the spherical basis, which in the zero-field limit introduces somewhat artificial separations between degrees of freedom, compared to the Cartesian basis where all three directions are equivalent. One example is the four-point vertex, which in the Cartesian basis has a mixed and purely longitudinal component, while in the spherical basis, one seemingly has to deal with three different vertices $\tilde{\Gamma}_{\Lambda}^{++++}$, $\tilde{\Gamma}_{\Lambda}^{+-zz}$, $\tilde{\Gamma}_{\Lambda}^{zzzz}$. Secondly, by taking the $H \rightarrow 0$ limit, one has to account for a plethora of frequency combinations, that lead to different outcomes via $\delta_{\omega_i, \dots}$, compared to continuous expressions, induced by a finite H . Instead, we will, as hinted, solve the equations of motion for the n -point correlation functions in the free limit of an isolated spin without external field, i.e. $\mathcal{H} = 0$, using static spin correlations as a boundary condition.

A.1 Equations of Motion

Equations of motions for connected correlation functions, as outlined in [7], can be derived with the help of generating equations. One starts with the imaginary time-evolution of a spin operator in the Heisenberg picture which is given by

$$\partial_{\tau} \mathcal{S}^{\alpha}(\tau) = [\mathcal{H}(h; \tau), \mathcal{S}^{\alpha}](\tau). \quad (\text{A.1})$$

Here $\mathcal{H} = \mathcal{H}_{\text{Heisenberg}} - (h, S)$ is the isotropic Heisenberg Hamiltonian in presence of finite space-time dependent source fields h . The commutator with the source-term (h, S) , defined

in Eq. (2.10), yields a coupling to fields and operators perpendicular to the α -direction,

$$[(h, S), S_i^\alpha(\tau)] = -i\epsilon_{\alpha\beta\gamma} h_i^\beta(\tau) S_i^\gamma(\tau), \quad (\text{A.2})$$

and the coupling to the isotropic Heisenberg Hamiltonian generates a quadratic, non-local term

$$[\mathcal{H}_{\text{Heisenberg}}, S_i^\alpha(\tau)] = i \sum_j J_{ij} \epsilon_{\alpha\beta\gamma} S_i^\beta(\tau) S_j^\gamma(\tau). \quad (\text{A.3})$$

Taking the time-ordered expectation value on both sides of (A.1), one can express those through functional derivatives of $\mathcal{G}[\mathbf{h}]$ and thus arrives at the following generating equation

$$\partial_\tau \frac{\delta \mathcal{G}}{\delta h_i^\alpha(\tau)} = -i\epsilon_{\alpha\beta\gamma} \frac{\delta \mathcal{G}}{\delta h_i^\beta(\tau)} h_i^\gamma(\tau) + i \sum_j J_{ij} \epsilon_{\alpha\beta\gamma} \left[\frac{\delta \mathcal{G}}{\delta h_i^\beta(\tau)} \frac{\delta \mathcal{G}}{\delta h_j^\gamma(\tau)} + \frac{\delta^2 \mathcal{G}}{\delta h_i^\beta(\tau) \delta h_j^\gamma(\tau)} \right]. \quad (\text{A.4})$$

By functionally differentiating (A.4) with respect to the source fields one can therefore generate first order differential equations for arbitrary connected correlation functions. In K -representation the generating equation (A.4) becomes purely algebraic

$$\begin{aligned} \omega \frac{\delta \mathcal{G}}{\delta h^\alpha(K)} &= -T \int_q \sum_\nu \epsilon_{\alpha\beta\gamma} \frac{\delta \mathcal{G}}{\delta h^\beta(Q)} h^\gamma(Q - K) + \frac{T\epsilon_{\alpha\beta\gamma}}{2} \int_q \sum_\nu [J(\mathbf{q}) - J(\mathbf{q} - \mathbf{k})] \\ &\times \left[\frac{\delta \mathcal{G}}{\delta h^\beta(K - Q)} \frac{\delta \mathcal{G}}{\delta h^\gamma(Q)} + \frac{\delta^2 \mathcal{G}}{\delta h^\beta(K - Q) \delta h^\gamma(Q)} \right]. \end{aligned} \quad (\text{A.5})$$

Note that the interacting terms vanish for $\mathbf{k} \rightarrow 0$, which is a consequence of the total spin being a constant of motion, i.e. $[\mathcal{H}_{\text{Heisenberg}}, S(\mathbf{0})] = 0$. Differentiating (A.5) once and setting $h = 0$ one obtains for instance the equation of motion for the two-point function

$$\omega G(K) = \int_Q [J(\mathbf{q}) - J(\mathbf{q} + \mathbf{k})] G^{xyz}(K, -K - Q, Q), \quad (\text{A.6})$$

which implies its vanishing for $\mathbf{k} = \mathbf{0}$ (2.71). Taking another functional derivative of (A.5) one extracts one of the equations of motion (3.33) for the three-point function G^{xyz} . For correlations between three and more spin operators the terms in the upper line of (A.5), remain finite even for a vanishing h and J , i.e. a completely free model. Their origin lies in the non-trivial time-ordering, which creates different arrangements of non-commuting operators. Only lower order correlations contribute to these terms, allowing thus for a recursive solution of the free problem, once the boundary conditions at vanishing frequencies are fixed. The contribution in (A.5), which is proportional to two powers of the first derivative $\delta_h \mathcal{G}$, generates in the physical limit a purely local term, without frequency and momentum sum, due to conservation of total energy and momentum. It contains then two correlation functions, which have, either less or the same amount of legs as the correlation function on the left-hand side. This implies that solely in its presence the hierarchy of equations of motion is exactly soluble, which is also known as the tree approximation [7]. It is equivalent to the 0th order result by Vaks, Larkin and Pikin in their perturbation theory [5, 6], where one expands interaction-irreducible vertices $\Phi^{(n)}$ in loop integrals. In fact we will

demonstrate that by switching to their parametrization these terms are entirely eliminated in the dynamic equations of the vertices, consistent with the infinite resummation in the tree approximation that is performed by taking the non-interacting VLP-vertices. Accordingly, the term with the second functional derivative in (A.5) is the loop contribution, because it contains an explicit integration and furthermore couples to a higher order-correlation function, thus making the solution of this hierarchy highly non-trivial. Note that a full determination of an n -point function with $n - 1$ independent time arguments requires the same amount of first order equations or more general time derivatives, together with a boundary condition for itself or its partial derivatives on appropriate manifolds at fixed τ_i . The multitude of equations gives rise to consistency conditions, because by virtue of singling out a particular time or frequency τ_i, ω_i , one obtains a right-hand side, which is not symmetric with respect to permutations $K_i \leftrightarrow K_j$. Hence one is obliged to reconcile both right-hand sides after division with ω_i , implying therefore additional constraints concerning the correlations which appear in this equation of motion.

A.2 Initial condition

For a connected correlation function $G^{(m+n+l)} = G^{(m,n,l)}$, containing $m \times S_x, n \times S_y, l \times S_z$, one equation of motion reads at vanishing source field

$$\begin{aligned} \omega_1 G^{x_1 \dots x_m y_1 \dots y_n z_1 \dots z_l}(K_1 \dots K_m; K'_1 \dots K'_n; K''_1 \dots K''_l) &= \sum_{\nu=1}^n G^{(m-1, n-1, l+1)}(K_2 \dots K_m; K'_1 \dots K'_n; \\ &K''_1 \dots K''_l, K_1 + K'_\nu) - \sum_{\nu=1}^l G^{(m-1, n+1, l-1)}(K_2 \dots K_m; K'_1 \dots K'_n, K_1 + K''_\nu; K''_1 \dots K''_l) \\ &+ \mathcal{O}(J). \end{aligned} \tag{A.7}$$

Note that we did not explicitly write out the contribution, containing the exchange coupling, as it is irrelevant for the present purpose of calculating the initial condition. The free equations of motion feature only a frequency dependence and can be solved recursively for all correlation functions, which contain at least two non-vanishing frequencies in its arguments. It resembles a Wick-Theorem, with the major difference, that a single contraction of two operators, producing a commutator, generates again an operator and not a number [5].

The static components have to be obtained by other means. They can be all related to odd derivatives of the spin- S Brillouin function $b(\beta H)$ at vanishing external field H . For the purely longitudinal components $G^{(0,0,2l)} = G^{(0,2l,0)} = G^{(2l,0,0)}$ one simply has, due to the absence of non-commuting operators,

$$G_0^{(0,0,2l)}(\omega_1, \dots, \omega_{2l}) = \beta^{2l-1} \prod_{j=1}^{2l} \delta_{\omega_j, 0} b_0^{(2l-1)}, \tag{A.8}$$

e.g.

$$G_0^{zz}(0, 0) = \beta b'_0 = G_0, \tag{A.9}$$

$$G_0^{zzzz}(0, 0, 0, 0) = \beta^3 b_0''', \tag{A.10}$$

$$G_0^{zzzzzz}(0, 0, 0, 0, 0, 0) = \beta^5 b_0^{(5)}. \tag{A.11}$$

For static correlations, involving different spin operators, for instance G^{xxyy} , one also finds that they are proportional to these derivatives, albeit with prefactors that are smaller than

unity. One way to extract these prefactors, is given by taking a magnetic field in an arbitrary direction, thus replacing $H \rightarrow |H| = \sqrt{H_x^2 + H_y^2 + H_z^2}$ in the Brillouin function. One can then generate mixed connected correlations by differentiating with respect to different components of \mathbf{H} , since one can interpret the Zeeman-term as a coupling to static source fields. One obtains

$$G_0^{xxyy}(0,0,0,0) = \frac{\beta^3 b_0'''}{3}, \quad (\text{A.12})$$

$$G_0^{xxyyzz}(0,0,0,0) = \frac{\beta^5 b_0^{(5)}}{15}, \quad G_0^{xxxxyy}(0,0,0,0) = \frac{\beta^5 b_0^{(5)}}{5}, \quad (\text{A.13})$$

while static correlations with an odd number of legs are zero, as expected with an intact symmetry. The corresponding static vertices are therefore given by

$$\Sigma_0 = G_0^{-1} = (\beta b_0')^{-1}, \quad (\text{A.14})$$

$$\tilde{\Gamma}_{\Lambda_0}^{\alpha\alpha\gamma\gamma}(0,0,0,0) = -[A_0^{(2)}(0)]^{-4} A_0^{\alpha\alpha\gamma\gamma}(0,0,0,0) = \frac{|b_0'''}{3\beta(b_0')^4}, \quad (\text{A.15})$$

$$\tilde{\Gamma}_{\Lambda_0}^{\alpha\alpha\alpha\alpha}(0,0,0,0) = -[A_0^{(2)}(0)]^{-4} A_0^{\alpha\alpha\alpha\alpha}(0,0,0,0) = \frac{|b_0'''}{\beta(b_0')^4}, \quad (\text{A.16})$$

$$\tilde{\Gamma}_{\Lambda_0}^{\alpha\alpha\gamma\gamma\sigma\sigma}(0,0,0,0,0,0) = -\frac{\beta}{15(b_0')^6} \left(b^{(5)} - 10 \frac{(b_0''')^2}{b_0'} \right) = \frac{\tilde{\Gamma}_{\Lambda_0}^{\alpha\alpha\alpha\alpha\gamma\gamma}(0,0,0,0,0,0)}{3}. \quad (\text{A.17})$$

The equations for the three-point functions are

$$\omega G_0^{xyz}(\omega, -\omega - \nu, \nu) = G_0^{zz}(\nu) - G_0^{yy}(\omega + \nu), \quad (\text{A.18})$$

$$\nu G_0^{xyz}(\omega, -\omega - \nu, \nu) = G_0^{yy}(\omega + \nu) - G_0^{xx}(\nu), \quad (\text{A.19})$$

from which we read off

$$G_0^{xyz}(\omega, -\omega - \nu, \nu) = \frac{\beta b_0'}{\omega} (\delta_{\nu,0} - \delta_{\nu,-\omega}) - \frac{\beta b_0'}{\nu} \delta_{\omega,0}, \quad (\text{A.20})$$

i.e. a totally antisymmetric form $G_0^{\alpha\beta\gamma}(\omega, -\omega - \nu, \nu) = \epsilon_{\alpha\beta\gamma} G_0^{xyz}(\omega, -\omega - \nu, \nu)$. Note that there are no free and non-zero correlation functions without any constraints regarding the combinations of frequencies, which is a consequence of the absent time-evolution. The initial 3-point vertex in our hybrid formalism is thus

$$\begin{aligned} \tilde{\Gamma}_{\Lambda_0}^{\alpha\beta\gamma}(\omega, -\omega, 0) &= -[\tilde{A}_0^{(2)}(i\omega)]^{-2} [\tilde{A}_0^{(2)}(0)]^{-1} \tilde{A}_0^{xyz}(\omega, -\omega, 0) = -G_0^{-1}(0) G_0^{xyz}(\omega, -\omega, 0) \\ &= -\frac{\epsilon_{\alpha\beta\gamma}}{\omega}, \end{aligned} \quad (\text{A.21})$$

where we used that

$$\tilde{A}_0^{(2)}(0) = G_0 = -[\tilde{A}_0^{(2)}(i\omega \neq 0)]^{-1}. \quad (\text{A.22})$$

For the four-point correlation functions we first check that

$$\omega_1 G_0^{xxyy}(\omega_1, \omega_2, \omega_3, -\omega_1 - \omega_2 - \omega_3) = G_0^{xyz}(\omega_2, -\omega_1 - \omega_2 - \omega_3, \omega_1 + \omega_3) + G_0^{xyz}(\omega_2, \omega_3, -\omega_2 - \omega_3), \quad (\text{A.23})$$

which can be non-zero, only if one of the frequencies in the three-point correlation functions on the right-hand side is zero. This means that we either have two pairs of frequencies

APPENDIX A. DERIVATION OF INITIAL CONDITIONS AND RELATIONS
BETWEEN VERTICES

$\omega, -\omega$ and $\nu, -\nu$, or that one of the frequencies is zero with arbitrary, energy-conserving combinations for the three remaining ones. The respective configurations are

$$\begin{aligned}\omega G_0^{xxyy}(\omega, -\omega, 0, 0) &= 2G_0^{xyz}(-\omega, 0, \omega) \\ \rightarrow G_0^{xxyy}(\omega, -\omega, 0, 0) &= \frac{2\beta b'_0}{\omega^2},\end{aligned}\tag{A.24}$$

$$\begin{aligned}\omega G_0^{xxyy}(\omega, 0, -\omega, 0) &= G_0^{xyz}(0, -\omega, \omega) + G_0^{xyz}(0, 0, 0) \\ \rightarrow G_0^{xxyy}(\omega, 0, -\omega, 0) &= -\frac{\beta b'_0}{\omega^2},\end{aligned}\tag{A.25}$$

$$\begin{aligned}\omega G_0^{xxyy}(\omega, -\omega, \omega, -\omega) &= G_0^{xyz}(-\omega, -\omega, 2\omega) + G_0^{xyz}(-\omega, \omega, 0) \\ \rightarrow G_0^{xxyy}(\omega, 0, -\omega, 0) &= -\frac{\beta b'_0}{\omega^2},\end{aligned}\tag{A.26}$$

$$\begin{aligned}\omega G_0^{xxyy}(\omega, -\omega, \nu, -\nu) &= G_0^{xyz}(-\omega, \omega + \nu, -\nu) + (\nu \leftrightarrow -\nu), \quad |\nu| \neq |\omega|, \quad 0 \\ \rightarrow G_0^{xxyy}(\omega, -\omega, \nu, -\nu) &= 0,\end{aligned}\tag{A.27}$$

$$\begin{aligned}\omega G_0^{xxyy}(\omega, \nu, -\omega, -\nu) &= G_0^{xyz}(\nu, -\nu, 0) + G_0^{xyz}(\nu, -\omega, \omega - \nu), \quad |\nu| \neq |\omega|, \quad 0 \\ \rightarrow G_0^{xxyy}(\omega, \nu, \omega, -\nu) &= \frac{\beta b'_0}{\nu\omega},\end{aligned}\tag{A.28}$$

$$\begin{aligned}\omega G_0^{xxyy}(\omega, \nu, -\nu - \omega, 0) &= G_0^{xyz}(\nu, -\nu, 0) + G_0^{xyz}(\nu, -\omega - \nu, \omega), \quad \nu \neq 0, \quad -\omega \\ \rightarrow G_0^{xxyy}(\omega, \nu, -\nu - \omega, 0) &= \frac{\beta b'_0}{\omega\nu}.\end{aligned}\tag{A.29}$$

All other 4-point correlation functions are zero. Note also that $G^{\alpha\alpha\gamma\gamma}(\omega_1, \omega_2, \omega_3, \omega_4)$ does not depend on the flavors $\alpha \neq \gamma$, meaning that we have only one mixed 4-vertex. Other 4-vertices, featuring unpaired spin operators, are inconsistent with spin-rotational invariance and thus also zero. The corresponding dynamic 4-point vertices are

$$\begin{aligned}\tilde{\Gamma}_{\Lambda_0}^{\alpha\alpha\gamma\gamma}(\omega, -\omega, 0, 0) &= -[\tilde{A}_{\Lambda_0}^{(2)}(i\omega)]^{-2}[\tilde{A}_{\Lambda_0}^{(2)}(0)]^{-2}\tilde{A}_{\Lambda_0}^{\alpha\alpha\gamma\gamma}(\omega, -\omega, 0, 0) \\ &\quad + 2\Gamma_{\Lambda_0}^{xyz}(\omega, 0, -\omega)\Gamma_{\Lambda_0}^{xyz}(-\omega, 0, \omega)\tilde{A}_{\Lambda_0}^{(2)}(i\omega) = 0 \\ &= \Gamma_{\Lambda_0}^{\alpha\alpha\gamma\gamma}(\omega, 0, -\omega, 0),\end{aligned}\tag{A.30}$$

$$\begin{aligned}\tilde{\Gamma}_{\Lambda_0}^{\alpha\alpha\gamma\gamma}(\omega, 0, -\omega, 0) &= -[\tilde{A}_{\Lambda_0}^{(2)}(i\omega)]^{-2}[\tilde{A}_{\Lambda_0}^{(2)}(0)]^{-2}\tilde{A}_{\Lambda_0}^{\alpha\alpha\gamma\gamma}(\omega, 0, -\omega, 0) + F_{\Lambda_0}^{(2)}(i\omega)[\Gamma_{\Lambda_0}^{xyz}(\omega, -\omega, 0)]^2 \\ &= 0,\end{aligned}\tag{A.31}$$

$$\begin{aligned}\tilde{\Gamma}_{\Lambda_0}^{\alpha\alpha\gamma\gamma}(\omega, -\omega, \omega, -\omega) &= -[\tilde{A}_{\Lambda_0}^{(2)}(i\omega)]^{-2}[\tilde{A}_{\Lambda_0}^{(2)}(0)]^{-2}F_{\Lambda_0}^{xxyy}(\omega, -\omega, -\omega, \omega) \\ &\quad + \Gamma_{\Lambda_0}^{xyz}(\omega, -\omega, 0)\Gamma_{\Lambda_0}^{xyz}(-\omega, \omega, 0)\tilde{A}_{\Lambda_0}^{(2)}(0) = 0 \\ &= \Gamma_{\Lambda_0}^{\alpha\alpha\gamma\gamma}(\omega, \omega, -\omega, -\omega),\end{aligned}\tag{A.32}$$

$$\Gamma_{\Lambda_0}^{\alpha\alpha\gamma\gamma}(\omega, -\omega, \nu, -\nu) = 0, \quad |\nu| \neq |\omega|,\tag{A.33}$$

$$\begin{aligned}\tilde{\Gamma}_{\Lambda_0}^{\alpha\alpha\gamma\gamma}(\omega, \nu, -\omega, -\nu) &= -[A_{\Lambda_0}^{(2)}(i\omega)]^{-2}[A_{\Lambda_0}^{(2)}(i\nu)]^{-2}A_{\Lambda_0}^{\alpha\alpha\gamma\gamma}(\omega, \nu, -\omega, -\nu) \\ &\quad + \Gamma_{\Lambda_0}^{xyz}(\nu, -\nu, 0)\Gamma_{\Lambda_0}^{xyz}(\omega, -\omega, 0)A_{\Lambda_0}^{(2)}(0) = 0,\end{aligned}\quad (\text{A.34})$$

$$\begin{aligned}\tilde{\Gamma}_{\Lambda_0}^{\alpha\alpha\gamma\gamma}(\omega, \nu, -\nu - \omega, 0) &= -[A_{\Lambda_0}^{(2)}(i\omega)A_{\Lambda_0}^{(2)}(i\nu)A_{\Lambda_0}^{(2)}(i\omega + i\nu)A_{\Lambda_0}^{(2)}(0)]^{-1}A_{\Lambda_0}^{\alpha\alpha\gamma\gamma}(\omega, \nu, -\nu - \omega, 0) \\ &= \frac{1}{\nu\omega}, \quad \omega, \nu, \omega + \nu \neq 0.\end{aligned}\quad (\text{A.35})$$

The five-point and six-point correlation functions will be only considered in the purely static configuration or the combination, where two frequencies are finite, since all other do not appear in the flow equations of interest. For the mixed five-point vertex we have

$$\begin{aligned}\omega G_0^{xyzzz}(\omega, -\omega, 0, 0, 0) &= G^{zzzz}(0, 0, 0, 0) - 3G^{yzzz}(\omega, -\omega, 0, 0) \\ \rightarrow G_0^{xyzzz}(\omega, -\omega, 0, 0, 0) &= \frac{b_0'''}{\omega} - \frac{6b_0'}{\omega^3},\end{aligned}\quad (\text{A.36})$$

$$\begin{aligned}\omega G_0^{xyzzz}(\omega, 0, -\omega, 0, 0) &= G^{zzzz}(\omega, -\omega, 0, 0) - 2G^{yzzz}(\omega, 0, -\omega, 0) - G^{yzzz}(0, 0, 0, 0) \\ \rightarrow G_0^{xyzzz}(\omega, 0, -\omega, 0, 0) &= -\frac{b_0'''}{3\omega} - \frac{2b_0'}{\omega^3},\end{aligned}\quad (\text{A.37})$$

where we made use of $G^{\alpha\gamma\sigma\sigma} = \epsilon_{\alpha\gamma\sigma}G^{xyzzz}$, see also the next section. Combinations involving an even number of spin operators of a given component are thus zero. After inverting the tree expansion one obtains for the corresponding vertices

$$\begin{aligned}\Gamma_0^{xyzzz}(\omega, -\omega, 0, 0, 0) &= -G_0^{-3}G_0^{xyzzz}(\omega, -\omega, 0, 0, 0) + \Gamma_0^{zzzz}(0, 0, 0, 0)G_0\Gamma_0^{xyz}(0, -\omega, \omega) \\ &\quad - 6(-G_0)^{-2}[\Gamma_0^{xyz}(\omega, -\omega, 0)]^3 \\ &= 0,\end{aligned}\quad (\text{A.38})$$

$$\begin{aligned}\Gamma_0^{zzzyx}(0, 0, -\omega, 0, \omega) &= -G_0^{-3}G_0^{xyzzz}(\omega, 0, -\omega, 0, 0) + \Gamma_0^{yzzz}(0, 0, 0, 0)G_0\Gamma_0^{xyz}(\omega, 0, -\omega) \\ &\quad - 2(-G_0)^{-2}[\Gamma_0^{xyz}(\omega, -\omega, 0)]^3 \\ &= 0.\end{aligned}\quad (\text{A.39})$$

The six-point functions of relevance are

$$\begin{aligned}\omega G_0^{xxxxzz}(\omega, -\omega, 0, 0, 0, 0) &= -4G_0^{xyzzz}(-\omega, \omega, 0, 0, 0, 0) \\ &= \frac{4b_0'''}{\omega} - \frac{6b_0'}{\omega^3},\end{aligned}\quad (\text{A.40})$$

$$\begin{aligned}\omega G_0^{xxxxzz}(\omega, -\omega, 0, 0, 0, 0) &= -2G_0^{xxyyz}(-\omega, 0, 0, \omega, 0) \\ &= \frac{2b_0'''}{3\omega} - \frac{4b_0'}{\omega^3},\end{aligned}\quad (\text{A.41})$$

$$\begin{aligned}G_0^{xyyyz}(\omega, -\omega, 0, 0, 0, 0) &= 2G_0^{xyzzz}(-\omega, 0, \omega, 0, 0) - 2G_0^{xyyyz}(-\omega, 0, \omega, 0, 0) \\ &= \frac{4b_0'''}{3\omega} - \frac{8b_0'}{\omega^3}.\end{aligned}\quad (\text{A.42})$$

The respective vertices are given by

$$\begin{aligned}
 \tilde{\Gamma}_0^{xxxxzz}(\omega, -\omega, 0, 0, 0, 0) &= -G_0^{-4}G_0^{zzzzxx}(0, 0, 0, 0, \omega, -\omega) \\
 &\quad + 8\Gamma_0^{zzzz}(0, 0, 0, 0)[\Gamma_0^{xyz}(\omega, -\omega, 0)]^2 \\
 &\quad + 24[\Gamma_0^{xyz}(0, -\omega, \omega)]^4(-G_0)^{-3}, \\
 &= -\frac{4|b_0''|}{\beta(b_0')^4\omega^2}, \tag{A.43}
 \end{aligned}$$

$$\begin{aligned}
 \tilde{\Gamma}_0^{xxxxzz}(\omega, -\omega, 0, 0, 0, 0) &= -G_0^{-4}G_0^{xxxxzz}(\omega, -\omega, 0, 0, 0, 0) \\
 &\quad + 4\Gamma_0^{xxxx}(0, 0, 0, 0)[\Gamma_0^{xyz}(\omega, -\omega, 0)]^2 \\
 &\quad + 4(-G_0)^{-3}[\Gamma_0^{xyz}(\omega, -\omega, 0)]^4 \\
 &= -\frac{2|b_0''|}{3\beta(b_0')^4\omega^2}, \tag{A.44}
 \end{aligned}$$

$$\begin{aligned}
 \tilde{\Gamma}_0^{xyyyzz}(\omega, -\omega, 0, 0, 0, 0) &= -G_0^{-4}G_0^{xyyyzz}(\omega, -\omega, 0, 0, 0, 0) \\
 &\quad + 8\Gamma_0^{xyyy}(0, 0, 0, 0)[\Gamma_0^{xyz}(\omega, -\omega, 0)]^2 \\
 &\quad + 8(-G_0)^{-3}[\Gamma_0^{xyz}(\omega, -\omega, 0)]^4 \\
 &= -\frac{4|b_0''|}{3\beta(b_0')^4\omega^2}. \tag{A.45}
 \end{aligned}$$

Note the frequent cancellations of terms after applying the tree expansion, such that most irreducible vertices are zero, in contrast to the corresponding n -point functions. These can be attributed to the fact that a Wick-contraction is equivalent to multiplying a lower order vertex with a non-interacting mixed 3-vertex $\sim \frac{1}{\omega}$. Such terms occur in the tree expansion too and have a sign opposite to the contributions in the free correlation functions, thus often cancelling them, due to the same combinatorics. For the six-point vertices this does not work out entirely, because there are more tree-terms than Wick-contractions, which produce a finite residue. Conversely for some vertices one cannot write down additional trees, due to the absence of a purely quantum three-point vertex, for example the four-point vertex $\tilde{\Gamma}_{\Lambda_0}^{\alpha\alpha\gamma\gamma}(\omega, \nu, -\nu - \omega, 0)$.

Recently Halbinger *et al.* presented a new method for calculating time-ordered correlation functions [199, 200]. It is based on the spectral representation of $G_{\Lambda}^{(n)}$ and was applied to the atomic limit of the Hubbard model and the case of an isolated spin as well. A potential advantage compared to our method is the fact, that it does not rely on a sufficiently simple structure of the equations of motion as made use of in this section but only on knowledge of the eigenspectrum [199, 200].

A.3 Relations arising from symmetries

We can use the equations of motion to read off symmetry relations between the vertex functions, that are a consequence of spin-rotational invariance, some of which were already observed in the initial condition. Quite generally, setting both the momentum and frequency

to zero in the generalized equation of motion (A.5) to zero and taking appropriate functional derivatives one finds

$$\begin{aligned} & \sum_{\nu=1}^n G^{(m-1, n-1, l+1)}(K_2 \dots K_m; K'_1 \dots K'_n; K''_1 \dots K''_l, K'_\nu) \\ = & \sum_{\nu=1}^l G^{(m-1, n+1, l-1)}(K_2 \dots K_m; K'_1 \dots K'_n, K''_\nu; K''_1 \dots K''_l). \end{aligned} \quad (\text{A.46})$$

This is a relation between lower order correlations, that appeared in the equation of a correlation function with one more leg, see Eq. (A.7). Here we also used that the $\mathcal{O}(J)$ -contributions vanish for $k \rightarrow 0$ due to total spin conservation. Using an appropriate initial correlation function, for which the equation of motion is formulated, we can therefore obtain such relations. From the dynamics of the 3-point function G^{xyz} we read off

$$G^{\alpha\alpha}(K) = G^{\gamma\gamma}(K). \quad (\text{A.47})$$

Similarly we obtain from the equation of motion for the mixed 4-point function

$$\omega_4 G^{yyxx}(K_1, K_2, K_3, \omega_4) = G^{yzx}(K_1, K_2 + \omega_4, K_3) + G^{zyx}(K_1 + \omega_4, K_2, K_3), \quad (\text{A.48})$$

i.e.

$$G^{yzx}(K_1, K_2, K_3) = -G^{zyx}(K_1, K_2, K_3). \quad (\text{A.49})$$

From that one can infer, by considering all possible combinations,

$$G^{\alpha\gamma\sigma}(K_1, K_2, K_3) = \epsilon_{\alpha\gamma\sigma} G^{xyz}(K_1, K_2, K_3), \quad (\text{A.50})$$

which leads to the only possible rotationally invariant product of three fields $\sim \mathbf{h}_1 \cdot (\mathbf{h}_2 \times \mathbf{h}_3)$ in the functional series expansion of $\mathcal{G}[\mathbf{h}]$. For the 4-point function one first considers the equation for $\nu G^{xyzzz}(K_1, K_2, \nu, K_3, K_4)$, which implies

$$G^{xyyy}(K_1, K_2, K_3, K_4) = G^{xxzz}(K_1, K_2, K_3, K_4), \quad (\text{A.51})$$

i.e. that $G^{\alpha\alpha\gamma\gamma}(K_1, K_2, K_3, K_4)$ does not depend on the explicit values of α, γ , in accordance with isotropy. Furthermore the EoM of $G^{xyzzz}(\nu, K_1, K_2, K_3, K_4)$ with respect to ν , yields the following relation

$$G^{\alpha\alpha\alpha\alpha}(K_1, K_2, K_3, K_4) = \mathcal{S}_{K_2; K_3, K_4} G^{\alpha\alpha\gamma\gamma}(K_1, K_2, K_3, K_4), \quad (\text{A.52})$$

where \mathcal{S} is the symmetrization operator introduced in Eq. (2.105). Thus one only has to deal with one mixed 4-point function. The above relations imply fourth order contributions of the type $(\mathbf{h}_1 \cdot \mathbf{h}_2)(\mathbf{h}_3 \cdot \mathbf{h}_4)$ in the expansion of $\mathcal{G}[\mathbf{h}]$, again fully conforming with spin-rotational invariance. Progressing with the 5-point function, we find, based on equations of the type $\nu G^{xyyzz}(\nu, K_1, K_2, K_3, K_4, K_5) = \dots$, i.e. by placing ν in each spin operator, that

$$G^{\alpha\gamma\sigma\sigma\sigma}(K_1, K_2, K_3, K_4, K_5) = \epsilon_{\alpha\gamma\sigma} G^{xyzzz}(K_1, K_2, K_3, K_4, K_5), \quad (\text{A.53})$$

thus corresponding to rotationally invariant combinations of the form $\mathbf{h}_1 \cdot (\mathbf{h}_2 \times \mathbf{h}_3)(\mathbf{h}_4 \cdot \mathbf{h}_5)$. In complete analogy to the longitudinal 4-point function one obtains for the longitudinal six-point function, by taking a look at the equation for $\nu G^{xyzzzzz}(\nu, K_1, K_2, K_3, K_4, K_5, K_6)$

$$G^{\alpha\alpha\alpha\alpha\alpha\alpha}(K_1, K_2, K_3, K_4, K_5, K_6) = \mathcal{S}_{K_2; K_3, K_4, K_5, K_6} G^{\gamma\gamma\alpha\alpha\alpha\alpha}(K_1, K_2, K_3, K_4, K_5, K_6), \quad (\text{A.54})$$

where we already used that $G^{\gamma\gamma\alpha\alpha\alpha}$ does not depend on the actual values of $\gamma \neq \alpha$. By considering $\nu G^{xxyyzz}(K_1, K_2, K_3, K_4, K_5, K_6, \nu)$ we also find

$$G^{\alpha\alpha\alpha\gamma\gamma}(K_1, K_2, K_3, K_4, K_5, K_6) = \mathcal{S}_{K_2;K_3,K_4} G^{xxyyzz}(K_1, K_2, K_3, K_4, K_5, K_6), \quad (\text{A.55})$$

implying that one only needs G^{xxyyzz} . The purely longitudinal correlation function can then be written as

$$G^{\alpha\alpha\alpha\alpha\alpha}(K_1, K_2, K_3, K_4, K_5, K_6) = \mathcal{S}_{K_2;K_3,K_4,K_5,K_6} \mathcal{S}_{K_4;K_5,K_6} G^{xxyyzz}(K_1, K_2, K_3, K_4, K_5, K_6). \quad (\text{A.56})$$

Note that as relations, which simply arise from spin-rotational invariance, the above equations can be directly transferred to irreducible vertices $\tilde{\Gamma}^{(n)}$. One can check their validity explicitly by inserting the tree expansion of the correlation function on both sides.

A.4 Hierarchy for interaction-irreducible vertices

We want to present an alternative way of writing the hierarchy of dynamic equations, by expressing the connected correlation functions $G_\Lambda^{(n)}$ via the interaction-irreducible vertices $\Phi_\Lambda^{(n)}$, that are generated by the VLP-functional $\Phi_\Lambda[\eta]$. For this purpose, we have to write the expectation values of the spin operators and the magnetic sources in terms of the new degrees of freedom η , i.e.

$$\langle \mathcal{T}(\mathbf{S}) \rangle = -\mathbf{J}_\Lambda^{-1} \boldsymbol{\eta} - \mathbf{s} = -\mathbf{J}_\Lambda^{-1} \boldsymbol{\eta} - \frac{\delta \Phi_\Lambda}{\delta \eta} - \mathbf{R}_\Lambda \boldsymbol{\eta}, \quad (\text{A.57})$$

$$\langle \mathcal{T}(S^\beta S^\gamma) \rangle = [\mathbf{J}_\Lambda^{-1} \mathbf{F}_\Lambda^{(2)} \mathbf{J}_\Lambda^{-1}]_{\beta\gamma} + [\mathbf{J}_\Lambda^{-1}]_{\beta\gamma} + \langle \mathcal{T}(S^\beta) \rangle \langle \mathcal{T}(S^\gamma) \rangle, \quad (\text{A.58})$$

$$\mathbf{h} = -\mathbf{J}_\Lambda \mathbf{s} = -\mathbf{J}_\Lambda \left(\frac{\delta \Phi_\Lambda}{\delta \eta} + \mathbf{R}_\Lambda \boldsymbol{\eta} \right), \quad (\text{A.59})$$

$$\mathbf{F}_\Lambda^{(2)} = [\Phi_\Lambda^{(2)} + \mathbf{R}_\Lambda]^{-1} = \mathbf{R}_\Lambda^{-1} [\mathbf{1} + \Phi_\Lambda^{(2)} \mathbf{R}_\Lambda^{-1}]^{-1}, \quad (\text{A.60})$$

where $\mathbf{R}_\Lambda = -\mathbf{J}_\Lambda^{-1}$. The linear relation between $\langle \mathcal{T}(\mathbf{S}) \rangle$ and $\frac{\delta \Phi_\Lambda}{\delta \eta}$ in Eq. (A.57) allows to use (A.4) directly as a generating equation after plugging in the above expressions. Thus by differentiating both sides with respect to η or applying a vertex expansion with a subsequent comparison of properly symmetrized coefficients, one can obtain equations of motion for all $\Phi_\Lambda^{(n)}$. Explicit insertion yields that some contributions from the magnetic source term compensate the finite interaction tree level part in (A.4), which is consistent with the irreducible nature of the VLP-vertices. One obtains from (A.4) in space-time

$$i\partial_\tau \left(\frac{\delta \Phi_\Lambda}{\delta \eta_i^\alpha(\tau)} \right) = -\epsilon_{\alpha\beta\gamma} \eta_i^\beta(\tau) \frac{\delta \Phi_\Lambda}{\delta \eta_i^\gamma(\tau)} - \epsilon_{\alpha\beta\gamma} [\mathbf{J}_\Lambda^{-1} \mathbf{F}_\Lambda^{(2)}]_{\beta\gamma,ii}(\tau, \tau) \quad (\text{A.61})$$

and thus in K -representation

$$\omega \left(\frac{\delta \Phi_\Lambda}{\delta \phi_K^\alpha} \right) = -\epsilon_{\alpha\beta\gamma} \int_Q \eta_{K-Q}^\beta \frac{\delta \Phi_\Lambda}{\delta \eta_Q^\gamma} + \epsilon_{\alpha\beta\gamma} \int_Q [1 - \Phi_\Lambda^{(2)} \mathbf{J}_\Lambda]_{\beta\gamma}^{-1}(Q, K - Q). \quad (\text{A.62})$$

As already stated we have eliminated the tree-contributions, implied by J , in these new equations of motion, consistent with $\Phi_\Lambda^{(n)}$ being one-interaction line irreducible. This leaves us with the Spin-Wick-theorem contributions, also present in the free case, and terms which contain one explicit loop integration. Setting $J = 0$ one therefore obtains free correlation functions, i.e. generalized blocks, for the $\Phi_\Lambda^{(n)}$. The diagrammatic structure of the one-loop term is somewhat similar to the one in the Wetterich equation, but the diagonal two-point vertex $\partial_\Lambda \mathbf{R}_\Lambda$ is replaced by a chiral three-point vertex, with a marked frequency and momentum, due to the applied derivative. Moreover the functional derivative on the left-hand side implies that one will only encounter vertices with at most one more leg in the loops. Taking another functional derivative we obtain the equation of motion of the dynamic polarization $\Pi_\Lambda(K)$

$$\omega \Pi_\Lambda(K) = \int_Q [J_\Lambda(\mathbf{k} + \mathbf{q}) - J_\Lambda(\mathbf{q})] L_\Lambda(Q) L_\Lambda(K + Q) \Phi_\Lambda^{xyz}(Q, -Q - K, K), \quad (\text{A.63})$$

which vanishes for $\mathbf{k} \rightarrow \mathbf{0}$, as expected from the conservation of the total spin. Here we have introduced

$$L_\Lambda(K) = \frac{1}{1 + \Pi_\Lambda(K) J_\Lambda(\mathbf{k})} = \Pi_\Lambda^{-1}(K) G_\Lambda(K) = -J_\Lambda^{-1}(\mathbf{k}) F_\Lambda(K). \quad (\text{A.64})$$

Note that the subtracted polarization $\tilde{\Pi}_\Lambda(K) = [\Pi_\Lambda^{-1}(K) - \Sigma_\Lambda(\mathbf{k})]^{-1}$, that is generated by the hybrid functional $\tilde{\Gamma}_\Lambda[\mathbf{m}^c, \boldsymbol{\eta}^q]$, satisfies an analogous equation

$$\omega \tilde{\Pi}_\Lambda(K) = \int_Q [J_\Lambda(\mathbf{k} + \mathbf{q}) - J_\Lambda(\mathbf{q})] \tilde{L}_\Lambda(Q) \tilde{L}_\Lambda(K + Q) \tilde{\Gamma}_\Lambda^{xyz}(Q, -Q - K, K), \quad (\text{A.65})$$

where

$$\tilde{L}_\Lambda(\mathbf{k}, i\omega) = \delta_{\omega,0} G_\Lambda(\mathbf{k}) + \frac{1 - \delta_{\omega,0}}{1 + \tilde{\Pi}_\Lambda(K) G_\Lambda^{-1}(\mathbf{k})} = \delta_{\omega,0} \Sigma_\Lambda^{-1}(\mathbf{k}) L_\Lambda(\mathbf{k}) + \frac{(1 - \delta_{\omega,0}) L_\Lambda(K)}{1 + \tilde{\Pi}_\Lambda(K) \Sigma_\Lambda(\mathbf{k})}. \quad (\text{A.66})$$

Furthermore we used for the hybrid three-point vertex

$$\tilde{\Gamma}_\Lambda^{xyz}(Q, -Q - K, K) = X_\Lambda(Q) X_\Lambda(K) X_\Lambda(Q + K) \Phi_\Lambda^{xyz}(Q, -Q - K, K), \quad (\text{A.67})$$

where we defined $X_\Lambda(K) = \delta_{\omega,0} \Sigma_\Lambda(\mathbf{k}) + (1 - \delta_{\omega,0}) [1 + \tilde{\Pi}_\Lambda(K) \Sigma_\Lambda(\mathbf{k})]$. However, the structural similarity observed here is a coincidence. For vertices with more than two legs, additional factors $\propto [1 + \Sigma_\Lambda(\mathbf{k}) \tilde{\Pi}_\Lambda(K)]$, $\Sigma_\Lambda(\mathbf{k})$ are generated in their equations of motion, compared to the pure interaction-irreducible parametrization. The one- J -irreducible three-vertex satisfies for instance

$$\begin{aligned} \omega'' \Phi_\Lambda^{xyz}(K'', P, Q) &= \Pi_\Lambda(P) - \Pi_\Lambda(Q) + \int_K [J_\Lambda(\mathbf{k}) - J_\Lambda(\mathbf{k}'' - \mathbf{k})] L_\Lambda(K) L_\Lambda(K'' - K) \\ &\quad \times \Phi_\Lambda^{zyy}(K, Q, K'' - K, P) + \int_K [J_\Lambda(\mathbf{k}) - J_\Lambda(\mathbf{k}'' - \mathbf{k})] L_\Lambda(K) \\ &\quad \times L_\Lambda(K'' - K) L_\Lambda(P + K) J_\Lambda(\mathbf{p} + \mathbf{k}) \Phi_\Lambda^{xyz}(P + K, K'' - K, Q) \\ &\quad \times \Phi_\Lambda^{xyz}(-P - K, P, K). \end{aligned} \quad (\text{A.68})$$

In contrast to $\tilde{\Pi}_\Lambda$ the equations for $\tilde{\Gamma}_\Lambda^{xyz}$ will contain the aforementioned factors. Nevertheless one can for instance infer that $\tilde{\Gamma}_\Lambda^{xyz}$ at all momenta vanishing is equivalent to

its non-interacting expression. Taking a look at Eq. (A.65) for the subtracted polarization, we obtain from approximating $\tilde{\Gamma}_\Lambda^{xyz}$ by its non-interacting value $\propto \omega^{-1}$ and $\tilde{L}_\Lambda(K) \approx \delta_{\omega,0}G_\Lambda(\mathbf{k}) + (1 - \delta_{\omega,0})$, the following expression

$$\tilde{\Pi}_\Lambda(K) = \frac{2T}{\omega^2} \int_{\mathbf{q}} [J_\Lambda(\mathbf{q} + \mathbf{k}) - J_\Lambda(\mathbf{q})] G_\Lambda(\mathbf{q}), \quad (\text{A.69})$$

which to leading order in J_Λ/T yields the exact result for the second moment given in Eq. (2.123) [31, 100]. At lower temperatures it amounts to neglecting frequency sums, that contribute to the static structure factor $\langle S^z(\mathbf{q})S^z(-\mathbf{q}) \rangle$ contained in the exact expression Eq. (4.54), which is equivalent to using the classical form of the fluctuation-dissipation theorem [98, 136]. As discussed in Sec. 4.2, this approximation only makes sense, as long as the static susceptibility is clearly known to be gapless for sufficiently low temperatures. Note that retaining the self-consistency in $L_\Lambda(\mathbf{q} + \mathbf{k}, i\omega)$ already leads to problems at $T \gg |J_\Lambda|$, since beyond leading order in ω^{-2} it is not clear how to treat the terms arising from $G_\Lambda(\mathbf{q}) \approx b'_0/T$. The proper way to go beyond ω^{-2} would thus require the renormalization of $\tilde{\Gamma}_\Lambda^{(3)}$, including a finite pure quantum 3-vertex.

Returning to the pure VLP three-point vertex and setting $\omega'' = 0$ in its equation of motion (A.68) we obtain the following relation for the polarization

$$\begin{aligned} \Pi_\Lambda(Q + \mathbf{k}'') &= \Pi_\Lambda(Q) + \int_K [J_\Lambda(\mathbf{k}) - J_\Lambda(\mathbf{k}'' - \mathbf{k})] L_\Lambda(K) L_\Lambda(\mathbf{k}'' - K) \Phi_\Lambda^{zzyy}(\mathbf{k}'' - K, Q, K, P) \\ &+ \int_K [J_\Lambda(\mathbf{k}) - J_\Lambda(\mathbf{k}'' - \mathbf{k})] L_\Lambda(K) L_\Lambda(\mathbf{k}'' - K) L_\Lambda(P + K) J_\Lambda(\mathbf{p} + \mathbf{k}) \\ &\times \Phi_\Lambda^{xyz}(P + K, \mathbf{k}'' - K, Q) \Phi_\Lambda^{xyz}(-P - K, P, K). \end{aligned} \quad (\text{A.70})$$

Expanding to linear order in the momentum \mathbf{k}'' we then arrive at

$$\begin{aligned} \nabla_{\mathbf{q}} \Pi_\Lambda(\mathbf{q}, i\nu) &= \int_K \nabla_{\mathbf{k}'} J_\Lambda(\mathbf{k}')|_{\mathbf{k}'=\mathbf{k}} L_\Lambda(K)^2 \Phi_\Lambda^{zzyy}(K, Q, -K, -Q) \\ &+ \int_K \nabla_{\mathbf{k}'} J_\Lambda(\mathbf{k}')|_{\mathbf{k}'=\mathbf{k}} L_\Lambda(K)^2 L_\Lambda(Q - K) J(\mathbf{q} - \mathbf{k}) \\ &\times \Phi_\Lambda^{xyz}(K - Q, -K, Q) \Phi_\Lambda^{xyz}(Q - K, -Q, K) \\ &= \int_K \nabla_{\mathbf{k}'} J_\Lambda(\mathbf{k}')|_{\mathbf{k}'=\mathbf{k}} L_\Lambda(K)^2 \Phi_\Lambda^{zzyy}(K, Q, -K, -Q) \\ &+ \int_K \nabla_{\mathbf{k}'} J_\Lambda(\mathbf{k}')|_{\mathbf{k}'=\mathbf{k}} L_\Lambda(K)^2 F_\Lambda(Q - K) [\Phi_\Lambda^{xyz}(K - Q, -K, Q)]^2, \end{aligned} \quad (\text{A.71})$$

which includes the static component $\nu = 0$ too. This has a similar shape to the corresponding flow equation for $\Pi_\Lambda(\mathbf{q}, i\nu)$ [2], if one replaces the single-scale propagator $\dot{F}_\Lambda(K)\delta_{\alpha\gamma}$ by the non-diagonal object $\nabla_{\mathbf{k}} J_\Lambda(\mathbf{k}) L_\Lambda^2(\mathbf{k}) \epsilon_{\alpha\sigma\gamma}^+$, i.e. $\partial_\Lambda J_\Lambda$ by the gradient of the exchange interaction, which connects to different components of the spin in the respective vertex. The origin of these relations lies again in the conservation laws, implied by spin-rotational invariance. Analogous relations can be written down for higher order vertices, involving one gradient for each independent momentum. From the relation $\Pi_\Lambda(\mathbf{k}, i\omega) = \tilde{\Pi}_\Lambda(\mathbf{k}, i\omega) [1 + \tilde{\Pi}_\Lambda(\mathbf{k}, i\omega) \Sigma_\Lambda(\mathbf{k})]^{-1}$ one sees that the corresponding equation for the subtracted polarization $\tilde{\Pi}_\Lambda(\mathbf{k}, i\omega)$ contains additional terms, e.g. the gradient of $\Sigma_\Lambda(\mathbf{k})$. Note that the approximate fulfillment of similar identities was invoked in order to justify the Katanin truncation [75, 76] for fermionic systems with two-body interaction in the weak coupling limit.

Appendix B

Additional calculations regarding spin dynamics

B.1 High temperature spin dynamics on lattices with cubic symmetry

In this section we present additional results for the $T = \infty$ -dynamics of spin- S Heisenberg models with nearest and next-nearest neighbor coupling J_1 and J_2 on several lattices with hypercubic symmetry in $d \leq 3$. In all cases we will use that the leading J^2/T -correction to the static self-energy $\Sigma(\mathbf{k})$ is for finite-ranged exchange couplings given by

$$\Sigma_2(\mathbf{q}) - \Sigma_2(\mathbf{q} + \mathbf{k}) = \sum_i \frac{c_i (J_i)^2}{12} \left[\gamma^{(i)}(\mathbf{q}) - \gamma^{(i)}(\mathbf{q} + \mathbf{k}) \right]. \quad (\text{B.1})$$

Here J_i is the coupling to i -th nearest neighbors with corresponding form factors $\gamma^{(i)}(\mathbf{k})$ that are orthogonal to each other, $\int_{\mathbf{k}} \gamma^{(i)}(\mathbf{k}) \gamma^{(j)}(\mathbf{k}) = c_i^{-1} \delta_{ij}$, and c_i is the number of sites on the i -th shell. All quantities with units of energy will be rescaled with $|J_1| \sqrt{b'_0}$.

B.1.1 $J_1 - J_2$ model on a hypercubic lattice

Linear chain

For a linear $J_1 - J_2$ -chain the exchange coupling in \mathbf{k} -space is given by

$$J(\mathbf{k}) = 2J_1[\gamma(\mathbf{k}) + \mu\gamma(2\mathbf{k})], \quad (\text{B.2})$$

where $\mu = J_2/J_1$ and $\gamma(\mathbf{k}) = \cos(k_x a)$. $\Delta(\mathbf{k}, i\omega)$ can then be written in terms of four independent amplitudes

$$\tilde{\Delta}(k_x, i\omega) = \sum_{j=1}^4 [1 - \cos(jk_x a)] \tilde{\Delta}_j(i\omega), \quad (\text{B.3})$$

which in turn satisfy

$$\tilde{\Delta}_1(i\omega) = \frac{1}{3b'_0} \int_{q_x} \frac{\cos(q_x a)}{|\tilde{\omega}| + \tilde{\Delta}(q_x, i\omega)} + 2 \int_{q_x} \frac{1 + \cos(2q_x a)}{|\tilde{\omega}| + \tilde{\Delta}(q_x, i\omega)} - \tilde{\Delta}_3(i\omega), \quad (\text{B.4a})$$

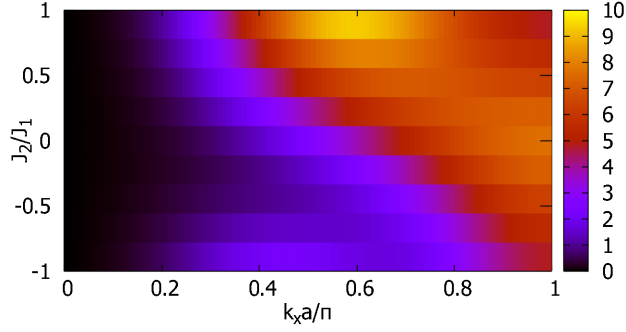


Figure B.1: Momentum dependence $\tilde{\Delta}(k_x)$ of the dimensionless dissipation energy in the low-frequency limit at $T = \infty$, defined by Eq. (B.6), for a $S = 1/2$ J_1 - J_2 Heisenberg Model in $d = 1$ as a function of $\mu = J_2/J_1 \in [-1, 1]$. Reprinted with permission from Ref. [10] © [2021] American Physical Society.

$$\begin{aligned} \tilde{\Delta}_2(i\omega) = & \left(\frac{\mu^2}{3b'_0} - 1 \right) \int_{q_x} \frac{\cos(2q_x a)}{|\tilde{\omega}| + \tilde{\Delta}(q_x, i\omega)} + 2\mu \int_{q_x} \frac{\cos(q_x a) + \mu}{|\tilde{\omega}| + \tilde{\Delta}(q_x, i\omega)} \\ & - \tilde{\Delta}_3(i\omega) - 2\tilde{\Delta}_4(i\omega), \end{aligned} \quad (\text{B.4b})$$

$$\tilde{\Delta}_3(i\omega) = -2\mu \int_{q_x} \frac{\cos(3q_x a)}{|\tilde{\omega}| + \tilde{\Delta}(q_x, i\omega)}, \quad (\text{B.4c})$$

$$\tilde{\Delta}_4(i\omega) = -\mu^2 \int_{q_x} \frac{\cos(4q_x a)}{|\tilde{\omega}| + \tilde{\Delta}(q_x, i\omega)}. \quad (\text{B.4d})$$

The anomalous diffusion coefficient can be expressed via these amplitudes as

$$\mathcal{D}(i\omega) = \frac{|J_1| \sqrt{b'_0} a^2}{4} \left[\tilde{\Delta}_1(i\omega) + 4\tilde{\Delta}_2^\parallel(i\omega) + 2\tilde{\Delta}_2^\perp(i\omega) \right]. \quad (\text{B.5})$$

Note that the leading low-frequency behavior is driven by the self-energy term $\propto 1/b'_0$. This term is an even function of μ , in contrast to contributions which are generated by $[J(\mathbf{q}) - J(\mathbf{q} + \mathbf{k})]^2$, and emerge only at $\mathcal{O}(k^4)$. One therefore obtains $\mathcal{D}(i\omega)$ for $J_2 \neq 0$ by replacing $|J_1| \rightarrow |J_1| \sqrt{1 + 4\mu^2}$ in the $J_2 = 0$ -expression. Moreover the solution for the amplitudes in $d \leq 2$ is simply determined by the $\omega \rightarrow 0$ -divergence times the coefficients on the right-hand side of their self-consistency equations, as implied by Eq. (3.108).

In Fig. B.1 the general momentum dependence of the low-frequency dissipation energy, defined as

$$\tilde{\Delta}(k_x) \equiv \frac{2}{\sqrt{3}} |\tilde{\omega}|^{\frac{1}{3}} \text{Re} \tilde{\Delta}(k_x, \omega + i0), \quad (\text{B.6})$$

is shown for $\mu \in [-1, 1]$. Quite generally we just replicate the momentum dependence of the kernel at vanishing loop momenta $V(\mathbf{k}, 0)$, see also Eq. (3.109). In Fig. B.2 a plot of the inverse is displayed for large momenta $ka \sim \mathcal{O}(1)$, which yields in this case also the k -dependence of the dynamic structure factor at sufficiently small frequencies $|\omega| \ll |J_1|$

$$\tilde{S}(k_x, \omega) = \frac{\sqrt{3} b'_0 |\tilde{\omega}|^{\frac{1}{3}}}{2\pi \tilde{\Delta}(k_x)}. \quad (\text{B.7})$$

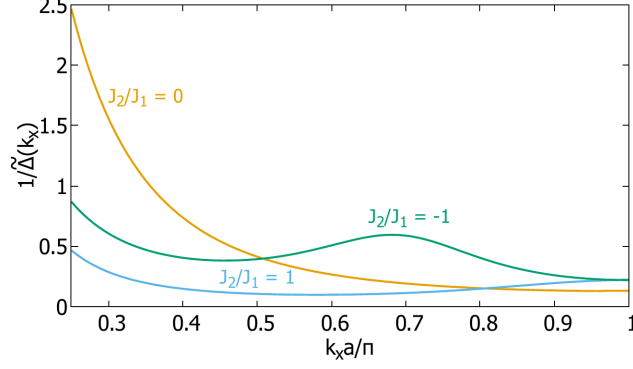


Figure B.2: $\tilde{\Delta}^{-1}(k_x)$, which is the inverse of the k_x -dependent part of the rescaled dissipation energy in the low-frequency limit for a linear $S = 1/2 J_1 - J_2$ Heisenberg magnet at $T = \infty$, shown for $k_x a > \pi/4$ and $J_2/J_1 = -1, 0, 1$. We display this quantity, since for $|\omega| \ll |J_1|$ it is proportional to the dynamic structure factor $S(\mathbf{k}, \omega)$, see Eq. (B.7). Reprinted with permission from Ref. [10] © [2021] American Physical Society.

For $\mu = 0$ the quantity $\Delta(k_x)$ simply has a global maximum at $k_x a = \pi$ and exhibits no other features of interest. There are some qualitative differences in the shape of $\tilde{\Delta}(k_x)$ at short wavelengths $1/k_x \sim a$ between negative and positive μ . For instance, below $\mu_- \approx -0.67$ the dissipation energy has two maxima, one at $k_x a = \pi$ and the other at $k_x a < \pi/2$ with an intermediate local minimum in $[\pi/2, \pi]$. The second maximum becomes global for some value of μ smaller than -1 (not included in Fig. B.1). For $\mu > 0$ no additional maximum is generated. Instead we observe above $\mu_+ \approx 0.28$ that the global maximum, initially located at $k_x a = \pi$, moves to a position $\in [\pi/2, \pi]$, with a local minimum forming in its place at π . The local minima which are generated in both cases, therefore imply a local peak in $S(\mathbf{k}, 0)$ at the same position, which is either found at $k_x a = \pi$ ($\mu > \mu_+$) or an intermediate value ($\mu < \mu_-$). In the latter case this maximum is surrounded by two minima, i.e. maxima of $\tilde{\Delta}(k_x)$. In the interval $\mu_- < \mu < \mu_+$ no additional local maximum is present.

Square lattice

The exchange interaction of a Heisenberg model with nearest-neighbor coupling J_1 and next-nearest neighbor coupling $J_2 = \mu J_1$ on the square lattice reads in momentum space

$$J(\mathbf{k}) = 4J_1[\gamma(\mathbf{k}) + \mu\gamma^\perp(\mathbf{k})], \quad (\text{B.8})$$

with the normalized form factors of nearest

$$\gamma(\mathbf{k}) = \frac{1}{2} [\cos(k_x) + \cos(k_y)], \quad (\text{B.9})$$

and next-nearest neighbors

$$\gamma^\perp(\mathbf{k}) = \cos(k_x) \cos(k_y). \quad (\text{B.10})$$

The solution for $\Delta(\mathbf{k}, i\omega)$ can then be expressed in terms of five independent form factors,

$$\begin{aligned} \tilde{\Delta}(\mathbf{k}, i\omega) = & (1 - \gamma(\mathbf{k}))\tilde{\Delta}_1(i\omega) + (1 - \gamma(2\mathbf{k}))\tilde{\Delta}_2^\parallel(i\omega) \\ & + (1 - \gamma^\perp(\mathbf{k}))\tilde{\Delta}_2^\perp(i\omega) + (1 - \gamma^\perp(2\mathbf{k}))\tilde{\Delta}_{2,2}^\parallel(i\omega) \\ & + (1 - \gamma^{(2,1)}(\mathbf{k}))\tilde{\Delta}_{2,1}(i\omega), \end{aligned} \quad (\text{B.11})$$

where the mixed form factor

$$\gamma^{(2,1)}(\mathbf{k}) = \frac{1}{2} \left[\cos(2k_x a) \cos(k_y a) + \cos(k_x a) \cos(2k_y a) \right], \quad (\text{B.12})$$

was introduced. The corresponding self-consistency equations for the amplitudes are given by

$$\tilde{\Delta}_1(i\omega) = \frac{2}{3b'_0} \int_{\mathbf{q}} \frac{\gamma(\mathbf{q})}{|\tilde{\omega}| + \tilde{\Delta}(\mathbf{q}, i\omega)} + 4 \int_{\mathbf{q}} \frac{1 + \gamma(2\mathbf{q}) + 2\gamma^\perp(\mathbf{q})}{|\tilde{\omega}| + \tilde{\Delta}(\mathbf{q}, i\omega)} - \tilde{\Delta}_{2,1}(i\omega), \quad (\text{B.13a})$$

$$\tilde{\Delta}_2^\parallel(i\omega) = -2(1 + 2\mu^2) \int_{\mathbf{q}} \frac{\gamma(2\mathbf{q})}{|\tilde{\omega}| + \tilde{\Delta}(\mathbf{q}, i\omega)}, \quad (\text{B.13b})$$

$$\begin{aligned} \tilde{\Delta}_2^\perp(i\omega) &= \left(\frac{2\mu^2}{3b'_0} - 4 \right) \int_{\mathbf{q}} \frac{\gamma^\perp(\mathbf{q})}{|\tilde{\omega}| + \tilde{\Delta}(\mathbf{q}, i\omega)} + 8\mu \int_{\mathbf{q}} \frac{\gamma(\mathbf{q})}{|\tilde{\omega}| + \tilde{\Delta}(\mathbf{q}, i\omega)} \\ &+ 4\mu^2 \int_{\mathbf{q}} \frac{1}{|\tilde{\omega}| + \tilde{\Delta}(\mathbf{q}, i\omega)} + 8\mu^2 \int_{\mathbf{q}} \frac{\gamma(2\mathbf{q})}{|\tilde{\omega}| + \tilde{\Delta}(\mathbf{q}, i\omega)} \\ &- \tilde{\Delta}_{2,1}(i\omega) - 2\tilde{\Delta}_{2,2}^\parallel(i\omega), \end{aligned} \quad (\text{B.13c})$$

$$\tilde{\Delta}_{2,2}^\parallel(i\omega) = -2\mu^2 \int_{\mathbf{q}} \frac{\gamma^\perp(2\mathbf{q})}{|\tilde{\omega}| + \tilde{\Delta}(\mathbf{q}, i\omega)}, \quad (\text{B.13d})$$

$$\tilde{\Delta}_{2,1}(i\omega) = -8\mu \int_{\mathbf{q}} \frac{\gamma^{(2,1)}(\mathbf{q})}{|\tilde{\omega}| + \tilde{\Delta}(\mathbf{q}, i\omega)}. \quad (\text{B.13e})$$

The k^2 -coefficient is therefore

$$\mathcal{D}(i\omega) = \frac{|J_1| \sqrt{b'_0} a^2}{4} \left[\tilde{\Delta}_1(i\omega) + 4\tilde{\Delta}_2^\parallel(i\omega) + 2\tilde{\Delta}_2^\perp(i\omega) + 8\tilde{\Delta}_{2,2}^\parallel(i\omega) + 5\tilde{\Delta}_{2,1}(i\omega) \right] \quad (\text{B.14})$$

As in $d = 1$ one obtains the leading low-frequency limit for $J_2 \neq 0$ by replacing $|J_1| \rightarrow |J_1| \sqrt{1 + (a'/a)^2 \mu^2}$, where a' is the distance to next-nearest neighbors on the lattice, with $a'/a = \sqrt{2}$ for the square lattice and $a' = 2a$ for a chain. Note that in the limit $\mu \rightarrow \infty$ the equations in one and two dimensions map again onto a square lattice and linear chain with spacing a' .

In Fig. B.3 we show the momentum-dependent part of the dimensionless dissipation energy in the low-frequency limit, defined here as

$$\tilde{\Delta}(\mathbf{k}) \equiv \frac{\text{Re} \tilde{\Delta}(\mathbf{k}, \omega + i0)}{\sqrt{\ln \left(\frac{\sqrt{J_1^2 + 2J_2^2}}{\sqrt{24\pi|\omega|}} \right)}}, \quad (\text{B.15})$$

in the quadrant $k_{x,y} \geq 0$ of the first Brillouin zone for select $\mu \in [-1, 1]$. Again, the dependence of $\tilde{\Delta}(\mathbf{k})$ on momentum is just proportional to $V(\mathbf{k}, \mathbf{0})$. Complementary, the inverse of $\tilde{\Delta}(\mathbf{k})$ is shown in Fig. B.4 along a path $\mathbf{k}(p)a = \pi(1, p)$ at the edge of the zone, focusing on the illustrative cases $\mu = -1, 0, 1$. The dynamic structure factor for non-hydrodynamic momenta is then directly proportional to that inverse, i.e.

$$\tilde{S}(\mathbf{k}, \omega) = \sqrt{\ln \left(\frac{\sqrt{J_1^2 + 2J_2^2}}{\sqrt{24\pi|\omega|}} \right)} \frac{b'_0}{\pi \tilde{\Delta}(\mathbf{k})}. \quad (\text{B.16})$$

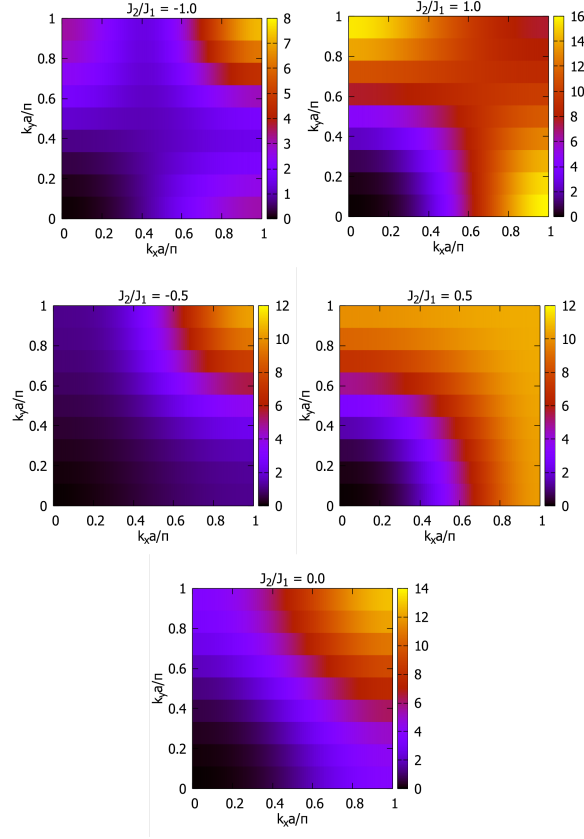


Figure B.3: Momentum dependence $\tilde{\Delta}(\mathbf{k})$ in the relevant quadrant of the Brillouin zone $k_{x/y} > 0$ of the low-frequency dissipation energy, defined by Eq. (B.15), of a $S = 1/2$ J_1 - J_2 Heisenberg magnet on the square lattice at $T = \infty$. The ratios of couplings used above are $J_2/J_1 = -1, -0.5, 0, 0.5, 1$ (counterclockwise, starting from top left). Reprinted with permission from Ref. [10] © [2021] American Physical Society.

Concerning the dependence of the shape on μ we observe features similar to one dimension. For sufficiently negative $\mu < \mu_- \approx -0.52$ the dissipation energy exhibits two maxima at both $\mathbf{k}a = (\pi, 0)$ and $\mathbf{k}a = (\pi, \pi)$ with a local minimum on the connecting path. This translates into a local maximum along that path in $S(\mathbf{k}, 0)$, surrounded by two local minima at the aforementioned corners. On the other hand, for $\mu > \mu_+ \approx 0.52$ the position of the global maximum switches from $\mathbf{k}a = (\pi, \pi)$ to $\mathbf{k}a = (\pi, 0)$. The former peak at (π, π) becomes then a local minimum, therefore implying a maximum at the same position in $S(\mathbf{k}, 0)$. For $\mu_- < \mu < \mu_+$ we observe only a saddle point at $(\pi, 0)$. The position of the global maximum of $\tilde{\Delta}(\mathbf{k})$ at (π, π) is again more stable for negative μ , with degeneracy occurring only below a $\mu < -1$.

Simple cubic lattice

The Fourier transform of the exchange interaction for an Heisenberg Model on a sc lattice with nearest neighbor coupling J_1 and next-nearest neighbor coupling $J_2 = \mu J_1$ reads

$$J(\mathbf{k}) = 6J_1[\gamma(\mathbf{k}) + 2\mu\gamma^\perp(\mathbf{k})], \quad (\text{B.17})$$

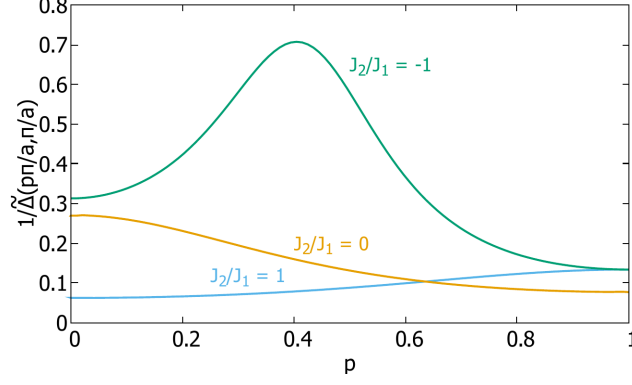


Figure B.4: Inverse of the \mathbf{k} -dependent part $\tilde{\Delta}(\mathbf{k})$ of $\Delta(\mathbf{k}, i\omega)$ for a $S = 1/2$ J_1 - J_2 Heisenberg magnet on the square lattice at $T = \infty$. Its \mathbf{k} -dependence is explicitly depicted along the path $\mathbf{k}(p) = \frac{\pi}{a}(1, p)$ at the edge of the Brillouin zone for $J_2/J_1 = -1, 0, 1$. These curves are then proportional to $S(\mathbf{k}, \omega)$ for $|\omega| \ll |J_1|$, as implied by Eq. (B.16). Reprinted with permission from Ref. [10] © [2021] American Physical Society.

with the nearest neighbor simple cubic form factor

$$\gamma(\mathbf{k}) = \frac{1}{3} \left[\cos(k_x a) + \cos(k_y a) + \cos(k_z) \right], \quad (\text{B.18})$$

and its pendant for next-nearest neighbors

$$\gamma^\perp(\mathbf{k}) = \frac{1}{3} \left[\cos(k_x a) \cos(k_y a) + (x \leftrightarrow z) + (y \leftrightarrow z) \right]. \quad (\text{B.19})$$

The Fourier decomposition of $\tilde{\Delta}(\mathbf{k}, i\omega)$ involves then seven different form factors

$$\begin{aligned} \tilde{\Delta}(\mathbf{k}, i\omega) = & (1 - \gamma(\mathbf{k}))\tilde{\Delta}_1(i\omega) + (1 - \gamma(2\mathbf{k}))\tilde{\Delta}_2^\parallel(i\omega) + (1 - \gamma^\perp(\mathbf{k}))\tilde{\Delta}_2^\perp(i\omega) \\ & + (1 - \gamma^\perp(2\mathbf{k}))\tilde{\Delta}_{2,2}^\parallel(i\omega) + (1 - \gamma^{(2,1,0)}(\mathbf{k}))\tilde{\Delta}_{2,1,0}(i\omega) \\ & + (1 - \gamma^{(2,1,1)}(\mathbf{k}))\tilde{\Delta}_{2,1,1}(i\omega) + (1 - \gamma^{(1,1,1)}(\mathbf{k}))\tilde{\Delta}_{1,1,1}(i\omega), \end{aligned} \quad (\text{B.20})$$

where we have introduced three additional form factors

$$\gamma^{(2,1,0)}(\mathbf{k}) = \frac{1}{6} \left[\cos(2k_x a) \cos(k_y a) + \cos(k_x a) \cos(2k_y a) + (x \leftrightarrow z) + (y \leftrightarrow z) \right], \quad (\text{B.21a})$$

$$\gamma^{(2,1,1)}(\mathbf{k}) = \frac{1}{3} \left[\cos(2k_x a) \cos(k_y a) \cos(k_z a) + (x \leftrightarrow z) + (y \leftrightarrow z) \right], \quad (\text{B.21b})$$

$$\gamma^{(1,1,1)}(\mathbf{k}) = \cos(k_x a) \cos(k_y a) \cos(k_z a). \quad (\text{B.21c})$$

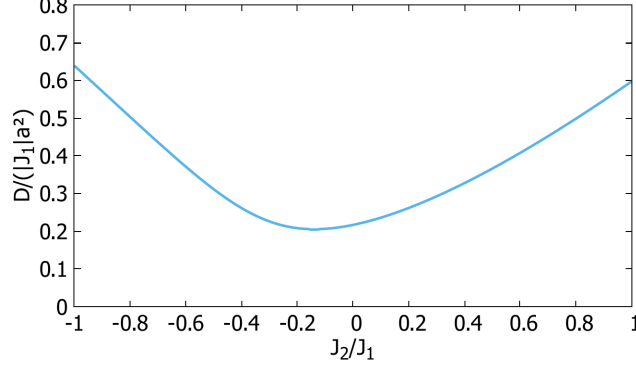


Figure B.5: $\mathcal{D}/(|J_1|a^2)$ as a function of $\mu = J_2/J_1$ for the $S = 1/2$ $J_1 - J_2$ Heisenberg Model on a sc lattice at infinite temperature. The location of the minimum at $\mu \neq 0$ clearly shows the asymmetry with respect to $\text{sign}(\mu)$. Reprinted with permission from [10] © [2021] American Physical Society.

The amplitudes obey then the following set of coupled self-consistency equations

$$\begin{aligned} \tilde{\Delta}_1(i\omega) = & \frac{1}{b'_0} \int_{\mathbf{q}} \frac{\gamma(\mathbf{q})}{|\tilde{\omega}| + \tilde{\Delta}(\mathbf{q}, i\omega)} + 6 \int_{\mathbf{q}} \frac{1 + \gamma(2\mathbf{q}) + 4\gamma^\perp(\mathbf{q})}{|\tilde{\omega}| + \tilde{\Delta}(\mathbf{q}, i\omega)} \\ & - \tilde{\Delta}_{2,1,0}(i\omega) - \tilde{\Delta}_{1,1,1}(i\omega), \end{aligned} \quad (\text{B.22a})$$

$$\tilde{\Delta}_2^\parallel(i\omega) = -3(1 + 4\mu^2) \int_{\mathbf{q}} \frac{\gamma(2\mathbf{q})}{|\tilde{\omega}| + \tilde{\Delta}(\mathbf{q}, i\omega)}, \quad (\text{B.22b})$$

$$\begin{aligned} \tilde{\Delta}_2^\perp(i\omega) = & \left(\frac{2\mu^2}{b'_0} + 24\mu^2 - 12 \right) \int_{\mathbf{q}} \frac{\gamma^\perp(\mathbf{q})}{|\tilde{\omega}| + \tilde{\Delta}(\mathbf{q}, i\omega)} \\ & + 24\mu \int_{\mathbf{q}} \frac{\gamma(\mathbf{q})}{|\tilde{\omega}| + \tilde{\Delta}(\mathbf{q}, i\omega)} + 12\mu^2 \int_{\mathbf{q}} \frac{1 + 2\gamma(2\mathbf{q})}{|\tilde{\omega}| + \tilde{\Delta}(\mathbf{q}, i\omega)} \\ & - \tilde{\Delta}_{2,1,0}(i\omega) - \tilde{\Delta}_{1,1,1}(i\omega) - 2\tilde{\Delta}_{2,2}^\parallel(i\omega) - 2\tilde{\Delta}_{2,1,1}(i\omega), \end{aligned} \quad (\text{B.22c})$$

$$\tilde{\Delta}_{2,2}^\parallel(i\omega) = -6\mu^2 \int_{\mathbf{q}} \frac{\gamma^\perp(2\mathbf{q})}{|\tilde{\omega}| + \tilde{\Delta}(\mathbf{q}, i\omega)}, \quad (\text{B.22d})$$

$$\tilde{\Delta}_{2,1,0}(i\omega) = -24\mu \int_{\mathbf{q}} \frac{\gamma^{(2,1,0)}(\mathbf{q})}{|\tilde{\omega}| + \tilde{\Delta}(\mathbf{q}, i\omega)}, \quad (\text{B.22e})$$

$$\tilde{\Delta}_{2,1,1}(i\omega) = -24\mu^2 \int_{\mathbf{q}} \frac{\gamma^{(2,1,1)}(\mathbf{q})}{|\tilde{\omega}| + \tilde{\Delta}(\mathbf{q}, i\omega)}, \quad (\text{B.22f})$$

$$\tilde{\Delta}_{1,1,1}(i\omega) = -24\mu \int_{\mathbf{q}} \frac{\gamma^{(1,1,1)}(\mathbf{q})}{|\tilde{\omega}| + \tilde{\Delta}(\mathbf{q}, i\omega)}. \quad (\text{B.22g})$$

The spin-diffusion coefficient at infinite temperature is therefore given by

$$\begin{aligned} \mathcal{D} = & \frac{|J_1|\sqrt{b'_0}a^2}{6} \left[\tilde{\Delta}_1(0) + 4\tilde{\Delta}_2^\parallel(0) + 2\tilde{\Delta}_2^\perp(0) + 8\tilde{\Delta}_{2,2}^\parallel(0) \right. \\ & \left. + 5\tilde{\Delta}_{2,1,0}(0) + 6\tilde{\Delta}_{2,1,1}(0) + 3\tilde{\Delta}_{1,1,1}(0) \right]. \end{aligned} \quad (\text{B.23})$$

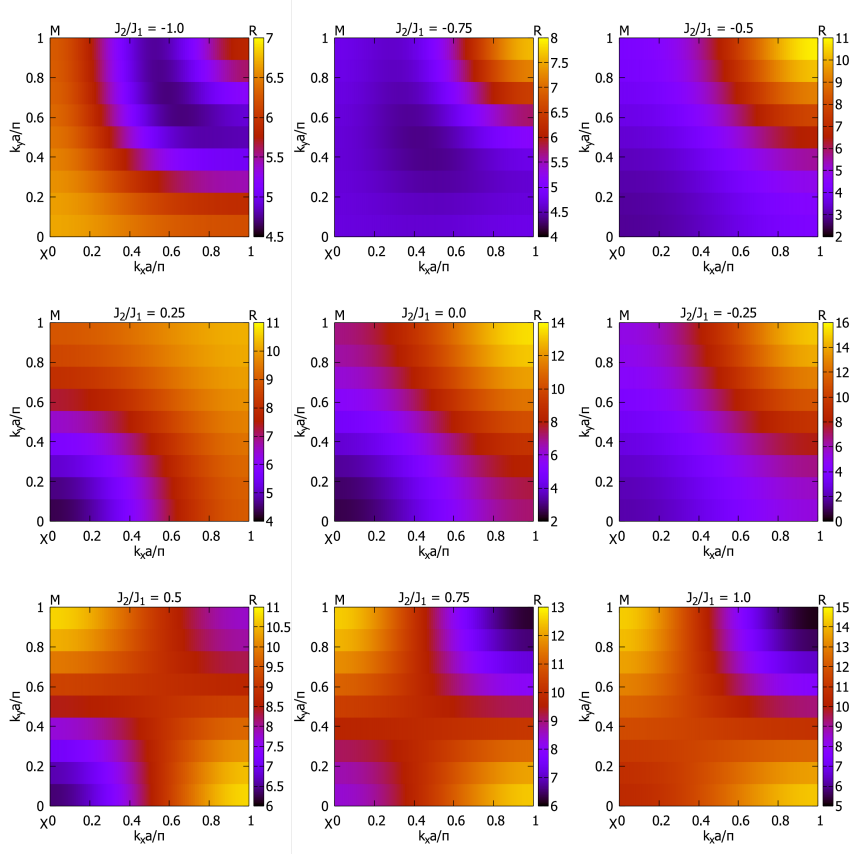


Figure B.6: Static limit of the dimensionless dissipation energy in the plane $k_z a = \pi$ of a $S = 1/2$ J_1 - J_2 Heisenberg magnet on a sc lattice at $T \gg |J_{1/2}|$. In the upper row it is shown for the ratios $J_2/J_1 = -1.0, -0.75, -0.5$, in the central row for $J_2/J_1 = 0.25, 0.0, -0.25$ and in the lowest for $J_2/J_1 = 0.5, 0.75, 1.0$. Reprinted with permission from Ref. [10] © [2021] American Physical Society.

In contrast to $d \leq 2$ the low-frequency solution cannot be reduced to $V(\mathbf{k}, \mathbf{0})$, because all momenta yield non-negligible contributions to the integrals in the self-consistency equations. The spin diffusion coefficient which is thus a non-symmetric function of J_2/J_1 is shown in B.5. Experiments in an effective $T = \infty$ -regime are unavailable for systems, that can be modeled by an isotropic Heisenberg model on this lattice. However, for the simple cubic nearest-neighbor Heisenberg antiferromagnet RbMnF_3 measurements were performed at room temperature, which is $\approx 3.5T_c$ and already accessible by a high-temperature expansion [120]. Including corrections up to linear order in J_1/T to the mode-coupling [128] and extrapolation results [97] at $T = \infty$ one finds deviations smaller than 10 percent between the experimentally measured value and these theoretical estimates. This supports the notion that our value for \mathcal{D} is simply too small, as was inferred from the second moment (3.96).

Going beyond the hydrodynamic regime, we display in Fig. B.6 the \mathbf{k} -dependence of the dissipation energy in the plane $k_{x,y} \geq 0, k_z a = \pi$ for different ratios $J_2/J_1 \in [-1, 1]$. We have designated in these plots the characteristic points at the corners of the first Brillouin zone, namely $\mathbf{X} = \frac{\pi}{a}(0, 0, 1)$, $\mathbf{M} = \frac{\pi}{a}(0, 1, 1)$ and $\mathbf{R} = \frac{\pi}{a}(1, 1, 1)$. For further elucidation we present in Fig. B.7 the \mathbf{k} -dependence of $\frac{1}{\Delta(\mathbf{k}, 0)}$ along the closed path $\mathbf{X} - \mathbf{M} - \mathbf{R} - \mathbf{X}$

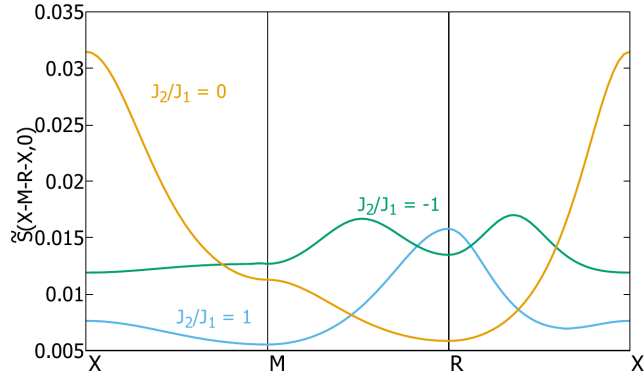


Figure B.7: Zero-frequency limit of the dimensionless dynamic structure factor $\tilde{S}(\mathbf{k}, 0)$, see Eq. (B.24), for a $S = 1/2$ $J_1 - J_2$ Heisenberg magnet on a sc lattice at $T \gg |J_{1/2}|$. Depicted is its momentum-dependence along the closed path $\mathbf{X} - \mathbf{M} - \mathbf{R} - \mathbf{X}$ for $J_2/J_1 = -1, 0, 1$, see also Fig. B.6. Reprinted with permission from Ref. [10] © [2021] American Physical Society.

for $\mu = -1, 0, +1$. As previously discussed, the dimensionless dynamic structure factor for $\omega \rightarrow 0$ and $ka \sim 1$ is simply given by

$$\tilde{S}(\mathbf{k}, 0) = \frac{b'_0}{\pi \tilde{\Delta}(\mathbf{k}, 0)}. \quad (\text{B.24})$$

The main qualitative features are similar to those observed in reduced dimensions. Around $J_2 = 0$ we find saddle points at \mathbf{X} and \mathbf{M} while \mathbf{R} is the sole global maximum of $\Delta(\mathbf{k}, 0)$. Note that the maximum at \mathbf{R} is again more persistent for negative J_2/J_1 compared to $J_2/J_1 > 0$. A two-peak structure formed by \mathbf{R} and \mathbf{X} with an intermediate saddle point remaining at \mathbf{M} , arises for sufficiently negative J_2/J_1 . Degeneracy of these maxima occurs for $J_2/J_1 = \mu_- \approx -0.97$ which is larger than -1 compared to low dimensions. In the case of positive J_2/J_1 we observe that \mathbf{M} assumes the role of the global maximum for $J_2/J_1 = \mu_+ \approx 0.32$, whereas \mathbf{R} becomes a local minimum. Taking a look at $S(\mathbf{k}, 0)$ along the path $\mathbf{X} - \mathbf{M} - \mathbf{R} - \mathbf{X}$ in the Brillouin zone, as shown in Fig. B.7 we see that for $\mu > \mu_+$ it has a local peak at \mathbf{R} . Conversely for $\mu < \mu_-$ maxima appear at intermediate positions on the connecting paths $\mathbf{M} - \mathbf{R}$ and $\mathbf{X} - \mathbf{R}$. We close this discussion by remarking that in our approximation $\Delta(\mathbf{k}, i\omega)$ is a finite number of lattice harmonics (3.64), whereas the expressions for its low-frequency form, extracted by extrapolation schemes [95, 98] or mode-coupling theory [74] are capable of exhibiting more complex \mathbf{k} -dependences.

B.1.2 $J_1 - J_2$ model on a body-centered cubic lattice

The body-centered cubic (bcc) lattice is of particular interest, since experiments that are performed at large enough temperatures, such that corrections at $\mathcal{O}(J/T)$ were negligible, are available for magnetic systems on this lattice [123], in contrast to the other cubic lattices [120, 121]. The exchange interaction of the $J_1 - J_2$ model on the bcc lattice is in momentum space given by

$$J(\mathbf{k}) = 8J_1 \left[\gamma^{\text{bcc}}(\mathbf{k}) + \frac{3}{4} \mu \gamma(\mathbf{k}) \right], \quad (\text{B.25a})$$

where $\mu = J_2/J_1$ and we defined the normalized nearest neighbor form factor of the bcc lattice as

$$\gamma^{\text{bcc}}(\mathbf{k}) \equiv \cos\left(\frac{k_x a}{2}\right) \cos\left(\frac{k_y a}{2}\right) \cos\left(\frac{k_z a}{2}\right), \quad (\text{B.26})$$

while $\gamma(\mathbf{k})$ is the nearest neighbor form factor of the sc lattice. Note that a is the lattice spacing of the conventional unit cell, a cube containing two sites. The dissipation energy can then be written in terms of six normalized form factors

$$\begin{aligned} \tilde{\Delta}(\mathbf{k}, i\omega) &= (1 - \gamma_{\mathbf{k}}^{\text{bcc}}) \tilde{\Delta}_1^{\text{bcc}}(i\omega) + (1 - \gamma_{\mathbf{k}}) \tilde{\Delta}_1^{\text{sc}}(i\omega) \\ &+ (1 - \gamma_{2\mathbf{k}}^{\text{bcc}}) \tilde{\Delta}_2^{\text{bcc},\parallel}(i\omega) + (1 - \gamma_{\mathbf{k}}^\perp) \tilde{\Delta}_2^{\text{sc},\perp}(i\omega) \\ &+ (1 - \gamma_{\mathbf{k}}^{\text{bcc,sc}}) \tilde{\Delta}_2^{\text{bcc,sc}}(i\omega) + (1 - \gamma_{2\mathbf{k}}) \tilde{\Delta}_2^{\text{sc},\parallel}(i\omega), \end{aligned} \quad (\text{B.27})$$

with $\gamma^\perp(\mathbf{k})$ being the off-diagonal form factor on the sc lattice, while the 'mixed' form factor is defined as

$$\gamma_{\mathbf{k}}^{\text{bcc,sc}} \equiv \frac{1}{3} \left[\cos\left(\frac{3k_x a}{2}\right) \cos\left(\frac{k_y a}{2}\right) \cos\left(\frac{k_z a}{2}\right) + (x \leftrightarrow z) + (x \leftrightarrow y) \right]. \quad (\text{B.28})$$

The corresponding amplitudes satisfy the following self-consistency equations

$$\begin{aligned} \tilde{\Delta}_1^{\text{bcc}}(i\omega) &= \frac{4}{3b'_0} \int_{\mathbf{q}} \frac{\gamma^{\text{bcc}}(\mathbf{q})}{|\tilde{\omega}| + \tilde{\Delta}(\mathbf{q}, i\omega)} + 8 \int_{\mathbf{q}} \frac{1 + 3\gamma(\mathbf{q}) + 3\gamma^\perp(\mathbf{q})}{|\tilde{\omega}| + \tilde{\Delta}(\mathbf{q}, i\omega)} \\ &- \tilde{\Delta}_2^{\text{bcc,sc}}(i\omega) - 2\tilde{\Delta}_2^{\text{bcc},\parallel}(i\omega), \end{aligned} \quad (\text{B.29a})$$

$$\tilde{\Delta}_2^{\text{bcc},\parallel}(i\omega) = -4 \int_{\mathbf{q}} \frac{\gamma^{\text{bcc}}(2\mathbf{q})}{|\tilde{\omega}| + \tilde{\Delta}(\mathbf{q}, i\omega)}, \quad (\text{B.29b})$$

$$\tilde{\Delta}_2^{\text{bcc,sc}}(i\omega) = -24\mu \int_{\mathbf{q}} \frac{\gamma^{\text{bcc,sc}}(\mathbf{q})}{|\tilde{\omega}| + \tilde{\Delta}(\mathbf{q}, i\omega)}, \quad (\text{B.29c})$$

$$\begin{aligned} \tilde{\Delta}_1^{\text{sc}}(i\omega) &= -12 \int_{\mathbf{q}} \frac{\gamma(\mathbf{q})}{|\tilde{\omega}| + \tilde{\Delta}(\mathbf{q}, i\omega)} + 24\mu \int_{\mathbf{q}} \frac{\gamma^{\text{bcc}}(\mathbf{q})}{|\tilde{\omega}| + \tilde{\Delta}(\mathbf{q}, i\omega)} - \tilde{\Delta}_2^{\text{bcc,sc}}(i\omega) \\ &+ \frac{\mu^2}{b'_0} \int_{\mathbf{q}} \frac{\gamma(\mathbf{q})}{|\tilde{\omega}| + \tilde{\Delta}(\mathbf{q}, i\omega)} + 6\mu^2 \int_{\mathbf{q}} \frac{1 + \gamma(2\mathbf{q}) + 4\gamma^\perp(\mathbf{q})}{|\tilde{\omega}| + \tilde{\Delta}(\mathbf{q}, i\omega)}, \end{aligned} \quad (\text{B.29d})$$

$$\tilde{\Delta}_2^{\text{sc},\perp}(i\omega) = -12(1 + \mu^2) \int_{\mathbf{q}} \frac{\gamma^\perp(\mathbf{q})}{|\tilde{\omega}| + \tilde{\Delta}(\mathbf{q}, i\omega)}, \quad (\text{B.29e})$$

$$\tilde{\Delta}_2^{\text{sc},\parallel}(i\omega) = -3\mu^2 \int_{\mathbf{q}} \frac{\gamma(2\mathbf{q})}{|\tilde{\omega}| + \tilde{\Delta}(\mathbf{q}, i\omega)}. \quad (\text{B.29f})$$

Note that all integrals run over the Brillouin zone corresponding to the primitive unit cell. For $\mu \rightarrow \infty$ one obtains the equations for a nearest-neighbor model on a simple cubic lattice with spacing a . The diffusion coefficient of the bcc lattice at $T = \infty$ can then be written as

$$\begin{aligned} \mathcal{D} &= \frac{|J_1| \sqrt{b'_0} a^2}{6} \left[\frac{3}{4} \tilde{\Delta}_1^{\text{bcc}}(0) + 3\tilde{\Delta}_2^{\text{bcc},\parallel}(0) + \frac{11}{4} \tilde{\Delta}_2^{\text{bcc,sc}}(0) + \tilde{\Delta}_1^{\text{sc}}(0) \right. \\ &\left. + 4\tilde{\Delta}_2^{\text{sc},\parallel}(0) + 2\tilde{\Delta}_2^{\text{sc},\perp}(0) \right]. \end{aligned} \quad (\text{B.30})$$

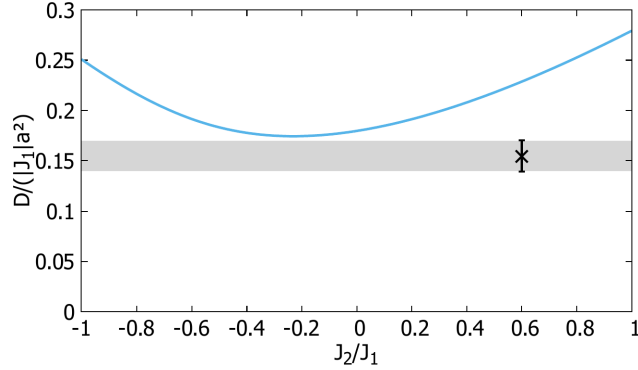


Figure B.8: $\mathcal{D}/(|J_1|a^2)$ as a function of $\mu = J_2/J_1$ for the $S = 1/2$ $J_1 - J_2$ Heisenberg Model on a bcc lattice. The cross with error bars marks the experimental value for $\mu = 0.6$ from Ref. [123]. Like the bars the shaded area indicates the experimental error for \mathcal{D} given in Ref. [123], reflecting a potential uncertainty in the values of the exchange couplings J_1, J_2 [201]. Reprinted with permission from [10] © [2021] American Physical Society.

S	$\frac{1}{2}$	1	$\frac{3}{2}$	2	$\frac{5}{2}$	3	$\frac{7}{2}$	∞
$\frac{\mathcal{D}}{ J a^2\sqrt{4b'_0}}$	0.180	0.160	0.153	0.15	0.149	0.148	0.147	0.145

Table B.1: Diffusion coefficient \mathcal{D} for the nearest-neighbor spin- S Heisenberg Model on a bcc lattice.

The spin diffusion coefficient of a $J_1 - J_2$ -model on the bcc lattice with $S = 1/2$ is shown in Fig. B.8 as a function of J_2/J_1 . In Table B.1 results are given for the normalized quantity $\mathcal{D}/(\sqrt{4b'_0})$ for $S \geq 1/2$ and $J_2 = 0$. Our $S = 1/2$ -value at $J_2/J_1 = 0.6$

$$\mathcal{D}_{\text{theor}} = 0.23|J_1|a^2, \quad (\text{B.31})$$

is about 35 percent larger than the experimental result

$$\mathcal{D}_{\text{exp}} = (0.16 \pm 0.02)|J_1|a^2, \quad (\text{B.32})$$

determined by Labrujere *et al.* [123] for the spin-1/2 Heisenberg ferromagnet $\text{Rb}_2\text{CuBr}_4 \cdot 2\text{H}_2\text{O}$ at temperatures $T = 20$ K and 77 K, which are both \gg than $J_1 = 0.49$ K, $J_2 =$

Method	$J_2/J_1 = 0.0$	$J_2/J_1 = 0.6$
Experiment [123]		0.16 ± 0.02
our result	0.18	0.23
Mori <i>et al.</i>	0.295	0.32
Resibois <i>et al.</i>	0.22	0.27
Tahir-Kheli <i>et al.</i>	0.295	0.275

Table B.2: Comparison with some other estimates for $\mathcal{D}/|J_1|a^2$ on the bcc lattice for $S = 1/2$ and $J_2/J_1 = 0.0, 0.6$ [123]. The deviation of our \mathcal{D} from other theoretical approaches is ~ 30 -40 percent and therefore consistent with the result for the sc lattice.

0.29 K. Other theoretical results, listed in Table B.2, show even larger deviations. However, the difference between our results and older predictions may be, to a significant portion, attributed to a lacking factor of two in the second moment, see Eq. (3.96). In turn this implies a \mathcal{D} which is smaller by a factor $\sqrt{2}$, and the better performance of our solution might be therefore accidental. Note that for solid bcc ^3He , the experimental value for the spin diffusion coefficient [122] was found to be within the range of a few percent of estimates from extrapolation schemes [94, 96] under the assumption of an isotropic nearest-neighbor Heisenberg model for its spin degrees of freedom. One can argue that the values of the exchange couplings in $\text{Rb}_2\text{CuBr}_4 \cdot 2\text{H}_2\text{O}$ and especially their ratio may, as parameters of the model, actually depend on temperature. Such a behavior was indeed observed for the related compound $\text{K}_2\text{CuCl}_4 \cdot 2\text{H}_2\text{O}$ [201]. In that system the nearest neighbor-coupling decreased by a factor of five between $T = 77$ K and $T = 300$ K, with its cause ascribed to an optical phonon with a small gap. However, the good agreement of the short-time behavior exhibited by other theoretical solutions, which is heavily sensitive to the values of $J_{1/2}$, with the experimental results, raises doubts about this attempt at explaining the discrepancy. The authors of Ref. [123] noted that all of the theoretical results failed to reproduce the experimentally measured frequency/time-dependence of the autocorrelation function at intermediate scales, so that the deviations at low frequencies/large times are probably connected to that deficiency.

Moreover we should be cautious in comparing our result with the long-time asymptotics of the autocorrelation function $S(\mathbf{0}, t)$, which in the case of $\text{Rb}_2\text{CuBr}_4 \cdot 2\text{H}_2\text{O}$ were employed [123] to extract \mathcal{D} , see Eq. (3.82). This is due to the discussed non-analytic corrections in $\Delta(\mathbf{k}, i\omega)$ for $\omega \neq 0$, which modify for instance the long-time coefficient in $S(\mathbf{r}, t)$ by non-hydrodynamic terms that depend on short-range properties. In principle this can even lead to a fully incompatible result on our side, like negative autocorrelations. Our comparison of the coefficients should therefore be restricted to the strict hydrodynamic limit, where the experimental result for \mathcal{D} , extracted from the long-time behavior of $S(\mathbf{0}, t)$, is also valid. In fact, Labrujere *et al.* compared their result for \mathcal{D} to the calculation of Resibois and De Leener, whose solution for $S(\mathbf{0}, t)$ does not exhibit a $t^{-3/2}$ -decay for $t \rightarrow \infty$ with their notion of \mathcal{D} being only valid in the aforementioned scaling limit [90].

B.2 Time-dependent correlations

In the following sections time-dependent correlations are calculated from our low-frequency solution for $S(\mathbf{k}, \omega)$ in one and three spatial dimensions at infinite temperature.

B.2.1 Non-analytic corrections in $d = 3$

We have already discussed in some lengths the presumed effects of the branch point on $S(\mathbf{k}, t)$ in $d = 3$, see Sec. 3.2.2. Here we want to quantify it a little further. For this purpose, consider first

$$S(\mathbf{k}, t) = \int_0^\infty \frac{d\omega}{\pi} S(\mathbf{k}, \omega) \cos(\omega t) \approx \frac{b'_0}{2\pi} \int_0^\infty \frac{d\omega}{\pi} \frac{2 \cos(\omega t) [\Delta(\mathbf{k}) + \Delta'(\mathbf{k})|\omega/2|^{1/2}]}{\omega^2 + \Delta(\mathbf{k})^2 + 2\Delta(\mathbf{k})\Delta'(\mathbf{k})|\omega/2|^{1/2}}, \quad (\text{B.33})$$

where we inserted the 'distorted' Lorentzian (3.102) on the right-hand side and $\Delta(\mathbf{k}) = \Delta(\mathbf{k}, 0)$. Moreover we neglected contributions $\sim |\omega|$, $|\omega|^{3/2}$ in the denominator because these terms will produce contributions in the time-domain that decay with larger exponents

than $3/2$. In fact, we can isolate the branch-cut contribution for arbitrary momentum \mathbf{k} , by expanding (3.102) to leading order in $\Delta'(\mathbf{k})|\omega|^{1/2}$ around the Lorentzian, which yields

$$2\pi S(\mathbf{k}, t) \approx 2b'_0 \int_0^\infty \frac{d\omega \cos(\omega t) [\Delta(\mathbf{k}) + \Delta'(\mathbf{k})|\tilde{\omega}/2|^{1/2}]}{\pi (\omega^2 + \Delta(\mathbf{k})^2)} - 4b'_0 \int_0^\infty \frac{d\omega \cos(\omega t) \Delta(\mathbf{k})^2 \Delta'(\mathbf{k})|\tilde{\omega}/2|^{1/2}}{\pi (\omega^2 + \Delta(\mathbf{k})^2)^2}. \quad (\text{B.34})$$

The term containing no square-roots is the contribution from the diffusion pole, which evaluates to

$$2\pi S_{\mathcal{D}}(\mathbf{k}, t) = b'_0 \exp(-\Delta(\mathbf{k})t). \quad (\text{B.35})$$

The other two contributions will be $\sim t^{-3/2}$. To see this we first substitute $u = \omega t$, so that

$$\int_0^\infty \frac{d\omega \cos(\omega t) \Delta'(\mathbf{k})|\tilde{\omega}/2|^{1/2}}{\pi (\omega^2 + \Delta(\mathbf{k})^2)} = \frac{\Delta'(\mathbf{k})}{\Delta(\mathbf{k})^2 \tilde{t}^{3/2}} \int_0^\infty \frac{du \cos(u) |u/2|^{1/2}}{\pi \left(\frac{u}{\Delta(\mathbf{k})t}\right)^2 + 1}, \quad (\text{B.36})$$

$$\int_0^\infty \frac{d\omega \cos(\omega t) \Delta(\mathbf{k})^2 \Delta'(\mathbf{k})|\tilde{\omega}/2|^{1/2}}{\pi (\omega^2 + \Delta(\mathbf{k})^2)^2} = \frac{\Delta'(\mathbf{k})}{\Delta(\mathbf{k})^2 \tilde{t}^{3/2}} \int_0^\infty \frac{du \cos(u) |u/2|^{1/2}}{\pi \left(\left(\frac{u}{\Delta(\mathbf{k})t}\right)^2 + 1\right)^2}. \quad (\text{B.37})$$

For $t \rightarrow \infty$ we can use then that

$$\lim_{b \rightarrow \infty} \int_0^\infty du \frac{f(u) b^{2n}}{(u^2 + b^2)^n} = \lim_{b \rightarrow \infty} \left(F(u) \frac{b^{2n}}{(u^2 + b^2)^n} \Big|_0^\infty + \int_0^\infty du \frac{F(u) 2nb^{2n}u}{(u^2 + b^2)^{n+1}} \right) = -F(0), \quad (\text{B.38})$$

where $n \geq 1$, $b = \Delta(\mathbf{k})t$ and it was used that the indefinite integral of the oscillatory function $f(u)$, denoted by $F(u)$, exhibits a weaker growth than u^2 for $u \gg 1$. For $f(x) = \cos(x)\sqrt{x}$, we find $F(0) = \sqrt{\pi}/8$. Adding up all terms we obtain

$$S(\mathbf{k}, t) = \frac{b'_0}{2\pi} \left(\exp(-\Delta(\mathbf{k})t) + \frac{1}{2\sqrt{\pi}} \frac{\Delta'(\mathbf{k})}{\Delta(\mathbf{k})^2 \tilde{t}^{3/2}} \right). \quad (\text{B.39})$$

As shown in Fig. 3.3 of Sec. 3.2.2 $\Delta'(\mathbf{k})$ is < 0 for $ka \sim 1$, which reflects the tendency of $S(\mathbf{k}, t)$ to oscillate at short wavelengths. For small k the non-hydrodynamic term in (B.39) behaves as $1/k^2$. In $d > 2$ dimensions this singularity is fully neutralized by a \mathbf{k} -integration, so that it suffices to consider the $t \rightarrow \infty$ -limit of $S(\mathbf{k}, t)$. This applies to the omitted terms $\sim \mathcal{O}(t^{-2})$ as well, which justifies their exclusion from $S(\mathbf{r}, t \rightarrow \infty)$. Hence one can calculate the long-time limit of $S(\mathbf{r}, t)$ by taking the Fourier-transform of (B.39). Our estimate for the correlation function in real space at long times becomes

$$\frac{2\pi S(\mathbf{r}, t)}{b'_0} \approx \frac{1}{2\pi^2} \int_0^\infty dk k^2 e^{-\mathcal{D}k^2 t + i\mathbf{k} \cdot \mathbf{r}} + \frac{1}{2\sqrt{\pi} \tilde{t}^{3/2}} \int_{\mathbf{k}} \frac{\Delta'(\mathbf{k})}{\Delta(\mathbf{k})^2} e^{i\mathbf{k} \cdot \mathbf{r}}, \quad (\text{B.40})$$

where we used that for the diffusion pole the integral is dominated by momenta $k \sim t^{-1/2}$. The first term yields a Gaussian with variance $(\Delta r)^2 \sim \mathcal{D}t$ and a long-time tail $\sim t^{-3/2}$, as already encountered in the solution of the diffusion equation for a sharply localized initial condition [35]

$$\frac{1}{2\pi^2} \int_0^\infty dk k^2 e^{-\mathcal{D}k^2 t + i\mathbf{k} \cdot \mathbf{r}} = \frac{1}{8(\pi \mathcal{D}t)^{3/2}} e^{-\frac{r^2}{4\mathcal{D}t}}. \quad (\text{B.41})$$

\mathbf{r}	$\frac{1}{2}$	1	$\frac{3}{2}$	∞
(0, 0, 0)	-0.52	-0.24	-0.12	0.08
$\frac{\pi}{a}(1, 0, 0)$	0.56	0.92	1.08	1.32

Table B.3: Ratio between non-hydrodynamic and Gaussian contribution in the $t^{-3/2}$ -long time tail for the auto- and nearest neighbor pair-correlation functions $S(\mathbf{r}, t)$ on a sc lattice with different S .

As expected the coefficient in front of the hydrodynamic result for the correlation function is modified. Moreover the value of the coefficient depends explicitly on \mathbf{r} , due to the Fourier transform of the non-hydrodynamic term. The latter is influenced by microscopic details, e.g. the type of exchange interaction and lattice on which the spins are placed. We have quantitatively checked the influence of these contributions for nearest-neighbor couplings on a simple cubic lattice by solving (3.101) for $\Delta'(\mathbf{k})$ and subsequently evaluating the second integral in (B.40). We found that the contribution to the autocorrelation function $S(\mathbf{0}, t)$ is negative for $S = 1/2$, and has a smaller magnitude than the Gaussian term, so that in total the $t^{-3/2}$ -coefficient remains > 0 . For correlations between nearest neighbors, the non-hydrodynamic contribution is > 0 and has a larger amplitude than for $\mathbf{r} = \mathbf{0}$. Furthermore both quantities become more positive with increasing S , with the $\mathbf{r} = \mathbf{0}$ -contribution being even > 0 for $S \rightarrow \infty$.

B.2.2 Superdiffusion in $d = 1$

In this section we will use the Laplace-transform $\tilde{\mathcal{R}}_L(\mathbf{k}, s)$ on the imaginary axis to calculate $S(\mathbf{k}, t)$ in $d = 1$ at elevated temperatures, i.e. [109]

$$2\pi S(\mathbf{k}, t) = \frac{b'_0}{2\pi i} \int_{c-i\infty}^{c+i\infty} ds \tilde{\mathcal{R}}_L(\mathbf{k}, s) e^{st}, \quad (\text{B.42})$$

where $\text{Re}(c) > \text{Re}(z_*)$ with z_* being the pole with the largest real part and

$$\tilde{\mathcal{R}}_L(\mathbf{k}, s) = \int_0^\infty dt e^{-st} \tilde{\mathcal{R}}(\mathbf{k}, t). \quad (\text{B.43})$$

The contour along the shifted imaginary axis is then closed by an infinite half-circle with a keyhole detour around the branch axis and branch point. Then one can directly use the residue theorem as long as the poles do not lie on the same axis as the branch cut

$$\frac{1}{2\pi i} \int_C \tilde{\mathcal{R}}_L(\mathbf{k}, s) e^{st} = \sum_a \text{Res}_{s=a} \tilde{\mathcal{R}}_L(\mathbf{k}, s) e^{st}. \quad (\text{B.44})$$

In the case of poles lying on the branch axis, C should include additional detours around these poles. In contrast to $d > 2$ the branch cut is already part of the scaling form and is therefore not suppressed relative to contributions from ordinary poles in a strict hydrodynamic limit of the form $k^z t = \text{const}$. The Laplace-transform for the superdiffusive form in $d = 1$ is given by

$$\tilde{\mathcal{R}}_L(\mathbf{k}, s) = \frac{1}{\Delta(\mathbf{k}, s) + s} = \frac{s^{1/3}}{\Delta'(\mathbf{k}) + s^{4/3}}, \quad (\text{B.45})$$

where we used that $\Delta(\mathbf{k}, s) = \Delta'(\mathbf{k})s^{-1/3}$. This expression has two simple poles in the complex plane, given by the solution of $s^{4/3} = -\Delta'(\mathbf{k})$, namely $s/\Delta'(\mathbf{k})^{3/4} = e^{\pm i\frac{3\pi}{4}} = \cos(\frac{3\pi}{4}) \pm i\sin(\frac{3\pi}{4})$. By virtue of the theorem of residues we thus find

$$\begin{aligned} & \int_{c-i\infty}^{c+i\infty} ds \frac{e^{s\Delta'(\mathbf{k})^{3/4}t} s^{1/3}}{s^{4/3} + 1} + \int_{-\infty}^{-\epsilon} \frac{duu^{1/3}e^{u\Delta'(\mathbf{k})^{3/4}t}}{u^{4/3} + 1} + \int_{-\epsilon}^{-\infty} \frac{duu^{1/3}e^{u\Delta'(\mathbf{k})^{3/4}t}}{u^{4/3} + 1} \\ & + i\epsilon \int_{\pi}^{-\pi} d\phi e^{i\phi} \frac{e^{\epsilon e^{i\phi}\Delta'(\mathbf{k})^{3/4}t} (\epsilon e^{i\phi})^{1/3}}{1 + (\epsilon e^{i\phi})^{4/3}} = 2\pi i \operatorname{res} \frac{e^{s\Delta'(\mathbf{k})^{3/4}t} s^{1/3}}{s^{4/3} + 1}. \end{aligned} \quad (\text{B.46})$$

Here we have already neglected the arcs in the limit $R \rightarrow \infty$, as the integrand decays exponentially for $\operatorname{Re}(s) < 0$. Furthermore the fourth integral over the branch point at $s = 0$ vanishes for $\epsilon \rightarrow 0$. The two integrals parallel to the branch cut along the real negative half-axis are

$$\int_{-\infty}^{-\epsilon} \frac{duu^{1/3}e^{u\Delta'(\mathbf{k})^{3/4}t}}{u^{4/3} + 1} = \int_{\epsilon}^{\infty} \frac{duu^{1/3}e^{\frac{i\pi}{3}e^{-u\Delta'(\mathbf{k})^{3/4}t}}}{u^{4/3}e^{\frac{4i\pi}{3}} + 1}, \quad (\text{B.47})$$

$$\int_{-\epsilon}^{-\infty} \frac{duu^{1/3}e^{u\Delta'(\mathbf{k})^{3/4}t}}{u^{4/3} + 1} = - \int_{\epsilon}^{\infty} \frac{duu^{1/3}e^{-\frac{i\pi}{3}e^{-u\Delta'(\mathbf{k})^{3/4}t}}}{u^{4/3}e^{-\frac{4i\pi}{3}} + 1}, \quad (\text{B.48})$$

and therefore

$$\int_{-\infty}^{-\epsilon} \frac{duu^{1/3}e^{u\Delta'(\mathbf{k})^{3/4}t}}{u^{4/3} + 1} + \int_{-\epsilon}^{-\infty} \frac{duu^{1/3}e^{-u\Delta'(\mathbf{k})^{3/4}t}}{u^{4/3} + 1} = 2i \operatorname{Im} \left(\int_0^{\infty} du \frac{u^{1/3}e^{-u\Delta'(\mathbf{k})^{3/4}t} e^{-i\pi}}{u^{4/3} + e^{-\frac{4i\pi}{3}}} \right), \quad (\text{B.49})$$

so that

$$\int_{c-i\infty}^{c+i\infty} \frac{dz}{2\pi i} \frac{e^{z\Delta'(\mathbf{k})^{3/4}t} z^{1/3}}{z^{4/3} + 1} = \operatorname{res} \left(\frac{e^{s\Delta'(\mathbf{k})^{3/4}t} s^{1/3}}{s^{4/3} + 1} \right) + \frac{\sin(\frac{4\pi}{3})}{\pi} \int_0^{\infty} \frac{duu^{1/3}e^{-u\Delta'(\mathbf{k})^{3/4}t}}{(u^{4/3} + \cos(4\pi/3))^2 + \sin^2(4\pi/3)}. \quad (\text{B.50})$$

The contribution from the poles is simply an exponentially damped oscillation

$$\operatorname{res} \left(\frac{e^{s\Delta'(\mathbf{k})^{3/4}t} s^{1/3}}{s^{4/3} + 1} \right) = \frac{3}{2} e^{-\frac{\Delta'(\mathbf{k})^{3/4}t}{\sqrt{2}}} \cos \left(\frac{\Delta'(\mathbf{k})^{3/4}t}{\sqrt{2}} \right). \quad (\text{B.51})$$

The term generated by the branch cut is negative, due to $\sin(4\pi/3) = -\sqrt{3}/2$ and is either of the same order or much larger than the pole contribution. Furthermore its magnitude decreases monotonously as a function of $\Delta'(\mathbf{k})^{3/4}t$. One can straightforwardly evaluate it for $\Delta'(\mathbf{k})^{3/4}t \rightarrow \infty$, by neglecting the u -dependence in the denominator. The contribution behaves then as $(\Delta'(\mathbf{k}))^{-1}t^{-4/3}$, which for $ka \ll 1$ is $\sim k^{-2}t^{-4/3}$ and is therefore the leading term in $S(\mathbf{k}, t)$ for large times. However, in an integral over k to determine $S(\mathbf{r}, t)$ the dependence on k^{-2} also implies a singular behavior $\sim 1/k$ for $k \ll \mathcal{O}(t^{-2/3})$. Hence the contribution from the branch cut to $S(\mathbf{r}, t)$ is actually $\sim t^{-2/3}$, same as the tail of the Fourier-transformed pole terms. Moreover this means that the contribution from the branch cut to real-space correlations is actually dominated by the small momentum regime $k \lesssim \mathcal{O}(t^{-2/3})$ like the superdiffusion poles, instead of the aforementioned long-time limit in $S(\mathbf{k}, t)$, as is the case in $d = 3$. Hence we evaluate the contribution of the branch cut to the autocorrelation function $S(\mathbf{0}, t)$ by calculating

$$\frac{2\pi}{b'_0} \int_{\mathbf{k}} S_{\text{B}}(\mathbf{k}, t) = \frac{-3\sqrt{3}}{8\pi^2(\mathcal{D}'t)^{-2/3}} \int_0^{\infty} dy \int_0^{\infty} dk \frac{e^{-y^{3/4}k^{3/2}}}{(y - \frac{1}{2})^2 + \frac{3}{4}}, \quad (\text{B.52})$$

where the integral over k and y is, as anticipated, finite, e.g.

$$\int_0^\infty dy \int_0^\infty dk \frac{e^{-y^{3/4}k^{3/2}}}{(y - \frac{1}{2})^2 + \frac{3}{4}} = \Gamma(5/3) \int_0^\infty \frac{dy y^{-1/2}}{(y - \frac{1}{2})^2 + \frac{3}{4}} \approx 2.84 \quad (\text{B.53})$$

so that

$$2\pi \int_{\mathbf{k}} S_B(\mathbf{k}, t) = -\frac{0.19b'_0}{(\mathcal{D}'t)^{-2/3}}, \quad (\text{B.54})$$

while the contribution from poles evaluates to

$$2\pi \int_{\mathbf{k}} S_D(\mathbf{k}, t) = \frac{3 \times 2^{1/3} b'_0}{2\pi (\mathcal{D}'t)^{2/3}} \int_0^\infty dk e^{-k^{3/2}} \cos(k^{3/2}) = \frac{0.37b'_0}{(\mathcal{D}'t)^{-2/3}}. \quad (\text{B.55})$$

The autocorrelation function for $t \rightarrow \infty$ is therefore positive with a, in contrast to $d = 3$, universal renormalization of the coefficient caused by the branch cut.

One can also estimate the effect of the $\Delta''(\mathbf{k})\omega^{1/3}$ -correction to $\Delta(\mathbf{k}, i\omega)$. For $t \rightarrow \infty$ its contribution to $S(\mathbf{k}, t)$ is $\sim \Delta''(\mathbf{k})(\Delta(\mathbf{k})t)^{-2}$, which for $ka \ll 1$ behaves as $\sim k^{-2}t^{-2}$. Even with the singular behavior $\sim 1/k$ at the lower boundary $k \sim t^{-2/3}$ this implies only a $t^{-4/3}$ -term in $S(\mathbf{r}, t)$ and is therefore of subleading order. This is consistent with the suppression of this term as $\Delta''(\mathbf{k})(\Delta(\mathbf{k}))^{-1/2} \sim k \rightarrow 0$ in the scaling regime, which translates into an additional power $t^{-2/3}$. In contrast to $d = 3$ the long-time solution is therefore solely determined by small momenta $k \lesssim \mathcal{O}(t^{-1/z})$, i.e. the scaling regime, which also applies to correlations between different sites, that will all exhibit the same asymptotics to leading order in $t^{-2/3}$.

Note that the above results may be applied to any superdiffusive power-law singularity $\Delta(\mathbf{k}, s) \sim \Delta'(\mathbf{k})s^{-\alpha}$, $\alpha < 1$. One finds the following superposition of poles and branch cut

$$\begin{aligned} \mathcal{R}(\mathbf{k}, t) &= \frac{2}{1 + \alpha} e^{\cos(\frac{\pi}{1+\alpha})\Delta'(\mathbf{k})^{3/4}t} \cos\left(\cos\left(\frac{\pi}{1 + \alpha}\right)\Delta'(\mathbf{k})^{\frac{1}{1+\alpha}}t\right) \\ &+ \frac{\sin(\pi(1 + \alpha))}{\pi} \int_0^\infty \frac{du u^\alpha e^{-u\Delta'(\mathbf{k})^{\frac{1}{1+\alpha}}t}}{(u^{1+\alpha} + \cos(\pi(1 + \alpha)))^2 + \sin^2(\pi(1 + \alpha))}. \end{aligned} \quad (\text{B.56})$$

Calculating the right-hand side in general as a function of $\Delta'(\mathbf{k})t$, we obtain for the previously discussed case $\alpha = 1/3$ an exponentially damped oscillation, a feature shared with the KPZ scaling function [113], although for the latter quantity it is much less pronounced. For $\alpha = 3/5$, which is exhibited by the critical scaling function in $d = 3$ for $\omega \ll \omega_k$ and $\gg \omega_k$ (with different numeric factors) one obtains a similar time-dependence. in qualitative agreement with a mode-coupling solution [129]. Both functions are shown in Fig. B.9. For $t \rightarrow \infty$ we extract $\mathcal{R}(\mathbf{k}, t) \sim t^{-1-\alpha}$ from (B.56). Note that one should obtain the same asymptotic t -dependence for the full scaling functions near T_c by employing an argument similar to the one used in Eq. (B.38) for the branch cut-correction in $d = 3$.

B.3 Spin dynamics at intermediate temperature in $d = 3$

In order to connect our results at high temperatures and in the critical region, we compute several zero-frequency amplitudes, including the spin diffusion coefficient \mathcal{D} by solving the integral equation (3.50) for $\Delta(\mathbf{k}, 0)$ of a three-dimensional paramagnet on a grid. We will focus on a nearest-neighbor antiferromagnet on a simple / body-centered cubic lattice,

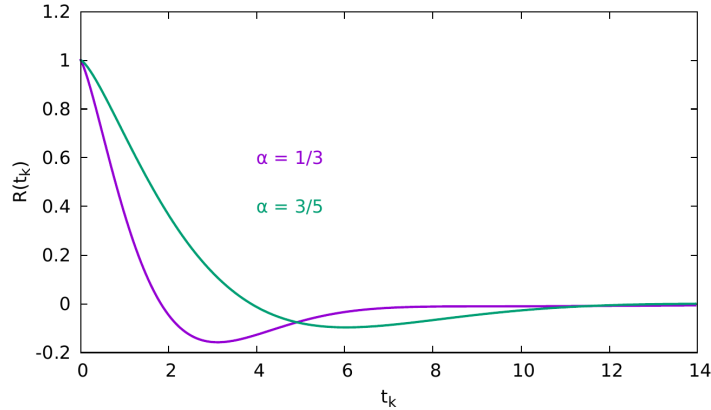


Figure B.9: $\mathcal{R}(\mathbf{k}, t) = \mathcal{R}(t_k = \Delta'(\mathbf{k})^{\frac{1}{1+\alpha}} t)$ from Eq. (B.56) for $\alpha = 1/3$ and $\alpha = 3/5$.

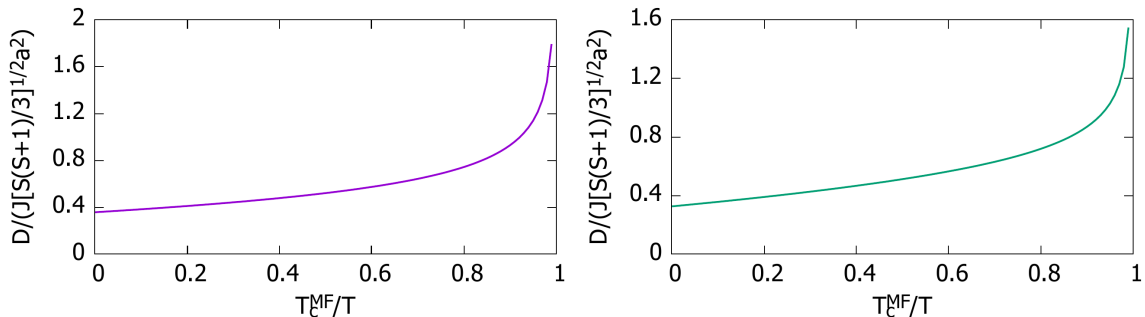


Figure B.10: Dimensionless spin diffusion coefficient as a function of T_c^{MF}/T for a nearest neighbor Heisenberg antiferromagnet on the sc (left) and bcc (right) lattice from the numerical solution of (3.50), using a mean-field ansatz for the static susceptibility $G(\mathbf{q})$.

since up to this point we did not perform any explicit calculation with $J > 0$ at $T < \infty$. For simplicity we have chosen to approximate the static susceptibility $G(\mathbf{q})$ by the tree-approximation (4.3) where $T_c = T_c^{\text{MF}}$. This ansatz does not yield quantitatively correct thermodynamics, but it suffices for a qualitative description of how \mathcal{D} depends on temperature. Note that approximations like a static sum rule $b'_0/T = \int_{\mathbf{q}} G(\mathbf{q})$ [64, 128], which also neglect the momentum dependence of $\Sigma(\mathbf{k})$, yield more accurate critical temperatures. On the other hand, the critical exponents still deviate substantially from the benchmark values, e.g. $\nu = 1$ [64, 128] instead of $\nu \approx 0.7$ [26].

Plots of $\mathcal{D}(T)/(|J|\sqrt{b'_0}a^2)$ as a function of $g = T_c/T$ for both lattices are shown in Fig. B.10. We see that, in qualitative agreement with neutron scattering experiments on antiferromagnets [120] and theoretical calculations [92], \mathcal{D} grows when T is lowered. In particular, one sees the divergence of the diffusion coefficient in the vicinity of the critical point. This is consistent with the prediction of dynamic scaling $\mathcal{D} \sim (T - T_c)^{-\nu/2}$, where $\nu = 1/2$ in the mean-field approximation. For large temperatures the leading deviation from the $T \rightarrow \infty$ -limit is linear in βJ , i.e. [92, 97]

$$\mathcal{D}(T) = \mathcal{D}(\infty)(1 + \mathcal{D}^{(1)}\beta J), \quad (\text{B.57})$$

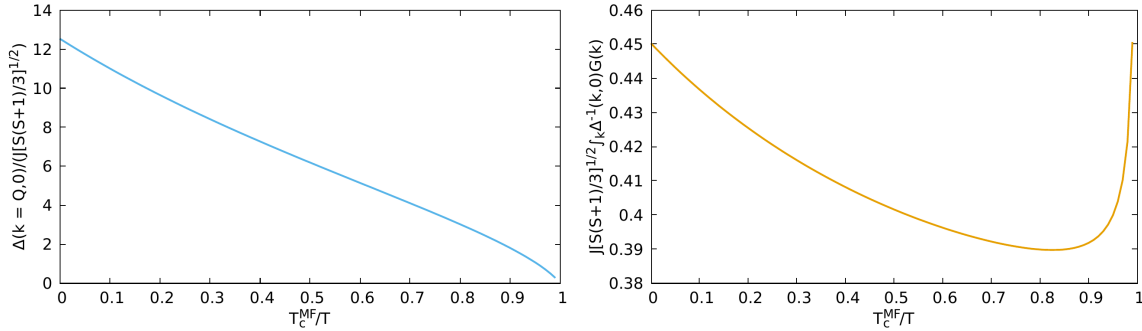


Figure B.11: Dimensionless staggered relaxation rate $\Delta(\mathbf{Q}, 0)$ (left) and zero-frequency autocorrelation function $S(\mathbf{r} = \mathbf{0}, 0) \propto \int_{\mathbf{q}} \frac{G(\mathbf{q})}{\Delta(\mathbf{q}, 0)}$ (right) as a function of T_c^{MF}/T for a nearest neighbor Heisenberg antiferromagnet on the simple cubic lattice from the numerical solution of (3.50), using again a mean-field ansatz for the static susceptibility $G(\mathbf{q})$.

with $\mathcal{D}^{(1)} > 0$. Its numerical value depends on the lattice and ansatz for $G(\mathbf{q})$. Note that $\mathcal{D}^{(1)}$ can be also calculated by expanding the right-hand side of (3.77) to next-leading-order in βJ . This yields a set of linear equations for the corrections to the Fourier amplitudes in $\Delta(\mathbf{k}, i\omega)$, with additional harmonics, i.e. form factors, generated at this order. In Fig. B.11 we show the temperature dependence of two other quantities, the relaxation rate of the staggered magnetization $\Delta(\mathbf{k} = \mathbf{Q}, 0)$ and the autocorrelation function at vanishing frequency. Both functions are consistent with the scaling behavior found in the vicinity of T_c . Interestingly $S(\mathbf{0}, 0)$ is a non-monotonous function of T , first decreasing down to a global minimum, before it diverges for $T \rightarrow T_c$. This may be explained by two competing processes, first the increase of the diffusion coefficient, which drives the diminishing of $S(\mathbf{0}, 0)$ for high to intermediate temperatures, before this trend is reversed by the singularities of $G(\mathbf{Q})$ and $\Delta^{-1}(\mathbf{Q}, 0)$ contained in the product $\frac{G(\mathbf{Q} + \delta\mathbf{q})}{\Delta(\mathbf{Q} + \delta\mathbf{q}, 0)}$. The described T -dependence is in qualitative agreement with a moment-based calculation [202]. Such a non-monotonous behavior does not occur for the ferromagnet, where $\Delta(\mathbf{k})^{-1}$ and $G(\mathbf{k})$ are peaked in the same region, implying thus a monotonous growth of $S(\mathbf{r} = \mathbf{0}, 0)$ as T is lowered.

B.4 Spin dynamics in the critical region

B.4.1 Dynamic scaling in low-dimensional antiferromagnets

Analogous to ferromagnets we want to briefly discuss the low-temperature spin dynamics of antiferromagnets below three dimensions. Like in $d = 3$ one has to consider two different dissipation energies for fluctuations around $\mathbf{q} = \mathbf{0}$ and $\mathbf{q} = \mathbf{Q}_N$. On the square lattice the order parameter susceptibility χ_N and correlation length ξ exhibit the same leading exponential divergence [164, 175, 203, 204, 205] as for the ferromagnet. For the antiferromagnetic chain, one should keep in mind that only systems with half-integer spin are gapless with $\xi^{-1} \sim T \rightarrow 0$, while for integer spin the correlation length and thus the Néel susceptibility remain finite [164, 196, 197]. However, even half-integer chains do not exhibit true magnetic order with a finite order parameter, as can be inferred from a simple spin wave analysis [16]. Ignoring these subtleties in $d = 1$ for the moment, as was done by Takahashi in his modified spin-wave theory [205], and working with naive expressions for χ_N , ξ , we write in

reduced dimensions

$$\Delta(\mathbf{k}, i\omega) = \tau^{-1} A_0(k\xi, i\omega\tau), \quad (\text{B.58})$$

$$\Delta(\mathbf{k} + \mathbf{Q}, i\omega) = \tau^{-1} A_N(k\xi, i\omega\tau). \quad (\text{B.59})$$

The characteristic hydrodynamic times are given by

$$\tau = \sqrt{\frac{2\chi\xi}{aT}}, \quad d = 1 \quad (\text{B.60})$$

$$\tau = \sqrt{\frac{2\chi\xi^2}{a^2T}}, \quad d = 2, \quad (\text{B.61})$$

where χ is the non-singular uniform susceptibility and we used that $[\chi^{-1} - \chi_N^{-1}]^{-1} \approx \chi$ leading to the same τ for fluctuations near $\mathbf{0}$ and \mathbf{Q} . In one dimension, where $\xi \sim T^{-1}$ [197], the dynamic exponent $z = 1$ agrees with the result of modified spin-wave theory [205], in line with the naive expression for the magnon dispersion. On the other hand, in $d = 2$, we have that $\tau \sim T^{-1/2}\xi \sim \xi \ln^{1/2}(\xi/a)$, which coincides with the Ornstein-Zernicke result for the ferromagnet and is at odds with modified spin-wave theory [205]. One concludes that it is impossible to obtain simultaneously dynamic scaling for the two-dimensional ferro- and antiferromagnets with a plain integer z from our equations. Note that the shape of τ in $d = 2$ agrees with an RG analysis by Chakravarty *et al.* [203]. The integral equations determining the above scaling functions are explicitly given by

$$A_0(x, iy) = \int \frac{d^d r}{(2\pi)^d} g(r) g(|\mathbf{x} + \mathbf{r}|) \frac{[g^{-1}(r) - g^{-1}(|\mathbf{x} + \mathbf{r}|)]^2}{A_N(r, iy) + |y|}, \quad (\text{B.62})$$

$$A_N(x, iy) = g^{-1}(x) \int \frac{d^d r}{(2\pi)^d} \left(g(|\mathbf{x} + \mathbf{r}|) \frac{1}{A_0(r, iy) + |y|} + g(r) \frac{1}{A_N(r, iy) + |y|} \right), \quad (\text{B.63})$$

where the static scaling functions in the vicinity of \mathbf{Q}_N are assumed to be [205, 206]

$$g(x) = [1 + x^2]^{-1}, \quad d = 1 \quad (\text{B.64})$$

$$g(x) = \frac{\ln(x + \sqrt{x^2 + 1})}{x\sqrt{x^2 + 1}}, \quad d = 2. \quad (\text{B.65})$$

From the analytic continuation of their solution one obtains then the scaling functions

$$\Phi_0(x, y) = \frac{1}{y} \text{Im} \left(\frac{A_0(x, y + i0)}{A_0(x, y + i0) - iy} \right), \quad (\text{B.66})$$

$$\Phi_N(x, y) = \frac{1}{y} \text{Im} \left(\frac{A_N(x, y + i0)}{A_N(x, y + i0) - iy} \right). \quad (\text{B.67})$$

We did not explicitly evaluate the self-consistency equations, but it is clear that the low-frequency ($\omega\tau \rightarrow 0$) asymptotics are characterized by diverging static dissipation energies, in complete analogy to the ferromagnet. For large $k\xi$ one expects that the scaling functions Φ_0 , Φ_N in $d = 1$ feature broad peaks dispersing as $y_* \propto x$. In two dimensions the x -dependence of this peak position will be due to the logarithmic correction in τ more complicated, i.e. $y_* \sim x \ln^{1/2}(x)$, in order to obtain $\omega_*(k) \sim k$ at $T = 0$, see also appendix B.4.2. In $d = 2$ the damping is probably overestimated, similar to mode-coupling theory [117]. A vanishing damping is predicted by modified spin-wave theory ($d = 1, 2$) [205] and Schwinger-Boson mean-field theory ($d = 2$) [67], where the ratio of width to excitation

energy scales as $(k\xi)^{-1}$ [206], similar to ferromagnets. The mean-field theory was shown to be equivalent to Takahashi's spin-wave approach [205]. In contrast to the ferromagnet, neither the exact ground state nor the low-lying excited eigenstates are exactly known, which makes arguing in favor of a vanishing width much harder. More recent calculations indeed show, that the zero-temperature dynamic structure factor of a square-lattice antiferromagnet hosts high-energy continua besides a sharp one-magnon peak with reduced spectral weight [191, 192, 207]. These continua are associated with multimagnon processes and more recently are also interpreted in terms of deconfined fractionalized quasiparticles, known as spinons [191]. For $d = 1$ the naive assumptions of spin wave theory are inherently invalid [16]. In fact, expansions of $S(\mathbf{k}, \omega)$ at $T = 0$ in terms of spinon-continua are available for the integrable $S = 1/2$ -chain, thus definitely ruling out sharp peaks [208].

B.4.2 Zero-temperature solution for low-dimensional Heisenberg magnets

We briefly discuss the solution implied by (3.46) for $S(\mathbf{k}, \omega)$ in the limit $T \rightarrow 0$. First we note that for $\xi \rightarrow \infty$ the static susceptibility in $d \leq 2$ dimensions satisfies a sum rule

$$T \int_{\mathbf{q}} G(\mathbf{q}) = \text{const.} \equiv (\tilde{S})^2. \quad (\text{B.68})$$

Furthermore the inverse correlation length acts in this limit as an cutoff for all momentum integrations around the peaks of the static susceptibility. For any function in the integrand $f(\mathbf{q}, \mathbf{k})$ that is slowly varying for $|\mathbf{q} - \mathbf{Q}| \lesssim \xi^{-1}$, one can therefore approximate

$$T \int_{\mathbf{q}} G(\mathbf{q}) f(\mathbf{q}, \mathbf{k}) \approx f(\mathbf{Q}, \mathbf{k}) (\tilde{S})^2. \quad (\text{B.69})$$

On the other hand by rewriting the modified kernel in (3.46) as

$$V(\mathbf{k}, \mathbf{q}) = \frac{T G^{-1}(\mathbf{k})}{2} [G^{-1}(\mathbf{q}) - G^{-1}(\mathbf{q} + \mathbf{k})][G(\mathbf{q} + \mathbf{k}) - G(\mathbf{q})], \quad (\text{B.70})$$

and using (B.69) one obtains

$$\begin{aligned} \Delta(\mathbf{k}, i\omega) &= -\frac{G^{-1}(\mathbf{k})}{2} \left(\frac{[G^{-1}(\mathbf{Q}) - G^{-1}(\mathbf{Q} + \mathbf{k})]}{|\omega| + \Delta(\mathbf{k} + \mathbf{Q}, i\omega)} + \frac{[G^{-1}(\mathbf{Q}) - G^{-1}(\mathbf{Q} + \mathbf{k})]}{|\omega| + \Delta(\mathbf{Q}, i\omega)} \right) (\tilde{S})^2 \\ &= \frac{G^{-1}(\mathbf{k}) G^{-1}(\mathbf{k} + \mathbf{Q}) (\tilde{S})^2}{2} \left(\frac{1}{|\omega|} + \frac{1}{|\omega| + \Delta(\mathbf{k} + \mathbf{Q}, i\omega)} \right), \end{aligned} \quad (\text{B.71})$$

where we used that $\Delta(\mathbf{Q}, i\omega) = 0$. Furthermore, by considering the equation for $\mathbf{k} + \mathbf{Q}$ we see that, due to $2\mathbf{Q}$ being a reciprocal lattice vector, the solution obeys

$$\Delta(\mathbf{k} + \mathbf{Q}, i\omega) = \Delta(\mathbf{k}, i\omega). \quad (\text{B.72})$$

By defining the 'dispersion'

$$\epsilon(\mathbf{k}) = \sqrt{G^{-1}(\mathbf{k}) G^{-1}(\mathbf{k} + \mathbf{Q})} (\tilde{S})^2, \quad (\text{B.73})$$

and the dimensionless frequency $\tilde{\omega} = \omega / \epsilon(\mathbf{k})$ we thus find that

$$\Delta(\mathbf{k}, i\omega) = \epsilon(\mathbf{k}) \tilde{\Delta}(i\tilde{\omega}). \quad (\text{B.74})$$

Note that for $|\mathbf{k} - \mathbf{Q}|a \ll 1$ or $ka \ll 1$, we infer from $\epsilon(\mathbf{k})$ the already obtained scaling of the characteristic energies with either $z = 2$ (FM) or $z = 1$ (AF). The scaling function satisfies thus

$$\tilde{\Delta}(i\tilde{\omega}) = \frac{1}{2} \left(\frac{1}{|\tilde{\omega}|} + \frac{1}{|\tilde{\omega}| + \tilde{\Delta}(i\tilde{\omega})} \right) \leftrightarrow \Delta(i\tilde{\omega})^2 + \left(|\tilde{\omega}| - \frac{1}{2|\tilde{\omega}|} \right) \Delta(i\tilde{\omega}) - 1 = 0. \quad (\text{B.75})$$

Hence

$$\Delta(i\tilde{\omega}) = \frac{1}{2} \left(\frac{1}{2|\tilde{\omega}|} - |\tilde{\omega}| \right) + \sqrt{\frac{1}{4} \left(\frac{1}{2|\tilde{\omega}|} - |\tilde{\omega}| \right)^2 + 1}. \quad (\text{B.76})$$

Taking the analytic continuation one therefore finds

$$\Delta(\tilde{\omega}) = \frac{i}{2} \left(\frac{1}{2\tilde{\omega}} + \tilde{\omega} \right) + \sqrt{-\frac{1}{4} \left(\frac{1}{2\tilde{\omega}} + \tilde{\omega} \right)^2 + 1}. \quad (\text{B.77})$$

The only way to obtain a finite real part $\Delta_R(\tilde{\omega}) > 0$, is by ensuring that the square-root on the right-hand side of (B.77) is real and positive. For large and small $\tilde{\omega}$ one finds that its discriminant is always negative, implying thus a purely imaginary solution. Hence the window where it is positive is determined by

$$\frac{1}{4} \left(\frac{1}{2\tilde{\omega}} + \tilde{\omega} \right)^2 = 1 \leftrightarrow \tilde{\omega}^4 - 3\tilde{\omega}^2 + \frac{1}{4} = 0, \quad (\text{B.78})$$

so that

$$\frac{3}{2} - \sqrt{2} \leq \tilde{\omega}^2 \leq \frac{3}{2} + \sqrt{2}, \quad (\text{B.79})$$

i.e. $1 - 1/\sqrt{2} \lesssim \tilde{\omega} \leq 1 + 1/\sqrt{2}$. In this region of frequencies $S(\mathbf{k}, \omega)$ is non-zero and forms a broad continuum. Note that outside this window, there is no δ -distribution implied by $\Delta_I(\tilde{\omega}) - \tilde{\omega} = 0$, since

$$\tilde{\omega} - \frac{1}{2} \left(\frac{1}{2\tilde{\omega}} + \tilde{\omega} \right) \mp \sqrt{\frac{1}{4} \left(\frac{1}{2\tilde{\omega}} + \tilde{\omega} \right)^2 - 1} \neq 0, \quad (\text{B.80})$$

where \mp depends on the choice of branch for the square-root in order to reproduce the correct small or large- $\tilde{\omega}$ behavior of $\Delta_I(\tilde{\omega})$. In Fig. B.12 we show our result for the frequency dependence of $S(\mathbf{k}, \omega)$, namely the shape-function

$$\Psi(\tilde{\omega}) = \frac{\tilde{\Delta}_R(\tilde{\omega})}{(\tilde{\omega} - \Delta_I(\tilde{\omega}))^2 + \tilde{\Delta}_R(\tilde{\omega})^2}. \quad (\text{B.81})$$

Note that at $T = 0$ the detailed-balance factor $[1 - \exp(-\beta\omega)]^{-1}$ is simply a step function $\Theta(\omega)$, in contrast to the classical expression, which is valid only for $\omega/T \ll 1$.

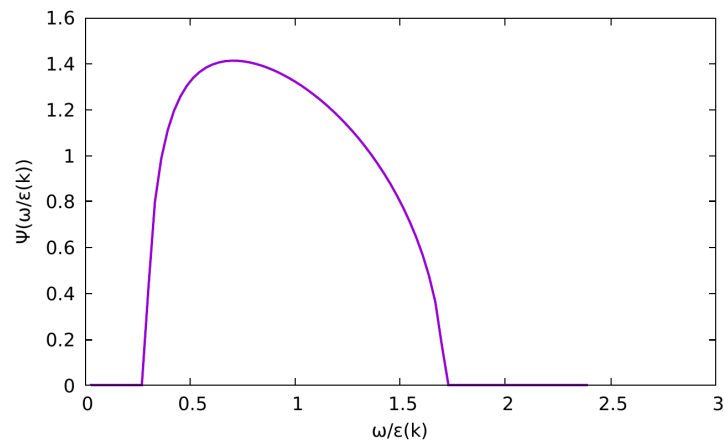


Figure B.12: Our $T = 0$ -solution for the frequency dependence of the line-shape, given by (B.81). It does not contain sharp peaks that are implied by well-defined magnon excitations which are at least anticipated in two dimensions and for the linear ferromagnet.

Appendix C

Additional calculations concerning thermodynamics

C.1 Fixed point in $d \geq 3$

We want to give a short discussion of the flow equations in the Level 2-truncation (4.34) and (4.35), using rescaled variables in order to relate them to an ordinary RG flow for the relevant couplings in the corresponding classical field theory. For simplicity, let us assume a non-frustrated model, $J_{\min} = -J_{\max}$, e.g. with nearest-neighbor coupling on a d -dimensional hypercubic lattice, $J(\mathbf{k}) = 2dJ\gamma(\mathbf{k})$, $J_{\min} = -2d|J|$. Dimensionless vertices are defined as follows

$$r_\Lambda = \frac{\Sigma_\Lambda}{2d|J|} - 1, \quad u_\Lambda = \frac{5U_\Lambda T}{6(2d|J|)^2}, \quad v_0 = \frac{7V_0 T^2}{6(2d|J|)^3}. \quad (\text{C.1})$$

Using a Litim-cutoff (4.9), the Level-2 flow equations (4.34) and (4.35) thus become

$$\partial_\Lambda r_\Lambda = -u_\Lambda I_\Lambda \left[\frac{1}{[1 + \Lambda + r_\Lambda]^2} - \frac{1}{[1 - \Lambda + r_\Lambda]^2} \right], \quad (\text{C.2})$$

$$\partial_\Lambda u_\Lambda = -\frac{v_0 I_\Lambda}{2} \left[\frac{1}{[1 + \Lambda + r_\Lambda]^2} - \frac{1}{[1 - \Lambda + r_\Lambda]^2} \right] + \frac{22u_\Lambda^2 I_\Lambda}{5} \left[\frac{1}{[1 + \Lambda + r_\Lambda]^2} - \frac{1}{[1 - \Lambda + r_\Lambda]^3} \right], \quad (\text{C.3})$$

where

$$I_\Lambda = \int_\Lambda^1 d\epsilon \rho(\epsilon), \quad (\text{C.4})$$

yields the number of states with energies between the lower / upper band edge and the cutoff Λ . For the further analysis of fixed points we are interested in the flow for $\Lambda \rightarrow 1$, such that the interval at the boundaries is very slim. In that case, one can use for the behavior of the density of states in the vicinity of the edges $\rho(\epsilon) \approx (1 - \epsilon)^{(d-2)/2}$ and therefore

$$I_\Lambda \approx I_d (1 - \Lambda)^{d/2}, \quad (\text{C.5})$$

with $I_d = \frac{K_d (2d)^{d/2}}{d}$ and $K_d = \frac{1}{2^{d-1} \pi^{d/2} \Gamma(d/2)}$. Introducing now the logarithmic RG time l via $\Lambda = 1 - e^{-2l}$ and rescaled variables according to the usual procedure [3]

$$r_l = e^{2l} r_\Lambda, \quad u_l = e^{(4-d)l} I_d u_\Lambda, \quad v_l = e^{(6-2d)l} I_d^2 v_0 \quad (\text{C.6})$$

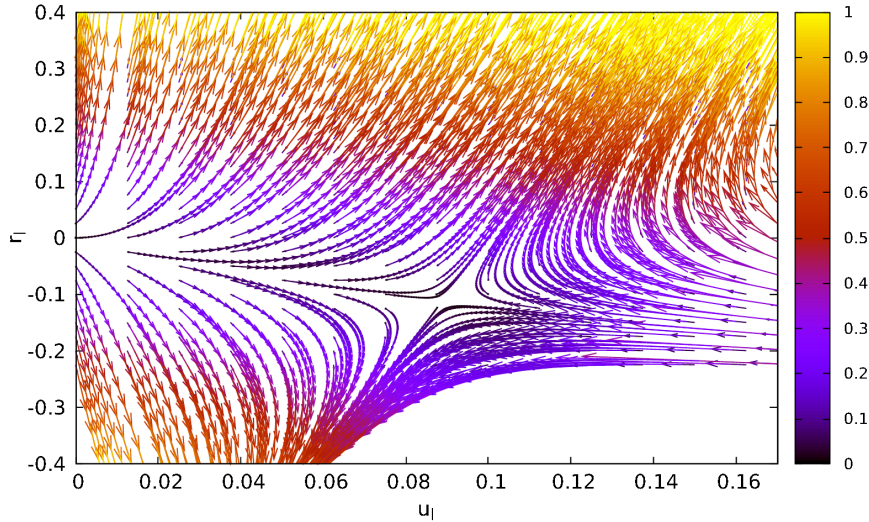


Figure C.1: Flow of the rescaled couplings for $l \rightarrow \infty$ in $d = 3$ dimensions, for $S = 1/2$ and the temperature $T = 0.2 T_c^{\text{MF}}$.

we obtain in the asymptotic limit $e^{-2l} \ll 1$ the following RG equations

$$\partial_l r_l = 2r_l + \frac{2u_l}{[1+r_l]^2}, \quad (\text{C.7})$$

$$\partial_l u_l = (4-d)u_l + \frac{v_l}{[1+r_l]^2} - \frac{44u_l^2}{5[1+r_l]^3}, \quad (\text{C.8})$$

$$\partial_l v_l = (6-2d)v_l. \quad (\text{C.9})$$

Here we have already dropped the high-energy modes at the upper band edge, whose contribution is negligibly small in the $l \rightarrow \infty$ -limit, in contrast to low energy fluctuations near the ordering vector. The resulting differential equations are thus autonomous in l , as expected after the rescaling. Fixed points (r_*, u_*, v_*) of these equations are determined by a simultaneously vanishing flow of all couplings, $\partial_l(r_l, u_l, v_l) = 0$. One sees that above three dimensions the six-point vertex is always irrelevant and thus negligible, whereas for $d = 3$ it is marginal. Thus one obtains the same RG flow equation as for the three-component ϕ^4 -model in $d > 3$. Besides the trivial Gaussian fixed point at $\tilde{r}_* = \tilde{u}_* = 0$, which describes the critical properties for $d > 4$ but is unstable in $d < 4$, one finds for $d < 4$ the Wilson-Fisher fixed point with $\tilde{r}_* < 0$, $\tilde{u}_* > 0$ and one attractive scaling variable, characterizing the true critical behavior below the upper critical dimension [3]. In $d = 3$, we have a non-flowing six-point coupling $v_l = v_0$, thus introducing a third direction, perpendicular to the (r_l, u_l) -plane. Indeed we find for $T < T_c$, i.e. sufficiently small v_0 , the Wilson-Fisher fixed point with $\tilde{r}_* < 0$ and $\tilde{u}_* > 0$ and a relevant scaling variable with positive RG eigenvalue y_t . The repulsive Gaussian fixed point is shifted to slightly positive values of \tilde{r}_* . Slightly above 3 dimensions, where v_l is irrelevant, one finds $\tilde{r}_* \approx -0.102$ and $\tilde{u}_* = 0.197$ with the RG matrix

$$\mathcal{R} = \begin{pmatrix} 2 - \frac{4\tilde{u}_*^*}{[1+\tilde{r}_*^*]^3} & \frac{2}{[1+\tilde{r}_*^*]^2} \\ \frac{132(\tilde{u}_*^*)^2}{5[1+\tilde{r}_*^*]^4} & 1 - \frac{88\tilde{u}_*^*}{5[1+\tilde{r}_*^*]^3} \end{pmatrix} \approx \begin{pmatrix} 1.55 & 2.48 \\ 0.27 & -0.99 \end{pmatrix}. \quad (\text{C.10})$$

The positive eigenvalue is then given by $y_t \approx 1.79$, implying a critical susceptibility exponent $\gamma = 2/y_t \approx 1.12$ and therefore $\nu \approx 0.56$ for ξ . This is simply the result of the one-loop RG approximation [3] evaluated at $\epsilon = 1$, and hence it is not surprising, that it deviates significantly from the established value $\gamma \approx 1.4$ in three dimensions [26]. The RG flow of the rescaled couplings in the (r_t, u_t) -plane is depicted in Fig. C.1 for $T = 0.2 T_c^{\text{MF}}$.

C.2 Flow equation of static four-point vertex at finite S

For the sake of completeness we provide the additional quantum diagrams in the flow of the classical four-point vertex $\Gamma_\Lambda^{\alpha\alpha\gamma\gamma}(\mathbf{k}_1, \mathbf{k}_2, \mathbf{k}_3, \mathbf{k}_4)$. The respective diagrams are depicted in Fig. C.2.

C.3 Integration of flow using self-consistent high-temperature spin dynamics

Besides the high temperature/frequency expansion for $\tilde{\Pi}_\Lambda(\mathbf{k}, i\omega)$ we have also tried a different, more elaborate ansatz, namely the solution of the self-consistency equation (3.50), derived by us for arbitrary frequencies. In this process we make however another approximation, by considering solely the $T = \infty$ -solution for the dissipation energy $\Delta_\Lambda(\mathbf{k}, i\omega)$, i.e. neglecting its temperature dependence. This is mostly done out of convenience, because in this case $\Delta_\Lambda(\mathbf{k}, i\omega)$ can be written as a superposition of a finite number of lattice harmonics, whereas solving for $\Delta_\Lambda(\mathbf{k}, i\omega)$ at arbitrary temperatures requires the calculation of an a priori unknown \mathbf{k} -dependence. Such a simplification has, compared to the high-temperature ansatz for $\tilde{\Pi}_\Lambda(\mathbf{k}, i\omega)$ in (2.123), the advantage that $\Delta_\Lambda(\mathbf{k}, i\omega)$ is always proportional to J_Λ , so that the magnitude of this quantity cannot explode for too low temperatures. Moreover it contains information about dynamics at all timescales, not only the short-time window. Conversely a non-trivial dependence on ω also implies that the frequency sums appearing in the flow equations cannot be evaluated analytically. Hence one has to rely on numerics in this regard too, increasing the computational effort by the number of Matsubara frequencies below a chosen frequency cutoff. Another shortcoming, shared with the high- T and ω -approximation is the absence of any features in the dynamics that can be attributed to a different global sign of J , since all states are equally probable at $T = \infty$. Under this $\{J_i\} \leftrightarrow \{-J_i\}$ symmetry, one cannot for instance distinguish between a frustrated antiferromagnet or a plain ferromagnet with additional couplings to neighbors of higher order. The difference in the response of finite frequency diagrams onto $\Sigma_\Lambda, U_\Lambda$ is then solely determined by purely static numerators in $\tilde{F}_\Lambda(Q)$, whereas the denominators containing $\Delta_\Lambda(\mathbf{k}, i\omega)$ do not depend on the global sign of the exchange coupling.

We have integrated the flow equations numerically, using a linear interaction cutoff (4.4), for nearest neighbor Heisenberg magnets on a simple cubic lattice. As before we do not use the Litim-cutoff, because for intermediate scales, it necessitates solving for a complicated momentum dependence of the dissipation energy, even at $T = \infty$. For the largest frequency we have chosen $\omega_m = 50\pi T$ or $\omega_m = 100\pi T$ and found the difference in outcomes to be negligible, thus confirming convergence. Results for transition temperatures of $S = 1/2$, 1-Heisenberg models are given in Table C.1. The outcomes are quite similar to the previous approximation, except for the $S = 1/2$ -ferromagnet, where this ansatz for the dynamics performs significantly worse. From this we conclude that a simple expression

S	J_1	J_3/J_1	T_c/T_c^{MF}		rel. error / %
			switch	benchmark	switch
1/2	< 0	0	0.521	0.559	6.8
1/2	> 0	0	0.641	0.629	1.9
1	< 0	0	0.649	0.650	0.2
1	> 0	0	0.698	0.684	2.0

Table C.1: Results for T_c as in Table 4.3, but now the self-consistent ansatz for $\tilde{\Pi}_\Lambda(K)$ from the integral equation (3.44) at $T = \infty$ is employed for the numeric integration of Eq. (4.45) and Eq. (4.46).

S	J	T_c/T_c^{MF}		rel. error / %
		switch	benchmark	switch
1/2	< 0	0.624	0.630	1.0
1/2	> 0	0.708	0.688	2.9
1	< 0	0.723	0.710	1.8
1	> 0	0.759	0.738	2.8
3/2	< 0	0.755	0.739	2.2
3/2	> 0	0.773	0.754	2.5
∞		0.793	0.770	3.0

Table C.2: Critical temperatures for the nearest neighbor spin- S Heisenberg model on a body-centered cubic lattice. Benchmark values are taken from an Padé-approximated high temperature series expansion [182].

for the spin dynamics in Matsubara representation like (2.123) is quite sufficient to obtain sensible results for the thermodynamics of non-frustrated systems in $d = 3$.

C.4 T_c on other cubic lattices

In these section results for T_c of isotropic magnets on other cubic Bravais lattices in three dimensions, namely the bcc and fcc lattice, are presented. They are obtained from a numerical integration of the flow equations (4.57), using the interaction-switch cutoff (4.4) and approximating the dynamic polarization $\tilde{\Pi}_\Lambda(K)$ by its high-frequency and temperature limit (2.123).

C.4.1 Magnets with nearest-neighbor interaction on a bcc lattice

The exchange coupling on a body-centered cubic lattice is given by

$$J(\mathbf{k}) = 8J\gamma^{\text{bcc}}(\mathbf{k}), \tag{C.11}$$

where the next-neighbor coupling J can be positive or negative, since the lattice is bipartite, thus being compatible with Néel order for $J > 0$. Note that in momentum space the Néel state is characterized by an instability at the ordering vector $\mathbf{Q} = \frac{2\pi}{a}(1, 1, 1)$. The

S	J	T_c/T_c^{MF}		rel. error / %
		switch	benchmark	switch
1/2	< 0	0.666	0.669	0.5
∞	< 0	0.815	0.795	2.5

Table C.3: Critical temperatures for the nearest neighbor Heisenberg ferromagnet on a face-centered cubic lattice with $S = 1/2$ and $S = \infty$. Benchmark values are taken from an extrapolated high temperature series expansion for $S = 1/2$ [210] and a Monte Carlo simulation for the classical model [211].

momentum dependence of the corresponding polarization function is

$$\tilde{\Omega}_\Lambda(\mathbf{k}) = \frac{4G_\Lambda^{-1}(\mathbf{k})(6\Lambda Jb'_0)^2}{9T^3} \left(1 - \gamma^{\text{bcc}}(\mathbf{k})\right). \quad (\text{C.12})$$

Critical temperatures for both signs of J and different values of S are shown in Table C.4.1. One achieves an accuracy that is comparable to the results for the sc lattice. The case $S = 1/2$ with $J < 0, > 0$ was also investigated by means of the PF-FRG in Ref. [209]. The deviations from the benchmark values were found to be larger than in our method, even within a more sophisticated two-loop truncation [209].

C.4.2 Ferromagnet with next-neighbor interaction on a fcc lattice

The exchange interaction on the face-centered cubic lattice is given by

$$J(\mathbf{k}) = 12J\gamma^{\text{fcc}}(\mathbf{k}), \quad (\text{C.13})$$

with the nearest-neighbor form factor

$$\gamma^{\text{fcc}}(\mathbf{k}) = \frac{1}{3} \left[\cos(k_x a) \cos(k_y a) + (x \leftrightarrow z) + (y \leftrightarrow z) \right]. \quad (\text{C.14})$$

We consider only a ferromagnetic coupling $J < 0$, because the lattice is not bipartite. As a consequence one cannot construct a Néel state with a finite staggered magnetization. Instead the exchange coupling assumes for $J > 0$ its global minimum on a continuous manifold in \mathbf{k} -space, namely $\mathbf{Q}(x)a = (2\pi, x, 0)$, $x \in [0, \pi]$ [156]. In the light of this degeneracy our employed approximations seem hardly appropriate for the antiferromagnet. The dynamic polarization is proportional to

$$\tilde{\Omega}_\Lambda(\mathbf{k}) = \frac{2G_\Lambda^{-1}(\mathbf{k})(6\Lambda Jb'_0)^2}{3T^3} \left(1 - \gamma^{\text{fcc}}(\mathbf{k})\right). \quad (\text{C.15})$$

Results for the critical temperature of the $S = 1/2$ and classical ferromagnet are displayed in Table C.4.2. The accuracy is again quite similar to the outcomes for the bcc and sc lattices.

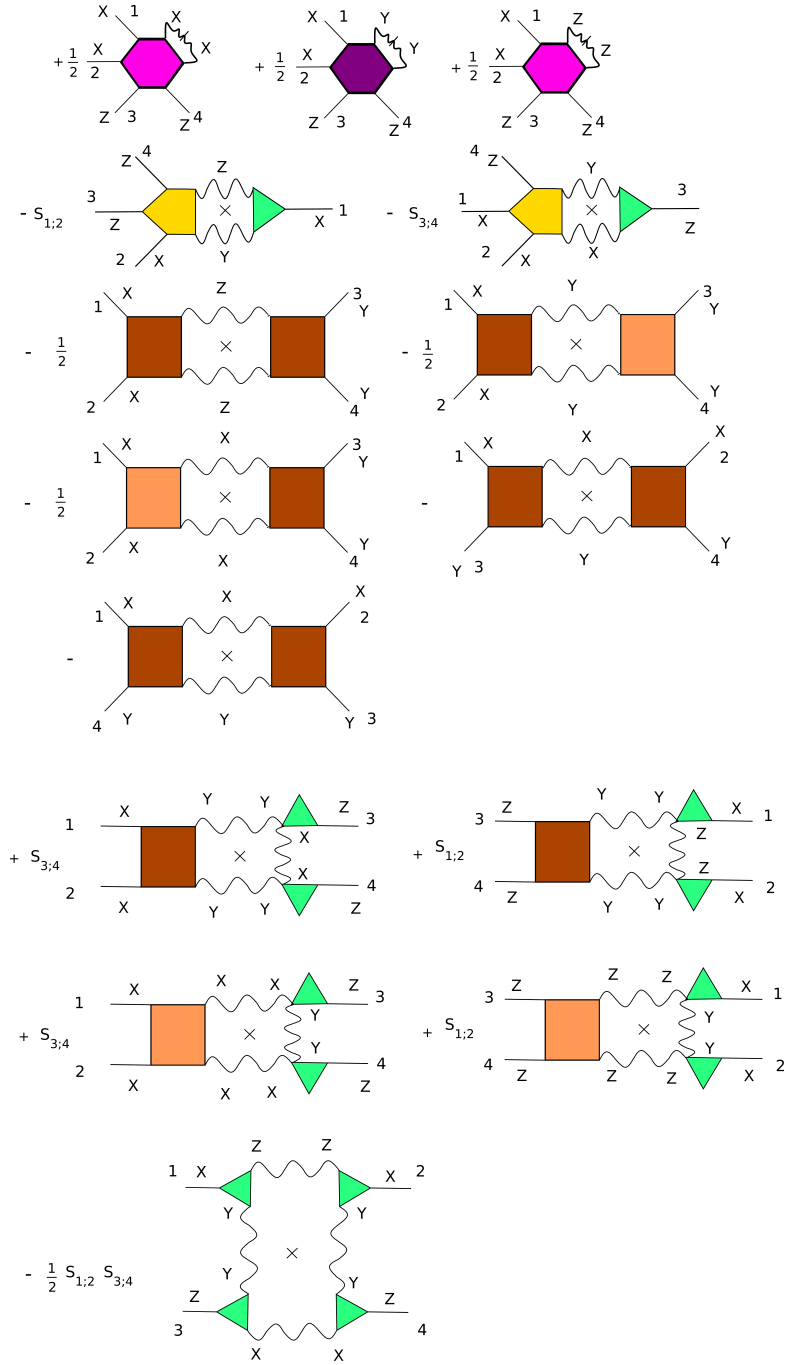


Figure C.2: Quantum diagrams in the flow equation of the mixed static 4-legged vertex $\Gamma_{\Lambda}^{xxxx}(\mathbf{k}_1, \mathbf{k}_2, \mathbf{k}_3, \mathbf{k}_4)$. $S_{K_1\dots}; Q_{1\dots}$ denotes here again the action of a symmetrization operator for two different tupels.

Appendix D

Deutsche Zusammenfassung

D.1 Funktionale Spin-Renormierungsgruppe

In dieser Arbeit befassen wir uns mit der Berechnung der statischen und dynamischen Eigenschaften isotroper Heisenberg-Paramagneten mithilfe einer neuen Implementierung der Funktionalen Renormierungsgruppe (FRG) für Quantenspinsysteme. Das untersuchte Modell ist explizit gegeben durch

$$\mathcal{H} = \frac{1}{2} \sum_{i,j} J_{ij} \mathbf{S}_i \cdot \mathbf{S}_j, \quad (\text{D.1})$$

wobei $\mathbf{S}_i = (S_i^x, S_i^y, S_i^z)$ Vektoroperatoren auf einem Bravais-Gitter mit Plätzen $i = 1 \dots N$ sind, die die Drehimpulsvertauschungsrelationen erfüllen

$$[S_i^\alpha, S_j^\gamma] = i \delta_{ij} \epsilon_{\alpha\gamma\sigma} S_i^\sigma, \quad (\text{D.2})$$

welche ursächlich für eine nichttriviale Quantendynamik sind. J_{ij} ist die Austauschkopplung, dessen Ursprung rein quantenmechanischer Natur ist, eine Folge des Pauli-Prinzips für ununterscheidbare Fermionen. Dieses effektive Modell ist in der Lage viele Eigenschaften realer magnetischer Systeme, insbesondere Isolatoren, zu erklären.

Unser Zugang zur nicht-perturbativen Untersuchung dieses Modells basiert auf der funktionalen Spin-Renormierungsgruppe (SFRG), die zuerst von Krieg und Kopietz formuliert und verwendet wurde [1, 2]. Man beachte, dass die SFRG komplett ohne die sonst üblichen Pfadintegrale auskommt. Die Hauptidee besteht darin J_{ij} in \mathcal{H} durch eine deformierte Kopplung J_{ij}^Λ zu ersetzen und dann die Evolution der verbundenen zeitgeordneten Spin-Korrelationsfunktionen $G_\Lambda^{(n)}$ in Imaginärzeit mit dem Flussparameter Λ , ausgehend von einer exakt oder kontrolliert lösbaren Anfangsbedingung wie $J_{ij}^{\Lambda_0} = 0$, zu berechnen. Die fließenden Korrelationsfunktionen $G_\Lambda^{(n)}$ können dabei durch Ableitungen eines erzeugenden Funktionals

$$\mathcal{G}_\Lambda[\mathbf{h}] = \ln \text{Tr} \left(\mathcal{T} \left(e^{(h,S) - \int_0^\beta d\tau \mathcal{J}_\Lambda(\tau)} \right) \right), \quad (\text{D.3})$$

nach passend eingeführten Quellenfelder \mathbf{h} ausgedrückt werden. Von besonderem Interesse ist die Zweipunktfunktion oder Propagator, aus dem bei $\omega = 0$ Ordnungstendenzen, z.B. Temperaturen für Phasenübergänge, als auch für $\omega \neq 0$ die Spindynamik extrahiert werden können. Das Funktional $\mathcal{G}_\Lambda[\mathbf{h}]$ erfüllt eine komplizierte Integro-Differentialgleichung, welche dessen zweiten Ableitung beinhaltet [1, 2]. Unter der Annahme, dass $\mathcal{G}_\Lambda[\mathbf{h}]$ in Potenzen

der Quellen \mathbf{h} um den physikalischen Punkt $\mathbf{h} = \mathbf{0}$ entwickelt werden kann, ist dessen Flussgleichung equivalent zu einer unendlichen Hierarchie gekoppelter Gleichungen für die $G_\Lambda^{(n)}$, die man mittels Trunkierung näherungsweise lösen kann. Es stellt sich jedoch heraus, dass gewisse Teile der Hierarchie, nämlich solche ohne explizite Schleifenintegration, exakt resummiert werden können. Üblicherweise geschieht dies über eine Reparametrisierung mittels 1-Teilchen (Propagator) irreduzibler (1-PI) Vertizes $\Gamma_\Lambda^{(n)}$ [2, 3]. Diese werden von der subtrahierten Legende-Transformierten, auch bekannt als effektive mittlere Wirkung, erzeugt. Explizit ist dieses neue Funktional gegeben durch

$$\Gamma_\Lambda[\mathbf{m}] = (\mathbf{m}, \mathbf{h}) + \mathcal{G}_\Lambda[\mathbf{h}] - \frac{1}{2}(\mathbf{m}, \mathbf{J}_\Lambda \mathbf{m}). \quad (\text{D.4})$$

Die neue unabhängige Variable \mathbf{m} steht hierbei für die Magnetisierung oder Einpunktfunktion. Die effektive 1-PI Wirkung erfüllt die wohlbekannte Wetterich-Gleichung [1, 4]

$$\partial_\Lambda \Gamma_\Lambda[\mathbf{m}] = \frac{1}{2} \text{Tr} \left(\partial_\Lambda \mathbf{R}_\Lambda [\Gamma_\Lambda^{(2)}[\mathbf{m}] + \mathbf{R}_\Lambda]^{-1} \right), \quad (\text{D.5})$$

die eine Einschleifen-Form besitzt, ebenso die Flussgleichungen der Vertizes. Allerdings hat $\Gamma_\Lambda[\mathbf{m}]$ eine pathologische Anfangsbedingung falls die Kopplung verschwindet, was an einer fehlenden Zweipunkt-Dynamik isolierter Spins liegt.

Um dieses Problem zu umgehen führten Krieg und Kopietz ein Funktional $\mathcal{F}_\Lambda[\mathbf{s}]$ ein, das amputierte Korrelationen $F_\Lambda^{(n)}$ erzeugt und betrachteten die Flussgleichung der Legendre-transformierte $\Phi_\Lambda[\boldsymbol{\eta}]$, die wieder eine Wetterich-Form besitzt, wobei die neuen Vertizes $\Phi_\Lambda^{(n)}$ irreduzibel bezüglich einer (effektiven) Wechselwirkungslinie sind [1, 2]. Diese Vertizes haben eine wohldefinierte Anfangsbedingung und es lässt sich zeigen, dass die Iteration der Hierarchie an Flussgleichungen eine Entwicklung nach Schleifenintegralen, die von Vaks, Larkin und Pikin [5, 6] mittels einer komplizierten diagrammatischen Methode berechnet wurden, reproduziert. Allerdings hat sich ebenso gezeigt, dass für Näherungen, die nicht auf perturbativen Entwicklungen basieren, 1-PI-Zugänge immer bessere Ergebnisse produzieren, sofern die Vergleichsmöglichkeit zwischen beiden Fällen bestand, zum Beispiel bei der Thermodynamik klassischer Spinsysteme [2].

Wir konstruieren, basierend auf diesen Erfahrungen, ein statisch-dynamisches Hybrid-Funktional $\tilde{\mathcal{A}}_\Lambda[\mathbf{h}^c, \mathbf{s}^q]$, welches statische Fluktuationen durch verbundene Korrelationen und damit korrespondierende 1-PI Vertexfunktionen ausdrückt, während der dynamische Sektor weiterhin mittels Amputation behandelt wird. Jedoch wird letztere nicht mittels der fließenden Kopplung wie bei Krieg und Kopietz durchgeführt, sondern mit der inversen statischen Suszeptibilität. Diese Wahl ist motiviert durch die Annahme, dass dynamische Korrelationen $G(\mathbf{k}, i\omega)$ zwischen nicht-erhaltenen Operatoren für $\omega \rightarrow 0$ kontinuierlich in die statische Suszeptibilität $G(\mathbf{k})$ übergehen, was oft als Folge einer postulierten Ergodizität des Systems verstanden wird [28, 36, 72]. Die dazu korrespondierende effektive Wirkung $\tilde{\Gamma}_\Lambda[\mathbf{m}, \boldsymbol{\eta}]$ erfüllt eine modifizierte Wetterich-Gleichung,

$$\begin{aligned} \partial_\Lambda \tilde{\Gamma}_\Lambda[\mathbf{m}^c, \boldsymbol{\eta}^q] &= \frac{1}{2} \text{Tr} (\dot{\mathbf{R}}_\Lambda [\tilde{\Gamma}_\Lambda^{(2)}[\mathbf{m}^c, \boldsymbol{\eta}^q] + \mathbf{R}_\Lambda]^{-1}) + \frac{1}{2} \text{Tr}_{\omega \neq 0} (\tilde{\mathbf{J}}_\Lambda \partial_\Lambda \mathbf{J}_\Lambda) \\ &\quad - \frac{1}{2} \left(\frac{\delta \tilde{\Gamma}_\Lambda}{\delta \boldsymbol{\eta}^q}, [\partial_\Lambda \boldsymbol{\Sigma}_\Lambda] \frac{\delta \tilde{\Gamma}_\Lambda}{\delta \boldsymbol{\eta}^q} \right)_{\omega \neq 0}, \end{aligned} \quad (\text{D.6})$$

die einen zusätzlichen Term mit der Ableitung des statischen 2-Punkt-Vertex Σ_Λ enthält, als Folge der modifizierten Amputation. Die daraus folgende Hierarchie, die im klassischen Limes $S \rightarrow \infty$ in die 1-PI Gleichungen übergeht, dient als Basis für unsere weiteren Rechnungen.

D.2 Spin-Dynamik im Heisenberg-Paramagneten

Auf Basis des Konzepts der Hydrodynamik wird in der Literatur regelmäßig argumentiert, dass bei hohen Temperaturen und verschwindendem Magnetfeld die Langzeitdynamik der Korrelationsfunktionen zwischen Spin-Fluktuationen bei langen Wellenlängen, durch langsam ablaufende, dissipative Prozesse, in der Regel Diffusion des magnetischen Moments, dominiert wird [41]. Hierbei wird *lang* im Vergleich zu mikroskopischen Skalen, die mit Parametern des Hamiltonians wie der Gitterkonstante und Austauschwechselwirkung zusammenhängen, oder emergenten Größen wie der Korrelationslänge ξ , bestimmt. Eine Magnetisierung, die durch eine Störung des thermodynamischen Gleichgewichts erzeugt wird, gehorcht dann der Diffusionsgleichung [35, 41]

$$\partial_t M(\mathbf{k}, t) = -\mathcal{D}k^2 M(\mathbf{k}, t) \quad (\text{D.7})$$

wobei \mathcal{D} der Spin-Diffusionskoeffizient ist und die Lösung dieser Gleichung exponentiell abklingt. Ein analoges Resultat wird für die Korrelationsfunktionen $\langle S^z(\mathbf{k}, t) S^z(\mathbf{k}, 0) \rangle$ postuliert [35]. Der dynamische Strukturfaktor [32]

$$S(\mathbf{k}, \omega) = \int_{-\infty}^{\infty} \frac{dt}{2\pi} \langle S^z(\mathbf{k}, t) S^z(\mathbf{k}, 0) \rangle e^{i\omega t}, \quad (\text{D.8})$$

welcher in Experimenten als Wirkungsquerschnitt inelastischer Neutronenstreuung gemessen werden kann [31, 32], ist dann durch eine bei $\omega = 0$ zentrierte Lorentzkurve gegeben [35, 41]

$$S(\mathbf{k}, \omega) \propto \frac{\mathcal{D}k^2}{(\mathcal{D}k^2)^2 + \omega^2}. \quad (\text{D.9})$$

In der Nähe des kritischen Punktes schrumpft das hydrodynamische Regime aufgrund einer stark anwachsenden Korrelationslänge. Es ist dann durch die Bedingungen $k\xi \ll 1$ und $\omega \ll \tau^{-1}(\xi)$ eingegrenzt, mit einer charakteristischen Zeitaskala $\tau(\xi)$ die für $T \rightarrow T_c$ divergiert. Die hydrodynamische Zerfallsrate von Fluktuation um $\mathbf{k} = \mathbf{0}$ ist dann $\mathcal{D}k^2 \sim (k\xi)^2/\tau$. Im Ferromagneten verschwindet als Folge der Singularität in $\tau(\xi)$ zum Beispiel der Diffusionskoeffizient \mathcal{D} für $T = T_c$. Dies kann als Manifestation des *critical slowing down* aufgefasst werden, ein Phänomen, welches auch erklärt wieso das statische kritische Verhalten für $T_c \neq 0$ unabhängig von dynamischen Eigenschaften ist [3]. Einfachere Theorien [32] postulieren $\mathcal{D} \sim \chi^{-1} \sim \xi^{-2}$, wobei in drei Dimensionen tatsächlich ein schwächeres Verschwinden eintritt, $\mathcal{D} \sim \xi^{-1/2}$. Letzteres ist eine Vorhersage der *Dynamic scaling hypothesis* (DSH) für Phasenübergänge bei endlicher Temperatur in mehr als zwei Dimensionen [58], und ist ein Effekt singularer Fluktuationen des Ordnungsparameters auf die Dynamik [54, 55]. Allgemeiner postuliert *Dynamic scaling*, dass für makroskopisch lange Wellenlängen und Zeiten der dynamische Strukturfaktor proportional zu einer Skalenfunktion ist, in der Frequenz, Impuls sowie die Korrelationslänge nicht unabhängig voneinander, sondern in kombinierten Argumenten auftreten, zum Beispiel $k\xi$ und $\omega/\omega(\mathbf{k})$, wobei $\omega(\mathbf{k}) \sim k^z$ eine charakteristische Frequenz mit dynamischen Exponenten z ist [58]. Der Exponent z bestimmt auch die Singularität der hydrodynamischen Skala $\tau(\xi) \sim \xi^z$, aus der entsprechend das modifizierte Verhalten des Diffusionskoeffizienten für $T \rightarrow T_c$ folgt.

Im Rahmen unserer Implementierung der SFRG wurden Näherungen für den Fluss des dynamischen Zwei-Punkt Vertex $\tilde{\Pi}_\Lambda(K)$, auch Polarisation genannt, hergeleitet. Dabei mussten zahlreiche Bedingungen für eine physikalische Lösung beachtet werden, wie die bereits erwähnte Stetigkeit des Propagators bei verschwindender Frequenz und endlichem

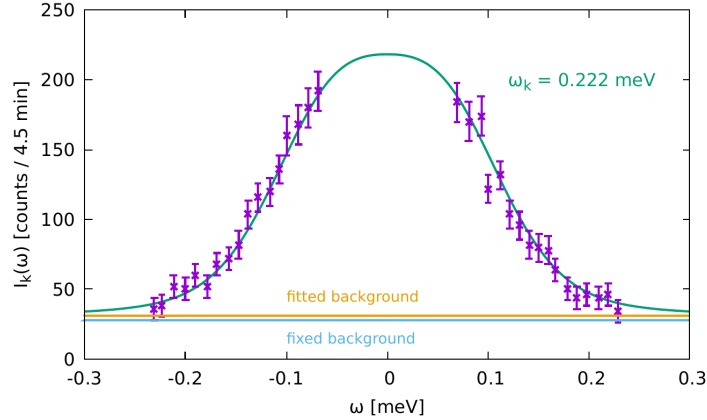


Figure D.1: Fit unseres Ergebnisses für $S(\mathbf{k}, \omega)$ an inelastische Neutronenstreudaten [144] bei konstantem Impuls $k = 0.15 \text{ \AA}^{-1}$ und hinreichend hohen Frequenzen für das ferromagnetische Material EuO bei der kritischen Temperatur $T = T_c$. Mit Genehmigung aus Ref. [11] übernommen © [2022] American Physical Society.

Impuls, als auch die Erhaltung des Gesamtspins, sowie weitere Eigenschaften, wie Positivität der Polarisierung oder korrekte Hochtemperatur-Asymptotiken. Anstatt der Polarisierung ist es zweckmäßiger eine Dissipationsenergie definiert als

$$\Delta(\mathbf{k}, i\omega) = |\omega|G^{-1}(\mathbf{k})\tilde{\Pi}(\mathbf{k}, i\omega), \quad (\text{D.10})$$

zu betrachten, die als charakteristische Zerfallsrate der skizzierten Prozesse im Paramagneten aufgefasst werden kann und mit dem Gedächtniskern in *mode-coupling*-Zugängen eng verwandt ist [74]. Die am intensivsten diskutierte der betrachteten Näherungen ist die Integralgleichung

$$\Delta(\mathbf{k}, i\omega) = \int_{\mathbf{q}} \frac{V(\mathbf{k}, \mathbf{q})}{\Delta(\mathbf{q}, i\omega) + |\omega|}, \quad (\text{D.11})$$

wobei der Integralkern $V(\mathbf{k}, \mathbf{q})$ durch anderweitig bekannte Größen wie $J(\mathbf{q})$ und $G(\mathbf{q})$ bestimmt wird. Man beachte die lokale Struktur dieser Gleichung bezüglich ω , die es zum Beispiel erlaubt die analytische Fortsetzung $\Delta(\mathbf{k}, \omega) = \Delta_R(\mathbf{k}, \omega) + i\Delta_I(\mathbf{k}, \omega)$ direkt auszuführen. Der dynamische Strukturfaktor ergibt sich dann als

$$S(\mathbf{k}, \omega) = \frac{1}{\pi} \frac{\omega G(\mathbf{k})}{1 - e^{-\beta\omega}} \frac{\Delta_R(\mathbf{k}, \omega)}{\Delta_R^2(\mathbf{k}, \omega) + (\omega - \Delta_I(\mathbf{k}, \omega))^2}, \quad (\text{D.12})$$

und Diffusion liegt vor falls

$$\mathcal{D} = \lim_{\omega \rightarrow 0} \lim_{k \rightarrow 0} \Delta(\mathbf{k}, \omega)/k^2, \quad (\text{D.13})$$

nicht-singulär und endlich ist. Anomale Diffusionsprozesse werden durch verschwindende oder divergierende Grenzwerte in der obigen Relation charakterisiert. Diffusion erhalten wir tatsächlich in $d > 2$, in Einklang mit dem hydrodynamischen Postulat [41, 77]. Die Größenordnung des Diffusionskoeffizienten bei $T = \infty$ stimmt dabei mit anderen theoretischen Methoden, wie *mode-coupling theory* [74] oder extrapolierten Hochfrequenz-Entwicklungen [95] sowie experimentellen Studien [122, 123] überein. In reduzierten Dimensionen finden wir anomale Diffusion, sodass \mathcal{D} für $\omega \rightarrow 0$ divergiert. Zumindest in

integriblen Spinketten konvergieren die Ergebnisse verschiedener Methoden Richtung superdiffusives Verhalten [50, 85]. In der kritischen Region ist die Lösung konsistent mit dem postulierten Skalenverhalten der DSH inklusive der selben dynamischen Exponenten für Ferro- und Antiferromagnete in $d > 2$. Dies ist auch das Result anderer theoretischer Methoden [128, 157] und wurde in Streuexperimenten bestätigt [62, 144]. Bei den expliziten Formen der Skalenfunktionen für $\Delta(\mathbf{k}, i\omega)$ und $S(\mathbf{k}, \omega)$ finden wir, für nicht zu kleine Frequenzen oder große Impulse, gute Übereinstimmung mit Approximationen wie einer extrapolierten ϵ -Entwicklung in drei Dimensionen [134]. Im entgegengesetzten Fall treten Abweichungen auf, wie das Verschwinden von $S(\mathbf{k}, 0)$ oder Deformation der Kurven durch nicht-analytische Terme um $\omega = 0$. Diese Beobachtungen bestätigen sich beim Vergleich mit experimentell gemessenen Streuintensitäten [144] und numerischen Spindynamik-Simulationen [155]. Wir identifizieren die Diskrepanzen bei sehr kleinen Frequenzen als Folge der verhältnismäßig einfachen Form der Integralgleichung.

D.3 Thermodynamik oberhalb der kritischen Temperatur

Die thermodynamischen Eigenschaften des Heisenberg-Modells wurden bereits angeschnitten. Wir konzentrieren uns im Folgenden auf die paramagnetische Phase. Für $T \gg |J|$ ist das statische Verhalten des Modells durch exakt bekannte Hochtemperatur-Entwicklungen gegeben, mit dem isolierten magnetischen Moment als führenden Limes. Ein Beispiel ist das Curie-Gesetz für die Suszeptibilität [14, 15]

$$G(\mathbf{k}) = \frac{S(S+1)}{3T}. \quad (\text{D.14})$$

Von tieferen Temperaturen kommend, sollen alle hier diskutierten Modelle einen geordneten Grundzustand haben. Beispiele sind ein Ferromagnet ($\mathbf{Q} = \mathbf{0}$) oder Antiferromagnet ($\mathbf{Q} = \mathbf{Q}_N$) mit Neel-Ordnung auf bipartiten Bravais-Gittern. Die Zustände werden durch einen eindeutigen Ordnungsvektor \mathbf{Q} in der ersten Brillouin-Zone charakterisiert, an dem die Austauschkopplung ihr globales Minimum annimmt. In drei oder mehr Dimension tritt ein Phasenübergang bereits bei einer endlichen Temperatur $T_c \sim |J(\mathbf{Q})|S(S+1)$ auf. In reduzierten Dimensionen, kann es, nach dem Mermin-Wagner Theorem langreichweitige Ordnung nur bei $T = 0$ geben [24]. Das ergibt je nach Art des Modells unterschiedliche Ausdehnungen der symmetrischen Phase. Signalisiert werden kritischen Punkte durch eine Divergenz der statischen Suszeptibilität $G(\mathbf{k})$ beim Ordnungsvektor \mathbf{Q} . Das singuläre Verhalten der Suszeptibilität in der kritischen Region ist durch einen charakteristischen Exponenten γ gekennzeichnet,

$$G(\mathbf{Q}) \propto |T - T_c|^{-\gamma}, \quad (\text{D.15})$$

der nicht nur dem Heisenberg-Modell, sondern allen Modellen gleicher Symmetrieklasse inhärent, also universell ist. Letzteres ist eine Konsequenz langreichweitiger Korrelationen nahe T_c , sodass mikroskopische Details keine Rolle spielen. Für endliche Impulse gilt in guter Näherung [3]

$$G(\mathbf{k} + \mathbf{Q}) \propto \frac{1}{k^2 + \xi^{-2}}, \quad (\text{D.16})$$

wobei $\xi \gg a$ die bereits erwähnte Korrelationslänge ist, die hier $\xi \sim G(\mathbf{Q})^{1/2}$ erfüllt und damit mit dem Exponenten $\nu = \gamma/2$ divergiert. Ergebnisse für T_c und den Exponenten γ sind bereits durch die einfache Molekularfeld-Näherung zu erhalten, bei der \mathcal{H} durch einen Zeeman-Operator mit effektivem selbstkonsistenten Austauschfeld $\sum_j J_{0j} \langle S^z \rangle$ ersetzt

[15]. Unser Ziel ist es über diese Näherung hinauszugehen, die in physikalisch zugänglichen Dimensionen und/oder der diskutierten kritischen Region nur sehr grobe Ergebnisse liefert und für quantitative Vorhersagen damit ungeeignet ist [3, 15].

Wie schon für die Berechnung der Dynamik verwenden wir auch hier das Hybrid-Funktional $\tilde{\Gamma}_\Lambda[\mathbf{m}^c, \boldsymbol{\eta}^q]$. Dabei starten wir zunächst mit einer rein klassischen Näherung, in der Quantenfluktuationen komplett vernachlässigt werden. Dies ist äquivalent zu einem reinen 1-PI Zugang, in dem nur statische Vertexfunktionen mit gerader Zahl an Beinen auftreten. Flussgleichungen für die statische Selbstenergie $\Sigma_\Lambda(\mathbf{k})$ werden gelöst, aus der die statische Suszeptibilität berechnet werden kann

$$G_\Lambda(\mathbf{k}) = \frac{1}{\Sigma_\Lambda(\mathbf{k}) + J_\Lambda(\mathbf{k})}, \quad (\text{D.17})$$

wobei am kritischen Punkt $\Sigma_\Lambda(\mathbf{Q}) + J_\Lambda(\mathbf{Q}) = 0$ gilt. In der simpelsten Näherung wird der 4-Vertex $\Gamma_\Lambda^{(4)}$ nicht renormiert, und wir erhalten keine magnetische Ordnung bei endlichen Temperaturen in $d \leq 4$. Jedoch lassen sich aus dem Kurvenverlauf der inversen Suszeptibilität Ordnungstemperaturen abschätzen, die insbesondere mit einem Bandweiten-Cutoff für die deformierte Kopplung [176, 177]

$$J_\Lambda(\mathbf{k}) = J_{\mathbf{k}} - \Theta(J(\mathbf{k})) (J(\mathbf{k}) - J_{\max}\Lambda) \Theta(J(\mathbf{k}) - J_{\max}\Lambda) \\ + \Theta(-J(\mathbf{k})) (-J(\mathbf{k}) + J_{\min}\Lambda) \Theta(-J(\mathbf{k}) + J_{\min}\Lambda), \quad (\text{D.18})$$

nur um wenige Prozent von etablierten Ergebnissen auf dem kubischen Gitter abweichen. Unter Berücksichtigung des 4-Vertex in einfacher impulsunabhängiger Form $\Gamma_\Lambda^{(4)} \approx U_\Lambda$ und der Näherung $\Gamma_\Lambda^{(6)} \approx V_0$ für den 6-Vertex, erhalten wir zwei gekoppelte Flussgleichungen

$$\partial_\Lambda \Sigma_\Lambda = -\frac{5TU_\Lambda}{6} \int_{\mathbf{q}} \frac{\partial_\Lambda J_\Lambda(\mathbf{q})}{[J_\Lambda(\mathbf{q}) + \Sigma_\Lambda]^2}, \quad (\text{D.19})$$

$$\partial_\Lambda U_\Lambda = T \int_{\mathbf{q}} \dot{G}_\Lambda(\mathbf{q}) \left[\frac{7}{10} V_0 - \frac{11}{3} U_\Lambda^2 G_\Lambda(\mathbf{q}) \right]. \quad (\text{D.20})$$

Die Lösung dieser Gleichungen ergibt wieder ein endliches T_c in drei Dimensionen. Wir finden unter Verwendung eines linearen Deformationsschemas $J_\Lambda(\mathbf{k}) = \Lambda J(\mathbf{k})$ die beste Übereinstimmung mit Benchmarkwerten für T_c auf dem einfach kubischen Gitter [181, 182]. Mithilfe eines Bandweiten-Cutoffs lassen sich aus den obigen Gleichungen zudem die Einschleifengleichungen der Renormierungsgruppe für die $\mathcal{O}(3)$ -Universalitätsklasse, zu der das Heisenberg-Modell gehört, extrahieren. Diese besitzen mit dem Wilson-Fisher Fixpunkt einen nicht-Gausschen Fixpunkt, der die kritischen Eigenschaften des Heisenberg-Modells beschreibt [3].

Zum Abschluss wird die Quantendynamik des Systems durch einen einfachen Ansatz für die Polarisationsfunktion $\tilde{\Pi}_\Lambda(K)$ berücksichtigt,

$$\tilde{\Pi}_\Lambda(\mathbf{k}, i\omega) = \frac{2(b'_0)^2}{T\omega^2} \int_{\mathbf{q}} J_\Lambda(\mathbf{q}) [J_\Lambda(\mathbf{q}) - J_\Lambda(\mathbf{q} + \mathbf{k})], \quad (\text{D.21})$$

was einer Hochtemperatur- und Hochfrequenz-Näherung entspricht, die für unsere Zwecke in drei Dimensionen ausreicht. Über das Feedback der Dynamik ist es dann möglich Effekte wie unterschiedliche Übergangstemperaturen für Ferro- oder Antiferromagneten bei endlichem Spin abzubilden, die in einem rein statischen Zugang nicht auftreten konnten

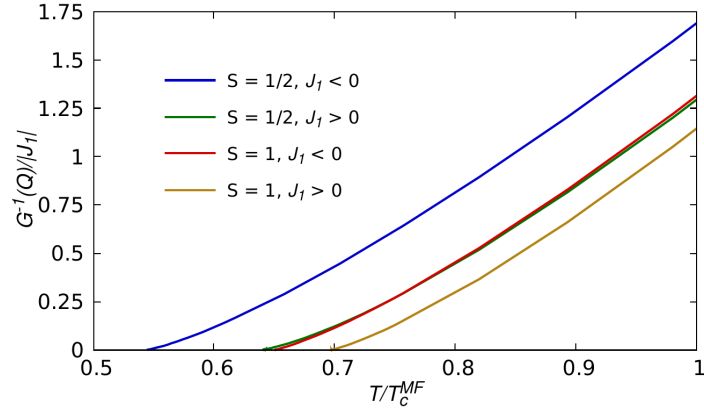


Figure D.2: Temperaturabhängigkeit der inversen Suszeptibilität $G^{-1}(\mathbf{Q})$ unter Berücksichtigung von Quantenkorrekturen nach Integration der Flussgleichungen. Ein Nulldurchgang $G^{-1}(\mathbf{Q}) = 0$ impliziert hierbei einen Phasenübergang.

[182]. Wie im statischen Fall wird die Impulsabhängigkeit der Vertizes ignoriert, was für nicht-frustrierte Systeme ohne konkurrierende Wechselwirkungen keine zu grobe Näherung darstellt. Unter Verwendung einer linearen Deformation finden wir Abweichungen $< 5\%$ von den etablierten Werten für T_c [179, 182]. Dies wird mit der in jüngerer Zeit populären und vielfach angewandten Pseudofermion-FRG kontrastiert, welche mit signifikant höherem numerischen Aufwand eine ähnliche oder schlechtere Genauigkeit erzielt [181, 184, 190]. Zukünftige Anwendungen auf frustrierte Systeme, die bessere Ansätze für die Quantendynamik und Impulsabhängigkeit der Vertizes benötigen, werden diskutiert.

Bibliography

- [1] J. Krieg and P. Kopietz, *Exact renormalization group for quantum spin systems*, Phys. Rev. B **99**, 060403(R) (2019).
- [2] J. Krieg, *Functional renormalization group approach to classical and quantum spin systems*, (PhD thesis, Johann Wolfgang Goethe-Universität, Frankfurt am Main, 2019).
- [3] P. Kopietz, L. Bartosch, and F. Schütz, *Introduction to the Functional Renormalization Group*, (Springer, Berlin, 2010).
- [4] C. Wetterich, *Exact evolution equation for the effective potential*, Phys. Lett. B **301**, 90 (1993).
- [5] V. G. Vaks, A. I. Larkin, and S. A. Pikin, *Thermodynamics of an ideal ferromagnetic substance*, Zh. Eksp. Teor. Fiz. **53**, 281 (1967) [Sov. Phys. JETP **26**, 188 (1968)].
- [6] V. G. Vaks, A. I. Larkin, and S. A. Pikin, *Spin waves and correlation functions in a ferromagnetic*, Zh. Eksp. Teor. Fiz. **53**, 1089 (1967) [Sov. Phys. JETP **26**, 647 (1968)].
- [7] R. Goll, D. Tarasevych, J. Krieg, and P. Kopietz, *Spin functional renormalization group for quantum Heisenberg ferromagnets: Magnetization and magnon damping in two dimensions*, Phys. Rev. B **100**, 174424 (2019).
- [8] R. Goll, A. Rückriegel, and P. Kopietz, *Zero-magnon sound in quantum Heisenberg ferromagnets*, Phys. Rev. B **102**, 224437 (2020).
- [9] A. Rückriegel, J. Arnold, R. Goll and P. Kopietz, *Spin functional renormalization group for dimerized quantum spin systems*, Phys. Rev. B **105**, 224406 (2022).
- [10] D. Tarasevych and P. Kopietz, *Dissipative spin dynamics in hot quantum paramagnets*, Phys. Rev. B **104**, 024423 (2021).
- [11] D. Tarasevych and P. Kopietz, *Critical spin dynamics of Heisenberg ferromagnets revisited*, Phys. Rev. B **105**, 024403 (2022).
- [12] D. Tarasevych, A. Rückriegel, S. Keupert, V. Mitsioannou, and P. Kopietz, *Spin-functional renormalization group for the $J_1J_2J_3$ quantum Heisenberg model*, Phys. Rev. B **106**, 174412 (2022); *Erratum: Spin-functional renormalization group for the $J_1 J_2 J_3$ quantum Heisenberg model*, *ibid*, **107**, 019904(E) (2023).
- [13] W. Pauli, *Zur Quantenmechanik des magnetischen Elektrons*, Z. Phys. **43**, 601 (1927).
- [14] N. W. Ashcroft and N. D. Mermin, *Solid state physics*, (Saunders College Publishing, New York, 1976).

-
- [15] G. Czycholl, *Theoretische Festkörperphysik 2*, (Springer, Berlin, 2017).
- [16] P. Kopietz, *Theorie zur Supraleitung, Magnetismus und elektronische Korrelation*, (Lecture Notes, Johann Wolfgang Goethe-Universität, Frankfurt am Main, 2021).
- [17] W. Heisenberg, *Zur Theorie des Ferromagnetismus*, Z. Phys. **49**, 619 (1928).
- [18] W. Nolting, *Vielteilchentheorie*, (Springer, Berlin, 2009).
- [19] P. W. Anderson, *Antiferromagnetism. Theory of Superexchange Interaction*, Phys. Rev. **79**, 350 (1950).
- [20] J. Kanamori, *Superexchange interaction and symmetry properties of electron orbitals*, J. Phys. Chem. Solids, **10**, 87 (1959).
- [21] F. Bloch, *Zur Theorie des Ferromagnetismus*, Z. Phys. **61**, 206 (1930).
- [22] J. Goldstone, A. Salam, and S. Weinberg, *Broken Symmetries*, Phys. Rev. **127**, 965 (1962).
- [23] P. W. Anderson, *An Approximate Quantum Theory of the Antiferromagnetic Ground State*, Phys. Rev. **86**, 694 (1952).
- [24] N. D. Mermin and H. Wagner, *Absence of Ferromagnetism or Antiferromagnetism in One- or Two-Dimensional Isotropic Heisenberg Models*, Phys. Rev. Lett. **17**, 1133 (1966).
- [25] B. Widom, *Surface tension and molecular correlations near the critical point*, J. Chem. Phys. **43**, 3892, (1965).
- [26] C. Holm and W. Janke, *Critical exponents of the classical three-dimensional Heisenberg model: A single-cluster Monte Carlo study*, Phys. Rev. B **48**, 936, (1993).
- [27] L. P. Kadanoff, *Scaling laws for Ising models near T_c* , Physics **2**, 263, (1966).
- [28] R. Kubo, *Statistical-Mechanical Theory of Irreversible Processes. I. General Theory and Simple Applications to Magnetic and Conduction Problems*, J. Phys. Soc. Japan **12**, 570 (1957).
- [29] P. Kopietz, *Vielteilchentheorie*, (Lecture Notes, Johann Wolfgang Goethe-Universität, Frankfurt am Main, 2022).
- [30] T. Holstein and H. Primakoff, *Field dependence of the intrinsic domain magnetization of a ferromagnet*, Phys. Rev. **58**, 1098 (1940).
- [31] M. F. Collins and W. Marshall, *Neutron scattering from paramagnets*, Proc. Phys. Soc. **92**, 390, (1967).
- [32] L. Van Hove, *Time-Dependent Correlations between Spins and Neutron Scattering in Ferromagnetic Crystals*, Phys. Rev. **95**, 1374 (1954).
- [33] U. Balucani, M. Howard Lee and V. Tognetti, *Dynamical correlations*, Phys. Rep. **373**, 409, (2003).
- [34] R. Kubo, *The fluctuation-dissipation theorem*, Rep. Prog. Phys. **29**, 255 (1966).

-
- [35] D. Forster, *Hydrodynamic Fluctuations, Broken Symmetry, and Correlation Functions*, (Benjamin, Reading, 1975).
- [36] P. C. Kwok and T. D. Schultz, *Correlation functions and Green functions: zero-frequency anomalies*, J. Phys. C **2**, 1196 (1969).
- [37] H. Falk, *Lower Bound for the Isothermal Magnetic Susceptibility*, Phys. Rev. **165**, 602 (1968).
- [38] R. Zwanzig, *Memory Effects in Irreversible Thermodynamics*, Phys. Rev. **124**, 93 (1961).
- [39] H. Mori, *Transport, Collective Motion, and Brownian Motion*, Prog. Theor. Phys. **33**, 423 (1965).
- [40] T. Matsubara, *A New Approach to Quantum-Statistical Mechanics*, Prog. Theor. Phys. **14**, 351 (1955).
- [41] L. P. Kadanoff and P. C. Martin, *Hydrodynamic equations and correlation functions*, Ann. Phys. **24**, 419 (1963).
- [42] P. Kopietz, *Thouless number and spin diffusion in quantum Heisenberg ferromagnets*, Mod. Phys. Lett. B **7**, 1747 (1993).
- [43] X. Zotos and P. Prelovšek, *Evidence for ideal insulating or conducting state in a one-dimensional integrable system*, Phys. Rev. B **53**, 983 (1996).
- [44] Y. Pomeau and P. Résibois, *Time dependent correlation functions and mode-mode coupling theories*, Phys. Rep, **19**, 64 (1975).
- [45] D. Forster, D. R. Nelson, and M. J. Stephen, *Long-Time Tails and the Large-Eddy Behavior of a Randomly Stirred Fluid*, Phys. Rev. Lett. **36**, 867 (1976).
- [46] D. Forster, D. R. Nelson, and M. J. Stephen, *Large-distance and long-time properties of a randomly stirred fluid*, Phys. Rev. A **16**, 732 (1977).
- [47] M. Žnidarič, *Spin Transport in a One-Dimensional Anisotropic Heisenberg Model*, Phys. Rev. Lett. **106** 220601, (2011).
- [48] M. Ljubotina, M. Znidaric, and T. Prosen, *Spin diffusion from an inhomogeneous quench in an integrable system*, Nat. Commun. **8**, 16117 (2017).
- [49] S. Gopalakrishnan, R. Vasseur, and B. Ware, *Anomalous relaxation and the high-temperature structure factor of XXZ spin chains*, PNAS **116**, 16250 (2019).
- [50] S. Gopalakrishnan and R. Vasseur, *Kinetic Theory and Spin Diffusion and Superdiffusion in XXZ Spin Chains*, Phys. Rev. Lett. **122**, 127202 (2019).
- [51] R. J. Sanchez, V. K. Varma, and V. Oganesyan, *Anomalous and regular transport in spin- $\frac{1}{2}$ chains: ac conductivity* Phys. Rev. B **98**, 054415 (2018).
- [52] E. Ilievski and J. De Nardis, *Microscopic Origin of Ideal Conductivity in Integrable Quantum Models*, Phys. Rev. Lett. **119**, 020602, (2017).

-
- [53] J. De Nardis, D. Bernard and B. Doyon, *Diffusion in generalized hydrodynamics and quasiparticle scattering*, SciPost Phys. **6**, 049 (2019).
- [54] P. C. Hohenberg and B. I. Halperin, *Theory of dynamic critical phenomena*, Rev. Mod. Phys. **49**, 435 (1977).
- [55] E. Frey and F. Schwabl, *Critical dynamics of magnets*, Adv. Phys., **43:5**, 577 (1994).
- [56] R. Folk and G. Moser, *Critical dynamics: a field-theoretical approach*, J. Phys. A: Math. Gen. **39** R207 (2006).
- [57] S.-K. Ma and G. F. Mazenko, *Critical dynamics of ferromagnets in $6 - \epsilon$ dimensions: General discussion and detailed calculation*, Phys. Rev. B **11**, 4077 (1975).
- [58] B. I. Halperin and P. C. Hohenberg, *Scaling Laws for Dynamic Critical Phenomena*, Phys. Rev. **177**, 952 (1969).
- [59] B. I. Halperin and P. C. Hohenberg, *Hydrodynamic Theory of Spin Waves*, Phys. Rev. **188**, 898 (1969).
- [60] K. Kawasaki, *Kinetic equations and time correlation functions of critical fluctuations*, Ann. Phys. **61**, 1 (1970).
- [61] P. Böni and G. Shirane, *Paramagnetic neutron scattering from the Heisenberg ferromagnet EuO* , Phys. Rev. B **33**, 3012 (1986).
- [62] R. Coldea, R. A. Cowley, T. G. Perring, D. F. McMorrow and B. Roessli, *Critical behavior of the three-dimensional Heisenberg antiferromagnet RbMnF_3* , Phys. Rev. B **57**, 5281 (1998).
- [63] N. N. Bogolyubov and S. V. Tyablikov, Dokl. Akad. Nauk SSSR **126**, 53 (1959) [Sov. Phys.-Dokl. **4**, 604 (1959)].
- [64] R. A. Tahir-Kheli and D. Ter Haar, *Use of Green Functions in the Theory of Ferromagnetism. I. General Discussion of the Spin-S Case*, Phys. Rev. **127**, 88 (1962).
- [65] J. Kondo and K. Yamaji, *Green's-Function Formalism of the One-Dimensional Heisenberg Spin System*, Prog. Theor. Phys. **47**, 807 (1972).
- [66] L. Siurakshina, D. Ihle, and R. Hayn, *Magnetic order and finite-temperature properties of the two-dimensional frustrated Heisenberg model*, Phys. Rev. B **64**, 104406, (2001).
- [67] A. Auerbauch and D. P. Arovas, *Spin Dynamics in the Square-Lattice Antiferromagnet*, Phys. Rev. Lett. **61**, 617 (1988).
- [68] J. Reuther and P. Wölfle, *J_1 - J_2 frustrated two-dimensional Heisenberg model: Random phase approximation and functional renormalization group*, Phys. Rev. B **81**, 144410 (2010).
- [69] B. Schneider, D. Kiese, and B. Sbierski, *Taming pseudofermion functional renormalization for quantum spins: Finite temperatures and the Popov-Fedotov trick*, Phys. Rev. B **106**, 235113 (2022).

-
- [70] R. M. Wilcox, *Bounds for the Isothermal, Adiabatic, and Isolated Static Susceptibility Tensors*, Phys. Rev. **174**, 624 (1968).
- [71] M. Suzuki, *Ergodicity, constants of motion, and bounds for susceptibilities*, Physica **51**, 277 (1971).
- [72] Y. Chiba, K. Asano, and A. Shimizu, *Anomalous behavior of Magnetic Susceptibility by Quench Experiments in Isolated Quantum Systems*, Phys. Rev. Lett. **124**, 110609 (2020).
- [73] L. D'Alessio, Y. Kafri, A. Polkovnikov, and M. Rigol, *From quantum chaos and eigenstate thermalization to statistical mechanics and thermodynamics*, Adv. Phys. **65**, 239 (2016).
- [74] M. Blume and J. Hubbard, *Spin Correlation Functions at High Temperatures*, Phys. Rev. B **1**, 3815 (1970).
- [75] A. A. Katanin, *Fulfillment of Ward identities in the functional renormalization group approach*, Phys. Rev. B **70**, 115109 (2004).
- [76] M. Salmhofer, C. Honerkamp, W. Metzner and O. Lauscher, *Renormalization Group Flows into Phases with Broken Symmetry*, Prog. Theor. Phys. **112**, 943 (2004).
- [77] P. G. De Gennes, *Inelastic magnetic scattering of neutrons at high temperatures*, J. Phys. Chem. Solids **4**, 223 (1958).
- [78] M. Chertkov and I. Kolokolov, *Long-time dynamics of the infinite-temperature Heisenberg magnet*, Phys. Rev. B **49**, 3592 (1994).
- [79] S. W. Lovesey and E. Balcar, *A theory of the time-dependent properties of Heisenberg spin chains at infinite temperature*, J. Phys.: Condens. Matter **6**, 1253, (1994).
- [80] S. W. Lovesey and E. Balcar, *Time-dependent spin correlations in the Heisenberg magnet at infinite temperature*, J. Phys.: Condens. Matter **6**, L521, (1994).
- [81] M. Ljubotina, M. Žnidarič, and T. Prosen, *Kardar-Parisi-Zhang Physics in the Quantum Heisenberg Magnet*, Phys. Rev. Lett. **122**, 210602, (2019).
- [82] J. De Nardis, M. Medenjak, C. Karrasch, and E. Ilievski, *Anomalous Spin Diffusion in One-Dimensional Antiferromagnets*, Phys. Rev. Lett. **123**, 186601 (2019).
- [83] J. De Nardis, M. Medenjak, C. Karrasch, and E. Ilievski, *Universality Classes of Spin transport in One-Dimensional Isotropic Magnets: The Onset of Logarithmic Anomalies*, Phys. Rev. Lett. **124**, 210605 (2020).
- [84] U. Agrawal, S. Gopalakrishnan, R. Vasseur, and B. Ware, *Anomalous low-frequency conductivity in easy-plane XXZ spin chains*, Phys. Rev. B **101**, 224415, (2020).
- [85] M. Dupont and J. E. Moore, *Universal spin dynamics in infinite-temperature one-dimensional quantum magnets*, Phys. Rev. B **101**, 121106(R) (2020).
- [86] E. Ilievski, J. De Nardis, S. Gopalakrishnan, R. Vasseur, and B. Ware, *Superuniversality of Superdiffusion*, Phys. Rev. X **11**, 031023, (2021).

-
- [87] H. Mori and K. Kawasaki, *Theory of Dynamical behaviors of Ferromagnetic Spins*, Prog. Theor. Phys. **27**, 529 (1962).
- [88] H. S. Bennett and P. C. Martin, *Spin diffusion in the Heisenberg paramagnet*, Phys. Rev. **A138**, 608 (1965).
- [89] P. Résibois and M. De Leener, *Irreversibility in Heisenberg Spin Systems. I. General Formalism and Kinetic Equations in the High-Temperature Limit*, Phys. Rev. **152**, 305 (1966).
- [90] P. Résibois and M. De Leener, *Irreversibility in Heisenberg Spin Systems. II. Approximate Solution of the High-Temperature Kinetic Equations*, Phys. Rev. **152**, 318 (1966).
- [91] G. F. Reiter, *Spin Fluctuations in Heisenberg Paramagnets. I. Diagrammatic Expansion for the Moments of the Spectral Density at Finite Temperature*, Phys. Rev. B **5**, 222 (1972).
- [92] G. F. Reiter, *Spin Fluctuations in Heisenberg Paramagnets. II. Kinetic Theory and Approximate High Temperature Solutions*, Phys. Rev. B **7**, 3325 (1973).
- [93] C. W. Myles and P. A. Fedders, *Dynamical two-point correlation functions in a high-temperature Heisenberg paramagnet*, Phys. Rev. B **9**, 4872 (1974).
- [94] A. G. Redfield and W. N. Yu, *Moment-method calculation of magnetization and interspin-energy diffusion*, Phys. Rev. **169**, 443 (1968).
- [95] R. A. Tahir-Kheli and D. G. McFadden, *Space-Time Correlations in Exchange-Coupled Paramagnets at Elevated Temperatures*, Phys. Rev. **182**, 604 (1969).
- [96] T. Morita, *Spin Diffusion in the Heisenberg Magnets at Infinite Temperature*, Phys. Rev. B **6**, 3385 (1972).
- [97] T. Morita, *Spin Diffusion Constant for the Heisenberg Magnet at High Temperatures*, J. Phys. Soc. Jpn. **39**, 1217 (1975).
- [98] S. W. Lovesey and R. A. Meserve, *Dynamic properties of Heisenberg paramagnets*, J. Phys. C: Solid State Phys. **6**, 79 (1973).
- [99] H. Mori, *A Continued-Fraction Representation of the Time-Correlation Functions*, Prog. Theor. Phys. **34**, 399 (1965).
- [100] K. Tomita and H. Tomita, *A Dynamic Approach to Phase Transition Based on Moments*, Prog. Theor. Phys. **45**, 1407 (1971).
- [101] M. F. Collins, *Series expansion of High-Temperature Dynamics of Heisenberg Paramagnets*, Phys. Rev. B **4**, 1588 (1971).
- [102] J. W. Tucker, *Relaxation-shape function of a Heisenberg paramagnet based on the method of moments*, J. Phys. C: Solid State Phys. **7**, 4089 (1974).
- [103] C. G. Windsor, *Spin correlations in a classical Heisenberg paramagnet*, Proc. Phys. Soc. **91** 353 (1967).

-
- [104] G. Müller, *Anomalous Spin Diffusion in Classical Heisenberg Magnets*, Phys. Rev. Lett. **60**, 2785 (1988).
- [105] R. W. Gerling and D. P. Landau, *Comment on "Anomalous Spin Diffusion in Classical Heisenberg Magnets"*, Phys. Rev. Lett. **63**, 812 (1989).
- [106] G. Müller, *Reply to Comment on "Anomalous Spin Diffusion in Classical Heisenberg Magnets"*, Phys. Rev. Lett. **63**, 813 (1989).
- [107] M. Theodosopulu and P. Résibois, *Kinetic approach to the long-time behavior in fluids III. The One-particle propagator*, Physica **82A**, 47, (1976).
- [108] Y. Pomeau, *Low-Frequency behavior of transport coefficients in fluids*, Phys. Rev. A **5**, 2569 (1971).
- [109] P. Borckmans, G. Dewel and D. Walgraef, *Long time behavior of correlation functions in Heisenberg paramagnets*, Physica A, Volume **88**, 2261 (1977).
- [110] H. C. Fogedby and A. P. Young, *On correlations at long times in Heisenberg paramagnets*, J. Phys. C: Solid State Phys. **11**, 527 (1978).
- [111] M. Manson, *The memory function in the mode-mode coupling theory for the Heisenberg paramagnet*, J. Phys. C: Solid State Phys. **7**, 4073 (1974).
- [112] M. Kardar, G. Parisi, and Y. Z. Zhang, *Dynamic scaling of growing interfaces*, Phys. Rev. Lett. **56**, 889 (1986).
- [113] M. Prähofer and H. Spohn, *Exact scaling functions for one-dimensional stationary KPZ growth*, J. Stat. Phys. **115**, 255 (2004).
- [114] H. Bethe, *Zur Theorie der Metalle I. Eigenwerte und Eigenfunktionen der Hnearen Atomkette.*, Z. Phys. **71**, 205 (1931).
- [115] T. E. Wainwright, B. J. Alder, and D.M. Gass, *Decay of time correlation in two dimensions*, Phys. Rev A **4**, 233, (1971).
- [116] K. Kawasaki, N. Miyamoto and R.A. Tahir-Kheli, *Dynamics of quasi-one- and two-dimensional spin systems in the high-temperature limit*, J. Phys. C: Solid State Phys. **15**, 2735 (1982).
- [117] T. Nagao and J. Igarashi, *Spin Dynamics in Two-Dimensional Quantum Heisenberg Antiferromagnets*, J. Phys. Soc. Jpn. **67**, 1029 (1997).
- [118] S. Hild, T. Fukuhara, P. Schauß, J. Zeiher, M. Knap, E. Demler, I. Bloch, and C. Gross, *Far-from-Equilibrium Spin Transport in Heisenberg Quantum Magnets*, Phys. Rev. Lett. **113**, 147205 (2014).
- [119] A. Tucciarone, J. M. Hastings, and L. M. Corliss, *Theoretical and Experimental Spin-Relaxation Functions in Paramagnetic RbMnF₃*, Phys. Rev. Lett. **26**, 257 (1971).
- [120] A. Tucciarone, J. M. Hastings, and L. M. Corliss, *Spin Diffusion in RbMnF₃*, Phys. Rev. B **8**, 1103 (1973).

-
- [121] L. Passell, O. W. Dietrich, and J. Als-Nielsen, *Neutron scattering from the Heisenberg ferromagnets EuO and EuS. III. Spin dynamics of EuO*, Phys. Rev. B **14**, 4897 (1976).
- [122] J. R. Thompson, E. R. Hunt and H. Meyer, *Spin diffusion in solid ^3He* , Phys. Lett. A, **25**, 4, 313 (1967).
- [123] J. Labrujere, T. O. Klaassen, and N. J. Poulis, *Spin dynamics in a 3D Heisenberg ferromagnet in the paramagnetic state II*, J. Phys. C: Solid State Phys. **15**, 999 (1982).
- [124] T. Morita and T. Horiguchi, *Singular behavior of the Spectral-Weight Function of the Spin-Pair Correlation Function*, Phys. Rev. B **8**, 414 (1973).
- [125] M. Böhm, H. Leschke, M. Henneke, V. S. Viswanath, J. Stolze, and G. Müller, *Spectral signature of quantum spin diffusion in dimensions $d = 1, 2$ and 3*, Phys. Rev. B **49**, 417 (1994).
- [126] K. Kawasaki, *Anomalous spin diffusion in ferromagnetic spin systems*, J. Phys. Chem. Solids **28**, 1277 (1967).
- [127] F. Wegner, *On the Heisenberg model in the paramagnetic region and at the critical point*, Z. Phys. **216**, 433 (1968).
- [128] J. Hubbard, *Spin-correlation functions in the paramagnetic phase of a Heisenberg ferromagnet*, J. Phys. C: Solid State Phys. **4**, 53 (1971).
- [129] C. Aberger and R. Folk, *Shape crossover in the correlation function of isotropic ferromagnets above T_c* , Phys. Rev. B, **38**, 6693 (1988).
- [130] A. Cuccoli, V. Tognetti, and S. W. Lovesey, *Critical and paramagnetic spin fluctuations in Heisenberg magnets*, Phys. Rev. B **39**, 2619 (1989).
- [131] V. Dohm, *Dynamical spin-spin correlation function of an isotropic ferromagnet at T_c in $6 - \epsilon$ dimensions*, Solid State Commun. **20**, 657 (1976).
- [132] J. K. Bhattacharjee and R. A. Ferrell, *Dynamic scaling for the isotropic ferromagnet: ϵ expansion to two-loop order*, Phys. Rev. B **24**, 6480 (1981).
- [133] P. Résibois and C. Piette, *Temperature Dependence of the Linewidth in Critical Spin Fluctuation*, Phys. Rev. Lett. **24**, 514 (1970)
- [134] R. Folk and H. Iro, *Paramagnetic neutron scattering and renormalization-group theory for isotropic ferromagnets at T_c* , Phys. Rev. B **32**, 1880(R) (1985).
- [135] H. Iro, *The Dynamical Correlation Function for Isotropic Ferromagnets for $T \geq T_c$* , Z. Physik B **68**, 485 (1987).
- [136] B. S. Shastry, D. M. Edwards and A. P. Young, *The paramagnetic state of BCC iron*, J. Phys. C: Solid State Phys., **14** L665, (1981).
- [137] M. J. Nolan and G. F. Mazenko, *Dynamic structure factor for a ferromagnet in the scaling region to first order in $\epsilon = 6 - d$* , Phys. Rev. B **15**, 4471 (1977).
- [138] K. Chen and D. P. Landau, *Spin-dynamics study of the dynamic critical behavior of the three-dimensional classical Heisenberg ferromagnet*, Phys. Rev. B **49**, 3266 (1994).

-
- [139] D. P. Landau and M. Krech, *Spin dynamics simulations of classical ferro- and anti-ferromagnetic model systems: comparison with theory and experiment*, J. Phys. C: **11** R179 (1999).
- [140] X. Tao, D. P. Landau, T. C. Schulthess, and G. M. Stocks, *Spin Waves in Paramagnetic bcc Iron: Spin Dynamics Simulations*, Phys. Rev. Lett. **95**, 087207 (2005).
- [141] H. A. Mook and J.W. Lynn, *Measurements of the magnetic excitations above T_c in iron and nickel*, J. App. Phys. **57**, 3006 (1985).
- [142] X. Tao, *Spin Dynamic Simulations of Body-Centered Cubic Iron*, (PhD thesis, University of Georgia, Athens, 2005).
- [143] L. Passell, O. W. Dietrich, and J. Als-Nielsen, *Neutron scattering from the Heisenberg ferromagnets EuO and EuS. I. The exchange interactions*, Phys. Rev. B **14**, 4897 (1976).
- [144] P. Böni, M. E. Chen, and G. Shirane, *Comparison of the critical magnetic scattering from the Heisenberg system EuO with renormalization-group theory*, Phys. Rev. B **35**, 8449 (1987).
- [145] P. Böni, G. Shirane, H. G. Bohn, and W. Zinn, *Spin fluctuations in EuS above T_c : Comparison with asymptotic renormalization-group theory*, J. Appl. Phys. **63**, 3089 (1988).
- [146] J. P. Wicksted, P. Böni, and G. Shirane, *Polarized-beam study of the paramagnetic scattering from bcc iron*, Phys. Rev. B **30**, 3655 (1984).
- [147] G. Shirane, P. Böni, and J. L. Martínez, *Propagating spin waves in Ni above T_c : Evidence against their existence*, Phys. Rev. B **36**, 881 (1987).
- [148] P. Böni, H. A. Mook, J. L. Martínez, and G. Shirane, *Comparison of the paramagnetic spin fluctuations in nickel with asymptotic renormalization-group theory*, Phys. Rev. B **47**, 3171, (1993).
- [149] E. Frey, F. Schwabl, and S. Thoma, *Shape functions of dipolar ferromagnets at and above the Curie point*, Phys. Rev. B **40**, 7199 (1989).
- [150] J. Hubbard, *The magnetism of iron*, Phys. Rev. B **19**, 2626 (1979).
- [151] J. Hubbard, *Magnetism of nickel*, Phys. Rev. B **23**, 5974 (1981).
- [152] F. Mezei, *Critical Dynamics in EuO at the Ferromagnetic Curie Point*, Physica **B**, 136, 417 (1986).
- [153] H. Iro, *The dynamical correlation function of an isotropic heisenberg ferromagnet in the critical region*, J. Magn. Magn. Mater. **73**, 175 (1988).
- [154] R. Folk and H. Iro, *Temperature dependence of paramagnetic neutron scattering from Heisenberg ferromagnets above T_c* , Phys. Rev. B **34**, 6571 (R) (1986).
- [155] S-H. Tsai and D. P. Landau, *Critical dynamics of the simple-cubic Heisenberg anti-ferromagnet $RbMnF_3$: Extrapolation to $q = 0$* , Phys. Rev. B **67**, 104411 (2003).

-
- [156] R. Schick, O. Götze, T. Ziman, R. Zinke, J. Richter, and M. E. Zhitomirsky, *Ground-state selection by magnon interactions in a fcc antiferromagnet*, Phys. Rev. B **106**, 094431 (2022).
- [157] F. Wegner, *On the Dynamics of the Heisenberg Antiferromagnet at T_N* , Z. Physik **218**, 260 (1969).
- [158] A. Cuccoli, S. W. Lovesey and V. Tognetti, *Critical and paramagnetic spin dynamics in an antiferromagnetically coupled Heisenberg magnet: results for $RbMnF_3$* , J. Phys.: Condens. Matter **6**, 7553 (1994).
- [159] R. Freedman and G. F. Mazenko, *Critical dynamics of isotropic antiferromagnets using renormalization-group methods: $T \geq T_N$* , Phys. Rev. B **13**, 4967 (1976).
- [160] H-K. Janssen, *Renormalized Field Theory of the Critical Dynamics of $O(n)$ -Symmetric Systems*, Z. Physik B **26**, 187 (1977).
- [161] M. Takahashi, *Quantum Heisenberg Ferromagnets in One and Two Dimensions at Low Temperature*, Prog. Theor. Phys. Suppl. **87**, 233 (1986).
- [162] M. Takahashi, *Few-Dimensional Heisenberg Ferromagnets at Low Temperature*, Phys. Rev. Lett. **58**, 318 (1987).
- [163] M. Yamada and M. Takahashi, *Critical behavior of Spin-1/2 One-Dimensional Heisenberg Ferromagnet at Low Temperatures*, J. Phys. Soc. Jpn. **55**, 2024 (1986).
- [164] D. P. Arovas and A. Auerbach, *Functional integral theories of low-dimensional quantum Heisenberg models*, Phys. Rev. B **38**, 316 (1988).
- [165] P. Kopietz, *Low-temperature behavior of the correlation length and the susceptibility of the ferromagnetic quantum Heisenberg chain*, Phys. Rev. B **40**, 5194 (1989).
- [166] M. Takahashi, *Dynamics of Heisenberg ferromagnets at low temperature*, Phys. Rev. B **42**, 766 (1990).
- [167] F. B. McLean and M. Blume, *Spin Dynamics of Linear Heisenberg Magnetic Chains*, Phys. Rev. B **7**, 1149 (1973).
- [168] S. W. Lovesey, *Dynamic properties of one-dimensional Heisenberg magnets*, J. Phys. C: Solid State Phys. **7**, 2008 (1974).
- [169] M. Dupont, N. E. Sherman, and J. E. Moore, *Spatiotemporal Crossover between Low- and High-Temperature Dynamical Regimes in the Quantum Heisenberg Magnet*, Phys. Rev. Lett. **127**, 107201 (2021).
- [170] S. W. Lovesey and A. Megann, *A Coupled-Mode Theory of Heisenberg Paramagnets*, Z. Physik B **63**, 437 (1986).
- [171] G. Reiter, *Spin-wave theory of critical dynamics in one- and two-dimensional Heisenberg models: Failure of the dynamic-scaling hypothesis and the mode-coupling theory*, Phys. Rev. B **21**, 5356 (1980).
- [172] G. Reiter, *Comment on “Dynamics of Heisenberg ferromagnets at low temperature”*, Phys. Rev. B **47**, 8335 (1993).

-
- [173] M. Takahashi, *Reply to “Comment on ‘Dynamics of Heisenberg ferromagnets at low temperature’ ”*, Phys. Rev. B **47**, 8336 (1993).
- [174] P. Kopietz and S. Chakravarty, *Low-temperature behavior of the correlation length and the susceptibility of a quantum Heisenberg ferromagnet in two dimensions*, Phys. Rev. B **40**, 4858 (1989)
- [175] A. Chubukov, *Schwinger bosons and hydrodynamics of two-dimensional magnets*, Phys. Rev. B **44**, 12318, (1991).
- [176] A. Rançon and N. Dupuis, *Nonperturbative renormalization group approach to the Bose-Hubbard model*, Phys. Rev. B **83**, 172501 (2011).
- [177] D. F. Litim, *Optimized renormalization group flows*, Phys. Rev. D **64**, 105007 (2001).
- [178] W. Metzner, M. Salmhofer, C. Honerkamp, V. Meden, and K. Schönhammer, *Functional renormalization group approach to correlated fermion systems*, Rev. Mod. Phys. **84**, 299 (2012).
- [179] A. W. Sandvik, *Critical Temperature and the Transition from Quantum to Classical Order Parameter Fluctuations in the Three-Dimensional Heisenberg Antiferromagnet*, Phys. Rev. Lett. **80**, 5196 (1998).
- [180] M. Troyer, F. Alet, and S. Wessel, *Histogram Methods for Quantum Systems: from reweighting to Wang-Landau Sampling*, Braz. J. Phys. **34**, 377 (2004).
- [181] Y. Iqbal, R. Thomale, F. P. Toldin, S. Rachel, and J. Reuther, *Functional renormalization group approach for three-dimensional quantum magnetism*, Phys. Rev. B **94**, 140408(R) (2016).
- [182] J. Oitmaa and W. Zheng, *Curie and Néel temperatures of quantum magnets*, J. Phys. Condens. Matter **16**, 8653 (2004).
- [183] S. Yabunaka and B. Delamotte, *Surprises in $O(N)$ Models: Nonperturbative Fixed Points, Large N Limits, and Multicriticality*, Phys. Rev. Lett. **119**, 191602 (2017).
- [184] M. Rück and J. Reuther, *Effects of two-loop contributions in the pseudofermion functional renormalization group method for quantum spin systems*, Phys. Rev. B **97**, 144404 (2018).
- [185] D. Kiese, T. Müller, Y. Iqbal, R. Thomale, and S. Trebst, *Multiloop functional renormalization group approach to quantum spin systems*, Phys. Rev. Research **4**, 023185 (2022).
- [186] M. K. Ritter, D. Kiese, T. Müller, F. B. Kugler, R. Thomale, S. Trebst, and J. von Delft, *Benchmark Calculations of Multiloop Pseudofermion fRG*, Eur. Phys. J. B **95**, 102 (2022).
- [187] M. L. Baez and J. Reuther, *Numerical treatment of spin systems with unrestricted spin length S : A functional renormalization group study*, Phys. Rev. B **96**, 045144 (2017).

-
- [188] T. Müller, D. Kiese, N. Niggemann, B. Sbierski, J. Reuther, S. Trebst, R. Thomale and Y. Iqbal, *Pseudo-fermion functional renormalization group for spin models*, arXiv:2307.10359.
- [189] N. Niggemann, B. Sbierski, and J. Reuther, *Frustrated quantum spins at finite temperature: Pseudo-Majorana functional renormalization group approach*, Phys. Rev. B **103**, 104431 (2021).
- [190] N. Niggemann, J. Reuther and B. Sbierski, *Quantitative functional renormalization for three-dimensional quantum Heisenberg models*, SciPost Phys. **12**, 156 (2022).
- [191] H. Shao, Y. Q. Qin, S. Capponi, S. Chesi, Z. Y. Meng, and A. W. Sandvik, *Nearly Deconfined Spinon Excitations in the Square-Lattice Spin-1/2 Heisenberg Antiferromagnet*, Phys. Rev. X **7**, 041072 (2017).
- [192] F. Ferrari and F. Becca, *Spectral signatures of fractionalization in the frustrated Heisenberg model on the square lattice*, Phys. Rev. B **98**, 100405(R) (2018).
- [193] H. Shackleton, A. Thomson, and S. Sachdev, *Deconfined criticality and a gapless \mathbf{Z}_2 spin liquid in the square-lattice antiferromagnet*, Phys. Rev. B **104**, 045110 (2021).
- [194] S. Morita, R. Kaneko, and M. Imada, *Quantum Spin Liquid in Spin 1/2 J_1 - J_2 Heisenberg Model on Square Lattice: Many-Variable Variational Monte Carlo Study Combined with Quantum-Number Projections*, J. Phys. Soc. Jpn. **84**, 024720 (2015)
- [195] Y. Nomura and M. Imada, *Dirac-Type Nodal Spin Liquid Revealed by Refined Quantum Many-Body Solver Using Neural-Network Wave Function, Correlation Ratio, and Level Spectroscopy*, Phys. Rev. X **11**, 031034 (2021).
- [196] F. D. M. Haldane, *Nonlinear Field Theory of Large-Spin Heisenberg Antiferromagnets: Semiclassically Quantized Solitons of the One-Dimensional Easy-Axis Néel State*, Phys. Rev. Lett. **50**, 1153 (1983).
- [197] T. Xiang, *Thermodynamics of quantum Heisenberg spin chains*, Phys. Rev. B **58**, 9142, (1998).
- [198] J. Oitmaa, *Frustrated $J_1 - J_2 - J_3$ Heisenberg antiferromagnet on the simple cubic lattice*, Phys. Rev. B **95**, 014427 (2017).
- [199] J. Halbinger, B. Schneider and B. Sbierski, *Spectral representation of Matsubara n -point functions: Exact kernel functions and applications*, SciPost Phys. **15**, 183 (2023).
- [200] A. Rückriegel, J. Arnold, R. Krämer, and P. Kopietz, *Functional renormalization group without functional integrals: Implementing Hilbert space projections for strongly correlated electrons via Hubbard X -operators*, Phys. Rev. B **108**, 115104 (2023).
- [201] T. A. Kennedy, S. H. Choh, and G. Seidel, *Temperature Dependence of the Exchange Interaction in $K_2\text{CuCl}_4 \cdot 2\text{H}_2\text{O}$* , Phys. Rev. B **2**, 3645 (1970).
- [202] J. W. Tucker, *Temperature Dependence of Nuclear Magnetic Resonance Linewidths in RbMnF_3* , Phys. Lett. A **61** 3, 195 (1977).
- [203] S. Chakravarty, B. I. Halperin, and D. R. Nelson, *Two-dimensional quantum Heisenberg antiferromagnet at low temperatures*, Phys. Rev. B **39**, 2344 (1989).

- [204] J. Kim and M. Troyer, *Low Temperature Behavior and Crossovers of the Square Lattice Quantum Heisenberg Antiferromagnet*, Phys. Rev. Lett. **80**, 2705 (1998).
- [205] M. Takahashi, *Dynamics of Antiferromagnetic Heisenberg Model at Low Temperatures*, Prog. Theor. Phys. **101**, 487 (1990).
- [206] P. Kopietz, *Comment on "Spin Dynamics in the Square-Lattice Antiferromagnet"*, Phys. Rev. Lett. **64**, 2587 (1990).
- [207] C. M. Canali and M. Wallin, *Spin-spin correlation functions for the square-lattice Heisenberg antiferromagnet at zero temperature*, Phys. Rev. B **48**, 3264 (1993).
- [208] J.-S. Caux and R. Hagemans, *The four-spinon dynamical structure factor of the Heisenberg chain*, J. Stat. Mech.: Theory Exp. P12013 (2008).
- [209] P. Ghosh, T. Müller, F. P. Toldin, J. Richter, R. Narayanan, R. Thomale, J. Reuther, and Y. Iqbal, *Quantum paramagnetism and helimagnetic orders in the Heisenberg model on the body centered cubic lattice*, Phys. Rev. B **100**, 014420, (2019).
- [210] J. Oitmaa and E. Bornilla, *High-temperature-series study of the spin-1/2 Heisenberg ferromagnet*, Phys. Rev. B **53**, 14228 (1996).
- [211] M. P. Nightingale and H. W. J. Blöte, *Monte Carlo Calculation of Free Energy, Critical Point, and Surface Critical behavior of Three-Dimensional Heisenberg Ferromagnets*, Phys. Rev. Lett. **60**, 1562 (1988).